

## **X-ray Fluorescence Spectroscopy for Laboratory Applications**

# **X-ray Fluorescence Spectroscopy for Laboratory Applications**

*Michael Haschke*

*Jörg Flock*

*Michael Haller*

**WILEY-VCH**

## Authors

### *Dr. Michael Haschke*

Günter Allee 11  
15345 Eggersdorf  
Germany

### *Dr. Jörg Flock*

Thyssen Krupp Stahl AG  
Kaiser-Wilhelm-Str. 100  
47166 Duisburg  
Germany

### *Dipl.-Min. Michael Haller*

CrossRoads Scientific LLC.  
Middletown  
CT  
United States

■ All books published by **Wiley-VCH** are carefully produced. Nevertheless, authors, editors, and publisher do not warrant the information contained in these books, including this book, to be free of errors. Readers are advised to keep in mind that statements, data, illustrations, procedural details or other items may inadvertently be inaccurate.

**Library of Congress Card No.:**  
applied for

### **British Library Cataloguing-in-Publication Data**

A catalogue record for this book is available from the British Library.

### **Bibliographic information published by the Deutsche Nationalbibliothek**

The Deutsche Nationalbibliothek lists this publication in the Deutsche Nationalbibliografie; detailed bibliographic data are available on the Internet at <<http://dnb.d-nb.de>>.

© 2021 Wiley-VCH Verlag GmbH & Co. KGaA, Boschstr. 12, 69469 Weinheim, Germany

All rights reserved (including those of translation into other languages). No part of this book may be reproduced in any form – by photoprinting, microfilm, or any other means – nor transmitted or translated into a machine language without written permission from the publishers. Registered names, trademarks, etc. used in this book, even when not specifically marked as such, are not to be considered unprotected by law.

**Print ISBN:** 978-3-527-34463-5

**ePDF ISBN:** 978-3-527-81660-6

**ePub ISBN:** 978-3-527-81662-0

**oBook ISBN:** 978-3-527-81663-7

**Cover Design** Formgeber, Mannheim, Germany

**Typesetting** SPi Global, Chennai, India

**Printing and Binding**

Printed on acid-free paper

10 9 8 7 6 5 4 3 2 1

## Contents

	<b>Preface</b>	<i>xvii</i>
	<b>List of Abbreviations and Symbols</b>	<i>xix</i>
	<b>About the Authors</b>	<i>xxiii</i>
<b>1</b>	<b>Introduction</b>	<i>1</i>
<b>2</b>	<b>Principles of X-ray Spectrometry</b>	<i>7</i>
2.1	Analytical Performance	<i>7</i>
2.2	X-ray Radiation and Their Interaction	<i>11</i>
2.2.1	Parts of an X-ray Spectrum	<i>11</i>
2.2.2	Intensity of the Characteristic Radiation	<i>13</i>
2.2.3	Nomenclature of X-ray Lines	<i>15</i>
2.2.4	Interaction of X-rays with Matter	<i>15</i>
2.2.4.1	Absorption	<i>16</i>
2.2.4.2	Scattering	<i>17</i>
2.2.5	Detection of X-ray Spectra	<i>20</i>
2.3	The Development of X-ray Spectrometry	<i>21</i>
2.4	Carrying Out an Analysis	<i>26</i>
2.4.1	Analysis Method	<i>26</i>
2.4.2	Sequence of an Analysis	<i>27</i>
2.4.2.1	Quality of the Sample Material	<i>27</i>
2.4.2.2	Sample Preparation	<i>27</i>
2.4.2.3	Analysis Task	<i>28</i>
2.4.2.4	Measurement and Evaluation of the Measurement Data	<i>28</i>
2.4.2.5	Creation of an Analysis Report	<i>29</i>
<b>3</b>	<b>Sample Preparation</b>	<i>31</i>
3.1	Objectives of Sample Preparation	<i>31</i>
3.2	Preparation Techniques	<i>32</i>
3.2.1	Preparation Techniques for Solid Samples	<i>32</i>
3.2.2	Information Depth and Analyzed Volume	<i>32</i>
3.2.3	Infinite Thickness	<i>36</i>
3.2.4	Contaminations	<i>37</i>
3.2.5	Homogeneity	<i>38</i>

3.3	Preparation of Compact and Homogeneous Materials	39
3.3.1	Metals	39
3.3.2	Glasses	40
3.4	Small Parts Materials	41
3.4.1	Grinding of Small Parts Material	42
3.4.2	Preparation by Pouring Loose Powder into a Sample Cup	43
3.4.3	Preparation of the Measurement Sample by Pressing into a Pellet	44
3.4.4	Preparation of the Sample by Fusion Beads	48
3.4.4.1	Improving the Quality of the Analysis	48
3.4.4.2	Steps for the Production of Fusion Beads	49
3.4.4.3	Loss of Ignition	53
3.4.4.4	Quality Criteria for Fusion Beads	53
3.4.4.5	Preparation of Special Materials	54
3.5	Liquid Samples	55
3.5.1	Direct Measurement of Liquids	55
3.5.2	Special Processing Procedures for Liquid Samples	58
3.6	Biological Materials	58
3.7	Small Particles, Dust, and Aerosols	59
<b>4</b>	<b>XRF Instrument Types</b>	<b>61</b>
4.1	General Design of an X-ray Spectrometer	61
4.2	Comparison of Wavelength- and Energy-Dispersive X-Ray Spectrometers	63
4.2.1	Data Acquisition	63
4.2.2	Resolution	64
4.2.2.1	Comparison of Wavelength- and Energy-Dispersive Spectrometry	64
4.2.2.2	Resolution of WDS Instruments	66
4.2.2.3	Resolution of EDS Instruments	68
4.2.3	Detection Efficiency	70
4.2.4	Count Rate Capability	71
4.2.4.1	Optimum Throughput in ED Spectrometers	71
4.2.4.2	Saturation Effects in WDSs	72
4.2.4.3	Optimal Sensitivity of ED Spectrometers	73
4.2.4.4	Effect of the Pulse Throughput on the Measuring Time	74
4.2.5	Radiation Flux	75
4.2.6	Spectra Artifacts	76
4.2.6.1	Escape Peaks	76
4.2.6.2	Pile-Up Peak	77
4.2.6.3	Diffraction Peaks	77
4.2.6.4	Shelf and Tail	79
4.2.7	Mechanical Design and Operating Costs	79
4.2.8	Setting Parameters	80
4.3	Type of Instruments	80
4.3.1	ED Instruments	81
4.3.1.1	Handheld Instruments	82
4.3.1.2	Portable Instruments	83

4.3.1.3	Tabletop Instruments	84
4.3.2	Wavelength-Dispersive Instruments	85
4.3.2.1	Sequential Spectrometers	85
4.3.2.2	Multichannel Spectrometers	87
4.3.3	Special Type X-Ray Spectrometers	87
4.3.3.1	Total Reflection Instruments	88
4.3.3.2	Excitation by Monoenergetic Radiation	90
4.3.3.3	Excitation with Polarized Radiation	91
4.3.3.4	Instruments for Position-Sensitive Analysis	93
4.3.3.5	Macro X-Ray Fluorescence Spectrometer	94
4.3.3.6	Micro X-Ray Fluorescence with Confocal Geometry	95
4.3.3.7	High-Resolution X-Ray Spectrometers	96
4.3.3.8	Angle Resolved Spectroscopy – Grazing Incidence and Grazing Exit	96
4.4	Commercially Available Instrument Types	98
<b>5</b>	<b>Measurement and Evaluation of X-ray Spectra</b>	<b>99</b>
5.1	Information Content of the Spectra	99
5.2	Procedural Steps to Execute a Measurement	101
5.3	Selecting the Measurement Conditions	102
5.3.1	Optimization Criteria for the Measurement	102
5.3.2	Tube Parameters	103
5.3.2.1	Target Material	103
5.3.2.2	Excitation Conditions	104
5.3.2.3	Influencing the Energy Distribution of the Primary Spectrum	105
5.3.3	Measurement Medium	107
5.3.4	Measurement Time	108
5.3.4.1	Measurement Time and Statistical Error	108
5.3.4.2	Measurement Strategies	108
5.3.4.3	Real and Live Time	109
5.3.5	X-ray Lines	110
5.4	Determination of Peak Intensity	112
5.4.1	Intensity Data	112
5.4.2	Treatment of Peak Overlaps	112
5.4.3	Spectral Background	114
5.5	Quantification Models	117
5.5.1	General Remarks	117
5.5.2	Conventional Calibration Models	118
5.5.3	Fundamental Parameter Models	121
5.5.4	Monte Carlo Quantifications	124
5.5.5	Highly Precise Quantification by Reconstitution	124
5.5.6	Evaluation of an Analytical Method	126
5.5.6.1	Degree of Determination	126
5.5.6.2	Working Range, Limits of Detection (LOD) and of Quantification	127
5.5.6.3	Figure of Merit	129
5.5.7	Comparison of the Various Quantification Models	129

5.5.8	Available Reference Materials	131
5.5.9	Obtainable Accuracies	132
5.6	Characterization of Layered Materials	133
5.6.1	General Form of the Calibration Curve	133
5.6.2	Basic Conditions for Layer Analysis	135
5.6.3	Quantification Models for the Analysis of Layers	138
5.7	Chemometric Methods for Material Characterization	140
5.7.1	Spectra Matching and Material Identification	141
5.7.2	Phase Analysis	141
5.7.3	Regression Methods	143
5.8	Creation of an Application	143
5.8.1	Analysis of Unknown Sample Qualities	143
5.8.2	Repeated Analyses on Known Samples	144
<b>6</b>	<b>Analytical Errors</b>	<b>149</b>
6.1	General Considerations	149
6.1.1	Precision of a Measurement	151
6.1.2	Long-Term Stability of the Measurements	153
6.1.3	Precision and Process Capability	154
6.1.4	Trueness of the Result	156
6.2	Types of Errors	156
6.2.1	Randomly Distributed Errors	157
6.2.2	Systematic Errors	158
6.3	Accounting for Systematic Errors	159
6.3.1	The Concept of Measurement Uncertainties	159
6.3.2	Error Propagation	160
6.3.3	Determination of Measurement Uncertainties	161
6.3.3.1	Bottom-Up Method	161
6.3.3.2	Top-Down Method	162
6.4	Recording of Error Information	164
<b>7</b>	<b>Other Element Analytical Methods</b>	<b>167</b>
7.1	Overview	167
7.2	Atomic Absorption Spectrometry (AAS)	168
7.3	Optical Emission Spectrometry	169
7.3.1	Excitation with a Spark Discharge (OES)	169
7.3.2	Excitation in an Inductively Coupled Plasma (ICP-OES)	170
7.3.3	Laser-Induced Breakdown Spectroscopy (LIBS)	171
7.4	Mass Spectrometry (MS)	172
7.5	X-Ray Spectrometry by Particle Excitation (SEM-EDS, PIXE)	173
7.6	Comparison of Methods	175
<b>8</b>	<b>Radiation Protection</b>	<b>177</b>
8.1	Basic Principles	177
8.2	Effects of Ionizing Radiation on Human Tissue	178
8.3	Natural Radiation Exposure	179

8.4	Radiation Protection Regulations	181
8.4.1	Legal Regulations	181
<b>9</b>	<b>Analysis of Homogeneous Solid Samples</b>	<b>183</b>
9.1	Iron Alloys	183
9.1.1	Analytical Problem and Sample Preparation	183
9.1.2	Analysis of Pig and Cast Iron	184
9.1.3	Analysis of Low-Alloy Steel	185
9.1.4	Analysis of High-Alloy Steel	187
9.2	Ni–Fe–Co Alloys	188
9.3	Copper Alloys	189
9.3.1	Analytical Task	189
9.3.2	Analysis of Compact Samples	189
9.3.3	Analysis of Dissolved Samples	189
9.4	Aluminum Alloys	191
9.5	Special Metals	192
9.5.1	Refractories	192
9.5.1.1	Analytical Problem	192
9.5.1.2	Sample Preparation of Hard Metals	192
9.5.1.3	Analysis of Hard Metals	193
9.5.2	Titanium Alloys	194
9.5.3	Solder Alloys	194
9.6	Precious Metals	195
9.6.1	Analysis of Precious Metal Jewelry	195
9.6.1.1	Analytical Task	195
9.6.1.2	Sample Shape and Preparation	196
9.6.1.3	Analytical Equipment	197
9.6.1.4	Accuracy of the Analysis	198
9.6.2	Analysis of Pure Elements	198
9.7	Glass Material	199
9.7.1	Analytical Task	199
9.7.2	Sample Preparation	200
9.7.3	Measurement Equipment	202
9.7.4	Achievable Accuracies	202
9.8	Polymers	203
9.8.1	Analytical Task	203
9.8.2	Sample Preparation	204
9.8.3	Instruments	205
9.8.4	Quantification Procedures	205
9.8.4.1	Standard-Based Methods	205
9.8.4.2	Chemometric Methods	206
9.9	Abrasion Analysis	209
<b>10</b>	<b>Analysis of Powder Samples</b>	<b>213</b>
10.1	Geological Samples	213



10.1.1	Analytical Task	213
10.1.2	Sample Preparation	214
10.1.3	Measurement Technique	215
10.1.4	Detection Limits and Trueness	215
10.2	Ores	216
10.2.1	Analytical Task	216
10.2.2	Iron Ores	216
10.2.3	Mn, Co, Ni, Cu, Zn, and Pb Ores	217
10.2.4	Bauxite and Alumina	218
10.2.5	Ores of Precious Metals and Rare Earths	219
10.3	Soils and Sewage Sludges	221
10.3.1	Analytical Task	221
10.3.2	Sample Preparation	221
10.3.3	Measurement Technology and Analytical Performance	222
10.4	Quartz Sand	223
10.5	Cement	223
10.5.1	Analytical Task	223
10.5.2	Sample Preparation	224
10.5.3	Measurement Technology	225
10.5.4	Analytical Performance	226
10.5.5	Determination of Free Lime in Clinker	227
10.6	Coal and Coke	227
10.6.1	Analytical Task	227
10.6.2	Sample Preparation	228
10.6.3	Measurement Technology and Analytical Performance	229
10.7	Ferroalloys	230
10.7.1	Analytical Task	230
10.7.2	Sample Preparation	230
10.7.3	Analysis Technology	232
10.7.4	Analytical Performance	234
10.8	Slags	235
10.8.1	Analytical Task	235
10.8.2	Sample Preparation	235
10.8.3	Measurement Technology and Analytical Accuracy	236
10.9	Ceramics and Refractory Materials	237
10.9.1	Analytical Task	237
10.9.2	Sample Preparation	237
10.9.3	Measurement Technology and Analytical Performance	238
10.10	Dusts	239
10.10.1	Analytical Problem and Dust Collection	239
10.10.2	Measurement	242
10.11	Food	242
10.11.1	Analytical Task	242
10.11.2	Monitoring of Animal Feed	243
10.11.3	Control of Infant Food	244
10.12	Pharmaceuticals	245
10.12.1	Analytical Task	245

10.12.2	Sample Preparation and Analysis Method	245
10.13	Secondary Fuels	246
10.13.1	Analytical Task	246
10.13.2	Sample Preparation	247
10.13.2.1	Solid Secondary Raw Materials	247
10.13.2.2	Liquid Secondary Raw Materials	249
10.13.3	Instrumentation and Measurement Conditions	250
10.13.4	Measurement Uncertainties in the Analysis of Solid Secondary Raw Materials	251
10.13.5	Measurement Uncertainties for the Analysis of Liquid Secondary Raw Materials	252
<b>11</b>	<b>Analysis of Liquids</b>	<b>253</b>
11.1	Multielement Analysis of Liquids	254
11.1.1	Analytical Task	254
11.1.2	Sample Preparation	254
11.1.3	Measurement Technology	254
11.1.4	Quantification	255
11.2	Fuels and Oils	255
11.2.1	Analysis of Toxic Elements in Fuels	256
11.2.1.1	Measurement Technology	256
11.2.1.2	Analytical Performance	258
11.2.2	Analysis of Additives in Lubricating Oils	258
11.2.3	Identification of Abrasive Particles in Used Lubricants	260
11.3	Trace Analysis in Liquids	261
11.3.1	Analytical Task	261
11.3.2	Preparation by Drying	261
11.3.3	Quantification	262
11.4	Special Preparation Techniques for Liquid Samples	263
11.4.1	Determination of Light Elements in Liquids	263
11.4.2	Enrichment Through Absorption and Complex Formation	264
<b>12</b>	<b>Trace Analysis Using Total Reflection X-Ray Fluorescence</b>	<b>267</b>
12.1	Special Features of TXRF	267
12.2	Sample Preparation for TXRF	269
12.3	Evaluation of the Spectra	271
12.3.1	Spectrum Preparation and Quantification	271
12.3.2	Conditions for Neglecting the Matrix Interaction	272
12.3.3	Limits of Detection	273
12.4	Typical Applications of the TXRF	274
12.4.1	Analysis of Aqueous Solutions	274
12.4.1.1	Analytical Problem and Preparation Possibilities	274
12.4.1.2	Example: Analysis of a Fresh Water Standard Sample	275
12.4.1.3	Example: Detection of Mercury in Water	277
12.4.2	Analysis of the Smallest Sample Quantities	278
12.4.2.1	Example: Pigment Analysis	278

12.4.2.2	Example: Aerosol Analysis	279
12.4.2.3	Example: Analysis of Nanoparticles	279
12.4.3	Trace Element Analysis on Human Organs	280
12.4.3.1	Example: Analysis of Blood and Blood Serum	280
12.4.3.2	Example: Analysis of Trace Elements in Body Tissue	282
12.4.4	Trace Analysis of Inorganic and Organic Chemical Products	283
12.4.5	Analysis of Semiconductor Electronics	284
12.4.5.1	Ultra-Trace Analysis on Si Wafers with VPD	284
12.4.5.2	Depth Profile Analysis by Etching	285
<b>13</b>	<b>Nonhomogeneous Samples</b>	<b>287</b>
13.1	Measurement Modes	287
13.2	Instrument Requirements	288
13.3	Data Evaluation	290
<b>14</b>	<b>Coating Analysis</b>	<b>291</b>
14.1	Analytical Task	291
14.2	Sample Handling	292
14.3	Measurement Technology	293
14.4	The Analysis Examples of Coated Samples	294
14.4.1	Single-Layer Systems: Emission Mode	294
14.4.2	Single-Layer Systems: Absorption Mode	297
14.4.3	Single-Layer Systems: Relative Mode	298
14.4.3.1	Analytical Problem	298
14.4.3.2	Variation of the Specified Working Distance	298
14.4.3.3	Sample Size and Spot Size Mismatch	299
14.4.3.4	Non-detectable Elements in the Layer: NiP Layers	300
14.4.4	Characterization of Ultrathin Layers	302
14.4.5	Multilayer Systems	304
14.4.5.1	Layer Systems	304
14.4.5.2	Measurement Technology	305
14.4.5.3	Example: Analysis of CIGS Solar Cells	305
14.4.5.4	Example: Analysis of Solder Structures	306
14.4.6	Samples with Unknown Coating Systems	307
14.4.6.1	Preparation of Cross Sections	308
14.4.6.2	Excitation at Grazing Incidence with Varying Angles	309
14.4.6.3	Measurement in Confocal Geometry	311
<b>15</b>	<b>Spot Analyses</b>	<b>313</b>
15.1	Particle Analyses	313
15.1.1	Analytical Task	313
15.1.2	Sample Preparation	314
15.1.3	Analysis Technology	315
15.1.4	Application Example: Wear Particles in Used Oil	315
15.1.5	Application Example: Identification of Glass Particles by Chemometrics	316
15.2	Identification of Inclusions	318

15.3	Material Identification with Handheld Instruments	318
15.3.1	Analytical Tasks	318
15.3.2	Analysis Technology	319
15.3.3	Sample Preparation and Test Conditions	320
15.3.4	Analytical Accuracy	320
15.3.5	Application Examples	321
15.3.5.1	Example: Lead in Paint	321
15.3.5.2	Example: Scrap Sorting	321
15.3.5.3	Example: Material Inspection and Sorting	322
15.3.5.4	Example: Precious Metal Analysis	322
15.3.5.5	Example: Prospecting and Screening in Geology	323
15.3.5.6	Example: Investigation of Works of Art	323
15.4	Determination of Toxic Elements in Consumer Products: RoHS Monitoring	324
15.4.1	Analytical Task	324
15.4.2	Analysis Technology	325
15.4.3	Analysis Accuracy	327
15.5	Toxic Elements in Toys: Toys Standard	328
15.5.1	Analytical Task	328
15.5.2	Sample Preparation	328
15.5.3	Analysis Technology	330
<b>16</b>	<b>Analysis of Element Distributions</b>	<b>331</b>
16.1	General Remarks	331
16.2	Measurement Conditions	332
16.3	Geology	333
16.3.1	Samples Types	333
16.3.2	Sample Preparation and Positioning	333
16.3.3	Measurements on Compact Rock Samples	334
16.3.3.1	Sum Spectrum and Element Distributions	334
16.3.3.2	Object Spectra	335
16.3.3.3	Treatment of Line Overlaps	336
16.3.3.4	Maximum Pixel Spectrum	339
16.3.4	Thin Sections of Geological Samples	340
16.4	Electronics	342
16.5	Archeometric Investigations	344
16.5.1	Analytical Tasks	344
16.5.2	Selection of an Appropriate Spectrometer	346
16.5.3	Investigations of Coins	347
16.5.4	Investigations of Painting Pigments	349
16.6	Homogeneity Tests	350
16.6.1	Analytical Task	350
16.6.2	Homogeneity Studies Using Distribution Analysis	351
16.6.3	Homogeneity Studies Using Multi-point Measurements	352
<b>17</b>	<b>Special Applications of the XRF</b>	<b>355</b>
17.1	High-Throughput Screening and Combinatorial Analysis	355

17.1.1	High-Throughput Screening	355
17.1.2	Combinatorial Analysis for Drug Development	357
17.2	Chemometric Spectral Evaluation	358
17.3	High-Resolution Spectroscopy for Speciation Analysis	361
17.3.1	Analytical Task	361
17.3.2	Instrument Technology	361
17.3.3	Application Examples	362
17.3.3.1	Analysis of Different Sulfur Compounds	362
17.3.3.2	Speciation of Aluminum Inclusions in Steel	363
17.3.3.3	Determination of SiO <sub>2</sub> in SiC	365
<b>18</b>	<b>Process Control and Automation</b>	<b>367</b>
18.1	General Objectives	367
18.2	Off-Line and At-Line Analysis	369
18.2.1	Sample Supply and Analysis	369
18.2.2	Automated Sample Preparation	371
18.3	In-Line and On-Line Analysis	376
<b>19</b>	<b>Quality Management and Validation</b>	<b>379</b>
19.1	Motivation	379
19.2	Validation	380
19.2.1	Parameters	384
19.2.2	Uncertainty	385
<b>Appendix A Tables 387</b>		
<b>Appendix B Important Information 419</b>		
B.1	Coordinates of Main Manufacturers of Instruments and Preparation Tools	419
B.2	Main Suppliers of Standard Materials	422
B.2.1	Geological Materials and Metals	422
B.2.2	Stratified Materials	423
B.2.3	Polymer Standards	424
B.2.4	High Purity Materials	424
B.2.5	Precious Metal Alloys	425
B.3	Important Websites	425
B.3.1	Information About X-Ray Analytics and Fundamental Parameters	425
B.3.2	Information About Reference Materials	426
B.3.3	Scientific Journals	427
B.4	Laws and Acts, Which Are Important for X-Ray Fluorescence	427
B.4.1	Radiation Protection	427
B.4.2	Regulations for Environmental Control	428
B.4.3	Regulations for Performing Analysis	428
B.4.4	Use of X-ray Fluorescence for the Chemical Analysis	428
B.4.4.1	General Regulations	428

B.4.4.2 Analysis of Minerals 429  
B.4.4.3 Analysis of Oils, Liquid Fuels, Grease 430  
B.4.4.4 Analysis of Solid Fuels 432  
B.4.4.5 Coating Analysis 433  
B.4.4.6 Metallurgy 433  
B.4.4.7 Analysis of Electronic Components 434

**References** 435

**Index** 453

## Preface

The discovery of X-rays by Wilhelm Conrad Röntgen dates back to nearly 125 years. Despite their “age,” the research and discoveries that have been made in the past and today make X-rays one of the most powerful analytical tools available today. The discovery of this part of the electromagnetic spectrum has seen many applications. First, used for medical purposes by Röntgen himself, who found that the newly discovered rays can penetrate and at the same time can be absorbed by different types of matter. Therefore, it was now possible to image the human body. Later, Max von Laue showed that they are a higher-frequency part of the electromagnetic spectrum where natural light is also a part of. This led to his work on diffraction of X-rays, which to this day is used to investigate the crystalline and amorphous structure of solids. Finally, Moseley found that every element emitted characteristic X-ray radiation that can be used to determine the qualitative and quantitative elemental composition of materials of different types. This is the application that is most interesting for us – the spectroscopists.

X-ray fluorescence spectroscopy has now developed into an analytical technique that, due to its robustness and flexibility, can be used in almost all scientific areas, in research, and above all in quality control in industrial production. The technique has become so powerful because of its ability to analyze many different material types, having a wide range of elements and concentrations. The sample preparation is mostly simple or even not required, therefore making it possible to fully automate the entire analysis process.

Even when one has many years of experience with the method, specific expertise is still required to achieve reliable results, especially since the applications for X-ray fluorescence spectrometry have been significantly expanded in recent years due to new components being developed and becoming commercially available for X-ray spectrometers. Examples of such are X-ray optics, new types of detectors, and the availability of powerful computing technique and software solutions.

A combination of theoretical knowledge and practical know-how about the materials to be examined, the best practices for sample preparation, and the most suitable measuring instrument at optimal measurement conditions is required to make the most precise and true analysis results. The intention of this book is to summarize the experiences of the analytical community working with X-ray fluorescence. For many years this community has convened at global annual user meetings and conferences for X-ray fluorescence spectrometry, covering all types of applications of X-ray spectroscopy. The work presented

at these meetings shares new developments in the field of device technology and provides information on the analytical capabilities of X-ray fluorescence for known applications, for instance, in the analysis of metallurgical or mineralogical samples. Interesting new applications are presented as well. These experiences are the basis of this book in which we tried to summarize but also to preserve this knowledge.

The book is addressed to current and future users of X-ray fluorescence analysis. It strives to provide suggestions and examples on how to use X-ray fluorescence and what kind of results can be expected, as well as advice on suitable preparation techniques and measurement conditions. Accordingly, in addition to the method-specific basics, the book contains information about the essential preparation techniques and a variety of material-specific applications that can serve as the basis for your own current and future measurement concepts.

Many inspiring discussions and joint projects with numerous users and instrument manufacturers have been included in this book. The authors want to especially thank Prof. A. Janßen, Ms.Sc. S. Hanning and many other colleagues not mentioned here for their support of this work. Our special acknowledgement goes to Dr. A. von Bohlen, he not only supported the project by a lot of discussions but also provided our work with elaborated information about conditions and applications for total reflection X-ray spectrometry.

Michael Haller dedicates his work in this book to the late Dr. Volker Rößiger. Friend, mentor, and true Renaissance man, his enthusiasm and kindness were an inspiration to all who had the privilege to know him.

Finally, thanks to the publisher Wiley-VCH for their support and smooth completion of this project.

We hope that this book will inspire and fascinate all readers using X-rays as an analytical tool.

February 2020

*Michael Haschke, Jörg Flock, Michael Haller  
Eggersdorf, Schwerte and Middletown*



## List of Abbreviations and Symbols

AAS	atomic absorption spectrometry
AES	atomic emission spectrometry
BG	background
$c$	velocity of light
$C_{\text{det}}$	detector capacitance
CR	counting rate
CRM	certified reference material
$d$	d-spacing of the scattering lattice, thickness
$d_{\text{information}}$	information depth
D	dose
$e$	charge of an electron
$E$	energy
$E_{\text{C}}$	energy of the absorption edge
ED	energy dispersive
EDS	energy-dispersive spectrometry
ENC	electronic noise contribution
EPMA	electron probe microanalysis
EXAFS	extended X-ray absorption fine structure
$f$	functional relation, degrees of freedom
$F$	Fano factor
FOM	figure of merit
FT-IR	Fourier transform infrared
FWHM	full width at half maximum
$G$	gain
GEXE	grazing exit X-ray emission
GIXE	grazing incident X-ray emission
$h$	Planck's constant
HOPG	highly oriented pyrolyzed graphite
HTS	high throughput analysis
$i$	current
$I$	intensity
$I_{\text{o}}$	primary intensity
$I_{\text{d}}$	leakage current
$I_{\text{scat}}$	scattered intensity
ICP	inductively coupled plasma spectrometry

$k$	factor of confidence, proportionally coefficient
keV	kiloelectron volt
LA-ICP	laser ablation inductively coupled plasma spectrometry
LIBS	laser-induced breakdown spectrometry
LN <sub>2</sub>	liquid nitrogen
LOD	limit of detection
LOI	loss of ignition
$m$	atomic mass
$m_0$	mass of an electron
μ-XRF	micro-X-ray fluorescence analysis
$M$	matrix interaction
MC	Monte Carlo
MCA	multichannel analyzer
MPS	maximum pixel spectrum
MS	mass spectrometry
MXRF	macro-X-ray fluorescence analysis
$n$	refraction index, number (channels, pixels), order of diffraction
$N$	number of photons
NAA	neutron activation analysis
OES	optical emission spectrometry
$p$	probability
PC	proportional counter
PCA	principal component analysis
PCB	printed circuit board
PIXE	proton-induced X-ray emission
PMI	positive material identification
$Q$	mass per area
$R$	intensity ratio
$R^2$	correlation coefficient
RM	reference material
RoHS	Restriction of Hazardous Substances
SDD	silicon drift detector
SIMS	secondary ion mass spectrometry
SML	synthetic multilayer
SRM	standard reference material
$t$	thickness of a layer, measurement time
$T$	temperature
TXRF	total reflection X-ray fluorescence spectrometry
$U$	voltage, uncertainty
$v$	measured value
VPD	vapor phase deposition
$w$	mass fraction
WD	wavelength dispersive
WDS	wavelength-dispersive spectrometry
XANES	X-ray absorption near edge structure
XPS	X-ray induced photoelectron spectrometry
XRF	X-ray fluorescence

$Z$	atomic number
$\Delta$	difference
$\eta$	efficiency
$\varepsilon$	energy for generation of a charge carrier
$\kappa$	overlapping factor
$\lambda$	wavelength
$\mu$	mass attenuation coefficient
$\rho$	density of the absorbing material
$\vartheta$	scatter angle
$\sigma$	standard deviation, scattering coefficient
$\Theta$	angle
$\tau$	shaping time, linear absorption coefficient
$\psi$	incidence/take-off angle
$\omega$	fluorescence yield
$\Omega$	captured angle

## About the Authors



**Dr. Michael Haschke** has worked for more than 35 years in several companies in the field of product management for the development of new products and the market introduction of new methods in X-ray fluorescence. These were mainly instruments in the field of energy-dispersive spectroscopy. During the market introduction it was every time necessary to deal with competition element analysis methods but also with the new applications. He, therefore, has both knowledge in the field of X-ray fluorescence and analysis method and for the wide range of applications for X-ray fluorescence.



**Dr. Jörg Flock** was for many years the head of the central laboratory of ThyssenKrupp Steel AG and therefore familiar with several analytical methods, in particular with X-ray fluorescence spectroscopy. He has a lot of practical knowledge for the analysis of various sample qualities.



**Michael Haller, M.S.**, has been using X-rays as an analytical tool for over 30 years, first in X-ray crystallography and then later in the development and application of polycapillary X-ray optics. During the majority of his career, he has developed new applications for coating thickness instruments in industrial process control. In 2018 he became co-owner of CrossRoads Scientific, a company specializing in the development of analytical X-ray software.

## 1

## Introduction

X-ray spectrometry has been known as a method for element analyses for more than 70 years and can be regarded as a routine method since the 1960s. This means that there is a broad range of instruments available, and numerous analytical tasks are carried out routinely by X-ray fluorescence (XRF) analysis. For example, XRF is used for the characterization of metallic or geological materials or for analyses of solid or liquid fuels despite the fact that other elemental analytical methods have been developed and are readily available for these applications. Among them are optical emission spectrometry with excitation both by sparks and by inductively coupled plasmas and mass spectrometry. The high importance of using XRF is due to the fact that one can achieve very high precision over a wide concentration range. XRF also requires little effort with sample preparation and the method can be automated.

Especially in the last 15–20 years, XRF has experienced a new boom mainly because the technology has further developed, and new fields of applications could be opened up. These include, among others, the analysis of layered materials and high-resolution position-sensitive analysis. This was made possible by the availability of new components for X-ray spectrometers.

The development of high-resolution energy-dispersive detectors with good count rate capability now allows precision measurements also with energy-dispersive spectrometers. The simultaneous detection of a wide energy range over a large solid angle made possible with these detectors allows not only short measuring times but also special excitation geometries. It is therefore now possible to achieve higher sensitivities in the detection of traces; further, the fluorescence radiation of small surface areas can be detected with sufficient intensity.

The development of various X-ray optics allows shaping of the primary X-ray beam and thus the concentration of high excitation intensity on small sample surfaces; this development was the key to opening up new applications in the field for a spatially resolved analysis.

These developments have significantly expanded the range of applications of XRF analysis.

However, the most important influence in the further development of XRF into a routine method was the advances in data processing technology. These made it

possible to automate instrument control as well as the evaluation of measurement data. Not only was it possible to reduce subjective influences by a manual operator but also the processes during instrument control and measurement data acquisition could largely be automated and made more effective. The evaluation of the measurement data, such as the peak area calculation in case of overlapping peaks, or the calculation procedures for the quantification could be expanded and significantly refined by the available computing power.

These improvements have been particularly important because X-rays strongly interact with the sample matrix, which requires complex correction procedures. Nevertheless, in contrast to other analytical methods, the physics of these interactions is very well understood and can be exactly modeled mathematically. Consequently, in principle, standard-less analysis is possible, which again requires a high computing effort.

As a result of these developments, new methodical possibilities for XRF emerged, combined with an expansion of their field of applications. For this reason, it seems to be meaningful to carry out an up-to-date compilation of the applications currently being processed by XRF, in combination with a discussion of both the necessary sample preparation and instrument-related efforts and the achievable analytical performance. There are several very good books available, which however, due to their date of publication, have not been able to take into account the developments of the last 15–20 years (Erhardt 1989; Hahn-Weinheimer et al. 2012) or they do not adequately address frequently used routine applications, in particular in industrial analyses (Beckhoff et al. 2006; van Grieken and Markowicz 2002).

The goal of this book is to focus on the practical aspects of the various applications of XRF. This leads to the discussion of the requirements necessary for the analysis of the very different sample qualities, such as the type of sample preparation, the available measurement technique or the required calibration samples, as well as the type and quality of the results to be expected with these efforts. This appeared to be important, in particular, because XRF is often used in many laboratories, but methodical studies are carried out only in very few of them.

This leads to the application aspects often not being understood very well. Consequently, the analytical results are accepted without scrutinizing the influence of sample state, preparation methods, and measurement parameters. This becomes especially true because complete results are often available as the outcome of an instrumental analysis and their quality cannot be correctly comprehended.

In order to assure the quality of the applications and their results, the analyst must critically question all aspects of the test method. For this purpose, a basic understanding of the influences of sample condition, preparation methods, measurement parameters, and evaluation models used on the quality of the analytical result is imperative.

Therefore, we are deliberately focusing on the daily laboratory work with commercially available instruments. On the other hand, the interesting but not routine applications of the method utilizing synchrotron radiation excitation are not addressed. Nevertheless, methodical developments obtained on a synchrotron are often incorporated into laboratory analysis, such as micro-X-ray fluorescence ( $\mu$ -XRF) or applications with grazing beam geometry. However,

this book treats only laboratory applications. If any of these newly developed methods have been implemented into special laboratory instruments these are also presented as examples.

Despite the focus on the various applications, a brief introduction to the fundamentals of X-ray spectrometry and a comprehensive presentation of the basic steps for a complete analysis are required in order to be able to relate in the following discussion of the individual applications.

The book therefore starts with a discussion of the analytical capability of X-ray spectrometry in Chapter 2. The most important relations that describe the generation of the characteristic radiation are presented, and the individual steps in the execution of an analysis follow, along with a brief characterization of their influence on the analysis result. Deeper descriptions of the physical bases are comprehensively given in other publications (e.g. Erhardt 1989; Hahn-Weinheimer et al. 2012; van Grieken and Markowicz 2002; Beckhoff et al. 2006).

In Chapter 3, the various sample preparation procedures typical for X-ray spectrometry are presented and their influence on the precision and trueness of the analyses is discussed. Even though the sample preparation is generally regarded as being very simple for XRF, it is important to carry it out carefully, appropriate to the expectations of the analysis result.

In Chapter 4, the different types of X-ray spectrometers are discussed. On the one hand, the general differences and application characteristics of wavelength-dispersive and energy-dispersive instruments are examined; on the other hand, the different instrument types as well as the instruments currently available on the market are presented.

In Chapter 5, the essential steps for the measurement of a spectrum are reviewed, in particular, the optimum selection of the measurement parameters and the steps for the evaluation of the measured data. The first step is the determination of the intensities of the fluorescence peaks, where different procedures are used for wavelength- and energy-dispersive spectrometers. Then quantification models and factors concerning the consideration of matrix interaction, both in the analysis of homogeneous samples and in the characterization of layers, are presented. Here, a comprehensive and detailed description of the theory of X-ray spectrometry is not required, since a series of detailed papers are available (see, for example, Hahn-Weinheimer et al. 2012; Jenkins et al. 1981; Lachance and Claisse 1994; Mantler 2006) and only very few new ideas have been added in the last few years. In this chapter, further possibilities for the evaluation of spectra are presented, in which the individual spectral components are not considered separately, but the spectrum as a whole is evaluated by means of chemometric methods.

Chapter 6 is devoted to the discussion of the classification, determination, and evaluation of errors. The achievable analytical precision of XRF is determined by the errors. In addition to the traditional treatment of errors with the Gaussian error model, the principle of measurement uncertainty is also discussed. This chapter is intended to qualify the expectations of an analytical result.

In Chapters 7 and 8, a brief comparison is made with other element analysis methods, in particular atomic absorption and emission spectrometry as well as mass spectrometry. The fundamentals of radiation protection when dealing with

X-ray radiation, in particular when carrying out X-ray analysis experiments, are compiled as well.

Based on these fundamentals, various applications of XRF, which have been used already over a long time period or were introduced recently, are presented and discussed. The presentation here is carried out according to the different sample qualities or according to the analytical question.

Typical XRF applications are discussed first. Chapter 9 discusses the analysis of homogeneous solid samples, such as various metallic materials, glasses, or plastics. Chapter 10 describes the investigation of powdered samples, such as geological samples, soil, building materials, slags, and dusts.

In Chapter 11, the different possibilities for analyzing liquids are presented, either by direct analysis or, for example, by different enrichment procedures to answer specific analytical questions. Applications with total reflection XRF (TXRF) are dealt with in Chapter 12. Here, in addition to ultra-trace analyses of liquids the analysis of very small sample quantities is the focus.

Descriptions of the analysis of nonhomogeneous materials cover a wide range of analytical questions. This concerns inhomogeneities normal to the sample surface, i.e. the characterization of layered materials (Chapter 14) along with their different applications, as well as inhomogeneities in the sample plane and the analysis of irregularly shaped samples (Chapter 15). In this case, only small sample areas are to be analyzed, which means a point analysis has to be carried out. This is important when identifying particles or inclusions as also when analyzing inhomogeneous materials.

Handheld instruments are increasingly being used for element analysis. Based on this fact, the applications that up to now have been typical for this instrument technology are presented in Section 15.4. It was possible to increase the efficiency of this type of instruments significantly in recent years due to the miniaturization of all hardware assemblies. In this way, their range of measurement applications could be expanded continuously. An important factor for that expansion is the possibility for “on-site” analysis, i.e. materials for analysis are no longer required to be taken to a laboratory. However, the quality of the analyses is not as high, mainly because of a very simplified or even completely missing sample preparation, undefined sample geometry, or contamination in the measuring environment.

A further important field of application of spatially resolved analysis, the determination of element distributions, is dealt with in Chapter 16. This method allows not only the analysis of small areas on structured materials, but also the investigation of their element distributions and therefore their more detailed characterization. Presentation of the examples for the distribution analysis is carried out according to the different analytical tasks. For example, the analysis of geological samples and of electronic assemblies as well as homogeneity tests of reference samples is presented.

A specific problem is the analysis of archeological objects, because they cannot be modified by preparation due to their uniqueness. Examples for such analytical tasks are discussed in Section 16.5.

In Chapter 17, special applications of the XRF analysis are described. This implies the high-throughput analysis (HTS) for the characterization of



small sample quantities, chemometric spectral evaluation with the resulting possibilities for material characterization, as well as speciation analysis.

Chapter 18 presents the requirements and conditions for the use of the XRF in process analysis, with particular attention to the automation of sample preparation. Requirements and possibilities of automated analyses are given, but the associated problems are pointed out as well.

Finally, in a brief discussion in Chapter 19 the assurance of the quality of analyses by means of a corresponding quality management system in test laboratories and also the requirements for the validation of test methods are mentioned.

All these applications are intended to demonstrate the wide range of possible measurement applications of XRF as well as the analytical performance that can be achieved.

At the end of the book, in Appendix A numerical data required for X-ray spectrometry is compiled in a comprehensive set of tables, and in Appendix B important references with information on instrument manufacturers, basic literature for the field of XRF spectrometry, important websites, as well as magazines, standards, and laws that help readers quickly find the right information and contacts for solving their analytical tasks can be found.

## 2

## Principles of X-ray Spectrometry

### 2.1 Analytical Performance

X-ray analysis has been established as an important method for element analysis. Already since Moseley's discovery in 1913 that the energies of the X-ray lines of individual elements differ from each other and depend on the square of the atomic number of the emitting atoms, preconditions for using this method for element analyses were given. However, it took several years until the first usable equipment for routine analyses was available. In the 1930s the first laboratory instruments were available, but they were not yet suited for routine analyses.

To this purpose, various instrumental prerequisites had to be developed, such as an effective excitation source with sufficient intensity and high stability, the supply of dispersive elements, i.e. crystals with high reflectivity and sufficient size, and then also synthetic multilayers with larger d-spacings, detectors with sufficient counting capacity, instruments that allow for simple and safe operation, in particular for sample positioning, and later also for radiation protection, possibilities for measurement in vacuum, as well as the effective recording of the measurement data and their evaluation. The first applications focused on the identification of the elements present in a sample, i.e. a purely qualitative analysis. In this way, some elements could even be discovered, such as hafnium in 1923 (Coster, v.Hevesy), rhenium in 1925 (Tacke 1925), and technetium in 1947 (Perrier and Segrè 1947).

However, very soon the mass fractions of the different elements in the examined materials became interesting, mainly for the quantitative assessment of the investigated materials.

After the availability of the first commercial equipment, very fast development and distribution of X-ray spectrometry began. The following characteristics of X-ray spectrometry have undoubtedly been of assistance in this process:

- X-ray spectra have much less lines per element than optical spectra. This means that the lines in the spectrum are easy to identify and due to the corresponding small number of line interferences the requirements for the spectrometer resolution are not very high.
- All important parameters for the spectrometry depend on the atomic number of the considered element, which significantly supports the interpretation and evaluation of the spectra.

- The analysis can be carried out on very different sample qualities. Both compact solid samples and powder samples as also liquids and layered materials can be directly examined.
- The analysis is nondestructive, i.e. the material to be examined is not consumed or changed by the analysis. Therefore, the sample is available for further or repeated examinations.
- A large element and concentration range is covered. All elements except very light elements can be analyzed. The detectable element contents range from a few milligrams per kilogram to pure elements, i.e. at least 5 orders of magnitude. In cases of specific excitation geometries, instrument designs, or preparation methods, the detection limits can even be lowered to the sub-milligram per kilogram range.
- The development of novel components for X-ray analysis, such as X-ray optics and energy-dispersive (ED) detectors, initialized a strong dynamic in the development of new methodical possibilities. In recent years, therefore, a clear extension of the application range of X-ray spectrometry could be observed.

The analytical performance of X-ray fluorescence spectrometry (XRF), however, is characterized by further properties, which, in some cases, have a limiting character.

- The analysis can be carried out with very high precision because the statistical error can be kept very small due to the high measurable intensities. Typical analytical errors for the analysis of homogeneous samples are between 0.3 and 0.5 rel. wt%. With corresponding methods, these limits can be even further reduced.
- The analytical accuracy can be influenced by the type of sample preparation, the selection of measurement conditions, the measurement sequences, and the effort on data processing.
- The abovementioned high accuracies can be achieved only by comparative measurements with samples of exactly known composition, i.e. by calibrations using reference samples or primary substances (pure substances).
- The strong matrix dependence of the method can be considered as a limiting factor. This means that the element intensities have a nonlinear dependence on the sample composition. This makes quantifications more difficult and complex.

During the development of X-ray spectrometry, it has been found that most of the interactions of both the incident radiation and the fluorescence radiation with the sample are physically very well understood and mathematically describable.

This means that X-ray spectrometry is a very well understood analytical method, which now can be used even standard-less, i.e. quantifications are possible without the use of reference samples, only based on fundamental parameters such as absorption cross sections, transition probabilities, fluorescence yields, and others. This widely reduces the effort for the analyses

of unknown samples, but it can also reduce the accuracy of an analysis. In particular, exact knowledge of the fundamental parameters and of the measuring geometry is required for high accuracy. On the other hand, in the case of inaccurate knowledge of these parameters, the analysis accuracy is limited.

- Typically, the analyzed sample volume is not very large. It is determined by the size of the area under investigation and the information depth, i.e. the thickness of the material that can be penetrated by the excited fluorescence radiation and contributes therefore to the measurement signal. For correct analysis, this volume should be representative of the material to be characterized.

The size of the excited area can be easily adjusted and depends substantially on the homogeneity of the sample. The depth of penetration depends on the energy of the fluorescence radiation of the investigated element as well as on its absorption in the sample, i.e. from the composition of the matrix of the sample.

- X-ray fluorescence is known as a nondestructive analysis method that is capable of analyzing materials in various aggregate states, i.e. liquids, solid samples, or powders. Nevertheless, in many cases modifications of the material to be examined may be necessary for the analysis. These preparation procedures may be necessary, for example,
  - to adjust the material to be investigated to the instrument geometry, for example, by detaching parts from a larger piece of the material, by filling loose powder into a sample cup, or by pressing it into tablets;
  - to generate a sufficient representativity of the analyzed sample volume for the entire sample material, for example, by producing a planar sample surface or by cleaning the surface from contaminations; or
  - to avoid or reduce the influence of inhomogeneities of the sample material on the analysis result, for example, by homogenization through grinding, by dilution, or by the manufacturing of fusion beads.
- However, the analyses can mostly be carried out without any changes in the aggregate state of the sample, i.e. the dissolution of solid samples is not required. Therefore, the effort for sample preparation compared to optical methods is relatively low and no or only slight dilution effects reduce the sensitivity of trace detection and therefore avoid analytical errors by contaminations.

Nevertheless, it should be noted that even in the case of XRF, sample preparation must be carried out very carefully in order to achieve the desired analytical accuracy.

- Besides the analysis of homogeneous volume samples, the characterization of layered systems with XRF is also possible. Under certain conditions, both thickness and composition of layers can be determined. In this case, the mass per unit area can be determined by measurement, which then has to be converted into layer thicknesses and mass fractions by using the material density. The determination of layer thicknesses is a very common analytical problem in industrial process control of mechanical and electronic components or many other electroplated products.

- Another very important property of X-ray spectrometry is the possibility of automation, in particular, the automation of the measurement process, including data evaluation. In case there is no change in the sample type even sample preparation can be automated. This results in a fast analysis, but above all it provides for an analysis independent of subjective influences. Sample preparation and measuring operation can then be carried out under equivalent conditions, which reduces the uncertainty range of the measurement.

Apart from this effect, the ongoing costs for analyses are reduced by means of automation.

- The analytical problem of X-ray spectrometry can be very different and can be classified into various “degrees of difficulty.”

Qualitative analysis can be considered as a simple task. In this case, it is only necessary to determine whether certain elements are present in the sample or not.

The next stage involves the monitoring of concentration ranges for selected elements. In this instance, it must be determined whether the mass fractions of the elements under consideration in the sample material are below or above a certain limit. Here, often no direct quantitative analyses are required but only a monitoring of the intensity level of the analyte. In this case, the matrix influence can be neglected because samples of similar qualities are investigated and their matrices do not change significantly.

Without doubt, the most demanding analytical problem is the quantitative analysis. Here, the elements present in a sample have to be identified at first – for samples of same quality as in the case of quality control in the production process, this is not necessary – and then their mass fractions or their layer parameters have to be determined.

- The requirements regarding accuracy and sensitivity of the analysis can be very different, resulting in the selection of
  - the sample preparation method (homogenization of the sample, elimination of influences of the surface roughness or of mineralogical effects)
  - the measuring conditions (excitation conditions, measuring times, measuring medium)
  - the evaluation model and, if available, of the reference samples to be used for the calibration to the accuracy requirements.
- Further, X-ray spectrometry can also determine element distributions of large sample areas by using specific excitation conditions. For this purpose, the incident beam has to be concentrated on a small sample area. The sample then needs to be moved under the fixed beam into the measuring position. This offers the possibility for the analysis of non-regular sample surfaces and additionally for the characterization of inhomogeneous materials.
- By using specific excitation geometries and conditions, it is possible to influence the sensitivity of the method. For example, in the case of a grazing incidence of the primary beam, the spectral background is greatly reduced and hence the sensitivity of the measurement is significantly increased. A similar effect can be obtained by using monoenergetic radiation for the excitation. Here also, the spectral background is reduced and an improvement in sensitivity can be achieved.

- A large number of different X-ray spectrometry instruments are available, each of which is designed for specific analytical tasks. A more detailed discussion of the individual instrument types can be found in Section 4.3.
- The radiation sources used in laboratory analyses today are X-ray tubes. In the past, isotope sources have been used as well. Another radiation source includes synchrotrons. Their radiation properties, i.e. the high beam brilliance, the polarization of the synchrotron radiation, or the possibility of generating monoenergetic radiation by means of appropriate X-ray optics, allow the use of very dedicated measuring geometries and measurement methods. As a result, new analysis methods are often developed at these radiation sources, which subsequently can be transferred into routine practice. However, these special analyses methods are not discussed within this scope since the very high instrumental effort and the limited availability of measurement time at these sources restrict their routine use.

Another type of interesting X-ray source are plasmas in which atoms are ionized by extremely high temperatures. These atoms then emit X-radiation when transferred back to the ground state. It is usually radiation in the lower energy range. Because the plasma is often generated by a laser impact, these sources can be pulsed and consequently be used for time-resolved studies. However, these sources are not yet suitable for real routine use.

## 2.2 X-ray Radiation and Their Interaction

### 2.2.1 Parts of an X-ray Spectrum

X-radiation is electromagnetic radiation in the energy range of approximately 0.1–100 keV or with wavelengths in the range of approximately 25 to 0.01 nm. X-radiation is therefore characterized either by its energy  $E$  or by its wavelength  $\lambda$ . Both quantities are mutually transferable through the following relationship:

$$E \text{ (keV)} = 1.242 / \lambda \text{ (nm)} \quad (2.1)$$

X-ray radiation can be generated by several processes. A continuous broad-band spectrum is emitted by the stepwise deceleration of highly energetic charged particles but also by highly ionized plasmas (bremsstrahlung). Line-like spectra (characteristic radiation) are generated when transitioning excited atoms back into the ground state, if the energy difference of the energies involved is within the range described above. For the excitation of X-rays in the laboratory scale, accelerated charged particles, i.e. electrons or protons, as well as high-energy ionizing radiation, i.e. X-rays themselves are used. In the beginning, radioactive elements were also used as radiation sources in laboratory equipment. However, these sources are now used not very often because of the high safety requirements.

The most common way of producing X-ray radiation is the deceleration of accelerated electrons. This is used in X-ray tubes and electron microscopes. The deceleration of the electrons results in both a continuous spectrum and a line-like spectrum.

The continuous spectrum results from the deceleration of the electrons on the tube target by scattering on the atomic nuclei. The intensity of the emitted radiation is described in detail by Kramers' law.

$$I_{\text{cont}}(E) = k \cdot i \cdot Z (E - E_0)/E \quad (2.2)$$

with

- $I_{\text{cont}}$  intensity of the emitted radiation
- $K$  proportionality coefficient
- $I$  electron current
- $Z$  atomic number of the decelerating material
- $E_0$  maximum energy of the electrons

If this process is carried out in an X-ray tube, the generated radiation must be directed at the sample through an exit window. The exit window of the tube absorbs the low-energy parts of the primary spectrum. This process is described by the following addition to Kramers' law, in which  $\mu$  is the mass attenuation coefficient,  $\rho$  is the density, and  $d$  is the thickness of the tube window:

$$I_{\text{emit}}(E) = k \cdot I \cdot Z \frac{E - E_0}{E} \exp(-\mu(E) \cdot \rho \cdot d) \quad (2.3)$$

The proportions of this relation are shown in Figure 2.1. It shows the continuous spectrum (emission) generated at the target, the low transmission through the tube window in the low-energy range (transmission) as well as the resulting radiation emitted by the tube (tube output).

In addition to the continuous radiation, there are also line-like spectral components in the energy range of X-rays, which are generated by electron transitions in an atom. For this purpose, an internal electron level must be ionized by an energy input, which is higher than the binding energy of the electron. This excitation is possible by radiation, i.e. electron, proton, or even X-rays themselves or by the generation of a high-energy plasma. The resulting electron vacancy in an inner shell is filled by electrons of outer shells, in order to transfer the atom to a stable state again. These transitions can occur from different electron levels, resulting in a series of X-ray lines being emitted. The energy level differences depend on the type of the emitting atom; therefore, this radiation is called the characteristic

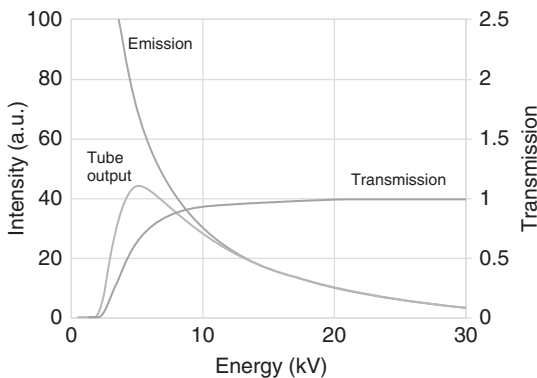
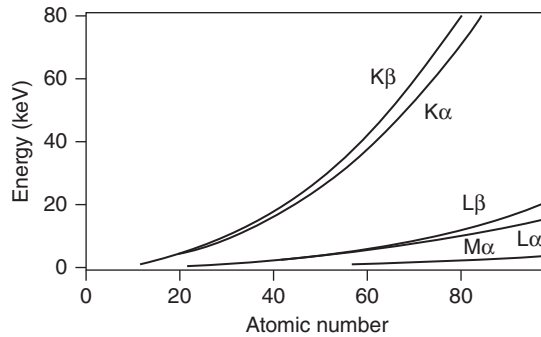


**Figure 2.1** Parts of the continuous spectrum of an X-ray tube.

**Figure 2.2** Line energy as a function of the atomic number.



radiation. The labeling of these lines starts with the designation of the primary vacancy, i.e. when the innermost K-shell is ionized it is K-radiation, when the L-shell is primarily ionized it is L-radiation, etc.

The energies of the electron levels depend mainly on the number of protons of the atom, i.e. on the atomic number. This means that the energy differences depend on the type of the atoms. These energy differences are described by Moseley's law.

$$E = C_1 \cdot (Z - C_2)^2 \quad (2.4)$$

with

- $E$  = energy difference between the electron levels
- $Z$  = atomic number of the atom
- $C_1, C_2$  = constants

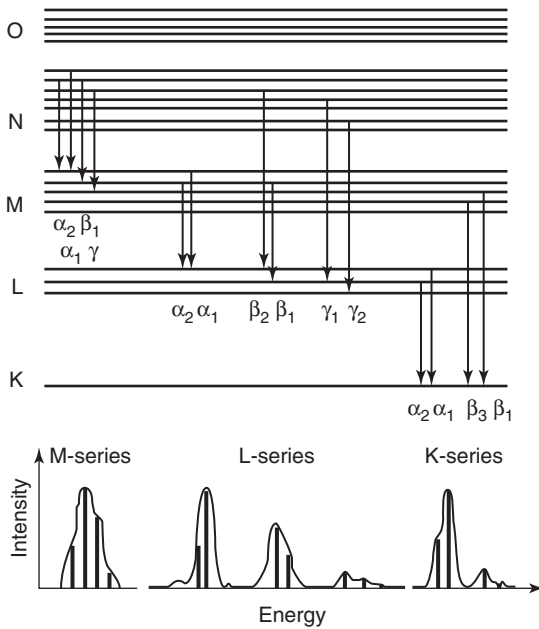
This relation is shown for different lines as a function of the atomic number in Figure 2.2. Detailed information can be found in Tables A.4–A.9.

Figure 2.2 shows that the energy of the characteristic radiation increases with the atomic number; it also shows that the line energies of an element decrease from the K series over the L series to the M series, and that in the energy range of approximately 1–40 keV, which is commonly used for X-ray spectrometry, almost all elements emit their characteristic radiation. Exceptions are only elements with very low atomic numbers ( $Z \leq 7$ ).

### 2.2.2 Intensity of the Characteristic Radiation

The intensity of the characteristic radiation is determined by the number and type of the atoms in the excited volume; in other words, the intensity depends on their mass fraction  $w$ . It is further influenced by the intensity  $I_0$  of the primary radiation. The photo-absorption coefficient  $\tau(E)$  describes the probability for the excitation of an atom by X-rays with energy  $E$ . If an inner electron shell is ionized, the transition from an outer electron shell is described by the transition probability  $p$ . For shells that are close together,  $p$  has the greatest value; therefore, the  $\alpha$ -lines are the most intense within a series. For energy levels with a larger difference the transition probabilities are smaller, i.e. the intensities of the  $\beta$ -lines are correspondingly lower; however, their energies are higher. Special electron





**Figure 2.3** Electron transitions with the corresponding line names.

transitions can be excluded as a result of quantum selection rules; for these transitions, the transition probabilities are  $p = 0$ . For the main electron transitions, the labels of the corresponding X-ray lines are shown in Figure 2.3.

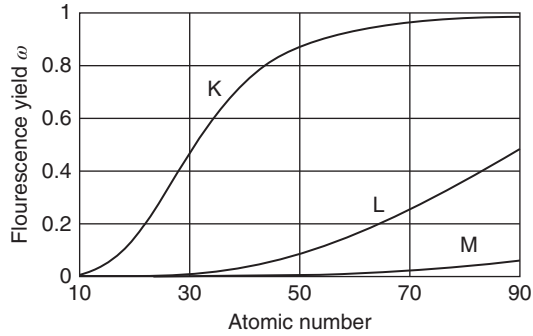
The approximate intensity ratios within a series as well as between the main lines of the different series (dependent on the excitation conditions) are shown in Table 2.1.

**Table 2.1** Approximate relative line intensities of main X-ray lines.

K-series			L-series			M-series		
100			Approx. 5–10			Approx. 1		
$K\alpha_1$	K–L3	100	$L\alpha_1$	L3–M5	100	$M\alpha_1$	M5–N7	100
$K\alpha_2$	K–L2	50	$L\beta_1$	L2–M4	50	$M\alpha_2$	M5–N6	100
$K\alpha_{1,2}$	K–L2,3	150	$L\beta_2$	L3–N5	12	$M\beta$	M4–N6	52
$K\beta_{1,3}$	K–M2,3	15	$L\gamma_1$	L2–N4	6	$M\gamma$	M3–N5	5
$K\beta_{2,4}$	K–N2,3	3	L1	L3–M1	5			
			$L\beta_3$	L1–M3	10			
			$L\beta_4$	L1–M2	7			
			$L\eta$	L2–M1	5			

After an electron transition, the released energy is emitted. This is possible by the emission of characteristic radiation, which is due to the large energy differences of the involved electron levels in the range of X-ray radiation. Another

**Figure 2.4** Fluorescence yield as a function of the atomic number.



possibility is the transfer of the energy to an outer electron of the atom under consideration and its emission. This process is called Auger effect. The probability for the emission of an X-ray photon again depends on the atomic number and is called fluorescence yield  $\omega_{\text{fluo}}$ . This probability is shown in Figure 2.4; more precise values for the fluorescence yield of the individual elements can be taken from Table A.11. Since an ionized atom always goes into the stable basic state,

$$\omega_{\text{fluo}} + \omega_{\text{Auger}} = 1$$

The relation shows that the fluorescence yields are very small for elements with low atomic numbers. Most of the atoms then emit the energy released by the transition to the ground state as Auger electron and only very few as X-ray photons. This is the main reason for the low sensitivity of X-ray spectrometry for light elements. For higher radiation energies, the fluorescence yield increases significantly.

### 2.2.3 Nomenclature of X-ray Lines

Two nomenclatures are used to designate the X-ray lines. The older is based on the fixed intensity ratios of the individual lines and was introduced by Siegbahn (1923). It also shows the development of the performance of X-ray spectrometers, in particular their energy resolution. For the first instruments, only the distinction between K-, L-, and M-lines was possible. With the improvement of the resolution, a splitting of these lines was then discovered, i.e.  $\alpha$ -,  $\beta$ -, and  $\gamma$ -lines could be distinguished. Later, further splittings were detected, which are denoted by indices.

There is also the nomenclature introduced by the IUPAC, which is based on an exact designation of the respective electron levels from which the X-ray lines are generated. A comparison of the designations for the most important X-ray lines can be found in Table 2.2.

### 2.2.4 Interaction of X-rays with Matter

X-radiation interacts with matter – it will be scattered and absorbed. This process is described by Lambert–Beer’s law.

$$I = I_0 \exp(-\mu \cdot \rho \cdot d) \quad (2.5)$$

with

$I$  intensity after absorption in a layer

$D$  thickness of the layer

$P$  density of the layer

$M$  mass attenuation coefficient of the layer material

$I_0$  primary intensity

The mass attenuation coefficient  $\mu$  has several contributions. At low energies, the absorption described by the photoionization coefficient  $\tau$  is dominant; the influence of the scattering characterized by the scattering coefficient  $\sigma$  increases with energy, and in the case of energies  $>1.2$  MeV the electron pair production described by  $\kappa$  gains importance. However, this is outside the range of energy that is of interest for X-radiation.

$$\mu = \tau + \sigma + \kappa \quad (2.6)$$

All these interactions depend on both the analyzed material and the energy of the radiation, as shown in the diagrams in Figure 2.5 for the elements (a) carbon and (b) lead. They show that in the energy range of about 0.5–40 keV, absorption dominates. Rayleigh scattering contributes a fraction of less than 1% for low energies. At higher energies, Compton scattering dominates the radiation attenuation coefficient.

### 2.2.4.1 Absorption

Absorption will be understood merely as the attenuation of the incident X-ray radiation by the ionization of atoms. This process is described by the element- and

**Table 2.2** Comparison of line designations for the main X-ray lines.

Siegbahn	IUPAC	Siegbahn	IUPAC	Siegbahn	IUPAC
$K\alpha_1$	K-L3	$L\alpha_1$	L3-M5	$M\alpha_1$	M5-N7
$K\alpha_2$	K-L2	$L\alpha_2$	L3-M4	$M\alpha_2$	M5-N6
$K\beta_1$	K-M3	$L\beta_1$	L2-M4	$M\beta$	M4-N6
$K\beta_2$	K-N3	$L\beta_2$	L3-N5	$M\gamma$	M3-N5
$K\beta_3$	K-M2	$L\beta_3$	L1-M3	$M\xi$	M4,5-N2,3
$K\beta_4$	K-N5,4	$L\beta_4$	L1-M2		
$K\beta_5$	K-M4,5	$L\beta_5$	L2-O4,5		
		$L\beta_6$	L3-N1		
		$L\gamma_1$	L2-N4		
		$L\gamma_2$	L1-N2		
		$L\gamma_3$	L1-N3		
		$L\gamma_4$	L1-O3		
		$L\gamma_5$	L2-N1		
		$L\gamma_6$	L2-O4		
		$L\eta$	L2-M1		

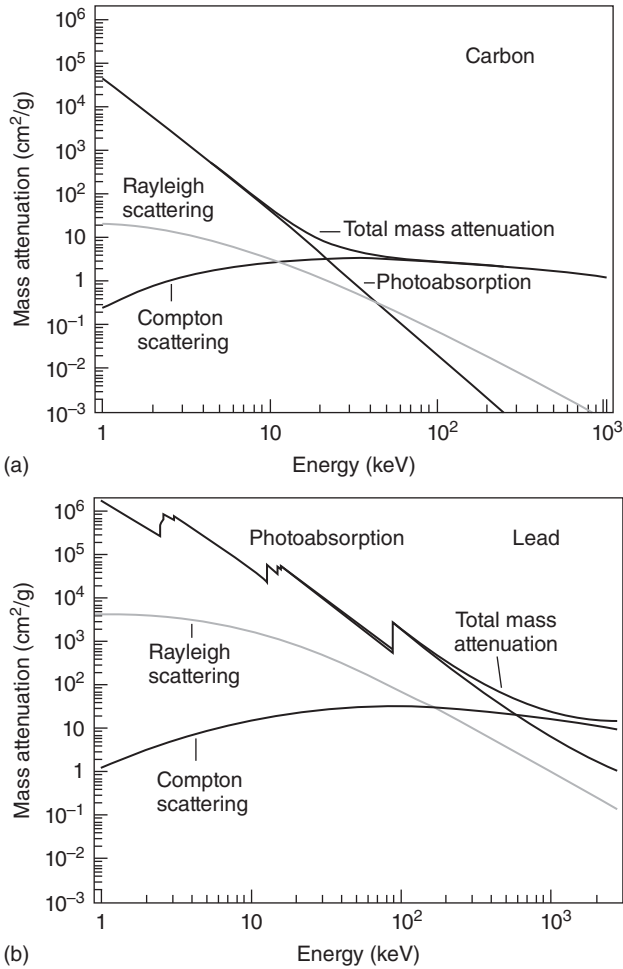


**Figure 2.5** Contributions to the attenuation coefficient for X-radiation of (a) carbon and (b) lead.

energy-dependent photoionization coefficient. It increases with higher atomic number and decreases with increasing energy as can be seen in Figure 2.5. This energy dependence can be approximated by  $\tau \approx E^{-3}$ . The curve does show discontinuities that manifest themselves as jumps. They occur when the energy of the absorbed radiation is sufficient to ionize a new electron shell, i.e. a new interaction mechanism is added. In the diagrams in Figure 2.5, this applies to Pb for the excitation of M, L, and K radiation at energies of approximately 3, 15, and 88 keV, respectively. The energy of the K-absorption edge of C, on the other hand, is 0.283 keV and is therefore not displayed in the diagram.

#### 2.2.4.2 Scattering

Scattering is the most important origin of the spectral background in X-ray spectrometry. The incident radiation is scattered at the electrons of the atoms of

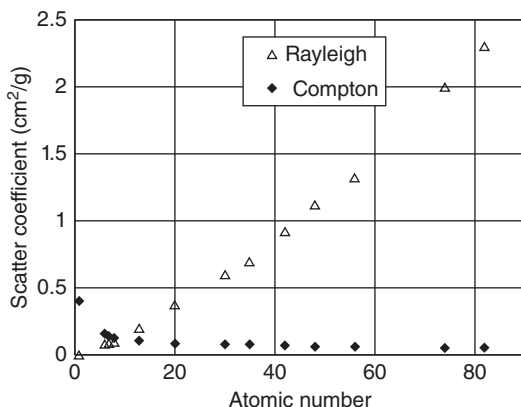


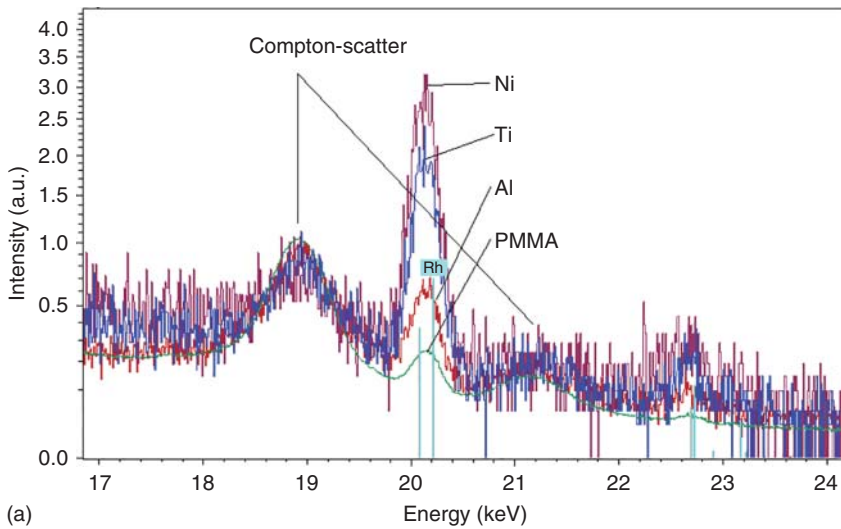
**Figure 2.6** Elastic and inelastic scattering coefficients for selected elements at 20 keV.

the sample. The scattering can be both elastic (Rayleigh or coherent scattering) and inelastic (Compton or incoherent scattering). All electrons of an atom contribute to the elastic scattering, i.e. the scattering intensity is proportional to the number of electrons or to the atomic number. Inelastic scattering can occur only at weakly bonded, i.e. outer electrons. Therefore, its intensity is mostly independent of the atomic number. This is demonstrated in Figure 2.6 showing the scatter coefficients for a few elements for an energy of 20 keV, which is close to Rh- $K\alpha$ -radiation, the most often used target material for spectroscopic X-ray tubes (Section 5.3.2.1). The coefficients for the Rayleigh (elastic) scattering increase approximately proportionally with the atomic number whereas the coefficients for the Compton (inelastic) scattering show only a small dependence on atomic number; only for the lightest elements they are slightly larger than for most other elements.

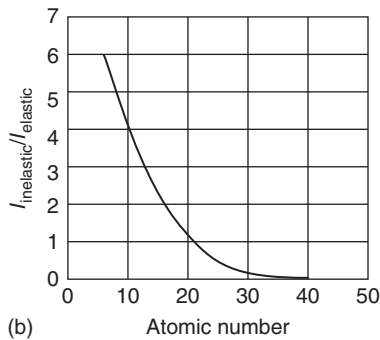
This means, that the ratio  $I^{\text{inelastic}}/I^{\text{elastic}}$  is dependent on the sample composition. For light matrices the ratio is large due to the small contribution of elastic scattering, and for heavy matrices it is small due to the larger contribution of elastic scattering. This is demonstrated in Figure 2.7. Panel (a) shows the elastically and inelastically scattered fluorescence radiation of the X-ray tube for four different samples normalized to the Compton peak of the scattered Rh- $K\alpha$ -radiation of the tube. Panel (b) shows the ratio of inelastic and elastic scattered fluorescence radiation of the X-ray tube as a function of the mean atomic number of the sample for a given measurement geometry. This different scattering behavior can be helpful in the quantitative analysis of the sample.

With the help of the Compton–Rayleigh ratio the mean atomic number of the sample can be determined. The mean atomic number can then be used for an averaged description of the absorption properties of the sample. Another application is the normalization of the fluorescence intensity of analytes to the Compton intensity. Knowledge of the mean atomic number of the sample can be further used to determine elements that cannot be measured by XRF, such as oxygen in oxides, as a difference to 100 wt%.

The continuous background of a spectrum is mainly caused by the scattered continuous bremsstrahlung of the X-ray tube at the sample, both by elastic and inelastic scattering. As demonstrated in Figure 2.7, the elastic scattering decreases with decreasing average atomic number of the sample. Nevertheless,



(a)



(b)

**Figure 2.7** (a) Influence of the sample type on the intensity of the scattered radiation (y axis in square root scale) and (b) ratio of elastic and inelastic scattering intensities on the average atomic number of the sample.

the intensity of the scattered tube radiation is considerable in relation to the fluorescence intensity of the light matrix elements. This is also caused by the limited excitation efficiency and the very small fluorescence yield for these elements (see Figure 2.4). On the other hand, due to the high fluorescence yield for heavier elements the ratio between fluorescence radiation and the spectral background is larger even if here the elastic scattering and consequently also the spectral background have a higher intensity. This is demonstrated in Figure 2.8 for the spectra already shown in Figure 2.7a. However, Figure 2.8 shows the direct measured, non-normalized spectra. Here it can be clearly seen that the background of the spectra of polymethylmethacrylate (PMMA) and Al are large compared to the fluorescence lines. On the other hand, the spectra of Ti and Ni have higher fluorescence intensities and therefore a lower spectral background.

In addition to the fluorescence lines of the metal samples diffraction lines can also be detected as a result of Bragg-reflection of the continuous tube radiation at crystalline structures of the sample, see also Section 4.2.6.3.

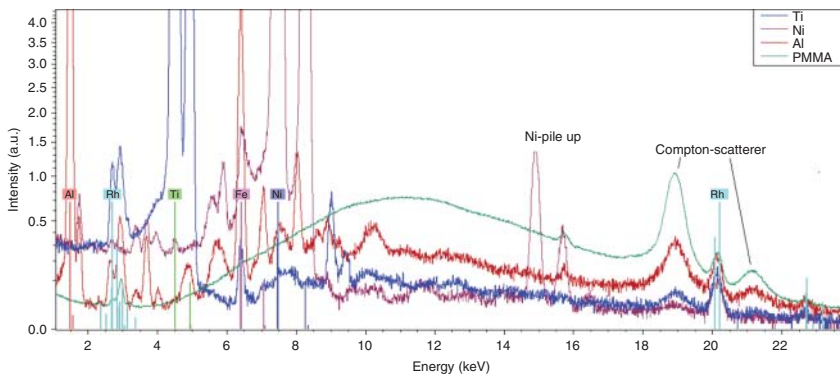


**Figure 2.8** Spectra of PMMA, Al, Ti, and Ni demonstrating the different scatter behavior (y-axis in square root scale).

The intensity of the elastic scattered radiation depends on the direction of the scattered radiation. The scattering intensity of non-polarized radiation on a sphere with the diameter  $R$  and the scattering object in its center can be described by the following formula,  $\Theta$  being the scatter angle:

$$I = I_0/R^2 \cdot (1 + \cos^2 \Theta) \quad (2.7)$$

As a result, the scatter intensity has a maximum in the forward and backward directions, while it is reduced perpendicular to the direction of irradiation.

Inelastic scattering means a loss of energy of the scattered radiation compared to the original incident radiation. The energy is transferred to the scattering particle, most often an electron, which is then emitted as photoelectron. Because the conservation laws for both energy and momentum apply, the energy loss  $\Delta E$  depends on the scatter angle  $\Theta$  and on the energy  $E$  of the scattered radiation. For scattering on an electron this dependence is described by the following formula:

$$\Delta E = E_0 - E_{\text{scat}} = 1 - (1 - 0.001957 \cdot (1 - \cos \Theta))^{-1} \quad (2.8)$$

### 2.2.5 Detection of X-ray Spectra

The radiation emitted by a sample is detected by an X-ray spectrometer. The spectrometer separates energetically different beam components and determines their intensity within narrow energy ranges; they can be, for example, individual element peaks as well as background areas with narrow energy ranges of a few electronvolts. In principle, two instrument types for spectrometry are in use where the dispersion takes place by different means:

- In the case of wavelength-dispersive spectrometers (WDSs – see Section 4.3.2), the separation of the radiation components takes place via a dispersive element, for example, a crystal, or, at low energies, by special multilayer structures, on which the fluorescence radiation of the sample is diffracted. The “reflection” of individual energies takes place only at defined diffraction angles, following Bragg’s law, see Eq. (4.1).

- In the case of energy-dispersive spectrometers (EDSs – see Section 4.3.1.3), the dispersion is performed directly in the detector and its associated electronics. This generates an energy-dependent signal from each individual absorbed X-ray photon. By means of pulse-height analysis, the probability distribution of the photon energies absorbed in the detector can be generated, creating an image of the emitted spectrum.

For analytical purposes, element identification, i.e. qualitative analysis, is possible due to the element dependence of the energies of the characteristic radiation (see Eq. (2.4)).

The intensity of this characteristic radiation depends on the number of atoms in the analyzed material, i.e. on their contents  $w$ . In a first approximation, therefore, the mass fraction  $w = \varepsilon \cdot I$ , where  $\varepsilon$  is the element-dependent sensitivity, and  $I$  is the measured fluorescence intensity of the element under consideration. Unfortunately, the conditions are more complex than this, as all other elements in the sample influence through absorption and secondary excitation the measured fluorescence intensities. For a quantitative analysis this matrix influence has to be considered. It leads to complex corrections of the above linear dependency (see Section 5.5).

## 2.3 The Development of X-ray Spectrometry

The period from the beginnings of early X-ray spectrometry to today's powerful instrument technology has been long. The first stage was characterized by the development of sufficiently powerful instrument components and the development of basic mathematical models for matrix interaction. In the next step, the use of computing technology for data preparation as well as for instrument control was an important step for the establishment of the method for automated industrial use. Finally, the application areas of the method have been significantly expanded in the last 20 years by the availability of various X-ray optic elements as well as more powerful detectors.

The development of X-ray fluorescence is briefly described by Niese (2007). The foundations for the use of X-ray spectrometry for element analysis were laid out by the discoveries of Moseley and Laue, and by using X-ray radiation for the screening of the human body for medical purposes. Experience was gained in making components such as X-ray tubes for the emission and X-ray films for the detection of the radiation. These were the preconditions for the initial use of X-ray spectrometry for element analysis.

The first attempts for an element analysis with X-rays, still utilizing electron excitation, were carried out by v.Hevesy for determining the content of tantalum (Hevesy et al. 1930; Hevesy and Böhm 1927). The excitation of the sample with X-rays was first published by Glocker and Schreiber (1928) but also used by v.Hevesy. Nevertheless, the transition from simple laboratory designs to the first serial production of instruments required a few more years. Siemens and Philips built the first commercial instruments in the early 1950s. Taking advantage of the experiences gained during the initial designs, these instruments already showed





**Figure 2.9** PW 1540 from Philips.

an acceptable ease of operation and sufficient radiation protection. The successful and ever-widening use of X-ray fluorescence spectrometry in laboratory analysis began with these instruments. Significant progress has been made in Europe, in particular by companies such as Siemens, Philips, and Bausch & Lomb. Through successive development steps, such as the expansion of the detectable element range by the use of different crystals, the improvement of analytical accuracy by the increased performance of the X-ray tubes, the improvement of precision by more powerful evaluation models or by simplifying the sample management by means of sample carriers or magazines, improvements in the analytical performance and in range the applications were achieved. A typical instrument from the beginnings of commercial X-ray spectrometry is shown in Figure 2.9, the PW 1540 from Philips.

Significant progress could be made by the introduction of electronic data processing, which began in the 1970s. At the beginning, it was mainly used for complex data processing, and later also for the control of instrument functions. As a result, XRF became much more powerful, not only regarding the analytical performance but also in regard to the ease of use, the sample throughput, and the ability to automate the analytics. This was of extraordinary importance for the acceptance of X-ray spectrometry as an analytical method and its wide use in quality control in industrial production. A further important step was the integration of automated sample preparation, measurement, and instrument monitoring for the improvement of analytical quality and the reduction of the subjective influence of human work.

These developments were mainly carried out by the companies mentioned above, some of which in the meantime underwent changes in ownership, but even now with the new name they are the current major players, such as

Bruker (formerly Siemens), Malvern Panalytical (formerly Philips), and Thermo Fisher (formerly Bausch & Lomb). Parallel developments were also made in Japan – here mainly Rigaku has to be mentioned.

Another important development step for XRF was the availability of effective ED solid-state detectors. These Si- or Ge-based detectors, first used for  $\gamma$ -spectrometry, continuously achieved improved energy resolution through the development of low-noise signal electronics, the cooling of the detectors down to  $-200\text{ }^{\circ}\text{C}$ , and the refinement of the manufacturing technologies. Owing to the improvements in energy resolution they were able to be used for lower radiation energies, and lastly even for the X-ray energy range.

These detectors were first used for X-ray microanalysis in electron beam instruments. Up to this time, the fluorescence intensity generated in an electron microscope was too low for WDSs. Therefore, X-ray micro-analyzers had to be built with a sufficiently high beam current. The high electron intensity however saturated the electron detectors quickly, increased the volume analyzed, and thus reduced image resolution. As a result, these instruments did not have good imaging quality and often had to be operated in parallel to electron microscopes with their good imaging function. For ED detectors, however, the fluorescence intensity in a scanning electron microscope is sufficient. This has made it possible to combine the good imaging function of electron microscopes with the analytic function of X-ray spectrometry in one instrument.

The manufacturing of these detectors required special technologies, which were only developed by a few companies, primarily in the United States by EDAX and KEVEX, and by Link in the United Kingdom. These companies also manufactured and sold the first XRF instruments with ED detectors. The detectors again had to be cooled with liquid nitrogen to  $-200\text{ }^{\circ}\text{C}$ , which was complicated by the required Dewar vessel and the handling of liquid gas. One of the first-generation instruments, the KEVEX Analyst 0700, is shown in Figure 2.10.

EDSs were first mainly used for screening tasks, i.e. for qualitative analyses. In the course of time, the analytical performance of these ED instruments could be significantly improved. This was possible not only using special excitation geometries (grazing incidence, use of monochromatic or polarized radiation), but also by the improvement of the performance of the detectors (energy resolution, pulse throughput) and the improvement of the data evaluation methods. The precise determination of the line intensities, for example, by fitting or deconvolution methods, was of particular importance, since the limited resolution of ED detectors causes line overlaps, which may limit the accuracy of the analysis. On the other hand, improvements in quantification were possible by the availability of the entire spectrum including the background.

The availability of silicon drift detectors (SDDs), with their high count rate capability, gave EDS another boost, since now statistical errors could be achieved comparable to those of WDS instruments. The development of ED spectrometry was especially advanced by companies such as Spectro, Oxford, and Thermo.

A special application for X-ray spectrometry is the analysis of layered materials. Here, we have special analytical conditions, that are reflected in the measurement equipment as well as in the evaluation routines. The measurements are carried



**Figure 2.10** Analyst 0700 from KEVEX.

out usually on finished products, on which layers have been applied for decorative or functional purposes. This means that the samples are rarely flat and homogeneous over a large area, as it is necessary for conventional XRF. Therefore, the analysis must be carried out on small sample areas. This requires collimation of the exciting beam, thereby reducing the excitation intensity. The intensity loss associated with collimation must be compensated by large solid angles for the detection of the fluorescence radiation. Therefore, mostly ED instruments are used for coating thickness measurements. The associated loss of spectroscopic performance is acceptable, since layer systems usually contain only a few elements that are even known, since this analysis is usually carried out as quality control of the coating process.

As a result of the different analytical tasks, but primarily due to the different equipment requirements for WDS and EDS instruments, the development of coating thickness analyzers was for a long time independent from that of conventional X-ray spectrometers. The main companies were UPA, TwinCity, and CMI in the United States, Helmut Fischer in Germany, and Hitachi and Seiko in Japan. In the meantime, companies that had previously concentrated on the development of WDSs have recognized the high demand for coating thickness analyzers and therefore have also focused on this application. This development is also supported by the increased use of EDSs for the analysis of bulk samples at these companies. On the other hand, the companies, which were

once primarily focused on layer analysis, are increasingly turning to applications on compact samples, for example, the analysis of precious metal in jewelry, the determination of toxic elements in consumer products or toys, i.e. samples which are finished products and therefore are not homogeneous or do not have flat surfaces. As previously mentioned, these measurements require small sample areas. Fischer and Bruker in Europe, Hitachi in Japan, and Bowman in the United States are currently the leading companies for this type of equipment.

A continuous trend in the development of X-ray spectrometers has always been the reduction of instrument size. The first commercially produced X-ray spectrometers were filling a complete room, in particular due to the elaborate electronics. Today, a table is often sufficient for setting up the instruments. Further, increase in the integration of the electronics has not only resulted in an increase in performance but also in a significant reduction of instrument footprint.

A significant step in this direction is the use of instruments that can be held in one hand. This development began shortly after the turn of the millennium with the demand in the United States for the determination of lead pigments in wall paints. This task was important because lead as a toxic element was to be identified, in order to be replaced in wall paint. The requirement was that the analysis is done on site in order to avoid the logistical effort necessary for the analysis of pieces of paint in the laboratory. The first instruments still operated with radioactive sources for excitation; they were later replaced by low power tubes. Owing to the very small distances between radiation source, sample, and detector the tube power can even be less than 5 W. This not only assures a higher safety of the instruments, but also a good analytical performance and higher flexibility. The integration of powerful computing technology has further also contributed significantly to the improvement of performance. In the meantime, handheld instruments have been used for a wide range of analytical tasks. The possibility of on-site analysis has played a decisive role in the selection of analytical tasks.

Typical applications of handheld instruments are sorting of scrap, the determination of toxic elements in consumer products, the tracking of ores in mining explorations, or the investigation of art objects. Equipment is offered by companies such as Thermo, Bruker, Hitachi, Olympus, or Spectro; these companies usually also carry ED X-ray spectrometers in their portfolio. They all work with comparable components and the performance achieved in the meantime is remarkable as well as comparable for all companies. The available computing technology on the instruments is limited by the battery power supply but allows for quantification of predefined material classes by means of standard-based calibrations. The analytical accuracy however is mainly limited due to the lack of sample preparation, and due to sample contaminations on site. In special cases, the transfer of measurement data to an external computer is possible, on which more powerful evaluation algorithms and procedures for data management are available.

A further important influence on the development of XRF analysis was the availability of various X-ray optics. First, there were multilayer systems with large lattice constants for the detection of light elements in WD spectrometry. Increasingly, however, optics was used for beam shaping and influencing the properties of the primary radiation. The performance and application range of EDSs therefore could be continuously improved, for example, by the excitation of very small

sample areas with high intensity or by reducing the scattering of the exciting radiation to improve the sensitivity.

All these assemblies are now used in modern X-ray spectrometers. A more detailed description and compilation of the most important instrument classes is given in Section 4.3.

## 2.4 Carrying Out an Analysis

### 2.4.1 Analysis Method

In order to carry out an analysis various steps have to be taken starting with asking the right analytical questions – this applies not only to X-ray spectrometry.

In the following discussions, unless otherwise stated, it is assumed that the sampling has already taken place and the material to be analyzed is available; this means that sampling here is not a part of the analysis. The sample material available in the laboratory is called laboratory sample (see DIN-51418-1 2008, Part 2, DIN-51418-2 2014).

For carrying out an analysis it is required to determine the analytical strategy and the analytical method to be used. It is based on the material to be analyzed as well as the analytical task requested, specifically the definition of the elements to be analyzed, the estimation of the concentration range to be detected, and the desired uncertainties. Of course, one must take into account the available equipment and the required time. Therefore the following steps are necessary:

- Determination of the type of sample preparation, namely, manufacturing of the measurement specimen from the laboratory sample, taking into account the analytical task
  - the parameters that have to be determined with the analysis
  - the time available for the entire analysis, including preparation, measurement, and data evaluation
  - the required analytical accuracy
- Definition of analysis conditions (e.g. excitation parameters and measurement time) and of the quantification model to be used
- Carrying out the measurements on the sample as well as, if necessary, on reference or monitor samples
- Qualitative and quantitative evaluation of results
- Estimation of measurement uncertainties
- Preparation of a report of the analytical results

In the case of unknown samples and high accuracy requirements this process can take up a considerable amount of time; in the case of repetitive measurements on known sample material it is possible to obtain an analysis result in a very short time even with low measurement uncertainties.

The individual steps can be summarized as follows:

- The actual *measurement* includes the determination of the test conditions as well as the measurement of the test sample itself and, if necessary, of the calibration samples with the available analytical technique.

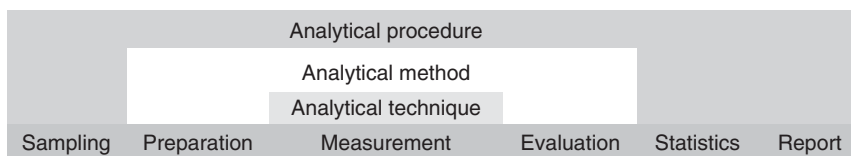


**Figure 2.11** Steps for an analytical procedure.

- The *analytical method* includes the measurement, sample preparation, and evaluation of the measured data. The analytical method can be used in an identical way for comparable analytical questions.
- The *analytical procedure* includes additionally the sampling procedure and the data processing, namely, the preparation of the analysis report including a possible statistical evaluation of the results.

This situation is demonstrated in Figure 2.11.

The individual steps of an analytical method and their influence on the analysis results are discussed in more detail in the following sections. In addition to the various possibilities of sample preparation, the influence of the analytical technique must be discussed as well. In both cases, the analytical problem itself, as well as the analytical accuracy that is required, has a great influence on their selection.

When performing the measurement itself, the selection of the optimal measuring conditions as well as the processing and evaluation of the spectra, including quantification, is important. Finally, the estimation of the analysis errors and the uncertainties is an important part of an analysis procedure in order to assess the quality of the results. These considerations essentially depend on the respective analytical task.

## 2.4.2 Sequence of an Analysis

The first step in an analysis is to define its goal. Several separate problems have to be considered.

### 2.4.2.1 Quality of the Sample Material

The laboratory sample, i.e. the sample material that is available in the laboratory, can have different forms: it can be compact, it can be small-particle size granule or powder-like, or it can be a paste or even a liquid. Increasingly, finished products have to be analyzed for quality assurance or fault identification purposes. As far as possible, they should not be modified for the analysis. Knowing the sample material, important information about the sample matrix can be obtained for the evaluation, such as information about non-measurable light elements.

### 2.4.2.2 Sample Preparation

For the various material qualities, the possibility of different sample preparation techniques is required. They also depend on the type of the spectrometer as well as on the desired analytical accuracy.

The simplest method of sample preparation is to cut the laboratory sample into a shape appropriate for the spectrometer. Nonetheless, it may also be necessary to homogenize, compress, or clean the sample surface so that the analyzed sample volume represents the material to be characterized. In special cases, it can be advantageous to change the state of the sample by dissolution, digestion, or deposition to achieve better analytical results.

These options are discussed in detail in Chapter 3.

#### 2.4.2.3 Analysis Task

Analytical tasks for element analyses can vary broadly. They can be

- a simple determination of the elements present in the laboratory sample (qualitative analysis);
- a monitoring of the content of one or more elements with respect to a predetermined threshold value (semiquantitative analysis);
- a comparison of the measured intensities of one or several elements with those of reference samples for identifying a material class (positive material identification – PMI);
- the quantitative determination of the mass fractions of some or all elements in the sample material with a predetermined uncertainty level as an overview analysis, as well as for an accurate or even highly accurate analysis (quantitative analysis);
- the characterization of layer systems on the sample with respect to layer thickness and layer composition, again with different accuracy requirements;
- the determination of element distributions in inhomogeneous samples.

Starting from these very different objectives, the individual steps for the analytical method are to be defined, such as the selection of

- the equipment to be used for the measurement
- the reference samples to be used to calibrate the method
- the selection of appropriate measuring conditions as well as
- the procedures for data processing and evaluation.

#### 2.4.2.4 Measurement and Evaluation of the Measurement Data

In accordance with these definitions, the measurements shall be carried out both on the unknown sample and, if necessary, on reference samples with the selected measuring conditions.

Thereafter, a processing of the raw data is required, i.e. the measured intensities must be corrected for overlap with other lines, for detector artifacts as well as for the spectral background. The resulting net intensities can then be converted into mass fractions or layer thicknesses using appropriate quantification models. By comparison with reference samples, the analytical result can be improved, or the measurement uncertainty can be reduced.

Finally, before using the test method it can be essential to validate the entire analytical process. According to ISO EN DIN 17025 (DIN-EN-ISO-17025 2005) the validation is defined as “*the confirmation by examining and providing proof that the special requirements for a specific intended use are met.*” For that

purpose, the required statistical parameters can be determined with the help of suitable reference samples or by comparing the analyses results of different samples with those of other independent analytical methods. These include the validity range of the method, and parameters such as trueness, repeatability and comparability, specificity and selectivity, as well as in the case of the detection of low mass fractions, the detection and determination limits. Validation is necessary to demonstrate the quality of an analytical method and to determine the achievable uncertainty of the analytical results.

#### **2.4.2.5 Creation of an Analysis Report**

Often, in addition to the analysis, a report must be prepared about all procedures and results of the analysis. It should include

- the analytical instrument and measuring conditions used
- the results of the individual measurements
- the description of the evaluation method of the measurement results and a result summary
- the discussion and estimation of possible errors in order to understand the contribution of every step of the analysis to the analytical uncertainties.



## 3

### Sample Preparation

#### 3.1 Objectives of Sample Preparation

It is generally assumed that the effort for sample preparation for X-ray spectrometry is very small, in particular since very different sample qualities can be analyzed and therefore, as with other analytical methods, the transfer of the starting material into a specific aggregate state is not necessary. Another common fact is that the sample is not modified by X-ray fluorescence (XRF). This is only true, however, insofar as the sample, which is used for measurement in the instrument, will not be changed and will be consequently available for further analytical procedures. Yet, significant changes to the sample material may be required during the preparation procedure itself.

The types of materials that can be analyzed by X-ray spectrometry range from compact homogeneous solids to small samples and liquids, as well as nonhomogeneous samples. Careful preparation of these different materials is the prerequisite for correct analytical results. With the sample preparation, different goals are pursued:

- At first, the sample must be adapted geometrically to the instrument. For this purpose, it may be necessary to cut samples to size or prepare them such that they can be positioned in the measuring instrument, for example, cutting disks from the material, pressing powder samples into tablets, or filling fluids into suitable measuring cells.
- On the other hand, the result of the sample preparation must be a laboratory sample for which the analyzed volume corresponds to the material to be characterized and for which the surface texture does not influence the measurement result. Owing to the limited penetration depth of X-rays, in particular for light elements, this means that in the case of solid-state samples, the surface must be free of corrosion layers. In addition, the surface roughness should be less than the information depth of the fluorescence radiation with the lowest energy emanating from the sample, or in the case of powder samples, the grain sizes should be of the same order of magnitude as the information depth.
- An important objective of sample preparation can be the production of a homogeneous sample in order to reduce the influence of mineralogical effects, and the influence of matrices or surface roughness. In this way, the analytical accuracy can be influenced by the different preparation methods.

- The sample composition should not change during analysis, i.e. both chemical reactions and influences by the excitation radiation are to be avoided by suitable preparation as far as possible. However, it is also possible to make selective changes to the sample type in order to prepare them for measurement. In this case, however, a determination of the recovery rates through intensive studies is recommended.

Different preparation methods are available for the various sample qualities – they are used depending on the desired analytical accuracy as well as the time available for the analysis. In this chapter, we will give examples of the commonly used preparation techniques for different sample qualities including their time and effort, but also with their effect on the achievable analytical accuracies. Where applicable, more detailed descriptions of the preparation techniques are discussed in connection with the presentation of individual analytical tasks.

Problems of sampling are not covered here since they are very much dependent on the respective analytical questions. It is assumed that the material to be examined is already available and has been processed by the initial preparation steps, e.g. crushing and, if applicable, multiple milling and separation. It is available not only in sufficient quantity, but also in quality that adequately represents the material to be investigated.

The samples produced prior to preparation as well as those produced by the preparation are named differently according to their state and their intended purpose according to DIN 51418-2 (DIN-51418-2 2014). The material that is provided for analysis is called a laboratory sample. This sample can be analyzed either with or without further preparation.

The measuring sample is the sample measured with the analyzer; the retained sample is the sample that is archived for necessary traceability. It can be either the measuring sample itself or a sample prepared in parallel. The measuring samples are distinguished according to their purpose; there are analyte samples, calibration samples, recalibration samples, drift correction samples, blank samples, and others.

## 3.2 Preparation Techniques

### 3.2.1 Preparation Techniques for Solid Samples

The variety of solid samples is very large. This results in a corresponding high number of different preparation techniques. Caused by the large influence of sample preparation to the analytical result not only the measurement methods but also the preparation techniques for special sample qualities are standardized. Table 3.1 summarizes the typical preparation techniques for the most common sample types.

### 3.2.2 Information Depth and Analyzed Volume

The information depth is an important parameter for the assessment of sample preparation. It depends on the energy of the fluorescence radiation of the elements of interest as well as on the matrix of the sample. In the case of XRF, the incident radiation penetrates into the material, is absorbed on its way through the

**Table 3.1** Preparation technologies for solid samples.

Sample type	Compact and homogeneous	Compact and inhomogeneous	Powder-like	Liquid
Example	Metals, glasses	Minerals (ores, rocks, etc.), glasses, metal alloys, metal swarfs	Minerals (ores, slags, soil, sludge, etc.) powder, dust	Solutions, melts
Homogenization	Usually not necessary, where appropriate remelting	<i>Metals, glasses:</i> remelting ⇒ transfer into compact homogeneous material (from here see compact and homogeneous)  <i>Minerals:</i> crushing, grinding ⇒ transfer into powder-like material or direct analysis ⇒ position-sensitive analysis (see Chapter 13)	Grinding, digestion, melting, solution	Stirring, shaking, where appropriate, filtering of solid components (as powder-like material)
Shaping	Sawing, cutting, turning, drilling, milling		Pouring of the powder in sample cups, pressing of disks, preparation of melted disks	Pouring in sample cups
Surface preparation	Polishing or milling with a roughness adapted to the elements to be analyzed		Realized with shaping	Given by covering of the sample cup

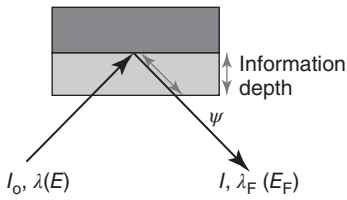


**Figure 3.1** Information depth of fluorescence radiation.

sample, and thereby generates fluorescent radiation. The radiation must reach the sample surface in order to be detected by the spectrometer. On its way, the fluorescence radiation is attenuated, i.e. only the radiation from a well-defined sample layer reaches the sample surface. This is referred to as the information depth.

Because the energy of the primary radiation must be higher than that of the fluorescence radiation, the penetration depth is always greater than the information depth. These geometric relations are shown in Figure 3.1.

The information depth  $d_{\text{information}}$  of the radiation can be estimated from Lambert–Beer’s law (2.5), as well as from the measurement geometry shown in Figure 3.1. If it is assumed that about 95% of the fluorescence radiation comes from this layer, the information depth is calculated as

$$d_{\text{information}} = \frac{0.05}{\mu \cdot \rho \cdot \sin \psi} \quad (3.1)$$

This relation for a few different matrices and  $\psi = 90^\circ$  is shown in Figure 3.2.

For the fluorescence energy of a specific element, the information depth is shown here for different matrices. Since the information depth is only an approximate measure of the layer thicknesses contributing to the measurement signal, this representation is sufficient for an estimation. For other matrix compositions,

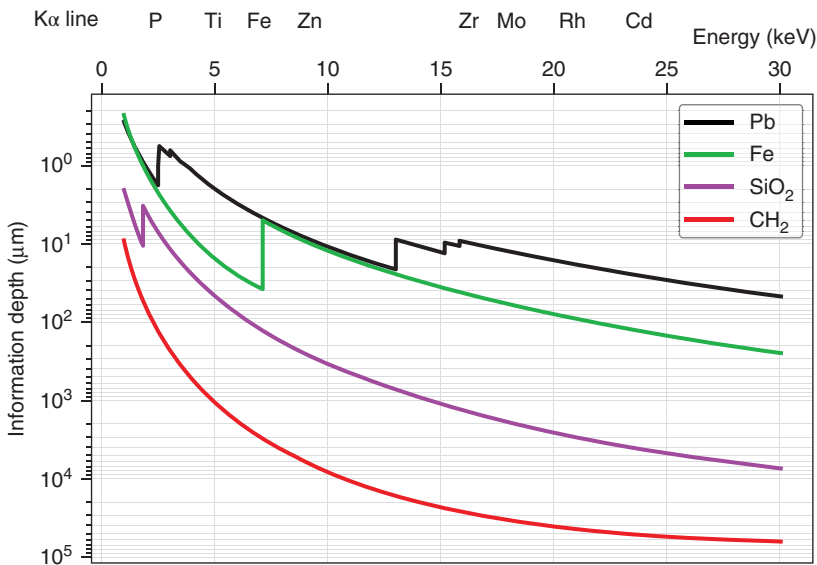


**Figure 3.2** Information depth for different matrices.

**Table 3.2** Information depth for different fluorescence lines in various materials.

Fluorescence line	Energy (keV)	Graphite ( $\mu\text{m}$ )	Silicon oxide ( $\mu\text{m}$ )	Steel ( $\mu\text{m}$ )	Lead ( $\mu\text{m}$ )
B-K $\alpha_1$	0.18	4	0.13	0.01	0.01
F-K $\alpha_{1,2}$	0.68	3.7	1.7	0.4	0.3
Mg-K $\alpha_1$	1.25	20	7	2	1
S-K $\alpha_1$	2.31	116	15	10	5
Cr-K $\alpha_1$	5.41	1 600	100	104	7
Ni-K $\alpha_1$	7.48	4 000	300	30	17
Cd-K $\alpha_1$	23.17	14 500	8 000	700	77

**Table 3.3** Information depth and accumulated intensity in the case of 10 wt% Ni in different matrices.

Matrix	Mass absorption coefficient ( $\text{g}/\text{cm}^2$ )	Information depth ( $\mu\text{m}$ )	Count rate in case of 10 wt% (cps)
Steel	333	10.3	6 000
Aluminum	60	170	35 000
Polyethylene	15	1 300	170 000

it is possible to interpolate between these relations. It should also be taken into account that the information depth in Figure 3.2 is given for a perpendicular incidence. Usually however, there is an incident angle close to  $45^\circ$ , which reduces the information depth according to (3.1) by a factor of about 1.4.

Table 3.2 gives an overview of the information depth of different fluorescence lines in various materials. It shows, the information depth covers 6 orders of magnitude for these materials. This has to be considered for the sample preparation. The surface layer of the material to be analyzed needs to be homogeneous and representative of the corresponding fluorescence line in this material.

The influence of a different absorption of fluorescence radiation in the matrix on the information depth and the measured intensity is demonstrated in Table 3.3 for the element Ni. It shows very strong changes not only in information depth but also in accumulated intensity depending on the matrix. A factor of almost 30 is observed for the same content of Ni in different matrices. These changes must be considered in case of quantification.

Considering these information depths, the volume contributing to the measurement signal as well as the corresponding sample mass can be estimated depending on the excited sample surface, the sample matrix, and the element under consideration. Table 3.4 summarizes the volume and the analyzed mass in metallic and mineral matrices for different spot diameters. These volumes and masses are very small in metallic or mineral matrices, i.e. only a few  $\text{mm}^3$ ; or mg contribute to the measurement signal, but in the case of light matrices such as aqueous solutions or polymers they can be relatively large.

**Table 3.4** Estimations of the sample volume and mass that contribute to the measured signal.

Excited area (mm)	Volume/analyzed mass for				Cd in aqueous solution
	Si in SiO <sub>2</sub>	Si in steel	Fe in SiO <sub>2</sub>	Fe in steel	
∅ 20	6 mm <sup>3</sup>	0.6 mm <sup>3</sup>	72 mm <sup>3</sup>	23 mm <sup>3</sup>	7500 mm <sup>3</sup>
	16 mg	5 mg	190 mg	175 mg	7.5 g
∅ 0.3	0.001 mm <sup>3</sup>	0.0001 mm <sup>3</sup>	0.005 mm <sup>3</sup>	0.0015 mm <sup>3</sup>	1.7 mm <sup>3</sup>
	0.003 mg	0.0016 mg	0.015 mg	0.04 mg	1.7 mg

The sample preparation must therefore guarantee that the material of this surface layer within its information depth sufficiently characterizes the material to be analyzed. This means

- that in the case of surface contamination it is important to ensure that their thicknesses are small compared to the information depth and thus cannot influence the analytical result too much;
- that the surface roughness should be small against the information depth so that the absorption lengths of the fluorescence radiation are not influenced by topological effects – this influence can be reduced by rotating the sample during the measurement; or
- that for light matrices and high fluorescence energies, the information depth can exceed the sample thickness. Then the measured fluorescence intensity depends not only on the concentration of the analyte but also on the sample thickness. This is shown in Figure 3.3 for the intensities of Cd in polymer samples of different thicknesses. This problem can be solved by using the same amount of sample material for all analyzed samples, i.e. both measured and reference samples.

However, this problem is somewhat mitigated because both the incident and the fluorescence radiation hit the sample at an angle less than 90° and, therefore, the analyzed volume is limited (see Figure 3.4). This means that the sample thickness does not have to be greater than the saturation thickness and in the case of the detection of heavy elements in light matrices, sample thicknesses that are less than the information depth can also generate sample-independent fluorescence intensities in case of an appropriate excitation geometry. Nevertheless, this analyzed sample volume defined by the excitation geometry must also be considered during quantification.

### 3.2.3 Infinite Thickness

The infinite thickness of a sample is another important parameter to consider, in particular for the analysis of layered samples (see Chapter 14). Like the information depth it depends on the element in question, other elements in the matrix, and the respective measuring geometry but it is largely independent of the spectrometer type. Typical  $d_{\text{infinite}}$  is assumed as three times  $d_{\text{information}}$ , since

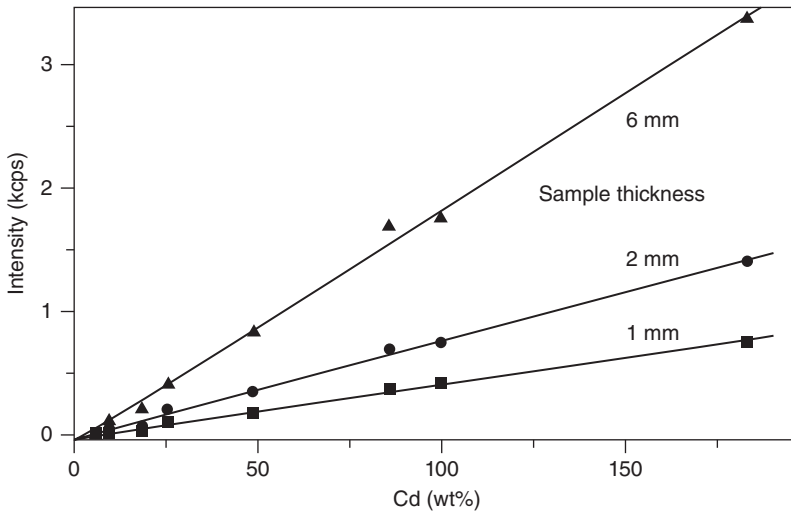
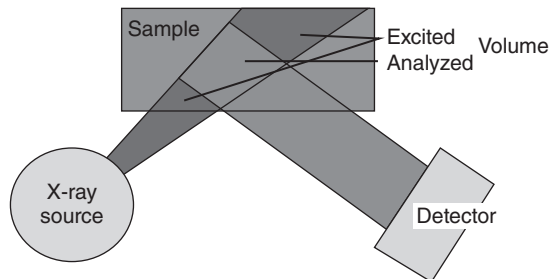


**Figure 3.3** Cd intensities measured on polymer samples of different thicknesses. Source: Courtesy of S. Hanning, FH Münster.

**Figure 3.4** Analyzed volume limited by the measurement geometry.




the usable thickness range cannot be expanded to infinity, because the slope of the calibration curve for thick layers approaches asymptotically the infinite value. Infinite thickness does not mean that no other radiation can penetrate this layer – radiation of higher energy will not completely be absorbed in layers of this thickness. The infinite thickness, for example, of Si is about  $15\ \mu\text{m}$ , but only approximately 21% of the fluorescence radiation of Cu will be absorbed in this layer. In the matrix, backscattered Cu radiation can even enhance the fluorescence intensity of Si.

### 3.2.4 Contaminations

For all preparation steps, the sample material comes into contact with other materials as well as with the laboratory environment. This can cause contaminations. These should, however, be avoided as far as possible in order not to influence the analytical result. Contaminations by the laboratory environment are usually in the range of trace amounts, in case of observing good laboratory practice. Another source of impurities is the contaminations by the sample preparation

**Table 3.5** Contaminations in the range of traces by preparation tools (main contaminations in bold).

Preparation tool	Possible contaminations
Jaw crusher	
Grinding tools made from carbon steel	C, Si, <b>Cr</b> , Mn, <b>Fe</b> , Ni, Mo
Grinding tools made from chromium steel	C, Si, <b>Cr</b> , Mn, <b>Fe</b> , Ni
Grinding tools made from agate	<b>Si</b>
Grinding tools made from zirconium oxide	Mg, <b>Zr</b> , Hf
Grinding tools made from tungsten carbide	C, <b>Co</b> , <b>W</b>
Sieves made from brass	<b>Ni</b> , <b>Cu</b> , Zn
Pressing tools (steel)	C, Si, <b>Cr</b> , Mn, <b>Fe</b> , Ni
Crucible made from platinum	Pt
Crucible made from carbon	C, Si, Fe
Abrasion by polishing	<b>C</b> , <b>Si</b> , <b>Al</b> , <b>Zr</b>
Abrasion by milling	C, Si, <b>Cr</b> , Mn, <b>Fe</b> , Ni in case of steel tools C, Si, Zr, Hf in case of ceramic tools



tools (e.g. mills, crushing tools, melting crucibles, etc.). Furthermore, if the preparation tools are not sufficiently cleaned, cross-contamination can occur as a result of transfers between the individual samples.

Because contamination cannot be completely avoided, such as by abrasion of the preparation tools, it is important that these contaminations do not affect the analyte. This is especially the case when the analytes are present in trace amounts. Changes in the contents of the main components due to traces can be neglected as well as any noticeable influence on the matrix.

Table 3.5 summarizes some typical impurity elements that can be introduced during the different steps of sample preparation.

### 3.2.5 Homogeneity

The homogeneity of samples for bulk specimens as well as glasses or metals and also for powder pellets can be determined by measurements at different specimen positions with a position-sensitive instrument; some examples are shown in Section 16.6. It is also possible to determine inhomogeneities by repeated measurements after the removal of sample layers. In this case, inhomogeneities perpendicular to the surface of the sample can be identified, in other words, layer structures. Furthermore, three-dimensionally distributed inhomogeneities can be detected in this way.

Minor sample inhomogeneities as well as surface roughness can be partially compensated by a rotation of the sample during the measurement.

One possibility for the determination of the reproducibility of the preparation procedure is to repeat several times the entire analysis process including sample preparation, measurement, and evaluation. One can then compare the results obtained from the repeated measurements.



Sufficient homogeneity or reproducibility is achieved if the average value and standard deviation of the results of repeated measurements at the same sample position or on the same sample differ only insignificantly from the results obtained from different sample positions or at different samples. The calculation of the mean value and the standard deviation is shown in Section 6.1.1. Examples for homogeneity tests are discussed in Section 16.6.

### 3.3 Preparation of Compact and Homogeneous Materials

#### 3.3.1 Metals

Metals here mean both pure metals and metal alloys. This may be a wide variety of iron alloys, nonferrous metal alloys, or hard metals.

The preparation of metals for a measurement depends on the starting material as well as on the analytical task. Casting from the melt is possible. In the case of inhomogeneous alloys, remelting is also possible. The resulting specimens first have to be adapted to the geometry of the respective measuring instrument by mechanical processing, such as cutting, drilling, or sawing and then a clean and plane surface must be prepared by milling, grinding, or polishing. For the sampling from liquid melts, probe samplers are available with which, under reproducible conditions, homogeneous samples can be produced whose external form is directly fitted for the measuring instruments (see Figure 3.5). For castings, depending on the casting mold, removal of a surface layer is required to eliminate the influence of surface segregation and corrosion. Castings should always be produced under the same conditions, i.e. temperature and mixing of the melt, cooling rate, and sample geometry to ensure high reproducibility.

Conversely, the material to be analyzed can also present a compact metal body that already has been subjected to mechanical deformation, e.g. plates, bars, or



Figure 3.5 Specimen generated by sampling from a melt.

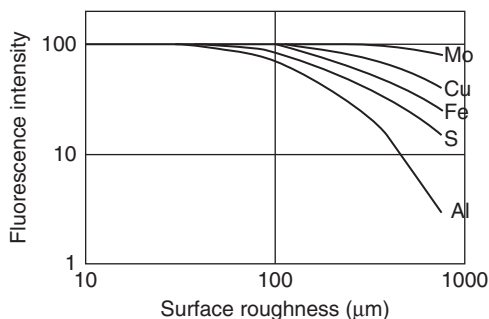


**Figure 3.6** Influence of surface roughness on the measured fluorescence intensity. Source: According to Willis et al. (2014).

tubes; they must be prepared by modifying the shape and by processing the surface to a measurement sample. The aim is always to produce a homogeneous sample with low surface roughness.

Usually, the surface roughness obtainable by grinding or milling is sufficient for the analytical task. If a surface treatment is required by polishing, care must be taken that the polishing agent does not penetrate into the sample and cause contamination. This is especially likely in the case of relatively soft sample matrices, such as aluminum samples, in conjunction with hard polishing agents. This effect can be avoided by using other surface processing methods, such as milling. For hard sample matrices, polishing is often the only way to process the sample surface. Here, the risk of contamination is relatively low and can be largely avoided by subsequent cleaning procedures, for example, washing in an ultrasonic bath.

The measured intensities can be influenced by the surface roughness of the samples. It should be taken into consideration that this influence is greater for small fluorescence energies, in particular for heavy matrices, but smaller for high fluorescence energies in light matrices. The dependence of the measured fluorescence intensities of pure metals on the surface roughness of the sample is shown in Figure 3.6.

### 3.3.2 Glasses

Glasses are amorphous substances that can contain very different elements, usually in the form of oxides; they are dissolved in glass formers and have typically a good homogeneity and a high surface quality. Glasses are available in very different forms for the analysis: commercial flat glasses, molded glass, and glass in art objects. Glassy beads are also frequently produced with the goal to obtain homogeneous samples from minerals or other small-particle materials. In this way, not only surface effects but also mineralogical influences can be neglected.

To keep contaminations small during the melting process, Pt crucibles are used. During the melting of the glasses, low melting temperatures are required in order to avoid or reduce the loss of easily volatile elements in the melting process.  $\text{LiBO}_2$  (lithium metaborate),  $\text{Li}_2\text{B}_4\text{O}_7$  (lithium tetraborate), or  $\text{Na}_2\text{B}_4\text{O}_7$  (sodium tetraborate or borax) are used as melting agents and glass formers (see Section 3.4).

Flat glasses usually only require shaping to fit the sample to the geometry of the measuring instrument; they already have a flat surface and are also homogeneous.

The shaping can be carried out by cutting, breaking, or sawing. Remelting should be avoided, because a possible loss of easily volatile elements can occur.

For the preparation of glasses, the procedures described for metals can also be required to remove surface layers or for improving the surface quality, in particular to avoid the effects of laminations in the glass composition. As a result of the generally light matrices of glasses, the requirements for the surface quality are typically comparatively low, in particular when determining elements with high fluorescence energies due to their large information depths. The specific preparation techniques are again strongly dependent on the sample type and the analytical task. More detailed information on the preparation techniques for glasses can be found in the descriptions of the appropriate applications in Section 9.7.

Shaped glasses or art objects are often irregularly shaped, which means that sufficiently large areas are not available for a conventional large area analysis. In the case of valuable objects, sample preparation usually is not possible in order to avoid any damage to the object. Here, spatially resolved methods are recommended.

### 3.4 Small Parts Materials

Powder-like materials can be of various nature – minerals such as ores, rocks, or sands, slags or metal swarfs, but also polymer granules or secondary raw materials.

The sample preparation starts usually with crushing of the samples, which is usually combined with a mixture and division of the crushed material, in order to achieve sufficient representativity. For geological samples it is recommended to remove metallic components; Fe-containing particles for example can be removed by a magnetic separator, and other metals for example by flotation. After further grinding or cutting steps, the final making of the test sample can be carried out by filling the test particles into a sample cup or vessel, by pressing a tablet, or by producing a fusion bead. Depending on the starting material, the processing methods and sample quantities given in Table 3.6 are usually used.

In the following, it is to be assumed that sample particles exist in a size of 2 mm, which means that they were prepared by breaking or cutting.

**Table 3.6** Steps for processing and sampling of small part materials.

Primary material	Processing step	Sample amount	Grain size
Rocks, ores, slags	Coarse crushing, dividing	10 kg c. 1:10	150 mm => 20 mm
Waste and pre - crushed rocks, ores, or slags	Fine crushing cutting dividing	1 kg c. 1:20	20 mm => 2 mm
Soils and fine crushed materials	Grinding dividing	50 g	2 mm => 40 µm
Finished material	Pouring in cuvettes pressing fusion beads	10 – 20 g 10 – 20 g 1 g	

### 3.4.1 Grinding of Small Parts Material

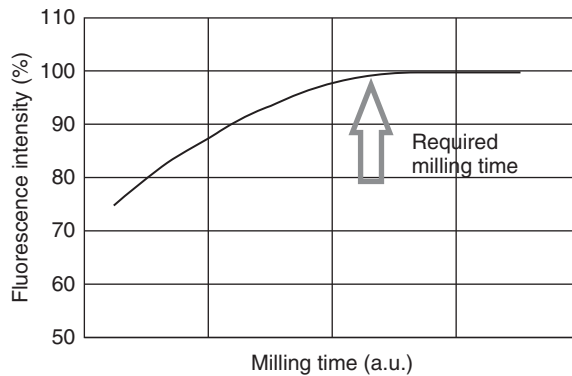
The pre-crushed materials for further processing should have a grain size of approximately 1–2 mm for hard materials; for soft materials the grain sizes can be up to 10–20 mm. Further processing is then carried out by cutting or grinding. Depending on the material quality, various mills are available for this purpose. Table 3.7 summarizes the available mills for the different materials to be ground.

The selection of an appropriate mill depends essentially on the type of material to be ground. Hard and brittle materials are most effectively crushed by friction

**Table 3.7** Mills for fine grinding of powder-like material.

Type of material	Type of mills	Functional principle
	Milling materials Milling speed/ revolution speed	Size of the starting material  Final grain size
Soft to medium hard, brittle as well as fibrous material	Rotating mill	Comminution by cutting
	Steel 200–3000 min <sup>-1</sup>	Up to 10–20 mm 100–200 μm
Soft material, fibers, cloth, textile	Cutting mill	Comminution by cutting
	Steel 2000–20 000 min <sup>-1</sup>	Up to 10–20 mm 0.25–10 mm
Medium hard, hard, brittle or fibrous materials (dry or in suspension)	Disk mills	Comminution and homogenization by thrusting and milling between rotating disks
	Steel, agate 400–1500 min <sup>-1</sup>	Up to 15 mm 10–20 μm
Dry samples or solids in suspension	Ball mill	Comminution and homogenization by thrusting and milling by beating balls
	Steel, agate, tungsten carbide <i>Frequency: 3–25 Hz</i>	Up to 5 mm 10 μm
Hard to soft materials (dry or in suspension)	Planet mill	Finest comminution and homogenization by thrusting and milling in rotating milling molds
	Steel, agate, tungsten carbide 100–1000 min <sup>-1</sup>	Up to 5 mm 1 μm
Medium hard to soft-brittle materials (dry or in suspension)	Mortar grinder	Finest comminution and homogenization by thrusting and milling between mortar and mold
	Steel, agate, tungsten carbide up to 80 min <sup>-1</sup>	Up to 8 mm 1 μm

**Figure 3.7** Dependence of fluorescence intensity on grinding time.



or thrusting, and soft and fibrous materials rather by cutting. Cooling of soft and fibrous materials to low temperature, e.g. by liquid nitrogen ( $\text{LN}_2$ ), can temporarily convert these materials into a hard and brittle state. When selecting the grinding vessels for very hard samples to be ground one should look for a high-density material (for example tungsten-carbide). For medium-hard specimens good milling results can also be achieved with lighter material grinding tools (steel, agate).

The milling times required must be determined by tests. They depend on the sample type, the type of mill, the material of the grinding vessels, and the grinding medium. For preparation as loose material or as a pressed tablet the required fineness of the grinding material and thus the duration of the grinding process should be determined from the measurement of the fluorescence intensity of the analyte as a function of the grinding time. Such a determination is illustrated exemplarily in Figure 3.7. The grinding time can range from a few tens of seconds to a few minutes. It should be noted that samples containing a percentage of oxidizable material (e.g. metals) can absorb oxygen due to the heating during grinding, whereby the composition of the sample material changes.

### 3.4.2 Preparation by Pouring Loose Powder into a Sample Cup

Powder-like material can be filled directly into sample cups and analyzed there. In the case of excitation from below, the measurement sample rests on a thin polymer film (see Figure 3.17). Since the sample material can only slightly be compacted by pressure, the sample density can vary for the same sample material. The surface roughness of such samples depends essentially on the grain size. This preparation technique is simple and allows for very fast analyses, but usually does not allow for high precision.

The following factors influence the analysis accuracy most:

- The film of the sample cup absorbs both the incident and the analyte radiation. This means that low-energy radiation of lighter elements in particular cannot or can only badly be detected. This can lead to significant analytical errors if the analyzed materials have a high content of light elements. In addition, it is possible that contaminations in the film of the sample cup counterfeit elements or their content in the sample.

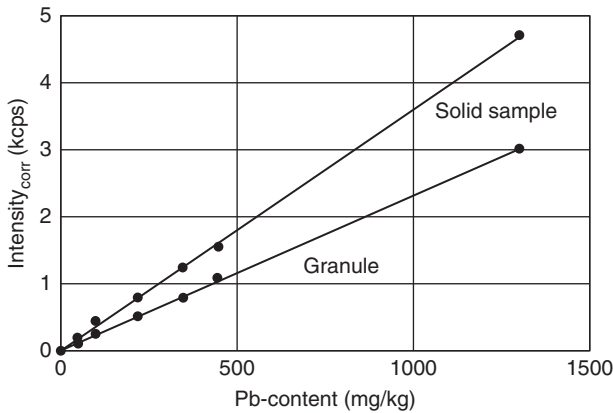


**Figure 3.8** Dependence of fluorescence intensity on the morphology of the sample. Source: Courtesy of S. Hanning, FH Münster.

- The measurement often takes place in air, on the one hand, in order to save the time pumping down the sample chamber, but on the other hand also to avoid contamination of the spectrometer by swirling sample particles. Air in the beam path acts as an absorber. The contamination of the spectrometer during evacuation with sample particles can be avoided by covering the sample cup with a lid, see Figure 3.17.
- The relatively large surface roughness of loose samples influences the analytical accuracy for light elements. Different information depths of the fluorescence radiation result in their varying absorption.
- Owing to the filling process the sample density is not uniform. This significantly influences the reproducibility of the analytical result. This is illustrated in Figure 3.8, which shows the measured intensities of Pb in a loose powder of synthetic granules and correspondingly in a pressed pellet of the same material.

This type of sample preparation is usually used for waste or secondary raw materials. High analytical accuracy is not expected here in the first place due to the low reproducibility and representativeness of the sampling. Variations of the analytical results caused by this simple preparation technique are still small compared to the variations generated by the actual sampling and are therefore negligible. Typical uncertainties for the measurement of loose powder samples are in the range of 3–5% relative to the main components; accordingly, for traces they are larger and depend on the element, the matrix, and the grain size.

It needs to be considered that in case of wavelength-dispersive spectrometry (WDS) instruments the film is thermally stressed by the high excitation intensity, i.e. long measurement times should be avoided.

### 3.4.3 Preparation of the Measurement Sample by Pressing into a Pellet

Higher analytical accuracies are possible by the manufacturing of pressed pellets, since these can produce relatively smooth sample surfaces and uniform sample densities. For this purpose, the ground material is filled into a press mold

**Figure 3.9** Press die for to produce pellets from small-sized materials. Source: Courtesy of Specac Ltd.



having a diameter that corresponds to the respective size of the sample holder of the spectrometer. Pressures of 100–200 kN for pellet diameters of 32 mm and of 200–300 kN for pellet diameters of 40 mm have to be typically applied for up to one minute to compress the material. As a result, pellets with a relatively high density are prepared, which are stable and can be stored over a longer period. In order to avoid contamination by the mold, the pressing surfaces can be covered with a thin plastic film, which is removed after pressing the pellet. Figure 3.9 shows a press die. This die allows evacuation of the sample material during the pressing operation. As a result, gas inclusions are avoided, which can destroy the pressed pellets during the pressure changes in the course of vacuum measurements.

Various possibilities exist for the manufacturing of a pressed pellet, which are distinguished, in particular, by the stability of the pressed pellet, but also by the effort for its production; it depends on the starting material as well. Pressed pellets can be made by

- direct pressing of the ground raw material without any additives;
- mixing the sample with a binder and pressing the mixture into a pellet. The binder increases the strength and thus, if necessary, allows multiple use of the pellet. At the same time, a dilution of the matrix is achieved. The binders used are cellulose, wax, or other soft materials;
- pressing the sample material with a binder into solid sample holders such as rings or aluminum molds. The rings are made of steel or plastic. The material of the Al molds must have high purity in order to avoid superpositions of the sample spectrum with that of high-energy fluorescence radiation of impurities. This support of the sample material with molds is particularly useful for often used samples, where particles can flake off and contaminate the spectrometer. The pressing of small-particle material produces stable pellets with very smooth surfaces, as shown in Figure 3.10a;
- simultaneous pressing of the sample material into a substrate made of binder or boric acid utilized as a sample vessel. In this case, a test sample can also be produced with a small amount of sample material. Samples with a binder carrier pellet are shown in Figure 3.10b. Calibration samples can also be produced by this preparation method in order to ensure a high analytical accuracy

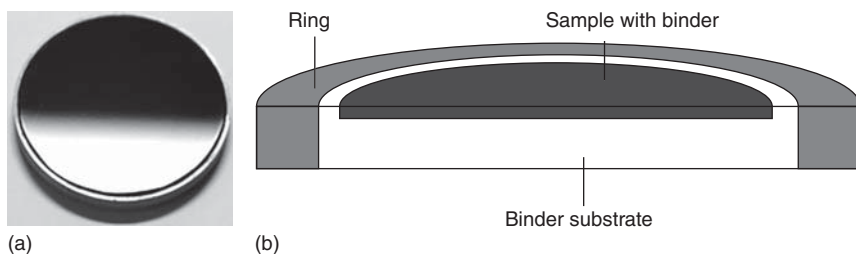


**Figure 3.10** Pressed pellet (a) and cross section of a pressed pellet in binder (b).

even in the case of small sample quantities. However, an increased spectral background has to be expected for samples prepared in this way because the high-energy incident radiation is scattered on the light matrix of the sample mold;

- pressing the sample material at elevated temperatures. Particularly in the case of organic materials, this can lead to a gluing of the individual sample particles and thus to stable pellets; see for example in Section 10.13.2.

In order to avoid the sample thickness influencing the analytical results, always the same sample quantities as well as the same mixing ratios with binders should be used for the production of pressed pellets. Depending on the size of the press die, the usual sample amount is 3–5 g. The binders are added in constant mixing ratios with proportions between 10% and 15%. As a result of the same sample masses, the sample thickness is either greater than the information depth of the analytes or the two parameters are always in the same relation to one another. The addition of binders must be considered for the quantification, both for the matrix interaction and for a possible normalization to 100%.

The durability of pressed pellets depends on the hardness of the sample particles as well as on their grain size distribution. Ultimately, the size of the surfaces of the individual particles contacting each other is important. If this area is large, then the van der Waals forces between the individual sample particles are sufficient and the pellet is mechanically stable. The various possibilities for producing stable pellets are demonstrated in Figure 3.11.

- In the case of hard particles with a narrow grain size distribution (for example, spheres of the same size as in Figure 3.11a), the closest sphere packing is obtained by pressing, but it has only relatively few and small points of contact between the individual sample particles. No stability of the pellet can thereby be expected.
- If the sample particles have a broader particle size distribution, smaller particles can be incorporated between the gaps of the larger particles. This increases the number of points of contact and thus the stability of the pellets. This case is illustrated in Figure 3.11b by the inclusion of small spheres in the interstices of the distribution of Figure 3.11a.



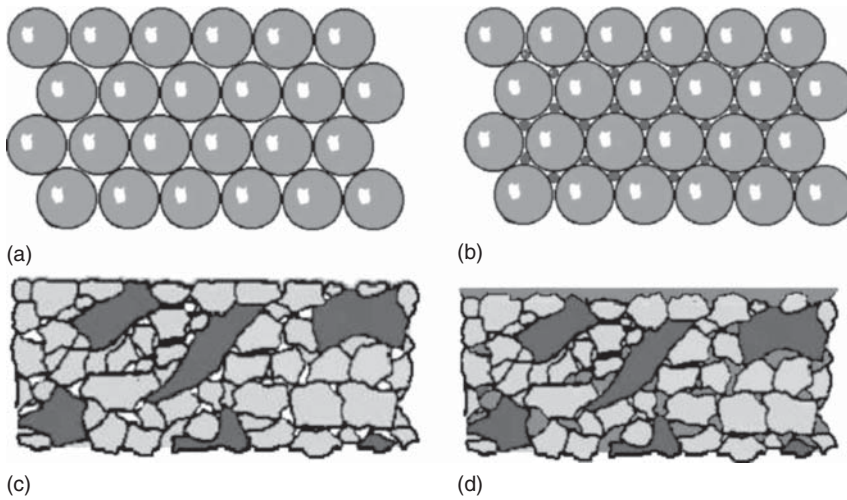


**Figure 3.11** Influence of grain size distribution and different hardness of sample particles on the durability of pressed pellets, (a) spheres of same size, (b) spheres of different sizes, (c) particles of differing hardness, and (d) incorporation of binders.

- If the hardness of the sample particles is different, the pressing can deform the softer sample parts. They then adhere to the harder parts so that the contact surfaces are significantly enlarged and thus improve the stability of the pellet (Figure 3.11c). If no soft components are present in the sample itself, a binder can be added to the sample. This has the same effect.

On the other hand, these soft components tend to segregate to the edges during pressing, i.e. also on the sample surface (see Figure 3.11d). These soft components, in particular the binder then forms an additional absorption layer, which especially influences the low-energy fluorescence radiation of the sample components and thus the analytical result.

Various binders are available. It is important that the binder does not contain any analyte elements. Binders usually are mixed into the sample during the last grinding process; they are ground with the sample material and thus homogenized. These additives often also support the grinding process by preventing particle aggregation. The binders are available as pellets with a defined weight; therefore, no additional weighing is necessary during portioning binder and sample. This is particularly important for an automation of workflows. Liquid binders are also used; they are often the only way to produce a stable pellet. In this case, it is necessary to check whether these binders dissolve elements from the sample; then the evaporation of the solvent can lead to a depletion of these elements.

The selection of an optimum binder as well as the mixing ratio with the sample for a given analytical problem usually requires tests, since there is a dependence

**Table 3.8** Binders and additives for pressed pellets.

Binder	Function	Properties/application
Boron acid Borax	Additive and binder Also advantageous for sample stabilization as sample mold	No longer allowed, slightly toxic
Paraffin wax	Mostly binder	Slightly toxic, no influence by moisture
Cellulose	Mostly binder	Absorption of moisture
Methylmetaacrylate in a solution of acetone	Binder for materials that enlarge their volume due to water absorption	Mixing with the sample and wait for evaporation of the acetone, then pressing
Polyvinyl alcohol solution	Additive and binder, avoids aggregation of the grounded material and cools down the mill	

between sample material, grain size distribution, and the available preparation technique. Table 3.8 shows a summary of the most commonly used binders.

The quality of sample preparation influences the analytical accuracy and the reproducibility of the analyses. The manufacturing of pressed pellets produces a much higher quality measurement sample compared to the simple loose powder samples of small size materials; it improves the analytical accuracy. For mineralogical material it is in the order of 0.5% for main components and <1% for secondary components.

### 3.4.4 Preparation of the Sample by Fusion Beads

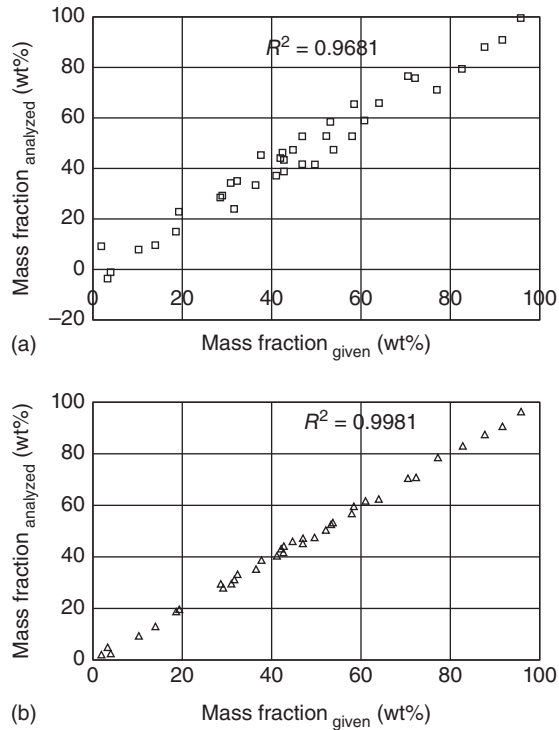
#### 3.4.4.1 Improving the Quality of the Analysis

The manufacturing of pressed pellets is fast and relatively easy; however, there still can be effects that influence the analytical accuracy, for example,

- grain size effects
- mineralogical effects
- preferential orientations
- surface roughness and
- segregations of the material.

The elimination of these effects is possible by the manufacturing of fusion beads. This type of sample preparation also results in a standardization of the matrix, since a considerable dilution of the sample material by the melting agent takes place. As a result, calibrations can be used for a wider range of sample qualities, which also means less reference samples are required for a standard-based calibration. Further, calibration samples can be produced synthetically from pure substances in the form of fusion beads, so that their traceability is possible. The influence that the preparation of the material has on the analytical accuracy is demonstrated in Figure 3.12, which shows the calibration curve for pressed pellets and fusion beads.

**Figure 3.12** Calibration curves for the same powder material prepared as pressed pellet (a) and fusion bead (b).



The following materials are required for the manufacturing of fusion beads:

- Crucible (platinum/gold 95/5)
- Chill molds (platinum/gold 95/5), nickel discs
- Cover for the molds (platinum/gold 95/5)
- Stirring bar (e.g. platinum/gold 95/5)
- Muffle furnace
- Fully or partially automated fusion machine heated inductively or with burners

The disadvantages of manufacturing fusion beads are the relatively long processing times, the higher costs, and the dilution of the sample materials, since this often leads to a reduction in the detection limits.

#### 3.4.4.2 Steps for the Production of Fusion Beads

The production of a fusion bead takes place in several steps. There are different detailed descriptions of the advantages and procedures for the manufacturing of fusion beads (Willis 2010; Claisse 1957):

- First, the sample material should be ground. Here the grain sizes are not required to be as small as for pressed pellets. Grain sizes  $<63\ \mu\text{m}$  are usually sufficient.
- As pre-treatment the material is often dried by annealing. This takes place usually at temperatures of approximately  $950\ ^\circ\text{C}$ , in the case of refractory materials in accordance with ISO 12677 at  $1025\ ^\circ\text{C}$ , and should be carried out until the

material mass is constant. For this purpose, the samples are placed in an  $\text{Al}_2\text{O}_3$  dish and heated in a muffle furnace. In this case, the loss of ignition (LOI) must be taken into account from the evaporation of moisture or volatile materials; see Section 3.4.4.3.

- Pre-oxidation of the sample material may be necessary if the sample contains pure metals that can attack or alloy with the crucible material, which can lead to a reduction in its melting point and thus damage the crucible material. The following oxidizing agents are used:
  - $\text{NH}_4\text{NO}_3$  for low concentrations of reducing materials (oxidation at temperatures of approximately  $300^\circ\text{C}$  for 1–2 minutes)
  - $\text{LiNO}_3$  for slags from steel production (oxidation at temperatures of approximately  $815^\circ\text{C}$  for 5 minutes)
  - $\text{NaNO}_3$  for metal sulfides (oxidation at temperatures of  $700^\circ\text{C}$  for 15 minutes). In this case, the nonvolatile Na has to be taken into account in the subsequent analyses or
  - $\text{SrNO}_3$ , which not only oxidizes the material but also increases the mass absorption of the fusion bead.

Further protection of the crucible material is possible by a layering of the oxidizing agent and the sample material, so that the crucible material only comes into contact with the melting agent, as shown in Figure 3.13.

- As melting agent, usually borates are used because they cannot be detected analytically by XRF and they reduce the melting point of the samples. Most commonly, lithium metaborate and lithium tetraborate are used depending on the sample composition. Samples with high contents of Al, Si, S, or Fe react better with metaborate, and samples with high contents of Na, Mg, K, and Ca better with tetraborate. Mixtures of these two melting agents are also frequently used. Further melting agents such as sodium tetraborate are available for special applications, in order to further reduce the melting point. It must be ensured that analyte elements are not also contained in these materials. The usual fluxes as well as their melting temperature can be found in Table 3.9.

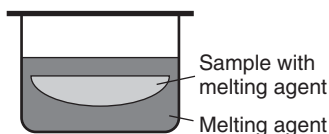


**Figure 3.13** Arrangement of layers of melting agent and sample in the fusion mold.

**Table 3.9** Flux agents for different applications.

Flux	Chemical notation	Melting temperature ( $^\circ\text{C}$ )
Lithium metaborate	$\text{LiBO}_2$	850
Lithium tetraborate	$\text{Li}_2\text{B}_4\text{O}_7$	925
Mixtures	$\text{LiBO}_2 + \text{Li}_2\text{B}_4\text{O}_7$	825 for a 50 : 50 mix
Sodium tetraborate	$\text{Na}_2\text{B}_4\text{O}_7$	741

**Table 3.10** Sample–flux ratios for typical materials in grams (valid for diameter of the fused bead of 32 mm).

Material	Ratio of sample to $\text{Li}_2\text{B}_4\text{O}_7$	Ratio of sample to $\text{Li}_2\text{B}_4\text{O}_7 + \text{LiBO}_2$ (mixture of 1 : 1)	Ratio of oxidizer ( $\text{LiNO}_3$ ) to the sample flux mix
Alumina		0.6 : 6	
Bauxite		0.5–1 : 6	
Cement	2–3 : 6		
Chromium oxide		0.1 : 10	
Coal ash	0.6 : 6		1 : 1
Ferric oxide		0.4 : 6	
Ferrous oxide		0.4 : 6	1 : 1
Magnesia	0.6 : 6		
Rocks		0.5–1 : 6	
Silica		1 : 6	
Slags	0.5–1 : 6		
Sulfate		1 : 6	
Sulfide concentrates	0.3–0.6 : 6		2–3 : 1
Sulfide ores	0.4–0.8 : 6		2 : 1
Titania		0.4–0.6 : 6	
Zirconia		0.4–0.6 : 6	

The fluxes are used in varying ratios to the sample and sometimes also with an additional oxidizer depending on the different sample qualities. Table 3.10 gives an overview of the different types of powder materials, the ratio of the amount of the flux to the amount of the sample to be used, and if an additional oxidizer is recommended. The weighing should be carried out with an uncertainty of approximately 1 mg. In any case, it is recommended to make tests in the preparation of the different sample qualities to ensure the manufacturing of high-quality fusion beads.

It has to be taken into account that due to the flux the sample is diluted, which means both the slope of the calibration curve and the sensitivity of the analysis will be reduced with increasing flux content.

Fluxes are hygroscopic, in particular lithium tetraborate. Therefore, the melting agents should be dried before use, and preheating at 105 °C over a longer period (overnight) is recommended.

- Other additives are sometimes also used in the melting process. These may be oxidizing agents and glass-forming agents, but also substances that aim to improve the quality of the fusion bead or have an influence on the analytical process.

By strong absorbers, such as BaO or  $\text{La}_2\text{O}_3$ , the matrix interaction is increased and fusion beads can then be treated as infinitely thick samples, in which the

intensity of the fluorescence signal does not depend on the sample thickness, i.e. their information depth is smaller.

- Sometimes, also lithium bromide (LiBr), lithium iodide (LiI), or ammonium iodide ( $\text{NH}_4\text{I}$ ) is added to the molten sample in small amounts (one or two drops) to increase the surface tension of the melt (especially when using lithium metaborate as flux). This allows for a loss-free pouring of the melt into the cooling mold and a subsequent simple separation of the sample from the mold. For these additives, care must be taken again that no interferences with analyte elements occur. Examples are overlaps of the Br- $L\alpha$  line with the Al- $K\alpha$  line or the Mg- $K\alpha$  line, and the I- $L\beta$  lines with the Ti- $K\alpha$  line. However, the contents of Br and I in the fused bead are very small, also caused by their high volatility. At the melting point of lithium metaborate half of the initial amount of Br or I is evaporated within approximately eight or two minutes, respectively.
- A good mixture of the sample material, additives, and the melting agent is very important. It should be carried out in ball mills in order to prevent segregation of the different components. Mixing in the melting vessel does not lead to a sufficient result and can also disturb the surface of the crucible, which can prevent the complete pouring of the sample or lead to its early destruction.
- The oxidation and melting process usually take place above a gas flame, but electrically heated muffle furnaces are also used. In order to increase the productivity of the sample preparation, usually several samples can be processed simultaneously.

A mound in the bottom of the Pt mold improves the mixing effect during the pivoting of the crucible.

- In order to increase the quality of the fusion beads and to standardize them, the temperature profiles of the ovens are mostly controllable. The temperatures for the melt process should be about 150–200 °C above the melting point of the melt. However, in order to reduce the loss of volatile elements such as alkali metals or sulfur, the melting temperatures should not be too high. This can be achieved using  $\text{Na}_2\text{B}_4\text{O}_7$  (see Table 3.9).

Equipment for fusion melting is offered by companies such as Claisse Inc., Fluxana GmbH, or XRF Scientific Ltd. (Table B.1). All of them are temperature controlled, mix the melt automatically by pivoting or rotating the crucible during the melting process, and pour the melt into a preheated casting mold, which is then cooled by a predetermined temperature profile. The casting mold then already has the required size of the X-ray spectrometer being used. The companies also offer prepared recipes for the preparation of a wide variety of sample materials.

Figure 3.14a shows the Pt crucible over a burner during the melting process, and Figure 3.14b a typical temperature profile for the complete melting process.

The cooling process strongly influences the quality of the glass beads as well. The aim is to prepare stress-free and homogeneous glass-like beads. The influence of the cooling rate on the quality of the glass beads is shown in the graph of Figure 3.15. In order to avoid crystallization of the sample material, sufficient rapid cooling is required. On the other hand, too rapid cooling can lead to high

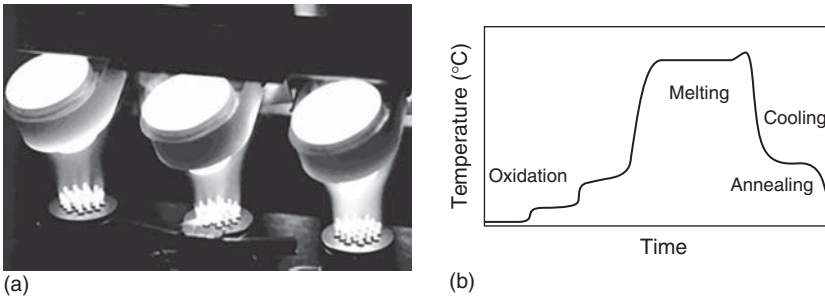
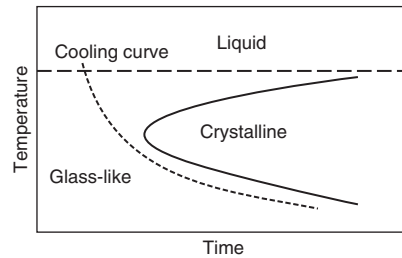


**Figure 3.14** (a) Pt crucibles over a gas burner. (b) Temperature profile of the melting process.

**Figure 3.15** Cooling curve to produce glass pellets.



stresses in the bead, which can result in the breakage of the bead; at a minimum it leads to micro-cracks or milky beads. Therefore, the casting molds are preheated before casting, and cooled by an air flow to appropriately control the cooling process. This procedure also depends on the respective melting agent, additives, and the sample material, and must be optimized by testing. In selecting the flux, a shift in the separation between amorphous and crystalline condensation along the time axis according to Figure 3.15 is possible, i.e. the cooling rate can be influenced. However, one has to take into account that the various melting agents have different dissolving properties.

The manufacturing of fusion beads requires not only a relatively long time, but also a high manual effort. Various efforts have been made to automate this process (see for example Flock and Ohls 1987).

#### 3.4.4.3 Loss of Ignition

During the melting process, the weight of the sample can be changed due to the loss of volatile elements or compounds, especially by the evaporation of moisture or gas inclusions in the sample material. This loss – LOI – must be taken into account in the later quantification. The following relationship is used:

$$C_{\text{corr}} = C_{\text{calc}} \cdot (100 - \% \text{ LOI})/100 \quad (3.2)$$

#### 3.4.4.4 Quality Criteria for Fusion Beads

Fusion beads of high quality are characterized by good transparency, a flat and smooth surface, and high homogeneity. Depending on the glass former, the fusion beads can be hygroscopic, i.e. their storage in desiccators is recommended if the samples should be available for follow-up measurements.

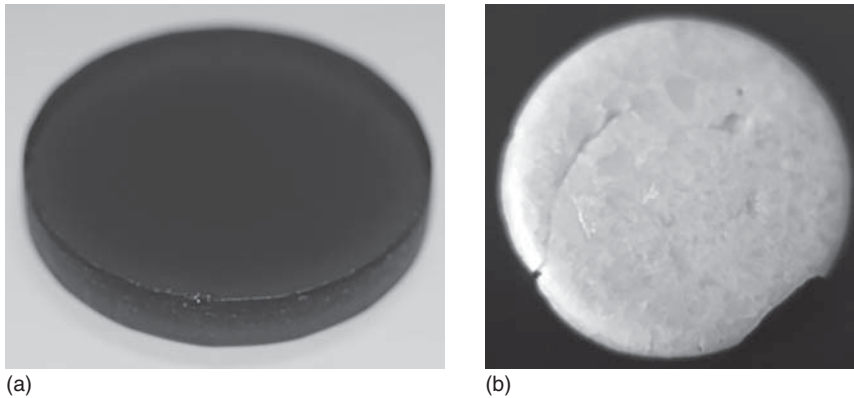


**Figure 3.16** Glassy (a) and milky, too quickly cooled fusion bead (b).

The following defects can occur in fusion beads:

- *Crystallization* can occur when a non-suitable flux for the analyzed material is used or when the cooling rate of the beads is too slow.
- *Cracking* occurs if the internal stress in the bead is too high. These can be caused by unsuitable annealing procedures or due to small inclusions, for example, after crystallization in the glassy sample.
- *Bubbles* can be generated if the material contains compounds that are volatile, if the material was not sufficiently dried, if the melt is too viscous, or if the melt captures air inclusions during the pouring process.
- *Distortion*, in cases where the mold has deviations from the correct shape these deviations are then transferred to the fusion bead and can lead, for example, to uneven surfaces.

All these influences must be tested and optimized for the various sample materials as well as for the available equipment.

Examples of a homogeneous (a) as well as a milky and cracked (b) fusion bead that was cooled too quickly can be seen in Figure 3.16.

Fusion beads can increase the analytical accuracy by reducing the matrix interaction as well as the avoidance of mineralogical effects in the sample. For main and secondary components analyses errors down to <0.2% are possible, and for traces <1%. However, it also has to be noted that the manufacturing of a fusion bead requires a relatively high effort in time and money and that the detection limits are decreased by the dilution of the sample with the melting agent.

To take advantage of a higher accuracy, any contamination by touching of the measurement surface of the sample must be avoided. Otherwise, traces of Na, K, Cl, and others will be transferred to the sample, contaminate it, and consequently influence the analytical result. The same care has to be used for pressed pellets.

#### 3.4.4.5 Preparation of Special Materials

The previously described procedures can be used for several material classes. However, for several materials special conditions must be fulfilled to produce fusion beads of high quality (Sear 1997). We will mention a few of them here:



- *Carbonates*: In the case of melting carbonates, the gas produced from the decomposition of the carbonate can have difficulties escaping from the melt because the flux has a lower melting temperature than the carbonate. This means that the gas is blocked by the viscous liquid and consequently produces foam that can completely fill the crucible. Calcium carbonate has a melting point of 900 °C. In this case, tetraborate has to be used since it has a higher melting point. If the flux is a coarse powder the gas can escape through the porous flux (Giles et al. 1995).
- *Carbon*: Pure carbon can be present in small amounts in the various sample qualities. It has to be removed before the fusion process. This is achieved by adding small amounts of ammonium nitrate. This will oxidize the carbon. The unused ammonium nitrate evaporates during the melting process. Its melting temperature is only 170 °C.
- *Metallic compounds*: The metallic particles should be milled to a very fine grain size. They then can be mixed with an oxidizer. Lithium carbonate has been proved to be very efficient. For the fusion procedure 5 g of tetraborate should be melted while the mold is rotated to coat the surface of the mold. Then the melt should be cooled down during rotation until the surface has solidified. Now 0.5 g of the metallic powder together with 1.25 g of  $\text{LiCO}_3$  can be added on the top of a layer of 1.8 g boron oxide ( $\text{B}_2\text{O}_3$ ). For oxidation and melting of the boron oxide it should be heated to an intermediate temperature, which prevents an outgassing of  $\text{CO}_2$ . After the complete oxidation of the material a standard fusion procedure can follow.
- *Sulfide minerals*: Sulfides are difficult because they can corrode and destroy the mold. This can be overcome by complete oxidation of the sample material to sulfate. The loss of sulfur due to evaporation is problematic, and therefore oxidants have to be used. Depending on the analyte elements potassium pyrosulfate or nitrates of lithium or sodium can be used. Ammonium iodide cannot be used for the improvement of the casting because sulfur evaporates with ammonium. Norrish and Thompson (1990) describe a procedure for the analysis of sulfides. They used 0.26–0.66 g of the sample, mixed that with 6.8 g of a 12 : 22 mixture of tetraborate to metaborate and 1.0 g of sodium nitrate, which was heated to 700 °C in a muffle furnace for 10 minutes with subsequent fusion at 1050 °C.

## 3.5 Liquid Samples

Liquid samples can be prepared in several ways. For instance, direct measurement of liquids is possible. Liquids can also be prepared by drying through evaporation of the solvents, by absorption, e.g. in cellulose or wax, by precipitation through a chemical reaction, or by filtration.

### 3.5.1 Direct Measurement of Liquids

For the direct measurement, the liquids are filled into special sample cups (see Figure 3.17). The sample cups are available in several styles, each one designed to

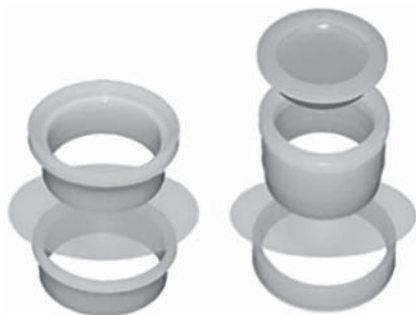


**Figure 3.17** Sample cup for the analysis of liquids. Source: Courtesy of Chemplex Industries, Inc.

fit the different types of instruments; they can have different sizes and can be used with or without a cover. They are made of polymers (PE, Teflon), which inherently are very clean, in order to avoid introducing any foreign measurement signal.

The cups are covered with polymer films, which must be pulled tightly onto the cup without any wrinkles; this is important in order to clearly define the distance between sample and spectrometer. On the one hand, the films should absorb the radiation as little as possible, i.e. they must be very thin and consist of elements with low atomic number. On the other hand, they must be stable against the liquids used. For the mostly organic solvents, this requires careful selection and testing before a measurement. It is therefore recommended to test the resistance of the window film of unknown samples, by filling the liquid into the sample cup and placing it on blotting paper for at least twice the measuring time. Thus, it can be verified whether the liquid reacts with the films or not. This is important in particular for wavelength-dispersive (WD) instruments; due to their high excitation intensity the thin films of the sample cup are thermally stressed. It is therefore essential to carry out these tests for WD spectrometers for a sufficiently long period.

This high excitation intensity of WDS instruments can also alter the sample, for example, by decomposition, which can then lead to generating bubbles in the liquid.

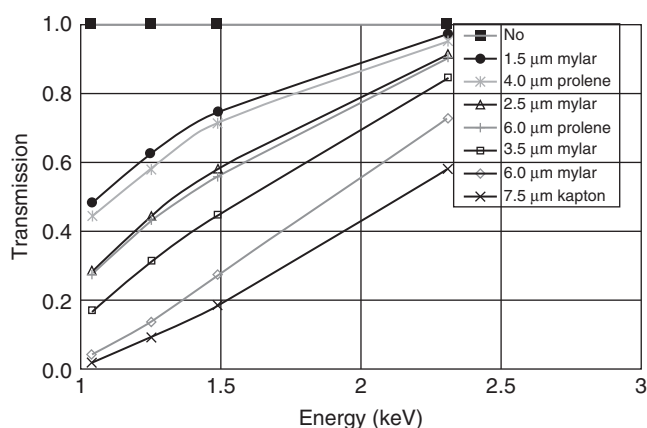
The samples should always be filled into the sample cups just before the measurement. For particularly aggressive solvents, it is also advisable to use a double film for covering the cup.

In the case of a defective foil, there is a high risk that the liquid enters the spectrometer, which then can lead to considerable damage, both by potential temperature shock to the X-ray tube and by contamination or reaction of the solvent with the spectrometer components.

Available window materials and their properties are summarized in Table 3.11. The transmission of low-energy radiation is shown in Figure 3.18 for different commonly used window materials. For light elements such as Na, Mg, or Al the transmission is fairly small, but for slightly higher energies, such as S, the transmission is already increased. However, this is not a real disadvantage because

**Table 3.11** Window materials for sample cups for liquid samples.

Material	Elements	Minimal thickness ( $\mu\text{m}$ )	Properties
Mylar (PET)	Hydrogen, carbon, oxygen	2.5	<ul style="list-style-type: none"> <li>• Very thin = &gt; small absorption</li> <li>• Low to no contaminations</li> <li>• Suitable for: aqueous solutions</li> <li>• Not suitable for aliphatic alcohols, alkaline solutions, ester, aromatic hydrocarbons, and ketones</li> <li>• Impurities of the film can have the following concentrations: Phosphorus – approx. 180 <math>\mu\text{g/g}</math>; calcium – approx. 45 <math>\mu\text{g/g}</math></li> </ul>
Polypropylene (PE)	Hydrogen, carbon	4	<ul style="list-style-type: none"> <li>• Small absorption due to light elements</li> <li>• Suitable: all organic solvents</li> <li>• Not suitable: aromatic and halogenated hydrocarbons, ketones, ether</li> <li>• Often contaminations from silicon, sulfur, or calcium</li> </ul>
Kapton	Hydrogen, carbon, nitrogen, oxygen	6	<ul style="list-style-type: none"> <li>• Stronger absorption due to heavier elements</li> <li>• High temperature resistance, high radiation resistance for continuous measurement</li> <li>• Suitable: aqueous solutions</li> </ul>

**Figure 3.18** Transmission of low-energy radiation of sample cup films.

liquids cannot be measured in vacuum, which means the radiation is absorbed also in air. In any case, the absorption in the different layers always has to be considered during analysis.

For highly volatile solutions, sample cups with a cover are offered to reduce the evaporation process (see right cup in Figure 3.17).

The preparation steps for liquids are generally determined by their state. In the case of a homogeneous liquid, the preparation is simple – the liquid can readily be filled into the sample cup and measured.

On the other hand, a multiphase liquid, having different densities, for example, can be homogenized by stirring or shaking. The measurement should then be carried out shortly after the homogenization in order to avoid a new segregation. Another possibility is the separation of the individual phases and their separate analysis.

If particulate material is suspended in liquid, homogenization by shaking and stirring is also required, in an ultrasonic bath, for example. The measurement should also be done quickly, in order to avoid new sedimentation. Another possibility is to filter the suspended particles in order to analyze the filtered particles and the liquid separately.

### 3.5.2 Special Processing Procedures for Liquid Samples

Various other preparation techniques are also being used for liquids. An increase in the detection sensitivity is obtained by drying up the solvent of a liquid dropped onto a sample carrier (see Sections 11.3.2 and 12.4.1). This method enriches the analytes, and at the same time reduces the spectral background, thereby increasing the analytical sensitivity.

Other possibilities are the transfer of a liquid directly into a quasi-solid body, for instance, by gel formation or by the absorption of the liquid in a porous material such as alumina or coal. The precipitation of solutes by a targeted chemical reaction and its recovery by filtering or the absorption of solutes and the analysis of the adsorbent is also possible. In all cases, depending on the composition of the primary material, the most favorable option and chemical reaction must be selected. To ensure sufficient analytical accuracy, test measurements on reference samples of known composition should be made, in order to determine parameters such as recovery rate and reproducibility before the actual analysis.

Some of the preparation procedures are described in connection with the corresponding applications in Chapter 11.

## 3.6 Biological Materials

Biological materials are generally inhomogeneous. For an analysis, it is therefore first necessary to decide whether these inhomogeneities are to be determined by the analysis or whether the mean composition of the sample is of interest and it therefore must be homogenized before the analysis.

If the inhomogeneities of the sample are to be recorded, the use of spatially resolved analyses techniques is required (see Section 4.3.3 for instrumentation, Chapter 13 for the measurement algorithms, and Chapter 16 for examples). The sample preparation for position-sensitive measurements depends on the texture of the primary materials. Solid materials, such as plant parts or bones, can directly

be analyzed in certain circumstances; alternatively, the samples are to be cut or ground in order to obtain flat surfaces for the analysis. In the case of tissues, it is possible to convert these into a solid sample by freeze drying, for example, or by preparing microsections for the analysis.

If, on the other hand, the primary material should be homogenized for the analysis, various preparation procedures are available, again depending on the sample state.

- For solid materials, such as wood or bone, direct analysis is possible if the samples are sufficiently large and not strongly structured. They can be polished and then directly analyzed.
- In the case of inhomogeneous solid samples, it is also possible to prepare pressed pellets. For this purpose, the material must be dried for several hours at 65–85 °C. Higher temperatures should be avoided to reduce the loss of easily volatile elements. After the material is crushed or cut (see Section 3.4.4), it can be pressed without binder, since it has low hardness and therefore produces stable pellets, where applicable also at elevated temperatures.
- Soft materials, such as human or animal tissues, should be first dried by heating or by freeze-drying. In this way, the prepared material can then be further processed by cutting or grinding and eventually pressed into pellets. If only a small amount of material is available, it is possible to press the sample into a binder tray (see Figure 3.10).
- Another possibility is the ashing of biological materials. For this purpose, the material is heated to temperatures above 900 °C under oxygen supply. Thus, all hydrocarbons escape from the sample, but also highly volatile elements such as P, S, and even important analytes such as As or Hg. The ashes can then be further processed like small-particle material, i.e. as pressed pellet or as a fusion bead.
- Another possibility to prepare tissue materials is to freeze them and then produce microsections. These can then be put on a sample carrier and analyzed. Glass slides as well as thin plastic films are suitable as sample carriers. Especially in the case of glass, care must be taken to ensure that the carrier material does not contain any analyte elements.
- Finally, biological fluids can be prepared for the analysis like other liquids. Examples of this are described in Section 12.4.3.

From this compilation, it becomes clear that a wide variety of preparation techniques for biological materials are available. Depending on the sample type as well as on the analytical targets, the most favorable option of sample preparation has to be selected. Like always, it is useful to carry out test preparations on comparable reference samples prior to the actual analysis in order to determine sensitivities and recovery rates.

### 3.7 Small Particles, Dust, and Aerosols

Dusts and aerosols are solid and liquid particles in the air, which occur in very different quantities depending on the location and the respective environmental

conditions. Usually they are only present in very small amounts in the range of 50–500 ng/m<sup>3</sup>. In order to achieve enough signal intensity an enrichment of the air components must be made by accumulation. This can be achieved by depositing the material from an air stream on filters or impactors. The filters can be analyzed directly. This means the preparation of dusts and aerosols already starts with the collection of the sample material and depends on the available amount, i.e. the collected material as well as the filters used. The amount of the collected material is determined by the amount of air throughput, i.e. the airflow and collection time.

Plastic films made of Teflon or polycarbonate (Nucleopore or Millipore) are often used as filters. The dust particles are deposited on these films. The filters do not contribute to the fluorescence signal but can increase the scattering background of the spectra if they are too thick. It is also important to ensure that the coverage is not too high in order to reduce the matrix interaction in the sample material and to allow a simple quantification. One should also keep in mind that larger particles do not adhere well to the filters.

Occasionally, cellulose or glass fiber filters are used. The collected particles and aerosols penetrate into these filters. They have a higher absorption capacity, but the elements contained in the glassy filters can interfere with the measurement signal and influence the analytical result. Further, these filters are not suitable for quantification, since the penetration of the dust into the filter increases the effects of matrix interaction and cannot be sufficiently modeled. They can be used for qualitative analyses.

A further possibility for the deposition of aerosol particles is the use of impactors. In this case, the air stream is directed onto impact plates on which the particles stick. It is also possible to separate different particle sizes by the stepwise change in the airflow. The particles collected on the impact plates can be analyzed directly or transferred to other sample carriers.

The optimal collection techniques and filter materials depend very much on the respective analytical problem and must be selected by appropriate tests. Some examples for the collection and preparation of dusts at different loads and with various analytical objectives are discussed in Section 10.10.1.

Small single particles can be positioned on a sample holder and fixed with a material that does not contain any of the analyte elements – selected hair sprays have produced good result – the small particle can also be embedded in suitable backing material. The final preparation strongly depends on the sample material, its size, and the analytical task. A few applications are described in Chapter 15.

## 4

### XRF Instrument Types

#### 4.1 General Design of an X-ray Spectrometer

Independent of the particular task, X-ray spectrometers always consist of the following components:

- The excitation source
- The sample to be analyzed, if necessary, with a sample positioning system
- A dispersing element, the actual spectrometer

The design of the individual components can vary greatly depending on the targeted application of the instrument. Usually, other assemblies are also required for the operation of the instrument, such as the following:

- Components to produce high voltages for the X-ray tube and the detector as well as for supplying the electronics
- Optic components for beam guidance and/or for influencing the spectral energy distribution of the incident radiation (primary optics) as well as the fluorescence radiation (secondary optics)
- Assemblies for shielding the X-ray radiation or for protecting the components against external interference and for the creation of a specific measurement environment (e.g. vacuum, helium purge, air)
- Modules for controlling the instrument as well as for recording and evaluating the measurement data

The geometry between the main components of an X-ray spectrometer, i.e. between excitation source, sample, and spectrometer, influences the analytical performance.

The essential differentiation of the instruments takes place by the type of dispersion of the fluorescence spectrum – this is the distinction between wavelength-dispersive spectrometers (WDSs) and energy-dispersive spectrometers (EDSs).

In the case of WDS instruments, the dispersion of the fluorescence radiation is carried out by Bragg diffraction on a periodic structure – usually a crystal lattice or for larger wavelengths (lower energies) also synthetically generated multilayer structures.

According to Bragg's equation

$$n \cdot \lambda = 2 \cdot d \cdot \sin \Theta \quad (4.1)$$

with

- $\lambda$  the wavelength of the diffracted radiation
- $n$  order of diffraction
- $d$  lattice spacing of the structure
- $\Theta$  angle of diffraction

The radiation of wavelength  $\lambda$  (or of the energy  $E$  (keV) = 1.24/ $\lambda$  (nm)) is only diffracted at the angle  $\Theta$ . A diffraction of the radiation is possible at different diffraction orders  $n$ . With every higher diffraction order the diffracted intensities are reduced by a factor of about 3. Therefore, first order of diffraction is usually used for analysis; higher orders of diffraction however can lead to interfering peak overlaps.

The discoveries of Laue and coworkers that X-ray radiation is diffracted at periodic grids (Friedrich et al. 1912) and by father and son Bragg that this property can be used for determining the energy composition of the radiation (Bragg and Bragg 1913) formed the basis for wavelength-dispersive (WD) spectrometry. They served as the fundamentals of wavelength-dispersive spectrometry, which was the only routinely used method of X-ray spectrometry for many years.

In WDS instruments, usually a parallel beam of the emitted fluorescence radiation, selected by means of collimators, is directed to the analyzer crystal at the incidence angle  $\Theta$ . If a radiation detector is brought to a position that corresponds to the diffraction angle, the Bragg-reflected radiation can be detected, and its intensity can be determined. By simultaneous variation of the angle of incidence and the angle of diffraction, a certain spectral region can be scanned sequentially. For this purpose, when the angle of incidence changes by  $\Delta\Theta$ , the diffraction angle must change by  $2 \cdot \Delta\Theta$ , i.e. the angular changes must take place at different speeds. If the diffracted intensity increases for energies corresponding to the fluorescence radiation of a specific element, the presence of this element in the examined sample is indicated.

The wavelength range (or energy range) that can be covered depends on the lattice constant  $d$  of the analyzer crystal. The largest wavelength (smallest energy) is reached for  $\Theta = 90^\circ$ . Crystals with larger lattice constants are required for larger wavelengths (smaller energies). If no natural crystals with such lattice constants are available, synthetic structures such as multilayer structures or synthetic crystals can also be used.

The diffraction angle must be smaller for smaller wavelengths (i.e. higher energies) of the examined radiation. No physical limits are set thereby for use, but the resolution decreases with decreasing diffraction angles, thus limiting the usability of a crystal.

For the detection of the radiation, simple counters are used, e.g. proportional counters or scintillation counters. These detectors can manage high count rates, i.e. they can detect high intensities. As a result, very small statistical measurement errors are achievable, which is ultimately the precondition for the achievable high accuracies attainable by X-ray spectrometry. The detection efficiency of these detectors is discussed in more detail in Section 4.2.3.



In EDS instruments, the radiation is dispersed in the detector. Here, the polychromatic beam coming from the sample directly interacts with the detector material. Each absorbed X-ray quantum is converted into a signal proportional to its energy, which can then be subjected to pulse-height analysis after appropriate amplification and filtering. This means that the measurement is quasi-simultaneous for a wide spectral range. The distribution of the heights of the collected pulses is an image of the energy distribution of the measured radiation, i.e. it corresponds to the spectrum emitted by the sample. However, by this detection process, the resolution, i.e. the ability for separation of neighboring element lines, is less than in the WDS method. This is mainly attributable to the very small primary signal generated by the absorption of only a single X-ray photon. By means of high amplification, these signals must be converted into a measurable range; however, the noise is also amplified and superimposes the signal. For the suppression of noise, filter techniques that require the availability of very low noise electronics are used. For this reason, (ED) X-ray spectrometry was not developed until the 1960s.

By developing better detectors and the use of special measuring geometries, the application range that can be covered by EDS instruments has constantly been expanded. This was accompanied by a continuous increase in the importance of ED X-ray spectrometry.

## 4.2 Comparison of Wavelength- and Energy-Dispersive X-Ray Spectrometers

A comparison of the most important properties of WDS and EDS X-ray spectrometers is given in Table 4.1.

The properties of the two methods will be discussed in more detail in the following sections.

### 4.2.1 Data Acquisition

For WDS instruments, the sampling of the spectrum must be carried out sequentially, i.e. the individual spectral regions must be adjusted by changing the Bragg angle. This means that a complete spectrum can only be acquired by a time-consuming scan. Time saving is possible by the so-called peak hopping; in this case, only the fluorescence intensities of the different elements are measured in the peak maximum. The determination of the spectral background requires separate measuring points. This method is suitable only for samples with known compositions; otherwise, unexpected elements could be overlooked in the case of peak hopping for unknown samples. The measuring times for the individual measuring points in WDS can be adapted for comparable statistics. They add up and result in relatively long overall measuring times. Therefore, multichannel instruments have been developed for very fast analyses, in which a separate spectrometer with a fixed Bragg angle is available for each element of interest and if necessary, also for individual background positions. However, this is associated with a considerable amount of mechanical effort in the instrument design.

**Table 4.1** Comparison of wavelength- and energy-dispersive X-ray spectrometer properties.

WDS	EDS
Complete spectrum requires scan, i.e. sequential measurement	Complete spectrum by simultaneous measurement
Simultaneous measurements only by use of several spectrometers on the same sample (multichannel instruments)	
Spectral resolution in the range of 10 eV, can be adapted by the selection of crystal and collimator	Spectral resolution in the range of 130 eV, depends on the detector, counting rate, and energy
High count capability up to 1000 kcps	Counting rate depends on the detector 2 to >400 kcps
Low radiation flux by collection radiation from a small solid angle (collimation) of the sample radiation $\Rightarrow$ high excitation intensity required	High radiation flux by large solid angle (short distances) between sample and detector and large sensitive area of the detector $\Rightarrow$ low excitation intensity sufficient ( $\approx$ reduced by a factor of approx. 100 in comparison to WDS)
Reflections of higher order can provoke peak overlaps	Detector artifacts (escape peak, sum peak) superpose the sample spectrum
Extensive mechanics due to synchronous and precise movement of analyzer crystal and detector	Low mechanical effort, only for sample positioning
Preferentially used for quantitative analyses	Used for both qualitative and quantitative analyses
Relative high effort in setting up measurement methods	Easy handling due to little setting parameters

EDSs acquire a large spectral range simultaneously, i.e. both the characteristic lines of present elements and the spectral background. This improves the determination of peak intensities and reduces the measuring times. For certain instruments, it is possible to select different measuring conditions for the optimal excitation of different element groups in certain energy ranges.

## 4.2.2 Resolution

### 4.2.2.1 Comparison of Wavelength- and Energy-Dispersive Spectrometry

The energy resolutions of the two spectrometer types, each with different crystals or detectors, are compared in Figure 4.1. WDSs show a significantly better resolution at low energies (large wavelengths). At higher energies, this difference becomes smaller and reverses at energies of approximately 15–20 keV. This means that, especially for light elements with long-wavelength fluorescence radiation, WDS instruments have a better peak-to-background ratio and, therefore, are much more sensitive in this range. Another reason for this higher sensitivity in the low-energy range are much thinner windows of the respective detectors.

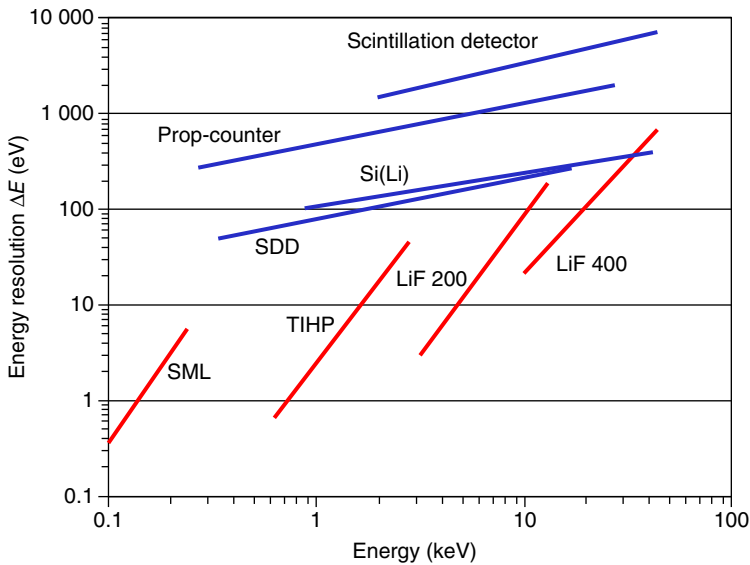


**Figure 4.1** Energy resolution of different ED spectrometer (blue) and WD spectrometer (red) arrangements (LiF, lithium fluoride; TIHP, thallium acid phthalate; SML, synthetic multilayer).

WDS instruments use detectors with extremely thin entry windows for the detection of radiation in the low-energy range. As a result, this radiation is only slightly attenuated by window absorption. These windows, however, are not gas-tight and therefore a continuous gas supply to the detectors is required.

For energy-dispersive detectors, the windows are usually thicker to maintain a certain atmosphere in the detector. For the usually used detectors, windows are made from beryllium. This limits the detection probability in the low-energy range, which goes not lower than to Sodium even in evacuated sample chambers. Nowadays new window materials like carbon (polymer-foils or Graphen), that can be prepared as thinner films, allow also the detection of even lower energies.

The effects that the different resolutions have on a spectrum are clearly demonstrated in Figure 4.2. It shows parts of the spectrum of stainless steel, measured by WDS and EDS.

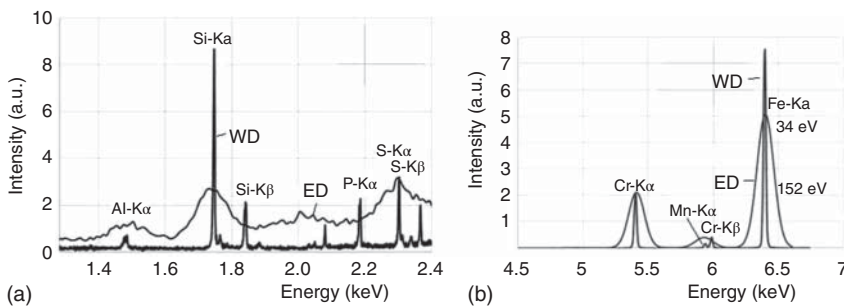


**Figure 4.2** Spectrum of stainless steel, measured by WDS and EDS: (a) low-energy range and (b) medium energy range.

each measured with a WDS and an EDS instrument. The comparison clearly shows that the peaks are narrower in the wavelength-dispersive spectrum and peak superpositions are much less pronounced, especially in the lower energy range (Figure 4.2a). In the middle-energy range (Figure 4.2b), these differences are less. As a result of the better resolution, the peaks are better separated and the peak-to-background ratio and thus the sensitivity are improved.

However, this also demonstrates that in the case of wavelength-dispersive measured spectra, the determination of the intensity in the peak maximum only is sufficient. Owing to the better resolution, most of the peak intensity is concentrated here. On the other hand, in the case of the broader energy-dispersive measured spectra, considering the entire peak area is appropriate since the statistical errors can then be reduced due to the larger pulse numbers.

The determination of peak intensities for both spectrometer types will be discussed in more in detail in Section 5.4.

#### 4.2.2.2 Resolution of WDS Instruments

The resolution in WDS instruments depends on the properties of the crystal used (i.e. its rocking curve) but also on the Bragg angle, i.e. from the crystal used. The dispersion can be derived from (4.1) as follows:

$$\Delta\Theta/\Delta\lambda = n/(2d \cdot \cos \Theta) \quad (4.2)$$

This means that the resolution of the spectrometer can be improved

- with the reflection order  $n$  (however, the intensity decreases by a factor of 3 with each reflection order);
- by increasing the Bragg angles  $\Theta$ ; or
- by a reduction of the lattice constants  $d$ .

Thus, the resolution can be influenced by the selection of the crystal or of the used lattice planes of a crystal. For identical crystals but different lattice planes, the lattice distance decreases with the sum of the Miller indices and the resolution increases for the same wavelength of the radiation; i.e. the crystal plane LiF 220 has a better resolution than the crystal plane LiF 200. On the other hand, the reflectivity decreases, since in higher indexed lattice planes there are fewer atoms and thus the number of scattering centers is decreased. This is shown in Figure 4.3a, which shows Fe- $K\alpha$  spectra measured with different crystal planes of a LiF crystal. The resolution is usually determined by the full width at half maximum (FWHM) of a peak, i.e. the width of the peak at half peak intensity. The FWHMs of the two lines shown in Figure 4.3a differ. For the LiF 200 it is 36 eV, while for the LiF 220 it is 29 eV, but also the intensities differ, here by a factor of approximately 2. As mentioned before, this means that a higher resolution is combined with a loss of intensity.

The improvement in resolution by a smaller lattice distance  $d$  is accompanied with a reduction of the wavelength range that can be acquired within a given Bragg angle range for same measuring conditions.

The longest wavelength detectable with a crystal is obtained for  $\Theta = 90^\circ$  according to (4.1). Larger wavelengths require crystals with a larger lattice spacing. The lattice spacings of natural crystals are no longer sufficient, especially

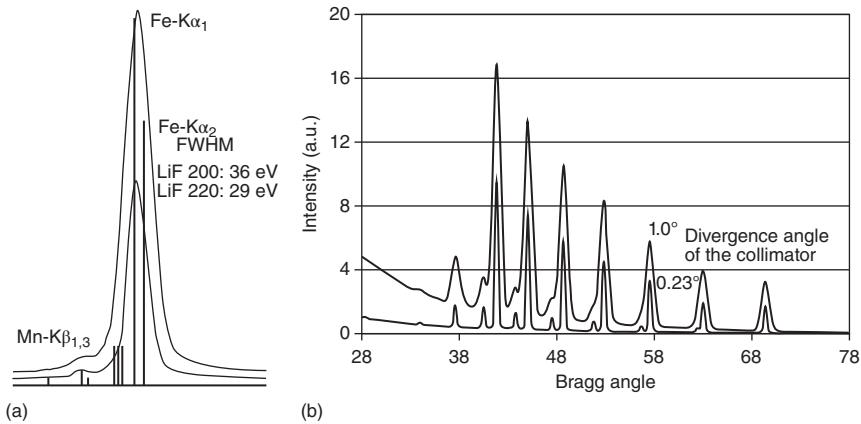


**Figure 4.3** Influence of the selected lattice plane (a) and the collimator size (b) on resolution.

for the long-wavelength (low-energy) lines. Consequently, organic crystals are often used. But they are not very stable, in particular their temperature stability is not good. Synthetic multilayer systems (SML), i.e. layer systems made from materials with different absorption properties, are another possibility; they were developed in the last 15–20 years. These can be optimized both by the elements used for the layers and by the layer thicknesses for a special analytic task.

Analyzer crystals can also be excited to fluorescence by the sample radiation. This isotropically emitted fluorescence superimposes with the measured spectrum and contributes to the spectral background. However, this contribution can be reduced by an electronic discrimination of the detector signals. Some typical crystals for WD spectrometry are listed in Table 4.2 with the elemental areas for their analysis.

**Table 4.2** Often used crystals for wavelength-dispersive spectrometry.

Crystal	2d (nm)	Reflectivity	Elements	Crystal fluorescence
LiF 420	0.1802	Medium	Ni–U	No
LiF 220	0.2848	High	V–U	No
LiF 200	0.4028	Very high	K–U	No
Ge 111	0.6532	High	P, S, Cl	Ge-L and Ge-K
Graphite	0.6715	Very high	P, S, Cl	No
InSb 111	0.7480	Very high	Si	In-L and Sb-L
PET 002	0.8742	High	Al, Si, Cl	No
ADP 101	1.064	Low	Mg	P-K
TIAP 1010	2.575	Medium	O–Mg	TI-M

Selecting an appropriate collimator size gives a further possibility to influence the resolution results in WDS instruments. With a smaller collimator the resolution can be improved since the divergence of the radiation striking the analyzer crystal is reduced. Nevertheless, here, again, the improvement of the resolution is associated with a decrease in intensity as seen on the right of Figure 4.3b.

#### 4.2.2.3 Resolution of EDS Instruments

The resolution of ED detectors is mainly determined by the type of detector used, but also by the energy of the detected radiation, as can be seen in Figure 4.1. Various types of detectors are available for EDS instruments. Proportional counters have the lowest resolution. Here, the FWHMs are about 1000 eV for Mn-K $\alpha$  radiation. For semiconductor detectors (PIN diodes, Si(Li) detectors or silicon drift detectors – SDDs) FWHMs from 200 eV down to 125 eV are achieved for the Mn-K $\alpha$  radiation. The resulting spectroscopic difference is evident from the two spectra of a gold alloy shown in Figure 4.4, measured with a proportional counter and an SDD.

With the proportional counter, the individual lines are not completely separated. This affects the correct identification of all elements but also the sensitivity. In most cases such detectors are only suited for quality monitoring in systems with a known qualitative composition. The spectrum measured with the SDD allows a clear identification of the individual peaks and guarantees higher sensitivity.

The resolution of EDS detectors consists of an energy-independent electronic noise contribution (ENC), which is largely determined by the electronics, as well as an energy-dependent component (4.3).

$$\Delta E = \sqrt{\text{ENC}^2 + 2.35^2 \cdot E \cdot F \cdot \epsilon} \quad (4.3)$$

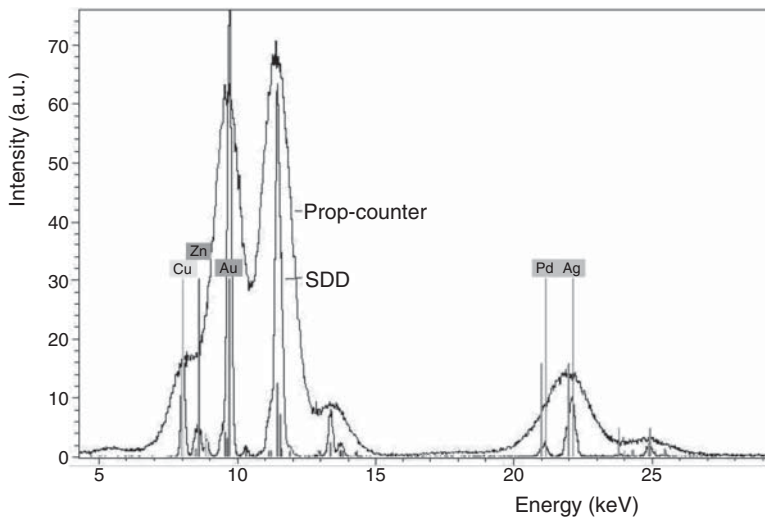


Figure 4.4 Spectra of a gold alloy measured with a proportional counter and an SDD.

with

$\Delta E$	FWHM of the peak
ENC	electronic noise contribution
$E$	energy of the detected radiation
$F$	Fano factor of the detector
$\varepsilon$	energy for generating a primary event

The energy  $\varepsilon$  for the generation of a primary event has an essential influence on the energy resolution. For proportional counters, this is the ionization energy of the counting gas. It depends on the counting gas and has the following values: Ne: 22 eV; Ar: 18 eV; Kr: 15 eV. In the case of semiconductor detectors, it is the energy required for the generation of an electron–hole pair by exciting a valence electron into the conduction band. It is about 2.7 eV for Si. Owing to this lower energy for the primary event, its number  $n = E/\varepsilon$  for semiconductor detectors is approximately 10 times higher than for proportional counters. This increases the number of registered events and, consequently, reduces the statistical error and improves the energy resolution.

The number of primary events is stochastically distributed; the variance  $\sigma_n^2$  of these events is described by the Fano factor  $F$  with  $\sigma_n^2 = F \cdot n$ . This factor describes the effectiveness of the generation of a primary event in the detector and depends on the material properties of the detector. For Si, the Fano factors are about 0.11.

The relationship given in (4.3) is shown in Figure 4.5. It can be seen that the ENC has an essential influence mainly on the resolution at low energies, whereas the influence is decreasing at higher energies. Particularly for the detection of low energies small ENC values are desirable. The ENC can be suppressed to below 40 eV for silicon-based detectors as Si(Li) and SDD.

In the case of electron beam-excited X-ray spectra this becomes important, since in this case the excitation of light elements is more effective. For the low-energy range the reduction of the ENC and the associated improvement

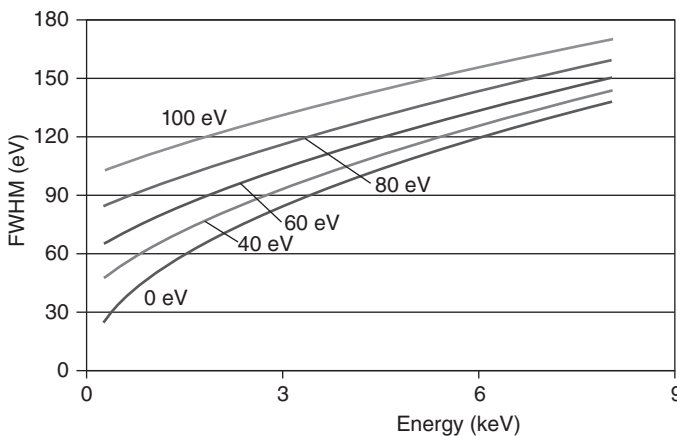


**Figure 4.5** Energy dependence of energy resolution of ED-detectors (FWHM, full width of half maximum).

in the resolution are equivalent to a reduction of the still detectable radiation energies since their signals must differ from the noise of the measuring channel.

### 4.2.3 Detection Efficiency

The detection efficiency, i.e. the probability to detect the photons depending on their energy, is determined by the absorption properties of the detector material but also influenced by the detector window.

In WDSs, prop-counters and scintillation counters are typically used to cover the complete energy range. Prop-counters are used for low energies. They can use different counting gases – Ar for the detection of lower energies and Xe for higher energies. In particular, Ar-filled detectors have typically very thin entrance windows to reduce the absorption of low energies. Because these windows are not completely vacuum-tight the counting gas has to be continuously refreshed by a special gas supply. Scintillation counters are used for the higher energies (see Figure 4.6).

In the past, both detectors were used in conjunction. In the former time prop-counter had windows both at the entrance and at the exit. High energetic radiation passing through the prop-counter could then be absorbed in the scintillation counter in a tandem arrangement. Nowadays, the detectors can be moved independently into the beam path.

As previously mentioned, both prop-counters and scintillation counters have a limited energy resolution, which is for prop-counters in the range of 1000 eV; for scintillation counters even worse. Nevertheless, this limited resolution is sufficient for the discrimination of lines of higher order. For that purpose, a discrimination of the pulse heights can be used in dependence of the energy of the analyte lines.

ED detectors have a higher detection efficiency than gas-filled detectors and scintillation counters in the medium energy range. Here, the efficiency is mainly determined by the absorption in the detector window. For higher energies the low absorption of the detector material – for ED-detectors it is mostly Si – is the limiting factor. Thicknesses of  $<500\ \mu\text{m}$  for SDD allow only a small sensitive volume. For the former usually used Si(Li) detectors the sensitive thickness was 3–5 mm (see Figure 4.7).

The low-energy behavior of the detectors is determined by the entrance windows. A light-element (LE) window has the best efficiency in the low-energy

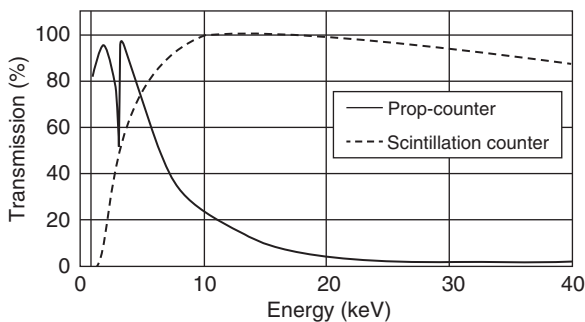
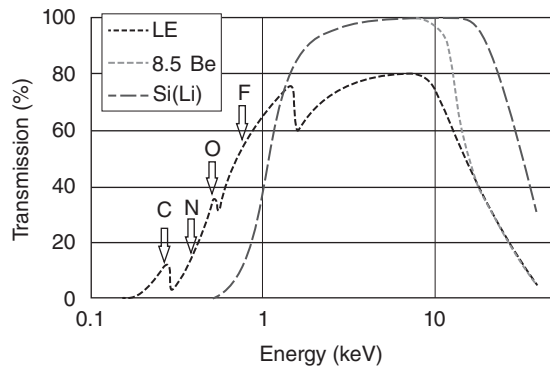


**Figure 4.6** Detection efficiency of prop-counter and scintillation counter.



**Figure 4.7** Detection efficiency of ED-detectors.



range, but does not reach 100% because the thin polymer film is supported by an Si grid of the same thickness as the SDD with 80% transmission. The Be windows of ED-detectors typically have a thickness of 8–12  $\mu\text{m}$  and have a higher absorption for low energies (see Figure 4.7). The thicker Si(Li) detectors have a better detection efficiency for high energies.

#### 4.2.4 Count Rate Capability

Since the measuring channels of WDS instruments have only the function of counting events, and no additional determination of the pulse height as in the case of ED systems is required, their count rate capability is significantly higher. This leads to higher number of acquired pulses and thus the statistical counting error can be reduced. However, this advantage is limited because the individual spectral ranges have to be recorded sequentially, as discussed in Section 4.2.1. The measurement times for every energy range therefore need to be added up. But they can be defined separately for the various measuring positions, i.e. for element and background positions to get comparable statistical errors.

The improvements in energy-dispersive detectors, in particular the signal electronics, continuously increased their count rate capability. The typical count rates of some  $10^3$  pulses for proportional counters and some  $10^4$  pulses for Si(Li) detectors are far exceeded by SDDs. Nowadays they can count up to  $10^6$  pulses which comes close to the capability of WDS instruments. EDS instruments are therefore increasingly an alternative to WDS with respect to the count-rate capability.

##### 4.2.4.1 Optimum Throughput in ED Spectrometers

The shaping time of the signal electronics influences the ENC and thus the energy resolution of the spectrometer, but also influences the pulse throughput of the detectors. This relationship is shown in Figure 4.8. It demonstrates that at low count rates, a widely complete registration of the incoming pulses occurs, but at higher count rates, the measurement channel is increasingly saturated. Pulses that are detected during the processing time of a previous pulse in the signal electronics are excluded from further processing; the measurement channel is “dead” during the shaping time. At a 63% dead time percentage the maximum throughput is reached. This maximum depends on the respective shaping time

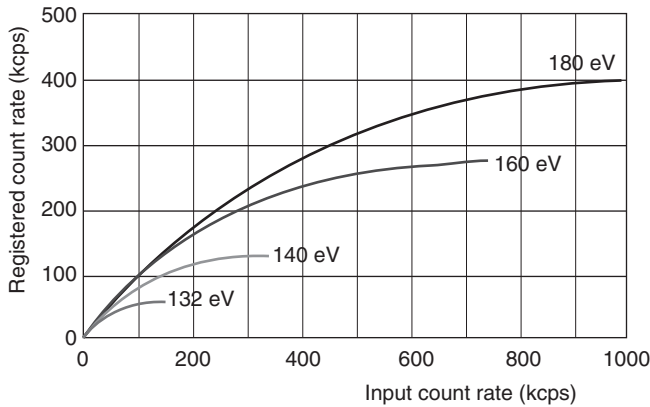


**Figure 4.8** Throughput of ED-detectors and their influence on the detector resolution.

of the detection electronics. As the length of the shaping time increases, the pulse throughput decreases, but at the same time the signal filtering and therefore the resolution (characterized by the displayed FWHM for Mn- $K\alpha$  radiation in Figure 4.8) are improved.

The influence of the dead times on the measured intensities has to be corrected, as shown in Eq. (5.3) (see Section 5.3.4). In order to keep the corresponding contribution to the measurement uncertainty small, it is recommended to work with up to 30% dead time for quantitative measurements; for qualitative measurements it can be up to 50%.

#### 4.2.4.2 Saturation Effects in WDSs

The counting rate capability of WDSs is generally much higher – counting rates over  $2 \times 10^6$  cps are possible. These high pulse rates are possible because in these instruments the dispersion is already occurring at the crystal and the absorbed photons only must be counted. Nevertheless, limits result from the collecting efficiency of the detectors. If the counting rates are too high, saturation effects can occur, which leads to distortions of the peak shape, as shown in Figure 4.9

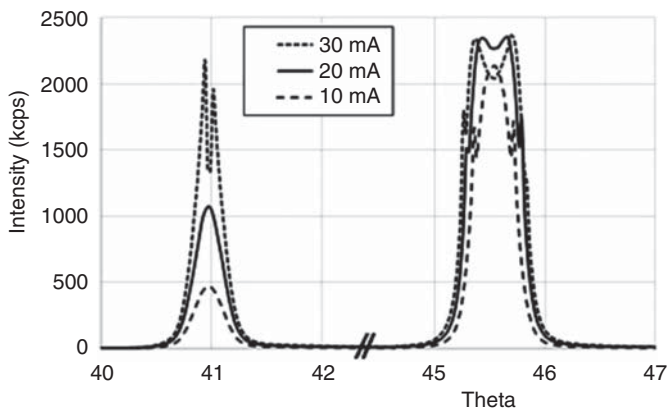


**Figure 4.9** Peak shape changes for very high count rates of WD spectrometers. Source: Courtesy of S. Hanning, FH Münster.

for a Cu sample. These measurements were carried out at 50 kV with different tube currents. It can be seen that only the spectrum measured at 10 mA (dotted line) is undisturbed. At higher tube powers, saturation effects occur, which can give highly false intensity values if the peak shape is not determined by a scan but determining only the peak maximum. It is therefore recommended to monitor the counting rates and, if necessary, to reduce the tube current in order to adjust the counting rates to the processing capacity of the electronics. In the case of multichannel instruments, the intensity needs to be adjusted to the highest intensity due to the simultaneous measurement of all elements; filters or collimators with different solid angles can be used to adjust the intensity for the individual elements.

#### 4.2.4.3 Optimal Sensitivity of ED Spectrometers

For the selection of optimal measuring conditions with EDS detectors, it is interesting whether an increase in the peak-to-background ratios required for an increase of sensitivity can be achieved either by an improvement in the resolution or by higher counting rates for a given measuring time. It should be noted that the improvements in the resolution due to different shaping times, which can be seen in the throughput curves in Figure 4.8, do not significantly improve the peak-to-background ratios. Higher pulse rates, on the other hand, which lead to higher pulse numbers at the same measurement times, have a much stronger influence on the peak-to-background ratio, as is demonstrated in Figure 4.10. These normalized spectra were calculated for counting rates of 1 and 100 kcps and one second measuring time for a Mn content of 5 wt% (Haschke et al. 2012).

It can be seen that the higher pulse throughput (red spectra) significantly reduces the statistical fluctuations and thus improves the peak-to-background ratios. A comparable result is not achieved by just improving the resolution, for example, by increasing the peak shaping time, which in addition limits the throughput. Selecting a detector with a smaller sensitive area and therefore a better resolution will also not have the desired effect because then the collection solid angle of the detected fluorescence radiation is reduced.

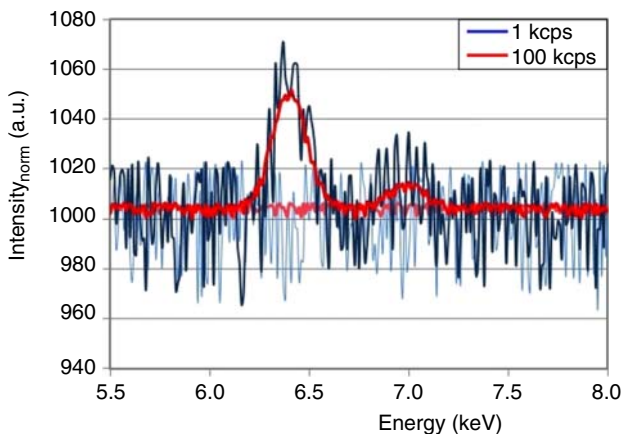


**Figure 4.10** Effect of the count rate on the peak-to-background ratios.

#### 4.2.4.4 Effect of the Pulse Throughput on the Measuring Time

When carrying out an analysis, often not only the achievable accuracy of the analysis is important, but also the time at which it can be achieved. The significantly improved count rate capability of SDDs has fundamentally changed this situation for ED-instruments because they not only allow for better instrument sensitivities, but one can also expect lower uncertainties in quantitative measurements due to the smaller statistical errors associated with higher count rates.

In the case of sequential WDS instruments, measuring times per measurement point (element or background position) are in the range of 5–10 s. In addition, the time necessary to adjust the correct angle and the electronic settings is a few seconds. The advantage of the sequential procedure is that the measurement times can be set individually for each element and background point; thus, the statistical errors can be matched as a function of the available count rate. In EDS the high pulse rate (up to 400 kcps) is distributed over the entire spectrum; however, usually only one or two different test conditions have to be set. Therefore, setup times are lower, and the entire analysis time can be used for the acquisition of a wide spectral range. Consequently, when measuring more than four to five elements modern EDS technology already has an advantage over the sequential acquisition.

Comparison to multichannel instruments results in the following situation. The maximum count rate capability for a WDS measuring channel is about twice as high as for an EDS instrument with SDD; however, the total count rate is collected on one element only, whereas in EDS instruments, the total count rate is dispersed over the entire acquired spectrum. Therefore, the count rate difference for each element at the same measuring time is about 30–50, but with the EDS instrument all elements are detected. This count rate difference can be partially compensated using multiple detectors whose spectra are added. The costs associated are still significantly lower than supplying several fixed WDS channels in one instrument.

Ultimately, it is also important to know what statistical uncertainties are still acceptable, especially since, in addition to errors from just counting, statistical influences of peak overlaps must also be considered in the calculation of peak intensities. Investigations were carried out on a multichannel spectrometer and an EDS instrument with two SDDs measuring the same stainless steel samples (Haschke et al. 2016), using standard deviations from repeated measurements (see Section 6.1.1). They show the following:

- The full tube power of multichannel instruments is often not usable in order to avoid saturation effects for elements with high concentrations and high excitation efficiency (in this case Fe). As a result of the simultaneous measurement, this affects all other elements to be measured.
- The number of counts collected in the same measuring time differs only by a factor of 3–5.
- For both analytical methods the relative standard deviations for the main components at 20 s acquisition times are about 0.1% – for the WDS measurements they are slightly smaller because of the higher count rates. Nevertheless, these statistical errors for both methods are sufficient for highly accurate analyses.

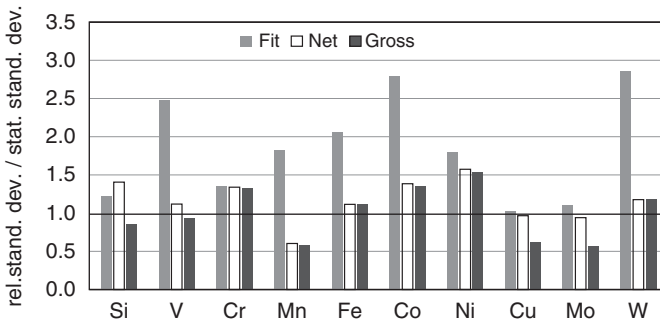


**Figure 4.11** Comparison of the ratios of the relative standard deviation (rel. stand. dev.) to the statistical error (stat. stand. dev.) in the peak area determination from gross and net intensities and from a peak fit.

- The method of peak area determination (gross intensities, net intensities due to background subtraction, and fitting of theoretical peaks) has an impact on the measurement uncertainties. Figure 4.11 shows the ratios of the relative standard deviation from the repeated measurements to the statistical standard deviations. These ratios show the increase in total uncertainty related to the unavoidable statistical error. At low peak overlaps (here, for example, Si, Cr, Ni, Mo), the values are comparable and are all close to or even less than 1. For elements with peak overlays (Mn and Cr, Fe and Mn, Co and Fe, W and Ni), an additional error contribution from the peak fitting has to be taken into account. It remains to be investigated to what extent gross intensities from EDS spectra can be used despite the stronger peak superposition in order to avoid this additional error contribution.

#### 4.2.5 Radiation Flux

A significant difference, which also affects the entire setup of the X-ray spectrometer, is the different radiation flux of the instruments. In a WDS instrument, only a small solid angle of the fluorescence radiation can be utilized, in order to guarantee high-resolution of the instruments through the reflection of a parallel beam. In addition, the acceptance angle of the primary collimator is limited. Furthermore, the reflectivity of the analyzer crystals or SML is in the order of  $<0.3$ , which limits the detected intensity further. To produce a sufficient fluorescence intensity the excitation intensities in a WDS instrument must therefore be relatively high. Tubes with outputs in the range of 1–4 kW are typically used for WDS instruments. These X-ray tubes require intensive cooling – in X-ray tubes only approximately 1% of the energy is converted into X-rays, and the rest has to be dissipated as heat – but also a complex radiation shielding to protect the operators. Further, this intensive irradiation can affect the sample.

The setup of EDS instruments, on the other hand, allows the detector to be positioned closely in front of the sample and a very large solid angle of the radiation can be detected. The difference between the acceptance angles of the two instrument types is typically 2 orders of magnitude. In addition,

the radiation emanating from the samples is almost completely absorbed in an energy-dispersive detector. Therefore, ED systems require much lower excitation intensities. Mostly they range within 50 W or even less and are therefore about 2 orders of magnitude smaller than in WDS, which the solid angles being larger. Air cooling for these tubes is sufficient, which considerably reduces the instrument design effort.

#### 4.2.6 Spectra Artifacts

Analytical lines can be superimposed by line-like artifacts. In the case of WDS instrument, these are mainly reflections of higher order. The Bragg equation (4.1) is then fulfilled for  $n > 1$ . Since the product  $n \cdot \lambda$  must remain the same, for  $n = 2$  the wavelength of the reflected radiation either has to be halved or its energy has to be doubled. The intensity of the reflected radiation decreases by a factor of approximately 3 with each order of reflection. Higher order lines can be recognized and eliminated by a pulse height discriminator that monitors and selects the correct pulse heights only. This is possible even with the low resolution of the detectors used in WDSs.

In the case of EDSs, other line artifacts occur, which must be taken into account in the evaluation of the spectrum. The following artifacts are discussed in detail.

##### 4.2.6.1 Escape Peaks

Escape peaks are produced by absorption of an incident X-ray photon by the detector material, generating fluorescence of the detector material itself. If this fluorescence photon “escapes” the detector its energy cannot be converted into charge carriers. The actual energy absorbed in the detector is then reduced by the energy of the fluorescence radiation of the detector material, resulting in a peak shifted by the energy of the fluorescence line of the detector material to the lower energy side of the originating peak. The probability of such an event depends on the energy of the absorbed radiation (van Espen et al. 1980). If the energy is high, the probable location for the absorption is deeper in the detector and the fluorescence radiation of the detector is reabsorbed within the detector. In the case of Si detectors, the escape peak probability for P-radiation is approximately 1.5% and decreases to negligible values for Zn. This escape process is shown in Figure 4.13 and is well understood. The instrument software at least can display the position of the escape peak or even better, directly correct these artifacts.

A similar escape effect generates a continuous background by the escape of Auger-electrons. Auger electrons are emitted when an excited atom goes into the ground state and the energy is transferred to an outer electron. However, the probability for this effect is very low due to the strong absorption of the low-energy electrons in the detector material. Therefore this effect only occurs close to the entrance window of the detector where parts of the generated electron-hole pairs are directly recombined at the entrance window itself.

The escape of a scattered Compton electron also reduces the absorbed energy in the detector. But in this case, a continuous artifact is produced in the low-energy range of the spectra because the energy loss depends on the scatter angle and can have different values. The probability for this effect is greater for higher energies

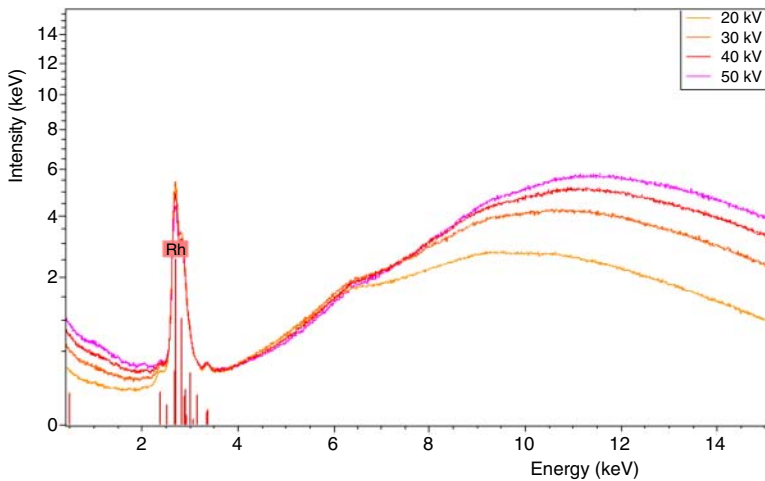


**Figure 4.12** Low-energy spectral background due to a Compton-induced escape effect ( $y$ -axis in square root scale).

of the incident radiation due to the increased Compton probability and is shown in Figure 4.12. It is described by Scholze and Procop (2009). The effect reduces the peak-to-background ratio for low-energy fluorescence radiation. Consequently, for the trace analysis of light elements lower excitation voltages are preferred.

#### 4.2.6.2 Pile-Up Peak

Pulses registered with very short time differences are recognized by the signal electronics and are rejected in order to prevent a pile-up of the second pulse on top of the first. The corresponding “closing” of the measuring channel is the reason for the dead time of the measuring channel. However, if the time interval between two X-ray photons is too short to be recognized as two separate pulses, the photons that are being absorbed almost simultaneously are added together. This then simulates a photon with the summed energy of the two individual photons. The probability of such an event increases with the excitation intensity. It will only be noticeable for the various combinations of the most intense lines of a spectrum. Pile-up lines can be identified by a lower tube current and the representation as current-normalized counting rates (see Section 5.4.1). Their positions are often identified by the instrument software, and corrected by most of them.

An example of escape and sum peaks is shown in Figure 4.13 for a Ti-spectrum. The Escape peak is superimposed onto the scattered Rh-L radiation of the X-ray tube and the Ti-K sum peaks occur with the line energy doubled. They would superimpose with the L-radiation of Hf or Os.

#### 4.2.6.3 Diffraction Peaks

Crystalline samples can diffract selected energies of the polychromatic incident spectrum in the direction of the detector according to the Bragg equation.

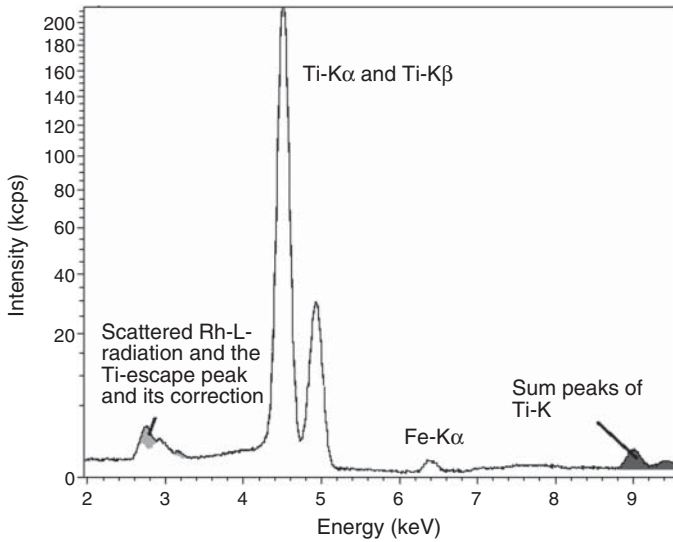


**Figure 4.13** Escape and pile-up peak of Ti radiation (y-axis in square root scale).

Depending on the diffraction plane of the crystal, different energies are diffracted, which leads to varying peak positions in the spectrum but also different peak shapes. For polycrystalline material this effect can be neglected in case of the examination of large sample areas (>10 mm) because every crystallite reflects another energy, however, for position sensitive analysis Bragg reflections are important because the complete excitation intensity is concentrated to a small sample area. Identification of the diffraction peaks can be made from their peak position (non-table positions or incomplete line series), by a mismatch of the FWHM of the peak or their non-Gaussian peak shape.

By changing the sample position, it is also possible to influence the position or shape of the diffraction peak in some lattice symmetries. However, these

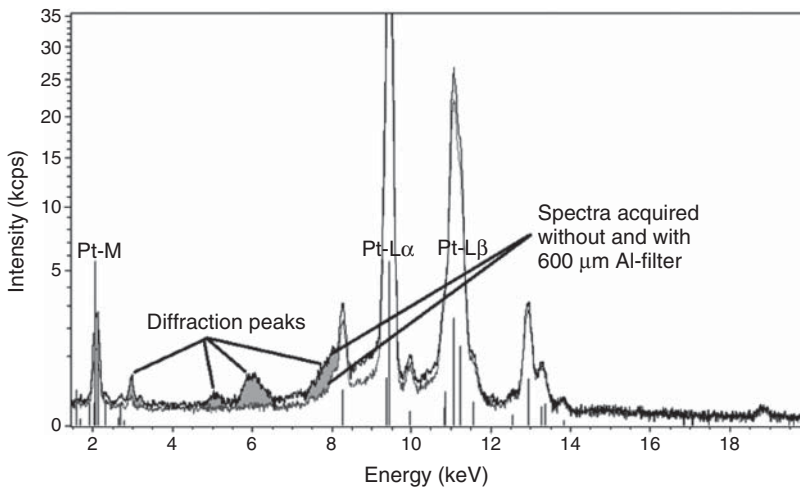


**Figure 4.14** Pt spectrum measured without and with Al filter (y-axis in square root scale).



techniques do not help in the case of their superposition with analyte lines. In this case, elimination of parts of the primary spectrum with a filter can be helpful simply because any eliminated part of the polychromatic excitation radiation cannot be Bragg-reflected. This is demonstrated in Figure 4.14, showing the spectra of pure Pt, measured without a filter and with a 600  $\mu\text{m}$  Al filter. Nevertheless, with the filter the fluorescence intensity of light element will be reduced because of the lower excitation intensity in this energy range.

#### 4.2.6.4 Shelf and Tail

Incomplete charge carrier collection in semiconductor detectors caused by a continuous escape effect (shelf) or by incomplete formation of the charge carrier cloud by absorption of the detected radiation near the detector window (tail) produces nonlinear, but describable and hence also correctable spectral contributions occurring in front of each measured peak. For Cu, these artifacts are shown in Figure 4.15. They are also described by Scholze and Procop (2009) and Wolff et al. (2018).

#### 4.2.7 Mechanical Design and Operating Costs

Finally, the mechanical effort for a precise adjustment of the angular position of the crystal and the detector in WDS instruments cannot be underestimated. Even if there are sufficiently precise and reliable mechanical solutions, the costs of precision mechanics and the service requirements for these are significantly higher than for just electronic systems. For EDS instruments, only the sample positioning needs a mechanical solution; in most cases, relatively low accuracies are sufficient.

Additionally, operating costs vary for the two types of instruments; they result from the previously described separate energy requirements and the additional water cooling required for the WDS units. The supply of counting gas in WD systems is an additional cost factor.

In summary, the instrumental effort, and thus the costs as well as the space requirement for a WDS, are usually significantly higher than for an EDS.

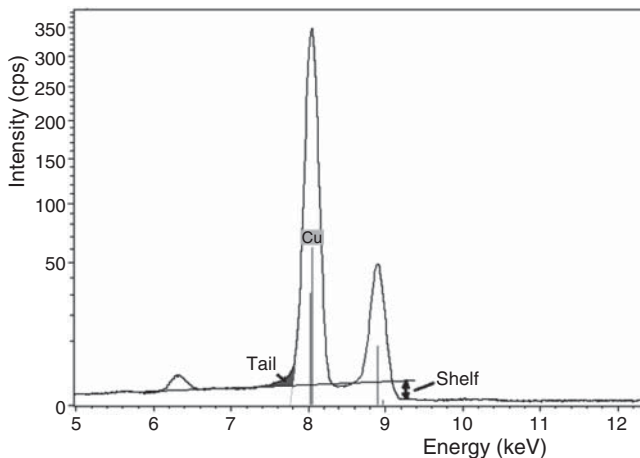


**Figure 4.15** Shelf and tail contributions to a Cu line (y-axis in square root scale).

**Table 4.3** Instrument setup parameters.

Instrument component	ED spectrometers	Sequential WD spectrometers
Excitation	Tube parameters (high voltage (HV), current, power) Target material given by the instrument If applicable: primary beam filter, secondary targets	Tube parameters (HV, current, power) Target material given by the instrument Primary beam filter
X-ray optics	Cylindrical collimator In case of position-sensitive instruments: limiting collimators of focusing optics	Slit collimators of different width in front of and behind the crystal, crystals, or SML
Detector	PIN, Si(Li), SDD (given by the instrument)	Flow counter, scintillation counter
Medium	Air, vacuum, He-flush (optional)	Vacuum, He-flush (optional)

However, higher analytical accuracy can be achieved with WDSs because of the higher count rate capability and better resolution at low energies. However, the accuracies cannot always be fully utilized, as the uncertainties associated with sampling and preparation are often significantly greater. Furthermore, the analytical advantages of WDS spectrometry are more and more overcome and compensated by improved ED system modules, special excitation geometries, and data processing methods. In particular, the high flexibility of EDSs is the main reason for their constantly increasing field of application.

#### 4.2.8 Setting Parameters

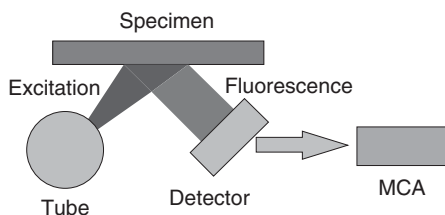
The number of parameters that must be set up for a measurement vary between WDS and EDS spectrometers. Consequently, the effort for preparing of a measurement and the required operator skills vary greatly. The following parameters have to be selected for the two methods (Table 4.3).

### 4.3 Type of Instruments

The final design of X-ray spectrometers and their main and subcomponents essential for the operation of an X-ray spectrometer depend strongly on the analytical goal. The following questions are important:

- Which materials are to be analyzed
- Can the sample be transferred to the instrument or is it necessary to carry out the analyses on site
- Which elements and concentration range need to be covered
- Which analytical accuracy is required and how much time is available for the analysis

**Figure 4.16** Principle layout of EDS instruments (MCA, multichannel analyzer).



The answers to these questions lead to the selection of the most suitable instrument.

In general, the following instrument types are available. The separating lines between the instrument types are not strictly drawn – some instruments can easily overlap in their use.

#### 4.3.1 ED Instruments

The principle layout of ED instruments is illustrated in Figure 4.16:

The general properties of EDSs can be characterized as follows:

- The sample is irradiated with the tube radiation. Sometimes, primary optics (collimators, filters or optical elements) are used for an optimization of the beam.
- The complete sample radiation (characteristic lines and scattered tube radiation) is detected by an energy-dispersive detector and transferred into a spectrum by pulse height analysis in the multichannel analyzer.
- The fluorescence spectrum is captured by energy-dispersive detectors, which means the resolution is limited and depends on the detector used.

- Proportional counters have a resolution of approximately 1000 eV. Consequently, no qualitative analysis of samples of unknown composition is possible (see Figure 4.4). However, accurate analyses are possible when the elements in the samples are known, for example, for quality control in production. In this case, the fluorescence intensities of overlapping peaks can easily be determined by well-established fitting procedures.

The reduced signal-to-noise ratio due to the lower resolution of the detectors and thus a reduced sensitivity for trace analysis is another limitation. Further, proportional counters also have a limited count rate capability.

- If, on the other hand, semiconductor detectors are used, the energy resolution is generally improved to less than 140 eV; as a result, the capability to separate individual lines is significantly enhanced. This also allows the analysis of samples of unknown composition. The improved signal-to-noise ratios compared to proportional counters also increases the sensitivity for the trace elemental analyses.

Various semiconductor detectors are available for X-ray spectrometry – in the beginning, Si(Li)s cooled with liquid nitrogen to reduce electronic noise were used. Then PIN diodes and nowadays SDDs are being used; they only require cooling with Peltier elements and are therefore easier to operate. Especially the count rate tolerances of SDDs are very high, reaching up to

- a few hundred kcps. On the other hand, these detectors are relatively thin and therefore have limited detection efficiency for higher energy radiation.
- EDSs do not require high excitation intensities due to their large captured solid angle. Therefore tube power can be below 50 W and air-cooling is sufficient, and if necessary, it can be supported by a fan.
  - The low tube power and small detectors allow for a compact design with a small footprint.
  - The instruments are usually controlled by powerful computers, which are either integrated into the instrument design or externally connected.

In addition, the computer is used to acquire the measurement data as well as for performing their evaluation. Nowadays, the performance of the computers is more than sufficient for extensive spectra processing and sophisticated spectra displays.

Now, the instruments are highly flexible and can be used for the analysis of unknown materials. For quantification standard-based models as well as fundamental parameter models that do not require standards are used.

ED-instruments are available at different levels, which will be described more in detail in the following sections.

#### 4.3.1.1 Handheld Instruments

These instruments can be characterized as follows:

- Mobile operation, i.e. they can be used on-site to perform fast analyses without sampling and elaborate sample preparation.
- Special attention must be given to radiation shielding and operator protection because of the open beam design of these instruments. Typically they are equipped with sensors that check the contact placement of the instrument on the sample, controlling locking mechanisms as well as require two hand operation. These safety measures prevent the unintentional use of the spectrometer and are usually standard to comply with safety regulations.
- Handheld instruments are always energy-dispersive and have very short operating distances, usually less than 5 mm. Consequently, the excitation powers can be very small – 1–5 W is already sufficient. This allows operation for a full day with a rechargeable battery at a still reasonable instrument weight that allows for easy handling.
- The on-site measurement capability makes it difficult to evacuate the measuring volume. This restricts the light element sensitivity. On the other hand, the working distances are so small that the absorption of low-energy radiation in air is very low and therefore analyses even down to Al are possible.
- The analyzed area of the sample is a few millimeters in diameter; the exact positioning is often supported by a video camera. The relatively small area analyzed also allows for the examination of nonhomogeneous materials; however, an averaging of the composition in somewhat nonhomogeneous samples is limited due to the small analyzed volume.
- The small excited area also allows the analysis of irregularly shaped samples, since plane surfaces with diameters of a few millimeters can usually be found on most sample surfaces.

- The instruments are usually controlled by integrated minicomputers that do not allow extensive calculations for quantification. Further, the implemented screen is too small for a reasonable spectral interpretation, in particular for a detailed qualitative analysis. For this reason, these instruments are often used for the analysis of known material classes with standard-based quantification models, or the material class must be first determined by a so-called positive material identification (PMI) in order to carry out a standard-based quantification in the second step. When the measured spectrum is classified by means of library spectra the corresponding stored standard-based quantification for this material class can be used for the quantification.
- Handheld instruments are usually used for specific tasks. For a long time, the determination of lead in wall paints was such a task. In the meantime, the identification of alloys, both for scrap metals and material stored in inventories is common. Other common tasks are the determination of the composition of ores in minings, the determination of toxic elements in consumer goods as well as the analysis of valuable artifacts that cannot be removed from their location. In the latter case, often only data acquisition with the handheld unit is carried out on site; the data can then be evaluated on a computer after transferring the measurement data. As a result, more complex evaluation methods can be applied utilizing the higher computing performance.
- With the instrument weight usually of less than 3 kg they can be easily handled.

In general, it can be stated that in recent years the performance capabilities of handheld instruments have made significant progress, both due to the improvements in individual components, in particular excitation sources and detectors, and due to more powerful computing technology. This offers the possibility to use handheld instruments for more and more applications. An important advantage is the analysis on-site, which allows quick decisions and avoids the logistics of sampling, transporting to, and preparing the material to be analyzed at the laboratory.

On the other hand, on-site analysis also has serious disadvantages. The achievable accuracy is often reduced because the possibilities for sample preparation are limited, contamination cannot be avoided, and the sample positioning does not guarantee sufficient reproducibility.

Handheld instruments are offered by various manufacturers (see Section 4.4), partly customized to the specific analysis tasks. Some of them are shown in Figure 4.17 (for information on the manufacturers, see Table B.1).

#### 4.3.1.2 Portable Instruments

In order to avoid any problems associated with inaccurate sample positioning as well as the risk of radiation exposure by means of the open beam path, and nevertheless to enable on-site use, portable instruments were developed. The instruments utilize similar components as handheld instruments, however the beam path is protected by an enclosure. The sample can now be placed on a table and as a result longer measuring times are possible. At first, this was realized through a holder for a handheld instrument (see Figure 4.18c, FlexStand from Olympus), but then more and more instruments were developed with a fixed housing, still



**Figure 4.17** Handheld instruments from various manufacturers: (a) XL5, Thermo Fisher Inc., (b) S1 Titan, Bruker Nano GmbH, and (c) XSORT, Spectro Analytical Instruments GmbH. Source: Courtesy of Thermo Fisher Inc., Bruker Nano GmbH and Spectro Analytical Instruments GmbH.



**Figure 4.18** Portable instruments of different manufacturers: (a) FXL, Thermo Fisher Inc., (b) SpectroScout, Spectro Analytical Instruments GmbH, and (c) FlexStand, Olympus. Source: Courtesy of Analyticon Instruments GmbH, Spectro Analytical Instruments GmbH and Olympus.

portable with weights of up to 15 kg, allowing on-site operation with just a battery supply. The same statements regarding their applications and analytical capabilities apply as for handheld instruments. Examples are shown in Figure 4.18 (for information on the manufacturers, see Table B.1).

#### 4.3.1.3 Tabletop Instruments

These instruments can be characterized as follows:

- Excitation of a relatively large sample surface, usually with 20–30 mm diameter. For an accurate analysis, this requires a homogeneous and flat sample, which must be ensured by a corresponding sample preparation.
- The instruments always enclose the sample, and therefore radiation protection is guaranteed. Depending on the instrument, the sample chamber can be evacuated or equipped with a helium flush. As a result, the analysis of light elements, usually down to Mg or even Na, is possible. However, this demands the use of a semiconductor detector.

If the sample chamber is not equipped for the measurement of light elements, the lightest element that can be analyzed depends on the length of the air path of the fluorescence radiation. Usually, this limits the range to S and Ca.



**Figure 4.19** Various energy-dispersive spectrometers: (a) Epsilon 3, Panalytical BV, (b) S2 Puma, Bruker AXS GmbH, and (c) QuantX, Thermo Fisher Inc. Source: Courtesy of Panalytical BV, Bruker AXS GmbH and Thermo Fisher Inc.

- The control of the instruments, the monitoring of compliance with the conditions for radiation protection, as well as sample management are carried out all at once; this also opens up the possibility to automate the measurement procedures.

Flexible and fast analyses with good accuracy, now offered by EDS instruments, have constantly extended their application areas and grown their market shares over the past two decades. Not to forget the much lower instrument design effort compared to WDS instruments.

Today EDS are commonly used for applications in environmental protection, waste analytics, jewelry analysis, the determination of toxic elements in consumer goods, and many other tasks.

There is a wide variety of EDS instruments that are tailored to specific applications. Some of the bench top instruments for the analysis of solid and liquid samples are shown in Figure 4.19 (for information on the manufacturers, see Table B.1).

## 4.3.2 Wavelength-Dispersive Instruments

### 4.3.2.1 Sequential Spectrometers

The principle layout of wavelength-dispersive instruments is illustrated in Figure 4.20.

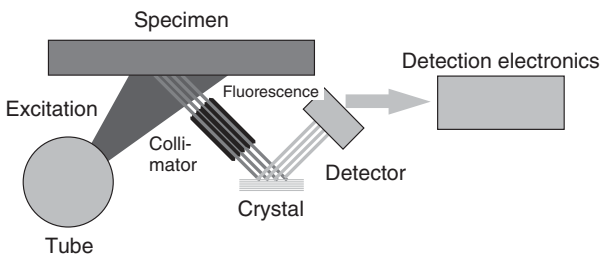


**Figure 4.20** Principle layout of WDS instruments.

Sequential WDS instruments can be characterized as follows:

- Similar to EDS instruments excitation takes place on a relatively large sample area, usually 20–40 mm in diameter. For an accurate analysis this requires the analyzed area to be flat and homogeneous, which can be achieved by suitable sample preparation.
- The dispersion of the fluorescence spectrum takes place on an analyzer crystal, which diffracted only the radiation of the energy fulfilling the Bragg equation (4.1). In order to cover different spectral regions, input and take-off angles on the crystal must be changed in an exact 1 : 2 ratio.  
In these spectrometers sequential sampling of the spectral range of interest is required. In order to achieve adequate energy resolution when covering a wide range of elements, it is necessary to change the analyzer crystal as well as the collimators.
- Owing to the low radiation flux of these instruments, which is a consequence of the small solid angle of the acquired sample radiation, high excitation power is required. It ranges between 1 and 4 kW. This results in higher expenses with respect to generating the tube power and its dissipation by cooling, commonly done by external water cooling. Radiation shielding as well as the additional space requirement add to the cost as well.
- The instrument is controlled by integrated or external computers; they perform the instrument control and safety monitoring, sample management, data acquisition, and data processing. Automation of the measurement procedures with WDS instruments is of course possible.
- The high precision of the analysis achievable with WDSs is a direct result of the high counting rates. To achieve comparable statistical errors for elements of different concentration the excitation conditions as well as measurement times can be accordingly adjusted.

This property as well as the good sensitivity of WDS instruments for the detection of light elements make these instruments especially interesting for their use in industry, where similar samples with short measuring times and high accuracies must be analyzed. The analyses accompanying production, for example, in metallurgy, in the cement industry, but also for the evaluation of minerals in the basic materials industry are typical applications for WDS.

The instrument performance of the most important suppliers differs only marginally. The key differences are in the software. Spectrometers of some manufacturers can be seen in Figure 4.21 (for information on the manufacturers, see Table B.1).

WDS instruments are equipped with a goniometer, i.e. with the ability to adjust the Bragg angle, which then enables a sequential sampling of certain spectral regions.

In most WDS as well as in EDS instruments the sample is irradiated from the bottom. In this case, the sample rests on a support and correct positioning is trusted by gravitation, independent of the sample thickness. However, this configuration has a disadvantage because parts from the sample can fall into the instrument and they can damage the tube window or the spectrometer.



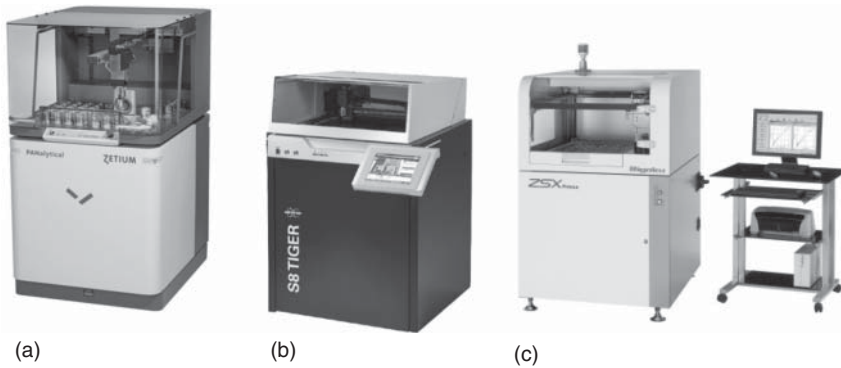


**Figure 4.21** A selection of wavelength-dispersive X-ray spectrometers: (a) Zetium, Panalytical B.V., (b) S8 Tiger, Bruker AXS GmbH, and (c) Primus, Rigaku Corp. Source: Courtesy of Panalytical B.V., Bruker AXS GmbH and Rigaku Corp.

#### 4.3.2.2 Multichannel Spectrometers

Multichannel spectrometers have the same principle layout as sequential instruments, but they have a separate spectrometer for every element to be analyzed. They can be characterized as follows:

- Simultaneous analysis of several elements, with every element to be analyzed in a separate spectrometer channel. Consequently, samples with only these elements can be analyzed. Background points would also require a separate spectrometer channel.
- Some multichannel instruments have an additional channel with an energy-dispersive detector to detect all other elements, at least to check that no unexpected elements are present.
- With such a spectrometer, very fast analyses are possible, however, only for a previously determined element spectrum and requiring a comparatively huge effort in instrument design.
- The simultaneous measurement of all analyte elements allows very short analysis times, but it is the same for all elements. Comparable statistical errors are possible by appropriate crystal–collimator combinations and by an adjustment of the measurement time.
- The instrumental effort for multichannel instruments is high; however, their flexibility for the analysis of various sample classes is very small.

Spectrometers of some manufacturers can be seen in Figure 4.22 (for information on the manufacturers, see Table B.1).

#### 4.3.3 Special Type X-Ray Spectrometers

In order to improve the analytical performance or to better match the instruments to specific analytical task, various special designs of the measurement geometry are used. The main goal usually is the improvement of sensitivity by increasing the signal-to-noise ratio.

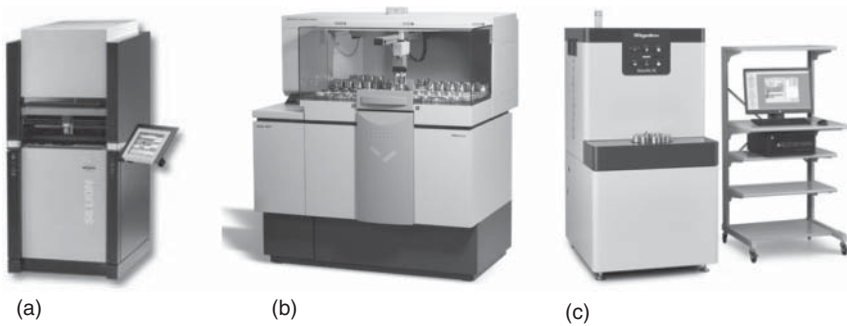


**Figure 4.22** A selection of multichannel X-ray spectrometers: (a) S8 Lion, Bruker AXS GmbH, (b) Axios, Panalytical B.V., and (c) Simultix 15, Rigaku Corp. Source: Courtesy of Bruker AXS GmbH, Panalytical B.V. and Rigaku Corp.

The most commonly used measurement geometry uses a  $90^\circ$  angle between the incident radiation to the sample and the take-off radiation to the detector. In this geometry, the scattering of the incident radiation on the sample is at its lowest (see Section 2.2.4) and thus leads to a good signal-to-noise ratio. The spectral background is essentially the result of the scattering of the tube radiation from the sample. This geometry is used in most of the instruments described so far.

Certain applications require the perpendicular incidence of the primary radiation to the sample surface. This is necessary for multichannel instruments (Section 4.3.2.2), in which several spectrometers are positioned at the same angle to the sample and, in the case of layer thickness measuring instruments in which sample positioning independent of the sample height is desirable.

It is also possible to influence the analytical performance using X-ray optics, which influences the primary radiation and thus can increase the sensitivity or enable a position-sensitive analysis.

Some of these options are discussed below.

#### 4.3.3.1 Total Reflection Instruments

The principle of total reflection X-ray fluorescence (TXRF) instruments is illustrated in Figure 4.23. Their essential principles are described in detail in DIN-51003, 2004-05 as well as by Klockenkämper and von Bohlen (2015).

In these instruments, the excitation results from a grazing incidence of the radiation. A very small sample amount is located on a very flat, usually polished, sample holder. Owing to the grazing incidence of the primary radiation with angles below  $0.5^\circ$ , the incident beam is totally reflected by the sample carrier and

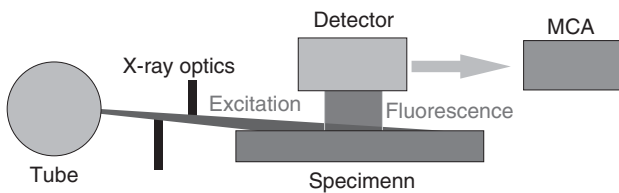


**Figure 4.23** Principle setup of a TXRF instrument (MCA, multichannel analyzer).

only the material on the sample holder is excited to fluorescence. The emitted radiation is recorded by an ED detector positioned close above the sample. As a result of the suppressed spectral background, this method results in a significant increase of sensitivity, which can be further improved when the primary radiation is monochromatized by primary beam optics. Detection limits in the lower microgram per kilogram range are readily achievable.

The analyzed sample amount however must be very low. It must be in the range of only a few micrograms. This can be considered as an advantage if only small sample quantities are available, but it requires special preparation procedures for assuring that the specimen is representative of a larger sample quantity. Possible methods are the digestion of solid materials and the evaporation of liquid drops on the flat sample carriers.

A further advantage of TXRF is the simple quantification. As a result of the very low sample masses, the matrix interaction is negligible so that the measured intensities are directly proportional to the mass fractions of the elements. In the case of liquid primary samples, the quantification can even be made independently of the analyzed sample amount by incorporating internal standards. This will be described in more detail in the section about the various quantification methods (see Section 5.5.2). Three commercially available TXRF instruments are shown in Figure 4.24 (for information on the manufacturers, see Table B.1).

TXRF is used for chemical analyses in the ultra-trace range and for the examination of the smallest sample amounts. Another area of application is the analysis of semiconductor wafers. In this case, the high sensitivity is suitable to detect the smallest amounts of surface contamination. By varying the incidence angle of the primary radiation even implantation profiles of semiconductor materials can be determined. These capabilities are also offered by the smaller laboratory instruments of the latest instrument generation. As a result, surface analysis on thin layer structures is possible (see also Section 4.3.3.8), where the radiation only penetrates into thin the surface layers of the material to be investigated.



**Figure 4.24** Total reflection X-ray spectrometers: (a) TXRF-310, Rigaku Corp., (b) S4 TStar, Bruker Nano GmbH, and (c) Nanohunter II, Rigaku Corp. Source: Courtesy of Rigaku Corp. and Bruker Nano GmbH.

The high sensitivity of TXRF requires an extremely clean working environment to avoid erroneous measurements potentially caused by contamination. Therefore, in this case the capability to automate the measurements is important. Some application examples of TXRF instruments are presented in Chapter 12.

#### 4.3.3.2 Excitation by Monoenergetic Radiation

If the excitation of X-ray fluorescence (XRF) results from monoenergetic radiation, only those elements whose absorption edges have lower energies than the monoenergetic radiation, and whose energy difference with respect to the excitation energy is not too large, are excited to fluoresce. Since there is only one excitation energy present, only this energy can be scattered by the sample, i.e. it cannot overlap with the fluorescence radiation of lower energies. In this way, similar to TXRF, an almost background-free spectrum is generated, thus enabling a high analytical sensitivity.

Monoenergetic incident radiation can be generated in various ways: first by excitation of an ultrapure material whose fluorescence radiation is then used for the excitation of the sample or secondly by the use of a monochromator between radiation source and sample, which allows only a small energy band of the polychromatic primary radiation to pass. However, in both cases significant losses in intensity are to be expected. Very narrow geometries, i.e. short working distances as well as the use of ED detectors, are necessary to compensate for this intensity loss.

The principle layout of an instrument with monochromatic excitation is illustrated in Figure 4.25.

An example of a sample excited with monoenergetic radiation is given in Figure 4.26; it shows the spectrum of an oil reference sample with about equal amounts of impurities of various elements. Despite the light matrix of the oil sample, the spectral background is very low due to the monoenergetic excitation. However, it can be easily seen that the fluorescence intensities decrease with increasing distance from the incident radiation even though the contents of the admixtures were about equal (500 mg/kg, each).

Both methods for generating monochromatic radiation, secondary targets as well as monochromators are utilized, for example, in the trace analysis of mineral oils, in the detection of toxic elements in toys, or in the investigation of traces in geological material. Monoenergetic excitation is helpful, if very low detection

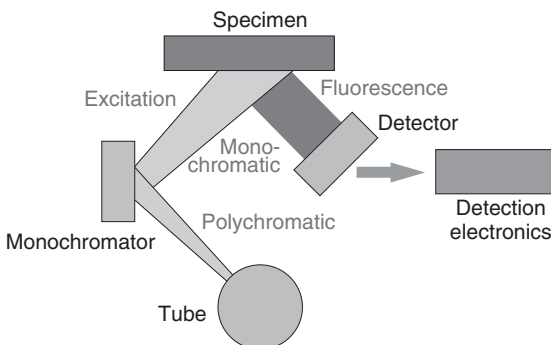


**Figure 4.25** Layout of an X-ray spectrometer with monoenergetic excitation.

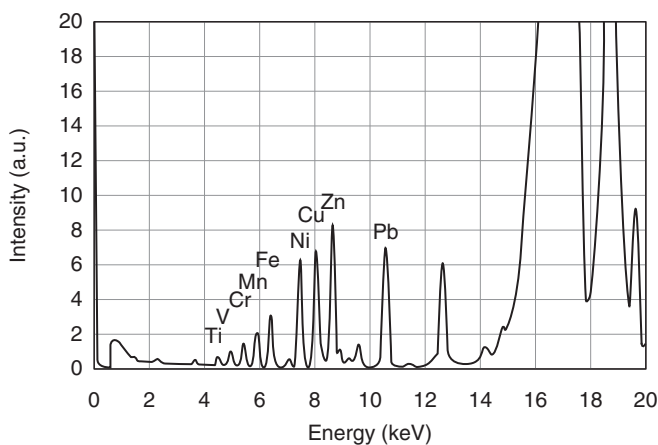


**Figure 4.26** Spectrum of an oil sample excited with Mo radiation. Source: Courtesy of Spectro Analytical Instruments GmbH.

limits of only a single element are required, specifically S in fuel oil, or if several elements have to be analyzed, such as different element groups in the analysis of geological materials.

#### 4.3.3.3 Excitation with Polarized Radiation

A further possibility to reduce the spectral background is utilizing polarized radiation for the excitation of the fluorescence. Polarized radiation will be scattered only in the polarization plane but not perpendicular to it. This means if the fluorescence radiation is measured perpendicular to the polarization plane, an improvement in the peak-to-background ratio can be expected. A reduction of the background intensity by a factor of 5–6 is possible. This reduction allows an improvement in the detection limits by a factor of 2. When detectors are used that are count-rate limited, as for example Si(Li) detectors, the effect is even larger, because, by reducing the spectral background, the percentage of relevant analytical radiation is increased in comparison to the scattered radiation.

Polarized radiation is generated in synchrotrons, but these are obviously not available as radiation sources for laboratory instruments. Another possibility is the scattering of non-polarized radiation at an angle of  $90^\circ$ . The scattered radiation is polarized in the scatter plane and can then be used for the excitation of the sample. The fluorescence radiation is then collected perpendicular to the polarization plane. This results in an orthogonal arrangement of the incident radiation, scattered radiation, and fluorescence radiation, as shown in Figure 4.27.

Light materials, such as boron carbide ( $B_4C$ ),  $Al_2O_3$ , or carbon in the form of highly oriented pyrolytic graphite (HOPG) are used as scattering targets, since their scattering efficiency is high. However, the loss of intensity is considerable; it is more than 2 orders of magnitude (Brumme ; Heckel et al. 1992; Heckel and Ryon 2002).

In the case of using HOPG, the Bragg-reflected L-radiation of a Pd or Rh tube can also be used for the excitation. Their Bragg angle is close to  $45^\circ$ , which

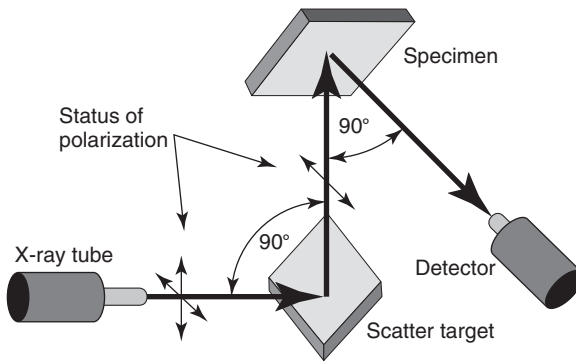


**Figure 4.27** Measurement geometry for the excitation with polarized radiation.

means that the radiation is also polarized and can be used for an effective and background-free excitation of light elements, i.e. Na to S, and thus improve their detectivity.

Again, the high loss of intensity during the generation of polarized radiation requires the use of ED detectors to compensate for this loss by collecting a large solid angle of the fluorescence radiation. However, very short distances between tube, scatter target, sample, and detector are necessary additionally. In this geometry, the use of X-ray tubes with powers in the range of 50–200 W is sufficient. They can be cooled by air (up to 50 W) or by an internal cooling system (up to 200 W). In the case of a more open geometry with larger distances, tubes with higher power with up to 4 kW are required; these inevitably have to be cooled by external systems.

Instruments using polarized or monoenergetic radiation for excitation are offered by three companies (see Table B.1). They are shown in Figure 4.28.

The sensitivity of XRF analysis can be significantly improved by using different excitation conditions, with each one exciting a specific group of elements with high efficiency and thereby achieving a very good peak-to-background ratio. The XEPOS from SPECTRO has an X-ray tube, which emits both Co-

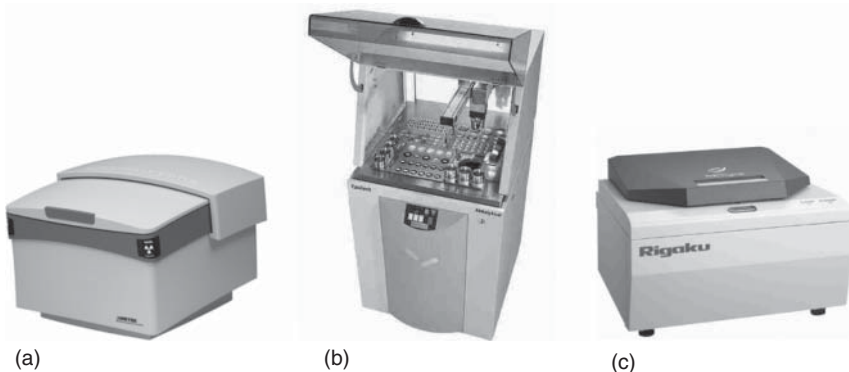


**Figure 4.28** Energy-dispersive instruments using polarized radiation: (a) XEPOS, Spectro Analytical Instruments GmbH, (b) Epsilon 5, Panalytical B.V., and (c) NEX CG, Rigaku Corp. Source: Courtesy of Spectro Analytical Instruments GmbH, Panalytical B.V., and Rigaku Corp.

and Pd radiation. The polarized Pd-L radiation can be used for the excitation of the light elements; with the Co radiation the elements up to Mn can be excited with high efficiency and the heavier elements can be excited with the Pd-K radiation. The availability of monoenergetic tube radiation increases the excitation intensity. By means of bandpass filters for the characteristic lines of the tube, their bremsstrahlung is suppressed and a further improvement in the peak-to-background ratio is achieved. This is reflected in a sensitivity gain that allows detection limits in the sub-parts per million range.

Similarly, in the HD Prime from XOS Inc. curved crystals are used for monochromatizing of the tube radiation via a Bragg diffraction. The diffracted radiation is then used for a highly efficient excitation of selected elements. Detection limits in the lower parts per million range are then possible even for light matrices.

#### 4.3.3.4 Instruments for Position-Sensitive Analysis

The demand to measure the elemental composition of finished goods is increasing; they often are nonhomogeneous or irregularly shaped, and therefore the analysis of a small homogeneous area of the sample surface is necessary. This can be achieved by limiting the primary radiation beam to a small area of the sample.

Using collimators, limiting the radiation to a spot of 0.2–2 mm diameter is possible. Using X-ray optics, e.g. polycapillary optics spot sizes of even  $<10\ \mu\text{m}$  can be achieved. The use of collimators is limited by the intensity, which decreases quadratically with the diameter of the collimator. X-ray optics collect the tube radiation from a large solid angle and then focus the radiation into a small area. As a result, sufficient high fluorescence intensities can be collected even from very small sample surfaces. The designation  $\mu\text{-XRF}$  has been established for this type of X-ray analysis.

The principle layout of these instruments is shown for an instrument with a collimator (a) and an instrument with a focusing optics (b) in Figure 4.29. This comparison demonstrates that the larger solid angle of source radiation, which can be achieved with focusing optics, leads to higher excitation intensity.

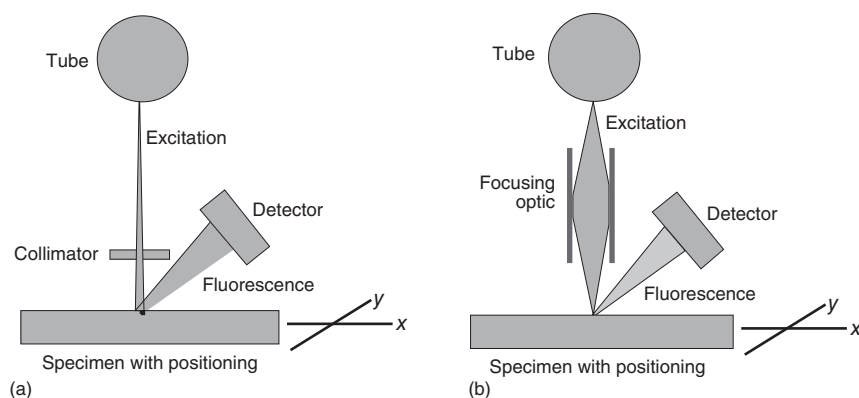


**Figure 4.29** Basic layouts of position-sensitive X-ray spectrometers with a collimator (a) and focusing optics (b).

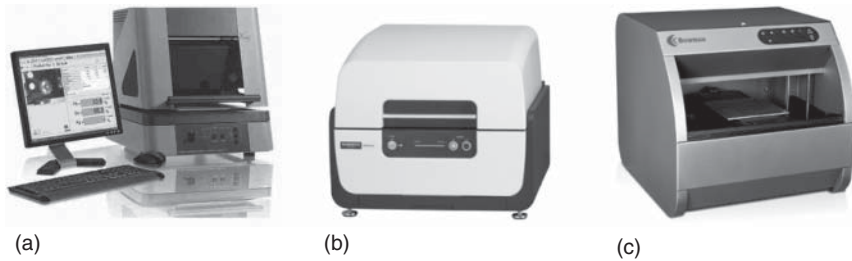


**Figure 4.30** Coating thickness instruments with collimators: (a) XDAL, Helmut Fischer GmbH, (b) AE1000, Hitachi High-Tech Science Corp., and (c) Bowman P-series. Source: Courtesy of Helmut Fischer GmbH, Hitachi High-Tech Science Corp., and Bowman.

In these instruments the sample is usually excited from the top. This is necessary because only then a correct sample positioning is possible and also irregular samples can be analyzed at different positions. On the other hand, this excitation direction requires an additional sample movement for an adjustment of the sample height.

These instruments are primarily used for the investigation of finished goods that cannot be destroyed for the analysis, either to determine their element composition or to characterize a layered material system.

Current instruments for the determination of layer thickness and layer composition, which are equipped with collimators with spot sizes down to 0.2 mm, are shown in Figure 4.30.

In addition to determining the mass fractions or layer thicknesses of selected sample areas, the elemental distribution can also be of interest. In this case, the sample is scanned under the incident beam and the data are displayed as linear or areal distributions.

For the analytical performance and its dependence on excitation intensity, detector type, or measuring medium (air, vacuum), the same statements hold true as for conventional EDSs. Using X-ray optics, excitation intensities are achieved that correspond to those of conventional EDS instruments.

Furthermore, these instruments require very precise sample positioning stages in order to position the very small spot accurately. This can only be achieved if the sample is positioned by a motorized stage and if the sample position can be controlled with the help of a microscope image. These capabilities are also required in order to correlate the measurement position with the corresponding spectrum and their calculated distribution images.

Some position-sensitive X-ray spectrometers with capillary optics for beam conditioning are shown in Figure 4.31.

#### 4.3.3.5 Macro X-Ray Fluorescence Spectrometer

A special type of small-spot instruments is offered for the investigation of art objects, especially when they are larger and cannot be moved. These instruments are called macro-X-ray fluorescence (MXRF) spectrometers. In these instruments the measuring head contains the excitation source with beam-shaping



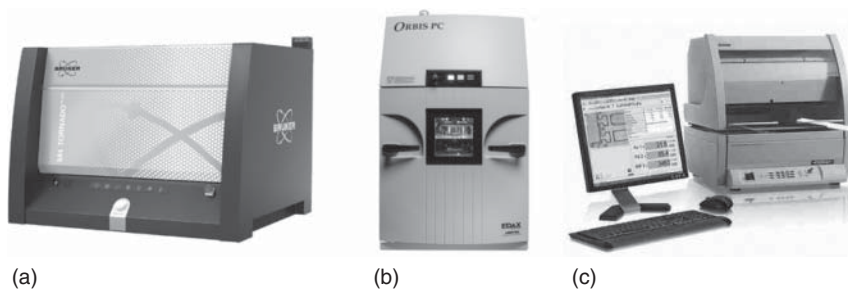


**Figure 4.31** Instruments utilizing X-ray optics for beam focusing: (a) M4 Tornado Plus, Bruker Nano GmbH, (b) Orbis, EDAX Inc., and (c) XDV- $\mu$ , Helmut Fischer GmbH. Source: Courtesy of Bruker Nano GmbH, EDAX Inc. and Helmut Fischer GmbH.

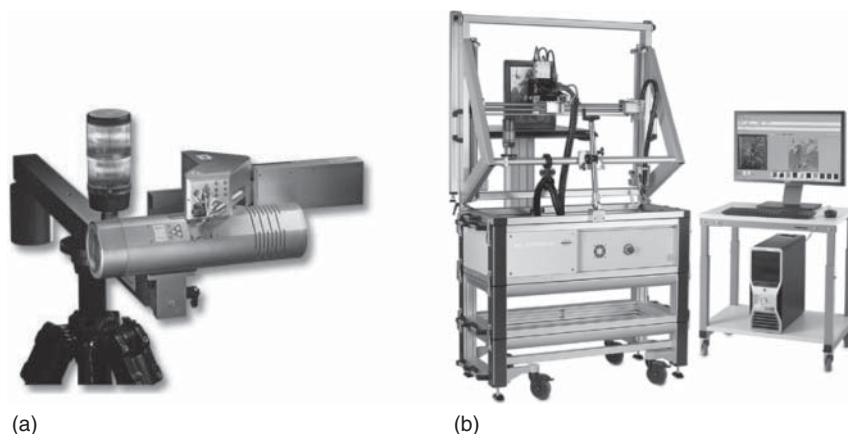


**Figure 4.32** Macro-X-ray fluorescence spectrometer for the investigation of large-area objects: (a) Artax and (b) M6 JetStream. Source: Courtesy of Bruker Nano GmbH.

optics, the detector, and usually an optical microscope; it is mounted on a motor-driven carriage that can be moved in front of the sample.

This enables both point measurements and distribution analyses of large samples; however, the measurement must be carried out in air, which limits the detectable element range. Special precautions are required for radiation protection purposes since the X-ray beam-guiding components are not covered. Data acquisition and processing is carried out similarly to  $\mu$ -XRF spectrometers. Examples of such commercially available instruments are shown in Figure 4.32.

In addition to the previously described commercially used spectrometer types, in R&D many other special excitation geometries are used in order to perform very specific analytic tasks utilizing XRF.

Only some of these solutions are discussed here.

#### 4.3.3.6 Micro X-Ray Fluorescence with Confocal Geometry

A special form for position-sensitive analysis is a confocal geometry. In this case, not only is the incident beam focused by an X-ray optic, but also the fluorescence radiation of the sample is detected only from a narrow beam that is defined by

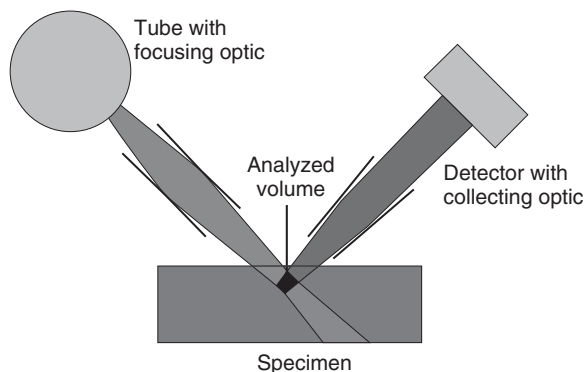


**Figure 4.33** Confocal geometry for the investigation of 3D elemental distributions.

an optical system in front of the detector. If these two beams intersect, an analytical volume (voxel) is defined that contributes to the fluorescence signal (see Figure 4.33).

If the sample is moved through this analytical volume, three-dimensional elemental distributions or depth profiles can be determined. However, the applications for such an arrangement are limited since the spot sizes of the available capillary optics are in the range of 10–15  $\mu\text{m}$ , i.e. the volume sizes contributing to the signal are at least 20  $\mu\text{m}$ . Since the penetration depth of the radiation in the case of metallic, mineral, or glass-like samples is of the order of magnitude of this voxel size, the application of this method is limited to light matrices. However, this method can yield interesting results when analyzing paint or lacquer coatings (see also Section 14.4.6).

#### 4.3.3.7 High-Resolution X-Ray Spectrometers

High-resolution X-ray spectrometers allow the very precise determination of the line shapes of X-ray lines. From this information the electron distribution in the outer shells or the surrounding electron state of the emitting atom can be obtained, i.e. information about the chemical bond of the emitting atom. This is especially possible when these lines are generated by transitions from the outermost energetic levels, which are influenced by the surrounding electron state of the atom. Thus, the determination of the chemical speciation of the atoms under analysis is possible; the determination of the line shape also allows the determination of the electron density of the electron levels (see also Section 17.3).

For this purpose, energy resolutions of less than 1 eV are required. This can be achieved largely with commercial WDS instruments. However, in addition to high-quality mechanics, suitable combinations of crystal and collimator as well as relatively long measuring times per measurement angle are necessary.

Shortened measurement times for high-resolution instruments can be achieved by special optimized measurement geometries. Examples of this are presented in Section 17.3.

#### 4.3.3.8 Angle Resolved Spectroscopy – Grazing Incidence and Grazing Exit

If the incidence of the primary radiation is similar to that of TXRF, but with angles slightly greater than the total reflection angle, the incident radiation penetrates

and generates fluorescence in thin surface layers of the sample (grazing incidence X-ray emission – GIXE). By changing the incidence angle, the penetration depth of the incident radiation and thus the sample volume contributing to the signal can be varied (see Figure 4.34).

By comparing spectra from different incident angles, the investigation of layer sequences of unknown layer systems or of composition gradients within the layer is possible (see also Section 14.4.6).

Using small incident angles for the primary radiation, very thin layers can be analyzed with high sensitivity since the path of the primary radiation in the top sample layers is very long and thus high fluorescence intensity can be achieved. The detection of the radiation is similar to TXRF, perpendicular above the sample.

This geometry is also used in the reverse. In this case, the excitation is more or less perpendicular to the sample and the fluorescence radiation will be picked up at low exit angles (Grazing Exit X-Ray Emission – GEXE). This is possible with strongly collimated beams at different angles or also simultaneously over a larger angle range with a position-sensitive detector (see Figure 4.35). Also with this measurement geometry a strong surface sensitivity can be achieved, since the depth of information is very small and varies by changing the angle of acceptance. Similarly to GIXE, this geometry allows the investigation of unknown layer systems and also of concentration gradients in layers.

**Figure 4.34** Grazing incident measurement geometry.

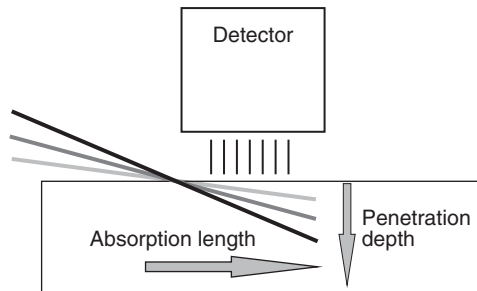
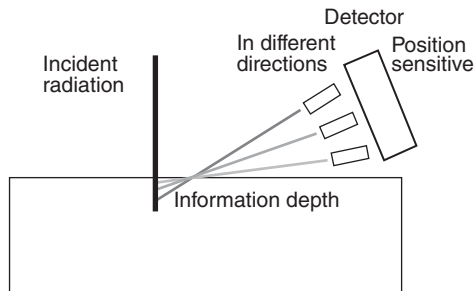


**Figure 4.35** Grazing exit measurement geometry.



## 4.4 Commercially Available Instrument Types

The most important manufacturers of X-ray spectrometers and the instrument types currently offered by them are listed in Table 4.4. More detailed information about the manufacturers is given in Table B.1.

**Table 4.4** Products offered by instrument manufacturers for different instrument types.

Manufacturer	WDS		EDS		μ-XRF		
	Multichannel	Sequential	Handheld	Tabletop	Poly-cap	Collimator	TXRF
Bruker AXS GmbH	X	X		X			
Bruker Nano GmbH			X		X	X	X
EDAX Inc. (Ametek)					X	X	
Helmut Fischer GmbH			X	X	X	X	
Hitachi former Oxford Instruments			X	X		X	
Panalytical B.V.	X	X		X			
Rigaku Corp.	X	X		X			X
Hitachi Corp.				X	X	X	
Shimadzu Corp. Sciaps	X	X		x			
SkyRay Instr. Co Ltd.		X	X	X		X	
Spectro Analytical Instruments GmbH (Ametek)			X	X		X	
Thermo Fisher Niton			X				
Thermo Fisher ARL	X	X					
Bowman				X		X	
XOS Inc.			X	X			

'X' for available from this manufacturer.

## 5

# Measurement and Evaluation of X-ray Spectra

## 5.1 Information Content of the Spectra

According to Moseley's law (see Eq. (2.4)), and based on the origination of characteristic X-rays, their energies are proportional to the square of the atomic number. By separating the individual lines, the identification of the emitting elements, i.e. a qualitative analysis, is possible.

The intensities of the lines, on the other hand, depend on the excitation and measurement conditions, but above all on the number of atoms of the emitting element in the analyzed sample volume. This allows the quantitative analysis of a sample. The measurement of the line intensity is a process based on counting statistics, i.e. it is associated with a statistical error, which can be reduced by increasing intensity. Therefore, for a precise analysis, it is desirable to obtain the highest possible number of measured pulses.

However, there is no linear relationship between the mass fraction of an element and its line intensity. Significant deviations from the linearity result from the secondary interactions of the X-ray radiation within the sample. These interactions are well understood and can be mathematically modeled very precisely and accounted for with high accuracy.

This interaction will be discussed using a well-known material system, the Cr–Fe–Ni alloy typical of stainless steels.

The situation for the binary material system Cr–Fe is shown in Figure 5.1. Panel (b) describes the dependence of the Fe intensity as a function of the Fe content. The curve shows a reduction in Fe intensity in relation to a linear dependency. The number of directly generated Fe photons is proportional to the Fe concentration, but some of them do not reach the spectrometer because they are absorbed by the Cr atoms on the path to the sample surface, i.e. Cr atoms are ionized and emit their characteristic radiation. The Cr intensity, on the other hand, exhibits behavior complementary to that of Fe, i.e. it increases above linearity due to this secondary excitation. Cr absorbs Fe-K-radiation with high efficiency because the energy of its absorption edge is only slightly smaller than that of the radiation.

Now, looking at the binary material system Fe–Ni, the Fe photons are also absorbed, but the absorption is less than that for the Cr–Fe system, since the mass-absorption coefficient of Fe radiation in Ni is smaller than that in Cr. In a second process the directly excited Ni radiation can be absorbed by the

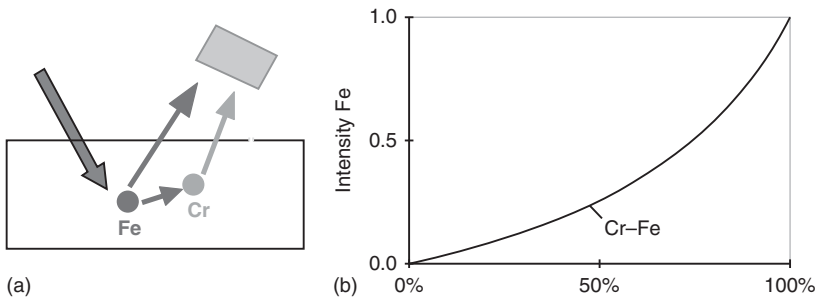


**Figure 5.1** Characteristics of the Fe intensity for the Cr-Fe binary material system.

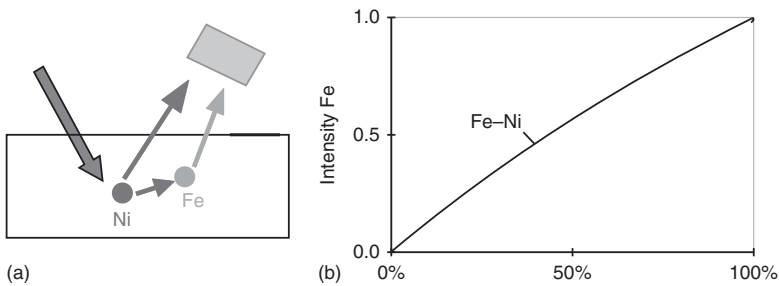


**Figure 5.2** Characteristics of the Fe intensity for the Fe-Ni binary material system.

Fe atoms, generating additional Fe radiation. This means that this secondary excitation of Fe atoms increases the Fe intensity disproportionately, as shown in Figure 5.2. The Ni radiation, on the other hand, is disproportionately reduced by its increased absorption.

Finally, consider the entire material system Cr-Fe-Ni. The Fe intensity depends primarily on the Fe content but also on both the secondary excitation by the Ni radiation and the absorption by the Cr atoms. This results in deviations of the Fe intensity from the linear behavior as a function of the concentrations of the two alloying elements, both to larger and smaller intensities, as shown in Figure 5.3b. For an accurate quantification this strong scattering of fluorescence intensity requires a correction of the Fe intensity based on the interaction of the

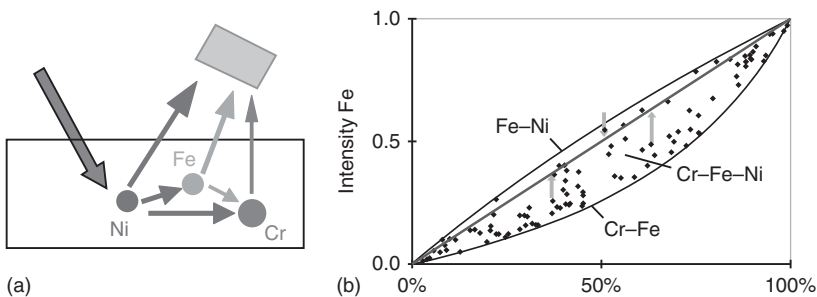


**Figure 5.3** Characteristics of the Fe intensity for the Cr-Fe-Ni material system.

**Table 5.1** Contributions to the Cr intensity by primary, secondary, and tertiary excitation in dependence of the alloy composition in Cr–Fe–Ni alloys.

Content (wt%)			Cr-K $\alpha$ -intensity, excited by... (%)		
Ni	Fe	Cr	Primary	Secondary	Tertiary
10	70	20	76	23	0.6
20	75	5	70	28	1.6
50	40	10	75	22	2.6
80	10	10	76	23	1.5

radiation with the matrix as shown for few measurements in Figure 5.3b by the arrows. As a result, the intensities then can be plotted as a linear calibration curve, as indicated in Figure 5.3.

The extent of the secondary effects depends on the concentrations of the elements involved but also on the interdependent attenuation and secondary excitation of the fluorescence radiation. In adverse cases as for the discussed Cr–Fe–Ni system, they can account for up to a quarter of the total intensity. With such strong influences, even tertiary effects have to be expected and considered, i.e. the secondary photons are subjected to a further interaction, which influences their intensity.

The percentages of the Cr intensity generated by primary, secondary, and also tertiary excitation are compiled in Table 5.1, as a function of a selected element composition of the Cr–Fe–Ni system. The proportions of the tertiary interaction are relatively small compared to the secondary effects but must be taken into account if the desired analysis error should be <0.5%.

It should be pointed out that the Cr–Fe–Ni system evaluated here is characterized by unusually strong interactions that even have a significant influence in the third order. On the other hand, this system consists of only three elements. In most common samples, the matrix influences are smaller so that tertiary effects are often negligible, but the number of elements involved in the matrix interaction is often higher. Consequently, the overall situation becomes more complex. For the evaluation of the matrix effects, different methods have been developed in order to ensure as accurate an analysis as possible. These are described in more detail in Section 5.5.

## 5.2 Procedural Steps to Execute a Measurement

High pulse rates ensure a small statistical measurement error. Therefore, determining the highest possible intensities of the fluorescence lines of an analyte is the goal of X-ray fluorescence (XRF) analysis. The following steps are required to prepare these measurements:

- Defining optimal measurement conditions in order to ensure the most favorable excitation of the analyte elements, i.e. guaranteeing a high sensitivity for the detection of trace elements or good statistics in the quantification of major and minor elements. The required good peak-to-background ratios and/or high counting rates can be achieved by optimizing the excitation and test conditions (tube parameters, crystal and collimator selection, filters, etc.).
- Selection of a suitable characteristic X-ray line, which has a high line intensity as well as little overlaps with other elements lines in the sample or the reference samples.

For wavelength-dispersive spectrometry (WDS) instruments, the selection of the analysis line also requires specifying the combination of analyzer-crystal and collimator as well as the determination of the background positions.

- Determination of the peak intensity. Here different methods are available, depending on the resolution of the spectrometer, i.e. the degree of peak overlap with other element lines.
- Calculation of the weight fractions of the individual elements in the sample using a suitable model, taking into account the matrix interaction.
- If necessary, measurement of reference samples for calibration and, if necessary, of monitor samples for compensating instrument instabilities.
- Estimation of the uncertainties of the analysis and, where required, an assessment of the quality of the analysis.

These individual steps are discussed in more detail in the following sections with their impact on the analytical result.

## 5.3 Selecting the Measurement Conditions

### 5.3.1 Optimization Criteria for the Measurement

The measurement of X-ray spectra is a counting statistics process, i.e. the count rate distribution of the detected photons over time obeys the Poisson statistics. This can be approximated very well by Gauss statistics for high pulse rates. It follows that the statistical distribution of the counts from repeated measurements can be described by their standard deviation. This is given for counts  $N$  by  $\sqrt{N}$ , i.e. the relative error is determined as follows:

$$\Delta N/N = 1/(\sqrt{N}) \text{ or } 100/\sqrt{N} (\%) \quad (5.1)$$

This statistical error occurs for every measurement, i.e. it cannot be avoided and thus, the complete analytical error cannot fall below this value. The dependence on the measured pulse number is shown in Table 5.2.

**Table 5.2** Relative statistical error as a function of the number of counts.

$N$	100	1 000	10 000	100 000	1 000 000
$\Delta N/N$ (%)	10	3.1	1	0.3	0.1



From these values, it can be concluded that the measured counts should be higher than 50 000 in order to keep the statistical error below 0.5%.

The measurement geometry influences the background of the measured spectrum. The intensity of the scattered primary radiation from the sample is angle dependent. It is determined by the incident angle of the primary radiation, the detector acceptance angle of the fluorescence radiation, as well as the solid angles of these radiation beams. If the scatter angle of the radiation, i.e. the angle between incidence and acceptance beam is close to  $90^\circ$ , the scatter intensity has a minimum. Usually, however, these parameters cannot be influenced since they are set by the available analytical instrument. The various types of instruments, with their measuring geometries, were discussed in Section 4.3.

### 5.3.2 Tube Parameters

#### 5.3.2.1 Target Material

X-ray tubes emit a continuous spectrum – the bremsstrahlung spectrum – as well as the characteristic fluorescence lines of the target material with a relatively high intensity.

The atoms in the sample to be examined are excited by both beam components. The excitation efficiency depends on the mass attenuation coefficient  $\mu$  of the excited atom and the intensity of the excitation spectrum. Components of the incident radiation with energies close to the absorption edge contribute most strongly to the excitation of the fluorescence, since the mass attenuation coefficient decreases strongly with the energy, according to  $\mu \sim E^{-3}$ . This was already illustrated in Figure 4.26, where the monoenergetic excitation of an oil sample led to very different fluorescence intensities for the different additives, even though their concentrations were essentially the same. An X-ray spectrometer, with a wide spectral band excitation, is useful for general, multipurpose use. In this case, reasonably good excitation conditions for all elements are available.

Consequently, the target material of the tube influences the intensity of the fluorescence lines of a sample. The following criteria are important for the selection of the target material:

- The target should provide an intensive bremsstrahlung intensity to ensure effective excitation of a wide range of elements. Since, according to (2.2), the bremsstrahlung intensity is proportional to the atomic number  $Z$  of the target material, a material with a high atomic number should be used. For this reason, tungsten, for example, would be a good choice.
- Only about 1–2% of the tube power is converted into X-ray radiation, and the remainder generates heat. This results in a high thermal load on the target, which either requires a high temperature melting point or a high thermal conductivity of the target material. Tungsten or molybdenum, with their high melting temperatures, would be a good choice or copper or silver for their high thermal conductivities.
- However, the most decisive criterion for the selection of a target material is the overlap of the fluorescence lines of the target material with the fluorescence lines of the sample. In this case, rhodium or palladium is suitable, since Rh

only influences Cl, and Pd only influences Rh. Both have an acceptable atomic number as well as a relatively high melting point.

For the laboratory user the option to select a tube is usually limited, since it is set by the available instrument. As a note, X-ray spectrometers are frequently equipped with Rh tubes.

### 5.3.2.2 Excitation Conditions

The tube parameters voltage and current influence the count rate, i.e. the number of counts per unit time. The count rate for an element on its own depends mainly on the intensity distribution of the incident radiation above the absorption edge of that element. For the most part, the range up to approximately 3–5 keV above the absorption edge has the highest impact. Spectral components with higher energies do not contribute very strongly to the excitation. This is the result of the already mentioned rapid decrease of the mass attenuation coefficients with energy. This means that most elements in a complex material are excited by the bremsstrahlung spectrum. The radiation of the fluorescence line of the target provides an essential contribution to the excitation for only a few elements whose absorption edges are just below the fluorescence energy of the target material, because here the fluorescence line has a higher intensity than the bremsstrahlung.

When selecting the excitation conditions, one can vary tube current and voltage. The target material of the tube is given by the instrument. The intensity of the entire tube spectrum varies proportionally with the current (see also Eq. (2.2)). A change in voltage also influences the energy distribution of the tube spectrum. This is illustrated in Figure 5.4 by showing various scatter spectra of a Rh tube. It has to be mentioned that these scatter spectra are not equivalent to the excitation spectrum, because the scattering of the radiation changes the energy distribution. Therefore, the spectra in Figure 5.4 show not only the elastically (Rayleigh) but also the inelastically scattered (Compton) Rh fluorescence of the tube. The continuous part is an overlap of both elastic and

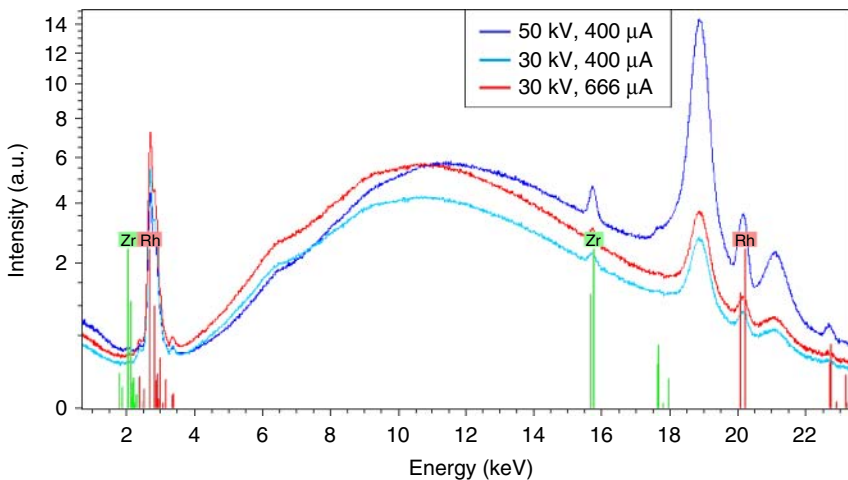


Figure 5.4 Excitation spectra for different tube parameters (y-axis in square root scale).

inelastic scattered bremsstrahlung. In general, however, the energy distribution is similar to the excitation spectrum. The small Zr peak (at 15.7 keV) is generated by a detector collimator.

Two of the displayed spectra (displayed in blue) are measured with the same tube current (400  $\mu\text{A}$ ) but with different tube voltages (30 and 50 kV). The high-energy part of the spectrum shifts accordingly toward the high excitation voltage; the maximum of the bremsstrahlung as well as its intensity increases with increased tube voltage. It is interesting to note that energy range from 3 to 10 keV, which is of interest for the excitation of most elements, is not significantly influenced by this change in tube voltage.

The third spectrum (displayed in red) was measured at a tube voltage of 30 kV and changing the tube current to 666  $\mu\text{A}$ . The result is an increase in the intensity of the complete primary spectrum that is proportional to the tube current. The excitation efficiency can thus be increased at a slightly lower high voltage by increasing the tube current but maintaining the same tube power. One should consider the operating conditions of the X-ray tube when making any changes to the excitation conditions. The X-ray tube only operates within a working envelope that includes maximum power, maximum filament current, and minimum and maximum high voltage.

When choosing the excitation conditions, the spectrometer's count rate capability must also be considered. For WDS instruments, it is very high since the detectors count the incoming pulses only. In the case of energy-dispersive detectors, the signal filtering requires additional time for the determination of the energy of the absorbed photon. Therefore, there are limitations to the count rate capability, which strongly depend on the instrument detector and its associated detector electronics. For a certain count rate, these are characterized by the so-called dead time, during which incoming pulses cannot be processed by the electronics. The dead time is significantly higher for energy-dispersive (ED) systems than for wavelength-dispersive (WD) systems.

The scatter spectra in Figure 5.4 show another feature, which is the increase in the low-energy background (below 2 keV) with increasing tube voltage; this is an effect due to the use of ED detectors. However, this low-energy background can adversely affect the traceability of elements in this energy range due to a decreased peak-to-background ratio. Low tube excitation voltages can be useful for certain analytical tasks, but one must be aware that potentially not all elements of interest are excited and therefore cannot be measured. For this reason, ED systems occasionally make use of multiple measurements with different excitation conditions to optimize excitation conditions for particular elements or element groups. Since WD systems already utilize the sequential detection of individual element lines, an optimization of the excitation conditions for each element is common.

### 5.3.2.3 Influencing the Energy Distribution of the Primary Spectrum

The use of secondary targets or monochromators to generate a monoenergetic excitation spectrum has already been described in Section 4.3.3.2. In the absence of the bremsstrahlung spectrum the spectral background is significantly reduced, resulting in an improved peak-to-background ratio for the elements that are

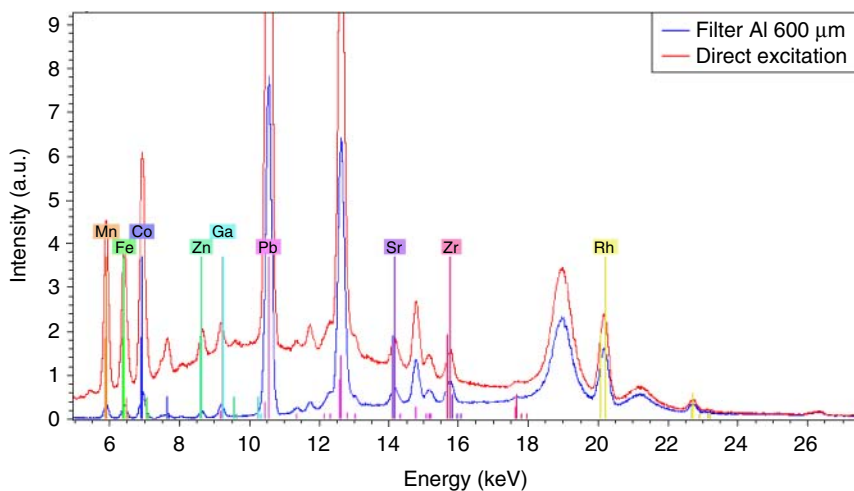


**Figure 5.5** Influencing the measured spectrum with an Al filter.

within the more selective narrow excitation range. Filters between tube and sample can also be used for the optimization of the excitation conditions. The selection of filters again influences the peak-to-background ratio of the primary radiation and therefore the sensitivity. Figure 5.5 shows spectra from a glass sample measured at 50 kV with and without a filter. The spectrum measured with an Al filter shows reduced background at low energies but also the peak intensities are reduced, progressively with lower energy. In sum, an improvement in the peak-to-background ratio and thus an improved detection sensitivity at the lower energy can be observed. By using filters in the incident beam path, the excitation spectrum is “hardened,” i.e. the mean energy of the spectrum shifts to higher energies. This allows for a better excitation of heavier elements and increases the sensitivity of their detection.

The use of filters also allows eliminating the characteristic tube radiation. This effect is often used in coating thickness measuring instruments. They employ W-tubes with a relatively thick glass window, which absorbs the W-L and the low-energy range of the primary beam spectrum. This is of little significance, because these instruments usually can only measure elements heavier than titanium due to the absorption of the fluorescence radiation in air in the complete beam path.

Another example of the use of filters is shown in Figure 5.6. The superposition of the scattered Rh-L radiation of the tube target with the Cl-K line of the sample prevents accurate peak area determination. Using a thin 12.5  $\mu\text{m}$  Al filter helps absorb the Rh-L radiation and the Cl line is unobstructed and can be evaluated easily.

Figure 5.6 illustrates also another effect of this filter. If the sample has a crystalline structure the primary radiation can be Bragg diffracted on these crystals, in particular if the exciting beam has a small diameter as in micro-X-Ray fluorescence ( $\mu\text{-XRF}$ ) instruments. In this case, the crystal selects the energy of the complete primary spectrum that can be diffracted into the detector direction.

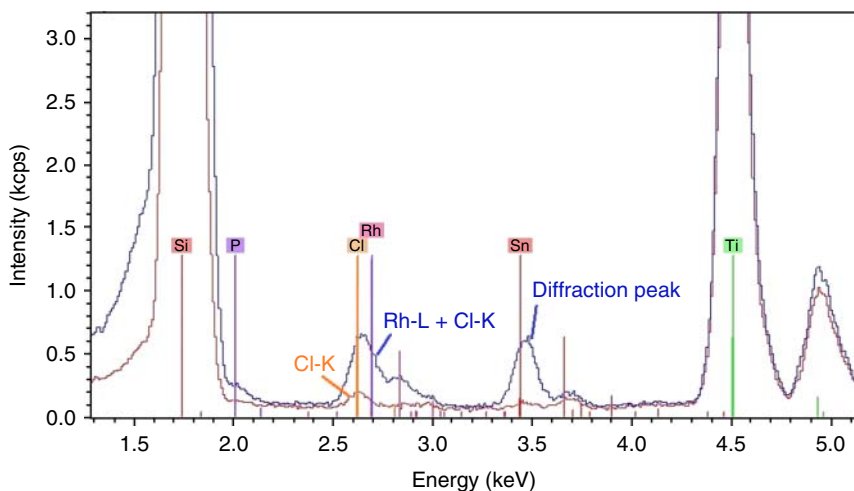


**Figure 5.6** Reduction of diffraction peaks and the scattered Rh-L radiation with direct excitation (blue) with a 12.5  $\mu\text{m}$  Al filter (red).

This generates small peaks in the measured spectrum, for example, in Figure 5.6 on the position of Sn-L. This complicates the correct peak identification and can influence the peak area determination when overlapping an element line (see Section 4.2.6.3). As already described, a filter eliminates the low-energy range of the bremsstrahlung. If no radiation is present in the excitation spectrum it cannot be diffracted, i.e. the diffraction peaks will be eliminated.

Most commercial instruments have the option to introduce different filters into the primary beam path. Often the instrument software suggests their optimum use.

### 5.3.3 Measurement Medium

The atmosphere in the X-ray path influences the intensity of the measured fluorescence lines, in particular the low-energy radiation. The measurement environment is therefore important for the measurement results. The absorption can be reduced by using helium or vacuum atmosphere. Of course, the absorption also depends on the distance between the sample and the spectrometer. Generally, it is necessary that measurement samples and reference samples are measured under the same conditions.

For a WD spectrometer the transmission probability is illustrated in Figure 5.7. Typically, the spectrometer itself is evacuated and only the atmosphere in the sample chamber must be considered.

In EDSs the distance between the sample and the detector is much smaller. Therefore, the spectrometers are often not evacuated. If the measurement chamber is evacuated or He-flushed the detector window influences mainly the absorption of low-energy radiation and thereby, the sensitivity for light elements (see also Figure 4.7).

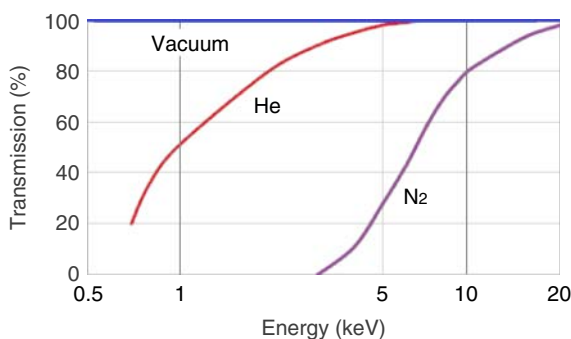


**Figure 5.7** Transmission of X-rays in different measurement atmospheres.

Of note, liquids cannot be measured in vacuum. They would evaporate and consequently can damage the instrument.

For WDS instruments it is recommended to measure volatile elements at the beginning of the measurement cycle. Then the analytical result will not be influenced by missing the evaporated mass fractions of these elements.

### 5.3.4 Measurement Time

#### 5.3.4.1 Measurement Time and Statistical Error

The measurement time directly influences the accumulated number of counts. Measurement time and count number are proportional to each other, i.e. by increasing the measurement time, both the precision and the sensitivity of the measurement can be improved.

As already mentioned in (5.1), the statistical error of a measurement depends on the detected number of counts  $N$  and is  $\Delta N = \sqrt{N}$ , i.e. the statistical error can be reduced to half by quadrupling the measured number of counts or the measurement time. A similar statement also applies for the detection limit – quadrupling the number of counts improves the detection limit by a factor of 2. Therefore, counting statistics sets limits to the ability to improve the analytical accuracy and sensitivity of the measurement.

In general, the statistical uncertainty should be matched to all other uncertainties, i.e. if possible, it should not be the dominant error contribution. On the other hand, it also does not need to be significantly below the other uncertainty contributions. A statistical uncertainty contribution, which is about a factor of 2–3 below the desired analysis error, is sensible. This requirement can usually be achieved for major and minor components, while it can become difficult for traces, since the number of counts depends on the mass fraction of the analyte. For sequential WDS instruments the measurement time can be adjusted for every element or background position, while for energy-dispersive spectrometry (EDS) instruments the measurement time is the same for the complete spectrum. Therefore, the measurement time needs to be set to meet the required error of the element with the lowest intensity.

#### 5.3.4.2 Measurement Strategies

An analysis can be carried out as a single measurement for all required elements or alternatively as repeated measurements. For repeated measurements mean

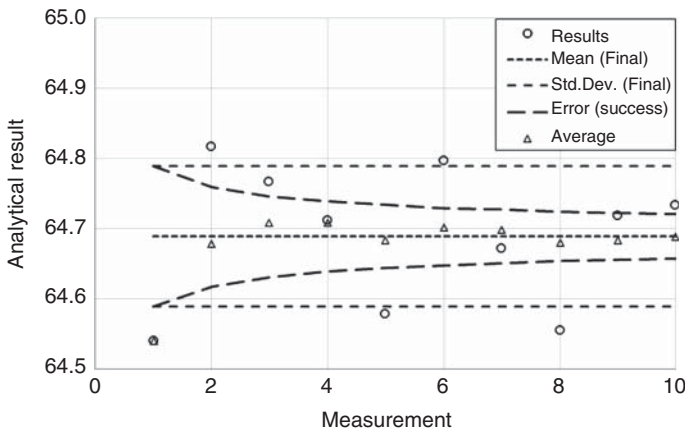


**Figure 5.8** Standard deviation and error of repeated measurements.

values and the standard deviation of the analytical results can be determined (see Section 6.1.1). If the standard deviation of a series of measurements is  $\sigma$  the error of the mean value  $\sigma_M$  for  $n$  repeated measurements is given by

$$\sigma_M = \frac{\sigma}{\sqrt{n}} \quad (5.2)$$

This result is demonstrated in Figure 5.8. It shows the analytical results of 10 repeated measurements, the corresponding mean value, the standard deviation of all measurements, the successive average of the measurements, and the error according to (5.2). It can be seen that the error is reduced with every measurement and the variations of the successive average are reduced.

From these results it can be concluded that repeated measurements give better results; however, they also require more measurement time. This is in particular true for WDS instruments where the test conditions (goniometer position, filter, tube parameters) have to be changed for every measurement position. Most often the extra time is not available, especially in the case of process control. Finally, the statistical error for a single measurement at time  $t$  or the error according to (5.2) for  $n$  repeated measurements at time  $t/n$  is the same.

Considering all the above, it is important to develop a measurement strategy to achieve the desired results before starting the measurements. In addition to the statistical error contributions there are also other contributions that can be better identified and reduced by multiple measurements. Further, outliers cannot be identified with a single measurement. Therefore, repeated measurements are recommended for analyses that demand high precision, for example, the preparation of reference material (RM).

#### 5.3.4.3 Real and Live Time

The measurement time can be displayed in real time or in live time. Detectors have a finite processing time  $\tau$  for an X-ray pulse. During this time the detector is busy and cannot process new X-ray photons. The sum of all processing times during the measurement is called dead time; it depends on the counting rate and

the characteristics of the measuring channel. It means that the measuring channel is not open during the complete measuring time (real time). The live time of the channel is shorter. In order to evaluate the acquired intensities correctly, after the measurement a dead time correction is required according to

$$t_{\text{live}} = t_{\text{real}} \cdot (1 - t_{\text{real}} \cdot \tau) \quad (5.3)$$

In newer instruments the dead time is determined by comparing the incident and processed count rate directly during the measurement; it is often displayed during the measurement. A measurement in live time is also possible, where the counting losses are taken into account by the dead time. A direct comparison of the intensities from different spectra is then possible independent of the contents of the elements to be analyzed including the matrix elements.

The dead time of WDS instruments is usually very small. For EDS instruments it is greater. It should not exceed 30% for a quantitative measurement; it can be greater for screening measurements, but should not exceed 50%.

### 5.3.5 X-ray Lines

The individual X-ray lines of an element have different intensities and are therefore associated with a different statistical error. The  $\alpha$ -lines are the most intense within a particular series and should preferably be used for the evaluation. In the K series, the intensities of the  $\beta$ -lines are about 20% of the  $\alpha$ -lines, and in the L-series they are about 50% (see Table 2.1).

Nevertheless, in certain cases, the use of less intense lines of a series may be advantageous to avoid overlaps with other element lines, and accordingly to reduce the error caused by the correction of the overlapping peaks by peak fitting or deconvolution procedures. Another reason can be to avoid saturation effects in WDS instruments in case of high mass fractions and high excitation efficiency.

The energies of the individual X-ray lines are given by Moseley's law. The energies for the  $\alpha$ -lines of every series have already been shown in Figure 2.2. Figure 5.9 now shows the energies for most lines of each series.

The figure illustrated that there is a concentration of X-ray lines in the low-energy region (<3 keV), since K-, L-, and M-lines occur in parallel. In the energy range from 3 to 20 keV there are only superpositions of K- and L-lines; above 20 keV there are only K lines. The resulting frequency distribution of only the main lines is shown in Figure 5.10. This illustrates that at energies less than 20 keV line interferences are most likely to be expected, most of them in the range <5 keV. In this range, the resolution of WD spectrometers is especially good (see Figure 4.1), i.e. the separation of the individual lines is also good. On the other hand, the separation of lines in this energy range is limited for EDSs.

The most important line overlaps of the main lines typical for energy-dispersive spectrometers are shown in Figure 5.11. As a result of the limited peak-to-background ratios secondary lines can often be neglected when their intensities are low.

On the one hand, the higher resolution of WDS instruments reduces the number of peak overlaps, but on the other hand, lines with lower intensity now have to be taken into account since the higher resolution improves the



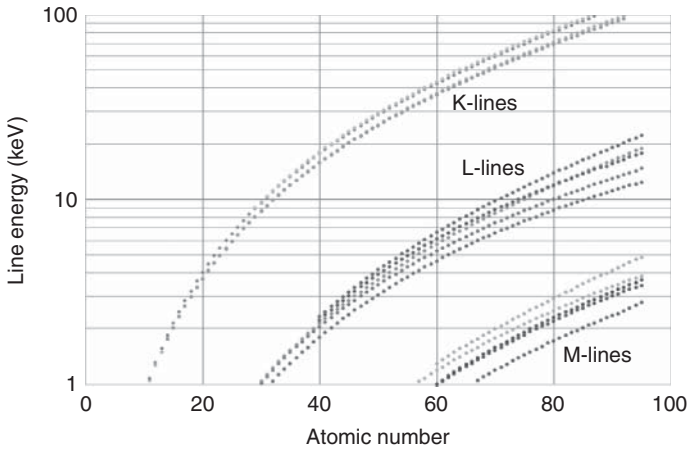


Figure 5.9 Energies of X-ray lines.

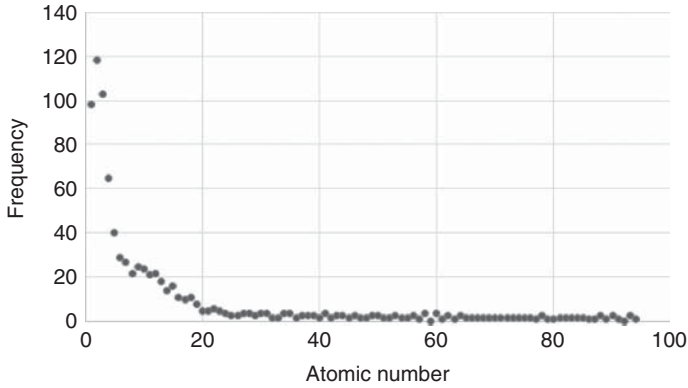


Figure 5.10 Frequency distribution of X-ray lines as a function of the atomic number.

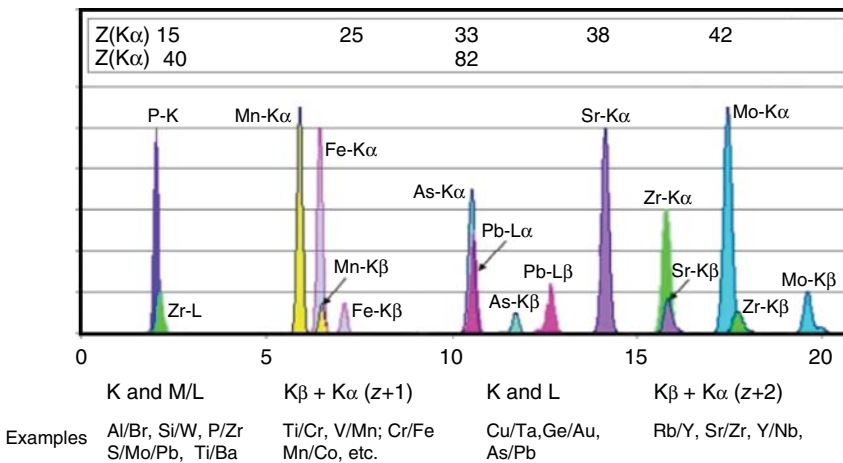


Figure 5.11 Typical line overlaps for energy-dispersive spectrometers.

peak-to-background ratio. As a result, significantly more line overlaps must be considered; this is particularly important when defining the support points for the background fit. The most important line overlaps are summarized in Table A.10.

## 5.4 Determination of Peak Intensity

### 5.4.1 Intensity Data

After the measurement, the determination of the peak intensity for the elements to be analyzed is necessary.

There are several possibilities for specifying the intensity data:

- Absolute intensities as count numbers  $N$ .
- Time-normalized intensities, as counting rate  $N/t$  with  $t$  being the measuring time. Counting rates allow the comparison of intensities, even if different measuring times were used.
- Intensities normalized to the measurement time  $t$  and the tube current  $i$ , as counting rate per current unit  $N/(t \cdot i)$ . Since the intensity of the tube spectrum is proportional to the tube current, these values allow the comparison of intensities even when measured with different tube currents.

The data are all equivalent, they can easily be converted from one to the other when the test conditions are known, and the dead time effects are included. The first two are the most frequently used.

When specifying intensities, a distinction is made between gross and net intensities.

Gross intensities comprise the total measured intensity of a line, which is composed of the actual peak intensity, the background intensity, as well as additional components.

Net intensity is the fraction that originates only from the element being analyzed.

To obtain the net intensity the following effects need to be corrected for:

- The tube spectrum scattered by the sample
- Peak overlaps, especially in the case of EDS due to its lower energy resolution
- Detector artifacts (mainly for energy-dispersive detectors)
- Higher order lines (in the case of wavelength-dispersive spectrometers)
- Artifacts generated by the sample, e.g. diffraction peaks

### 5.4.2 Treatment of Peak Overlaps

There are various methods to calculate peak intensities; they depend on the type of the spectrometer, in particular on its resolution.

In the case of WD spectrometers with good energy resolution, usually only the intensity in the peak maximum is determined (see Figure 5.12a). Owing to the small width of the peaks, the maximum contains most of the intensity. The

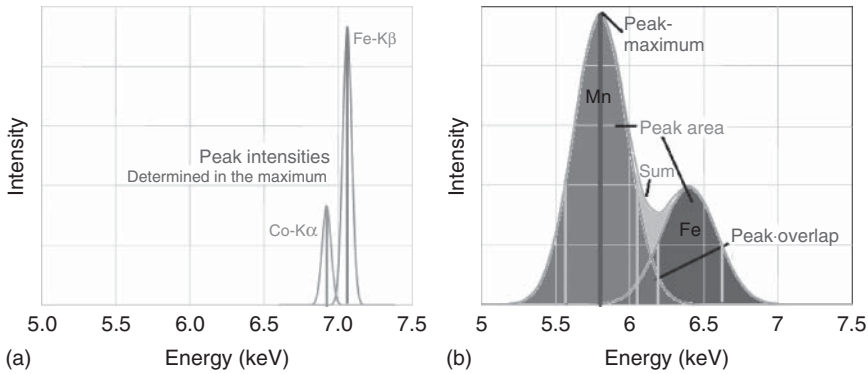


**Figure 5.12** Methods for the determination of the peak intensity: (a) WDS instrument – high resolution (overlap of Fe-K $\beta$  and Co-K $\alpha$ ) and (b) EDS instrument – medium resolution (overlap of Mn-K $\alpha$  and Fe-K $\alpha$ ).

peak intensity is usually directly measured by moving the spectrometer to the position of the peak maximum. This method is called peak-hopping. Sometimes, the peak maximum is first determined by a scan and then the peak intensity can be determined at this position.

The good resolution of WD spectrometers results in only relatively small peak overlaps. These can be corrected by the use of overlapping factors  $\kappa$  according to

$$I_{A,\text{corr}} = I_{A,\text{meas}} - \kappa_{AB} \cdot I_{B,\text{overlap}} \quad (5.4)$$

These overlap factors depend on the crystal–collimator combination – they must be determined only once, either by measurement or by calculation; they are usually stored in the instrument software. The better the resolution of the measuring setup, the smaller the correction factors are.

Owing to the EDS instrument's lower resolution, the peak maximum only represents a relatively small fraction of the total peak intensity. In order to still achieve small statistical uncertainties, the intensities in these spectrometers are usually determined as peak areas. For this purpose, the peak area is integrated within a defined energy range around the peak maximum. Most often the energy covers the range of the full width at half maximum (FWHM) of the peak, sometimes also a somewhat wider range.

As a result of the lesser energy resolution of these spectrometers, peak interferences are relatively frequent, and the corrections are more complex. Peak overlaps for energy-dispersive spectra can be corrected by the following:

- *Peak fitting*: In this case, either Gaussian peaks are fitted to the measured spectrum profile or the fitting process is carried out with measured pure element spectra. In the case of the fit with theoretical Gauss peaks, line-like spectral artifacts (escape, sum, and diffraction peaks; see Section 4.2.6) must be corrected beforehand. When using pure element spectra, the entire line series as well as detector artifacts are included and, therefore, automatically corrected. This, however, requires a high stability of the spectrometer.
- *Spectra deconvolution*: Since the measured spectrum results from a convolution of the radiation emitted from the sample with the spectrometer

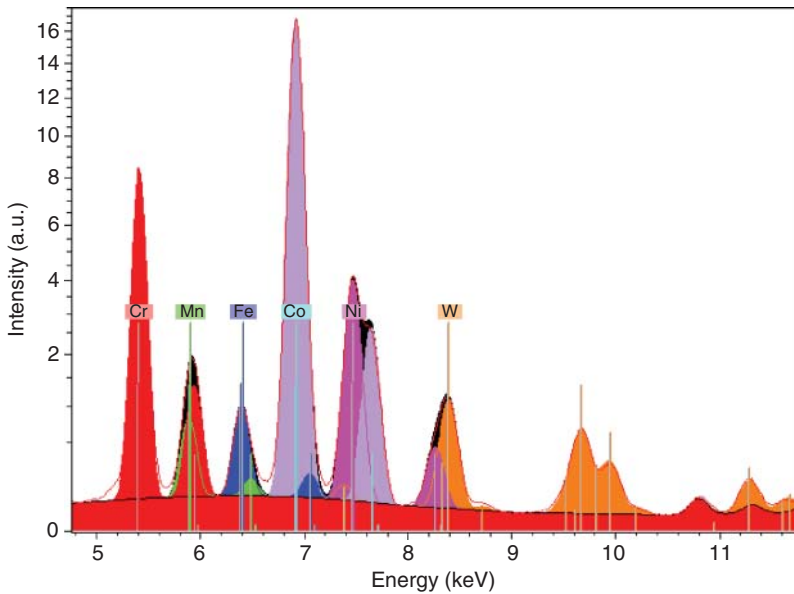


**Figure 5.13** Spectrum of a tool steel sample fitted with pure element peaks (every pure element spectrum in a separate color) (y-axis in square root scale).

response function it can be corrected by deconvolution. This makes it possible to separate the individual intensity contributions of both the line spectrum and the peak overlap area. For deconvolution the exact knowledge of the energy-dependent response function of the spectrometer is required.

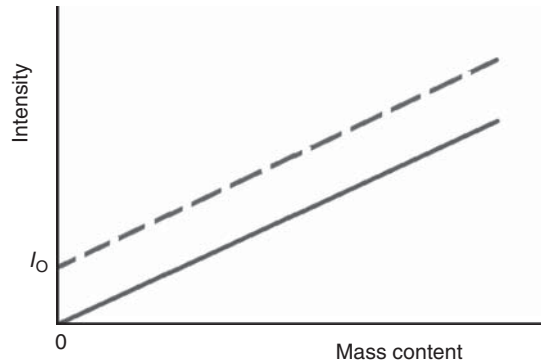
The peak intensities are then determined by integration over the defined energy range of the peak fitted to the measured spectrum, as illustrated in Figure 5.12b. When pure element spectra are used the intensity ratio of the fitted spectrum to the pure element spectrum can also be used.

A spectrum fitted with Gauss peaks is shown in Figure 5.13. The measured spectrum is shown as an (red) envelope. This is compared with the sum of the fitted colored single element spectra. A comparison of the measured and the fitted (black) spectrum permits a simple assessment of the quality of fit and assists in the identification of the elements included in the sample.

### 5.4.3 Spectral Background

The spectral background of a measured spectrum is defined by different contributions. There can be the spectrometer contribution such as higher order reflections or detector artifacts. A significant contribution results from the scattering of the primary radiation by the sample. The scattering depends on the measurement geometry, but mainly on the sample composition. As already discussed in Section 2.2.4.2 scattering from samples containing light elements is stronger than from heavy element samples (see also Figures 2.7 and 2.8).

**Figure 5.14** Calibration curves based on net intensities (continuous line) and with gross intensities (broken line).



The spectral background reduces the signal-to-background ratio and thus the sensitivity, but above all, the analyte signal, is distorted by the background.

Occasionally, only the uncorrected gross intensities are used for quantification, for example, in the case of multichannel spectrometers, which have no background measuring positions due to the fixed measurement geometry, or in the case of heavy metal alloys, which only have low scattering intensities. This means that there is a blank intensity  $I_0$  for zero concentration and the calibration curve does not go through the zero point (see Figure 5.14).

The calculation of the net intensities, i.e. the correction of intensity contributions that are not attributed to the fluorescence radiation, depends on the spectrometer type. First, all line type artifacts must be corrected in order to avoid their misinterpretation as analyte lines. These artifacts, such as higher order lines or detector artifacts (escape- or sum peaks), can either be avoided by hardware provisions or be corrected after the measurement by means of appropriate correction models during the processing of the spectra. The algorithms are implemented in the instrument software and are often automatically applied to the measured spectra.

For the correction of the scattering background in WD spectrometers, the background intensity must be measured at positions close to the analyte peak; the background can then be calculated by interpolation or extrapolation into the peak region. In order to achieve a good background fit, these measuring points must be carefully selected, especially in the case of peak interferences or a non-constant background. Peak overlaps can be avoided by improving the resolution of the spectrometer, i.e. by an appropriate choice of crystal and collimator. However, this results in a loss of intensity, which in turn leads to an increase in the statistical error or longer measurement time (see also Section 4.2.2.1). A non-constant background can only be properly corrected by the use of several background points, as shown in Figure 5.15. Consequently, the measurement time increases with the number of background points. Furthermore, one has to pay attention that the background intensity is not burdened with a significantly greater statistical error than the gross intensity; otherwise, the net intensity is encumbered with an additional error resulting from error propagation.

For EDSs, the background correction is simpler due to the simultaneous detection of the entire energy range, including the background. The simplest way to

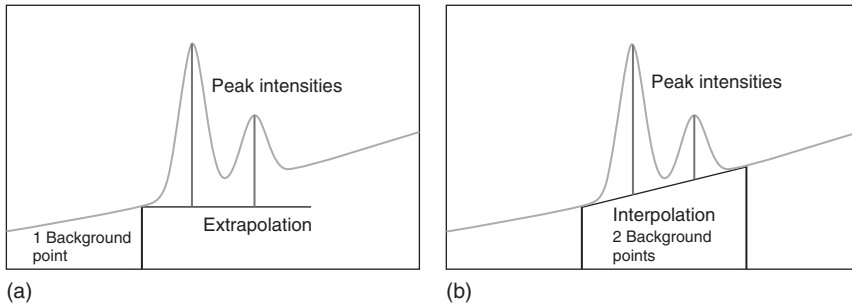


Figure 5.15 Setting of background points.

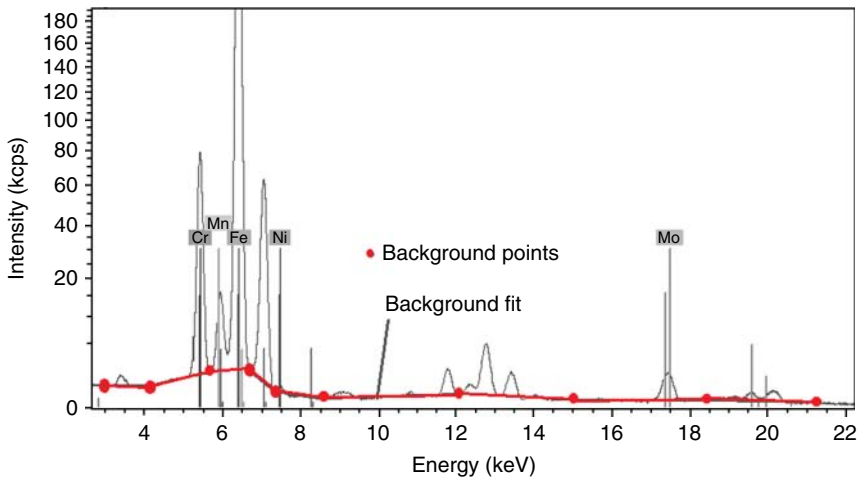


Figure 5.16 Background fit of an energy-dispersive measured spectrum (y-axis in square root scale).

fit the background is to set several background points in the measured spectrum and interpolate between them with simple linear or quadratic functions (see Figure 5.16).

Other possibilities are as follows:

- The measurement of a blank sample, i.e. a sample with a comparable matrix but without the analyte. Fitted to only a few supporting points, it can then easily be subtracted from the analyte spectrum.
- The modeling of the total scatter spectrum using the scatter properties of the sample concluded from the elastically and inelastically scattered fluorescence lines of the tube.

The net intensities thus determined can then be used for the quantification of the sample.

## 5.5 Quantification Models

### 5.5.1 General Remarks

In X-ray spectrometry the relationship between the mass content of an element and the fluorescence intensity is not linear. This complicates quantification. However, the different interactions that contribute to the nonlinearities are well known. They are described for example in the Sherman equation (Sherman 1955).

For only first-order terms, this equation can be written as follows:

$$I_i = G \cdot \int_E \frac{w_i \cdot \tau_i \cdot \frac{S-1}{S} \cdot p_i \cdot \omega_i}{A} \cdot I_0(E) \cdot dE \quad (5.5)$$

with

$G$	geometry and calibration factor
$(S-1)/S$	jump ratio
$\omega$	fluorescence yield
$\tau$	photoabsorption coefficient
$p$	transition probability
$\mu$	mass attenuation coefficient
$\psi$	incidence/take off angle
$I_0(E)$	primary spectrum
$w_i$	weight fraction of element $i$ , and
$A = \frac{\mu(E)}{\sin \psi_{in}} + \frac{\mu(i)}{\sin \psi_{takeoff}}$	consideration of absorption of incident and fluorescence radiation

At first sight, this equation looks relatively simple, but one problem is that the equation determines the opposite of what we are looking for. The intensities are calculated as a function of the mass fractions of all elements in the sample. For an analysis, however, the intensities are measured from which the mass fractions have to be calculated.

To further complicate things, terms of second order have to be additionally considered and significant computing power is required in order to solve the integral. When Sherman developed this equation, these calculations had to be carried out manually. The availability of computers reduces this effort but only with actual high-performance computers a direct solution of the Sherman equation, including several iteration steps, is possible within an acceptable time.

The criteria for an applicable quantification model are the achievable accuracy and the time that is required to calculate the result.

For calibration the measured intensities of reference samples with known compositions are used for the calculation of a calibration curve by regression analysis (see Figure 5.17). It is not trivial to mention that appropriate reference samples need to be available. This is often not the case and one will have to resort to a fundamental parameter-based standard-less analysis (see Section 5.5.3). The number of reference samples depends on the calibration parameters in the model as well as on the number of elements to be analyzed. The minimum number  $M$

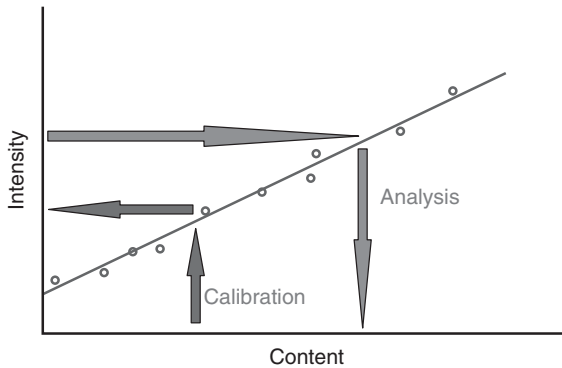


**Figure 5.17** Calculation and use of a calibration curve.

of mutually independent samples should be  $M = 2 \cdot (k + 1)$  if  $k$  is the number of free parameters, which is the sum of the number of coefficients of the calibration model and of the elements to be determined.

This means that a large number of well-characterized calibration samples are required for the preparation of a standard reference material (SRM)-based calibration. They must be prepared and measured in exactly the same way as the unknown sample. It is often an extensive and intricate procedure to prepare and measure all these samples.

Calibration samples are provided by various governmental organizations, for example, the National Institute of Standards and Technology (NIST) in the United States, the Bureau of Analyzed Samples (BAS) in the United Kingdom, the Federal Institute for Materials Research (BAM) in Germany, as well as by various companies for specific material classes (see Table B.2). As previously mentioned, calibration samples are not necessarily available for all analysis tasks. Therefore, it is often necessary to prepare one's own reference samples. This can be achieved by mixing known amounts of high-purity substances or substances with defined compositions. Reference samples can also be prepared by means of a complex analysis of samples with similar composition to the unknown material, for example, by reconstitution analysis (see Section 5.5.5), by round robin tests, or by cross-reference with results of other analytical methods.

In XRF different models can be used for the calculation of the calibration curve. They can be differentiated according to the sample matrix and the range of mass content of the different elements in the sample. These factors determine the calibration effort, i.e. in particular the number of required calibration samples as well as the time and effort for their measurement.

### 5.5.2 Conventional Calibration Models

A general description of the evaluation function can be made by

$$w_i = K_i I_i M_{ij} \quad (5.6)$$



with

- $w_i$  mass fraction of the element  $i$
- $K_i$  calibration coefficient for element  $i$
- $I_i$  intensity of element  $i$
- $M_{ij}$  matrix interaction of the element  $j$  on the analyte element  $i$

If the matrix correction can be neglected, i.e. if  $M_{ij} = 1$ , the simplest form of empirical models is obtained. They can be equations of first or second order, and can be written as

$$w_i = a_{i0} + a_{i1} \cdot I_i \quad (5.7)$$

or

$$w_i = a_{i0} + a_{i1} \cdot I_i + a_{i2} \cdot I_i^2 \quad (5.8)$$

A constant term  $a_0$  is used to take into account background contributions from scattering or peak overlaps. The  $a_{i1}$  terms are called calibration coefficients and describe the sensitivity for element  $i$ . By using second-order models, the error can be reduced and the range over which the calibration curve is valid can be somewhat extended; however, outside this range the deviations increase very fast.

The main drawback of empirical models, which do not consider any matrix interaction, is their limited validity. Sufficient accuracy is achieved only for a very narrow concentration range and considerable errors can occur outside these ranges. As a result, several calibrations are required – not only for different sample classes but also for different concentration ranges; all this is associated with high cost and effort.

By taking into account the matrix interaction the range over which the calibration is valid can be extended. The following approach is often used:

$$M_i = (1 + \sum_j a_j w_j) \quad (5.9)$$

It is assumed that the interaction depends on the concentration  $w_j$  of the matrix elements. Thus, (5.6) can be written as

$$w_i = K_i \cdot I_i (1 + \sum_j a_j \cdot w_j) \quad (5.10)$$

Here again, the  $a_j$  terms are calibration coefficients, which must be determined by calibration. This means that the matrix interaction depends on the mass fractions  $w_j$  of the other elements. Therefore, these models are referred to as concentration corrected. Their use is possible via iterative methods since the mass fractions of the matrix elements in the unknown sample are also not known.

If these mass fractions are approximated by their measured intensities, i.e.

$$w_i = a_i \cdot I_i$$

equation (5.9) can be written as

$$w_i = K_i \cdot I_i (1 + \sum_j a_j I_j) \quad (5.11)$$

In this case, the mass fractions  $w_i$  of the analyte element  $i$  depend only on the intensities of the element to be analyzed as well on the intensities of

the interacting elements. Now, the mass fractions can be calculated directly from the measured intensities without iterative methods. They are called intensity-corrected models.

The calculation of the calibration coefficients can be carried out purely empirically, i.e. they are determined by regression analysis from the measured calibration sample intensities. These approaches have a broader validity, but high accuracies can be achieved. In order to extend the validity range of the models further, various approaches have been developed to base the calibration coefficients on physical models using fundamental parameters.

The first approach was made by Lachance, which resulted in the Lachance–Traill model (Lachance and Traill 1966). Equation (5.10) was then written as

$$w_i = K_i \cdot I_i (1 + \sum_j \alpha_j \cdot I_j) \quad (5.12)$$

Here, the calibration coefficients  $a_i$  were substituted by influence factors, the so-called  $\alpha$  values.

Various models have been developed to determine these influence factors. They have been extensively described and compared in their applicability (see, e.g. Lachance and Claisse 1994 or Mantler 2006). The motivation to develop these various models was to extend the range over which the calibration is valid or to optimize the calibration for specific sample classes and at the same time find calculation procedures with relatively low complexity. It has to be taken into account that the available computing power at that time was not comparable with that available nowadays.

In general, the differences between the various models regarding their analytical accuracy are mainly determined by the quality of the available reference samples. The main differences between the individual models are their range of validity and the number of reference samples required. Calibration efforts are reduced with an increased use of physical models and the associated parameterization of these models.

A specific option to better account for the influence of the sample or to simplify the models is the use of intensity ratios in the form

$$w_i = a_{i0} + a_{i1} \cdot I_i / I_{\text{ref},1} \quad (5.13)$$

with

$a_{ij}$  calibration coefficients

$I_{\text{ref}}$  reference intensity

Such an approach is used for the following purposes:

- *As an internal standard:* In the analysis of liquids, i.e. solutions or melted samples, the analyte intensities can be normalized to the mass fraction of a known quantity of an element that has been added. This is a common method for total reflection X-ray fluorescence (TXRF) spectrometry.
- *For the correction of the matrix influence:* The intensity of the inelastically scattered incident radiation (Compton scattering) depends on the sample matrix. If this scattering is sufficiently strong, i.e. in the case of a light matrix, the matrix influence (for example, by varying matrices, grain size effects, filling density, and sample structure) can be corrected with help of Eq. (5.13).

- *For the simplification of quantification methods:* If the intensities of the analytes in an unknown sample as well as the intensities of the pure elements are measured under the same conditions, their intensity ratios  $R_i = I_i^{\text{analyt}}/I_i^{\text{pure}}$  are independent of the measurement geometry. Quantification by FP models then becomes much simpler.

This method is often used in coating thickness analysis. Usually, the number of elements in these samples is limited; therefore, the effort for measuring the pure elements is less. The pure element spectra can also be used during the peak fit to determine the peak area (see Section 5.4.2).

A special case is the quantification using TXRF. As a result of the very small analyzed sample volume the matrix influence is negligible. Therefore, a linear model can be used as shown in (5.6), usually even without the constant term. Only the linear calibration coefficients  $a_i$  must be determined; in this case, they are referred to as sensitivities  $\varepsilon$ . They have to be determined only once for an instrument. The mass fractions can then be calculated according to

$$w_i = \varepsilon_i \cdot I_i \quad (5.14)$$

The measured intensity, however, still depends on the total sample mass. The samples analyzed with TXRF are often in liquid form. They are dried on the sample carrier. Addition of internal standards, for example, an element solution of known concentration  $w_{\text{standard}}$ , allows for quantification even independent of the sample mass. In this case, the measured element intensities  $I_i$  are related to the intensity of the internal standard  $I_{\text{standard}}$ .

$$w_i = \varepsilon_i / \varepsilon_{\text{standard}} \cdot I_{\text{standard}} / I_i \cdot w_{\text{standard}} \quad (5.15)$$

Thus, quantification using TXRF can be very simple; it requires, however, that any matrix interaction can be neglected. This requires very small sample amounts, in particular in the direction normal to the sample surface. It has to be of the order of magnitude of the absorption lengths of the fluorescence radiation of the analyte elements (see also Section 12.3.2).

### 5.5.3 Fundamental Parameter Models

Despite the use of physical models for determining the influence factors, the validity of these calibrations is still limited to specific sample qualities. It is therefore always necessary to have the appropriate calibration samples for the various sample qualities available. With the availability of sufficient computing power, it is now possible to solve the Sherman equation directly, i.e. the intensity  $I_i$  for the element  $i$  can be calculated for an assumed sample composition. These calculated intensities  $I_i^{\text{calc}}$  can be compared with the measured intensities  $I_i^{\text{meas}}$  of the sample. By varying the starting values of the assumed sample composition  $w_i$  using an iterative calculation process according to (5.16) quick convergence to a solution for the unknown weight fractions can be achieved:

$$w_i^{n+1} = w_i^n \frac{I_i^{\text{meas}}}{I_i^{\text{calc}}} \quad (5.16)$$

A few iterations are usually enough for the calculated intensities to be almost equal to the measured intensities. It can then be assumed that the calculated composition will be almost equal to that of the analyzed material. The method can be used for a wide range of sample qualities with broad concentration ranges.

However, the achievable accuracy for this quantification method is limited for the following reasons:

- The measurement geometry is not exactly known and the specified conditions for the Sherman equation (narrow and parallel beams both for the excitation and fluorescence radiation) are not fulfilled. However, this can be partly compensated by an initial calibration for the geometry factor  $G$  in (5.5).
- The fundamental parameters are not sufficiently well known; there are several parameter errors, in particular for low energies.
- The exact energy density distribution of the excitation spectrum is not known.
- Not all elements can be measured, in particular light elements with atomic number with  $Z \leq 6$  for WDS instruments, and with  $Z \leq 11$  for EDS instruments.
- In most cases, only first and second order interactions are taken into account; third order effects are mostly ignored.
- The Sherman equation does not consider all interactions, for example, scattering effects and interatomic and intra-atomic effects.

In order to improve the analytical accuracy specific calibrations can be applied. In this case, the calibration method does not require a complete set of reference samples. For a sample with known composition, i.e. for a reference sample, the elements intensities can be measured ( $I_i^{\text{meas}}$ ) as well as calculated with the help of the quant-model ( $I_i^{\text{calc}}$ ). These intensities can then be used to determine an element sensitivity  $S_i$  according to

$$S_i = \frac{I_i^{\text{meas}}}{I_i^{\text{calc}}} \quad (5.17)$$

In the next step, these sensitivities can be used to correct the calculated intensities. Predicted intensities  $I^{\text{predict}} = S \cdot I^{\text{calc}}$ , which can then be used in the above-described iterative quantification procedures (5.16). For their determination the reference sample does not need to be equivalent to the unknowns, because the element sensitivities are largely independent of the sample type. It is further possible to use this procedure only for selected elements, for example, to avoid a negative impact on the accuracy of calibration, due to a high statistical error of certain elements caused by their low intensities.

Use of this quantification method requires operating under some basic conditions:

- The element intensities for all elements present in the sample must be determined. Otherwise, as a result of the missing elements errors will occur during the calculation of the matrix interaction. This requirement is difficult to fulfill, especially for light matrices, for example, for polymers or oils and for samples with organic ingredients but also for minerals with elements in different oxidation states or for carbonates, sulfides, etc. Here, however, the

matrix-dependent Compton scattering can be used for the characterization of the absorption of the fluorescence radiation for different matrices.

- For an accurate quantification, higher order terms, at least the second order, must be taken into account in the Sherman equation. This will complicate the Sherman equation and increase the computing effort. Third order terms are usually ignored, since their influence is only notable in very special cases.
- Fundamental parameters need to be known as accurately as possible. There are different data sets available that summarize them (Elam et al. 2002; Schoonjans et al. 2011). The accuracy of the data depends on the parameter itself and on the energy; line energies are relatively well known, while absorption or scatter coefficients are not so well known, in particular for lower energies. They are being continuously improved – the most current version will be shown in xraylab (see Table B.3.1)
- The Sherman equation does not take scattering effects into account and will therefore increase the uncertainty of the analysis result. However, scattering effects are relatively small, in particular for heavy matrices and for low energies.
- Cascade effects that influence the measured intensities of the L- and M-series lines are not considered and contribute to the measurement uncertainties. If possible, lines of higher energies should be used for quantification. Cascade effects can occur within an atom, for instance, when after the generation of a  $K\alpha$ -line the resulting vacancy in the L-shell is filled and an additional quantum is emitted. Cascade effects can also take place between atoms in a sample when the released photo- or Auger electron is absorbed in an adjacent atom and as a result this is ionized.
- The exact measurement geometry is usually not known. In order to determine the geometry factor the measurement of intensities of several pure elements or of reference samples is required. For the theoretical calculation of the geometry factor precise information about the opening angle of the incident beam and of the incidence and take off angle of the primary and fluorescence radiation would be required. The solid angle of the detector also needs to be known.
- On the other hand, quantification carried out with the help of the Sherman equation is not only independent of the sample type, but it can also be carried out for different excitation conditions when the excitation spectrum  $I_0(E)$  is known in (5.5). The excitation spectrum can either be theoretically calculated or derived from a measured scatter spectrum.

Fundamental parameter-based quantification models are often called as “standard-less.” However, this is only valid for the instrument user. Depending on the actual model a few or even a large number of calibration samples were measured for the calculation of the geometry factor and of individual influencing factors during the calibration procedure, respectively. However, this has to be carried out only during the initial installation; the corresponding spectra and the associated statistical data are stored for later use in libraries. These data can also be used for recalibration, which is necessary after a longer working period for the compensation of aging effects or, for example, in the case of exchanging instrument components, such as the tube. Then only a few setup samples must be measured, and the influence coefficients can be determined again.

### 5.5.4 Monte Carlo Quantifications

Owing to the detailed knowledge of all interactions of photons with matter it is possible to trace the path of a photon in the sample as well as in the detector. An exact tracing of an individual photon however is impossible because the probability for the different interaction processes is not an absolute value. Nevertheless, the paths of a very large number of individual photons will give an appropriate image about the complex processes when every interaction is considered as an uncertain response in the frame of the known probabilities by using random numbers. The number of individual photons paths that need to be calculated must be in the range of at least  $10^5$ , most often even more.

All interactions in the sample need to be modeled, i.e. the elastic and inelastic scattering, the absorption by the photoelectric effect and the emission of photoelectrons, Auger electrons and fluorescence photons and their absorption in the sample, and finally the recording of the fluorescence and the scattered radiation in the spectrometer.

For modeling, the composition of the sample also has to be taken into account. For a large number of individual photons this requires a very high computing effort, especially if for quantification the sample composition has to be iteratively changed until convergence between the measured and the calculated spectra is reached. For this reason, these models are currently used only in very special cases to quantify a sample. If increased computing power becomes available, it will be possible to also use Monte Carlo methods for quantification within an acceptable time. While the Sherman equation usually considers only the intensity of a single analyte line, Monte Carlo modeling takes into account the complete series. This also allows for example the analysis of non-infinity thick samples.

Currently, this method is used to model the analytical instrument performance for varying instrument or excitation parameters. The contributions of different interaction processes to the result can be modeled and the method can also aid in the optimal design of a measurement geometry or to model processes in the tube or the detector. A freeware software package for these methods is available (Vincze et al. 1993; Schoonjans et al. 2013; Schoonjans 2017).

### 5.5.5 Highly Precise Quantification by Reconstitution

The matrix interaction becomes negligible if the unknown and the reference samples are nearly identical. This means that the spectra of the sample and the reference sample must be compared. The two spectra should be as identical as possible. That can be achieved by a stepwise adaptation of the reference sample.

Reference samples that are identical to the unknown sample are usually not available; then they must be specifically prepared, i.e. their reconstitution is necessary. Step-by-step the composition of the unknown sample has to be matched by the composition of the reference samples. This type of quantification is therefore also called bracketing technique (Staats and Noack 1996; Michaelis 2005). This method can be used for samples such as metallic alloys or oxides. As a result, the calibration curve increasingly fits the conditions of the analysis sample (see Figure 5.18). The reference samples can be prepared from high-purity materials

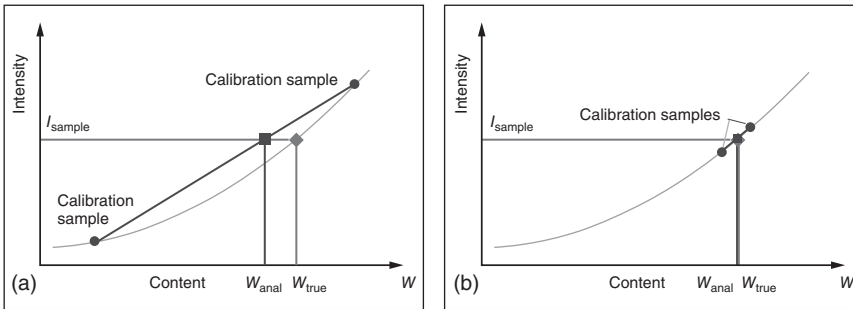


**Figure 5.18** Bracketing method for highly accurate analysis with two different distances between the calibration sample.

so that the composition can be traced back to basic units. This, however, requires a large effort in the sample preparation since the reference samples must be in the same form as the unknown samples. This not only applies to their composition but also to their homogeneity, the state of the sample surface, the grain size distribution as well as, if possible, the chemical bonding conditions.

By narrowing down the composition range in such a way, very high analytical accuracies can be achieved. Measurement uncertainties under 0.2% can be achieved provided that all other uncertainty contributions are kept correspondingly small, i.e. the statistical errors are very small, the instrument influence is negligible, etc.

This process does require much effort and it can require a period of several days or even weeks before the analysis can be completed. Therefore, this is not an analysis technique that can be used for many samples, but it is quite suitable for the characterization of reference materials.

Another possibility to precisely characterize a sample was described by Schramm (2016). He proposes that the well-prepared, i.e. sufficiently milled and homogenized, samples to be analyzed as well as a reference sample that is as close as possible in regard to the composition and consistency to the unknown are measured under the same conditions within short time intervals, for example, 10 times. The measurements on these samples has to be carried out in pairs in succession and under the same conditions. Then the mean deviations of the analyses results are determined from the measurements of both the unknown sample and the reference sample. For the reference sample, the deviation from the reference values is also determined. The scattering of the results from the unknown and the reference sample give information about the repeatability of the measurements from which the contribution to the total uncertainty can be obtained. The reason for drift or extreme deviations should be investigated, and those measurements may be omitted. Deviations of the results from the nominal values of the reference sample can be used for the correction of the results determined on the unknown sample. A highly accurate quantification is also possible in this way; however, the effort for sample preparation is less than that for the previously described method of reconstituting the sample.

### 5.5.6 Evaluation of an Analytical Method

Both the analytical accuracy of an analysis and its sensitivity are important criteria for assessing its quality. The accuracy can be evaluated by measuring reference samples of known composition. Comparing the known concentrations, or in the case of layer analyses, thicknesses with the measured values, the trueness of the values can be used as a measure of the quality of the calibration. Detection limits are a criterion of the sensitivity.

#### 5.5.6.1 Degree of Determination

An idea of the quality of an analytical method can be obtained by comparing the nominal and analyzed mass fractions. This is demonstrated for the same data set in the diagrams shown in Figure 5.19. In panel (a) the analyzed values are plotted against the nominal values. The identification of large deviations is possible here, but overall evaluation is difficult. A better measure is given by the correlation coefficient  $R^2$ , which allows for a good assessment of the results.

This correlation coefficient  $R^2$  can be calculated as

$$R^2 = \frac{\sum_i (x_i - \bar{x}) \cdot (y_i - \bar{y})}{\sqrt{\sum_i (x_i - \bar{x})^2 \cdot \sum_i (y_i - \bar{y})^2}} \quad (5.18)$$

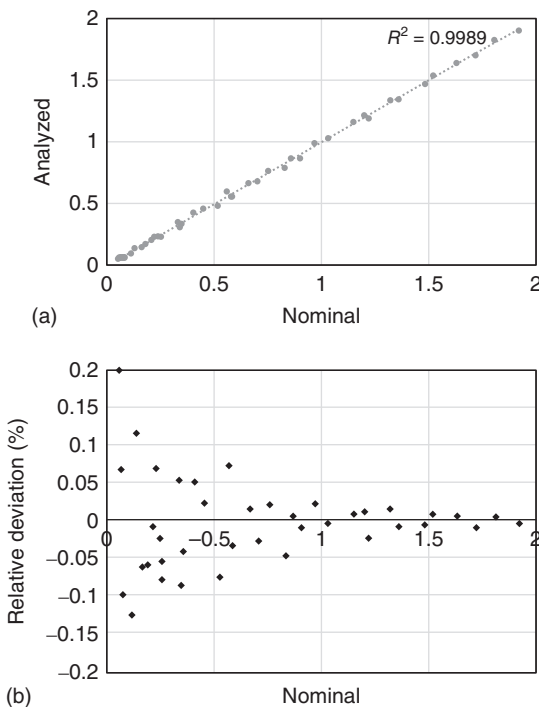


**Figure 5.19** Representation of the trueness of an analysis method: (a) comparison of nominal and analyzed and (b) relative deviations from the nominal values.



with

$x_i, y_i$  given and analyzed values  
 $\bar{x}, \bar{y}$  mean values of the given and analyzed values

If the value of  $R^2$  is close to 1, the correlation between the nominal and analyzed values is high. If the deviations are large, the correlation coefficient becomes smaller. The correlation coefficient however is dominated by deviations at higher concentrations. This means that deviations at higher concentrations affect it more strongly than those at lower concentrations. Nevertheless, it is frequently used, and it is a meaningful parameter for the quality of calibration. The correlation coefficient can easily be calculated, for example in Excel.

Figure 5.19b shows the relative deviations from the nominal values and thus gives a better overview of the trueness. The deviations are relatively small for large contents, but increase for small contents, since the smaller intensities with their larger statistical error result in a greater uncertainty.

### 5.5.6.2 Working Range, Limits of Detection (LOD) and of Quantification

The working range of an application depends on the element concentrations of the calibration samples used. For an empirical calibration this is especially important since the calibration curves that are determined by mathematical regression can show considerable deviations outside of this range.

In general, XRF has no upper concentration limit that can be analyzed in contrast to other analytical methods (see Table 7.1), and can therefore be used for the analysis of pure elements too.

Layer thicknesses analysis, however, has an upper limit to the measuring range, which is determined by the saturation thickness of the layer (see Figure 5.24).

The lower limit of the working range of an analytical method is determined by the limit of quantification of an analyte. It characterizes its sensitivity. The limit of quantification is the smallest concentration of an analyte that can be quantified within a defined statistical confidence. The limit of quantification  $w_{\text{LOQ}}$  is usually defined as three times the value of the detection limit  $w_{\text{LOD}}$ . The detection limit  $w_{\text{LOD}}$  is the concentration, which by using a calibration curve and under consideration of a given statistical confidence, is higher than in a blank sample (see DIN-32645 2008). The confidence level usually is 1% (i.e.  $3\sigma$ ).

The limits described above are illustrated in Figure 5.20. Shown is the calibration function

$$y = y_0 + b \cdot w \quad (5.19)$$

as well as an uncertainty interval, which is given by the level of significance. The calibration function at  $w = 0$  is equal to the blank value  $y_0$ . The uncertainty interval intersects the  $y$ -axis at the critical value  $y_{\text{crit}}$ . If this critical value is exceeded, based on the established error probability, the concentration of the component in the analysis sample is assumed to be greater than that in the blank sample. Using the established calibration function the detection limit  $w_{\text{LOD}}$  is then the associated concentration of the critical value  $y_{\text{crit}}$  of the measurand (DIN 32645).

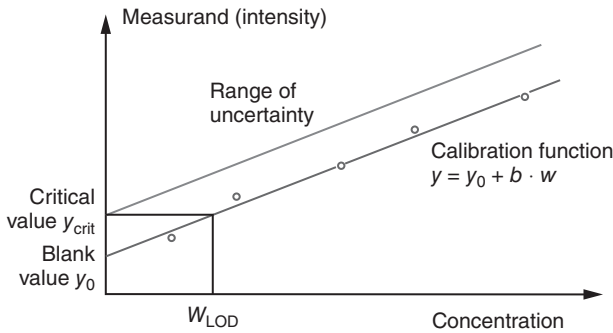


**Figure 5.20** Determination of the limit of detection from the calibration function.

Assuming a purely statistical distribution of the measurement value, the critical value is then  $y_{\text{crit}} = y_0 + 3\sqrt{y_0}$ . Equation (5.16) then becomes

$$w_{\text{LOD}} = \frac{3\sqrt{y_0}}{b} \quad (5.20)$$

where  $b$  is the slope of the calibration function near the detection limit. For the determination of the LOD in this way the calibration curve must be known close to this limit. Since the required calibration samples are not always available, the determination of the LOD is often carried out using the so-called blank value method or the  $3\sigma$  criterion (DIN 32645). It is assumed that

$$w_{\text{LOD}} = \frac{3 \cdot \sqrt{N_{\text{BG}}}}{N_{\text{sample}}} w_{\text{sample}} \quad (5.21)$$

with

$w_{\text{LOD}}$	Limit of detection for a given element
$N_{\text{BG}}$	background counts at the location of the count rate for the element
$N_{\text{sample}}$	count rate of the element
$w_{\text{sample}}$	concentration of the element in the sample

This method provides a useful value for the LOD, but only for small concentrations  $w_{\text{sample}}$ ; in addition, the LOD for a specific analyte can also depend on the other constituents of the sample. For example, peak overlaps or the increase of the spectral background by a light matrix is associated with a degradation of the LOD. On the other hand, it is also possible to improve the LOD by optimizing the measuring conditions, such as the excitation conditions or the measuring time. When the measured counts  $N$  in (5.21) are substituted by the product of the counting rate (CR) and time  $t$ , that is,  $N = \text{CR} \cdot t$ , the standard deviation of the background increases with the square root of time, but the counts of the reference sample increase proportionally with time, i.e. the LOD can therefore be reduced by  $1/\sqrt{t}$ .

### 5.5.6.3 Figure of Merit

For the best instrument performance, the instrument settings (see Section 4.2.8) have to be optimized. Often parameters such as the peak-to-background ratios or the LOD are used to gauge the measurement conditions. But these parameters do not allow for an optimal selection of the settings – a good peak-to-background ratio will not give the best LOD. Furthermore, it would be helpful to have only a single parameter – figure of merit (FOM) – for the assessment of test conditions or even for the general assessment of any analytical method. Willis et al. (2014) proposed the following relations for X-ray spectrometry for major and minor components,

$$\text{FOM} = \sqrt{\text{CR}_i^{\text{meas}}} - \sqrt{\text{CR}_i^{\text{background}}} \quad (5.22)$$

and the following for traces:

$$\text{FOM} = (\text{CR}_i^{\text{meas}} - \text{CR}_i^{\text{background}}) / \sqrt{\text{CR}_i^{\text{background}}} \quad (5.23)$$

where CR are the count rates for the analyte  $i$  and the corresponding background. The highest FOM values provide the smallest statistical error and the best LOD.

### 5.5.7 Comparison of the Various Quantification Models

An important condition for an accurate analysis is to obtain a high number of counts for the analyte, i.e. choosing the most effective excitation conditions for the analyte. On the other hand, the precise determination of the peak intensities is important as well. Because of the different resolution of ED and WD instruments this is achieved differently for the two types of instruments (see Section 5.4.2) – for WD instruments by measuring at the peak maximum, and for ED instruments by determining the peak area. The accuracy then depends on the resolution of the detector.

This is demonstrated by the measurements of more than 80 reference samples of precious metal alloys with gold concentrations in the 33–100 wt% range. They were analyzed using identical measurement geometries and excitation conditions, but with detectors with different resolutions – a proportional counter and a silicon drift detector (SDD). Owing to the smaller effective detector area of the SDD the count rates are smaller by a factor of 3. As a result, the statistical error for this detector is approximately 1.5 times higher. In each case an intensity-corrected matrix correction was used. Figure 5.21 shows the absolute deviations of the gold concentrations from the nominal values of the reference samples.

The differences between the two distributions are only marginal; the mean deviation of the measurements with the proportional counter is 0.145 and 0.122 wt% for the measurements with the SDD. Despite the smaller intensities in the measurements with an SDD and the associated larger statistical error, a smaller error is made in the peak area determination due to the better resolution of the SDD and the consequent smaller overlap of peaks. This more or less compensates the larger statistical error from the count rate by the smaller error associated with the peak area determination.

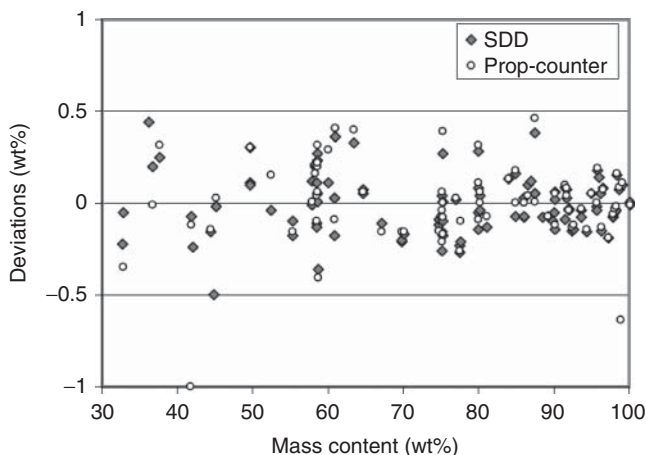


**Figure 5.21** Deviations of the gold concentrations measured with SDD and proportional counter instruments.

The achievable analytical accuracies are also influenced by the quantification model used. In particular, there is a difference between empirical models and fundamental parameter-based models.

The highest accuracies are usually achieved by sample-specific calibrations, i.e. standard-based calibrations prepared for a specific sample type. As previously described, their useful range is limited. For samples outside the calibrated concentration range, the results of the analysis can show strong deviations from the nominal values and the preparation of a sufficient number of calibration samples can be problematic.

Fundamental parameter-based models, on the other hand, have a wider range of validity and can also be used with only very few or even without standards. Since often a normalization of the concentrations to 100% is used it requires the measurement of all elements present. Only then the matrix interactions are considered correctly. For WDS instruments this requires a greater measurement effort in order to scan the entire wavelength range, while EDS instruments do not require any additional effort due to the simultaneous measurement of all elements. Unfortunately, very light elements such as carbon, oxygen, or nitrogen cannot be analyzed routinely with XRF; however, often they are in considerable concentrations in the sample and have a strong influence on the result.

In order to demonstrate the influence of the quantification model on the trueness of the analysis, the previously measured SDD data set of the precious metal samples was evaluated using an empirical and a fundamental parameter-based model. The results are illustrated in Figure 5.22. With standard-based models the deviations are significantly smaller. Since the range of the standard-based calibrations is limited, several calibrations had to be used to cover the entire concentration range, which typically ranges from about 30 to 100 wt% gold in jewelry. The different calibrations incorporate the most commonly used gold contents, i.e. 8–10, 14, 18, and 22–24 Karat. The mean deviations for the standard-based analysis are 0.12 wt%, and for the standard-free analysis 0.8 wt%. Despite the lower accuracies, in many cases standard-free models deliver satisfactory results for the analysis of materials.

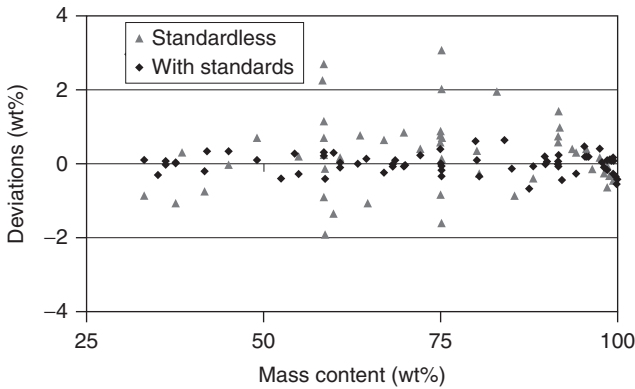


**Figure 5.22** Comparison of the accuracy of standard-based and standard-free models for the quantification of gold in jewelry.

### 5.5.8 Available Reference Materials

Reference materials are offered in a few grades. They can be differentiated as follows:

- *SRM – standard reference material*: Is a denomination reserved for certified reference material (CRM) that is issued, for example, by the NIST. One or more properties are certified, and the standards are accompanied by a certificate stating their uncertainty and traceability.
- *CRM – certified reference material*: Material with one or more certified properties, accompanied with a certificate stating their uncertainty and traceability.
- *RM – reference material*: Material having one or more characteristics characterized for a particular purpose.

In addition, there are other reference sample types that are not officially certified, but which can play an important role in an individual laboratory.

- Secondary reference materials or company standards, which are in-house, often very precisely characterized references using SRMs or CRMs, used for specific purposes.
- Instrument reference samples used for the characterization of the measuring instrument, such as drift correction, recalibration, etc. These samples do not have to be well characterized and their composition does not necessarily have to be known, but they need to be very stable and homogeneous.

SRMs, CRMs, and RMs are usually issued by government institutions. Usually a certificate is available, which provides information on the attested properties. For element analyses, the data includes the concentrations, the uncertainties of the data, the methods used for their determination, and any particular conditions to be considered when using them (drying, stability, etc.).

Company standards and instrument reference samples are not subject to these strict requirements. They can be manufactured or purchased by the company. Characterization may also be carried out by the company itself; for certain applications, a determination of the content can be omitted, for example, for drift correction.

Reference materials should be handled carefully in order that they will not be contaminated or damaged; they should be stored in a clean, cool, and dry environment. For the preparation of a measurement sample the same procedures should be used as for the unknown sample. The main suppliers of certified standard materials are summarized in Table B.2 with links to their catalogs.

An often used method to prepare reference samples is the round robin test. In this case, various laboratories with different methods characterize a material. By a statistical evaluation the reference values are defined. However, it is necessary to use the appropriate analytical methods because this type of “democratic” analytical results can easily give wrong results.

Calibration samples can also be prepared by the instrument user itself. One possibility was already described with the reconstitution method (Section 5.5.5), where the references are manufactured from pure materials. Another possibility is the quantification of samples with highly accurate analytical methods, for example, by using synchrotrons where the spectrum of excitation beam and the measurement geometry are exactly known.

Another possibility is to use the standard addition method for the preparation of calibration samples. In this method the mass fraction of one or more elements is increased by the admixture of specific oxides or compounds that contain the element. This procedure can easily be used for liquid samples, for geological samples and polymers it is applicable for both pressed pellets and fusion beads. It is crucial that the additives are very pure to avoid any contamination.

The known differences of mass fractions as well as the comparison with a blank sample allow the preparation of a calibration curve that is valid for a limited concentration range. The quantity of additives must be taken into account to obtain the correct relation between sample material and additives when mixing the sample material with a binder (for pressed pellets) or with a flux (for fusion beads).

Substances that can be used for this purpose are summarized in Table 5.3. Suppliers of pure materials are summarized in Table B.2.4.

According to a proposal by Schramm (2018) it is possible to prepare reference samples by a 3D-print procedure. The 3D-print process produces a pellet from a polymer. The pellet contains holes in which the reference materials as given in Table 5.3 can be added. The reference material in that case will not be homogeneous. This problem can be solved by the analysis of larger sample areas and by spinning the sample. The advantage of the method is that a wide range of mass fractions of many different materials can be added.

### 5.5.9 Obtainable Accuracies

Sampling and preparation effects strongly influence the quantification accuracies that are obtainable with XRF (see Section 6.1). If these influences are not considered, the precision of the measuring instrument is primarily responsible for the analytical error. The statistical error of the measurement and the stability of the instrument are therefore of crucial importance.

The quality of the calibration samples – in particular their homogeneity, stability, surface quality, and the accurate knowledge of their mass components, including their uncertainties – has great influence on the quantification process itself. Finally, the mass components themselves influence the measured intensities and thus the achievable analytical accuracies.

**Table 5.3** Substances suitable for standard addition.

Analyte	Substance	Analyte	Substance	Analyte	Substance
F	CaF <sub>2</sub>	Ni	NiO	Sb	Sb <sub>2</sub> O <sub>3</sub>
Na	NaCl	Cu	CuO	Te	Te <sub>2</sub> O <sub>3</sub>
Mg	MgO	Zn	ZnO	I	KI
Al	Al <sub>2</sub> O <sub>3</sub>	Ga	Ga <sub>2</sub> O <sub>3</sub>	Cs	CsCl
Si	SiO <sub>2</sub>	Ge	GeO <sub>2</sub>	Ba	BaCO <sub>3</sub>
P	KH <sub>2</sub> PO <sub>4</sub>	As	As <sub>2</sub> O <sub>3</sub>	La	La <sub>2</sub> O <sub>3</sub>
S	CaSO <sub>4</sub>	Se	SeO <sub>2</sub>	Ce	Ce <sub>2</sub> O <sub>3</sub>
Cl	NaCl	Br	NaBr	Hf	HfO <sub>2</sub>
K	KCl	Rb	RbCl	Ta	Ta <sub>2</sub> O <sub>5</sub>
Ca	CaCO <sub>3</sub>	Sr	SrCO <sub>3</sub>	W	WO <sub>3</sub>
Ti	TiO <sub>2</sub>	Y	Y <sub>2</sub> O <sub>3</sub>	Pb	PbO
Cr	Cr <sub>2</sub> O <sub>3</sub>	Zr	ZrO <sub>2</sub>	Bi	Bi <sub>2</sub> O <sub>3</sub>
Mn	MnO <sub>2</sub>	Nb	Nb <sub>2</sub> O <sub>5</sub>	Th	ThO <sub>2</sub>
Fe	Fe <sub>2</sub> O <sub>3</sub>	Mo	MoO <sub>3</sub>	U	U <sub>3</sub> O <sub>8</sub>
Co	Co <sub>3</sub> O <sub>4</sub>	Sn	SnO <sub>2</sub>		

For the various sample qualities, instrument types, and concentration ranges the typical achievable uncertainties are given in Table 5.4.

When specifying the results, the expected uncertainties should also be considered, i.e. the declaration of an analytical result should also reflect the expected analytical accuracy. For uncertainties <5%, the specification of two significant figures is sufficient and appropriate; three figures are only useful for uncertainties <0.5%.

## 5.6 Characterization of Layered Materials

### 5.6.1 General Form of the Calibration Curve

The characterization of thickness and composition of layered materials can also be performed by X-ray spectroscopic methods. Layer analysis is a very common

**Table 5.4** Analytical uncertainties for different sample qualities, measuring instruments, and quantification models (given in rel.%).

Sample composition	Content range (wt%)	WDS	EDS	FP-model	FP with type calibration
Traces	<1	1–5	1–10	>10	≈10
Minors	1–10	0.5–1.0	0.7–1.2	≈2.5	≈1
Majors					
Powder	>10	0.8–1.2	0.8–1.2	≈1.5	≈1.0
Pellets		0.3–0.5	0.5–0.8	≈1.0	≈0.7
Glass tablets		0.2–0.4	0.3–0.6	≈0.7	≈0.5

analytical task, especially in the quality control of finished products, since their surfaces are often coated for decorative or functional reasons.

When exciting a layer system, both the layer and the substrate are excited and emit fluorescence radiation. The substrate signal is absorbed by the overlaying layers. Both signals can be used for the evaluation. The absorption of X-rays is described by the Lambert–Beer’s law (2.5).

The intensity of the layer signal can be described by the Sherman equation given in (5.24) with an additional term that takes into account the finite thickness of the analyzed sample.

$$I_i = G \cdot \int_E \frac{w_i \cdot \tau_i \cdot \frac{S-1}{S} \cdot p_i \cdot \omega_i}{A} \cdot I_0(E) \cdot \{1 - \exp(-A \cdot \rho \cdot d)\} \cdot dE \quad (5.24)$$

Here,  $A = \mu(E)/\sin \psi_{\text{in}} + \mu(F)/\sin \psi_{\text{take off}}$  takes into account the absorption of the excitation radiation as well as of the fluorescence radiation, and  $\rho$  and  $d$  are the density and the thickness of the layer.

If the ratio of the layer intensity  $I_{\text{sample}}$  to the intensity of an infinitely thick layer  $I_{\infty}$  of the same element measured under the same conditions is used, the integral can be neglected, and the following simplified relationship can be used:

$$R = \frac{I_{\text{sample}}}{I_{\infty}} = 1 - \exp(-A \cdot \rho \cdot d) \quad (5.25)$$

Based on this formula, a general form of the calibration curve for layer systems can be established for the emission and absorption signal (see Figure 5.23). Their slope essentially depends on the absorption characteristics of the layer, i.e. their mass attenuation coefficients  $\mu$  and density  $\rho$ .

At first, the emission signal increases linearly with thickness, but then the intensity ratio  $R$  approaches asymptotically the value of 1 for an infinitely thick sample. The infinite thickness value is subject to the self-absorption of the fluorescence radiation in the layer material, i.e. it depends on the energy of the fluorescence radiation as well as the mass attenuation coefficient of the layer material. It ranges for pure elements from a few micrometers to a few tens of micrometers.

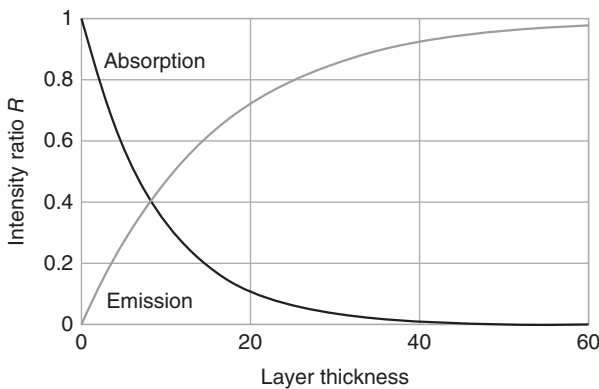


**Figure 5.23** Typical calibration curves for the emission and absorption signal of layered samples.



The substrate signal is absorbed in the layer, i.e. it is almost unaffected by a very thin layer, whereas with thicker layers the substrate intensity decreases. This signal can only be used with single layers since in multilayer systems, the contribution of the individual layers to the absorption cannot be uniquely determined. For single layers, the use of the substrate signal offers some advantages – for example, distance-independent analyses are possible and influences from the size of the analyzed area on the analysis result can be corrected. It should also be mentioned that with the help of the absorption method under certain conditions, it is also possible to analyze layers of very light elements from which no measurable signal is emitted.

As with the analysis of bulk materials these simple calibration curves become more complex by including secondary and tertiary interactions. In addition to the interactions within a layer, interactions between the layers and the substrate must also be considered. These interactions can strongly influence the characteristics of the calibration curve, particularly for multi-element layers.

In the case of layer analysis, the mass per unit area  $Q$  is determined, i.e. the mass or the number of atoms of an element per unit area. Since this is a slightly unusual parameter for a layer, it is usually converted into layer thickness  $d$  according to

$$d = Q/\rho \quad (5.26)$$

For this purpose, the density  $\rho$  of the layer material must be known. For pure element layers the density of the respective element can be used even if it can deviate from this value for very thin layers; for alloy layers the average density must be calculated as

$$\frac{1}{\rho_{\text{alloy}}} = \frac{1}{\rho_1} + \frac{1}{\rho_2} \quad \text{or} \quad \frac{1}{\rho_{\text{alloy}}} = \sum_i \frac{1}{\rho_i} \quad (5.27)$$

With very thin layers and depending on the coating method this density can vary. Variations in density can also occur in intermetallic or for different chemical states of the layer materials. This is important and needs to be kept in mind when evaluating layer thicknesses. Comparative measurements on cross sections perpendicular to the sample surface can be useful. However, this method is destructive, time consuming, and the obtainable accuracies are much less than with a well-designed XRF measurement.

### 5.6.2 Basic Conditions for Layer Analysis

The following specifics are unique for coating thickness analysis and must be considered during the analysis:

- The analysis is usually performed as a quality control tool in industrial process control. This means, the layer structures, in particular the layer sequence as well as the elements found in the layers, are known. This information is essential and must be used for the correct evaluation of the absorption conditions in the individual sample layers.
- Layer analyses are usually performed on finished or semi-finished products; they are often inhomogeneous and also irregularly shaped. Consequently, a

nondestructive analysis mostly has to be carried out on a small sample surface under set geometry conditions. Typical spot sizes are less than 1 mm, sometimes even as small as a few tens of micrometers. This limits the amount of radiation available for the excitation and also affects the sensitivity of the measurement. It is therefore required that a large solid angle of the fluorescence radiation is collected by the detector. This is possible with EDSs that have large-area detectors, or which can work at very short measuring distances.

- The individual layers often contain only one or a few elements. Their limited number and their knowledge simplify the spectroscopic requirements for layer analyses. For a long time, proportional counters were used for this task. They have large sensitive areas, in tens of square centimeters, but on the other hand only a limited energy resolution. However, knowing what elements to expect, a sufficiently precise determination of the peak area using fitting procedures is possible. Nevertheless, the analyses of very thin layers require the use of detectors with a better signal-to-noise ratio, i.e. with better energy resolution to meet the required sensitivity.
- For every unknown parameter one analyte line must be measured. That is, for every thickness as well as for every element concentration within a layer a separate line has to be available. Normalization of the element concentration to 100% within an alloyed layer is possible to reduce the number of lines by one. If possible, the X-ray lines should be selected such that they have a high sensitivity and allow for sufficient accuracy. For thin layers or small concentrations, a steep slope of the calibration curve is helpful. The X-ray line can be changed for the same layer system depending on the thickness and composition.
- The measurable layer thickness range covers up to 5 orders of magnitude and is strongly element dependent. For thick layers the limitation is given by the information depth of the fluorescence radiation. This is equivalent to the layer thickness, for which no significant signal increase is generated by increasing the layer thickness (see Section 3.2.3).

For thin films, i.e. close to the detection limits, the limitation again depends on the layer material, but also on the spectrometer type. Instruments with proportional counters can only analyze relatively thick layers since these detectors have a limited signal-to-noise ratio due to their low resolution. With high-resolution detectors, such as SDDs, better sensitivities are obtained due to their higher resolution.

For example, Au layers for printed circuit board (PCB) applications should be greater than 100 nm in order to be measurable with a proportional counter. The better peak-to-background ratio of SDD instruments allows the routine measurement of Au layers as low as 1 nm (see Figure 5.24).

- For certain elements the lowest detection limits can be achieved by means of vacuum measurements. By eliminating the air between the sample and detector the fluorescence radiation is less absorbed. As a result, lower energy X-ray lines (for example, L series instead of K series for elements with atomic numbers between 40 and 50 and the M series instead of the L series for elements with atomic numbers between 72 and 83) can be used for the analysis. For these low-energy lines, the information depth is significantly lower (for gold the information depth is about 0.5  $\mu\text{m}$  for the M-lines and about 5  $\mu\text{m}$  for the

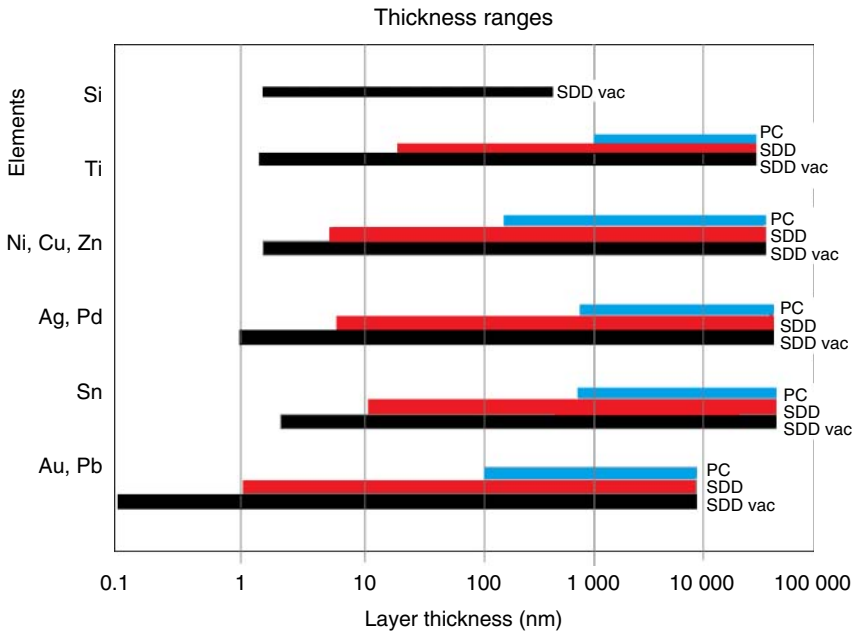


**Figure 5.24** Measurable layer thickness ranges for certain element groups and different instrument classes (PC, prop-counter; SDD, silicon drift detector; vac, measurement in vacuum).

L-lines). This means that the entire intensity range is shifted to a smaller layer thickness range, which leads to an increase of the slope of the calibration curve and thus its sensitivity.

The measurable layer thickness ranges for usual coating elements as well as for different instrument types are summarized in Figure 5.24.

- During measurements of multilayer systems, the sensitivities for buried layers are reduced as a result of both the absorption of the excitation radiation and the absorption of the emitted fluorescence radiation by the layers on the top. This means that the LOD, i.e. the thinnest layers measurable as well as the upper limit of the measurement range, are restricted.

The obtainable accuracies in layer analyses depend strongly on the layer thicknesses as well as the position of the layer within a layer stack, but also, of course, on the measurement time. The accuracy in the analysis of buried layers is usually lower. This is the direct result of the decrease in the intensity of the layer signal, but also because the errors made in the characterization of the upper layers have an additional influence on the buried layers.

- The layer thickness influences through the measured intensity the analytical error. Thinner layers generate only small intensities, which are associated with larger statistical errors. For thicker layers, the slope of the calibration curve decreases, i.e. small intensity changes are associated with large changes in layer thickness. Therefore, the best accuracies are obtained in the middle range of the calibration curve.

- The number of detectable layers depends primarily on the absorption of the fluorescence radiation in the upper layers, which depends on their composition and thickness.

The various possibilities for the characterization of layers are presented as examples in Chapter 14.

### 5.6.3 Quantification Models for the Analysis of Layers

The matrix interactions in layer characterization are more complex than for the analyses of homogeneous bulk samples; besides the interactions within every layer also the interactions between the layers, including the substrate, must be considered. Therefore, the Sherman equation has to be amended by a further term, which takes into account both the influence of a limited material thickness (see (5.24)) and the absorption of incident and fluorescence radiation in the upper layers (Mantler 1986; de Boer 1990; de Boer and Brouwer 1990; Rössiger and Nensel 2006). Moreover, it is necessary to add the term considering secondary interactions. This makes the mathematical model more complicated and requires additional computing time; however, it allows standard-free quantification for an iterative forward calculation.

Another possibility for quantification is a forward calculation of the intensities of all elements for varying layer thicknesses and compositions of a given layer system using the Sherman equation where the mentioned extensions are included. Theoretically determined calibration curves are obtained when these intensities are plotted against the layer thickness. These curves can be improved and adapted to the actual measurements by only a few standards (see Figure 5.25).

The achievable accuracies are limited due to the reasons already mentioned in Section 5.5.3. The use of reference samples typically improves the analytical performance. For the above-described procedure, the reference samples are only used for a correction of the theoretically determined calibration curve but not

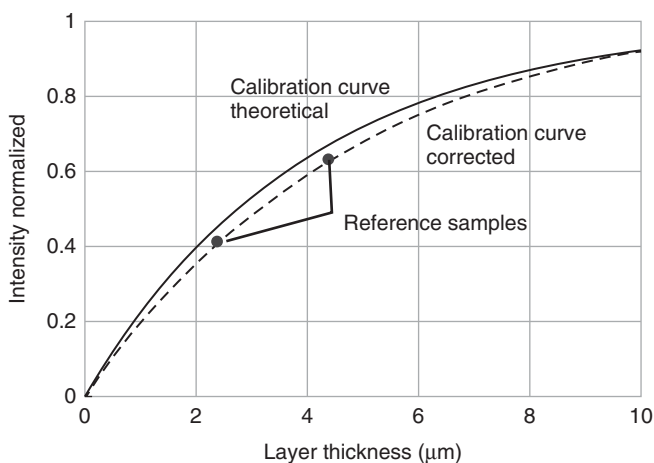


Figure 5.25 Corrected calibration curve using two reference samples.

for its complete calculation. It requires a small number of reference samples and only involves small changes to the theoretical calibration curve.

Another possibility to simplify the approach to Sherman's equation (5.24) for the quantification of layered materials is the use of relative intensities  $R_i$ , in reference to the intensities  $I_\infty$  of the pure infinite element  $i$  (see also Section 5.5.2). If these intensities are measured under the same conditions as the unknown samples the integral can be reduced to the ratio  $I_{\text{unknown}}/I_\infty$ . As a result, the calibration curves for all layers will all have a similar shape. Their slope and information depth are determined by the mass attenuation coefficient  $\mu$  and the density  $\rho$  of the respective layer elements (see Figure 5.23). The pure element spectra that are required for the calculation of the calibration curves are often also used for fitting the measured spectra for the peak area determination; this is often called reference deconvolution. This procedure automatically takes into account detector artifacts during the fitting process but requires stable instruments.

Finally, a strictly empirical method for the determination of a calibration curve is possible by using regression methods, which is a strictly empirical calibration and does not take any secondary excitation into account and therefore cannot be used universally. Further, a complete set of reference samples is required. The availability of suitable and well-characterized reference samples is required for any standard-based quantification models. This can be difficult because the possible types of layer systems are extremely large, both in terms of layer sequences and layer thicknesses and layer compositions.

In addition, the number increases even more by the possibility of using different substrate materials. Only a few certified layer thickness standards are available, especially since the stability, in particular, of very thin layers can be limited depending on the layer materials and the substrate they are plated on.

For thicker layers, the reference samples can be produced in the form of self-supporting films of known thickness placed onto different substrates. This allows for a relatively simple preparation. The influence of the thin air layers between the individual films is, in this case, negligible.

For very thin layers, in the range of less than  $1\ \mu\text{m}$ , the layers must be deposited onto substrates. The preparation of reference samples for variable layer systems is then possible only with significant effort. Therefore, the availability of suitable reference samples is limited. Consequently, standard-less quantification methods are of great importance for layer analysis.

One approach could be the iterative method used for the investigation of bulk materials as described in Section 5.5.3. Using sensitivities  $S_i$  for every element according to (5.17) allowance for the uncertainties of the measuring geometry, fundamental parameters, etc. is possible. For an efficient iteration process the differences between measured and calculated intensities has to be minimized. For single element layers the thickness can be determined according to

$$\text{Minimize} \left\{ \sum_{i=1}^{\text{no of lines}} \left( \frac{I_i^m - I_i^p(\mathbf{d})}{\sigma_i} \right)^2 \right\} \quad (5.28)$$

For the minimization calculation, known algorithms such as Levenberg–Marquardt can be used (Levenberg 1944; Marquardt 1963; Gill et al. 1981). For multiple element layers an additional term must be included, which considers the mass fractions of all elements.

The measurement uncertainties for the analysis of a layer system depend on the position of the layer within the layer stack. For the upper layers they are typically in the range of 3–5% (relative), largely independent of whether the analysis is carried out with or without a standard. Improvements in the analytical accuracy using standards are small; for the top layer the errors of the standards themselves are already of this order of magnitude.

In the case of an assessment of the accuracies, it must be taken into account that as a result of the relatively small layer thicknesses the absolute errors in the analysis of layers seem to be relatively large. Nevertheless, an error of 5% at a layer thickness of 3  $\mu\text{m}$  indicates an uncertainty range of  $\pm 0.15 \mu\text{m}$ ; for layer thicknesses of 300 nm it is then only  $\pm 15 \text{ nm}$ . This should be considered during a critical evaluation of the measurement results.

For all other layers, the errors are generally larger, approximately doubled for the second layer from the top because of the error propagation. For these layers an improvement in the accuracy can be achieved using standards; then the influences of the top layers can be better considered.

## 5.7 Chemometric Methods for Material Characterization

As described in the previous sections, X-ray spectrometry occupies an outstanding position when it comes to the understanding of the individual interactions and the possibility to model X-ray physics. However, other evaluation procedures can also be interesting and effective for certain problems, for example, if only material classifications are required. This is particularly true when the measured spectra do not show lines from every sample component or even no element lines because the sample consists only of light elements or because the intensities of the fluorescence lines do not clearly correlate with the corresponding element contents. This can occur, for example, if the sample size is smaller than the information depth of the radiation, i.e. if the intensities depend on the sample size as well as on the mass concentration in the sample, or if matrix variations strongly influence the peak intensities.

Also, for X-ray spectrometry chemometric methods can be used to characterize the materials. These methods can be very effective, even if the spectra show only small patterns. For these methods to work, a large number of spectra of the materials to be identified must be measured, prior to the actual analysis, in order to train the system. The materials have to be characterized according to the analytical problem and several samples must be available from each material type to be characterized. During the analysis, only the materials prepared in this way can be evaluated. On the other hand, the evaluation can then be very fast and also accurate. It is interesting that not only material identifications are possible

but also the characterization of special material properties can be achieved. The methods described in Section 5.7.1 are the simplest approaches for chemometric evaluation. Further information on these methods is given in Otto 2007, Danzer et al. 2001, and Brown et al. 2009.

### 5.7.1 Spectra Matching and Material Identification

The simplest method is to only compare spectra. The spectra of the unknown samples are compared with the spectra of the library. The similarity of the spectra is determined by a correlation coefficient; a ranking list of possible materials can then be established based on the correlation. The method achieves a very high hit rate when used for material identification. This method is called spectra matching. The simple algorithms allow for a very fast analysis but require the preparation of an extensive library of reference spectra and work only for the materials that are included in the library.

Another procedure that is called positive material identification (PMI) performs a quantification. The quantitative results are then compared with mass fractions of several predefined materials in the library. Finally, an identification of the material type is possible.

### 5.7.2 Phase Analysis

Another analytical problem can be the determination of material phases, i.e. of materials with fixed ratios of their components. Phase analysis provides additional information about the analyzed material and reduces the diversity of data. For phase analyses the following methods can be used.

- *Principal component analysis*: During the principal component analysis (PCA) a virtual multidimensional space is generated from the  $N$  intensities of the individual channels or certain spectral ranges, for example, element intensities, of the measured test spectra (variables), which are written at orthogonal axes. Each of the  $K$  spectra of the test materials can be represented by a point in this space. The linear combination of the variables with highest variation can be considered as first principle component (PC1). This means that this principal component corresponds to a certain combination of intensities, for example, a chemical phase or an alloy. In the next step, the next largest independent component to PC1 that is orthogonal to PC1 has to be determined as PC2 and so on (see Figure 5.26). This procedure mostly can be finished with few independent PCs, which are now the new variables.

The two-dimensional presentations of the relations between the different principal components, which are called scores, allow a classification of the examined materials according to different material groups. This transformation reduces the number of variables significantly and allows a fast identification of the analyzed materials according to specific properties, for example, for its composition.

Nevertheless, also PCA requires a comprehensive library of material spectra and in case of a new component (variable) the corresponding spectra have to be added to the library.

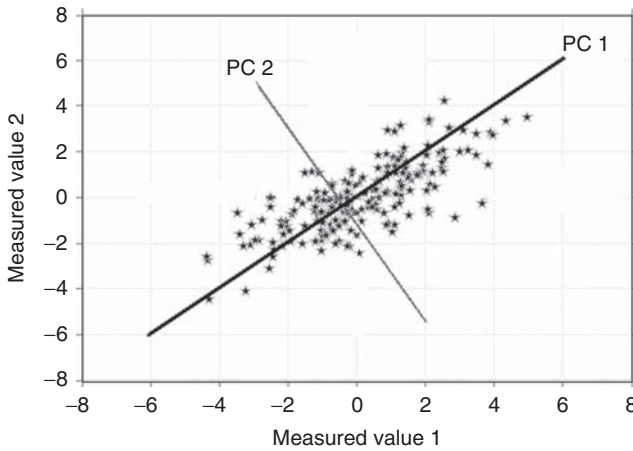


Figure 5.26 Scheme of a principal component analysis.

Examples of such type of analysis are the sorting of glass particles of different sizes and compositions or the identification of chemicals prepared in plastic bags described in Sections 15.2 and 17.2, respectively.

- *Cluster analysis*: For cluster analyses, again a virtual space is generated from the intensities of the individual channels or certain spectral regions. The distance  $\Delta I_{mn}$  between two points  $n$  and  $m$  can then be determined as follows:

$$\Delta I_{mn} = \sqrt{\sum_{j,n \neq m} (I_{j,m} - I_{j,n})^2} \quad (5.29)$$

The points with the smallest distance  $\Delta I_{mn}$  are then successively summarized to form a cluster. This procedure can be confined by setting a minimum distance between the individual clusters in the virtual space or a limitation to the number of clusters. In this way, similar spectra equating to similar materials are summarized. During the analyses of unknown samples, the measured spectrum can then be assigned to a respective cluster, i.e. the material can be identified.

Cluster analyses can take place both on the original data or after a PCA. In the case of an original data analysis the spectra background must be considered, whereas its influence is reduced by the PCA. It results in an easier and more precise identification.

In any case, a chemometric analysis of spectra has to be customized to the respective analytical task, which also means that a sufficient number of reference materials need to be available and measured. In addition, it is also necessary to adapt the evaluation procedures in order to provide optimal answers to the analytical questions. Then these methods can be very powerful and can provide the answers to various analytical questions, which are often not possible by conventional methods, or identify material properties that are not directly connected with the elemental composition, as for example the dampness of wood or the identification of organic compounds.



### 5.7.3 Regression Methods

Regression methods can determine the relations between a dependent and one or more independent variables, which can be further influenced by statistical fluctuations. The dependent data is compared with a model that can be a linear combination of the regression coefficients for a linear regression. More complex relations can be determined by multivariate regression.

Linear regression is often used for the calculation of the calibration function. In this case, the data is compared with the calibration function, and then the parameters of this calibration function as well as deviation and correlation parameters can be determined.

Other even more complex regression methods, for example, partial least square regression, can be used in the evaluation of spectroscopic data for material characterization (Beebe and Pell 1998; Danzer et al. 2001). It can be used for the suppression of signal noise, the determination of element mass fractions that cannot be directly measured (see Section 9.8.4.2), the characterization of small particles (see Section 15.1.5) or compounds (see Section 17.2), and even for the correlation of spectral data to material parameters such as mechanical strength and caloric value. Chemometric methods open up a wide range of new opportunities for the evaluation of spectral data and the compression of information. They are already widely used by other spectroscopic methods such as IR or UV spectroscopy.

Nevertheless, it has to be mentioned that the effectiveness of these methods depends on the availability of a sufficiently large number of well-characterized samples that can be used to train the system. The required effort to make all the measurements of these samples should not be underestimated. Further, it is necessary that for every new analytical problem the chemometric evaluation procedure has to be created, tested, and optimized. When all these conditions are fulfilled chemometric methods offer the possibility of a fast and problem-oriented data evaluation.

## 5.8 Creation of an Application

The creation of an application is largely determined by what the goal of the analytical question is, i.e. it is essentially determined by the nature of the sample material as well as by the desired analytical accuracy. Previous knowledge of the sample material as well as the analytical techniques available influences the approach on how to get the best answer to the analytical question.

Based on these goals, provisions for all steps of the analytical procedure must be predetermined, i.e. for sample preparation, test conditions, and evaluation of the measurement data. These will differ depending on the frequency of the measurements to be carried out as well as on the available measurement instruments.

### 5.8.1 Analysis of Unknown Sample Qualities

When analyzing unknown sample qualities, not only their quantitative composition but also their qualitative composition is unknown. For this reason, it is

necessary to capture the entire X-ray spectrum in order to determine all the elements contained in the sample. EDSs are particularly suitable for this purpose since they can simultaneously acquire the entire spectrum with one or more measurement modes. For WD spectrometers, the scan mode is required to capture the data for the entire element range. Changing the test conditions is possible to generate data with appropriate statistical errors for all elements.

When identifying unknown peaks, it is advisable to start with the highest intensity; the whole series can then be identified quickly. Another possibility is to start identification at lower energies or large wavelengths, since the intense  $\alpha$ -lines are on that side of a series.

For the quantification, standard-free models are often used since the availability of appropriate reference samples can be difficult. The achievable analytical accuracies will be somewhat lower compared to standard-based models, but the results of the analysis are readily available.

### 5.8.2 Repeated Analyses on Known Samples

A common task for XRF spectrometry is the control of a manufacturing process, where repeatedly similar samples have to be analyzed. These analyses often require a very high accuracy. The preparation of such an analytical method requires the following steps:

- At first, the specific analysis task has to be defined. This pertains to the determination of the elements and their concentration ranges to be analyzed, as well as the required analytical accuracy, taking into account the costs and the available time for the analysis.
- Thereupon, provisions for the sample preparation can be made. Possible influences on the analytical result from quality of the sample surface or mineralogical effects as well as the available time for the entire analysis have to be taken into account.
- The acquisition of the entire spectrum of a typical sample should then be performed under optimal conditions, for WDS instruments by a scan, and for EDS instruments by a simultaneous measurement.
- The optimal test conditions and the necessary measurement times for the given application can be derived from the initial measurements for all the elements to be analyzed. In this way, one can achieve the required statistical errors to match the accuracy requirements and achieve the sensitivities required to detect the low concentration elements.
- Furthermore, it is necessary to determine possible influences from the matrix or from mineralogical effects. Depending on the required analytical accuracy as well as available analysis time and cost, the optimal preparation procedures can be selected.
- It can also be useful to check whether there are ISO, DIN, or ASTM standards available for the specific analytical problem. These standards can, for example, aid in simplifying the setup of the application and make the results comparable with measurements in other laboratories. A selection of standards that provide guidelines for XRF measurements are summarized in Table B.4.

- In the next step, the selection of suitable reference samples is required. They should be as similar as possible to the sample to be analyzed, i.e. they should contain the same elements in comparable concentrations and have the same consistency. Additional elements should only be present in small amounts in order to have comparable matrix interactions as in the samples.
- For applications that will be used over a longer period of time, it is useful to set up monitor samples. With these monitor samples the stability of the spectrometer and the quality of the analyses can be monitored over time. These samples should of course be highly stable. Samples for quality assurance should be as similar as possible to the samples to be analyzed and they should be subjected to a thorough and complete analysis before being used. Drift correction samples are used to monitor the stability of the spectrometer. These can deviate more strongly from the sample type to be analyzed if they contain elements in the energy ranges of interest. They are then measured under the same test conditions as the unknown samples.
- In order to determine whether only the elements specified in the certificate are present, it is advisable to measure the complete spectra for all reference samples. This step will identify potential line overlaps that have to be taken into account when selecting the analyte lines and when defining the background point positions.
- When defining the analyte lines and background points as well as the conditions for their measurement, it is helpful to evaluate the spectra of all reference samples at the same time. Attention should be given to those that have as little line overlap as possible. Next, certain setup conditions for the analyte lines must be specified, especially in the case of WDS instruments.
- Measurement setup parameters for the analyte line: excitation conditions, filter selection, measuring time, goniometer position, crystal and collimator selection, detector and discriminator settings, sequence of the measurements – here it may be necessary to consider that volatile elements could be depleted by the influence of the incident radiation.
- The same setup conditions for the background points are to be made as for the analysis line. When determining the background positions, it should be noted once more that the positions do not overlap with peaks of both the sample to be analyzed and the reference specimens in order to enable a clear determination of the true background.

Since the background points usually have lower intensity they are associated with a larger statistical error. Therefore, longer measuring times can be necessary in order to reduce the influence of these larger statistical errors when determining the net intensities.

Better resolution settings of the spectrometer can reduce the issue of peak and background point overlaps. However, it should be noted that better resolution always comes at the expense of a remarkable loss of intensity.

- For EDS instruments, determining the measuring conditions is simpler since the entire spectrum or at least relatively large parts of the spectrum are recorded simultaneously under the same measurement conditions. The variation in the test conditions includes the selection of the tube parameters, the measuring time, as well as choice of filters or optical elements, such

as secondary targets, monochromators, or polarizers in the primary beam path, and finally the measurement environment in the sample chamber (air, vacuum, or helium flushing).

- Depending on the selected quantification model, the number of required reference samples has to be determined since they influence the range for which

**Table 5.5** Settings for the preparation of an analytical method.

Parameter	WDS	EDS
Analytical question	Elements, concentration range, accuracy, available time	Elements, concentration range, accuracy, available time
Optional settings	Check of the availability of standards (NIST, ASTM, DIN) and references Selection of monitor samples	Check of the availability of standards (NIST, ASTM, DIN) and references Selection of monitor samples
Sample preparation	Depending on accuracy requirements	Depending on accuracy requirements
Determination of elements present in unknown and references	Scan the complete spectrum from unknown and references	Simultaneous measurement of unknown and references
Excitation conditions	Definition of optimal conditions, separate for every measurement point (tube parameter, filter, measurement time)	Mostly one setting, depending on the instrument's different excitation conditions (tube parameter, filter measurement time)
Analyte line	Sensitivity – saturation? Overlapping with other lines both for unknown and reference samples	Mostly $\alpha$ -lines, only in a few situations $\beta$ -lines are used
Background points	Separate points by consideration of background distribution	Not necessary due to simultaneous measurement
Resolution	Crystal and collimator for every measurement point	No settings
Detector	Selection between two detectors Pulse height discriminator	Not necessary
Measurement medium	Air, vacuum (or He if available)	Air, vacuum, or He (if available)
Measurement	References, unknown sample, drift correction sample	References, unknown sample, drift correction sample
Evaluation	Peak area determination (background subtraction, overlap correction) Calibration Drift correction	Determination of background points and peak intensity Calibration Drift correction

the calibration is valid (see Section 15.1.5). For fundamental parameter-based correction models, the number of required reference samples is less and the range of validity of the calibration is wider. For many instruments, the spectra of many reference samples are stored in the instrument and can thus be used to create an application.

- Finally, when setting up an application, an estimate of the expected uncertainty budget that can be expected is useful. This can be done according to the methods described in Section 6.3.

These particular settings for the preparation of an analytical method (see Figure 2.11) are summarized in Table 5.5 separately for WDS and EDS measurements.

However, in most commercial instruments the software greatly supports the application setup. In small instruments that are prepared for single applications, often only the measurement time can be defined. For larger instruments the manufacturers often offer complete application packages including test conditions for all analytes and background points as well as reference samples. Nevertheless, for non-prepared applications the user mostly is guided through all necessary steps and the software makes very specific proposals for the correct selection of measuring conditions and instrument settings.

## 6

# Analytical Errors

## 6.1 General Considerations

Errors can be made at any stage of the analytical process. However, the errors of the individual contributions of the steps of the analysis process are very different. A typical distribution is illustrated in Figure 6.1. It shows that sampling contributes the largest error. This applies, in particular, when considering how well the sample taken represents the material to be characterized; large deviations can easily occur. In the following these sources of error are not to be considered; it is rather assumed that the laboratory sample is a good representative of the material to be analyzed and, if necessary, has sufficiently homogenized by a multistage milling, mixing, and division process for small parts material.

The next major source of errors is associated with the sample preparation. The sample material in the laboratory is processed in such a way that the measurement sample is produced. The many and potentially very different steps required depending on the sample and on the analytical problem have already been described in Chapter 3.

The errors from the actual measurement are relatively small compared with the first mentioned errors. They, however, will determine the analysis error in the case of exact sampling and error-free preparation. The statistical error contribution is a unique case, since, unlike other errors, it cannot be eliminated but can only be reduced.

The goal of an analysis is to provide a result that is as accurate as possible. However, accuracy in this context must be understood as an interaction of several parameters. This can be best explained with reference to the well-known target disk model in Figure 6.2, which illustrates the relation between a precise and a true measurement result as well as the influence of random and systematic errors.

In the first picture, the distribution deviates not only from the target value, but it is also strongly scattered, which means both large random and statistical deviations occur. In this case, the analytical method is not suitable or not correctly matched to the analytical task.

In the second picture, the scattering of the values is still considerable, but the measured values are uniformly distributed around the target value; the systematic deviations are reduced, but random deviations still dominate. The precision is still insufficient, but by taking the mean of the individual results, the true value is

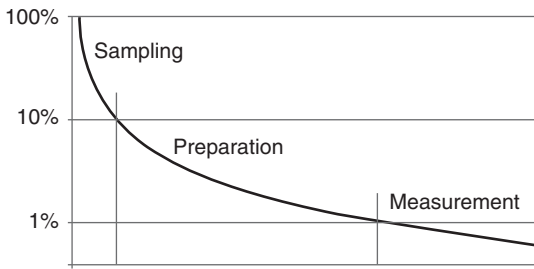


**Figure 6.1** Error distribution in the analytical process.

Precision Trueness	Bad Bad	Bad Good	Good Bad	Good Good
Deviations - Random - Systematic	Large Large	Large Small	Small Large	Small Small

**Figure 6.2** Target model for the illustration of random and systematic errors.

determined with relatively good accuracy in the case of a sufficiently high number of individual measurements. Still it would be better to improve the precision by changing the measurement conditions, for example, more efficient excitation or longer measurement time.

The third image represents a distribution that shows small random but a distinct systematic deviation from the target value. These systematic deviations can be easily corrected by means of an improved calibration or potentially just a recalibration.

Finally, the last image shows a distribution that is precise and true, i.e. the results are closely distributed around the target value. Even a single measurement would provide here a relatively true result. Since occasional outliers that are relatively far from the target value may occur, it is useful and advisable to take multiple measurements even in the case where there are only small random and systematic errors.

Based on these distributions it can be easily derived that for a correct result various conditions must be met.

The measurements must have good repeatability, i.e. repeated measurements of the same sample should preferably always give the same result. Repeatability needs to be achieved for both short-term periods (precision) and long-term periods (long-term stability of the measurement results).

Above all the analysis should have a high degree of trueness, i.e. the result should be as close as possible to the true value. Here it should be noted that even in certified reference samples, the true value is accompanied by errors. This

means that the position of the crosshair shown in Figure 6.2 is not exactly known. In general, this is valid for all unknown samples.

Various parameters are used to quantify the repeatability as a function of the time period of the observation as well as other measuring conditions.

### 6.1.1 Precision of a Measurement

The precision of a measurement describes the repeatability of a result in a short period of time. It can be determined by repeated measurements under identical conditions.

An example is given in Table 6.1. Here, the intensities of 10 repeated measurements of an Al alloy are presented.

Shown are total counts  $N$  (not counting rates  $N/t$ ) for some of the alloying elements, as well as the following quantities calculated from these intensities, where  $n$  is the number of measurements:

*Average:*

$$N_{\text{average}} = \sum_j N_j / n \quad (6.1)$$

*Standard deviation:*

$$\sigma = \sqrt{\frac{\sum_j (N_j - N_{\text{average}})^2}{n}} \quad (6.2)$$

*Relative standard deviation (%):*

$$\sigma_{\text{rel}} = \sigma / N_{\text{average}} \cdot 100 \quad (6.3)$$

**Table 6.1** Results of repeated intensity measurements.

Measurement	Mg	Al	Fe	Cu
1	1 827	300 772	9 693	2 920
2	1 897	299 465	9 564	2 776
3	1 746	300 124	9 566	2 821
4	1 883	299 658	9 941	2 904
5	2 037	300 507	9 583	2 960
6	1 994	299 652	9 556	2 736
7	1 734	299 776	9 550	2 901
8	2 029	300 851	9 803	2 767
9	1 759	298 730	9 720	2 781
10	2 134	299 787	10 006	2 973
$N_{\text{average}}$	1 904	299 932.2	9 698.2	2 853.9
$\sigma$	139.7	648.0	168.7	87.2
$\sigma_{\text{rel}}$ (%)	7.34	0.22	1.74	3.06
$\sigma_{\text{stat}}$ (%)	2.29	0.18	1.02	1.87
$\sigma_{\text{rel}}/\sigma_{\text{stat}}$	3.2	1.2	1.7	1.6



Relative standard deviation of the statistical error (%):

$$\sigma_{\text{stat}} = 100 / \sqrt{N_{\text{average}}} \quad (6.4)$$

Ratio between standard deviation of the measured intensities and the statistical error:

$$\sigma_{\text{rel}} / \sigma_{\text{stat}} \quad (6.5)$$

The results of Table 6.1 lead to the following conclusions:

- The measured intensities are relatively high for Al, the main element of the alloy, but lower for the elements with lower concentrations.
- The relative standard deviations for both the measurements ( $\sigma_{\text{rel}}$ ) and the individual counting statistics ( $\sigma_{\text{stat}}$ ) reflect this situation, i.e. for the greater number of counts for Al, these values are smallest; however, for the smaller intensities of the alloy elements, the relative standard deviations are larger.
- The ratios of the measured standard deviation and statistical error are interesting. The statistical error is the “minimum error” associated with every measurement. The total error cannot be smaller than this statistical error. Therefore, the ratio  $\sigma_{\text{rel}} / \sigma_{\text{stat}}$  shows the extent to which further error contributions have occurred during the measurement. In the specific example, the ratios for Al, Fe, and Cu are  $< 2$ . This can be considered a sufficiently good value, i.e. additional errors contributed by the instrument or the measuring procedure are of the same order of magnitude as the statistical error. On the other hand, the value for Mg is greater. In this case, a further error contribution must be assumed, probably caused by the overlap of the Mg and Al peaks. The measurements were carried out with an energy-dispersive spectrometry (EDS) instrument, in which the peaks of Mg and Al have a substantial overlap.

By means of such comparative measurements, it is possible to determine error contributions of certain instrument parameters or operations. If, for example, the individual measurements are carried out after the adjustment of an instrument parameter (for example, the excitation parameters) or after certain instrument operations functions have been carried out (for example, the positioning of the sample) and are compared with the values of the undisturbed repeatability measurements, the influence of the individual adjustment step on the overall error can be estimated. Another possibility is the characterization of the homogeneity of a sample by comparing repeated measurements at the same location with measurements done at different positions on the sample. An “analysis of variance” (ANOVA) test can be used to test the statistical significance of the result (Gelman 2005).

If the number of measurements is relatively small, the exact standard deviation  $\sigma$  of these separate measurement results is not known. Then the Student’s distribution can be helpful. It has a slightly larger variance than a normal distribution; however for larger numbers of tests ( $\approx 30$ ), it approaches to normal distribution.

The Student’s distribution  $t(p, f)$  can be used for the determination of the confidence interval  $\Delta x$  for a single or only very few measurements  $n$  with a selected

**Table 6.2** Student's  $t$ -distribution in dependence of the probability  $p$  and the number of degrees of freedom  $f$ .

$f$	$p = 0.50$	$p = 0.90$	$p = 0.95$	$p = 0.99$
1	1.000	6.31	12.70	63.70
2	0.816	2.92	4.30	9.92
5	0.727	2.01	2.57	4.03
10	0.700	1.81	2.23	3.17
30	0.683	1.70	2.04	2.75
$\infty$	0.674	1.64	1.96	2.58

probability  $p$  according to

$$\Delta x = s \cdot t(p, f) / \sqrt{n} \quad (6.6)$$

where

$s$	standard deviation
$t(p, f)$	Student's $t$ -distribution
$p$	probability for the occurrence of a measured value in the confidence interval
$f$	degrees of freedom
$n$	number of measurements

The values of the Student's distribution are tabulated. An abbreviated version is shown in Table 6.2 as a function of the number of degrees of freedom  $f$  and the probability  $p$  of the occurrence of the measured value (Bleymüller et al. 2015).

### 6.1.2 Long-Term Stability of the Measurements

The stability describes the long-term behavior of a measurement instrument. To monitor the stability, repeated measurements on a stable sample (monitor sample) under the same conditions are executed over an extended period of time, and the counts or the results of the analyses are recorded. The time between the individual measurements should be set such that the expected changes can be easily detected. Long-term changes to the instrument, such as inspection of the evaporation of the cathode material of the tube, can be determined by weekly or even monthly measurements. The influence of the instrument temperature or other ambient conditions is better checked in shorter cycles.

For easiest interpretation the results of these repeated measurements should be presented graphically. Examples of such measurements are illustrated in Figure 6.3. In panel (a), measurements are of a high stability. The plotted intensity values are mostly within the statistical uncertainty range of  $3\sigma$ . On the other hand, in panel (b), a decrease in the measured intensities over time on top of

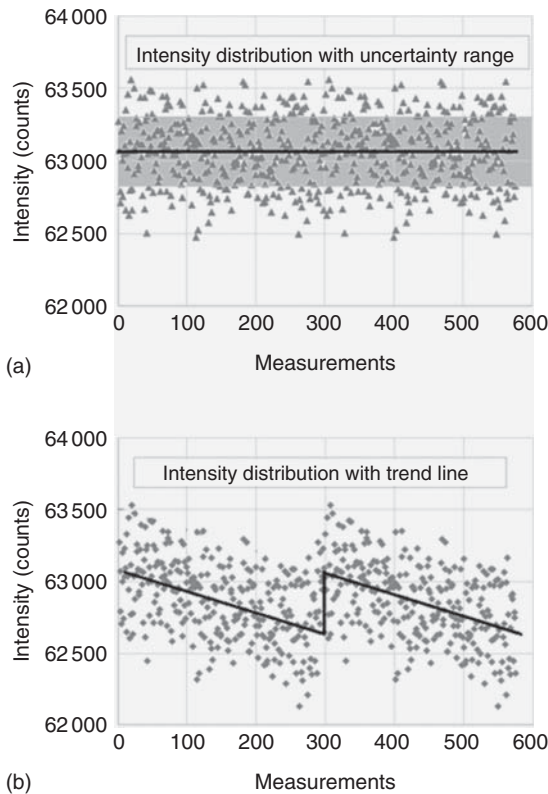


**Figure 6.3** Results of repeated measurement with a high (a) and lower (b) stability.

the previously described statistical fluctuation can be seen, which is also evident from the marked trend lines.

The ANOVA is also a commonly used statistical method to determine the long-term stability of a measurement instrument.

Such deviations can be detected and corrected by means of monitor measurements. The corrections can be achieved either by discrete corrections of the measured intensities after and according to a monitor measurement (as shown in Figure 6.3b) or by continuous corrections by an extrapolation-based model of predetermined and known changes.

### 6.1.3 Precision and Process Capability

Measurement precision is the closeness of agreement between measured quantity values obtained by replicate measurements on the same object under specified conditions (Brinkmann 2012). This parameter is often used to characterize the behavior of an analytical method to provide reliable and comparable results under different or changing conditions. To distinguish between repeatability and reproducibility, the following definitions are being used. Repeatability describes

the measurement precision of an analysis method under a set of identical working conditions (repeatability conditions) in a short time window. Reproducibility, on the other hand, describes the condition of measurement, out of a set of conditions that includes different locations, operators, measuring systems, and replicates measurements on the same object (Brinkmann 2012). It can also include the change of preparation tools or techniques, i.e. also the comparison of the results of different test laboratories. This can be used for the assessment of the stability of a complete analytical method.

This is comparable to the assessment of the process capability of a method, i.e. the investigation as to whether a (manufacturing) process delivers all the time high production quality over a long period of time. Various concepts have been developed for this purpose, which are summarized under the name “6 $\sigma$ ” (see, for example, Lunau 2013; DIN-EN-ISO-21747 2007).

The name 6 $\sigma$  indicates that certain parameters of a manufacturing part or component must be within six times standard deviation (6 $\sigma$ ) of the distribution. This means that only  $2 \times 10^{-9}$  of the results fall outside of the process limits. This appears to be a very strict requirement, but it is appropriate for safety-relevant components, such as automotive brake assemblies or microelectronic chips, considering product safety and as a result of the high number of units produced.

To define certain process parameters, the tolerance limits for the process must be specified. In the example shown in Figure 6.4, most of the results are within the tolerance limits, in this example 2 $\sigma$ ; however some values are outside the specification:

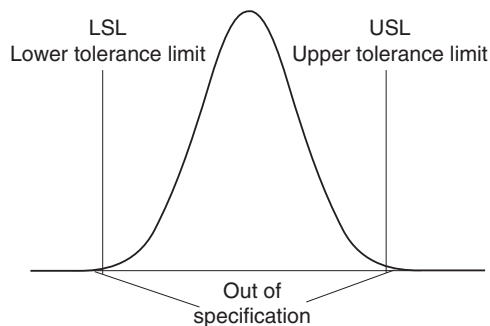
$$C_p = \Delta T / 6\sigma = (USL - LSL) / 6\sigma \quad (6.7)$$

USL – upper specification limit

LSL – lower specification limit

For the evaluation of the process capability, specific parameters are introduced. For example, the  $C_p$  value is a statistical index calculated from the upper and lower specification limits and the standard deviation of the process, which assumes a normal distribution about the target process value.

**Figure 6.4** Specification limits of a process.



The  $C_p$  value defines the width of the distribution. In the past  $C_p$  values of 1.33 were used as the acceptable target, which means that the specification limits were at  $\pm 4\sigma$ . Nowadays with improved production capabilities and increased quality demand, the requirements for  $C_p$  values are commonly set at 2 or even 4, i.e. the specification limits are  $\pm 6\sigma$  or even  $\pm 12\sigma$ .

If the mean value of the distribution  $\bar{w}$  and the target value do not match, then the  $C_{pk}$  value is used. It is a measure of how much the process deviates from the mean. It is calculated as follows:

$$C_{pk} = \min(w_{\text{average}} - \text{LSL}; \text{USL} - w_{\text{average}}) / 3\sigma \quad (6.8)$$

Since only the smaller unidirectional deviation is evaluated, only the  $3\sigma$  value is used in the denominator. These values are comparable with those of the  $C_p$  values.

To determine the process capability or to monitor a process, measurements are taken as already described in Section 6.1.1. Their results are plotted in trend charts, giving a quick overview of how much a process is in control (see Figure 6.3).

#### 6.1.4 Trueness of the Result

As in all measurement processes, the objective is to achieve the highest degree of trueness. In other words, for quantitative X-ray fluorescence analysis, the determination of the true value of the mass fraction or the mass per unit area is the goal. The “real” true value is usually unknown, since every measurement is associated with an uncertainty. A correct direct determination of the value is not possible. However, it is possible and common to make estimates of the trueness of an analytical method by using measurements on standards. Still, even when using standards, the values of the mass fractions have an uncertainty associated with them because they are also determined often by an analysis, usually obtained in the context of round robin tests using different methods in different laboratories and by averaging the results. Another possibility is to reconstitute reference samples, e.g. manufacture them from ultrapure materials (see Section 5.5.5). Due to the high accuracy of balances, very high accuracies then can be achieved.

Deviations from the predefined value are always superimposed by statistical fluctuations. To assess the trueness of a method, it is therefore useful to evaluate several samples with different compositions since deviations from the nominal values of the standards are always superimposed by statistical errors. The correlation between the nominal and the analyzed values can then be used to assess the trueness of the analytical method. A more detailed description has already been made in Section 5.5.6.1.

## 6.2 Types of Errors

Deviations of the analyses resulting from the true value are caused by various error contributions. A detailed estimation of the individual contributions allows for the assessment of the errors and helps in taking the selective steps to minimize them.

The errors can roughly be classified as random and systematic errors. However, few sources of errors can have both random and systematic characteristics.

### 6.2.1 Randomly Distributed Errors

Random errors are stochastically distributed in direction and magnitude; they fluctuate around the mean value and can be treated by the theory of probability. The most prominent random error is due to counting statistics. Errors that occur during sample preparation or sample positioning may also have a random character.

Random errors can usually be described by a Gaussian distribution. This means that for a large number of repeated measurements, the frequency of the individual results can be described by a normal distribution (also called a Gaussian distribution):

$$w = \frac{1}{\sigma\sqrt{2\pi}} \exp\left(-\frac{1}{2} \left(\frac{x-m}{\sigma}\right)^2\right) \quad (6.9)$$

where

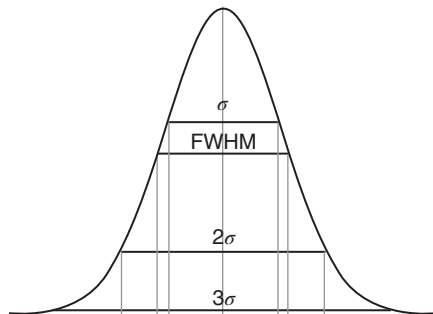
- $w$  probability for a measured value
- $\sigma$  standard deviation (full width at half maximum of the distribution)
- $m$  mean value of the distribution
- $x$  single measured value

As shown in Figure 6.5, approximately 68% of the events are within the single standard deviation  $\sigma$ . Using an extension factor  $k$  for the  $\sigma$  value, the probability for  $k = 2$  increases to approximately 95% and for  $k = 3$  to over 99%. Another frequently used variable is the full width at half maximum (FWHM) of the distribution, within which approximately 82% of the events are located. The relation between standard deviation and FWHM is

$$\text{FWHM} = 2 \cdot \sqrt{2 \ln 2} \cdot \sigma \approx 2.3548 \sigma \quad (6.10)$$

The magnitude of the occurring errors determines the standard deviation of the distribution or its FWHM. If the measurements yield results with larger deviations, the distribution is correspondingly broader. This is illustrated in Figure 6.6,

**Figure 6.5** Gaussian distribution of measuring results.



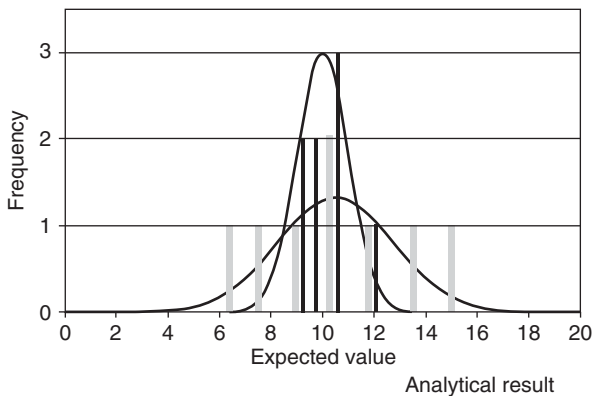


**Figure 6.6** Gaussian distributions with different standard deviations.

showing the results of two measurement series, each with 10 measurements, which are approximated by a Gaussian distribution. In this case, the distribution displayed by gray lines is broader, i.e. the deviations or the errors of the individual measurements are on average larger; on the other hand, the black lines represent a distribution of smaller deviations, which is correspondingly narrower.

In addition to the counting statistical error, other randomly distributed errors are possible during the measurement, for example:

- Instabilities of the excitation conditions (tube voltage and current)
- Changes of the analyzed sample volume, for example, caused by surface contaminations, surface roughness, mineralogical influences, or others
- Changes in working distance, for example, caused by fluctuations in the geometry between X-ray source, sample, and spectrometer due to inaccuracies in sample positioning

During the evaluation of the data, randomly distributed errors can occur, for example, during the determination of the peak area. The statistical distribution of the intensities in the individual channels of the spectrum results in variations in the peak areas during the peak fitting procedure. This error can be reduced by increasing the measured intensities, for example, by longer measuring times, resulting in a smaller statistical counting error of the individual channels.

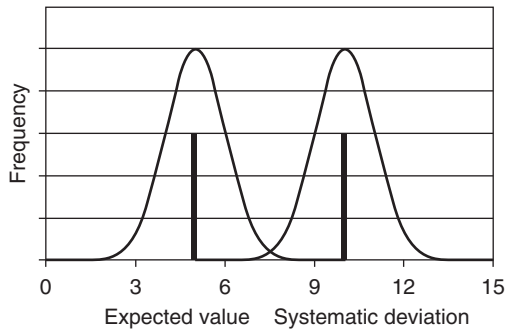
## 6.2.2 Systematic Errors

Systematic errors are recurring errors, which usually shift the target values “systematically” in the same direction as illustrated in Figure 6.7. Since these systematic errors are superimposed by the statistical errors, the analyses results still show a Gaussian distribution.

The reasons for systematic errors can be found in all steps of the analytical process. Without claiming to be complete, the following is a list of potential sources of systematic errors:

*Sample preparation:* Insufficient homogenization of the sample, contamination of the surface by oxide layers or impurities, influences from surface topology, segregation, sedimentation, etc.

**Figure 6.7** Statistical distribution around the expected value and shifted by a systematic error.



*Measurement:* Incorrect sample positioning, deviations from the specified excitation parameters, influences from the measurement environment as well as misalignment or contamination of the instrument itself. During the measurement, short-term changes affecting the components of the instrument, such as temperature changes, or long-term changes caused by aging processes, as well as changes in the sample, such as sedimentation, can systematically influence the analytical result.

*Evaluation:* Incorrect peak identifications (for example, a wrong or forgotten element during setup) can affect both the peak fit and a correct evaluation of the matrix interaction but can also cause an incorrect background calculation.

*Calibration:* Carrying out measurements on calibration samples and unknown samples with different sample preparation or different measurement conditions, use of insufficient number of calibration samples, use of inadequate evaluation models, etc.

Regarding the calibration samples, it must be pointed out that these can also be imperfect and are subject to the same measurement uncertainties as the laboratory sample itself. Calibration samples exist in different qualities (see Section 5.5.8).

## 6.3 Accounting for Systematic Errors

### 6.3.1 The Concept of Measurement Uncertainties

The conventional error treatment evaluates the measured data. It usually is statistically distributed and can be treated with statistical methods. Influences of a systematic nature are then often not sufficiently considered.

Due to a better understanding of the analytical processes, improved instrument technology as well as more powerful computing technology for the evaluation of the analytical results it is now also possible to take systematic deviations in the error analysis into account. As a result, the more comprehensive concept of measurement uncertainty has been introduced. Both random and systematic deviations are taken into account for the possibility of a more realistic assessment of the measurement results. This is also necessary since systematic errors are often the dominant factor when considering the high quality of today's measurement technology. The introduction of the concept of measurement uncertainty



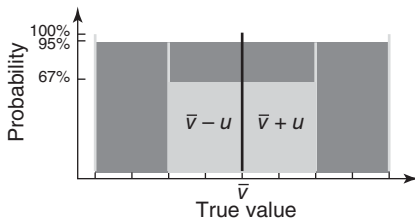


**Figure 6.8** Total measurement uncertainties of analytical results.

allows now to characterize the reliability of a measurement or the entire analytical method with one parameter only (ISO/IEC Guide 98-3 2008; Noack 2012).

This concept is also helpful since a sufficient number of measurements cannot always be made for a representative statistical treatment.

The uncertainty concept can also take into account influences that are not measurable. It should be noted, however, that any influence considered increases the range of uncertainty. When assessing the measurement uncertainties, the magnitude of the respective influencing variables must always be estimated in order to consider only the largest contributions.

The summation of uncertainties follows the same rules as conventional error propagations, which are described in (6.11–6.13). However, in contrast to statistically distributed errors, the probability of the occurrence of a measured value in the entire interval is equal and depends only on the width of the interval.

In this case, the uncertainty  $u$  is the probability that the true value  $\bar{v}$  lies within a certain interval. The probability is determined only by the expansion factor  $k$  of the width of the interval, but not by the measured value itself. This relationship is shown in Figure 6.8.

Similar to the treatment of statistical errors, the broadening of the value interval is given by the standard deviation. It can increase the likelihood that the correct result lies within this interval. For an interval width equal to the standard measurement uncertainty  $k = 1$ , it is 67%, and for  $k = 2$  according to  $\bar{v} \pm k \cdot U$ , it is 95%.

Various concepts have been developed for determining the uncertainty of measurements (Lira and Wöger 1998). For this purpose, however, the knowledge about the summation of measurement uncertainties and their error propagation is necessary (GUM 2008).

### 6.3.2 Error Propagation

If only statistical errors are present, the total error is determined by a summation of the individual error contributions. Fault propagation takes place according to Gauss:

$$\Delta v = \sqrt{\left(\frac{dv}{dx_1}\right)^2 \Delta v_1^2 + \left(\frac{dv}{dx_2}\right)^2 \Delta v_2^2 + \dots + \left(\frac{dv}{dx_n}\right)^2 \Delta v_n^2} \quad (6.11)$$

where  $v_i$  are the errors (uncertainties) and  $x_i$  are the individual influencing factors.

In the case of a multiplicative connection of the influencing factors, i.e. for  $v = x_1 \cdot x_2$ , the total error is according to

$$\frac{u}{v} = \sum_j \sqrt{\left(\frac{\Delta u}{x_j}\right)^2} \quad (6.12)$$

For an additive connection of the influencing factors, i.e.  $v = x_1 + x_2$ , the total error is according to

$$\Delta u = \sum_j \sqrt{\Delta u_j^2} \quad (6.13)$$

This relation for the addition of errors is shown in Table 6.3 for two respective error contributions.

**Table 6.3** Addition of error contributions.

$\Delta v_1$ (%)	5	5	5	5
$\Delta v_2$ (%)	5	3	1	0.1
$\Delta v_{\text{total}}$ (%)	$\approx 7$	5.8	5.1	5.01

This table shows that the overall error is dominated by the largest error contribution. In the example,  $\Delta v_1$  remains constant at 5%, while  $\Delta v_2$  significantly changes in each example. Nevertheless, the overall error mostly remains unchanged. This example shows that it is not advisable to concentrate on every error contribution in order to improve the measurement uncertainty, but always concentrate on the largest contributions. In particular, one must consider the statements made at the beginning of this chapter concerning the size of the error contributions of the individual steps of an analysis (see Figure 6.1).

### 6.3.3 Determination of Measurement Uncertainties

The measurement uncertainties are summarized in an uncertainty budget. Two different possibilities are used to determine this budget.

#### 6.3.3.1 Bottom-Up Method

In the bottom-up method, all error influences are considered separately, and an uncertainty budget is calculated as a sum of all of them. As described in the GUM (2008), for this purpose, comprehensive mathematical models are required (NordtestReport-TR537 2004). This estimation of the measurement uncertainty is based on the mathematical evaluation of each individual uncertainty component. It is necessary to determine all influences, to examine them, and to define their contributions. The determination of the total standard uncertainty can then be made by summing up the individual contributions according to (6.11). The final uncertainty is then determined by the expansion factor according to (6.15).

The bottom-up method is time consuming but provides a good indication of how the individual process steps influence the analytical result. In this way

the significant uncertainties can be recognized, and their influence reduced or corrected.

The effort for estimating the influences can be limited if only the most substantial contributions are considered. The disadvantages of the method are as follows:

- The effort to determine the individual contributions can be very high and requires a variety of measurements as well as complex mathematical procedures.
- An incomplete evaluation of the systematic deviations has to be avoided, since in that case overestimations of the overall uncertainties are possible.

The procedures for determining the uncertainties according to the bottom-up method require:

- A detailed description of the analysis procedure and the listing of all influencing factors
- The elimination of unimportant influences
- The determination of the distribution models for the individual distribution variables (experimental data are described by Gaussian distributions, and systematic deviations by rectangular distributions)
- The determination of the value ranges of the parameters as well as their standard deviations
- The determination of the combined uncertainties in accordance with the requirements in Section 6.3.2 and
- The determination of the expansion factors and thus the extended uncertainties.

The bottom-up method is very complex and should only be used where exact mathematical relationships between the individual sources of uncertainty are known and where a targeted improvement of the uncertainties is intended.

### 6.3.3.2 Top-Down Method

In the top-down method, the test method is considered as a whole. The influences of the various uncertainty components are summarized in one value by taking the parameters obtained from the analysis of reference materials, i.e. precision and trueness, or taking data obtained from round robin tests for the determination of the measurement uncertainty.

The top-down method is suitable for practical laboratory use because the individual uncertainty contributions do not have to be comprehensively mathematically recorded in complex multistage analytical procedures. Often, the exact mathematical correlations are simply missing to reasonably determine the uncertainty budget of all work steps. The individual contributions to the uncertainties are not the focus here, and the possibilities to correct the different error contributions are limited. Systematic deviations, however, can be well identified by measurements on standard samples.

The final uncertainty is a result from the uncertainties of the reference sample as well as the contributions from the analysis according to

$$U_{\text{total}} = \sqrt{\Delta_{\text{target-current}}^2 + \frac{\Delta v_{\text{reference}}^2}{n} + \frac{\Delta v_{\text{analysis}}^2}{m} + \frac{\Delta v_{\text{sample}}^2}{k}} \quad (6.14)$$

where

$U_{\text{total}}$	total measurement uncertainty
$\Delta_{\text{target-current}}$	difference from the expected value when analyzing the reference sample – systematic deviation (mass fraction or layer thickness)
$\Delta v_{\text{reference}}$	uncertainty of the reference value (from the certificate)
$\Delta v_{\text{analysis}}$	standard deviation when analyzing the reference sample
$\Delta v_{\text{sample}}$	standard deviation in the analysis of the unknown sample
$n, m, k$	number of respective measurements

The final measurement uncertainty can then again be determined by multiplying the total uncertainty by the expansion factor  $k$ :

$$U_{\text{expanded}} = k \cdot U_{\text{total}} \quad (6.15)$$

The uncertainties determined in this way can then also be used for the unknown samples if they are sufficiently similar to the reference sample and the same analysis method was used.

The top-down method for determining the uncertainties is relatively straightforward and requires a comparatively lower measurement effort because:

- All influences are automatically considered, even those that are not directly detectable or assignable
- The effort of their determination is relatively low and
- Systematic deviations are easily recognizable and can thus be corrected.

On the other hand, this method has also some disadvantages:

- The composition of the reference sample and the unknown sample should be as similar as possible.
- The procedures for determining the analytical values may differ, in particular in the case of reference samples characterized by round robin tests.
- The individual contributions to the uncertainty cannot be analyzed separately, however only their sum. This means that both the ability to reduce individual error contributions is not given and the ability to optimize the analysis method is made more difficult.

Despite the disadvantages mentioned, the top-down method can be regarded as a best-practice method because of the relatively simple workability. Comprehensive descriptions of the top-down method can be found in the Nordtest Report TR537 (2004-02). Also in the standard DIN-EN-ISO-11352 (2011:03) as well as in the German standard procedure DEV-AV-4 (2006), they both give good guidance on the use of the top-down method. The following additional references on this topic are recommended: DIN-V-ENV\_13005 (1999:06), EURACHEM Guide (1998), EURACHEM\_CITAC\_GUIDE (2004), and EUROLAB-TB\_2 (2006). They cover many analytical questions with well-defined examples which are beyond the scope of this book.

## 6.4 Recording of Error Information

There are many ways to specify errors. They can be specified as an *absolute error*. This is the difference of the analysis result from the true value, i.e.

$$\Delta w = w_{\text{analysis}} - w_{\text{true}} \quad (6.16)$$

This value is expressed in the unit of the analyzed parameter, i.e. for mass fractions, e.g. in wt%, or for layer thicknesses, e.g. in  $\mu\text{m}$ .

Another often used specification is in the form of the *relative error*, i.e. the deviation from the true value relative to this value, i.e.

$$\Delta w/w \quad (6.17)$$

The relative error is usually given in % [ $\Delta w/w \cdot 100$ ].

This information allows a comparison of uncertainties, regardless of the magnitude of the analytical value.

For a correct reporting of X-ray fluorescence results, that means the mass fraction, the area mass coverage, or the layer thickness should always be reported with their uncertainty interval  $\Delta w$  in the form  $w \pm \Delta w$ .

This is not always possible, but the uncertainty range can already be stated how the analysis results are presented. The specification of an analysis result with a certain number of significant digits implies according to the IUPAC

**Table 6.4** Number of significant figures typical for X-ray fluorescence.

Instrument/ analysis type	Sample quality	Statistical error (%)	Sample preparation (%)	Quant model (%)	Significant figures
Handheld		3–5	~10	2	2
ED-XRF					
Majors	Bulk	<0.2	>0.2	<1	3
	Powder pellet	<0.2	~1.0	>1	
	Glass fusion beads	>0.5	>0.5	~1	
Traces	Bulk	>5	>0.2	>5	2
	Powder pellet	>5	>0.5		
WD-XRF					
Majors	Bulk	~0.1	>0.2	0.2	3–4
	Powder pellet	~0.1	>0.5		3
	Glass fusion beads	>0.3	>0.2		3–4
Traces	Bulk	~1	>0.2	1	2–3
	Powder pellet	~1	>0.5		2–3
	Glass fusion beads	~1	>0.2		2
Precision		<0.1	~0.1	<0.1	4
Layer thickness		~3	~3–5	3–5	2

ED-XRF, energy-dispersive X-ray fluorescence; WD-XRF, wavelength-dispersive X-ray fluorescence.

(JCGM\_100:2008 2008) that half of the last significant digit identifies the uncertainty range, that is, a reported value of 45 would mean that  $w = 45.0 \pm 0.5$ . In the case of large numbers, the same convention applies; for an analytical result of 50 000 with two significant digits, the uncertainty specification then would be  $w = (50 \pm 0.5) \times 10^3$  or  $w = 50\,000 \pm 500$ .

Table 6.4 lists the uncertainties that can be expected for the various analytical and measuring tasks possible with X-ray fluorescence, and the significant figures are derived from there. It is very important to pay attention to these conventions since the quality of an analytical result is determined by it and thus its validity.

## 7

## Other Element Analytical Methods

### 7.1 Overview

If X-ray fluorescence (XRF) analysis is conducted with the aim to quantitatively determine the analytes, it is, in principle, a relative measuring method. Even for fundamental-parameter based quantifications independent methods are necessary to provide the basis for a calibration at least during the determination of the geometry parameters of the instrument. Reference materials are used for verification and control of the method.

Since the qualitative and quantitative determination of elements in different materials was one of the first analytical tasks, over the years, many analytical methods were developed, which still provide the basis for the calibration of relative measurement methods.

The classical methods include gravimetric and titrimetric methods, as well as various electrochemical methods such as coulometry, potentiometry, conductometry, and polarography. These methods can operate with simple instruments and are based on fixed stoichiometric relationships. Common to all is that they are time consuming and require a lot of experience from the user.

The most important reference methods for XRF analysis today are atomic spectroscopic methods such as atomic absorption spectrometry (AAS) and atomic emission spectrometry (AES). For metallic samples the emission is stimulated with a spark (Optical Emission Spectrometry [OES]) or in the case of liquid samples in an inductively coupled plasma (ICP). AAS and ICP have gained significance, as they primarily work with liquid samples and thus directly replace the wet-chemistry methods and they achieve an even higher accuracy and sensitivity as well as a significantly greater sample throughput. These methods are based on electron transitions, which occur, unlike than in XRF, between outer electron levels. As a result, the energy differences are significantly smaller, and correspondingly the radiation is of much smaller energy. Optical spectra also have many more lines than X-ray spectra; a suitable selection of the analytical lines allows to tune the sensitivity of the method to the analytical problem. On the other hand, high-resolution spectrometers are required in order to sufficiently separate the large number of individual lines (Cammann 2000).

Mass spectrometry is another analytical method that was developed. Here the analyte is transferred into a gas where the atoms then are ionized. The ions are

accelerated by an electric field and then separated in an electric or magnetic field and finally individually detected. This method is highly selective and sensitive and therefore primarily used for trace analyses.

There are a few additional elemental analytical methods, which are mostly used in research, due to the associated high instrumental complexity, the limited sample throughput, or even the limited application potential. These include methods such as X-ray induced photoelectron spectrometry (XPS), Auger electron spectrometry (AES), secondary ion mass spectrometry (SIMS), neutron activation analysis (NAA), and others.

The group of X-ray spectroscopic methods also includes various methods based on XRF, in which the excitation of the atoms is generated not by X-radiation but by other types of radiation, for example, by electrons in an electron microscope (scanning electron microscope–energy-dispersive spectrometry [SEM-EDS]) or by  $\alpha$  particles (proton-induced X-ray emission [PIXE]).

In addition, there are many one-element detection methods which are highly selective and in parts highly sensitive. They have been developed, for example, for highly toxic elements, like mercury or arsenic. Another method, the combustion analysis is used for elements whose sensitive detection presents difficulties with the usual spectroscopic methods such as carbon, nitrogen, oxygen, or sulfur. For these elements, the samples are burned in an oxygen stream or melted in an inert gas, and the escaping gases are transported to gas detectors. The detection may be carried out for example by the measurement of the thermal conductivity or with an IR spectrometer.

## 7.2 Atomic Absorption Spectrometry (AAS)

The principle of AAS is based on the fact that the mostly monochromatic emission radiation of the element to be analyzed is attenuated when passing through a gas mixture of its own atoms. If free atoms are formed in an atomizer and if the radiation from the analyte element emitted by a hollow cathode lamp (HKL) passed through this gas, the absorbed portion of this radiation is proportional to the number of identical atoms in the atomizer. The atomizer can be a simple flame, a graphite furnace, or others. The temperatures in the atomizer of an AAS can reach up to 3000 K. Under these conditions, the absorption in the flame is affected only by non-ionized atoms.

By comparing the intensities of the direct radiation and the absorbed radiation, it is possible to determine the amount of the element to be analyzed in the gas mixture. The schematic setup of an atomic absorption spectrometer is shown in Figure 7.1.

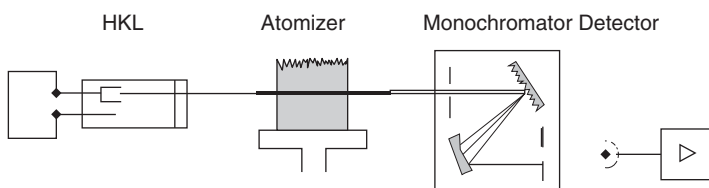


Figure 7.1 Setup of an atomic absorption spectrometer.



Some of the distinct features of the AAS can be concluded from the measuring principle – it is a one-element method, i.e. it is only possible to analyze one element at a time. For the analysis of another element, the excitation source must be changed, and the instrument has to be calibrated or a further instrument is required. Usually, volatile elements are difficult to analyze with AAS.

More recently, it is now also possible to use the AAS as a multi-element method. For this purpose, a light source is used, which emits a continuous spectrum. The analyte line is then selected by a spectrometer. However, this advantage of greater flexibility comes at the expense of reduced sensitivity.

Calibration samples must be measured for each analysis in order to be able to perform a standard-based quantification. The sensitivity of the AAS in the trace region is very high, but the detectable concentration range is only about 2 orders of magnitude. It may therefore be necessary to adjust the sample concentration to the measuring range of the method by dilution.

Despite these limitations, AAS has gained widespread use, also because the instrument design is very simple and can be used with linear calibration functions. A detailed description of the method and its analytical possibilities is provided by Welz and Sperling (1999).

## 7.3 Optical Emission Spectrometry

Optical spectra from an emission process also used for element analyses. The excitation can take place in different ways.

### 7.3.1 Excitation with a Spark Discharge (OES)

A very large amount of energy can be applied to solid metallic samples by means of a spark discharge, thereby creating a plasma at the location of the discharge. The material is evaporated, atomized, and ionized. During the transition to the ground state, an element-specific spectrum is emitted in the optical range. This method is called arc-spark spectrometry or arc optical emission. It requires an electrically conductive sample, i.e. the material be a metal or a pressed pellet containing conductive components. During the excitation, material is evaporated, and a mini crater is formed on the sample surface. The basic setup of an arc-spark spectrometer is shown in Figure 7.2. The method and its analytical possibilities are described extensively by Slickers (1992).

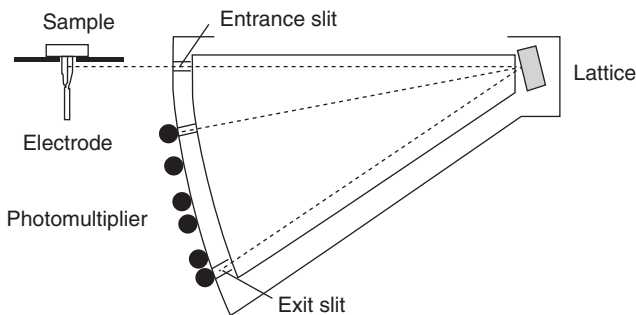


Figure 7.2 Principal setup of an arc-spark spectrometer.

Using arc-spark spectrometry, a wide range of elements can be analyzed with high sensitivity, including light elements which are not accessible to XRF, such as Beryllium, Boron, Carbon or Nitrogen. However, volatile elements do not have good recovery rates as they evaporate during plasma generation.

Arc-spark spectrometry also enables on-site analyses. Instruments are designed so that they are mobile and easy to transport. The sample then does not have to be extracted and transported to the laboratory for the analysis, but the analysis can be performed directly on the non-prepared material. This saves the elaborate task of separating the laboratory sample from the material to be analyzed and its transport to the laboratory. OES also allows for measurements in material storage as well as in plants and buildings.

The calibration is exclusively done with solid reference materials. Many certified reference samples are available for this purpose. Secondary standards or internal reference materials can be prepared using established reference methods.

### 7.3.2 Excitation in an Inductively Coupled Plasma (ICP-OES)

For liquid samples or small-sized materials, optical emission can also be stimulated with an ICP. For this purpose, the sample must be dissolved, atomized into an aerosol, and introduced into the high-frequency plasma through an argon gas stream, where it is heated to temperatures between 6000 and 10 000 K. The atoms, which are then ionized, again emit an optical spectrum when transitioning to the ground state. The optical spectra are dispersed via a lattice and then detected. Photomultipliers have been used as detectors for a long time, but they can only detect a single line. Nowadays, linear CCD detectors also used behind the dispending element for the detection of a wider range of the spectrum. This results in a higher flexibility of the instrument, but the sensitivity and the dynamic range of these detectors are somewhat lower. A detailed description of the method and its analytical capabilities is given, e.g. in Skoog and Leary (1996).

It is also possible to carry out atomization by laser ablation (evaporation) inductively coupled plasma (LA-ICP). Focusing the laser on small sample surfaces, a position-sensitive analysis is then also possible. The basic setup of an ICP-OES spectrometer is shown in Figure 7.3.

The precision and trueness of ICP-OES is usually very good. However, prerequisite is that the sample material is completely dissolved into a solution and contaminations, for example, by the solvent or the digestion instruments, or other influences are avoided.

Due to the use of solutions, it is possible to produce matrix-adjusted calibration solutions using primary substances, thus achieving excellent quantification results. The sensitivity for traces is very high. Nevertheless, it has to be taken into account that a dilution of at least 2 orders of magnitude occurs during the analysis of solids in solution. Correspondingly this leads to lower real detection limits. The digestion of a solid sample can also be very time consuming and has to be carried out complete and residue-free. During calibration and evaluation, the influence of the solution method and the sample matrix on the measurement result must be taken into account.

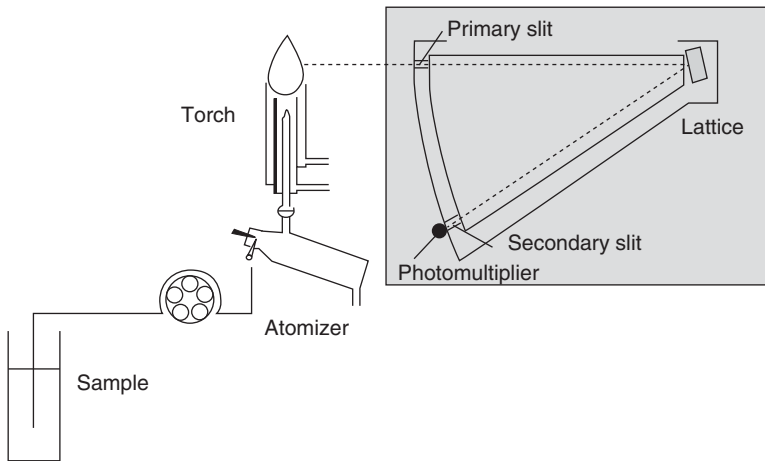


**Figure 7.3** Basic setup of an optical emission spectrometer with excitation by an inductively coupled plasma.

Both arc-spark spectrometry and ICP spectrometry are state-of-the-art analytical methods, they are used in many laboratories. The described optical emission methods, with exception of LA-ICP, are not suitable for a position-sensitive analysis, i.e. the samples to be tested must be homogenized by a suitable preparation technique. For arc-spark spectrometry of metallic samples, this can be done, for example, by remelting, in the case of ICP by dissolving of the material.

The detection with ICP excitation is also possible with a mass spectrometer. The ions in the plasma can be accelerated in an electric field and then separated (inductively coupled plasma mass spectrometry [ICP-MS]). Very high sensitivities for traces can be achieved in this way (see, for example, Thomas 2004).

### 7.3.3 Laser-Induced Breakdown Spectroscopy (LIBS)

Another possibility for the excitation of the optical emission is the generation of a plasma with a laser. This method is called Laser-Induced Breakdown Spectroscopy (LIBS) (Miziolek et al. 2006; Musazzi and Perini 2014). When a short laser pulse with sufficient intensity is applied, material is evaporated and ionized, i.e. a plasma is generated. With the transition to the ground state, the excited atoms emit optical spectra. The scheme of a LIBS instrument is shown in Figure 7.4

The advantage of this type of excitation is that also nonconductive solids but also liquids or gases can be analyzed. Further relatively large measurement distances are possible, i.e. the analysis can be performed for example on hot samples or dangerous regions. By the laser impact the material to be analyzed is evaporated. This can also be used to remove corrosive or contaminated surface layers of the sample.

However, the analytical performance of this method is still not sufficient enough to compete with the traditional methods, in particular due to its limited precision and reproducibility.

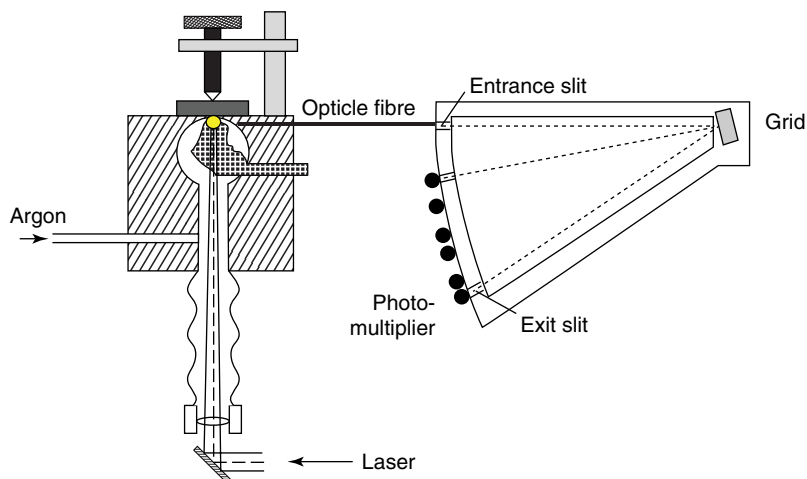


Figure 7.4 Basic setup of a laser-induced breakdown spectrometer.

## 7.4 Mass Spectrometry (MS)

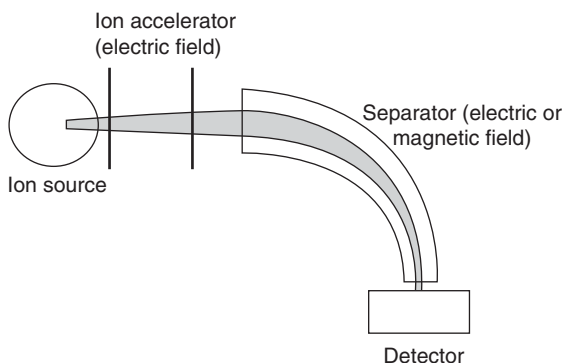
In Mass Spectrometry (MS), atoms or molecules (fragments) are sorted according to their ratio of mass to electrical charge by electric or magnetic fields. The fragments may be either single atoms or conglomerates of atoms or molecules. The ions can be produced in various ways dependent on the substance to be analyzed. Impact ionization, chemical ionization, photoionization, and other methods are used. Depending on the ionization source, a mass spectrometer can also be used as a detector for an upstream ionization or separation source, for example, in the combination ICP-MS, HPLC-MS, or GC-MS.

The ions are accelerated in an electric field and enter the separator. The first mass spectrometers used a changing electric field in which the accelerated ions were decelerated and the collected charges were detected as a function of the electric field (retarding field MS). It is also possible to deviate the ions by electric or magnetic fields acting perpendicular to the trajectory and to register them as a function of the field strength (sector field MS). This separation method ensures the highest resolution and thus the highest sensitivity. If all the ions have the same energy on entry into the analyzer but a different velocity due to their different masses, the time to fly across a certain distance can also be used for differentiation and separation (time-of-flight MS). There are various possibilities to detect ions, for example, photomultipliers, secondary electron multipliers, Faraday cups, microchannel plates, or channeltrons.

The basic setup of a mass spectrometer is illustrated in Figure 7.5 showing the essential components mentioned.

Mass spectrometers have become widely used not only due to their high sensitivity and good separation capability but also due to the simple and robust design of the spectrometers, in particular quadrupole mass spectrometers. A general

**Figure 7.5** Basic setup of a mass spectrometer.



description of the achievable analytical parameters is not possible due to the different ionization sources and separation methods. On the other hand, the method can be matched to various analytical requirements as result of its large setup variety (Budzikiewicz and Schäfer 2005; Gross 2013; Taylor 2001; Blackwell et al. 2005).

## 7.5 X-Ray Spectrometry by Particle Excitation (SEM-EDS, PIXE)

X-ray spectrometry can also be used with other excitation sources. A very often used excitation source is the electron beam in an electron microscope (SEM-EDS) or in an electron probe (electron Probe Micro-Analyzer, EPMA). The strongly focused electron beam produces not only an image of the sample topology but also vacancies in the electron shells of the irradiated atoms, which then emit X-rays as result of the transition into the ground state.

Coupling the high-resolution imaging capability of the electron microscope with a position-sensitive element analysis by XRF is often used. Depending on the strength of the electron beam, wavelength-dispersive (WD) spectrometers are used for the high electron currents in electron beam microanalyzers, and energy-dispersive (ED) spectrometers are used for the lower electron currents in electron microscopes.

The sensitivity of electron beam excitation compared with X-ray excitation is very different which is a result of different excitation probabilities. Figure 7.6 shows the K-shell cross sections for the excitation by electrons and X-rays of different energy in dependence of the element of interest. It can be seen, that electron excitation have significant larger cross sections for the light elements, however, vice versa X-ray excitation for the heavy elements. The analytical possibilities of electron probe microanalysis are described in detail by Eggert (2005) or Love et al. (1978). The excitation with electrons requires a very good vacuum, which excludes the analysis of liquid samples or materials with volatile elements.

Another possibility of X-ray excitation by particles is by protons (PIXE). Here, the protons must be accelerated to energies of several million electronvolts. They can then also create vacancies in inner electron shells of an atom. Depending

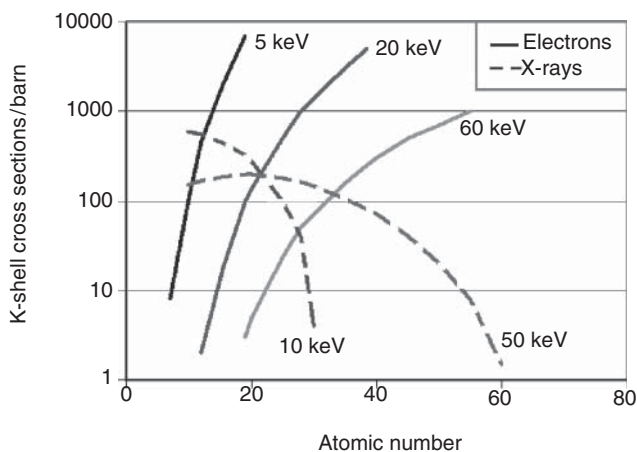


**Figure 7.6** Excitation cross-sections of different elements for monoenergetic electrons and photons.

on the proton energy, the penetration depth of the protons can be controlled relatively exact. Like the excitation by electrons, protons also have high efficiencies in the excitation of light elements (Verma 2007). However, one must take into account that the sample is stressed by the proton beam and the risk of damage, in particular for sensitive materials, is possible. The instrumental effort for a proton accelerator in the MeV range is rather high and can only be realized at certain laboratories.

## 7.6 Comparison of Methods

All described methods have a different analytical performance with respect to the detectable element range, the detectable mass quantities, the requirements on sample type, the analyzed volume, or the required instrumental effort. Therefore, a quality rating of a method over another is not possible. On the contrary, it is often necessary or useful to use several analytical methods side by side in order to characterize a material as comprehensive as possible. A very true statement say: One analytical method is no analytical method.

A comparison of the most important application properties of some of the most frequently used element analyses methods is summarized in Table 7.1. It has to be factored in that the sensitivity data refers to the sample as measured in the instrument. The effort for sample preparation, resulting changes, and contamination to the sample as well as required dilutions are not taken into account.

**Table 7.1** Comparison of methods for element analyses.

Method	Sample quality	Elemental range	Concentration range	Position-sensitive measurement
Combustion analysis	Solid	H, C, N, O, S	0.1–70%	Not possible
AAS	Liquid, solid	All elements, with only few exceptions	Few 0.01 to about 100 mg/l Adjustment of the concentrations range by dilution	Not possible
OES	Metallic samples (electric conductive)	All elements, with only few exceptions	Depending on the analyte line Limit of detection in the range of mg/kg	Possible, but limited resolution
ICP-OES	Liquid, paste-like	All elements, with only few exceptions	Depending on the analyte line 100 ng/l to few 100 mg/l In the case of solid samples, the dilution by digestion must be taken into account	Not possible
MS	Solid, liquid	All elements	<1 ng/l to 100 mg/l for majors the adaption of the concentration range is necessary	Possible; depends on ionization method
WD-XRF	Solid, powder, liquid	All elements with $Z > 5$ (boron)	Few mg/kg to 100%	Limited
ED-XRF	Solid, powder, liquid	All elements with $Z > 11$ (sodium)	Few mg/kg to 100%	Possible
EPMA	Solid	All elements with $Z > 5$ (boron)	From g/kg to 100%	Only position-sensitive, spotsize < 1 $\mu\text{m}$
PIXE	Solid	All elements with $Z > 4$ (Beryllium)	Depending on atomic number	Only position-sensitive, spotsize < 1 $\mu\text{m}$

## 8

## Radiation Protection

## 8.1 Basic Principles

X-ray radiation is an ionizing radiation that can cause damage to organic tissues, which can lead to serious health injuries. These damages depend not only on the absorbed radiation dose but also on its energy as well as of the irradiated tissue.

The absorption of radiation in a material layer of thickness  $d$  is described by Lambert–Beer law (Eq. (2.5)). This situation is shown in Figure 8.1. Not only the thickness  $d$  of the irradiated layer but also the density  $\rho$  and the mass attenuation coefficient  $\mu$  of the material influence the absorption. The mass attenuation coefficient describes both the absorption and the scattering of radiation. However, the scattering is largely negligible in the energy range of interest.

For the assessment of radiation exposure but also for protection for radiation protection shielding, the so-called half-width  $d_{1/2}$  is often used. It indicates the thickness of the material that reduces the radiation intensity to half. This half-width thickness can be calculated from (Eq. (2.5)) according to

$$d_{1/2} = -\ln 0.5 / (\mu \cdot \rho) = 0.693 / (\mu \cdot \rho) \quad (8.1)$$

The mass attenuation coefficient is energy dependent. For organic tissue, the half-width is shown as a function of radiation energy in Figure 8.2. A few fluorescence energies are given for reference. The penetration depth is  $<1$  mm for energies  $<8$  keV and therefore penetrates rarely through the skin, but the penetration depth increases rapidly for higher energies. However, this increase means also a decrease of absorption probability. The radiation penetrates deeper into the human body, but the absorbed radiation dose is smaller, causing less damage.

The absorbed radiation amount, “the dose,” is measured in energy per absorbing mass (Ws/kg). One Ws/kg corresponds to 1 Gray (Gy).

When assessing the radiation exposure to humans, in addition to the dose, the radiation type is also important. The radiation type is factored by the weighting factor  $w_s$ , which has the value 1 for X-rays. The dose absorbed by an organ is called the equivalent dose  $D_{\text{eq}}$  and is given in Sievert (Sv):

$$D_{\text{eq}} (\text{Sv}) = w_s \cdot D (\text{Gy}) \quad (8.2)$$



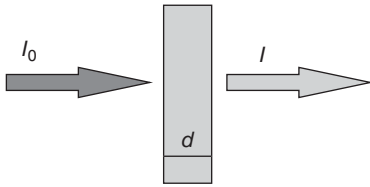


**Figure 8.1** Absorption of radiation in a material layer.

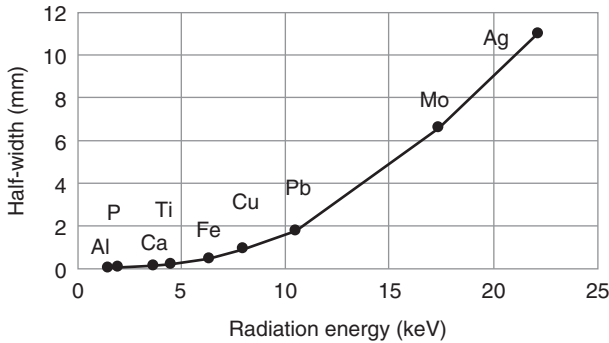


**Figure 8.2** Half-width of organic tissues for different energies.

The effective dose  $D_{\text{eff}}$  is calculated for the whole body and adds the equivalent doses to all organs, multiplied by a tissue weighting factor. It is used for the assessment of expected radiation damage. The equivalent dose rate is the radiation dose taken per time unit and is measured in Sv/h.

## 8.2 Effects of Ionizing Radiation on Human Tissue

The essential damage process in the tissue takes place by the ionization of atoms. The process of ionization also gives this radiation its name. The photoelectrons and Compton electrons produced in the process are absorbed in the immediate vicinity of the site where they are produced and can trigger physicochemical and biochemical reactions. This may be the generation of free radicals or the breaking up of chemical compounds in molecules.

The radiation damage caused thereby can be divided into:

- somatic damages occurring directly in the irradiated organism
- teratogenic damages caused by an embryo during pregnancy, and
- genetic damages, which are caused only in later generations by the damage to the genotype.

The damages occurring can be very diverse, both with respect to the irradiated organs and with respect to the absorbed radiation quantities.

The sensitivity of the individual organs for radiation damage is very different. This is described by relative sensitivities, which have been obtained by statistical investigations. However, they also vary individually as a result of different constitution and predisposition.

**Table 8.1** Relative sensitivities of different body parts.

Tissue	Sensitivity
Germ cells	0.20
Bone marrow, colon, lunge, stomach	0.12
Bladder, breast, liver, gullet, thyroid	0.05
Skin, bone surface	0.01

The relative sensitivities for some organs are summarized in Table 8.1.

The effect of ionizing radiation on the human body depends not only on the total dose absorbed but also on the temporal distribution of the individual doses. A dose of 6 Gy as a one-time irradiation already can be lethal, with partial irradiation of daily 0.5 Gy resistance already 10 times greater. The repair mechanisms of the cells are responsible for this behavior, which can compensate for minor radiation damage even in a relatively short time. These repair mechanisms works better in healthy cells than in diseased cells. The effect of radiation therapies for the treatment of cancer diseases by irradiation is based on this behaviour.

The somatic effects occurring during irradiation depends on the absorbed radiation dose. It is necessary to divide between deterministic and stochastic damages:

- At relatively low doses, i.e. up to about 2 mSv/a, stochastic damage such as cancer and leukemia or even damage to the genetic material can occur; the probability of stochastic damage is proportional to the received dose.
- For higher doses, i.e. up to about 6 Sv/a, direct damages to the irradiated person such as burns, organ failure, and even death can occur.

The health effects of irradiation are called radiation diseases, the course of which at higher beam loads are usually characterized by the following stages:

- *Primary period* (<2 days): Skin redness, burns, exhaustion, drop in blood pressure, sickness, vomiting
- *Latency period* (<14 days): No additional symptoms but changes in the blood count
- *Peak period* (~4 weeks): Sickness, vomiting, hair loss, fever, mucosal inflammation
- *Recovery period* (several month): Healing or defect healing, early aging, cancer

The course of the radiation disease depends on the dose received. The different steps are summarized in Table 8.2.

### 8.3 Natural Radiation Exposure

No one can escape irradiation by ionizing radiation caused by various natural radiation sources. The average environmental dose is, for example, about

**Table 8.2** Radiation levels depending on dose.

Dose (Sv)	Clinical effects	Increased cancer risk (%)	Lethality within 4–6 weeks
0.25	First clinical noticeable effects		
<1	Vomiting, tiredness, diarrhea	10	15%
2–3	Damage of hemopoietic cells and of cells in the gastrointestinal tract, hair loss	15	35–40%
3–4	Increased damage of cells, bleeding in mouth and kidney	20	50%
4–6	Heavy bleeding, extreme heavy sickness, infertility for woman	20	50–90%
6–10	Damaged bone marrow, collapse of the autonomic nervous system		Within 4 weeks
Up to 20	Damaged bone marrow, collapse of the autonomic nervous system		After 1–2 weeks
>20	Damaged bone marrow, collapse of the autonomic nervous system		After 7 days
>50	Damaged bone marrow, collapse of the autonomic nervous system		Within a few hours

2.2 mSv/a in Germany and about 3.1 mSv/a in the United States. It is composed of cosmic radiation, terrestrial radiation, and ingested radiation:

- The cosmic radiation is influenced by the Earth's magnetic field and therefore depends on the position of the Earth and on the altitude. It has a contribution of approximately 0.03  $\mu\text{Sv}$  at sea level, already 0.3  $\mu\text{Sv}$  at an altitude of 5 km, and even 15  $\mu\text{Sv}$  at 15 km altitude. This means that exposure at high altitude flights increases significantly. The total cosmic radiation exposure on Earth is about 0.3 mSv/a.
- Terrestrial radiation is emitted by natural radioactive deposits. Therefore, it is highly variable by location. Main sources are thorium ( $\text{Th}^{232}$ ), uranium ( $\text{U}^{235}$  and  $\text{U}^{238}$ ), and potassium ( $\text{K}^{40}$ ). In certain regions terrestrial radiation exposures to well above 1 mSv/a are possible.
- The ingested exposure is caused, for example, by the inhalation of radon, a radioactive decay product, or the ingestion of other radionuclides with food. This exposure also varies by region and is usually higher in the vicinity of natural deposits. This exposure can amount to about 2.0 mSv/a.

In addition to the natural radiation exposure, artificial radiation exposures must also be taken into account; they may occur by the abovementioned flights at high altitudes, by safety checks at airports or other sensitive security areas, and above all by medical procedure for diagnostic or therapeutic purposes. For example, the dose taken with a chest X-ray image is about 0.3 mSv. This means that it is about equivalent to the natural exposure of approximately 1.5 months, whereas that of an Atlantic flight is about 20 times less.

## 8.4 Radiation Protection Regulations

### 8.4.1 Legal Regulations

Due to the high danger of ionizing radiation, various legal regulations exist for the handling of radiation sources as well as for protection against radiation damage. These regulations are in the authority of the respective country and therefore vary from country to country. It is beyond the scope of this book to summarize the various legislations. The reader is advised to be educated about the legal requirements regarding radiation safety in their jurisdiction before operating any X-ray instrumentation. For a few countries, the main laws are summarized in Table B.4.1.

## 9

## Analysis of Homogeneous Solid Samples

Homogeneous solid materials may be metals, glasses, or even plastics. They are in solid form and a flat and smooth surface can be prepared by machining. Smooth surfaces can be produced by the most commonly used techniques such as appropriate processing, milling, or polishing. When polishing, one must make sure that the polishing material does not penetrate into the sample material and that the lubricant is removed by thorough cleaning. Cleaning in an ultrasonic bath in a slightly acidic medium has proved to eliminate possible surface contamination, which especially would influence the analysis of light elements. For fast-oxidizing metals, the cleaning should be done shortly before the analysis. To check the homogeneity, individual point analyses can be used at different sample sites (see Sections 3.2.5 and 16.6).

For metals, especially when they are in the form of chips, the homogeneity can be improved by a remelting process. However, then care must be taken to ensure that volatile elements are not lost by evaporation or that nonhomogeneous materials are produced by crystallization or phase formation during the cooling process.

Metal analyses are often carried out to assure the product quality. Then a fast but accurate analysis is required. There are a sufficient number of reference samples available for metal alloys; therefore standard-based quantification is preferred for this task. It will ensure high accuracy analyses for this sample type.

However, there is also the need to analyze very different sample qualities, for example, to determine whether the material specifications are met. In this case, it is again a requirement to carry out the analyses quickly, potentially even with a slightly lower accuracy. In this case, fundamental parameter-based quantification models are suitable since the sample qualities to be analyzed are not known and they can change frequently.

For the most common types of solid homogeneous materials, the analysis conditions and expected results are discussed in the following sections.

### 9.1 Iron Alloys

#### 9.1.1 Analytical Problem and Sample Preparation

Iron alloys are used in large quantities and for many types of applications. Therefore, there are a broad range of various alloy types; for the analysis they must be

considered separately. The most important types are pig and cast iron as well as low- and high-alloy steels. They are differentiated by their properties, which are based on the different alloying elements.

The sample preparation can be different for the different alloy types depending on the elements to be analyzed as well as on the hardness of the alloys. The time factor is also important as the analyses are often carried out for the quality control during the production process. Almost all iron alloys contain carbon, which influences their properties greatly. The analysis of carbon with X-ray fluorescence (XRF) is very limited and only possible with wavelength-dispersive spectrometry (WDS) instruments, but also then not very accurate. Therefore, combustion analysis and optical arc spectrometry are often used for the determination of carbon. A further difficulty for the determination of carbon by XRF is the very low information depth of the low-energy fluorescence radiation of carbon in iron; it is only about 0.3  $\mu\text{m}$ . In order to determine these light elements, a high quality of the sample surface is required, as already shown in Figure 3.6. The best procedure for this purpose is polishing with a fine sandpaper.

For both instrument types, i.e. for energy-dispersive spectrometry (EDS) and WDS instruments, the test conditions have to be selected such that no saturation of the detector occurs. Due to the high excitation efficiency for the main elements of these alloys, it is possible that the detectors of both spectrometer types can be saturated: for EDS instruments pile-up peaks are generated (see Section 4.2.6.2), while for WDS instruments peak shape deformation can occur (see Figure 4.9).

### 9.1.2 Analysis of Pig and Cast Iron

Pig and cast iron have a high carbon content, cast iron more than 2.06 wt% and pig iron even more than 4 wt%. The high carbon content makes the iron brittle. Other important elements are P and S, which always accompany Fe, as well as Si and Mn in higher concentrations. Further trace elements may be Ti, Cr, Ni, Nb, and Mo. Occasionally, the number of elements to be determined can be even higher. The contents of P and S are below 0.5 wt%, and that of Si and Mn for pig iron up to 3 and 6 wt%, respectively, while the remaining elements are only traces.

The measurement can be performed with WDS instruments as well as with EDS instruments. WDS instruments are more suitable for the determination of light elements due to their higher resolution and lower achievable detection limits. This also applies to the determination of the carbon content (ApplNote-WDXRF-Cast\_Iron n.d.); nevertheless the analysis is also possible with EDS instruments (ApplNote-EDXRF-Cast\_Iron n.d.). The detection limits for carbon determined with a WDS instruments are approximately 100 mg/kg, about a factor of 10 better than EDS instruments. The precision of the carbon determination, on the other hand, is comparable for both spectrometer types. The mean deviation is about 0.2 wt%, resulting in a mean relative deviation of about 10%. This precision is not sufficient for industrial process control, but alternative analysis methods are available. The mean deviations

**Table 9.1** Mean deviations for a cast iron calibration.

Element	Concentration range (wt%)	RMS WDS (wt%)	RMS EDS (wt%)
C	2–4.2	0.21	0.18
Si	0.3–3.5	0.09	0.12
P	0.009–0.78	0.005	0.01
S	0.006–0.14	0.004	0.006
Ti	0.003–0.12	0.0012	0.002
V	0.002–0.37	0.0012	0.004
Cr	0.018–1.92	0.0097	0.007
Mn	0.09–1.9	0.009	0.021
Ni	0.026–2.4	0.01	0.014
Cu	0.04–0.09	0.003	0.008
Mo	0.007–1.3	0.0055	0.007

(root mean square [RMS]) for Si for both instrument types are about a factor of 2 better than for carbon. For all other elements these values are clearly better. They range from 0.005 to 0.05 wt%, where the values for WDS instruments are slightly better as demonstrated in Table 9.1. Measurement times for WDS instruments are between 30 and 60 seconds for every element, and for EDS instruments, a total of approximately 10 minutes is required if several excitation conditions are used.

During the measurement, the samples should rotate to compensate for inhomogeneities both due to inconsistencies of the sample surface and in the composition. Despite these precautions the standard deviations of repeated measurements, especially for the light elements (C, Si, S), are significantly worse than the statistical error. The standard procedures for the analysis of low-alloy steels and cast iron with WDSs are summarized in ASTM-E\_322-12 (n.d.) and ASTM-E\_1085-16 (n.d.).

### 9.1.3 Analysis of Low-Alloy Steel

In low-alloy steels, the carbon content is below 2.06 wt% and the Fe content is at least 95 wt%, the maximum content of Si is about 1 wt%, and P and S are less than 0.1 wt%. V, Mn, Cr, Ni, Cu, or Mo may be in the range of 1–2 wt%. This also makes the analyses comparable with cast iron due to similar composition.

During production monitoring the sampling takes place directly from the melt using special dipping probes. Sampling is always done from the same part of the casting; the surface of the sample is then ground or more ideally milled (see Figure 3.6). Again, good and newly prepared surfaces are necessary to achieve the required precision.



**Figure 9.1** Pressed pellet of metals chips in a ring of steel.

**Table 9.2** Typical analytical performance of WD spectrometers for low-alloy steel.

Element	C	Si	P	S	V	Cr	Mn	Ni	Cu	Mo
Content (wt%)	0.39	0.22	0.072	0.055	0.37	1.34	0.95	0.36	2.16	0.36
$\sigma_{\text{rel/precision}}$ (%)	4.46	0.29	0.64	1.16	0.23	0.10	0.28	0.06	0.19	0.30
$\sigma_{\text{rel/stability}}$ (%)	1.77	0.32	0.49	2.10	0.20	0.18	0.44	0.06	0.22	0.31
$\sigma_{\text{stat}}$ (%)	0.45	0.17	0.47	0.57	0.16	0.07	0.15	0.03	0.09	0.26

Source: According to ApplNote-WDXRF-Low-Steel n.d.

If the sample material is only available as small parts or chips, the sample material can be pressed in a hardened steel ring into a stable, compact pellet (Figure 9.1). Due to the material properties, the sample is still porous, which can lead to a lower precision of the results. This effect can be reduced by spinning the sample during the measurement.

The lower carbon contents of low-alloy steels require WDS instruments for a sufficiently accurate determination; however, preferably other analyses methods such as combustion analysis or arc-spark spectrometry are used for the analysis of carbon. Multichannel instruments are also used to keep the analyses times low, especially in the case of production monitoring. The time to analyze then just depends on the accuracy requirements.

The various steel grades are standardized with their contents and properties (DIN-EN 10020: 2000-07, SAE Steel Grades n.d.). The concentrations are within narrow limits and require an accurate analysis, which is based on measurements of high precision and repeatability.

Typical results from 10 repeatability measurements of a low-alloy steel are given in (ApplNote-WDXRF-Low-Steel n.d.). They are summarized in Table 9.2, where  $\sigma_{\text{rel/precision}}$  is the repeatability, i.e. the precision taken from successive measurements (see Eq. (6.3));  $\sigma_{\text{rel/stability}}$  is the deviation of measurements taken over several days; and  $\sigma_{\text{stat}}$  is the statistical error calculated from the acquired counts (see Eq. (6.4)).



The repeatability measurements are related to the statistical error ( $\sigma_{\text{rel/precision}}$ ) and therefore strongly influenced by the element concentration. However, they are significantly larger for most elements compared to the statistical uncertainties  $\sigma_{\text{stat}}$ . This means that the contribution of the measuring method to the measurement uncertainty is larger than the statistical contributions. This is valid especially for carbon, which indicates that the sample volume contributing to the measurement signal changes during the measurements. This assumption is supported by the fact that, for stability measurements, where for every measurement the sample was newly grinded, the uncertainties ( $\sigma_{\text{rel/stability}}$ ) for the light elements are smaller than for the consecutive measurements for repeatability ( $\sigma_{\text{rel/precision}}$ ). Fe usually is determined as difference to 100%.

#### 9.1.4 Analysis of High-Alloy Steel

For high-alloy steels, the alloying elements have a content of at least 5 wt%. These elements determine the properties of the steel. The carbon contents are below 1.5 wt%, and those of P and S less than 0.05 wt%. Cr and Ni as main alloying elements produce a stainless steel since the high Cr content on the material surface builds up a passivation layer of  $\text{Cr}_2\text{O}_3$ . On the other hand, alloying elements like Ti, V, Cr, Co, Ni, Mo, and W produce hard and heat-resistant steels, which can be used for the manufacturing of tools. The concentrations of these elements can be relatively high: for stainless steel, the Cr content has to be at least 10.5 wt% and can be up to more than 25 wt%, and for tool steel the W content can be up to 20 wt%. Again, carbon content is often determined by a separate combustion analysis or by arc-spark spectrometry. The procedures for the analysis of stainless steels by WDS are summarized in ASTM-E\_572-13 (n.d.).

The samples are prepared as in the case of cast iron by grinding (100  $\mu\text{m}$  sandpaper) or milling. In both cases, careful cleaning of the sample is required to avoid surface contaminations. In particular, when grinding, it must be noted that the results of the main components depend strongly on the surface roughness, as shown in Figure 9.2 for the accessory element Cr (DIN-EN-10315 2006-10).

Usually multichannel WD spectrometers are used since the lab is under extreme time pressure from the mill to produce results. The high demand on the accuracy of the analyses is realized with WDS instruments. Typical analytical

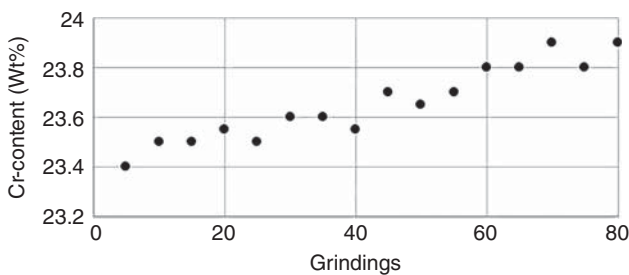


Figure 9.2 Change in measured Cr content as a function of grinding passes.

**Table 9.3** Analytical performance of WD spectrometers for stainless steel.

Elements	Si	P	S	Cr	Mn	Ni	Cu	Mo
Typical content								
Minimum (wt%)	0.2	0.005	0.004	9	0.24	0.25	0.01	0.01
Maximum (wt%)	1.4	0.03	0.04	25	1.7	20	0.35	3.5
$\sigma_{\text{rel/precision}}$ (%)	0.15	1.0	0.9	0.03	0.07	0.04	3.5	0.45
$\sigma_{\text{rel/stability}}$ (%)	0.14	1.1	0.7	0.03	0.1	0.07	2.7	0.9
$\sigma_{\text{stat}}$ (%)	0.13	0.95	0.95	0.01	0.06	0.03	0.45	0.16

Source: According to ApplNote-WDXRF-Stainless\_Steel n.d.

**Table 9.4** Analytical performance of WD spectrometers for tool steel.

Elements	Si	P	S	V	Cr	Mn	Co	Ni	Mo	W
Typical content										
Minimum (wt%)	0.14	0.009	0.006	0.18	0.25	0.19	0.007	0.045	0.06	0.03
Maximum (wt%)	2.0	0.04	0.1	1.9	11.5	1.2	10	1.45	9.4	20.4
$\sigma_{\text{rel/precision}}$ (%)	0.29	0.34	0.62	0.50	0.21	0.15	0.17	0.31	0.40	0.18
$\sigma_{\text{rel/stability}}$ (%)	0.34	0.47	0.36	0.44	0.24	0.10	0.13	0.22	0.40	0.18
$\sigma_{\text{stat}}$ (%)	0.19	0.42	0.49	0.50	0.15	0.10	0.08	0.21	0.48	0.12

Source: According to ApplNote-WDXRF-Tool\_Steel n.d.

results for a stainless steel are given in Table 9.3. Here trace elements such as Ti, V, Co, As, and Nb with mass fractions below 0.3 wt% are neglected. Again typical values for the standard deviations for precision  $\sigma_{\text{rel/precision}}$  and stability  $\sigma_{\text{rel/stability}}$  of repeated measurements and the respective statistical error  $\sigma_{\text{stat}}$  are presented. Precision and stability are not significantly different, but the statistical error for Cr, Ni, Cu, and Mo are more than a factor of 2 less than the standard deviation  $\sigma_{\text{rel/precision}}$  of the repeatability measurements. This can be caused by inaccurate intensity determinations due to peak overlaps or other systematic errors.

In Table 9.4 similar results are presented for tool steels. In this case all three standard deviations are in the same order of magnitude for the same element.

## 9.2 Ni–Fe–Co Alloys

This type of alloys is characterized by high durability, temperature resistance, and corrosion resistance. They are structural materials for high-temperature applications and are used wherever materials undergo high stresses and high reliability is required, for example, in steam and aircraft turbines and tools but also in heat exchangers in power plants. Their compositions vary widely. Many alloying elements such as Al, Si, Ti, Cr, Cu, Mn, Nb, Mo, Ta, or W are added to the main elements and influencing the mechanical or thermal properties.

The samples are usually prepared by polishing with a fine grind sandpaper or even with diamond powder. The removal of the polishing agent by careful cleaning is necessary.

The measuring conditions have to be selected such to avoid detector saturations (see the remarks in Section 9.1.1).

For the measurement predominantly WDS instruments are used since high accuracies are required as a result of the cost of the alloying components. The achievable precision and trueness are comparable to the analyses of high-alloy steels.

The measurement procedure for these alloys is standardized, for example, in ASTM-E\_2465-13 (n.d.).

## 9.3 Copper Alloys

### 9.3.1 Analytical Task

The composition of copper alloys varies greatly (DIN-EN-1652, 1998:03). Copper can be alloyed with tin (bronze), zinc (brass), nickel and zinc (nickel silver), manganese and nickel (constantan), and beryllium (copper–beryllium), but also combinations of these elements as well as other alloying components are common to accomplish a wide spectrum of properties.

In addition to the mentioned main alloying elements the most important additional components are Al, P, Cr, Mn, Fe, Ni, Zn, Sn, Pb, and Bi. Suitable traces are Mg, Si, S, Co, As, and Sb.

### 9.3.2 Analysis of Compact Samples

The sample preparation should be done by turning or milling, and the analysis should be performed shortly after the preparation. In the case of Cu alloys containing lead, it should be noted that the Pb can diffuse out of the Cu and is then being smeared over the surface during polishing. This has a significant influence on the measurement of light element since they will be heavily absorbed by the Pb.

The achievable accuracies are comparable with those obtained for high-alloy steels; relative deviations in the range of less than 0.2% are possible for the main components; for traces they are accordingly larger (DIN-EN-15063-1/2 (2007-01)).

Forceful analyses are not possible on copper–beryllium alloys; an exact determination of beryllium is not possibly caused by its low fluorescence energy and the associated very small information depth. Here arc-spark spectroscopy can be an appropriate analytical method.

### 9.3.3 Analysis of Dissolved Samples

In various cases, it may be helpful to dissolve alloys and measure them as a liquid. In this case, inhomogeneities of the material are not a factor, and the preparation of reference samples is simple. They can easily be prepared by solutions of the salts of the various elements, and different contents can then be obtained by varying

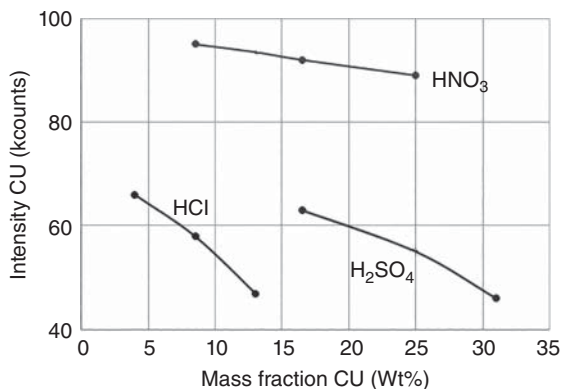


**Figure 9.3** Influence of acids on the measured signal of Cu. Source: Courtesy of A. Janßen, former FH Münster.

the amount of the solvent. However, it must be noted that this preparation procedure is time consuming and means a dilution of the sample that could complicate the analysis of traces. Janßen et al. (1997) have investigated the analysis of copper alloys in solution.

Acids were used in the preparation of the solutions. They are to be selected depending on the alloy to be analyzed. They should completely dissolve the alloy and influence the measuring signal very little. It was shown that nitric acid has the least influence, as shown in Figure 9.3. Small differences in the concentration of the acid that can occur during the preparation are then negligible. For preparing the samples, exactly 1 g of the alloy to be tested was dissolved in a solution of each 5 ml H<sub>2</sub>O and HNO<sub>3</sub>. The resulting nitrogen oxides evaporate during the digestion process, and the solution was let to cool and filled up to 100 ml with water. The samples were then filled into sample cups. The filling height should be determined such that no intensity increase is observed with further increasing the amount of the sample; at least the fill height should always be the same. The durability of the window films should also be ensured. In this study polyester films of 6 µm thickness were used. It is recommended to test the durability of the films before any measurement. This can be done by placing the filled cuvettes onto blotting paper. If no traces are visible on the blotting paper after approximately twice the measurement time, the so prepared cuvette can be measured. The influence of the film on the measurement signal depends on the analyte; for copper solutions it is largely negligible. For larger distances between sample and spectrometer, the measuring medium, i.e. air, can affect the measured signal (see Figure 5.7). Since the measurement of solutions in vacuum is not possible, only flushing with helium can reduce the absorption of the signal. For the measurement, it is also recommended to close the cuvettes in order to avoid evaporation of the solution, which can lead to corrosion of the instrument.

The measurements were done using a WD spectrometer. The measuring times were 10 seconds per element and background position. A relative statistical error of approximately 0.5% was achieved.

For the quantification both external and internal standards were used. For external standards, solutions with different concentrations were prepared in the same matrix. Co was used as internal standard; the same amount was added to

the unknown and calibration sample. In this way the matrix influence can be corrected by correlating the analyte intensities to the Co intensities.

Comparing the results shows that considering the matrix influence by including an internal standard or by using the appropriate intensity ratios of the analytes themselves provides the best results. The relative errors achieved are then in the range of <1% and are therefore adequate for most problems.

## 9.4 Aluminum Alloys

Aluminum is an abundant element and its alloys are widely used. Aluminum is a light metal, unalloyed; however it only has limited structural strength. The metal properties can be strongly influenced by alloying with Be, Mg, Si, Ti, Mn, Ni, Cu, and Zn, as well as traces of Ti and Mn. The mechanical properties are influenced by the composition of the alloys, by heat treatment, and through strain hardening. Aluminum also has very good corrosion resistance. The different alloys are standardized in EN-573\_3-2013-12 2013 and ANSI H35.1. Except for beryllium, all other elements can be determined by XRF. The contents are usually in the 1 wt% range; for certain alloys with Mg, Si, or Zn, they also can be significantly higher. The Si content should not be higher than ~12 wt%; otherwise the Si will be insoluble and crystallize.

The preparation of Al alloys should be done by turning or better by milling. During polishing, there is a risk that the abrasive, possibly even constituents of the alloy itself, can be worked into the alloy, which will then lead to a falsification of the analysis results. After the preparation by milling, the lubricants should be washed off, for example, with ethanol. The preparation should be carried out just before the analysis so that the measurement is not influenced by the formation of an Al oxide surface layer.

In the case of small particle or chip-shaped sample materials, it is easily possible to press them into a suitable mold (see Figure 9.1). Aluminum can be compressed to such an extent that stable, almost pore-free compact samples are produced. In the case of inhomogeneous samples, approximately 50 g of the material can be melted in a ceramic mold at about 800 °C in a muffle furnace and then cast into an appropriate mold. The melt can be solidified in the crucible. Due to the specific gravity, the oxidic impurities in the starting material are later found on the surface of the solidified sample. After mechanical cleaning of the sample, the amount of impurities in the starting material can be determined by differential weighing. In this way only the concentration of the metallic fraction is determined during the analysis of the melt. The final preparation is carried out as described above by turning or milling.

The analyses are usually done by WDS instruments since most alloying elements have low-energy X-ray lines that require higher-resolution instruments. Detection limits of 1 µg/g can be reached, which are adequate for most analytical problems. The relative mean deviations of the analyses from the certified values of the reference samples are in the range of 0.5%. Information on the typical analytical performance is given in Table 9.5.

**Table 9.5** Analytical performance of WD spectrometers for the analysis of Al alloys.

Element	Mg	Si	Ti	Mn	Fe	Ni	Cu	Zn
Typical content								
Minimum (wt%)	0.20	0.3	0.0	0.01	0.05	0.0	0.02	0.01
Maximum (wt%)	7.5	8.2	0.25	0.85	1.1	0.3	1.5	1.1
Mean deviation								
Absolute (wt%)	0.035	0.045	0.007	0.0055	0.009	0.012	0.007	0.008
Relative (%)	≈1	≈1	≈3	≈1	≈1	≈5	≈1	≈1

Source: According to ApplNote-WDXRF-Al-alloy n.d.

## 9.5 Special Metals

### 9.5.1 Refractories

#### 9.5.1.1 Analytical Problem

Refractory metals mainly belong to the fourth, fifth, and sixth subgroup of the periodic table. They are Ti, Zr, Hf and V, Nb, Ta and Cr, Mo, W, respectively. They have a very high melting point in common and are therefore highly temperature stable and exhibit a small thermal expansion. Not only the metals but also their carbides, silicides, or borides show a high wear and heat resistance. These compounds are usually mixed with a binder, e.g. Co, Ni, or Fe, and then sintered. The high hardness, high heat resistance, and high wear resistance make these materials ideal for use as cutting tools or where high abrasion resistance is required.

The analysis during the production and processing of these materials requires the determination of the content of the main components as well as the secondary elements in the raw materials, i.e. in ores, in hard-metal scrap and slags, as well as the characterization of the finished products.

Sample preparation of these hard metals is only possible with diamond tools or with electrical discharge machining. This complicates the preparation of the test samples. Therefore, refractories are often digested and then analyzed as a fusion bead.

Hard metals are frequently used as tool surface coatings, where steel often is the base material. In this case the analytical problem is the characterization of the hard-metal layers, i.e. the determination of their composition and thickness. For these measurements, dedicated coating thickness instruments are available. They have small measuring spot capability; the sample then does not require any special sample preparation.

#### 9.5.1.2 Sample Preparation of Hard Metals

Preparing refractories is dependent on the material to be analyzed, i.e. raw material, scrap metal, or hard metal. Samples are usually prepared using lithium borate ( $\text{Li}_2\text{B}_4\text{O}_7$  but also  $\text{LiBO}_2$ ) or sodium borate ( $\text{Na}_2\text{B}_4\text{O}_7$ ) fusion flux (Peters

and Schröder 1996). Additives of nitrate salts ( $\text{KNO}_3$ ,  $\text{NaNO}_3$ ) are frequently required to support the oxidation of the initial starting materials that can be added to increase the alkalinity. This additive also lowers the melting point of lithium tetraborate by the formation of an eutectic.

The following basic conditions must be considered when using a digestion method for the sample preparation of the various refractory materials (Peters and Schröder 1997):

- The raw sample must be in oxidic form. This can be achieved by extended annealing at about 800 °C in air. If this is not sufficient, for example, in the case of boron, silicon, or chromium carbides, pre-oxidation with 1 g of  $\text{Na}_2\text{CO}_3$  or  $\text{Li}_2\text{CO}_3$  in a Pt crucible is necessary. Afterward  $\text{Li}_2\text{B}_4\text{O}_7$  can be added to the sample up to a weight of 5 g; then this mixture can be melted.
- The grain size of the sample material must be very fine (<63  $\mu\text{m}$ ). When grinding, care must be taken that the grinding tools do not contaminate the sample. Larger particle size material can also be first dissolved directly in a mixture of hydrofluoric and nitric acid in a Pt crucible. After the drying process, the residue must be homogenized with  $\text{KNO}_3$ .
- Powder-like mixtures of borides and carbides of the refractory metals can easily be converted into oxides by a borate digestion. However, difficulties can arise in the digestion process of silicon refractory material, for mixtures of  $\text{Si}_3\text{N}_4$ , and for W/Re compounds.
- W/Re alloys cannot be prepared by fusion in a borate since rhenium oxide is highly volatile. Therefore, an alkaline digestion and the analysis of the solution are required. For this purpose, 50 mg of the alloy is dissolved in a mixture of each 5 ml HF (40%) and  $\text{HNO}_3$  (65%). After drying, the residue is mixed with 6 g of  $\text{K}_2\text{CO}_3$  and 4 g of  $\text{Na}_2\text{CO}_3$ , and the mixture is then leached in water. This solution can directly be analyzed.
- Mixtures of borides, carbides, nitrides, and oxides of Si are first dissolved in a 1 : 3 mixture of HCl (36%) and  $\text{HNO}_3$  (36%) in a porcelain crucible and then concentrated by evaporation with the addition of  $\text{H}_2\text{SO}_4$ . After calcination at 800 °C, a borate digestion can be carried out.
- Appropriate crucible materials shall be used for the digestion processes; Pt with 5 wt% Au is the most suitable.
- Digestion must be complete, that is, the digestion pellets must be homogeneous and stable.

### 9.5.1.3 Analysis of Hard Metals

There are only a limited number of elements that need to be analyzed in hard-metal products; however, strong overlaps of L-lines are possible for heavy metals. Analyzing the raw materials, in particular hard-metal scrap, the number of elements can be significantly expanded since carbides are often embedded in ductile phases.

Due to the required high spectral resolution, analyses are mostly carried out with WD spectrometers. The analytical accuracies that can be obtained are primarily determined by the uncertainties caused by the sample preparation as well as by statistical errors. For quantification, primarily standardized models

are used, and the calibration samples are often produced by the customers themselves (DIN-EN-ISO-12677 (2013-02), DIN ISO 4883:1991-06).

The procedures for the analysis of tungsten and tungsten alloys are summarized in ASTM-B\_890-07 (2012).

For the characterization of hard-metal coatings, the corresponding quantification models are used. Hard-metal layers usually contain only a few elements. For the characterization of layer thickness, EDS instruments can be used, and their spot size capability is also advantageous for the analysis of small areas as well as for the analysis of irregularly shaped surfaces of finished products.

### 9.5.2 Titanium Alloys

Titanium is similar to aluminum in that it is a metal with low density but in contrast it has a much higher melting point and higher strength. Ti is increasingly used in not only aviation and space industries because of its high strength to weight ratios but also in aggressive chemical environments because of its high corrosion resistance. Alloying with other metals in relatively low concentrations, mainly Al, V, Cr, Fe, Ni, Zr, Mo, and Sn, can change and optimize the mechanical properties.

Sample preparation can be carried out by milling or polishing with diamond paper. Preparation should be done before every measurement because buildup of a thin oxide layer can influence the measurement. The analysis of Ti alloys is standardized in ASTM-E\_539-11 (n.d.).

The accuracy that can be expected is comparable with that of Fe alloys.

### 9.5.3 Solder Alloys

The requirements for the **Restriction of Hazardous Substances (RoHS)** in consumer goods have increased the requirements for the analysis of soft solder alloys. Soft solder alloys are usually Sn based, which in the past had a high Pb content to achieve low melting points. The requirements were to reduce the Pb content in a new set of solder alloys, at the same time maintaining low melting points of the alloys in order to avoid excessive thermal load on the electronic components during their processing. Typical alloying elements for Sn are Cu, Zn, Ag, and Bi; it must however be possible to detect also traces of the toxic metals such as Pb or Cd. They must be quantified to meet the requirements of the RoHS regulation (see Section 15.4). Nevertheless, Pb concentrations of up to 3 wt% are necessary to avoid Sn whiskering. Low melting temperatures can be achieved in eutectics. In this case the Sn alloying elements have to be within a rather narrow concentration range. This requires highly accurate characterization of low mass fractions for which XRF is suitable. Typical compositions of these new soft solder alloys are shown in Table 9.6, also indicating the eutectic alloys.

The analysis required is usually done on the raw solder material in order to determine the composition of the solders that have not yet been processed. In this way their soldering properties can be ensured. Simple metal disks can be used for this purpose. The elements that need to be analyzed have relatively high fluorescence energies and therefore greater penetration depths; as a result, the



**Table 9.6** Composition of eutectics of soft solders.

Solder	Melting point (°C)	Eutectic
Sn96.5 Ag3.0 Cu0.5	217	
Sn96.3 Ag3.7	221	X
Sn99.3 Cu0.7	227	X
Sn99 Ag0.3 Cu0.7	227	X

'X' means that this are eutectics.

**Table 9.7** Analytical performance for the analyses of soft solders.

Element	Given content	LOD	Mean analytical results
Cu	1.01 ± 0.019 wt%	1.7 (mg/kg)	1.03 ± 0.00 wt%
Ag	2.98 ± 0.02 wt%	16 (mg/kg)	2.98 ± 0.01 wt%
Cd	88.0 ± 3.2 mg/kg	8 (mg/kg)	89.1 ± 7.0 mg/kg
Pb	520.9 ± 8.9 mg/kg	1.1 (mg/kg)	535 ± 4.1 mg/kg

Source: According to LabReport-XRF\_096 (n.d.).

requirements on the quality of the sample are pretty low. Both WDS and EDS instruments can be used for the measurements.

If the solders are already processed and mainly the compliance with the RoHS has to be controlled, then the areas that are available for the analysis are usually small. This involves measurements on finished printed circuit board. Therefore, position-sensitive analytical methods as described in Section 15.5 are required, but they are usually energy dispersive. An example for the analysis of solder points is discussed in Section 14.4.5.4.

Analysis results measured with WDS instruments on a reference sample are summarized in Table 9.7. The reported repeatability was determined by means of 10 repeated measurements at 300 seconds each.

## 9.6 Precious Metals

### 9.6.1 Analysis of Precious Metal Jewelry

#### 9.6.1.1 Analytical Task

In general terms, the same conditions apply to the analysis of precious metal as for other metal alloys. The main difference, however, is that these alloys are often mixed from pure gold and prepared additional alloys, melted, and then directly poured into jewelry piece molds. Therefore, analyses of precious metals in jewelry are mostly done on the finished products.

The elemental composition of jewelry is very closely controlled in many countries, not only in order to secure their monetary value but also because precious metals are strictly controlled as they are treated as financial reserves.

For the analysis of jewelry, the following conditions have to be considered:

- As a result of the precious metal value and the cost of manufacturing the jewelry, a destructive analysis is limited.
- Since jewelry pieces are often very intricate, only few small flat sample surfaces are available for the analyses. As a result, the fluorescence intensities are smaller compared with the analyses on large surfaces. For this reason, energy-dispersive (ED) spectrometers are usually used. Their spectroscopic performance is adequate to these analyses, since jewelry alloys usually only consist of a few elements that can be easily separated. The high concentrations of the alloy elements do not demand a high sensitivity instrument, and even relatively simple EDS instruments can be used.
- The monetary value of jewelry items can be very high due to the value of the precious metal used; as a result even small analytical errors affect the determination of their value considerably. Consequently, very high analytical accuracies are required.
- XRF competes with fire assay – a highly accurate analytical method to determine the content of gold and silver in precious metal alloys. Fire assay is a gravimetric method in which first the weight of the starting material is determined and then the sample material is depleted from all non-precious components and weighted again to determine the precious metal content by difference. The removal of all non-precious metal content is carried out by oxidation of the melted sample in an oxygen stream at temperatures of 1000–1200 °C. In a final step silver is dissolved by treating the sample silver in fuming nitric acid. By means of the differences in weights, both the gold and silver content of the sample can be determined very accurately.

Due to the availability of high precision balances, very high analytical accuracies can be achieved; repeatability and trueness are in the range of 0.02 wt%, i.e. approximately 1 order of magnitude better than what can be achieved by XRF. Some of the disadvantages of the method are as follows:

- The method is destructive; the analysis requires about 0.25 g of the sample material.
- It is time consuming; a fire assay takes at least four to six hours.
- The method only determines the gold and silver content; other elements that influence alloying properties such as color or machinability are determined only in sum.
- A characteristic of jewelry analysis is that usually the main components are of main interest, which means that the statistical errors are small using X-ray spectrometry.

### 9.6.1.2 Sample Shape and Preparation

The often intricate and irregular shapes of jewelry as well as the often varying composition of different parts of a piece of jewelry require the analysis of small sample surfaces. Spot sizes of 0.3–1 mm are required. Conventional incident beam shaping by collimators is sufficient.

The irregular shapes of the samples make it also difficult to position the sample in the instrument in the appropriate measuring geometry. For this purpose, the

excitation from the top has been proven as advantageous, since the sample can then be positioned in any desired position. The exact measuring position can then be adjustable by a three-axis movement of the sample support. A sample fixture can also aid in the proper positioning of the samples.

Usually there is no sample preparation since it can destroy the jewelry piece. However, this is not always an option since surface conditions, which are the result of a surface refinement made at the end of the manufacturing process – for example, a chemical polish – can influence the analytical result.

By means of such a polish, non-precious components can be leached from the material surface. This results in an enrichment of the precious metals on the surface of the jewelry, giving the impression of a more noble metal.

The crystalline structure of the material can also influence the measured intensities. By removing a very thin layer from the sample surface, such influences can be avoided. Since the analyzed areas are typically  $<1 \text{ mm}^2$  and the measurement can be taken place out at a location that is not visible, this type of sample preparation usually means no loss in value of the jewelry.

### 9.6.1.3 Analytical Equipment

EDS instruments are usually the best choice for measuring precious metals; they are well suited to measure the low intensity fluorescence radiation that can be expected from the small sample surfaces.

A tube voltage of 40 kV is usually sufficient for the excitation of all analytes. The absorption edges of gold and platinum as well as the common non-precious elements (nickel, copper, zinc) are in the range of  $<12 \text{ keV}$ , and that of alloying elements such as silver, palladium, or cadmium at  $<27 \text{ keV}$ . This radiation energy can excite all elements with sufficient efficiency.

Depending on the specific analytical task, both proportional counters and semiconductor detectors with higher resolution can be used.

For quality control in the production process, it can be assumed that the qualitative composition of the sample is known, i.e. the resolution for the separation of analyte lines does not need to be very high. The peak areas of overlapping peaks can be determined by deconvolution procedures with relatively high accuracy. For this purpose, even the resolution of proportional counters is sufficient. In addition, they have a large detection area, i.e. they can capture a large solid angle of the fluorescence radiation, and they are very stable and cost effective.

If, on the other hand, an unknown material must be analyzed in which the qualitative composition is unknown, a higher-resolution semiconductor detector is required. The smaller peak overlap then results in smaller errors in the determination of the peak area, as demonstrated in Figure 5.21. In addition, the better resolution is also helpful in accurately quantifying neighboring elements with small differences in line energies, for example, in dental alloys, which mostly contain platinum as well as gold.

Measurement times for precious metal analyses are usually in the range of minutes. This time is enough to collect sufficient intensities for the analysis of metal contents even from small sample surfaces. The statistical error will also be well within the range of  $<0.2\%$ .

**Table 9.8** Accuracies for the analysis of gold alloys.

Gold mass fraction (wt%)	Karat	Statistical error for Au (%)	Mean deviation (wt%)
33–45	8–12	0.45	0.24
24–60	12–16	0.37	0.14
60–85	14–20	0.33	0.14
85–100	20–24	0.30	0.07

#### 9.6.1.4 Accuracy of the Analysis

If it is assumed that the statistical error of the measurement can be kept sufficiently small and instrument errors are negligible, the analysis errors are then primarily the result of the peak area determination of the used quantification model, i.e. accounting for the correct matrix interaction as well as the quality of the calibration samples.

The complications of peak area determination as a function of the detector resolution have already been discussed. When using detectors with limited energy resolution, stronger peak overlaps have to be expected, which then also result in greater uncertainties in the determination of the peak area. The quantification model that is used also has an influence on the trueness of the analysis. Higher accuracies are achieved with evaluation models using standards.

The mean deviations that are achievable with such models as well as the statistical errors during measurement times of 120 seconds (which depend on the gold content and therefore on the accumulated intensity) are summarized in Table 9.8. It should be noted that the gold content often is expressed in karat. Twenty-four karats correspond to pure gold; correspondingly 1 karat (100/24) is about 4.17 wt%. This also results in the frequently used denomination for the gold contents of 333, 585, 750, or 916 (8, 14, 18, or 22 karats).

Calibration samples for the analysis of gold alloys are offered (for example, Fluxana, Fischer, Valcambi, or Goodfellow; see Table B.2.5). However, they are often also produced by the manufacturers themselves since fire assay provides a very precise analytical method for the analyses of gold and silver in these samples. Gold and silver alloys can also be manufactured with very good homogeneity.

#### 9.6.2 Analysis of Pure Elements

The production of precious metals with very high purity can be very costly. The increase in material value is not significant, but the cost of its refining. This becomes important, for example, for the production of precious metal bullions.

As discussed for the other samples, surface effects can influence the measured intensities. Therefore, the removal of a thin surface layer may be necessary. When analyzing gold bars, drilling chips are often used for the analysis. In this way inhomogeneities throughout the gold bar or even the use of lower-alloy content inside the ingot can be detected.

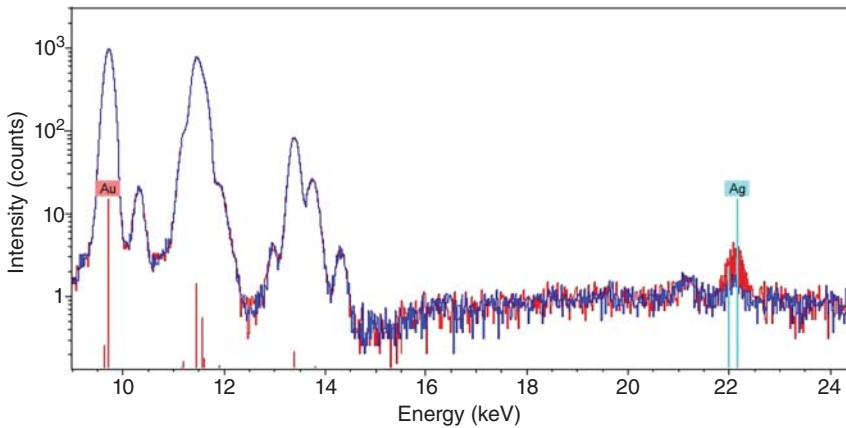


**Figure 9.4** Spectra of high-purity gold with varying small silver contents (y-axis in logarithmic scale).

The analysis of pure metals can be performed in different ways with XRF. One possibility is to directly determine the pure element content; then the statistical error dominates the quantification, i.e. uncertainties of at least 0.1–0.2% have to be expected.

The other possibility is to analyze the remaining traces in the material. If these values are in the range of <0.1% and can be determined with a relative uncertainty of only 5%, then the absolute errors are in the range of 0.005 wt%. Since these errors carry over to the main elements by difference to 100%, the error is significantly less than for the direct quantification.

As a result, the determination of the remaining traces is much more effective than the direct analysis, even when not all impurities can be detected. This becomes evident in the spectra of high-purity gold with different silver contents as shown in Figure 9.4. While the differences of the gold intensities are equal within their statistical uncertainty and are therefore not recognizable, the spectra clearly show recognizable differences in the silver intensities. These differences can be used for quantification.

This analysis method for pure substances cannot only be used for precious metals but also for other materials, since the absolute errors in the determination of traces are usually smaller than the uncertainties caused by the statistics in the determination of the main components. One should be aware, however, that the material analyzed can also contain elements such as nitrogen or oxygen, which cannot be detected with XRF. They of course can be analyzed by alternative methods, such as combustion analysis.

## 9.7 Glass Material

### 9.7.1 Analytical Task

The analytical task in the production and evaluation of glass can be very different. On the one hand, analyses of the raw materials are required in order to ensure

the desired quality of the final products. These raw materials are usually powders. The analyses of powdered materials are discussed in more detail in Chapter 10. Another task is of course the analysis of the final product – the glass itself – to determine its correct composition.

Depending on the specific use and the shape of the glass, the analytical questions as well as the methods of preparation can be very different. During the manufacturing of flat glass (often also called plate or float glass), the focus is primarily on the composition in order to ensure the product quality. It is also possible that impurities in the glass, for example, in the form of inclusions or inhomogeneous distributions of the elements, may be of interest. This requires a position-sensitive analysis is described in detail in Sections 15.2 and 16.6.2. Flat glass is often coated; the coatings are used to promote certain properties, such as the absorption or reflection of light, or they can have self-cleaning capability. The coatings can then be characterized by layer analyses, as described in Chapter 14.

The analytical questions regarding glassware are similar; however, the sample shape and thus the preparation effort can be very different. In historical glasses, not only the composition but also the identification of colorations is of interest. Environmental influences such as leaching or diffusion processes can cause changes of the glass; their characterization requires depth-dependent measurements. The available analytical methods are described in Section 14.4.6.

The focus in this section will be on the analysis of flat glass. Because of the wide range of use of flat glass, its elemental composition can vary considerably, which can make the analytical problem very complex, and in addition flat glass is not always homogeneous but can have layered structures. Flat glass is produced by pouring the molten mass onto a bath of tin, therefore the name float glass. This results not only in very smooth surfaces but also in an accumulation of tin in the surface exposed to the tin bath. Depletions of sodium and potassium oxides occur on the opposite side of the glass. In particular, the enrichment of tin is technically important since it makes the glass fluorescent. It can be controlled in the manufacturing process and needs to be monitored.

Glass formers are used in the production of glasses; they inhibit the melt to crystallize during the cooling so that it remains amorphous. The most important glass-forming agents are silicon oxide ( $\text{SiO}_2$ ), boron trioxide ( $\text{B}_2\text{O}_3$ ), or phosphorus pentoxide ( $\text{P}_2\text{O}_5$ ).

If boron is used in the manufacturing process of the glass, its determination is a particular challenge for XRF. The energy of its characteristic lines is very low, and therefore both excitation probability and fluorescence yield are extremely small. The information depth of boron is also extremely small since the boron radiation is readily absorbed.

### 9.7.2 Sample Preparation

Sample preparation, especially for flat glass, appears to be very simple since the glass already seems to be a “flat” and apparently homogeneous piece. In all cases, the glasses must be cut to fit the size of the sample holder suitable for the spectrometer.

For the determination of the thickness of the Sn layer, the sample can directly be analyzed on the coated side of the glass. On the other side of the sample, the depletion of glass constituents, which occurs during the cooling process, can be determined in the same way. For these analyses no sample preparation is necessary. For the determination of the bulk composition of the glass, a removal of the surface layer is necessary. For this purpose, the sample should be polished. The polishing abrasive should not contain any of the elements that are also in the glass, and it always should be removed by thorough cleaning after polishing.

In the case of homogeneous hollow glass, the measurement can be performed on the glass bottom, which can be ground and then polished. Another possibility is to prepare a glass pellet (Buchmeyer 1997). For this purpose, the glass is crushed in a vibratory disk mill with the addition of a binder, e.g. wax, and then pressed into a pellet. With this technique, the accurate analysis of light elements is made difficult because the relatively soft wax can form during the pressing process a surface film that absorbs their fluorescence radiation.

If a higher accuracy is required and if enough time for the analysis is available, a fusion process can be used to produce homogeneous pellets. The melting agents and mixing ratios that are used must be optimized for each sample type. The melting agents should not contain the elements that are to be determined in the glass. Lithium tetraborate is frequently added to the sample at a ratio of 6 : 1.

When analyzing boron in boron-silicate glasses, the sample preparation can only be done by very careful polishing. The information depth of boron in glass is only about 0.05  $\mu\text{m}$ , which means that a surface layer of this thickness must be representative for the bulk sample composition. The surface roughness is reduced by polishing with polishing agents having a 1–2  $\mu\text{m}$  grain size. The sample is then subsequently cleaned in an ultrasonic bath to remove the polishing agent. Through the polishing process the surface roughness will be reduced, and both the measured intensity and the reproducibility of the intensity determinations are improved. This effect has been demonstrated by studies on boron-silicate glass. Table 9.9 shows the results in the reduction in the relative standard deviations for repeated measurements for both boron and silicon using different sample preparation techniques.

Exposure to extended irradiation can change the composition at the surface by diffusion, which in turn will influence the measured intensities. This effect can be seen in Figure 9.5, which shows the change in boron intensity during repeated measurements.

**Table 9.9** Relative standard deviations of repeated measurements depending on their preparation technique.

Preparation	Boron (%)	Silicon (%)
Coarse grinding	0.4	0.10
Fine grinding	0.2	0.04
Polishing	0.1	0.05

Source: According to Walther (2005).

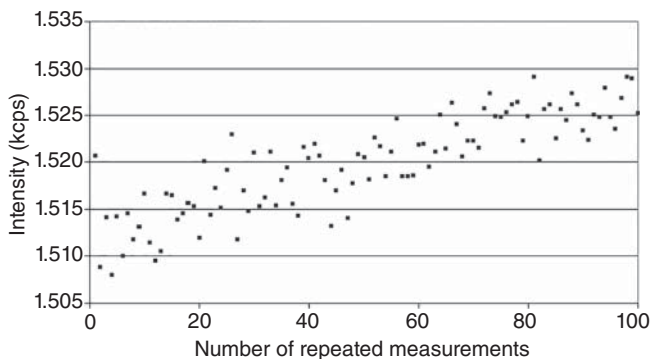


**Figure 9.5** Change of the boron intensity in a boron-silicate glass for several measurements. Source: According to Walther (2005).

These changes are reversible by re-polishing the sample. This effect is usually not a problem for a single measurement of a glass sample but can be significant for calibration or monitor samples. Therefore, repeated polishing is necessary before every set of measurements in order to obtain equal intensities. Similar effects are possible not only through the influence of the excitation radiation, in particular of the high primary intensity of WD spectrometers, but also by environmental influences.

### 9.7.3 Measurement Equipment

For the analysis of glass, mainly WDS instruments are used. The determination of the predominantly light elements in glass requires a higher-resolution instrument (see Section 4.2.2). Their better resolution ensures a high peak-to-background ratio and thus provides sufficient sensitivity for the detection of traces.

For the analysis of boron, it has been shown that the use of a fixed measurement channel leads to significantly improved results (Walther 2005). A multilayer structure optimized for the boron-K line at 183 eV was used for the dispersion channel, which means good resolution with high reflectivity at a favorable Bragg angle. In addition, the fluorescence radiation of boron can be collected during the measurement of all other elements, i.e. during the entire measurement time, since the fixed channel is independent of the rest of the sequentially operating spectrometer. Thus, despite the unfavorable excitation and measuring conditions, the collection of a sufficient fluorescence intensity of boron is possible.

EDS instrument are less frequently used for quality control in the glass industry, since the sensitivity to measure light elements is insufficient.

### 9.7.4 Achievable Accuracies

Primary beam X-rays can influence the concentrations in glass, in particular in thin surface layers. This was demonstrated by depth profile measurements using secondary ion mass spectrometry (SIMS) (Walther and Anderson 2002). However, due to the low information depth of the light elements, these thin surface layers are relevant for main components in the glass.



**Table 9.10** Typical composition and measurement uncertainties of flat glasses.

Element	Na <sub>2</sub> O	MgO	Al <sub>2</sub> O <sub>3</sub>	SiO <sub>2</sub>	K <sub>2</sub> O	CaO	S	TiO <sub>2</sub>	Fe
Mass fraction (wt%)	7	4	2	70	0.5	10	0.2	0.04	0.1
$\sigma$ (wt%)	0.3	0.05	0.05	0.3	0.01	0.05	0.005	0.001	0.005

Source: According to Walther (2005).

The achievable accuracies depend not only on the collected intensities but also on the quantification models used. In the case of glass, at least in the case of flat glass that does not contain much lead oxide, the matrix interactions are small because of the light element matrix. This means that the quantification models are valid over a relatively wide range. Nevertheless, a sufficiently large number of well-characterized calibration samples are required for calibration.

Table 9.10 shows a typical composition of silicate flat glass as well as measurement uncertainties for different elements achieved with a WD spectrometer.

## 9.8 Polymers

### 9.8.1 Analytical Task

The use of polymers is constantly increasing in consumer goods and in many areas of daily life. They are used as electronic instrument housings, as thermal insulation in building construction, and for car panels, packaging materials, credit cards, and toys. They are used everywhere and determine the functionality and appearance of many products. This variety is made possible by the very extensive, often even adjustable properties of plastics. The use of various hydrocarbon compound chains and the incorporation of various additives in concentrations ranging from milligram per kilogram, to the double-digit percentage enable to vary and control properties such as strength or plasticity, color and surface texture, and many others. In order to ensure the desired properties during the production process of the polymers, exact element analyses are required. This, however, is relatively complicated for polymers. A digestion process, in which results could then be used for an atomic spectroscopy analysis, is very difficult for polymers. Even with a successful digestion, only the additives can be determined, although the composition of the polymer itself remains unknown. The hydrocarbons of the polymer could be identified by molecular spectroscopy methods, but then the exact determination of additives will be problematic. Usually multiple analytical methods are required to achieve a complete characterization. X-ray spectrometry can be one of them.

Typical filler elements with a higher content in polymers are Na, Al, Si, P, S, Cl, Ca, and Ti; trace elements are V, Cr, Fe, Co, Ni, Cu, Zn, Br, Cd, Sb, Hg, and Pb; this presents a wide range of elements to be analyzed.

Using X-rays poses several challenges; polymers can have many very different matrices, which have an influence on the measured element intensities through the matrix interaction. The matrix itself cannot be determined directly due to

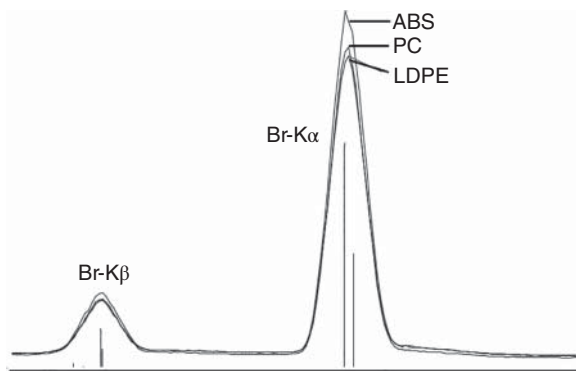


**Figure 9.6** Matrix influence of different polymers on the Br-K intensities (ABS, acrylonitrile butadiene styrene; PC, polycarbonate; LDPE, low density polyethylene). Source: Courtesy of S. Hanning, FH Münster.

the not measurable light elements that mainly make up the matrix. The influence of the matrix on the intensity of Br-K lines, for example, is demonstrated in Figure 9.6. For three different polymer matrices with the same Br contents, the measured intensities differ by several percent using the same measuring conditions. Consequently, a correct analysis result can only be expected if the matrix influences are taken into account correctly (Hanning and Bühler 2014).

However, the influences of the matrix can be considered either by an adjusted calibration or using matrix-dependent signals, for example, the Compton scattered tube radiation for normalization.

A further difficulty is that polymers can change under the influence of ionizing radiation; bonding bridges are broken, color changes or depletions of elements on the sample surface can occur, and associated changes in the material strength are possible. This also raises the question of the availability of reference samples, which in principle can be manufactured by reconstitution methods incorporating metal salts into the polymer, but then problems of homogeneity and durability still need to be considered.

The specific analytical tasks can be very different. A very common analysis task is the determination of toxic elements in consumer products, i.e. in polymers (see Section 15.4). Toxic elements are often used as fire retardants (bromine) or in pigments (chromium, lead, and cadmium) and require a monitoring of their contents; their limit values are given by regulatory directives and laws.

### 9.8.2 Sample Preparation

The sample preparation for polymers is relatively simple but differs on the kind of material to be analyzed, which either can be in the form of a foil, powder, granule, or solid. The preparation of fine powders is possible by cutting mills because polymers are too soft to be crushed; if necessary the material has to be cooled to become brittle (see Section 3.4.1). The quality of the cutting product depends not only on the hardness of the material but also on the cutting speed. Powders can then be measured directly after they are poured into a sample cup. But it is better to prepare pressed pellets to produce samples with comparable density. This is usually possible without the addition of binders, but heating during pressing can be helpful. Granules can be prepared by the same procedure; they can

also be pressed directly either under higher pressure or under heating in order to achieve sufficient compacting. Heating to about 100–150 °C should be carried out before pressing the sample and then slowly cooled down. The optimum procedure depends on the individual polymer and must be tested.

Solid polymers must be fit into the respective sample holders of the spectrometer, and their surface, if necessary, must be cleaned. No further effort usually is required for the sample preparation, i.e. the risks of contaminations caused by the preparation are relatively low.

The samples require a uniform thickness for their preparation since the information depth can be greater than the sample thickness, particularly for heavy elements in the light polymer matrices. Consequently, the measured intensities are then not only dependent on the concentration of the contents but on the sample thickness as well (see Figure 3.3). Therefore, when analyzing polymers with the help of standard-based quantification models, samples and the reference material should have the same thickness.

### 9.8.3 Instruments

Both WD and ED spectrometers can be used for the analysis of polymers. The required sensitivities are achieved by both instrument types since the additives are usually present not only as traces. One advantage of EDS is the simultaneous detection capability of a wide range of elements. This means that even unexpected additives can be recorded and evaluated. However, to have sufficient sensitivity for all additives, it can be necessary to use different excitation conditions, i.e. use different tube voltages and filters. Of course, the resulting measurement times will be longer than for one excitation condition only. On the other hand, the radiation load in an EDS instrument is about two orders lower than in WDS, which reduces the radiation damage of polymer samples and thus significantly prolongs the usability at least of the reference samples.

With WDS instruments, light elements should be measured first because the high energy input can lead to changes in the sample surface through diffusion. Especially the intensities of the light elements are influenced by this diffusion since the information depth of their signal is small.

### 9.8.4 Quantification Procedures

#### 9.8.4.1 Standard-Based Methods

Quantification can be carried out by using standard-based models. The achievable analytical accuracies for polymers then depend strictly on the correct consideration of the matrix influences. This is possible by using reference samples with similar matrices. Small differences of the matrices can compensate by corresponding corrections, for example, by a normalization of fluorescence intensities to the Compton scatter peak.

Reference samples with different matrices are offered by several suppliers (see Table B.2.3). However, the number of available calibration samples for polymers is not very high, due to the various matrices and the wide range of possible additives, as well as due to the problems of their correct characterization. Therefore,

calibration samples often are made synthetically from pure materials. For this purpose, pure polymer granules are carefully mixed with various metal salts, for example, in an extruder. This process has to be repeated several times in order to ensure an adequate homogenization (Hanning et al. 2010; Nakano et al. 2006). The homogenized material can then be used to prepare disk-sized reference samples.

The analysis of toxic elements in polymers, in particular in consumer goods, is described in Section 15.4 and in ASTM-F\_2617-15 (n.d.).

With these references and using standard-based quantification models, the achievable accuracies are comparable with those of other solid samples, i.e. with metals or glasses.

Pure fundamental parameter methods cannot be used because the information from all elements is required, but for polymers mainly light elements of the matrix do not give measurable signals. If, however, the matrix composition could be determined by other methods, this information can then be used in the fundamental parameter models for the exact determination of the mass contents of additives. Alternatively if only the additives are of interest one can obtain from the ratios of the Compton and Rayleigh scattered intensities an average  $Z$ -value of the light matrix elements, which then can also be used in the fundamental parameter model (see Section 2.2.4.2).

#### 9.8.4.2 Chemometric Methods

Even if the light elements produce no detectable X-ray lines that can be measured, they influence the spectral background due to their scattering of the incident radiation (see Section 2.2.4.2). The scattered tube radiation can also be used for a material characterization; however, it requires other evaluation procedures. Chemometric methods offer a possibility to quantify polymers. For this purpose, the differences in the scatter spectra of various hydrocarbons can be used for their identification. This knowledge about the matrix can then be used in the Sherman equation to quantify the mass fractions of additives and fillers in the material by using their fluorescence intensities. For high mass fractions of additives and fillers, their influence on the scatter spectra must be taken into account additionally in identifying the matrix.

Wacker (2015) used a partial least square (PLS) regression for the determination of the matrix composition, for the identification of the type of the hydrocarbon, and for a direct determination of the contents of light elements. For this purpose, the scatter spectra of several hydrocarbons with various additives in different concentrations were measured. These spectra were then classified with a PLS regression procedure.

Figure 9.7 shows the scattered tube spectra (Pd tube) of more than 80 different polymers measured with an ED spectrometer. The acquisition time of these measurements was relatively long for a clear identification of the spectral distribution and to minimize the influence of statistic fluctuations.

The polymers, shown in Table 9.11 together with their average composition, were used for the measurements. They were additionally doped with different amounts of Al, Zn, Br, Cd, Ba, and Pb, representing elements of atomic numbers ranging over the complete periodic table.

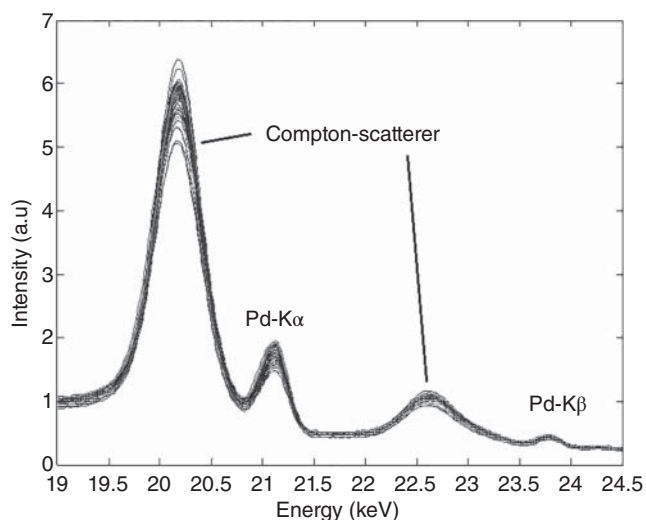


**Figure 9.7** Elastic and inelastic scattered tube radiation of various pure polymer samples. Source: Courtesy G. Wacker, former FH Münster.

**Table 9.11** Polymers and their approximate composition and mass fractions in wt%.

Polymer	Acronym	H	C	N	O
Polyethylene	PE	15	85	0	0
Polyethylene terephthalate	PET	4.2	61.5	0	34
Polypropylene	PP	14.6	85.2	0	0
Polymethylmethacrylate	PMMA	8	59.3	0	32.7
Polycarbonate	PC	5.6	75	0	19.6
Polyoxymethylene	POM	6.8	40.5	0	52.5
Acrylonitrile butadiene styrene	ABS	7.7	85.2	6.8	0
Polyamide	PA	10	63	12	15
Polyurethane	PUR	8.3	64.5	5	21

The behavior of the scattered radiation intensity varies clearly with the different compositions for both elastic and inelastic scattered radiation as well as in the exact shape of the Compton line. The scatter spectra can be measured with all types of instruments, i.e. ED spectrometers as well as WD spectrometers; however, the accuracy of the quantification results is better for higher-resolution spectra because they can separate more details. For the evaluation, gross intensities were used to avoid any additional error due to the subtraction of the background, further the information of the continuous background can also be used. Any outliers that can occur due to fluctuations of the scattered background were deleted.

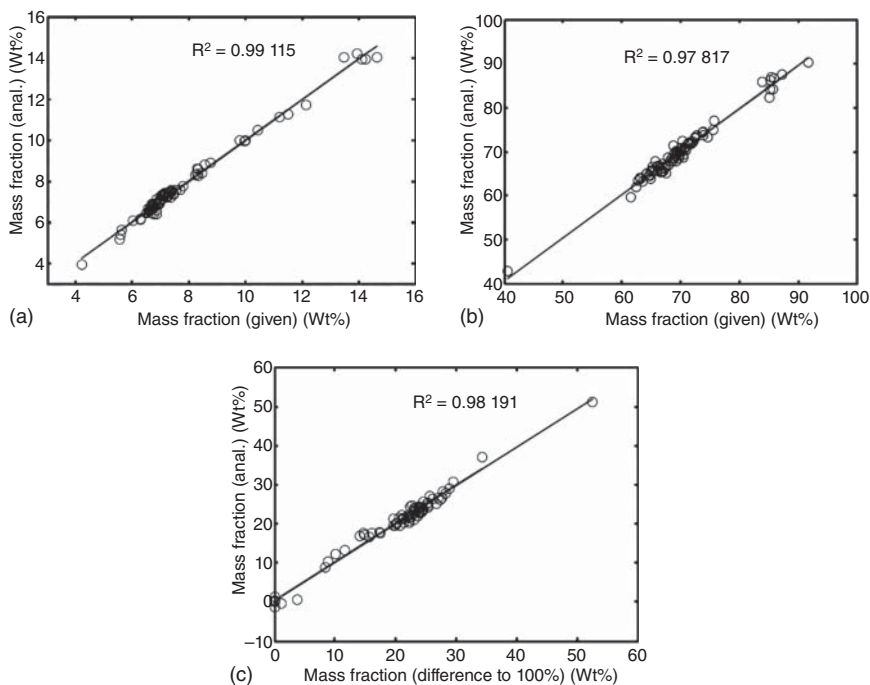


**Figure 9.8** Comparison between mass fractions of hydrogen (a), carbon (b), and oxygen (c) determined by IR spectroscopy and a chemometric evaluation of the scattered tube spectra.

**Table 9.12** Correlation coefficients  $R^2$  for different energy resolutions.

Resolution	Crystal	Collimator	H	C	N	O
Low	LiF 200	0.46	0.9875	0.9502	0.6102	0.9642
Medium	LiF 220	0.23	0.9942	0.9762	0.8237	0.9701
High	LiF 400	0.12	0.9919	0.9891	0.9648	0.9958

The relations between the given mass fraction of light elements determined by combustion analysis as well as Fourier transform infrared (FT-IR) spectroscopy and a chemometric evaluation of the scatter spectra are shown in Figure 9.8. They show an astonishing good agreement between data sets.

These quantification results can be improved with a higher-resolution spectrometer. This is demonstrated in Table 9.12 for measurements with WD spectrometers with different settings of crystal and collimator by using the correlation coefficients  $R^2$  (see Eq. (5.18)). With better resolution the intensity drops down; nevertheless this then has to be compensated by longer measurement times to achieve comparable statistical errors. For the medium resolution a factor of approximately 3, and for the high resolution even a factor in the range of 20 was required.

**Table 9.13** Mass fractions of hydrocarbon groups and H, N, and O for PUR and ABS in wt%.

Polymer	Polyurethane		Acrylonitrile butadiene styrene		Low density polyethylene	
	FT-IR	ED-XRF	FT-IR	ED-XRF	FT-IR	ED-XRF
Aliphatic	51.1 ± 8.6	46.9 ± 5.5	30.5 ± 5.2	40.0 ± 4.7	85.2 ± 14.5	81.4 ± 9.5
Aromatic	7.1 ± 0.7	9.0 ± 1.1	28.8 ± 2.6	21.2 ± 2.5	0.0 ± 0.0	2.9 ± 0.3
Carbonyl	5.1 ± 0.1	5.7 ± 0.7	0.9 ± 0.0	2.3 ± 0.3	2.2 ± 0.1	1.2 ± 0.1
C-rest	1.9 ± 0.0	8.1 ± 0.9	23.6 ± 0.0	20.7 ± 2.4	-2.0 ± 0.0	2.4 ± 0.3
N + O	26.3 ± 0.1	22.4 ± 2.6	7.95 ± 0.1	7.4 ± 0.9	0.03 ± 0.01	3.6 ± 0.4
H	8.55 ± 0.1	8.1 ± 0.9	8.25 ± 0.1	8.5 ± 0.1	14.6 ± 0.5	13.4 ± 1.6

The  $R^2$  values of the measurements with an ED spectrometer are only slightly worse than the results for the WD spectrometer with high resolution.

The chemometric method allows also a differentiation between the different carbon groups, i.e. between aliphatic, aromatic, and carbonyl groups that can occur simultaneously in polymers. The conventional method for the determination of these groups is FT-IR spectroscopy. But because of the different elastic and inelastic scattering coefficients, the evaluation of scattered X-rays can also give acceptable results. This was demonstrated by Wacker (2015). However, due to the similar scattering behavior of nitrogen and oxygen, the two elements were determined as their sum. The results for a few polymers are presented in Table 9.13. Shown are the mass fractions of carbon in aliphatic, aromatic, and carbonyl compounds as well as those for nitrogen and oxygen (N + O) and hydrogen (H) in wt% for three common polymers in comparison with the results of an FT-IR analysis. Even if the errors are relatively large, the agreement between the results is surprisingly good considering this special type of spectral evaluation.

With this information about the matrix, a standard-less quantification based on the Sherman equation is then also possible for additives and fillers in the polymer. It can be expected that these quantification results have a good reliability. The computing effort is relatively high, however considering the long measuring times required to achieve low statistical errors that are necessary for reliable spectral matching procedures it is acceptable. It is necessary not to forget the high effort to measure a large number of different samples for the spectral library.

## 9.9 Abrasion Analysis

The task often is to perform a quick material identification without much effort for sample preparation. The first choice certainly is the use of mobile X-ray spectrometers as described in Section 15.3. But handheld instruments are not always available. If only conventional X-ray spectrometers are available, quick sample analyses are possible without complex sampling, for example, by cutting out a laboratory-size sample from a larger piece of material with the necessary

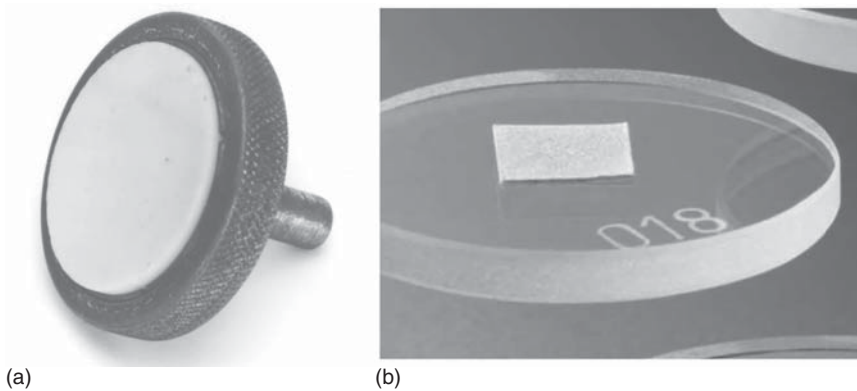


**Figure 9.9** Sample carriers for abrasion analyses: corundum disk for conventional instruments (a) and a quartz disk for TXRF instruments (b).

subsequent surface treatment. Also the sampling by abrasion of the material to be analyzed onto a suitable sample carrier is possible. This simplifies the sampling and accelerates the availability of the analyses result, but only for homogeneous materials such as metals.

In order to achieve enough removal of the material, the sample carriers should be somewhat rough and made from a material that, if possible, does not contain any analyte elements. Corundum disks are suitable as sample carriers for conventional excitation geometries, while quartz disks are also suitable for total reflection geometry. Such sample carriers are shown in Figure 9.9. Particularly when using total reflection X-ray fluorescence spectrometry (TXRF), care must be taken that no contamination occurs on the way from the sampling to the measurement since this can lead to significant falsification of the measurement result due to the very high sensitivity of the method.

The material applied to a corundum disk should be thicker than the saturation thickness. For light elements this is only a few micrometers, while for heavy elements this can mean much thicker layers; they might not always be achievable by

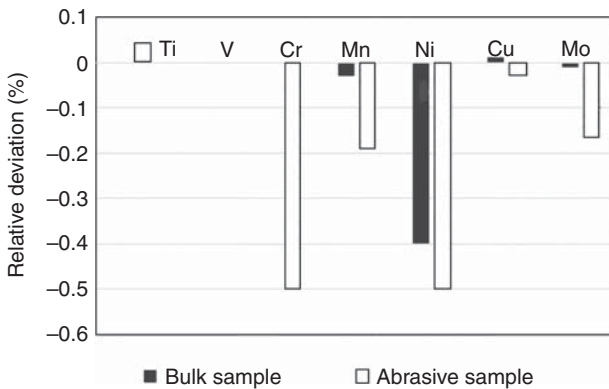


**Figure 9.10** Relative differences for a bulk and an abrasive analysis of steel.



abrasion. In this case one can expect to measure these elements too low, since for thicker layers the fluorescence intensity would increase for these elements.

Such a study was carried out on a steel sample (Flock et al. 2009). It was found that already approximately 1 mg of sample material applied by this method is enough to achieve constant fluorescence intensities. This corresponds to material thicknesses on the order of 10  $\mu\text{m}$ . In this case, similar to TXRF, there are no significant matrix interactions, at least for the purpose of a fast material identification. Figure 9.10 shows the relative deviations of the quantification results obtained from a bulk sample and an abrasion test sample of steel. The contents determined on the abrasion test sample are too small; this is the result of a not saturation thick sample and neglected matrix interactions.

This method of sample taking and preparation allows for a fast and sufficiently accurate analysis for a positive material identification. In order to take advantage of the quick sampling technique, EDS instruments are best suited due to the simultaneous acquisition of the entire energy range.

## 10

### Analysis of Powder Samples

Materials in powder form are a common sample type for X-ray analysis. They may be geological samples, such as minerals, sands, ores, rocks, or coal, industrial products, such as cement, dusts, and ferrous-alloys, or they can be polymer granules or waste products. The starting material can be quite dense, but also inhomogeneous, and cannot easily be melted like metals. In this case, the samples are first finely ground and then homogenized. Therefore, the material undergoes several cuttings, grinding, and dividing steps. The sample is first cut into smaller parts and then ground to a fine powder; mixing and dividing completes the homogenization process. Further sample preparation then depends on the respective analytical task, in particular on the required analytical accuracy as well as the time available.

In the simplest case, the sample is just filled into a cuvette. In the case of more stringent requirements, the production of a pressed pellet or even a fusion bead is necessary (see Section 3.4). Using these more elaborate preparation techniques, the uncertainty contributions from sample preparation, such as varying density, sample roughness, mineralogical effects, etc. are reduced, which thus leads to an improvement in the analytical accuracy.

#### 10.1 Geological Samples

##### 10.1.1 Analytical Task

Geological samples can be just as diverse in their composition as the motives for their being analyzed. Most of the time, the objectives are the exploration, localization, and assessment of mineral deposits. These may be minerals, rocks, or ores, which contain certain elements or compounds that can be used as fuels, as raw materials for smelting process, for the production of fertilizers, ceramic materials, or glasses.

In order to evaluate a mineral deposit based on certain indicator elements, prospecting requires a large number of samples to be analyzed for as large a number of elements as possible. Since sampling and analyses are carried out at different locations, time requirements for the measurement themselves are relatively low. However, the large number of samples that need to be measured limits the available time for a single analysis. During the exploitation phase of

the deposits, the focus lies on the determination of the elements of interest. They may be main or secondary components, often even trace elements. A high analytical accuracy is required in order to evaluate the mineability and to be able to identify the most effective processing technologies, at the same time also taking into account all the other components. These situations often require a fast analysis in order to be able to evaluate the mined materials. Because of the high added value, the requirements for precision and accuracy of the analytical data are very high. For a typical deposit an analysis error of 1 wt% relative to the main element can already influence the decision if developing a new mining field is an economic success. The application of XRF for this analytical task is described in DIN 51001:2003–08

Another interesting aspect is on-site analysis, in order to control and guide the excavation process along ore veins. Of interest is also the element content of already exhausted mining mineral, in order to avoid the mining of dead material.

All these questions can be answered very well with X-ray fluorescence (XRF). Relatively little sample preparation is required, and a wide range of elements and concentrations can be detected. XRF analysis for prospecting and evaluation of the deposits is usually done in the laboratory after the samples have been collected and prepared; on-site analysis of the materials on the other hand requires mobile XRF instruments.

In geological samples many elements need to be measured; more or less any element of the periodic table can be expected. The particular elements of interest to be analyzed depend on the actual analytical problem and the material to be analyzed.

### 10.1.2 Sample Preparation

The type of sample preparation determines the achievable analytical accuracy.

For a rapid analysis with medium accuracy, pressed pellets are suitable. The samples have to be milled, mixed with a binder, and then pressed into pellets. Wax or cellulose material is often used as a binder. Pressures of 100–250 kN are applied for up to one minute. During pressing, the surface of the pellet that is intended for the analysis should be protected from contamination from the pressing die by a thin plastic film. Using pressed pellets, analyses errors can occur, in particular for light element components due to matrix effects and grain size effects.

For more accurate analyses the samples should be prepared as fusion beads. The matrix interactions are reduced by the added glass former, which also homogenizes the sample. In addition, a uniform and flat sample can be produced in which grain size or mineralogical effects are negligible. Consequently, reproducibility and trueness of the analysis can be improved. However, the dilution of the samples and the conversion to a lighter matrix result in a decreased peak-to-background ratio, thereby reducing the sensitivity for traces.

The procedures for making fusion beads have already been described in Section 3.4.4 (see also Norrish and Hutton 1969). The choice of suitable oxidizing agents and glass formers depends on the specific sample type. These as well as the appropriate temperature regime for the fusion process should be determined by initial tests. The procedures thus established can then be used in the same way for the actual samples as well as for the preparation of the calibration samples. One has

to consider that due to the light matrix of fusion beads the information depth for heavy elements can be larger than the sample thickness. Therefore, both the unknown and reference samples should have the same mass. The information depth can be reduced by adding heavy oxides such as  $\text{BaO}_2$  (see also Section 3.4.4).

### 10.1.3 Measurement Technique

Both wavelength-dispersive spectrometers (WDSs) and energy-dispersive spectrometers (EDSs) are used for the analysis of geological samples. For prospecting work, in which potentially all elements are to be recorded, EDS instruments are more suitable, since they allow the simultaneous detection of the elements from Na to U. Measuring times can be shorter than for WDS instruments and, with suitable excitation conditions, sufficient sensitivities can be achieved.

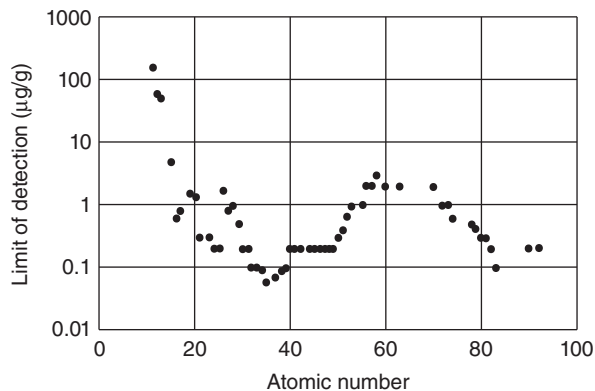
WD spectrometers are more likely to be used for the accurate analysis of the elements of interest during the refinement process. In particular, their higher sensitivity to measuring light elements, which are the main components in many geological samples, ensures a high degree of accuracy of the analyses.

For on-site analyses, often only the monitoring of threshold values is of interest. This can be achieved with mobile or even handheld instruments, without complex sample preparation.

### 10.1.4 Detection Limits and Trueness

Detection limits depend on sample preparation as well as on the measuring technique used. The detection limits shown in Figure 10.1 can be achieved for the most advanced EDS instruments with pressed pellets. It requires an optimal excitation of the element groups with different excitation conditions (polarized radiation, secondary radiation, direct excitation) and total measuring times in the range of 1500 seconds (ApplBrief-Geology 2015). The detection limits that can be achieved with WDS instruments are not significantly different. However, the measurement time can be longer when analyzing unknown materials, since then a scan to detect all elements is required.

**Figure 10.1** Limits of detection for geological material, measured with an ED spectrometer (Na to Ca and Fe as oxide), total measurement time approximately 1500 seconds. Source: According to ApplBrief-Geology (2015).



For trace elements, the reproducibility of the analyses is mainly dictated by the statistical error given by these measurement times. For concentrations  $>0.1$  wt% the uncertainties are primarily defined by irregularities in the sample preparation or instabilities of the instrument.

The trueness of the analyses can be estimated by comparing the results of the analyses against the certified mass fractions of reference samples. It is essentially determined by the quality of the reference samples, but also by the model used for matrix correction. For major and minor components, the matrix influence has to be regarded as the major contributor to uncertainty. The relative differences from the certified contents can be up to 1% for major and minor elements; for traces they can be even higher.

## 10.2 Ores

### 10.2.1 Analytical Task

Ores are rocks or sediment formations that contain the element of economic interest with other minerals. Determining the concentration of the value element(s) is important to assess the mineability of the ore. Ores are mined in large quantities, subsequently prepared for the smelting process, and often transported over long distances. In order to make these processes effective the exact knowledge of the concentrations of the elements of interest is also necessary. XRF is suitable for this task because a wide range of elements can be determined with high accuracy. For fast analyses the preparation of the material for the analysis is done as a pressed pellet. For higher requirements it is nowadays common to prepare the sample as a fusion bead. The following sections will describe the analyses conditions as well as the analytical performance for different ores.

### 10.2.2 Iron Ores

Iron occurs in nature in large concentrations as oxide, carbonate, or sulphides. The compounds with the largest iron content are magnetite ( $\text{Fe}_3\text{O}_4$ ) with up to 72 wt% Fe, hematite ( $\text{Fe}_2\text{O}_3$ ) with up to 70 wt% Fe, siderite ( $\text{FeCO}_3$ ) with up to 48 wt% Fe and limonite as a mixture of various iron oxides. These minerals are however usually mixed with a varying extent of dead rock. The determination of the Fe content is therefore of great importance.

When analyzing ores, attention should be given to taking a representative sample. Often, the requirement is to characterize a very large but also inhomogeneous amount of material with high accuracy. Specifications for the sampling are given, for example, in DIN-4021 (1990).

The preparation of iron ore is done either as a pressed pellet or as a fusion bead depending on the accuracy requirements and the available analysis time. A comparison of the two techniques was carried out by Janßen et al. (1994). For the preparation as pressed pellets, the material is finely milled to grain sizes  $<40$   $\mu\text{m}$  with the addition of milling aids. The material is then pressed at pressures of 150 kN. This preparation technique allows for a rapid analysis, but grain size

effects and mineralogical effects cannot be ruled out. The more elaborate preparation as fusion bead avoids these influences. For this purpose, the material must also be ground. After drying for about one hour at 105 °C, the material is then mixed in a ratio of 1 : 10 with a mixture of 34% LiBO<sub>2</sub> and 66% Li<sub>2</sub>B<sub>4</sub>O<sub>7</sub> and 0.2% LiBr to improve the casting behavior of the fusion. The use of pure Li<sub>2</sub>B<sub>4</sub>O<sub>7</sub> is also possible. The amounts used depend on the size of the required pellet. For a 40 mm diameter pellet, 1 g of sample and 10 g of glass formers are suitable amounts.

Both ED and WD instruments are used for the analyses of Fe ores. With sufficient measurement times, both types ensure small statistical uncertainties. Since the elements that need to be determined occur in high concentrations sensitivities down to the trace element level are not required. Peak overlaps can be solved by deconvolution procedures. The measurement time depends on the desired statistical uncertainty and the instrument type; they usually range from 30 to 400 seconds. In the case of EDS instruments most often various excitation conditions are used to achieve ideal excitation of the different element groups. For the light elements (Na, Al, S, P, S) the excitation voltage is reduced (10–15 kV) and the tube current is increased. For the heavier elements tube voltages are greater than 20 kV, with thin filters for the reduction of the low-energy spectral background being used.

The achievable reproducibility of the measurements is hardly influenced by the type of sample preparation. The relative standard deviations for repeated measurements are significantly better than 0.1% at an Fe content of approximately 80 wt%. For the lower concentrations, these values become worse due to the poorer counting statistics. For pressed pellets the light element results fluctuate more due to grain size influences, mineralogical effects, etc.

The trueness of the analyses results mainly depend on correct sample preparation and calibration. For EDS instruments, absolute standard deviations of about 0.3 wt% for Fe are achievable; for the other components, the relative deviations are larger, again due to the poorer statistics (ApplNote-EDXRF-Iron\_ore n.d.; LabReport-XRF\_110 n.d.; LabReport-XRF\_111 n.d.). As one can expect, the standard deviations achievable with WDS instruments using fusion beads are lower for both the main elements and the light elements. Deviations for the main element Fe can be 0.1 wt%.

Reference samples are offered by various vendors (see Table B.2.1). Manufacturing of synthetic references from pure reagents is also possible.

### 10.2.3 Mn, Co, Ni, Cu, Zn, and Pb Ores

In comparison to the iron ores, the concentrations of the elements of interest in these ores are significantly lower. With the exception of some special instances, for example Mn nodules, the concentrations are in the range of <40 wt%, often even lower, just a small wt% value. This results in not only a strong influence of the matrix on the analytes, but also in larger statistical uncertainties due to lower fluorescence intensities. For these ores, the preparation of the sample material can also be done as a pressed pellet or as a fusion disk. The suitable glass formers are determined depending on the composition of the ores. It may be necessary

to use larger amounts of glass formers in order to avoid damages to the melt crucibles.

In order to achieve sufficiently small statistical uncertainties, the measurement times for the low content elements need to be adjusted. Using an EDS instrument, it can be useful to work with different excitation conditions for the different element groups. The overall measurement time increases, thereby achieving comparable errors for all elements of interest. Depending on the kind of sample preparation the analytical performance varies in the same way as discussed for the iron ores. The preparation as fusion beads allows for a better precision and trueness. This is valid in particular for the light elements where matrix and mineralogical effects cause less of an influence when using fusion beads.

The trueness of the analysis is largely independent of the type of sample preparation. The more uniform sample preparation in a fusion bead apparently compensates the greater statistical uncertainty to be expected from the lower fluorescence intensities (ApplNote-EDXRF-Mn-Ore n.d.; ApplNote-EDXRF-Mn-ore\_Pellets n.d.; ApplNote-EDXRF-Ni-ore\_Beads n.d.; ApplNote-EDXRF-Ni\_ore\_Pellets n.d.; Banerjee and Olsen 1978).

Under these circumstances, it can be concluded that the simpler and faster preparation method, the preparation of pressed pellets, can be favored.

#### 10.2.4 Bauxite and Alumina

Bauxite, the world's main Al-ore, is a mixture of various, predominantly Al-containing minerals, mostly aluminum hydroxides ( $\text{Al}(\text{OH})_3$ ), with Al contents of up to 90 wt%. Other bauxite constituents are oxides of Si, Ca, Fe, and a few other elements, where the iron oxides strongly determine the coloration. Contents of at least 50–55% Al hydroxide are necessary for the ores to be commercially viable to be mined. Another mineral with high occurrence is alumina ( $\text{Al}_2\text{O}_3$ ), which is used as source for the exploitation of Al. The Al content in all these ores can be determined by XRF.

The exploration and mining process requires a fast feedback and a short analysis time; this can only be achieved by quick sample preparation in the form of pressed pellets. For this purpose, the material has to be milled into a small grain size and mixed with 10% wax binder. The material should be also dried to avoid an outgassing of water vapor in the vacuum.

To control an industrial process most effectively, the composition of the materials must be known as accurately as possible. Since Al is a very light main component that has only a small information depth, dilution of the matrix by means of a fusion process is reasonable. This dilution not only increases the information depth but also reduces the influence of any thin surface layer of the sample on the analysis result. It also achieves standardization of the test samples and reduces mineralogical influences.

For a fusion bead the finely ground bauxite must be carefully dried, because Al hydroxide is hygroscopic. After drying, the loss of ignition (see Eq. (3.2)) has to be accounted for. The sample material has to be mixed with a glass former in a relatively high dilution ratio (1 : 8 or 1 : 10). Both pure  $\text{Li}_2\text{B}_4\text{O}_7$  and mixtures

of  $\text{Li}_2\text{B}_4\text{O}_7$  with  $\text{LiBO}_2$  are suitable as glass formers. The melting temperature should be at least  $1150^\circ\text{C}$ .

For both preparation techniques it is necessary to consider the low absorption of radiation in the sample. This means that the amount of sample must be the same for references and unknowns; in the preparation of fusion beads heavy additives can be used to increase the absorption (see Section 3.4.4).

The analyses can be carried out with WD spectrometers, depending on the available time, both sequential and simultaneous instruments as well as with ED spectrometers. For measurements with WDS, setting the background points carefully is crucial because the light matrices of these materials generate a high spectral background. The measurement time needs to be chosen to match the statistical requirements.

When the samples are prepared as fusion beads the achievable relative standard deviation for repeated measurements of Al is in the range of  $<0.1$  wt%. For  $\text{SiO}_2$ , an important secondary component, the values are somewhat greater; for the oxides of the heavier elements, the values can also reach 0.1 wt% depending on their individual contents.

The accuracy is determined by measurements against standard samples. For  $\text{Al}_2\text{O}_3$  the mean deviations are typically in the range of 0.3 wt%; while comparable values are obtained for the light secondary components, for the heavier components the deviations are even smaller (ApplNote-Bauxite n.d.; LabReport-XRF\_100 n.d.).

### 10.2.5 Ores of Precious Metals and Rare Earths

Precious metals but also rare earth elements are only present in trace amounts in their ores. Their concentrations can be as low as a few tens of micrograms per gram, i.e. for a reliable determination of their content, limits of detection of a few micrograms per gram are required.

Special measurement procedures are required to achieve such sensitivities. First, optimal excitation conditions need to be selected. It would be the best to use the K-lines for the analytes. However, they require for these elements very high excitation energies. For gold, for instance, the energy of the absorption edge is 81 keV, and for the rare earth elements it is up to 65 keV. Therefore, tube voltages of approximately 100 kV would be required. Such high tube voltages are usually not available, and are not that easy to handle in a general-purpose commercial laboratory instrument. Therefore, L-lines are mostly used; the drawbacks are strong peak overlaps that can occur especially for the rare earth elements. The samples should also not be prepared as fusion beads, since the dilution with the glass former degrades the detection limits. A further possibility is the enrichment of the analyte. However, this is only useful in process control, and not for the prospecting.

The high excitation voltages required for the very low detection limits of the heavy metals are provided by one commercially available ED instrument (ApplNote-Rare\_earth\_elements n.d.). The excitation with polarized radiation, which is used in this case, also ensures high sensitivity due to the improved peak-to-background ratios. The Ge detector used in this instrument ensures



**Table 10.1** Detection limits for some heavy elements using K-radiation .

Elements	Cd	Sn	Sb	Cs	Ba	La	Ce	Nd
$w_{\text{LOD}}$ ( $\mu\text{g/g}$ )	0.42	0.46	0.49	0.74	0.88	1.1	1.2	1.8

Source: According to ApplNote-Rare\_earth\_elements (n.d.).

good detection probability for the high-energy fluorescence radiation of the analyte elements. The detection limits for a few heavy elements that can be achieved with this equipment are summarized in Table 10.1 (some elements were measured for 800 seconds).

While this technique is particularly suitable for the direct analysis of samples prepared as pressed pellets, with enriched samples both conventional EDS and WDS instruments can be used for monitoring the exploration process. In this case, the statistical uncertainties then essentially determine the achievable analytical accuracies.

For the quantification, usually standard-based models are used. For this analysis, plenty of reference samples are available (see Table B.2.1).

The automotive industry uses over 50% of the world production of Pt, Pd, and Rh in its catalysts. Such catalysts are applied as surface-active substances on a large-area substrate. The substrates are often ceramic materials such as  $\text{Al}_2\text{O}_3$  (Alumina) or  $(\text{MgFe})_2\text{Al}_4\text{Si}_5\text{O}_{18}$  (Cordierite) or honeycomb-shaped steel foils, which are coated with a temperature-stable primer of  $\text{CeO}_2$ ,  $\text{BaO}$ , or  $\text{ZrO}_2$ , on which the catalytic elements are applied in thin layers. The high monetary value of the catalytic elements necessitates their recycling. The average concentrations of precious metals in catalysts are similar to that of ores.

To prepare such old ceramic catalysts for the analysis they need to be crushed and milled. In the case of steel substrates, the catalysts are shredded, whereby the steel parts can be separated by a magnetic separator; the brittle precious metal coating will also be separated from the substrate by the shredding process. The milling time of the ceramic substrates must be adjusted such that the fluorescence intensities of the analytes become stable (see Figure 3.7). For the analysis, the powder can then be prepared as a pressed pellet or also as a fusion bead. Preparation as a melt is difficult since the noble metals tend to alloy with the material of the crucible, which can then be damaged.

Used catalysts can be contaminated by fuel additives; they must be taken into account in the analysis.

Both WDS and EDS instruments can be used for the analyses. The analyzing elements do not have any mutual overlapping peaks, although there may be overlaps with the substrate elements. For the quantification, normalization can be made to the spectral background; the Compton peak of the Rh tube cannot be used, since Rh itself is an analyte. Alternatively, standard models are used. Standard reference samples are offered, for example, by NIST and BAM.

## 10.3 Soils and Sewage Sludges

### 10.3.1 Analytical Task

Soils and dried sewage sludge have a similar consistency and can therefore be treated, for analytical purposes, similarly. Sewage sludge is a waste product when cleaning municipal wastewater. Non-contaminated sewage sludge contains about 50–70 wt% carbon, 21–24 wt% oxygen, and 15–18 wt% nitrogen, up to 1.5 wt% phosphorus, and up to 2 wt% sulfur. More than 2 million tons of dried sewage sludge is generated annually. These quantities must be prepared for further use. The high amounts of carbon suggest use as fuel, and the high contents of nitrogen and phosphorus also as fertilizer. However, since sewage sludge is frequently contaminated with toxic heavy metals as well as with organic compounds, in particular halogenated hydrocarbons, a determination of these components is necessary both for the application as fertilizer and for combustion use. This is regulated in Germany by the sewage sludge regulation (AbfklärV 2016).

This regulation stipulates both the maximum contamination of soils before fertilization with sewage sludge and those of the sewage sludge to be applied. These concentrations are summarized in Table 10.2. In addition, there are also specifications for the maximum concentrations of the sewage sludge with organic compounds, which however cannot be determined by XRF.

In addition to regulating the concentrations, requirements for sample collection and analysis are also included. For the toxic metals an aqua regia digestion according to DIN 38414, part 7 (DIN-38414-7 1983, p. 01) and an analysis according to DIN-38406 (1998, p. 07) by means of atomic absorption spectrometry (AAS) or inductive coupled plasma spectrometry (ICP–OES) is recommended. However, these methods are only partially suitable for the analysis of soils and sewage sludges as reported by Janßen et al. (1998). He found that a digestion does not completely decompose the material; in particular, Cr and Si from the matrix tend to be not dissolved in the digestion. This means that the concentrations of toxic metals are determined too high, since the undissolved residues still contain the elements to be monitored and therefore influence the analytical result. However, X-ray spectrometry completely records these contents. Therefore, in spite of the standard, investigations of soils and sludges are preferably carried out by XRF. If an efficient excitation by monochromatic radiation is used the required sensitivities for the toxic elements can be achieved; see for example (ASTM-D-8064-16 2016 and, DIN-EN-15309 (2007-08) and ISO 18227:2014-03), and for the analysis also of traces of U and Th (ASTM-C\_1255-11 n.d.).

### 10.3.2 Sample Preparation

Two preparation alternatives are available for the preparation of soils and sewage sludges for X-ray spectrometry. On the one hand, the preparation can be carried out as a pressed pellet. For this purpose, the dried starting materials are finely ground to <100 µm; they can then be pressed without or with only a low binder

**Table 10.2** Maximum loads of soils and sewage sludge.

Element	Soils ( $\mu\text{g/g}$ )	Sewage sludge ( $\mu\text{g/g}$ )
Cr	100	900
Cu	60	800
Ni	50	200
Zn	200	2500
Cd	1.5	10
Hg	1	8
Pb	100	900

Source: According to AbfklärV (2016).

content. Adequate durability is ensured by the soft organic components already present.

The other possibility is the preparation of fusion beads with lithium tetraborate ( $\text{Li}_2\text{B}_4\text{O}_7$ ) as a glass former. The dilution of the sample must be relatively high in order to obtain homogeneous pellets.

A comparison of the results of ICP–OES and XRF shows that due to the incomplete digestion as well as the loss of volatile elements, the results obtained with ICP can be up to 15–50 wt% below the XRF results (Janßen et al. 1998).

### 10.3.3 Measurement Technology and Analytical Performance

For the analysis of soils and sludges, both EDS and WDS instruments are used. The threshold values for Cd and Hg are a challenge for both instrument types. EDS instruments can meet the requirements for Cd with methods improving the peak-to-background ratios, for example, by excitation with monoenergetic or polarized radiation. For Hg, better resolution WDS instruments are required in the case of high Pb concentrations.

In addition to powerful laboratory instruments, handheld instruments were also tested for the screening of soil samples (Lück et al. 2012). Although the repeatability of the instruments themselves is good, several problems arise during the analysis of real soil samples, which are mainly caused by the lack of preparation. These problems, that result in reduced reproducibility, are caused by influences from the sample moisture, of inhomogeneities as a result of different sample densities as well as of grain size effects. The smaller the concentrations the larger the influences are. The relatively small analyzed sample volume is contributing to the low reproducibility. Furthermore, the sensitivity of handheld instruments is not sufficient for the detection of extreme traces, in particular of Cd and Hg. On the other hand, a quick screening with these instruments enables an on-site survey of the situation on the spot without an elaborate sampling, transport to the laboratory, and preparation.

The achievable reproducibility during actual measurements is up to a factor of 2 worse than the statistical uncertainty and is therefore sufficient. The trueness depends on the calibration. The average relative deviations are in the lower percentage range even for the elements in the lower concentration range.

Geological standards can be used as reference samples for the analysis of soils and sewage sludges, e.g. NIST: SRM (NIST-2709; NIST-2710; NIST 2711), the Canadian Certified Reference Material Project (SO-1 to SO-4), or the Chinese Institute of Geophysical and Geochemical Prospecting (People's Republic of China) from the GSS, GRS, and GSD series (see Section B.2).

## 10.4 Quartz Sand

Quartz sands are the raw material in the glass production process, for both daily use and technical glass. The quartz sand needs to be of high purity, since impurities such as oxides of Al, K, Ca, Ti, Fe, and Zr can lead to discoloration and streaks or inclusions in the glass. The purer the sands, the higher the prices that can be achieved. Therefore, a continuous control of the impurities is required.

The analytical requirements for monitoring are relatively high; the  $\text{Fe}_2\text{O}_3$  content should be below  $50 \mu\text{g/g}$  in order to produce clean glass. For a fast analysis, sample preparation efforts also need to be kept at a minimum. Preparing pressed pellets has proved to be sufficient. For this purpose, the material is milled, mixed with wax as a binder in a ratio of 5 : 1, and then pressed into aluminum rings. Care must be taken to ensure that no contamination occurs in the process; the grinding vessels should not contain the elements to be monitored. Owing to the hardness of quartz, grinding tools made of tungsten carbide are being used. During the pressing process the sample material should be protected by a thin polymer film avoiding contact with the pressing tool made of steel.

Both WDS and EDS instruments are suitable for the analysis. In order to analyze the light elements measurements under vacuum are necessary. The achievable reproducibility and trueness depend on the respective concentrations. For measurement times of about three minutes and concentrations in the range of  $<1 \text{ wt}\%$  for the elements to be monitored, relative reproducibilities of approximately 1% can be achieved. For lower concentrations in the range of  $100 \mu\text{g/g}$ , the relative reproducibility as well as the mean deviations from the certified contents are about 10% relative.

Suitable reference samples for calibration are offered by NIST and PT (Brazil) (see B.2.1).

## 10.5 Cement

### 10.5.1 Analytical Task

Cement is an important aggregate for building materials such as concrete or mortar, its annual worldwide production is over 2 billion tons. Since building materials must meet high standards with regard to their strength and stability,

**Table 10.3** Typical compositions of components for the cement production in wt%.

Oxide	Raw mix	Clinker	Cement	ASTM C114
Na <sub>2</sub> O	<1	<0.5	0.08–0.45	0.05
Al <sub>2</sub> O <sub>3</sub>	3.5–4	5–6	5–6	0.2
SiO <sub>2</sub>	13–14	19.5–21	18–21	0.2
SO <sub>3</sub>	0.1–0.3	0.3–0.6	3–4	0.1
CaO	42–44	63–66	62–64	0.3
Fe <sub>2</sub> O <sub>3</sub>	1.6–2	2–3	2–2.5	0.10

the composition of their most important binding agent, cement, is standardized including the methods for its determination (see for example ASTM-C\_114 2015; Frechette et al. 1979). This however only controls the composition of the finished product, and not of its starting materials. However, the analysis of the feedstock is equally important in cement production.

Cement is produced from a finely ground mixture of limestone, marl, sand, and iron oxide-containing substances. Under the constant increase of temperature in large rotary kilns, the material undergoes several chemical reactions. At a temperature of around 1450 °C it is burned into a clinker. The clinker is then ground with slag sand, limestone, and gypsum to cement. This material hardens by hydration, i.e. when it comes into contact with water. Depending on the additives, different hardnesses are achieved.

The elements to be monitored during cement production are Na, Mg, Al, Si, P, S, K, Ca, Mn, and Fe. The typical ranges of the most important oxide contents are given in Table 10.3 for the raw mix, clinker, and cement. Furthermore, the last column in the table lists the maximum allowable differences between double determinations on the same sample; the values are according to ASTM C114. These values illustrate the high demands on the repeatability and accuracy requirements of the analyses and are necessary for a clear assessment of cement quality.

The analyses of the starting materials are not time critical; they can be carried out on materials in inventory. On the other hand, the monitoring of the production is time critical; a feedback as short as possible is necessary for effective process control. As for the quality control of the finished product the time requirements are again not very critical, since the cement is available well in advance before delivery.

### 10.5.2 Sample Preparation

Depending on the requirements of the analysis quality and the available time, the samples can be prepared as pressed pellets or as fusion beads. The high number of analyses as well as the short response times in process monitoring often require rapid sample preparation.

For the production of pressed pellets, the material to be analyzed is finely ground. Since the main components of cement are light elements, considerable

grain size effects can be expected. The grain size of the milled samples should, therefore, not only be sufficiently small, recommended at  $<63\ \mu\text{m}$ , but also the distribution of grain sizes between samples to be analyzed should be the same, i.e. both for reference and unknown samples. The sample powder is mixed in a 5 : 1 ratio with a binder, usually wax, and then pressed at 200 kN for 30 seconds. For better stability the pellets can be pressed in aluminum cups; however, pellets pressed without this additive are sufficiently durable as well. If the material was dried before pressing, the measurement should start shortly after the preparation; otherwise, the material can absorb moisture causing the pellet to expand and crack.

For quality monitoring of the final product, fusion beads are recommended. To avoid any influence of moisture on the sample and the analyses results the sample as well as the glass former should be dried for several hours at about  $105\ ^\circ\text{C}$ . After a heat treatment of the sample at about  $950\ ^\circ\text{C}$  for about one hour, the loss of ignition can be determined gravimetrically. A mixture of 34% lithium metaborate ( $\text{LiBO}_2$ ) and 66% lithium tetraborate ( $\text{LiB}_4\text{O}_7$ ) in the ratio of at least 1 : 5 is mixed as a glass former and then melted as described in Section 3.4.4. The amounts of sample and glass former used depend on the diameter of the fusion bead but must always be the same for the reference sample and the unknown sample. The sample thickness should be at least 5 mm.

The production of fusion beads takes a relatively long time, but prevents influences of sample inhomogeneities, grain sizes, and mineralogical effects and thus permits high analytical accuracy.

For production monitoring in the cement industry, sample preparation will often be carried out by automatic systems. This guarantees reproducible sample type and high throughput.

### 10.5.3 Measurement Technology

For the element analyses, both EDS and WDS instruments are used, as well as sequential and even simultaneous measuring instruments. The decision on which instrument class to use is determined by the analytical requirements with respect to the analysis time and accuracy. EDS instruments have sufficient resolution to separate all elements of interest. In order to achieve comparable statistical uncertainties for all elements to be verified, it is useful to operate EDS instruments at different excitation conditions. This increases the analysis time but improves accuracy.

For WDS instruments, the measuring times for a sequential measuring spectrometer can be set to the accuracy requirements for each element. The measurement times are still relatively long – they can range up to 1000 seconds. This time can be significantly reduced with simultaneous measurement spectrometers, where intensities for all elements of interest are acquired at the same time. The measurement time is then determined by the smallest statistical error that needs to be achieved for the element with the smallest mass fraction or lowest excitation efficiency. In this case, measurement times in the range of 30–60 seconds are usually enough.

When WDS instruments are used for the analysis of sulfur, one has to pay attention to using the correct peak position. It differs for sulfide and sulfate compounds and in the case of an incorrect measuring position this can lead to errors. When using an EDS instrument, the small shifts in peak position are compensated by the integration over the peak area.

#### 10.5.4 Analytical Performance

The analytical performance is influenced by the type of sample preparation. The spectrometer type influences reproducibility and trueness.

The repeatability can be determined by repeated measurements of the same sample. EDS instrument measurements on pressed pellets and fusion beads of the same material are compared in the first two columns of Table 10.4 (ApplNote-WDXRF\_Cement n.d.). The measurements were repeated ten times using the same measurement time and the relative standard deviations were determined.

One can find that for measurements with EDS instruments for pressed pellets the repeatability is better, in particular for the light elements. This can be explained by the relatively high dilution of the analytes in the fusion beads resulting in a larger statistical error.

The third column lists the standard deviations for repeatability measurements for fusion beads, measured with a sequential WDS instrument. For the light elements these are comparable to the results on the pressed pellet, and for the heavier elements they are slightly better. This means that the use of an EDS instrument is adequate for cement analyses (ApplNote-EDXRF-Cement\_Pressed\_Pellets n.d.; ApplNote-EDXRF\_Cement\_beads n.d.; LabReport-XRF\_079 n.d.; LabReport-XRF\_093 n.d.).

The last column in Table 10.4 shows the relative standard deviations for repeated measurements over a longer period of time, i.e. the stability of the analysis. This characterizes the stability of the analytical process. The values

**Table 10.4** Relative standard deviations of repeated measurements for samples that were prepared separately.

Instrument type Oxide	Energy-dispersive		Wavelength-dispersive (only fusion beads)	
	Pressed pellet (%)	Fusion bead (%)	Repeatability (%)	Stability (%)
Na <sub>2</sub> O	2.0	10.3	2.3	3.6
Al <sub>2</sub> O <sub>3</sub>	0.3	0.42	0.3	0.4
SiO <sub>2</sub>	0.1	0.15	0.16	0.12
SO <sub>3</sub>	0.1	0.30	0.32	0.2
CaO	0.1	0.10	0.05	0.03
Fe <sub>2</sub> O <sub>3</sub>	0.1	0.10	0.05	0.04

Source: According to LabReport-XRF\_079 (n.d.) and LabReport-XRF\_093 (n.d.).

are approximately within the range of the repeatability results, which means there are no further influences on the analyses results. If there would be such influences, they could possibly be corrected by means of monitor measurements.

Various reference samples are available for calibration. For example, SRMs 1880–1889 from NIST or others from NCS can be used (see Section B.2.1).

### 10.5.5 Determination of Free Lime in Clinker

Clinker is a starting product in cement production, which contains various Ca compounds, for example, calcium silicates ( $\text{CaO}\cdot\text{SiO}_2$ ), calcium aluminoferrite ( $\text{CaO}\cdot[\text{Al}_2\text{O}_3, \text{Fe}_2\text{O}_3]$ ), and free limestone ( $\text{CaO}$ ). The free calcium is important for the quality and the production of cement. The optimum content should be in the range of 1–1.5 wt%. It is difficult however to determine the percentage of a particular Ca compound in a mixture with other Ca compounds from just the fluorescence intensity only.

Combining XRF and X-ray diffraction, the determination of the contents of the different phases in the clinker in particular the determination of free lime is possible. However, this is possible for example with multichannel spectrometers, which are supplemented by a separate channel just for the measurement of a diffraction line (LabReport-XRF\_094 n.d.). The tube radiation is diffracted on the crystallites of  $\text{CaO}$ . By measuring the intensity of this diffracted radiation, the determination of the content of free lime becomes possible. For measurement times of 60 seconds the detection limits can be within the range of  $<100$  mg/kg. The analytical results of this method deviate less than 5% relative when compared to chemical analyses; its reproducibility is better than 1%.

## 10.6 Coal and Coke

### 10.6.1 Analytical Task

Coal is an important energy source and is used both for heating and, above all, for generating electrical energy. In the field of metallurgy, coal is, to date, the most important reduction agent for refining metals, for example, iron, from the corresponding ores. Coal is a sedimentary rock produced by the carbonization of plant residues. The most important component of coal is therefore carbon. But other elements are also deposited in the sediment. They form the ash portion of coal and, like the water content, reduce the heating value of the coal. Depending on the degree of carbonization, brown coal, hard coal, and anthracite are distinguished from each other. With increasing carbonizing, the contents of moisture and liquid components are reduced and thus the heating value increases.

Coke is predominantly made from low-ash coal by a pyrolytic process, i.e. by heating, with the exclusion of oxygen. This results in a high carbon material with a high specific surface area, which has low gas content, and is used, for example, in the production of iron.

The heating value is crucial for the value of coal. Therefore, the analysis of moisture, of the ash content, but also of elements that can be released during



combustion and that can pollute the environment, for example phosphorus or sulfur, is required. Because of the high importance of coal, the corresponding analytical methods are standardized.

The main elements to be analyzed in coal are Na, Mg, Al, Si, P, S, K, Ca, Ti, Mn, and Fe as oxide; traces of interest are V, Cr, Co, Ni, Cu, Zn, As, Sr, Ba, and Pb. Further traces can also be present.

Coal often has a high moisture content; its determination is regulated in DIN-51718-06 (2002) or ASTM-D\_3173-17 (2017). In this case, a gravimetric method is used by drying the material. For the determination of the surface moisture, drying takes place at approximately 30 °C until no change in mass is measurable; for the determination of the hygroscopic moisture, subsequent drying takes place at about 106 °C for three hours. The mass differences are attributed to the vaporized moisture.

According to DIN-51719-07 (1997), the ash content is also determined gravimetrically, after the coal sample has been ashed in a muffle furnace, first at 500 °C and then for at least for one hour at 815 °C. In this way, only the total ash content can be determined, but not its composition.

The volatile constituents can also be determined gravimetrically after coking the coal under air exclusion for about 10 minutes at about 900 °C.

The content of combustible material can then be determined from the difference in weight of the initial sample and the content of moisture, the volatile elements, and the ash content.

These methods, however, only give summary information; a determination of the mass fractions of the different elements is not possible. For this purpose, XRF can be used, for both the raw and ash material.

In addition to being used as a fuel, coal is also used in industrial processes or in analytics, for example as electrode material in various electrolytic processes or as sample holder for various analytical methods. For these purposes, the purity requirements for the material are particularly high in order to avoid contamination in the processes. For this reason, special procedures for the preparation of the material may be necessary.

### 10.6.2 Sample Preparation

The preparation of carbon samples is often carried out as pressed pellets. First, the material must be dried as described above and then ground. For pressing, the sample is mixed with a binder (e.g. wax) in a 4 : 1 ratio and then pressed with 200 kN. The sample thickness should be relatively large, or the sample mass should always be the same since the absorption of higher energy fluorescence radiation in the light coal matrix is low. To get adequate reproducibility, both references and unknown samples should have the same mass; another possibility is to add a heavy element, for example Cr oxide, to increase the absorption. Depending on the type of coal, these pressed pellets have different mechanical stabilities.

The sample can also be prepared as fusion beads. For this purpose, however, a significant sample quantity must be incinerated. For a relatively low ash content of, for example, 4% and an initial weight of the ash of 0.6 g for a fusion bead, at least 30 g of coal must be incinerated to produce two samples for a repeat

determination. To produce a pressed ash pellet with a weight of 5 g at least 125 g of raw material must be incinerated. It is important to take into account the fact that not only carbon but also other volatile elements are lost during incineration and therefore cannot be considered for the analysis.

Pressed pellets can be produced directly from the ash after grinding; if necessary, a binder can be added. For the production of fusion beads, the glass formers depend on the composition of the ash;  $\text{Li}_2\text{B}_4\text{O}_7$  is more suitable for more CaO-containing ashes, and  $\text{LiBO}_2$  is more suitable for ashes containing  $\text{Al}_2\text{O}_3$  and  $\text{SiO}_2$ .

Coal ashes usually have a very low density, so that at a sample material weight of 0.6 and 5 g of flux, the crucibles are largely filled. Accordingly, the digestion process must be carried out very carefully in order to avoid any material losses.

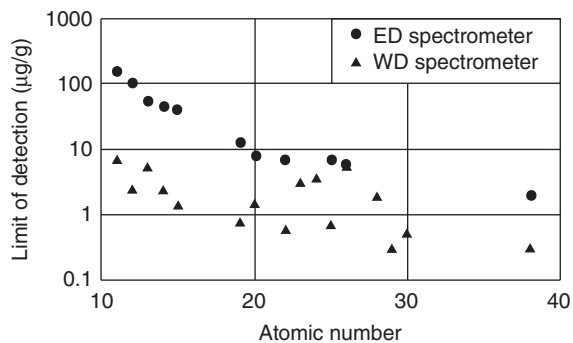
The analysis of ash is necessary in order to decide the possibilities for further use as, an additive to cement or as insulation material, which is dependent on the composition.

### 10.6.3 Measurement Technology and Analytical Performance

The analysis can be carried out by either EDS or WDS instruments. Except the carbon content, all the other elements of interest can be determined with sufficient precision by XRF. Their concentrations are high enough that no extreme trace sensitivity is required. Still, using different excitation conditions is useful for good precision using EDS instruments. The detection limits for the oxides of the elements for a total measurement time of approximately 1000 seconds are shown in Figure 10.2. This sensitivity is sufficient to fulfill all requirements for coal analysis.

The reproducibility of the analysis is characterized by the relative standard deviations of repeated measurements and depends on the concentrations of the different elements. For oxides with higher concentrations, they are in the range of <0.3%, but for oxides with smaller concentrations and for oxides of light elements they are in the range of 1%. The analytical accuracies can be determined by the mean deviations of analytical results of repeated analyses of reference samples. The relative mean deviations for the different elements are about twice as large as those of measurements under repeatability conditions except for the very light elements. Here, grain size effects are more pronounced, in particular in the case of pressed pellets (ApplNote-Coal n.d.).

**Figure 10.2** Limits of detection for element oxides in coal for EDS instruments and for pure elements with WDS instruments. Source: According to ApplNote-Coal (n.d.).



To achieve sufficient sensitivities when analyzing coals for industrial use, the use of WDS instruments is recommended. To avoid the loss of volatile elements, the samples can only be prepared as pressed pellets. The better energy resolution of WDS instruments, especially for the light elements, makes it possible to improve the detection limits down to the sub-parts per million range (LabReport-XRF\_115 n.d.; DIN-ISO-12980 2000).

Standard-based models are used for quantification. Matrix effects can be well compensated by normalization to the Compton intensity. Standard samples among others are issued by NCSCRM, NIST, and MINTEK, see Section B.2.

## 10.7 Ferroalloys

### 10.7.1 Analytical Task

Ferroalloys are iron alloys with very high concentrations of the alloying element. They are added during the steel-making process in order to obtain the desired elemental compositions of the material.

Typical ferroalloys are ferro-silicon (FeSi), ferro-chromium (FeCr), ferro-manganese (FeMn), silico-manganese (SiMn), electrolyte manganese (Mn), manganese metal (Mn), ferro-niobium (FeNb), ferro-molybdenum (FeMo), and molybdenum dioxide (MoO<sub>2</sub>).

Ferroalloys are additives for the smelting of ores; they are produced in large quantities. The exact analyses of their contents are necessary in order to correctly determine the required alloying amount to achieve the desired steel composition, but also for the determination of the material price.

Typical compositions of the main ferroalloys are summarized in Table 10.5. In addition to the main components, several additional elements are of analytical interest since they can influence the composition of the final product.

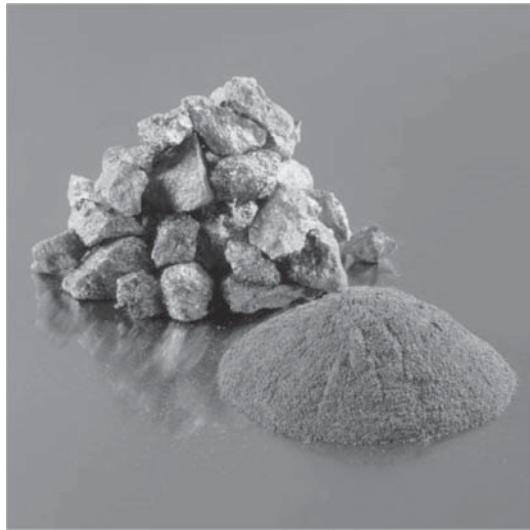
### 10.7.2 Sample Preparation

Ferroalloys are usually produced as coarse-grained granulates, which in some cases can be very hard. Examples of ferroalloys with different grain sizes are shown in Figure 10.3.

**Table 10.5** Concentrations of typical ferroalloys in wt%.

Ferroalloy	Fe-Si	Fe-Cr	Fe-Mn	Fe-Nb	Fe-Mo
Al	0.3–2.5			0.5–2	
Si	40–75	0.05–2	0.1–2.5		0.2–2.5
Ti				0.2–8	
Cr		70–85			
Mn	0.1–1		50–80	0.2–2	
Fe	25–60	15–30	20–50	45–35	30–35
Nb				50–65	
Mo					65–70

**Figure 10.3** Ferroalloy with different grain size.



To correctly characterize a large amount of a ferroalloy it is assumed that the available laboratory sample sufficiently represents the entire material to be analyzed.

The method of sample preparation depends on the required analytical accuracy and the time available for the analysis. Since the sample material usually exists as solid pieces, crushing with subsequent grinding is necessary. In principle, the sample material should have a grain size of  $<160\ \mu\text{m}$ . If the material is ground to a smaller grain size, there is a risk that during the grinding process the material will heat up and absorb oxygen. Experiments have shown that the oxygen content in ferro-vanadium can increase from 0.3% to 3% by grinding for too long. The oxidation correlates to the temperature of the grinding vessel. For the abovementioned fineness, only a short grinding time of approximately 30 seconds is required, so that the mill hardly warms up and oxidation is negligible.

Vibration mills or ball mills are suitable for the grinding process. The grinding tools should be sufficiently hard to achieve adequate grinding, and at the same time produce only a negligible amount of abrasion. Of course, the milling tools should not contain elements that are the analytes in order to avoid contamination. For ferroalloys grinding tools made of tungsten carbide (WC) fulfill these requirements. In order to obtain solid and stable pellets a binder should be introduced during the grinding process. The most commonly used binder is pure wax or cellulose, which is added in a mass ratio of 1 : 4 to the sample. Pressing is carried out at pressures of 200 kN. When using pressed pellets, influences from surface irregularities as well as from grain size and mineralogical effects can influence the analyses results.

A tried and tested preparation technique is the remelting of ferroalloys in an inert atmosphere. For this purpose, weighed sample amounts are placed in layers with pure iron into a ceramic crucible (Figure 10.4). The crucible is lined with an additional protective layer of refractory material to increase its temperature resistance. For the remelting process, an induction furnace should be used, which

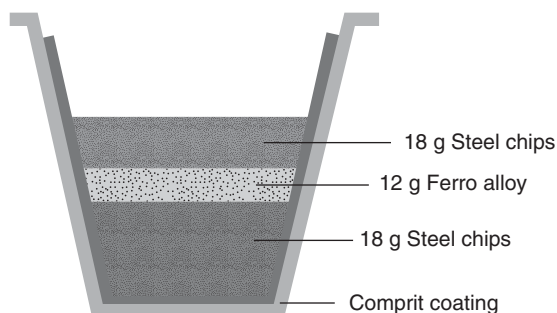


**Figure 10.4** Crucible for remelting ferroalloys.

can achieve the required melting temperatures of about 1500 °C within a very short time. The melt can be poured into a round sample mold. The solidified specimens can then further be prepared like any steel sample.

Since the alloys are usually available for a sufficiently long time prior to their use in the metallurgical process, preparation time is not critical and very often the material is prepared as a fusion bead. Their better homogeneity as well as elimination of mineralogical effects improves the analytical results. For the melt digestion, the sample material is therefore mixed with an oxidizing agent and a glass former.

The choice of oxidizing agents and glass formers to use, as well as their mixing ratios with the sample and the optimal temperature cycle, depends on the respective ferroalloy. Examples of the common ferroalloys are summarized in Table 10.6. As an example, the process for the digestion of ferro-silicon is shown schematically in Figure 10.5.

The costly and time-consuming procedures described for the sample preparation were the reason to test simpler preparation techniques, such as the measurement of a powder deposit. It was shown that there are strong influences due to particle size as well as the material structure. Satisfactory analytical results however can be achieved by a modified preparation procedure, when the particle size is <100 μm. This must be ensured by a sufficient milling time. Then segregations of the different phases can be avoided. Tests of this preparation method by repeated full analyses of a standard sample have shown that the trueness of the XRF measurements with this simplified preparation technique is comparable to a wet chemical analysis and the repeatability is only slightly worse compared to the wet chemical results (see Table 10.7; Saiz-Zens et al. 1998). With this technique the analytical results can be achieved with acceptable accuracy, much faster and with less effort.

### 10.7.3 Analysis Technology

Usually WDS instruments are used either sequential or multichannel instruments, depending on the respective laboratory availability. In the case of multichannel instruments, they need to have measuring channels available for all elements to be analyzed.

**Table 10.6** Digestion procedures for different Ferroalloys.

Ferroalloy	Sample weight	Pre-oxidation and pre-melt	Digestion
Fe-Si	0.500 g Na <sub>2</sub> CO <sub>3</sub> + 2% NaNO <sub>3</sub> 1.000 g CaCO <sub>3</sub> 0.300 g sample	Pre-oxidation at lower temperature for approx. six to seven minutes, then cover for about seven minutes	Compress oxide and melt for 10 minutes at 1150 °C w/o cover, after cooling add 5.00 g Na <sub>2</sub> B <sub>4</sub> O <sub>7</sub> , melt again at 1150 °C, homogenize by pivoting, pour into a preheated Pt-mold
Fe-Cr	5.000 g Na <sub>2</sub> B <sub>4</sub> O <sub>7</sub> 0.500 g KNO <sub>3</sub> 0.750 g NaNO <sub>3</sub> 0.500 g Na <sub>2</sub> CO <sub>3</sub> 0.200 g sample	Pre-oxidation at 800 °C for 15 minutes Pre-melting at 900 °C for 10 minutes	1100 °C for 15 minutes, homogenize by pivoting, pour into preheated (750 °C) molds, cool down slowly
MoO <sub>2</sub>	5.000 g Li <sub>2</sub> B <sub>4</sub> O <sub>7</sub> 0.200 g sample	Pre-melting at 1000 °C for three minutes	1100 °C for 12 minutes, pouring into preheated (750 °C) molds, cool down slowly
Fe-Mn, Si-Mn	<i>Method 1</i> 5.000 g Li <sub>2</sub> B <sub>4</sub> O <sub>7</sub> 0.500 g KNO <sub>3</sub> 0.050 g Na <sub>2</sub> CO <sub>3</sub> 0.200 g sample	Pre-oxidation at 700 °C for 15 minutes Pre-melting at 900 °C for 10 minutes	1150 °C for 15 minutes, homogenize by pivoting, pour into preheated (750 °C) molds, cool down slowly
	<i>Method 2</i> 0.200 g sample mixing in 1.000 g V <sub>2</sub> O <sub>5</sub> , place in a mold of 8.000 g Li <sub>2</sub> B <sub>4</sub> O <sub>7</sub> , adding of five drops of LiBr	Pre-oxidation at 700 °C for 15 minutes Pre-melting at 900 °C for 10 minutes	Same for both methods
Fe-Mo	0.500 g CaCO <sub>3</sub> 0.100 g Na <sub>2</sub> CO <sub>3</sub> 0.100 g NaNO <sub>3</sub> 0.300 g sample Cover with 0.500 g CaCO <sub>3</sub>	Pre-oxidation 900 °C for five minutes	1150 °C for six minutes, homogenize by pivoting, pour into preheated (750 °C) molds, cool down slowly
Fe-Nb	6.000 g Li <sub>2</sub> B <sub>4</sub> O <sub>7</sub> for a mold 0.700 g oxidation agent from KNO <sub>3</sub> , NaNO <sub>3</sub> , SrNO <sub>3</sub> , NaJO <sub>3</sub> (in a relation of 1 : 1 : 1 : 1) 0.200 g NaCO <sub>3</sub> 0.250 g sample	Pre-oxidation at 900 °C for 15 minutes Pre-melting at 950 °C for 10 minutes	1100 °C for 15 minutes, homogenize by pivoting, pour into preheated (750 °C) molds, cool down slowly

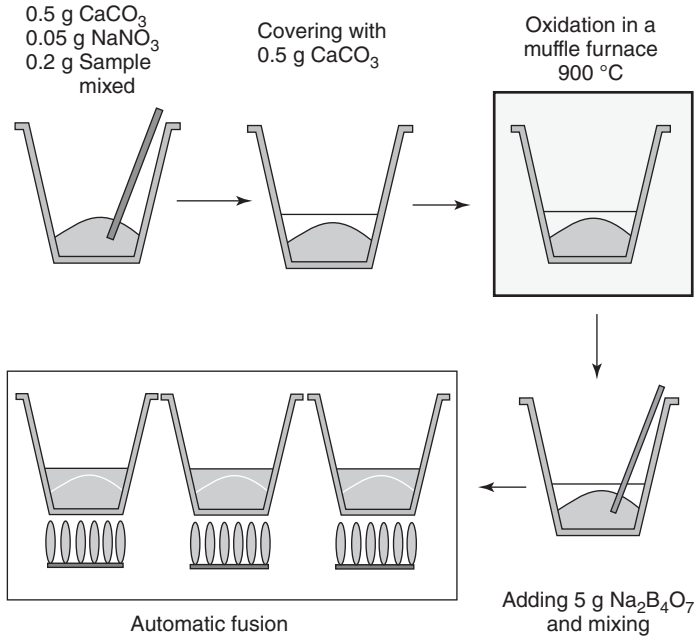


**Figure 10.5** Process scheme for the digestion of ferro-silicon.

**Table 10.7** Analyses results of ferro-silicon using powder samples in wt%.

Element	Si	Fe
Certified	$71.6 \pm 0.3$	$23.3 \pm (0.2)$
XRF (loose powder)	$71.3 \pm 0.5$	$21.9 \pm 0.5$
Wet chemical	$71.7 \pm 0.2$	$23.3 \pm 0.2$

### 10.7.4 Analytical Performance

Typical measurement times of sequential spectrometers for the analyses of ferroalloys are 60–100 seconds per element; this results in a total measurement time of at least 10–15 minutes for 15 analyte elements. The optimum measuring conditions can be set for each element in order to achieve similar statistical uncertainties. For a simultaneous measurement, the measuring conditions are identical for all elements. The excitation conditions and collimator size must be selected so that no saturation effects occur, and the measurement time must be selected to achieve the desired statistical uncertainties.

For evaluation, standard-based models are preferred, since the matrix interactions can be large, and a high analytical accuracy is required. Standard samples are offered by various suppliers, including NIST, NSC, BAS, and others, see Section B.2.

The achievable reproducibility is largely determined by the statistical uncertainty. The relative standard deviations for repeated measurements can range from 0.1% to 0.5%. If the entire analysis is carried out repeatedly, including the preparation as fusion beads, the standard deviations for the main components are of the same order of magnitude. However, the deviations for secondary components, in particular for light elements such as Na, Al, or Ca, can be significantly greater. The trueness for the main components ranges from 0.2% to 0.5%; for the secondary components the results can deviate as much as 5% (see also LabReport-XRF\_105 (n.d.); ApplNote-Ferrosilicon n.d.).

## 10.8 Slags

### 10.8.1 Analytical Task

Slags are by-products in metallurgy, which are produced in considerable quantities during most metallurgical processes. Slags have a glassy to porous structure. They are composed of different oxides and usually form a thin layer on top of the metal bath. Depending on the metallurgical process, various slags are produced; they can be distinguished by their composition. In all cases, slags contain high contents of Mg, Al, and Si oxides; they also always contain metallic components that diffuse into the slag during the various process steps. This consequently leads to a depletion of the melt.

Typical additional analytes are P, S, K, Ca, Ti, Mn, Fe, and Zn. Depending on the ores, secondary materials, and melting technology used, traces of several other elements can be of interest.

Slags are removed from the metal bath and can be used for various purposes after cooling and breakup. Depending on the source of the slags, their use is possible as fertilizers, as an admixture in the cement production, or in road substructure construction. Since slags have high hardness and, due to their porosity also good heat insulation, they are also used in road surfaces or house construction.

In order to monitor and control the metallurgical process, but also to ensure the quality of the slag for their various applications, their composition needs to be analyzed.

### 10.8.2 Sample Preparation

Analyses for process monitoring have to be fast; therefore the slags are most often only crushed, ground, and measured as loose material poured into a sample cup or mixed with a binder in a ratio of 5 : 1 and then pressed to a pellet in the same way as powder samples are.

Crone et al. (2005) carried out investigations solely on how to collect samples from a blast furnace slag to get an instrument sample that can be measured immediately without further preparation. For this purpose, the sample was directly skimmed from the melt, which then solidified in the sampling probe. The procedure is shown in Figure 10.6a; Figure 10.6b shows both the probe and a solidified sample. Measurements of samples taken repeatedly show that because of an



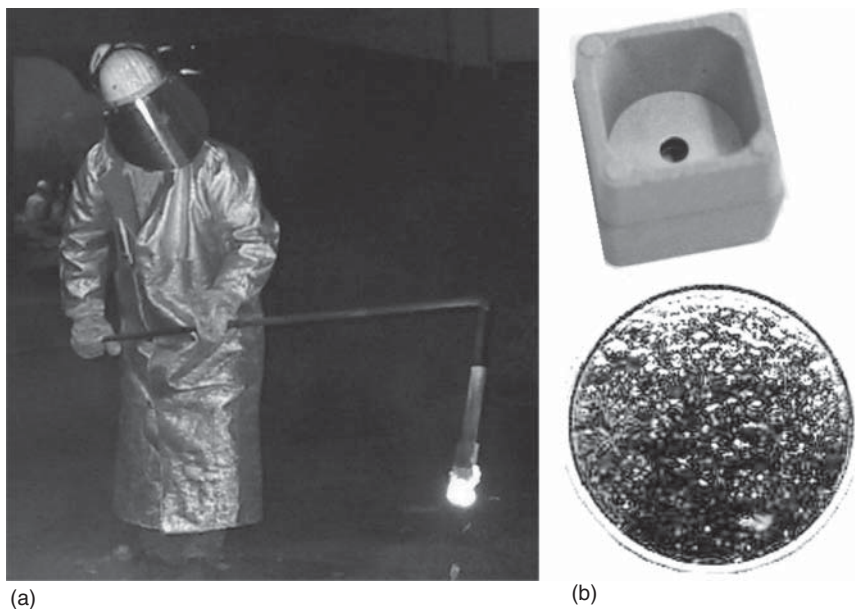


**Figure 10.6** Sampling of a slag sample from the melt with a sampling probe (a), probe head, and a glassy solidified sample (b).

incorrect cooling process, it is possible that crystallization of the sample occurs. Investigations of the homogeneity show only small variations in the concentrations; however, they can be overcome by analyzing relatively large sample areas. This preparation technique saves a lot of analysis time and cost.

For more accurate, but not time critical analyses, the material is prepared as fusion bead. Therefore, the material is ground to grain sizes less than 0.1 mm and mixed with sodium tetraborate ( $\text{Na}_2\text{B}_4\text{O}_7$ ) as well as potassium nitrate ( $\text{KNO}_3$ ) as fluxes in a ratio 1 : 12 : 1. After heat treatment at about 1200 °C for 10–15 minutes the melt can be poured into a mold. As expected, the reproducibilities of the results for pressed pellets and fusions beads are better than for loose powders but in general the differences are negligible (Doujak et al. 2002).

### 10.8.3 Measurement Technology and Analytical Accuracy

Both WDS and EDS instruments can be used for this analytical task. Bianchi et al. (2002) showed that the results are comparable when the measurement times are sufficient.

The achievable analytical accuracies depend on the type of sample preparation. They differ for loose powders, pressed pellets, and fusion beads. Table 10.8 shows the relative standard deviations for the three different preparation techniques for a few element oxides. They were determined by repeated measurements of a reference sample. As expected, the bulk powder sample shows the largest variation. The repeatabilities for the other two preparation methods are comparable, but are, as expected element dependent.

**Table 10.8** Relative standard deviation  $\sigma_{\text{rel}}$  of repeated measurements of slag samples, depending on preparation technique.

Element	MgO	Al <sub>2</sub> O <sub>3</sub>	SiO <sub>2</sub>	P <sub>2</sub> O <sub>5</sub>	CaO	TiO <sub>2</sub>	MnO	Fe
Sample mass fraction (wt%)	2.3	1.98	16.0	2.18	51.9	0.77	5.28	15.5
Loose powder (%)	2.9	2.5	1.0	1.7	0.8	2.9	1.7	1.35
Pressed pellet (%)	0.4	0.4	0.5	0.4	0.2	0.2	0.2	0.15
Fusion bead (%)	2.0	1.9	0.3	0.3	0.3	0.7	0.3	0.25

Source: According to Bianchi et al. (2002).

The trueness of the analyses not only depends on the preparation technique but also on the calibration. For the analysis of pressed pellets, the relative uncertainties of the main components are in the range of 1%. The uncertainties of the secondary components can reach up to approximately 5% (see also ApplNote-Slags\_Pellets n.d.; LabReport-XRF\_053 n.d.).

Reference samples for the analysis of slags are offered by NIST, NSC, Fluxana, and others (see also Section B.2.1).

## 10.9 Ceramics and Refractory Materials

### 10.9.1 Analytical Task

Ceramic materials that exhibit high strength up to temperatures of 1500 °C are referred to as refractory materials. These are ceramic materials, which consist predominantly of oxides of Mg, Al, Si, Ca, Cr, or Zr, but carbon or carbides can also be added. Refractory materials are mainly used as furnace linings in various production processes, for example, in the metallurgical industry or in manufacturing of glass. Owing to their high strength in association with their high temperature compatibility, the materials are also used as cutting tools. Typical concentrations of refractory materials are given in Table 10.9. Traces of Cr, Y, Zr, Hf, and Ce can be found as well. The concentrations of the individual oxides can vary a lot, which makes a standardized analysis very difficult.

The requirements for refractory materials are becoming ever higher with regard to their temperature range of use or their durability. Therefore, a continuous monitoring of the material quality is required. This applies to the raw materials, which usually are of geological origin, but above all to the finished products to ensure their product quality. For specific requirements, the raw materials are very often synthesized in order to ensure the required product properties by virtue of their sufficient purity.

### 10.9.2 Sample Preparation

Preparation as fusion beads is the preferred method. The main components of refractory materials are oxides of light elements, which are very hard. Grinding the material finely enough to prepare powder pellets is therefore difficult. Fusion

**Table 10.9** Mass fractions ranges of refractory materials.

Oxide	Na <sub>2</sub> O	Al <sub>2</sub> O <sub>3</sub>	SiO <sub>2</sub>	K <sub>2</sub> O	CaO	TiO <sub>2</sub>	Fe <sub>2</sub> O <sub>3</sub>
Content (wt%)	0.05–10	1–99	1–99	0.01–5	0.01–70	0.01–5	0.01–30

**Table 10.10** Results of repeated measurements on a refractory.

Oxide	Al <sub>2</sub> O <sub>3</sub>	SiO <sub>2</sub>	K <sub>2</sub> O	TiO <sub>2</sub>	Fe <sub>2</sub> O <sub>3</sub>
Nominal (wt%)	83.84	10.34	0.07	3.70	1.51
$\sigma_{\text{nominal}}$ (wt%)	0.23	0.16	0.007	0.015	0.057
Analyzed (wt%)	84.04	10.35	0.05	3.65	1.55
$\sigma_{\text{analysis}}$ (wt%)	0.047	0.042	<0.001	0.009	0.028
$\sigma_{\text{rel}}$ (%)	0.056	0.41	<0.001	0.26	1.78

Source: According to Körber (1998).

beads not only ensure a very even sample surface with a homogeneous depth profile, but grain size effects are also prevented. For the fusion process the material should be sufficiently crushed. Sufficiently hard grinding vessels and tools should be used that do not contain any analyte elements. For this reason, often tungsten carbide is used. When analyzing W, Ni, or Co, corrections in order to account for abrasions of the grinding tools might be necessary. The grain size should be at least less than 63  $\mu\text{m}$  after milling. The sample material is dried at 105 °C, and then mixed with Li<sub>2</sub>B<sub>4</sub>O<sub>7</sub> as flux in the ratio of at least 1 : 10. For challenging conditions, for example, for materials containing SiC or Cr<sub>2</sub>O<sub>3</sub>, adding of Na<sub>3</sub>PO<sub>4</sub> or NaNO<sub>3</sub> as well as a higher dilution of the sample with the flux is useful. The melting process should be carried out for about 10 minutes at temperatures of at least 1200 °C. The preparation procedure is described in detail EN ISO 12677:2011.

### 10.9.3 Measurement Technology and Analytical Performance

For the analyses of refractory materials usually WDS instruments are used, since the analytical focus is on the light elements. The better low-energy resolution of the instruments, in particular the higher fluorescence intensities due to the improved peak-to-background ratios, achieves smaller statistical errors.

Körber (1998) published repeated measurements made on refractory reference material that was individually prepared for every measurement. The results of three repeated analyses are summarized in Table 10.10.

The first two rows indicate the nominal values of the reference sample as well as the permissible standard deviations in accordance with DIN-EN-955-5 (n.d.). The following rows of Table 10.10 are the results of the repeated measurements.

The mean values of the concentrations, calculated using calibration with standard-based models, agree well within the permissible standard deviations. The standard deviations of the repeated measurements (fourth row) are

significantly smaller than the ranges specified by the DIN standard. The very small relative standard deviations (last row) show the high precision that is typical of XRF, not only for the individual measurements but also over the entire working range of the analytical method.

In addition to the use of standard models, standard-less fundamental parameter-based quantification models were also tested (Flock et al. 2008). The advantage of fundamental parameter-based models is their high flexibility, mainly when the composition of the analyzed materials is in question, which is important for refractories due to their highly varying compositions, but also with regard to the excitation conditions of the X-ray measurements. If the incident spectrum is known, quantification can be carried out at varying excitation conditions. The standard-less analyses were carried out on fusion beads prepared with lithium tetraborate. A comparison of the analytical results shows that satisfactory results for the main components can be achieved with fundamental parameter models; using standards in the quantification process does not lead to significant improvements. The accuracy is however limited for the secondary components and especially for traces when compared to standard-based analyses.

## 10.10 Dusts

### 10.10.1 Analytical Problem and Dust Collection

Dusts are liquid or solid components of the atmosphere, which may be of natural origin caused by erosion, volcanic activity or fires, but also of manmade sources, such as road and rail traffic or industrial sources. The distribution of the dusts depends on the individual weather conditions as well as on the intensity of the dust source and their altitude. Monitoring the dust load may be necessary for a variety of reasons, such as assessing the health hazard, to gauge the effectiveness of dust reduction, or to monitor compliance with certain limits of dust exposure. The analytical problem is always the same, determining the qualitative and quantitative composition of the dusts. The analytical methods however can be very different. They are determined by the amount of dust available for the analysis as well as by its composition. In addition to the actual measurement, the collection of the dust and its preparation must also be factored in. Some examples of the analyses of dusts, as a function of the dust load, are discussed below.

Very low dust loads can occur far away from manmade sources or in a particularly clean atmosphere, such as clean production rooms. Throughout their monitoring, the dust concentrations are very low; therefore their analysis also requires very sensitive analytical methods. In this case, total reflection X-ray spectrometry (TXRF) can be used. For this purpose, small sample quantities can be collected directly, on the sample carrier, for example by deposition in an impactor. Then the direct qualitative as well as quantitative analysis of the dusts is possible. Comparable analyses are described in Section 12.4.2.2.

Medium dust loads can occur during environmental monitoring in urban areas or also in workplaces with lower dust loads. In order to determine the dust load

in these areas and to have a sufficient amount of material for the analysis, larger quantities of air are pumped through a separation system via a dust collector and the dust is collected on filters. Different filters are used:

- Surface filters where the dust particles rest on the filter, such as membrane filters, Teflon<sup>®</sup> filters, or nitrate cellulose filters.
- Depth filters where dust particles infiltrate the filter, such as glass fiber or paper filters. When using depth filters, their influence on the matrix interaction during an X-ray analysis must be taken into account. Radiation of lighter elements is more readily absorbed, especially when the dust particles penetrate deep into the filter.

The filter can then be directly measured for the analysis. When measuring, make sure that the filters are flat and in the same position as a solid sample to avoid variations in intensity due to different distances of the sample to the spectrometer. In addition, the blank value of the filter material must also be factored. This means that the filters must be clean, should not contain elements that are expected in the dust, and their composition should not change from batch to batch. It is therefore recommended to measure the unloaded filters to clearly identify the differences between the loaded and unloaded filters. The spectra of a loaded filter and a blank filter are shown in Figure 10.7.

The collected amount of dust can be gravimetrically determined, i.e. from the weight difference between the loaded and the unloaded filters.

A further possibility is the ashing of the filters, for example in an oxygen plasma. The ash can then directly be analyzed, for example as a pressed pellet. Another possibility is adding nitric acid and an internal standard to the ash. This would allow for the analysis by TXRF (see Section 12.4.1), which can then provide not only qualitative but also quantitative information about the dust composition (Schmeling et al. 1995).

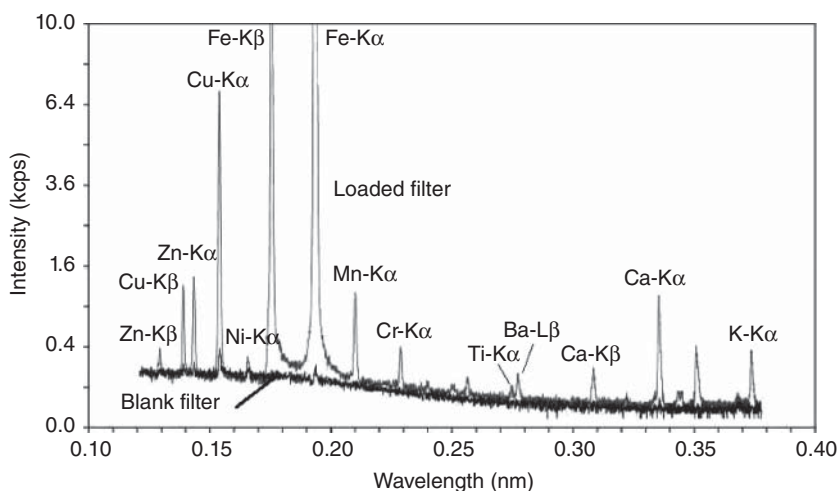
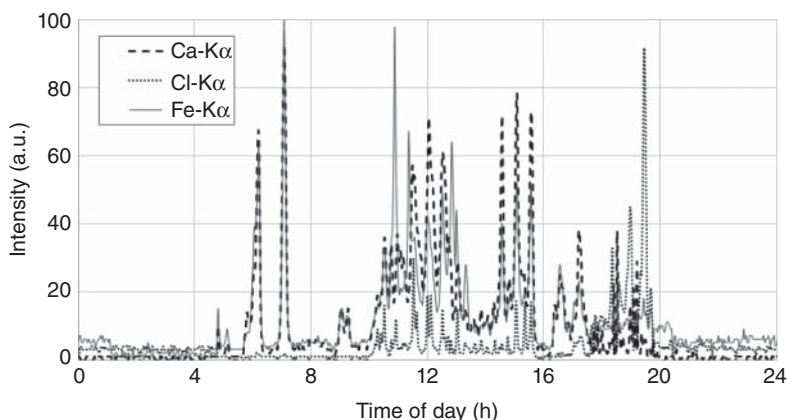


Figure 10.7 Spectra of a blank and a loaded filter.



**Figure 10.8** Element distribution along the trace of collected dust.

The advantage of XRF for this task is the simple preparation and measurement of the samples. However, quantifications are being complicated by the influence of the filters on the measured intensities and by the lack of appropriate reference samples. One way of producing standards is to deposit small particle powders of known composition onto the filters. Geological standards can be used for this purpose, but they do not correspond to the actual compositions of dusts. For the preparation of the reference sample, filters with real dust loads are also analyzed by means of alternative methods, such as ICP. For this purpose, homogeneously loaded filters are divided into several parts; one is used for the analysis with ICP, and the others can be used as reference for the XRF analysis.

For heavier loads it may also be interesting to examine the chronological sequence of the emissions and thus the dust loads (Lienemann 2009). For this purpose, the collected dusts are deposited on a tape that changes the deposition position with time. This creates traces that represent the time-based sequence of the load. An example of the deposition of urban dust over a period of 24 hours is shown for some elements in Figure 10.8. The recordings start at night with low loads; in the early morning hours, the first higher loads are noticeable, perhaps from the emission of heating or power plants. At approximately 7.00 a.m., the load increases significantly from the emissions of road traffic, and in the evening at around 8.00 p.m. the load decreases again.

The absolute quantity of dust is also important for the assessment of the hazards. A person breathes on average about 170 l/h of air. During the collection of dust, much higher throughputs – up to 100 times more – are targeted to be able to collect a sufficient amount of dust for an analysis in reasonable time.

In work environments, relatively large amounts of dust can be generated. Here, it is important not only to determine the chemical composition but also the particle size distribution – their respirability affects the potential health risk. At workplaces also larger particles can be generated, but these cannot reach the lung. However, smaller particles with sizes of less than 10  $\mu\text{m}$  are respirable and are therefore a health hazard. With cascade impactors a size separation of the dust particles is possible. In a cascade impactor the air stream is channeled through a

series of spray valves of different sizes onto impact plates. Only particles with inertia above a certain threshold value will be deposited on the impact plate; smaller particles will flow around the initial impact plate until their inertia is large enough to be collected by the next impact plate. After collecting the dust from the impact plates, it can be analyzed. The appropriate preparation method depends on the collected amount of dust or collection time.

Another possibility for separating the dust particles by their size is the cyclone separators in which the particles are separated by their inertia on the cyclone walls, which depends on their weight or size as well as on the air flux.

For a meaningful quantification, the samples should always have the same mass. This can be achieved by mixing the dust with a binder and pressing it into a pellet (see Figure 3.10) or by preparation as fusion bead.

### 10.10.2 Measurement

Both WDS and EDS instruments as well as the corresponding quantification models meet the analytical requirements. When EDS instruments are used, the simultaneous detection of the entire spectrum has the advantage that even unexpected elements are automatically detected. By optimizing the excitation conditions, sensitivities can be achieved that are significantly lower than the requirements of the EPA (EPA IO-3.3 1999; ApplBrief-Airborne\_particles n.d.). Using a WDS instrument for routine analysis, this would require a complete scan resulting in a relatively long analysis time.

The optimum test conditions must be selected for all elements of interest. This can require several excitation methods. The measurement times must be adjusted for the available amount of dust. For low amounts they are increased in order to achieve a sufficiently sensitivity and small statistical error. Where necessary it is also possible to use excitation methods in which the spectral background is suppressed, for example, an excitation with polarized radiation (Jonkers 2006) or with secondary target radiation.

For dust analyses the obtainable accuracies strongly depend on the total amount of dust analyzed, on the errors made during sample preparation, and on the correct treatment of the matrix interactions. The errors made during the actual measurement are usually small against these. The analytical accuracies are therefore usually not as good as for bulk materials or for powders.

## 10.11 Food

### 10.11.1 Analytical Task

Food may be contaminated with hazardous substances. These can already be present in the raw materials but can also be introduced into the foodstuffs during the production process. Toxic substances can be organic as well as inorganic. Therefore, a strict monitoring of these hazards is necessary. They are regulated by government regulations, for example (EU-regulation\_466 2001; EU-regulation\_22 2001). However, the diversity of the food and the possible

amounts of contaminations cover such a large range that comprehensive regulations are not possible.

Beverages take special position in the analyses of foodstuffs since they can be analyzed directly with the AAS or ICP. One of the best controlled beverages is drinking water. XRF methods can also be used for this purpose. Owing to the required low detection limits TXRF is used (see Section 12.4.1). For some beverages relatively complex sample preparation is required, in particular to isolate organic components.

Solid or pasty substances can be directly examined with XRF. Two examples with a high inorganic load and their analyses with XRF are discussed exemplarily below.

Some analytical questions in which the thresholds of the elements to be monitored are very small, require the use of XRF in total reflection, for example the detection of very toxic elements.

### 10.11.2 Monitoring of Animal Feed

The EU regulates the exposure of animal feed to undesirable substances by EU-regulation\_32 (2002). The maximum loads can be different for the various feed forms and apply to a variety of organic toxins as well as some toxic elements. A selection of values of these pure element limits are summarized in Table 10.11. These are (except for Hg) concentrations that are easily detectable with XRF. As a result of the very different matrices as well as the range of possible elements, energy-dispersive analysis is advantageous due to the simultaneous detection of the entire spectrum. This also facilitates quantification, since knowledge of the entire element spectrum is required when using standard-less models. A further advantage compared to the usual analyses using atomic spectroscopic methods, such as ICP–OES, is that the results of the analyses are available much faster, due to the simpler sample preparation, but also by potential on-site analysis.

The sensitivities for most elements are sufficient by simply pouring the sample into the sample cup. A sufficient precision of the analysis was demonstrated by repeated measurements on repeatedly prepared samples; the relative standard

**Table 10.11** Average limits for toxic elements in animal food.

Element	Limits (mg/kg)
As	<30
Cd	<10
K	<60
Hg	<0.5
Pb	<50
Ni	<20

Source: According to EU-regulation\_32 (2002).



deviations for the low contents of the toxic elements were in the range of 2% (ApplBrief-Animal-feed n.d.).

### 10.11.3 Control of Infant Food

Infant foods require very high standards with regard to hazardous substances. This includes not only the usual toxic elements but also other elements such as Na, Mg, P, Cl, K, Ca, Mn, Fe, or Zn.

In ApplNote-Cereals (n.d.), studies were carried out on children's soft food in which these elements were analyzed. The samples were prepared both as loose powders in a cuvette with a 4  $\mu\text{m}$  Prolene film cover, as well as pressed pellets, pressed at 100 kN without any binder. The measurements were carried out with an ED spectrometer using several excitation conditions to optimize the measured fluorescence intensities. The instrument was calibrated using reference samples, in which the element concentrations were determined with ICP-OES. For the heavier elements the detection limits for the two preparation methods were only marginally different. For the light elements (Na, Mg) they are better by a factor of 2 for the samples prepared as a pressed pellet. The light element radiation was easily absorbed by the film cover of the sample cup, resulting in lower collected fluorescence intensities. The two preparation methods have only a small effect on the trueness of the results. As demonstrated in Table 10.12, they are very similar and adequate for this analytical problem. The table shows the analyzed concentration range, the correlation coefficient  $R^2$  (see Eq. (5.18)) for the agreement between nominal and analyzed values of the used calibration standard, as well as the limits of detection for both types of sample preparation, i.e. for loose powder and pressed pellets. The loss of sensitivity for light elements and accuracy for the loose powder preparation is marginal, and for heavier elements even negligible.

**Table 10.12** Comparison between calibration results and limits of detection for two types of sample preparation.

Element	Concentration range (mg/100 g)	Correlation coefficient $R^2$		LOD (mg/100 g)	
		Pellet	Powder	Pellet	Powder
Na	6–276	0.9908	0.9867	14	71
Mg	16–137	0.9837	0.9864	5	25
P	120–560	0.9955	0.9934	2	2.5
Cl	25–455	0.9958	0.9964	2	2
K	84–945	0.9977	0.9973	2	2
Ca	163–630	0.9931	0.9899	1.2	1.2
Mn	0.13–3.4	0.9978	0.9980	0.2	0.2
Fe	4.30–26	0.9895	0.9872	0.2	0.2
Zn	1.3–5.5	0.9379	0.9697	0.2	0.2

## 10.12 Pharmaceuticals

### 10.12.1 Analytical Task

Pharmaceuticals are subject to strict controls to prevent exposures to toxic elements. They consist not only of the respective active ingredients but also of various fillers. The concentration of the essential elements such as Mg, Si, Ca, Fe, Zn, or Se is important; however, toxic elements such as V, Cr, Ni, As, Cd, Hg, or Pb are dangerous. In the often catalytic production process of the active ingredients, pharmaceuticals can become contaminated with elements such as Ru, Pd, Ir, or Pt, which also pose a hazard. The maximum exposure amounts are determined by the frequency at which the drugs need to be used and the content of toxic substances. This is specified by the maximum permitted daily exposure (PDE) (ICH Guideline Q3D on elemental impurities 2016). These values are summarized in Table 10.13 for different administrations of the drug taken. They vary far and wide for the various possibilities of administering the drug. The drugs vary in form and size. The various shapes and sizes also mean that the mass fractions that need to be detected also depend on the specific form of drug administration.

### 10.12.2 Sample Preparation and Analysis Method

Since not only the type of drug administration but also the matrices vary, universal guidelines for the analysis are not useful. These have to be specified based on the elements, their concentration as well as by the changing inorganic or organic matrices. Conventional analytical methods such as AAS or ICP have high sensitivity, but the processes producing measurable samples are different and their costs are often high. The analysis, however, often does not require very high sensitivity since the maximum loads indicated in the PDE are mostly concentrated in small-sized pharmaceuticals.

The European Pharmacopoeia proposes XRF as an appropriate analytical method (European-Pharmacopoeia 2008). XRF as an analytical method offers several advantages. Since the raw materials used for the preparation of the pharmaceutical are often fine-grained powders, they can be measured directly as a loose powder placed in sample cups; this ensures a short analysis time. Since energy-dispersive XRF instruments simultaneously detect a wide energy range of the spectrum, the risk of missing to detect any contaminations is very low. The light element matrices of pharmaceuticals produce a high scattering background. By normalizing the element intensities to the Compton-scattered intensity of the tube radiation, it is possible to take the different matrices into account during quantification. Utilizing fundamental parameter methods then simplifies the calibration effort that would be necessary for different matrices.

The achievable relative standard deviations under repeatability conditions and achievable accuracies are in the range of 1–5%. These results can be achieved even at concentration levels down to 10 times the detection limit. This is sufficient for the monitoring of the load level. However, for the analysis of pharmaceuticals exist special requirements in regards for data handling and archiving to avoid any type of manipulating the analytical results. This concerns the measurements

**Table 10.13** Maximal amount of intake of toxic elements per day in micrograms.

Element	Oral intake	Intake by injection or infusion	Intake by inhalation
V	100	10	1
Cr	11 000	1100	3
Ni	200	20	5
Cu	3000	300	30
Co	50	5	3
As	15	15	2
Se	150	80	130
Ru	100	10	1
Pd	100	10	1
Cd	5	2	2
Sb	1200	90	20
Ir	100	10	1
Pt	100	10	1
Au	100	100	1
Hg	30	3	1
Tl	8	8	8
Pb	5	5	5

of the samples itself but also all additional measurements for checking the instrument status, for example monitor measurements, recalibrations etc.

## 10.13 Secondary Fuels

### 10.13.1 Analytical Task

Industry and households are delivering a continuously increasing amount of waste, which is too valuable to be stored in landfills. It can be utilized for other purposes. Frequently they are used as secondary fuels, in particular when the calorific value of the waste is higher than 10 MJ/kg. Secondary fuels are mainly used in industrial heat generation, i.e. in cement or lime production plants, in the paper industry, or in steel mills, but also in the district central heating plants for domestic heating supply. Prior to combustion, in order to be able to control the combustion processes and to reduce or avoid the emission of toxic substances that are present in the waste or that can be formed by the combustion process, the composition of the waste must be determined. On the other hand, it is also necessary to protect the incineration plants against corrosive media and thus against damage. Most importantly, the emissions need to stay within the allowable limits of all legal regulations. Several factors determine

**Table 10.14** Reference values for the content of heavy metals in secondary fuels.

Element	Concentration (µg/g)
V	25
Cr	250
Mn	500
Co	12
Ni	160
Cu	350
As	13
Cd	9
Sn	70
Sb	60
Tl	2
Hg	1.2
Pb	200

Source: According to RAL-GZ-724 (2012).

the classification of secondary fuels – the heating value and the exposure to toxic substances take precedence. The calorific value is primarily given by the hydrocarbons contained in the waste; the maximal allowable contents of toxic elements are given by the RAL-GZ-724 (2012), and summarized in Table 10.14.

In addition, halogens, sulfur as well as phosphorus are important because these elements can be converted into aggressive substances during combustion, leading to accelerated corrosion of incineration plants and thus limiting their durability. Depending on the combustion temperature, highly toxic dioxins can also be produced.

The composition of secondary fuels is usually extremely nonhomogeneous, both in terms of their elemental composition and their material structure. XRF is therefore particularly well suited for the analyses of such materials because very different material qualities can be analyzed, and a broad element and concentration range can be detected.

## 10.13.2 Sample Preparation

### 10.13.2.1 Solid Secondary Raw Materials

The major challenge for the analyses of secondary fuels is still the sampling and the preparation of the material for the analyses. In the following, it is assumed that a representative sampling was used and that the sample material is available to the laboratory in sufficient quantities. Depending on the material quality, the preparation methods are very different. It is determined by the condition of the raw material, by the analytical task, but especially by the requirements regarding

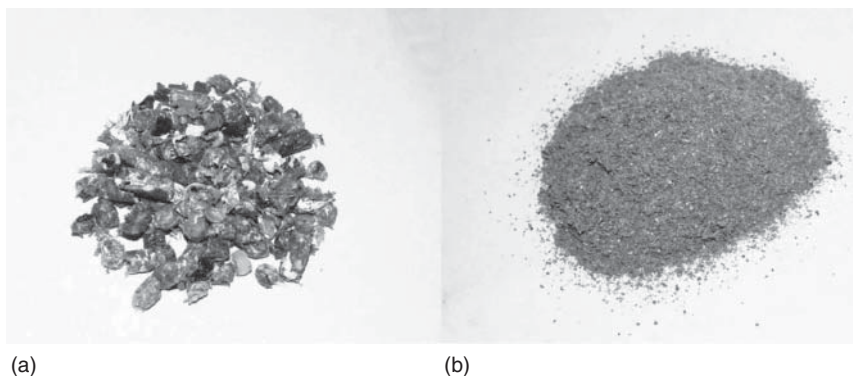


**Figure 10.9** Examples of raw secondary fuels (a) and crushed material (b).

the analytical accuracy. The sample material is usually very inhomogeneous, in terms of the size of the individual parts (see Figure 10.9a) and its composition.

To obtain a representative sample, as a first step, the sample is broken up, followed by often multistep successive mixings and dividings. Secondary raw materials are usually not hard and cannot easily be ground into smaller pieces; the following steps are therefore required to prepare the sample:

- Separation of metallic components, for example, magnetic separation of iron alloys.
- Crushing of soft materials by cutting, for example, with cutting mills. This can achieve good results even for soft materials, but with particle sizes that are still in the range of up to 0.3 mm (see Figure 10.9b). From this material, a representative sample can be obtained by mixing and dividing.
- This sample already would allow a fast analysis, however, with limited accuracy. The material can either be poured into a sample cup or pressed into a pellet. Since fibrous components are often present in the material, the pellets are usually not stable; over time their strength decreases due to volume expansion.
- A further breakup of the sample material, for example to produce reference samples, can only be achieved by grinding in ball or centrifugal mills. However, in order to achieve an effective grinding result, the hardness of the material should be increased. This is possible by freezing the material, for example with liquid nitrogen. This option also exists for the processing of the coarsely pre-processed raw material. The crushed material with grain sizes in the range of less than 300  $\mu\text{m}$  can then be pressed into pellets. Despite the mostly soft sample components, the pellets are not always stable. A mixture with a binder, such as cellulose, can increase the stability of the pellets. With such type of sample preparation, even if it might be more time consuming, more accurate results can be achieved because of the comparable sample mass and densities. These samples can also be archived and are then available for follow-up investigations.
- Pressing soft and organic materials under elevated temperatures can also increase the stability of the pellets. This was demonstrated for the preparation of wood flour (Füchtjohann et al. 2004). Figure 10.10 shows pressed wood flour pellets prepared without binder but at increased temperatures. At an

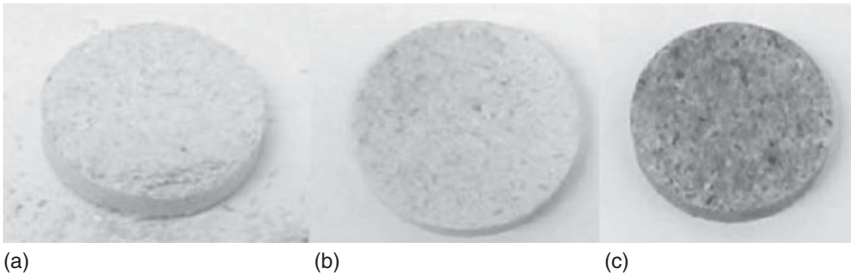


**Figure 10.10** Pellets produced at different temperatures have different strength: (a) 80 °C – not stable, (b) 140 °C – stable, (c) 180 °C – partly carbonized. Source: According to Füchtjohann et al. (2004).

optimum press temperature, stable pellets can be produced, which are even vacuum-capable. If the temperature is too low, the particles do not stick together sufficiently, and the pellets are not stable. If the temperature is too high, or the pressing time too long, there is a danger that organic parts of the sample can pyrolytically decompose and analytes evaporate from the sample. This is mainly the case for volatile elements such as F, Cl, As, or Hg. However, their contents are often subject to supervision, for example in accordance with the “Old-Wood” regulation (AltholzV 2002).

- Another possibility to prepare secondary raw materials is to carry out a digestion. However, there are several potential issues. On the one hand, the matrices can be very different, which makes it necessary to adapt the digestion process. On the other hand, there is a risk that the recovery rates are less than 100%, since not all substances are digested the same or elements can become lost. Furthermore, the sample is diluted by the digestion, which reduce the sensitivity for the detection of traces. In this case for some elements the requirements, summarized in Table 10.14, can no longer be met by XRF analysis.

#### 10.13.2.2 Liquid Secondary Raw Materials

Obtaining a representative sample from liquid secondary raw materials also offers a challenge, even though fluids in general are more homogeneous than solid waste. Nevertheless, the matrices can vary from low to high viscosity, phase formation can occur, emulsions can be formed, or suspended solids are present in the liquid.

However, for this purpose we assume that the laboratory sample is large enough to sufficiently represent the liquid to be analyzed.

For the measurement liquid cups are used (see Section 3.5.1). Since secondary raw materials can consist of various organic solvents, acids or bases, mineral oil products or even aqueous solutions, the selection of a suitable foil material for the sample cup window is of particular importance. It must have sufficient chemical resistance to the liquids, and at the same time the absorption of the fluorescence radiation of the light elements (P, S) that need to be measured must be as low as possible. A durability test of the foils is always recommended. The test sample should be sufficiently homogenized before the measurement, which can be achieved by mixing and by separating any phases or suspended matter (see also Chapter 11).

One possibility to standardize the different matrices of toxic liquids is described in ASTM-D\_6052 (2008). For this purpose, 5 g of the liquid to be analyzed should be mixed with 15 g of activated  $\text{Al}_2\text{O}_3$  powder (grain size  $< 150 \mu\text{m}$ ). The mixture can be prepared manually in a wide-necked 20 ml polypropylene bottle with two steel balls. The resulting mixture can easily be compressed into a bulk material and can then directly be analyzed. However, this preparation technique dilutes the sample, which can be disadvantageous when traces need to be analyzed.

### 10.13.3 Instrumentation and Measurement Conditions

The very inconsistent elemental compositions of secondary raw materials require a flexible analysis technique. EDS instruments are used for the analyses because simultaneous detection of a wide range of elements is possible. WDS instruments can also be used; however, they require a sequential measurement at several element and background positions; for unknown materials it is even necessary to perform a complete scan. With WDS instruments a better resolution of the individual elements is possible; however, it takes a long time to detect the large number of measurement points.

Even if the separation of the individual element lines in the energy range  $< 15 \text{ keV}$  is not as good when using EDS instruments, the spectra can be satisfiable deconvoluted. While this results in slightly larger errors in peak area determination, they are still small compared to the uncertainties introduced during the sampling and preparation of secondary raw materials, due to their large inhomogeneity. In the energy range larger than 15 keV, for example for the elements Ag, Cd, In, Sn, and Sb, the resolution is comparable to that of WDS instruments or even better (see Figure 4.1).

Important line overlaps for toxically relevant elements are summarized in Table 10.15.

The excitation conditions are to be selected for the elements or groups of elements to be investigated. This is possible by adjusting the tube parameters, by

**Table 10.15** Typical line overlaps for toxic elements.

Peak overlap	Solution
S-K $\alpha$ -Pb-M $\alpha$	WD: optimized resolution ED: deconvolution
V-K $\alpha$ -Ti-K $\beta$	WD: optimized resolution ED: deconvolution
As-K $\alpha$ -Pb-L $\alpha$	Evaluate the $\beta$ -lines of both elements Use of Pb-L $\beta$ and correction of As-K $\alpha$ with the help of the Pb-L $\beta$
Br-K $\alpha$ -As-K $\beta$ -Hg-L $\beta$	Switch to Br-K $\beta$ , Hg-L $\alpha$ , Pb-L $\beta$ As-K $\beta$ by deconvolution
Cd-K $\alpha$ -Rh-K $\beta$	Cd-K $\alpha$ by deconvolution
Sb-K $\alpha$ -Cd-K $\beta$	Switch to Sb-K $\beta$ and optimizing of measuring conditions for WD by increased resolution to filtering of the background

using filters to suppress the scattering background, or by optimizing the resolution of the spectrometer by the choice of crystal or collimator. In any case, the test conditions should be adjusted for the required accuracy.

#### 10.13.4 Measurement Uncertainties in the Analysis of Solid Secondary Raw Materials

The strong inhomogeneity of secondary raw materials presents a particular challenge not only with respect to the preparation of the material, but it also requires a particular approach in the evaluation of the measured spectra, caused by the large variability of the composition. Supplying suitable reference samples for this type of material is complicated and complex. Therefore, the use of standard-less models is simpler and more common. Although there are limitations to the analytical accuracy the higher flexibility does clearly compensate for this disadvantage. The measurement errors made are, in most cases, small against the uncertainties that have occurred before the measurement by sampling and preparation (DIN-51720-03 2001; DIN-51729-10 2011-04; DIN-EN-ISO-16967 2013-03).

In Table 10.16 the analyses results given for a sample prepared twice and measured on both sides are summarized. They give an indication of the limits of the analytical accuracies that are achievable.

**Table 10.16** Results of repeated measurements for secondary fuels.

Elem	Results prep 1 ( $\mu\text{g/g}$ )		Results prep 2 ( $\mu\text{g/g}$ )		Relative standard deviation (%)
	Front	Back	Front	Back	
Na	1200	1000	1100	1200	8.5
SiO <sub>2</sub>	27 400	19 900	21 100	25 900	15.4
P	300	200	200	300	23.1
S	2800	1900	1900	2600	20.4
Cl	9000	4400	4800	7900	34.8
CaO	10 300	8900	8900	10 000	7.7
TiO <sub>2</sub>	8500	7500	7600	8400	6.5
Cr	20.9	16.6	16.8	17	11.5
Ni	4.7	3.2	3.6	4.2	16.8
Cu	46.8	42.5	44.8	49	6.1
Zn	218	217	211	219	1.7
Br	717	540	614	750	14.7
Sn	33	29.6	33.2	30.8	5.5
Sb	17.4	17.9	16.7	16.2	4.4
Hg	20.6	21.0	20.8	20.7	0.8
Tl	3.1	3.2	3.1	2.9	4.1
Pb	76.4	70.6	68.3	77.2	6.0

Source: According to Hanning and Janssen (2005).



In Table 10.16, in addition to the individual analyses results, the respective relative standard deviations of the results are given in the last column. The following conclusions can be drawn from these results; they can also be applied to comparable sample types:

- The differences in results obtained from the front and back sides as well as the results between the two separately prepared samples are of the same magnitude. This leads to the conclusion that the reason for the relatively large variations in the results is mainly the nonhomogeneity of the samples.
- The relative standard deviations for the light elements are larger than for heavy elements. Their information depth is the smallest and thus the sample volume contributing to the analysis result is less. As a result, changes in the actual sample composition have a greater impact. For the heavier elements, the relative standard deviations of the results are lower since a larger sample volume contributes to the analysis result.
- How the results vary also depends on the concentration of the elements and therefore on the statistical error of the measured intensities; and also peak overlaps have an influence. Examples for the low measured intensities are Ni and Tl, and Br and Pb for a peak overlap.

### 10.13.5 Measurement Uncertainties for the Analysis of Liquid Secondary Raw Materials

Marx (2000) carried out studies on the reproducibility and trueness of the analyses results of liquid secondary raw materials on a real phase- and sediment-forming sample prepared according to ASTM D6052. To test the reproducibility the sample was prepared ten times and each preparation was analyzed three times. To test the accuracy, a further sample was prepared with known concentrations and analyzed three times. The results are summarized in Table 10.17. They show relative standard deviations in the order of 1–3%, both regarding the reproducibility and the trueness of an identical, multiple times prepared sample with concentrations in the trace region. For the analysis task at hand this is a satisfactory result, in particular, when considering the uncertainties that the effort to collect a representative sample contributes.

**Table 10.17** Reproducibility and trueness of the analyses of toxic liquids.

Element	S	Cl	Cd	Pb
Reproducibility				
$w_{\text{average}}$ (mg/g)	0.99	1.45	0.0056	0.0098
$\sigma_{\text{rel}}$ (%)	3.1	1.9	2.2	3.2
Trueness				
Nominal (mg/g)	0.85	1.65	0.046	0.0184
Analyzed (mg/g)	0.73	1.62	0.05	0.0182

Source: According to Marx (2000).

## 11

### Analysis of Liquids

X-ray fluorescence (XRF) is frequently used for the analysis of liquids. The range of applications can be very broad. The following problems must be considered for all applications:

- Liquids usually have a light matrix, which results in a strong scattering of the incident radiation. As a result, the spectral background increases and the sensitivity is reduced.
- For measurement, the liquids must be placed in special measurement cups within the X-ray spectrometer. Since, in most instruments the excitation is carried out from below, the measurement cup must be covered at the bottom, which means, both incident and fluorescent radiations are absorbed by this cover. Even if very thin films (PE, PET, etc., see Table 3.11) are used for this purpose, absorption is not negligible and detection is limited, in particular, for low-energy radiation, which restricts the analysis of light elements. The fact that the analysis of liquids is not possible in vacuum makes matter worse, especially since air readily absorbs the low-energy radiation.
- Liquids usually are homogeneous and therefore require no special sample preparation. In the case where liquids are nonhomogeneous, i.e. if they consist of liquids of different densities, or are emulsions or suspensions, preparation techniques to homogenize or to filter and separate can be required. Subsequently, the various phases or any incorporated particles can be analyzed separately.
- The analysis of liquids can also be required in close proximity to a manufacturing process. Then the measurements are often carried out in flow cells. The liquid continuously flows through the cell in order to be analyzed, i.e. a current process sample is always available.
- For light element and trace detection in liquids, special measurement or preparation techniques have been developed that reduce the spectral background and thus increase the sensitivity of the measurement.

## 11.1 Multielement Analysis of Liquids

### 11.1.1 Analytical Task

The analysis of liquids focuses on the determination of the substances contained. However, the solvents themselves can also provide an X-ray signal. The element contents are usually in the low concentration range, often only in trace amounts; therefore, the focus has to lie on performing measurements of high sensitivity.

The samples can be aqueous solutions as well as organic liquids. Other analytical methods, such as inductive coupled plasma spectrometry (ICP), are often used for this problem. However, for samples with high concentrations or specific elements, for example, salt solutions, or organic liquids such as oils or fuels, sample preparation for XRF can be simpler and faster. Nevertheless, using XRF with standard excitation conditions is often not sufficient to achieve satisfactory sensitivities. Special preparation methods or optimized excitation conditions and geometries can significantly increase the sensitivity.

### 11.1.2 Sample Preparation

The direct measurement of liquids is usually done with special sample cups, which are covered with polymer films (see Figure 3.17).

Depending on the consistency of the liquids, it may be necessary to carry out homogenization. This is possible by stirring or shaking the liquid. In the case of multiphase liquids, separation of the phases and their separate analysis is also possible. After filtration, the suspended matter can be analyzed directly or on the filter itself. The preparation methods are then similar to those for dust filters (see Section 10.10).

As mentioned before, liquids cannot be analyzed in vacuum; in order to still measure light elements the sample can be placed into a He atmosphere, which avoids the evaporation of the liquid and reduces the absorption of low-energy radiation. In this case, only the volume between the sample and the spectrometer has to be flushed with He. Additional preparation techniques for the same are described below.

### 11.1.3 Measurement Technology

Both wavelength-dispersive spectrometry (WDS) and energy-dispersive spectrometry (EDS) instruments are used for the analysis of liquids. The broad range of excitation energies allows the analysis of many elements. The scattering of the incident radiation at the usually light matrix of the solvent produces a high spectral background. This reduces the sensitivity for traces, which are common in solutions due to the high weight percentage of the solvent.

While using WDS special attention has to be paid to the sample cup window because the higher primary intensity in these instruments is an additional stress for the plastic films.

For the analysis of specific elements, single-element instruments can be used, which by means of special measuring geometries and optics achieve a significant

improvement in the peak-to-background ratios for individual elements and are thus highly selective and very sensitive (see Sections 11.3, 11.4, and Chapter 12).

#### 11.1.4 Quantification

Quantification is usually carried out using standard-based methods. Single and multielement standards for various matrices are commercially available. They can be adjusted by dilution or adding components to the desired concentration. Alternatively, it is possible to create calibration solutions tailored to a specific matrix, using primary substances. Compared to the analysis of solids, this is a big advantage, since this makes it possible to produce complete sets of calibration samples from only a few primary substances. This possibility exists for both aqueous solutions and oils and fuels.

The selection of the quantification model strongly depends on the respective matrix, i.e. the solvent. For aqueous solutions it can be assumed that the matrix influence is low and that the analytes are usually present in low concentrations. Therefore, for these types of samples, considering any matrix influences is not challenging.

On the other hand, the influence of the matrix in the various oils and fuels can vary and can be significant. Therefore, for an accurate analysis, either the matrices of standards and samples have to match, or quantification models with matrix correction have to be used. However, if the calibration factors are determined on the basis of fundamental parameters, these models are widely applicable (Bühler 2002).

If the matrix is correctly accounted for and the weight percentages of the analytes are comparable to those of solid samples, the achievable accuracies are also comparable, i.e. the statistical errors do not differ significantly.

## 11.2 Fuels and Oils

The analytical problems for the analysis of liquid oils and fuels are many. On the one hand, predominantly of interest is the monitoring of threshold values for hazardous additives in fuels, such as P, S, halogens, or Pb. On the other hand, analyzing the additives that give lubricating oils their special properties is of interest. Their exact concentration determines the quality of the finished product and is therefore of great analytical interest. Lastly, the determination of abrasive materials in used oils can be of interest, for example, in order to assess the status of an engine.

A key problem with these analyses is the composition of the basic oil, that is, of the matrix. Depending on the linking of the hydrocarbons, oils and fuels can have a very different consistency and thus also a very different matrix influence. Since the analytical problems discussed here are primarily relevant for the quality control of a production process, it can be assumed that the same products consist of the same matrices. For a standard-based calibration, the respective matrices are automatically taken into account, especially since for small concentrations the calibration curves are usually linear. When transferring

calibrations to other matrices, accounting for the matrix influence is also possible using Compton–Rayleigh ratios (see Sections 2.2.4 and 5.5.2).

The element range that needs to be detected in the analysis of oils and fuels depending on the specific task can be very wide. In the following, some of these questions will be discussed in more detail.

### 11.2.1 Analysis of Toxic Elements in Fuels

When burning fuels such as petroleum, diesel, or gasoline, combustion products are released, which are hazardous to the environment. For this reason, standards regulate the concentration of various elements; for example, P is regulated in DIN-51440 (2003, p. 03), S in DIN-EN-15485 (2007, p. 11), ASTM-D\_6334-12 (2012) and ASTM-D\_7039-15a (n.d.), halogens in DIN-51577 (1994, p. 02), and Pb in DIN-51769-10 (2013, p. 04) and DIN-EN-13723 (2002, p. 10), ASTM-D\_5059-14 (2014). The use of WDSs for the analysis of oils and fuels are described in ASTM-6376\_110 (2010) and for the sensitive excitation with monochromatic radiation in ASTM-D\_7039-15a. The use of EDS for this purpose is described in ASTM D6052 – 97(2016).

In the last few years, depending on the respective national legislation the maximum concentrations have been continuously reduced. They vary for the individual elements but are always in the lower milligrams per kilogram range. Therefore, the requirements concerning the sensitivity of the measuring technique were continuously raised in order to unambiguously identify the trace elements.

To achieve high accuracy and comparability of the analytical results, the methods for sampling (for example DIN-51750-02 (1990, p. 12) or DIN-EN-ISO-3170 (2004, p. 06)), for carrying out the measurements both with WDS instruments (for example ASTM-D\_2622-08 (2010)) and with EDS instruments (for example ASTM-D\_4294-16 (n.d.)), and also the regulations for the control of analysis quality (for example, DIN-EN-ISO-4259 (2006, p. 10) and ASTM-D\_5839-15 (n.d.)) are standardized.

#### 11.2.1.1 Measurement Technology

The relatively high spectral background due to the scattering of the incident radiation on the light matrices of the solvent makes the analysis difficult. Because the measurements are frequently carried out in an in-line production process there is not much time available, nor can elaborate preparation techniques be used. The simplest and fastest way is to fill the sample in a measuring cup and carry out the measurement or even use a flow cell as a bypass in the production flow (see for example Fig. 18.10). The measurement technique itself must then have sufficient sensitivity.

Trace analysis sensitivity is largely dependent on the peak-to-background ratio of the element of interest. In most of the analysis tasks described here, often only the detection of a single element is required. In that case there are several possibilities to improve the peak-to-background ratio.

The measurement signal of an element to be analyzed can be increased by an effective excitation condition. This requires that the excitation spectrum must have high intensity at the energy of the absorption edge of the element of interest. This can be achieved by optimizing the X-ray tube parameters or through monoenergetic excitation for example by radiation of an element whose

fluorescence energy is slightly higher than the absorption edge of the element to be analyzed.

Realizing a high peak-to-background ratio is not only achievable by a large signal intensity but also by a low spectral background. For this purpose, the following methods can be used.

- Filters in the excitation beam path can be used to reduce, within certain energy ranges, the bremsstrahlung intensity. This is possible with small effort. However, optimal filter materials are not available for all analyte elements and the achievable sensitivities using filters is not always sufficient.
- Using monochromatic radiation for the excitation of the analyte prevents the scattering of bremsstrahlung in the energy range below the peak of the analyte. The monoenergetic radiation can be generated by the fluorescence radiation of an element (secondary excitation) or by using a monochromator between excitation source and sample. The peak-to-background ratio then depends only on the excitation efficiency of the analyte; cf. Figures 4.25 and 4.26. While the range of applications for this instrument technology is limited to a small element range, it ensures high sensitivity for these elements.
- Reducing the intensity of the scattered radiation from the sample can also be achieved using polarized radiation for excitation. The fluorescence signal can then be measured in the polarization plane of the radiation with a low background (see Figure 4.27). In this case, high sensitivity is possible in a wide range of energies despite the broadband excitation.
- Finally, high sensitivity is also achievable with good resolution of the instrument. This condition is given using WD spectrometers with the appropriate crystal. It is then possible to use the Rh-L radiation of the tube for optimal excitation, for example, of P, S, and Pb-M lines. Ideally, if possible, a low excitation voltage and high tube current are used.

Instruments are commercially available that utilize each one of the methods described. Selecting an instrument depends on the required sensitivity and whether any other analytical task needs to be solved. In Table 11.1, detection limits for the element sulfur, which frequently must be measured and is strictly regulated in liquid fuels, are summarized. Thereby an assessment of the performance of the individual methods is possible.

To prepare the samples, cuvettes are used which should be filled with a sufficient and equal amount of sample material. When selecting a foil, ensure

**Table 11.1** Limit of detection for S in fuels depending on the measuring method.

Measuring method	Manufacturer	Limit of detection for S (mg/kg)
Filter method	For example, Horiba	20
Excitation with Rh-L	For example, Bruker	1
Polarized radiation	For example, Spectro	0.5
Monoenergetic radiation	For example, XOS, Horiba	0.2
WD spectrometer	For example, Bruker, Thermo, Panalytical, Rigaku	0.3

sufficient strength and chemical resistance against the fuel. The measurements should be made as soon as possible after filling the samples. In addition, measurements in He atmosphere are recommended to reduce the absorption of the low-energy radiation of the analyte elements.

### 11.2.1.2 Analytical Performance

Mostly standard-based models are used for the quantification of fuels. Base reference standards are available and can be prepared by dilution or addition. The matrices of the reference standard and the unknown samples should be comparable in order for the matrix influence to be similar.

For small weight percentages the achievable accuracies are mostly determined by the statistical error. This means that the measurement uncertainty can be reduced by a longer measurement time. Usually, the measurement time is set as a function of the measuring error that can be achieved for these tasks.

The previously mentioned standards specify the measurement procedure and the evaluation of the analytical data, and also the precision and long-term stability of the analytical process to be achieved. For example, ASTM D 2622-08 for WDS instruments defines that the difference between two successive determinations of sulfur in 19 of 20 cases must be less than 0.57 mg/kg when the concentration is in the range of 5.5 mg/kg. This determines both the sensitivity of the method and its precision.

DIN-EN-ISO-20884 (2011, p. 07) and DIN-EN-ISO-20847 (2004, p. 07) define as a function of the respective content the repeatability (analysis under identical conditions – instrument, measuring conditions, operator) as well as the reproducibility (same method but different instruments, operator, lab) for both WDS and EDS instruments. These values are summarized in Table 11.2.

The specifications show that the requirements for the analytical capabilities are high, but also prove that XRF analysis is well suited for a reliable detection of the smallest concentrations of light elements in a strongly scattering matrix.

## 11.2.2 Analysis of Additives in Lubricating Oils

Lubricating oils are primarily used to reduce friction, thus reducing the wear on machine parts, reducing noise, and rapidly dissipating heat. The base material

**Table 11.2** Repeatability and reproducibility limits for the detection of sulfur in gasoline and diesel fuels.

S-content (mg/kg)	Repeatability (mg/kg)		Reproducibility (mg/kg)	
	WDS	EDS gasoline/diesel	WDS	EDS gasoline/diesel
10	2		2	
30	3		3	
50	3	11/9	3	17/13
100	4	14/11	12	28/15
350	4	20/15	31	50/18
500	4	25/17	42	67/20

of lubricating oils can be very different – it can be of mineral or biological origin – but it can also be produced synthetically. In order to produce the desired properties of the lubricant, various additives are added to the base oil. These are intended to improve the tribological properties, such as reducing wear or friction, but also improving viscosity and corrosion protection. Additives can make up a large percentage of a lubricant. They can be organic compounds, usually also including inorganic constituents, which can be measured by XRF. Special properties of the lubricant can be assigned to certain elements; for example, Ca and Ba are anti-foaming agents and prevent the formation of antioxidants, P and S reduce wear, and together with Zn they prevent corrosion.

The analysis can be performed with EDS or WDS instruments. Sample preparation is simple, only equal sample amounts have to be filled into sample cups, and the analysis should be performed shortly thereafter to avoid segregation. The sensitivity of EDS instruments is adequate, and the simultaneous detection of a wide energy range allows for short measuring times. On the other hand, the sensitivity of WDS instruments is greater due to their better energy resolution; also, the measurement times are adjustable for each element, in order for the statistical errors of all elements to be comparable. Using WDSs the influence of the high excitation intensity to the sample cup window and the sample itself needs to be considered. The concentrations that need to be detected for the various elements that are characteristic of the additives of typical lubricating oils as well as the required repeatability and reproducibility requirements are summarized in Table 11.3. They are according to ASTM\_D 4927:2015 (n.d.) for WDS instruments as well as according to ASTM-D\_6481:2014 (n.d.) for EDS instruments. Repeatability limit is again the standard deviation under repeatability conditions, and the reproducibility limit is the standard deviation for measurements under varying conditions.

For WDS instruments, repeatability depends mainly on the statistical error, which is dependent on the concentration (ASTM-D\_6443 2010).

Table 11.4 summarizes the analyzed element concentration of the sample, the achievable detection limits for WDS instruments at a total measurement time of approximately 250 seconds, as well as the relative standard deviations for 20 successive measurements.

The summary demonstrates the performance, both in terms of sensitivity and precision of the analysis, and hence the ability of XRF to solve this analytical problem.

**Table 11.3** Requirements according to ASTM D 4927-05 and ASTM D6481.

Element	Percentage (wt%)	Repeatability limit		Reproducibility limit	
		WDS (wt%)	EDS (%)	WDS (wt%)	EDS (%)
P	0.001–0.5	0.004	≈4% rel	0.018	≈15% rel
S	0.001–1.5	0.006	≈2% rel	0.019	≈15% rel
Ca	0.001–0.8	0.003	≈10% rel	0.016	≈20% rel
Zn	0.001–0.5	0.002	≈2% rel	0.012	≈25% rel
Ba	0.001–1.0	0.001		0.016	



**Table 11.4** Analytical performance for additives with a WD spectrometer.

Element	Nominal content (wt%)	Limit of detection (wt%)	Analyzed content (wt%)
Mg	0.08	0.017	0.074 ± 0.0011
P	0.05	0.007	0.050 ± 0.0004
S	0.275	0.066	0.280 ± 0.0015
Cl	0.05	0.019	0.051 ± 0.0002
Ca	0.20	0.01	0.196 ± 0.0004
Cu	0.02	0.004	0.020 ± 0.0001
Zn	0.05	0.003	0.050 ± 0.0005

Source: According to Bühler (2002); LabReport-XRF\_101 (n.d.).

### 11.2.3 Identification of Abrasive Particles in Used Lubricants

Waste oils are often contaminated with abrasive particles. Their characterization can provide information about load and wear of an engine or transmission, thus providing an indication of possible failures. The information can also be used to make decisions on timely, but not too early replacement of the oil or of subassemblies. Therefore, the analysis of abrasive particles is of great interest. The wear debris usually consists of metallic particles with grain sizes of less than 0.3 mm. Several possibilities exist for their analysis with XRF.

One possibility is the direct measurement of the used oils or lubricant greases. For this purpose, they are filled into sample cups after homogenization by shaking or ultrasonic treatment. Note that the same sample amounts shall be used in order to avoid the measured analyte intensities being dependent on the sample quantity. The measurement should start shortly after preparation in order to avoid the sample segregation again. The mixtures can be stabilized by using a special emulsifier (for example, Triton B). Solid lubricants can be placed into special sample carriers. Again, it is important that the same sample amounts are used.

This type of analysis is also regulated by standards, for example (DIN-51396 2008, p. 11, DIN-51399 2010, p. 01, and DIN-51829 2013, p. 03). The standards describe the determination of the elements Al, Si, Cr, Fe, Ni, Cu, Mo, Sn, and Pb in lubricating oils and of the elements Na, Mg, Cl, Ca, Ti, and Ba in lubricating grease. According to the standards, the analysis can be carried out with both WDS and EDS instruments. First and foremost, the standards specify the repeatability and reproducibility requirements of the analysis. A precise analysis of spent oils is complicated since their matrices can vary a lot and are usually unknown. Therefore, the values for the relative repeatability is set at 10–20%, and for reproducibility at 30–50%.

A further possibility is the direct analysis of the debris particles themselves; in this way, wear-sensitive components can be identified. For this purpose, the debris particles must first be separated from the used oil. This is possible by sedimentation, filtration, or centrifugation. The separated sludge can then directly be analyzed. Larger particles can be separated and individually characterized using spatially resolved methods (see also Section 15.1).

## 11.3 Trace Analysis in Liquids

### 11.3.1 Analytical Task

Very often, the levels of toxic or environmentally relevant additives in liquids must be monitored. Their maximum concentrations are regulated by standards and their levels, for example, in waste water (DIN-EN-ISO-11885 2007) for elements such as Cr, Pb, and Cd can be very low. Since the concentrations that need to be detected are very low, the requirements for the sensitivity of the analysis are very high. Traces in the lower or even sub-milligram per kilogram range must be clearly identifiable. The relatively high spectral background from the scattering of the primary radiation at the light matrix of the solvent makes this task difficult.

For the simultaneous, sensitive detection of several elements in liquids, excitation over a wide energy range is necessary in order to excite all the elements to be analyzed with only one excitation condition. Consequently, this does not leave the option to improve the peak-to-background ratio by monoenergetic excitation. The reduction of the spectral background is therefore the best way to achieve high sensitivities. Within certain limits, using polarized radiation or a suitable but more time-consuming sample preparation technique makes this possible.

### 11.3.2 Preparation by Drying

When analyzing substances in liquids the focus is not on the solvent. Removing the matrix, i.e. the solvent, does not only result in higher concentrations of the sample but also in a reduction of the matrix influence. Removing the matrix of aqueous solutions and also of other solvents can easily be done by evaporation. After removing the light solvent, only the material of interest remains.

The analysis of light elements in liquids poses a further problem. Since their low-energy radiation is readily absorbed in air, measurements in vacuum would be necessary. This, however, is not possible since solutions rapidly evaporate in vacuum. Removing the liquid matrix, however, makes measurements in vacuum possible.

A proven technique for this type of preparation is the deposition of a defined number of drops with a micropipette onto a special sample holder. Depending on the subsequent measuring method, this holder may be a polished glass, a plastic disc, or a thin plastic film. For a polished glass holder the analysis is possible with total reflection XRF; otherwise, the glass substrate would produce a high scatter background (see Section 12.4.1). Plastic films are more suitable for measurement with conventional X-ray spectrometers. If these films have hydrophilic areas while the surrounding area is hydrophobic and the drops are applied in the hydrophilic area, the dissolved substances are confined to the hydrophilic area during drying (see Figure 11.1a). This process can be repeated several times in order to improve the detection limits by enriching the analyte by addition.

After evaporation of the solvent the dissolved substances remain as a very thin layer on the thin substrate holder. The incident radiation excites the residuals on the film; it is only insignificantly scattered by the plastic film. Therefore, the

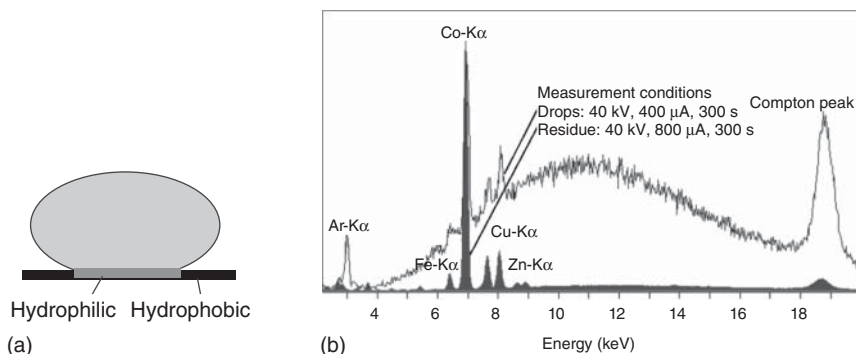


**Figure 11.1** Plastic film with a drop of a solution (a), spectra of a solution and the residual after drying (b).

spectral background is very small, and the peak-to-background ratios are significantly improved compared to the solution, i.e. the sensitivity is improved. This is illustrated in Figure 11.1b, which shows the spectra of a solution as well as the residuals of this solution, which were dried on a plastic film. The peak intensities of elements are comparable, but the spectral background shows significant differences.

When measuring such samples, one should pay attention that only the actual sample is excited and not the material of the sample chamber located underneath the sample holder. To avoid this, the plastic film carrying the sample can be prepared, for example, by mounting the film on a liquid cuvette (see, for example, Figure 15.2).

The evaporation of the solvent can be performed in several ways, either by storing the sample for a sufficiently long time under normal laboratory conditions or by increasing the temperature. However, it must then be ensured that volatile ingredients will not be depleted during heating. Another possibility is by increasing the surface area of the sample to be analyzed, for example, by applying the solution as droplets to the support. The large surface-to-volume ratio then promotes, as in the case of an inkjet printer, rapid evaporation of the solvent. Corresponding investigations were carried out by Fittschen and Havrilla (2010) and Fittschen et al. (2011). In this way, not only can the preparation time be significantly reduced but the sensitivity can also be optimized depending on the droplet size and their number. If the droplets are applied multiple times the sample can be enriched. Absolute mass fractions down to the lower nanogram range can then be detected. However, it is to be noted that the risk of cross-contamination with this preparation technique is very large. The droplets can be generated and deposited with inkjet printing heads. They require extensive cleaning after each preparation in order to avoid cross-contamination in the trace concentration range.

### 11.3.3 Quantification

With only a thin material layer on a plastic substrate, quantification is significantly simplified, since matrix interactions are largely negligible. This means that for

quantification it is possible to use the models that have already been discussed for TXRF (Eqs. (5.14) and (5.15)). Similar to TXRF, addition of internal standards is also possible for this analysis; in this way, the analysis becomes independent of the applied sample mass.

The detection limits can be improved by the already mentioned repeated application and drying of drops from the liquid sample. Various studies have shown that the detection limits for such a sample preparation on plastic films and measured with conventional ED spectrometers are only about one order of magnitude worse than for TXRF (see Section 12.4.1).

A general problem of this type of preparation can be the loss of volatile elements during evaporation. This is true for elements such as P, S, and As. It is therefore useful to determine the recovery rates for the individual elements based on comparable reference samples or methods.

Owing to the negligible matrix interactions, the uncertainties of the analysis are essentially determined by the statistical error, i.e. by adjusting the measurement time the required accuracies can be achieved.

## 11.4 Special Preparation Techniques for Liquid Samples

### 11.4.1 Determination of Light Elements in Liquids

A further approach for the analysis of light elements in liquids is a method patented under the name LiTrap by F. Rüttimann (2008b, 2011). The liquids are applied onto a porous solid-state absorber for example an  $\text{AlO}(\text{OH})$  substrate. The liquid permeates into the solid and can then be analyzed. Measurements are then also possible in vacuum, which means that also light elements with atomic numbers from 8 (oxygen) upwards can be analyzed with a WDS instrument. The elements of the sample carrier (primarily Al) are, of course, excluded from the analysis. Sample carriers of this type are shown in Figure 11.2.

Before any analysis with this type of sample preparation trials to determine the recoverability of the individual elements are recommended. How deep the solutions penetrate into the sample carrier depends on the viscosity of the liquid. The information depth of the individual elements is also affected by it. The achievable recovery rates with this method are at least 98% and the relative standard deviations of repeated analyses with WDSs are in the range of 1%, even for elements up to fluorine.

In addition to the analysis of liquids, this preparation method also makes it possible to determine suspended particles in solutions. They do not penetrate into the absorber, as in the case of filter paper, but they accumulate on the top of the sample holder (see Figure 11.2b). This then allows their direct analysis.

Quantification must be performed using standard-based methods that have been calibrated with similar sample types, since recovery rates and penetration depths strongly depend on the sample to be analyzed. The achievable accuracies strongly depend on the quality and comparability of the calibration samples with the samples to be analyzed.

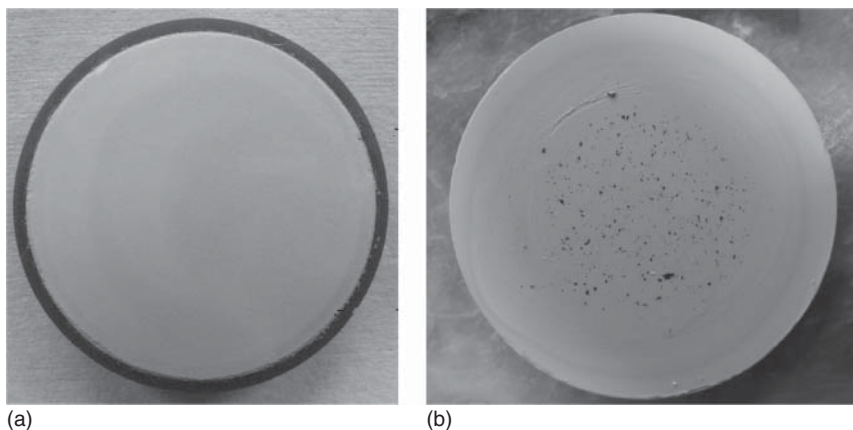


**Figure 11.2** LiTRap-sample holder, not used (a) and with metal particles from an oil sample (b). Source: Courtesy of F. Rüttimann.

#### 11.4.2 Enrichment Through Absorption and Complex Formation

Since traces can reach the human food chain via groundwater or soils and have a direct impact on health, their determination in water has become increasingly important. Several analytical methods have been developed for this purpose, but they are often not sensitive enough. By utilizing enrichment methods, XRF can provide an effective and efficient solution for these analytical questions (see also Cybik 2003; Janßen and Flock 2004).

Enrichments by a reduction in volume, for example, by evaporation of a solution, have already been discussed. However, enriching a sample is also possible by separating the matrix by chromatographic methods or by chemical reactions such as precipitation, complexing, and extraction.

After enrichment with a solid-phase absorber, the leaching of the adsorbed substances into a smaller volume is possible or alternatively a direct analysis of the solid phase itself. Suitable solid phases are activated carbon, silica gels, and microcrystalline naphthalene or Amberlite® XAD, a styrene-divinylbenzene compound (Nerin et al. 1995).

Chelate-forming ion exchangers are commercially available in many variants. In most cases they are made of cellulose, or synthetic resins with chelate-forming binding groups. They can either be used in the form of filter layers or short columns or they can directly be added to the solution in the so-called batch process. After the enrichment on the exchanger, the latter can then be pressed into mechanically stable pellets or further processed by adding a synthetic resin to form a sample. Figure 11.3a shows the pellet of an ion exchanger, which is mounted in synthetic resin, using the well-known ion exchanger Chelex® 100. A large number of cations can be analyzed with this ion exchanger and this preparation technique.

As complexing agents, dithiocarbonates (DTC), ammonium O,O-diethyldithiophosphate, or 1-pyridylazo-2-naphthol (PAN) can be used. The detectable cations in solution are complexed and can either be just filtered

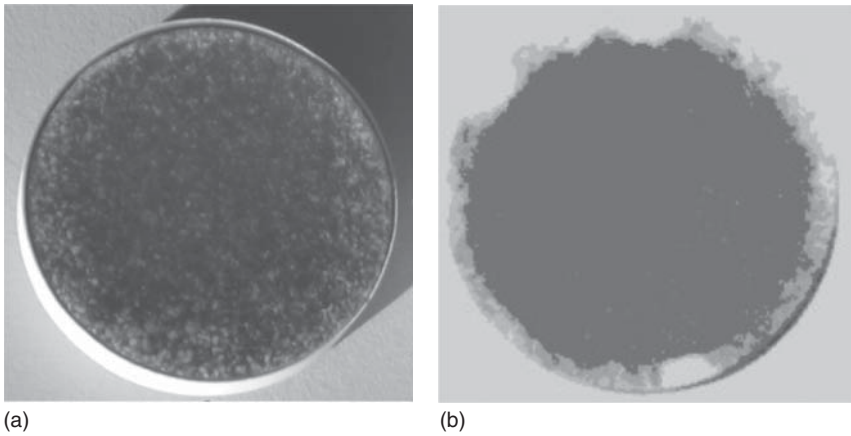


**Figure 11.3** Samples after complexation: a Chelex<sup>®</sup>-100-pellet with synthetic resin as binder (a), precipitated on a membrane filter (b).

(see Figure 11.3b) or absorbed on a collector material, for example, activated carbon. This procedure can usually be used for several elements, which then makes simultaneous detection of different elements possible.

For the analysis, the solid phase can directly be measured. To control the purity a preliminary blind sample analysis is recommended. To quantify, calibration with solutions of known composition that underwent the same preparation procedures is required. The absorption capacity is reflected in the recovery rates.

Using enrichment methods, a significant increase in sensitivity can be achieved and even the analysis of light elements in liquids is then possible.

## 12

# Trace Analysis Using Total Reflection X-Ray Fluorescence

## 12.1 Special Features of TXRF

First papers using grazing incidence radiation to reduce the spectrum background were published in the mid-1970s (Aiginger and Wobrauschek 1974; Knoth and Schwenke 1978). This reduction in the spectral background is illustrated in Figure 12.1. It shows two spectra measured on water fleas (Waldschläger 2016). The spectrum measured in conventional geometry is the sum spectrum of a distribution analysis carried out on a single water flea prepared on a thin plastic film, i.e. already with a reduced spectral background (see Section 11.2.3). The acquisition time for this spectrum was approximately 5.5 hours. For the spectrum measured in total reflection X-ray fluorescence (TXRF) geometry, a thin section of the sample prepared on a quartz disk was measured with grazing incidence of the excitation radiation; the measurement time was 500 seconds, about 40 times quicker. Nevertheless, the improvement of the peak-to-background ratio is significant. For Fe and Zn, which are detectable also in the conventional geometry, the improvement is on the order of 700. Other elements such as Mn, Cu, Pb, and Sr can only be seen in the TXRF spectrum. As the spectra proves, this can be primarily attributed to the reduction of the scatter background in the TXRF measurement.

The strong reduction of the spectral background in the total reflection geometry has two reasons: On the one hand, scattering of the incident radiation is reduced due to its total reflection on the sample holder, even compared to the relatively low background caused by the preparation on a thin polymer film. On the other hand, a further reduction of the spectral background can be achieved, using monoenergetic radiation for the excitation in total reflection; in our example, it is the Mo-K $\alpha$  line that is filtered from the tube spectrum with a monochromator, which results in a further reduction in the background since there is no radiation energy that can be scattered. A drawback however is that only elements with absorption edge energies close below the Mo line are excited effectively (see also Figure 4.26 and Section 4.3.3.2).

Since, for TXRF the scattering of the incident radiation at the sample is suppressed, the detector collects only the fluorescence radiation from the sample at the sample holder. Consequently, the signal-to-background ratio is significantly improved and finally also the sensitivity for traces. Furthermore, only

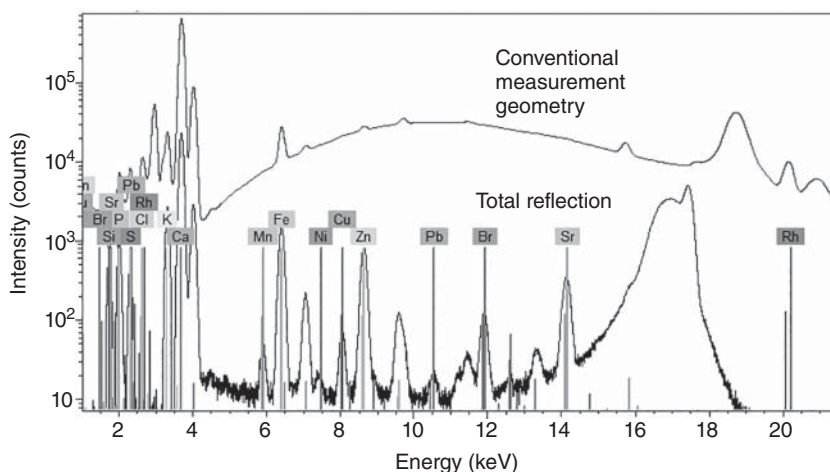


**Figure 12.1** Spectra of water fleas measured at conventional excitation geometry and below the critical angle of total reflection (y-axis in log scale). (Source: Waldschläger, U., personal information)

the smallest sample quantities are required for the analysis. However, for this excitation geometry some specific features must be considered:

- The incidence angle of the radiation must be very small in order to be totally reflected at the sample holder. The critical angle of total reflection depends on the radiation energy and the material of the sample carrier. For the frequently used quartz or acrylic glass holders and using Mo-K $\alpha$  radiation this angle is about 0.1°; for the lower energy of Cu-K $\alpha$  radiation it is about 0.2°.
- Such small incident angles enable the use of only a small solid angle of the source radiation. Therefore, intense point focus sources are required to produce sufficiently high excitation intensities.
- The sample holders must be very flat for a total reflection of the incident radiation. Highly polished quartz glasses or acrylic disks are therefore used.
- Only very small sample quantities are required for the analysis. The incident radiation would be scattered at larger sample quantities. The low sample amount can be an advantage for certain analytical questions; on the other hand, however, particularly in the case of a larger sample quantity high preparation effort is required in order to produce a representative sample.
- Very high care is required for sample preparation to avoid contaminations due to the high sensitivity of TXRF.
- The small sample quantities as well as the low concentrations to be analyzed with TXRF provide only low fluorescence intensities. This results in relatively long measuring times in order to ensure sufficiently small statistical errors.
- The basically background-free spectra allow for very high sensitivity. The achievable detection limits depend on the sample and the element to be analyzed. They are in the low micrograms per kilogram range, using special preparation methods even in the sub-micrograms per kilogram range.



- As a result of the small sample quantities, the matrix interaction is negligible and simple quantification models can be used (see Section 5.5.2, Eq. (5.14)). However, it must be ensured that the sample quantities are so small that matrix effects are negligible.
- The measurements are usually done in air. Since the detector is directly above the sample the absorption of the fluorescence radiation in air is low and the analysis of Si and even Al is possible.

The method is now being used in a wide range of applications. A detailed description of the physical basics, the specific instrument features, and various applications have already been summarized by Klockenkämper and von Bohlen in a second edition (2015).

## 12.2 Sample Preparation for TXRF

In principle, both solid and liquid samples can be analyzed with TXRF. It is, however, necessary to convert the material to be investigated into a suitable form. Herewith it is especially important that the very small measurement sample amount characterizes the material to be investigated sufficiently.

The sample preparation also requires extremely clean work, since the TXRF is very sensitive and even the smallest contaminants influence the analysis result. Contamination can be of different origin. Laboratory environment, touching the sample, cross-contamination by pre-prepared samples, and many other influences can lead to a falsification of the result. It is valid even more than for other analytical methods: Only a very clean work during the preparation ensures also correct analysis results!

The typical procedures for the preparation of different sample qualities are summarized in Table 12.1.

The preparation of very small particles is the simplest. They can be applied directly to the sample holder and analyzed. Other sample materials, such as solids, coarse grains, suspensions, or matrix-loaded solutions, must be converted into liquid form, that is, into solutions or suspensions.

Solids must first be broken and very finely milled and then transferred into a suspension. A further possibility would also be digestion, in which the sample is dissolved. However, the recovery rates depend on the matrix, the digestant, and the digestion method.

Suspensions need usually to be diluted, optionally with multi-distilled water or another high-purity solvent, and to be homogenized. The solutions generated in this way can be supplied with an internal standard to support quantification. No analyte elements should be used for this purpose. Yttrium or gallium is often used in acidic solutions, and germanium in basic solutions.

Aliquots of this solution can then be applied to the sample holder. The material of the sample holder is mostly polished quartz or acrylic glass, but boron nitride, sapphire, Si wafers, or glassy carbon are also used. The easiest way to do this is by pipetting. Sample quantities of about 10  $\mu\text{l}$  are dropped and dried by heating the sample holder or by evacuation. However, it is also

**Table 12.1** Preparation procedures for TXRF.

Analyzed material	Steps for preparation	Remarks
<i>Solid samples</i> Soils, sediments, minerals, food, pharmaceuticals, etc.	<i>Grinding</i> Milling, pestling, acid hydrolysis <i>Weighing</i> <i>Convert to a solvent</i> ⇒ Like suspension	Grain size < 20 μm <i>Mill material can generate contaminations</i> 20–100 mg <i>High pureness of the solvent necessary!</i>
<i>Suspensions</i> Sludge, wastewater, matrix-loaded solutions, blood serums, pigments	Shaking to a suspension  <i>Dilution</i> ⇒ Solution aliquotation ⇒ Like liquids	With aqua dest
<i>Liquids</i> Drinking water, beverages, urine, organic solvents	Addition of standards  Homogenization  Application to the sample holder <i>Drying</i> ⇒ Measurement	<i>High pureness necessary!</i>  <i>Use of highly pure materials (quartz, PTFE, PE) as tools</i> 5–20 μl, sample holder highly polished Heating or vacuum Required time: ≈10 minutes
<i>Small particles</i> Nano particles, gunshot residue, proteins, pigments, dusts	Transfer to sample holder  Carrying out the measurement	Q-Tip, scalpel  Required time: 5–15 minutes

possible to use sample-portioning systems that position small droplets on the sample holder (Fittschen et al. 2011) (see also Section 12.4.1). Owing to the large surface–volume ratio of the small droplets, the evaporation of the solvent does not need stimulation by heating or by vacuum. In addition, this preparation offers the possibility of several applications of the solution to be analyzed in several steps, which would increase the sensitivity of the method. Further, a smooth distribution of the sample on the sample holder is achieved, so that matrix effects can also be avoided even for stronger exposures. However, high care must be taken in order to avoid cross-contamination in these systems by a thorough purging of the positioning system.

In summary, it can be ascertained that the sample preparation for the TXRF in general is simple, but must in each case be adapted for the respective sample type and thus have high variability; and in any case it must be carried out under

the highest purity requirements. In Section 12.4, different applications with their preparation techniques are described in more detail. These can be used also for applications of comparable sample materials.

A general problem of TXRF is the representativeness of the measurement sample. Since only sample amounts in the range of only a few micrograms are analyzed, the preliminary preparation steps, that is, preparation, mixing, and dividing of the material, must be carried out not only without any contamination but also ensuring the representativeness of the test sample. If a sufficient amount of sample has been converted into a liquid and if this is homogeneous even the smallest amounts of liquid are aliquots of the sample solution produced.

## 12.3 Evaluation of the Spectra

### 12.3.1 Spectrum Preparation and Quantification

The evaluation of TXRF spectra is analogous to that of other ED spectrometers (see Section 5.4). Peak overlaps must be considered by fitting or deconvolution procedures; the treatment of the spectral background is easy since this has only marginal intensities and detector artifacts are corrected by the instrument software of commercial instruments automatically. If a background subtraction is required, a simple interpolation between background-free areas is sufficient.

A special feature of the TXRF is that the information depth should be large compared to the sample thickness caused by the very small sample amounts. Accordingly, the matrix interactions should be negligible. Therefore, for quantification linear calibration curves can be assumed (see Eq. (5.14)). The sensitivity  $\varepsilon_i$  depends on the element ( $i$ ) but also on the measuring conditions (excitation spectrum, geometry). The sensitivities can either be calculated by using fundamental parameters for a known excitation spectrum or they can also be determined experimentally for the specific measuring conditions. For this purpose, solutions of different elements  $i$  are measured under the same conditions and their peak intensities  $I_i$  are determined. Using the knowledge of the known concentrations  $w_i$ , the sensitivities of the individual elements can then be calculated according to Eq. (5.14) with

$$\varepsilon_i = (I_i/I_{\text{ref}}) \cdot (w_i/w_{\text{ref}}) \cdot \varepsilon_{\text{ref}} \quad (12.1)$$

The sensitivities for Mo excitation for Bruker's S2 Picofox are shown in Figure 12.2.

For quantification, usually internal standards are used, which can be applied in two kinds.

If only the concentration of one element has to be determined, a solution of this element can be added in different amounts to aliquots of the analyte solution. Displaying the intensities of these solutions over the known element concentrations results in a calibration line that can be used to determine the content in the unknown sample. In case an intensity is determined also for a blank sample, the calibration curve does not pass through the zero point but intersects the concentration axis at negative values (see Figure 5.14) and an additional constant term is required for the description of the linear calibration curve.

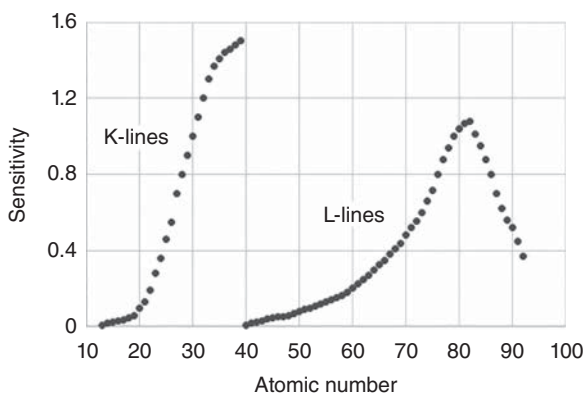


**Figure 12.2** Element-dependent sensitivities of a TXRF spectrometer.

If, however, several elements must be analyzed, it is more effective to add a known amount of a reference element to the sample as internal standard. If this element is not an analyte, the determination of the element quantity of each analyte element in the sample is possible, as already described in Eq. (5.15), with the aid of the sensitivities  $\varepsilon_i$ .

$$w_i = \varepsilon_i / \varepsilon_{\text{ref}} \cdot I_{\text{ref}} / I_i \cdot w_{\text{ref}} \quad (12.2)$$

### 12.3.2 Conditions for Neglecting the Matrix Interaction

Anyway, care must be taken that the matrix interaction is really negligible, which means the material amounts, in particular the thickness of the applied material to be analyzed, must be sufficiently low. To illustrate this requirement, it is assumed that this condition is fulfilled if the material layer absorbs only 1% of its fluorescence radiation. An estimate of this thickness  $d_{1\%}$  can be made from Lambert–Beer’s law (Eq. (1.5)).

$$d_{1\%} = 0.01 / (\mu \cdot \rho) \quad (12.3)$$

with  $\mu$  as the mass attenuation coefficient of the material under consideration and  $\rho$  its density. For some typical matrices these thicknesses are illustrated in Figure 12.3. They depend on the energy of the analyte radiation – the higher the energy, the less their absorption and the more the sample thicknesses can be. However, they also depend on the sample matrix – the matrix interaction is small for light matrices, for example in organic samples, accordingly the sample thicknesses may be larger. On the other hand, for heavier matrices, such as minerals or even metallic specimens – in Figure 12.3 an iron alloy is assumed – the interaction increases and the critical sample thicknesses correspondingly decrease. In general, these thicknesses are in the micrometer range, and in the case of metallic matrices even considerably less.

These are very small sample thicknesses. For illustration, a scanning electron microscope image of a dried water drop, a typical TXRF sample, is shown in Figure 12.4 (von Bohlen 2015). It can be seen that the sample thickness is in the range of several micrometers, in some areas even significantly more. This means

**Figure 12.3** Critical sample thicknesses for neglecting the matrix interaction.

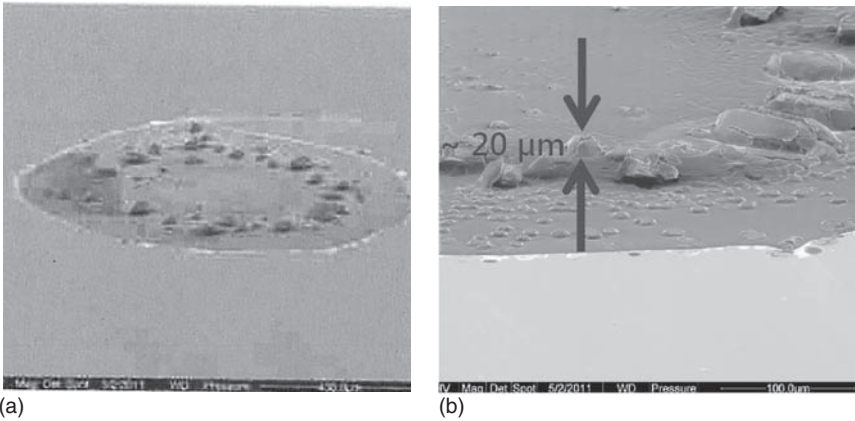
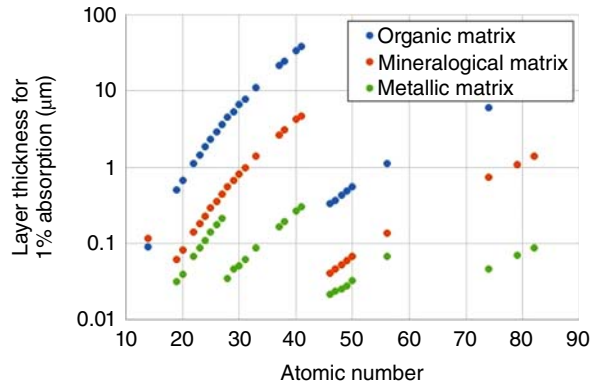


**Figure 12.4** Secondary electron microscope (SEM) image of a TXRF sample (dried drop of water) in two different magnifications. Source: Courtesy of A. von Bohlen.

that there is no interaction-free emission of fluorescence radiation. Consequently, quantification errors have to be expected.

In extreme cases, these effects can even be seen in the spectra. This is illustrated in Figure 12.5, which shows spectra of different amounts of a fine-grained Zn powder. At low amounts, the Zn particles are distributed separately on the sample carrier and the matrix interaction is negligible. For larger amounts the Zn particles conglomerate; therefore, matrix interaction cannot be neglected. This is illustrated by the increased spectral background, which is caused by the scattering of the tube radiation at massive sample areas.

### 12.3.3 Limits of Detection

The small sample quantities as well as the very limited usable solid angle of the incident radiation result in only very low fluorescence intensities. Therefore, measurement times up to 1000 seconds are common for TXRF. However, detection limits in the lower micrograms per litre range are achievable. Nevertheless, this

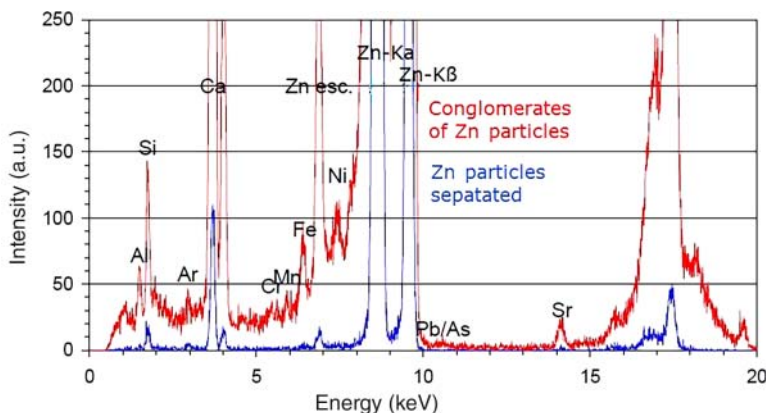


**Figure 12.5** Spectra of different amounts of fine-grained Zn-particles. esc, escape peaks of main components. Source: Courtesy of A. von Bohlen.

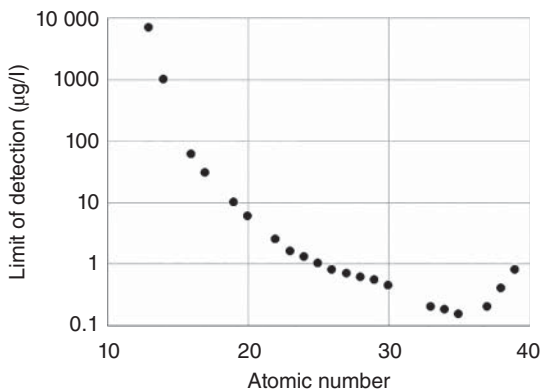


**Figure 12.6** Limits of detection in aqueous solutions. Source: According to LabReport-XRF\_425 (n.d.).

depends on the element under consideration, just as for conventional excitation geometries, caused by the different excitation probabilities and fluorescence yields. Furthermore, peak overlaps also influence the limits of detection for the current sample. Detection limits for aqueous solutions, determined from measurements on a standard for traces in water (NIST: SRM 1643), are summarized in Figure 12.6. These limits can even be improved by enrichment as described in Section 12.2, i.e. by a repeated application of the sample. For other sample systems, similar or slightly poorer detection limits are achieved, depending on the preparation.

## 12.4 Typical Applications of the TXRF

### 12.4.1 Analysis of Aqueous Solutions

#### 12.4.1.1 Analytical Problem and Preparation Possibilities

The analysis of aqueous solutions is a simple and often used application for TXRF. In this way, rainwater, groundwater, drinking water, and mineral water can be

analyzed almost directly, just as also dilutions of concentrated aqueous solutions. Such a solution (1–2 ml) should only be acidified (for example, with  $\text{HNO}_3$  to about pH 2) by adding a standard solution; then the sample can be applied to the sample carrier, dried, and measured.

The simplest way for sample application is by pipetting, which allows sample quantities in the microliter range. Drying is carried out by heating or vacuum drying. Repeated pipetting would increase the amount of the sample, but it can also lead to thicknesses of the residual that do not allow neglecting the matrix interaction.

Using small droplets, it is possible to increase the surface–volume ratio and reduce the evaporation time (Klockenkämper and von Bohlen 2015). These smaller droplets may, for example, be produced by pressing the solution through a capillary in nanoliter size (Miller and Havrilla 2004; M2-Automation 2016). The diameters of the capillary positioned tightly above the sample holder surface are in the range of 10  $\mu\text{m}$ . Drying times are between 20 seconds and 2 minutes, and the diameter of the dried remainders on the sample holder is 10–300  $\mu\text{m}$ , depending on the hydrophilic/hydrophobic properties of the sample holder. A further reduction in the droplet size is possible by the use of inkjet printer heads, which position the liquid sample in picoliter amounts onto the sample carrier by means of piezoelectric pulses (Fittschen et al. 2011). This further increases the surface area to volume ratio of the droplets and reduces the drying times to only a few seconds. The droplet volume then is adjustable to 1–200 pl and the sample amounts deposited are in the range of 1 pg–2 ng depending on the sample. The residues of the dried droplets have a size of 5–10  $\mu\text{m}$  and can be applied in patterns, so that a uniform distribution of the material to be analyzed on the sample carrier is possible. Even multiple depositions are then possible in order to improve the detection limits.

#### 12.4.1.2 Example: Analysis of a Fresh Water Standard Sample

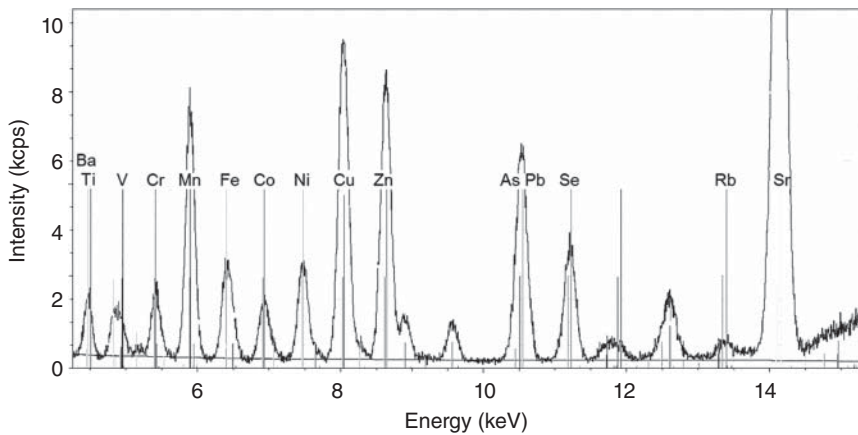
The requirements for monitoring drinking water are very high and are specified, for example, in the Drinking Water Ordinance (TrinkwV\_2001 2001; Klockenkämper et al. 1993). In Table 12.2 the threshold concentrations for inorganic elements are specified. Both toxic elements and indicator elements are listed, which themselves are nontoxic but are considered to be indicative of biological contaminations.

With a suitable sample preparation TXRF can meet these high requirements. The analysis of a freshwater reference sample (NIST: SRM 1640) was used as an example (LabReport-XRF\_425 n.d.). For this purpose, 1 ml of the sample was mixed with 20  $\mu\text{l}$  of a 10 mg/l Ga solution as an internal standard. A volume of 10  $\mu\text{l}$  of the solution was then pipetted on a quartz sample holder and dried. This procedure was repeated three times so that the total sample quantity was 30  $\mu\text{l}$ . The spectra shown in Figure 12.7 were acquired at 1000 seconds.

The entire analysis including sample preparation was repeated 10 times. This then provides information about the repeatability and reproducibility of the method. The analysis results are summarized in Table 12.3. They show the certified concentrations of the individual elements  $C_{\text{NIST}}$  together with their

**Table 12.2** Concentration limits of elements in drinking water.

Element	Limit (mg/l)
B	1.0
Al	0.2
Cr	0.05
Mn	0.05
Fe	0.2
Ni	0.02
Cu	2.0
As	0.01
Se	0.01
Cd	0.003
Sb	0.005
Hg	0.001
Pb	0.01
U	0.01

**Figure 12.7** Spectrum of NIST SRM 1640 – fresh water. Source: Courtesy by Bruker Nano GmbH.

uncertainties  $\Delta C_{\text{NIST}}$ , the mean values of the 10 repeated analyses  $C_{\text{meas}}$ , as well as their standard deviations  $\Delta C_{\text{meas}}$  and the calculated limits of detection  $C_{\text{LOD}}$ .

These results show that the trueness is very good for most of the elements, and deviations from the nominal values are in the range of the uncertainties. Slightly larger deviations are observed for the elements Mn, Co, Zn, and Se. One has to take into account that these analyses are in the range of ultra-traces and deviations in the range of 10% are easily possible. It is remarkable that the reproducibility of the results for the complete analysis, i.e. including sample preparation, is



**Table 12.3** Quantification results of the fresh water sample (NIST SRM 1640).

Element	$C_{\text{NIST}}$ ( $\mu\text{g/l}$ )	$\Delta C_{\text{NIST}}$ ( $\mu\text{g/l}$ )	$C_{\text{meas}}$ ( $\mu\text{g/l}$ )	$\Delta C_{\text{meas}}$ ( $\mu\text{g/l}$ )	$C_{\text{LOD}}$ ( $\mu\text{g/l}$ )
S	n/a		5012	21	40
Cl	n/a		2121	10	20
K	994	27	963	3.0	10
Ca	7045	89	7300	10.8	7
Ti	n/a		4.2	0.48	1.5
V	13.0	0.37	12.7	0.48	1.4
Cr	38.6	1.6	38.0	0.53	1.1
Mn	122	1.1	135	0.80	1.0
Fe	34.3	1.6	39.0	0.37	0.9
Co	20.3	0.31	13.8	0.18	0.7
Ni	27.4	0.8	31.5	0.28	0.6
Cu	85.2	1.2	80.9	0.55	0.5
Zn	53.2	1.1	61.9	0.32	0.4
As	26.7	0.41	29.2	0.21	0.3
Se	26.7	0.41	19.8	0.91	0.2
Rb	2.0	0.02	1.78	0.06	0.2
Sr	124.2	0.7	123	0.37	0.4
Y	n/a		0.76	0.12	0.8
Ba	148	2.2	163	1.59	
Pb	27.9	0.14	28.5	0.21	

Source: According to LabReport-XRF\_425 (n.d.).

extremely good. For most elements, it is below 1%, which is usually even below the uncertainties of the certificate.

The detection limits for freshwater samples have already been shown in Figure 12.7. They are listed in the last column of the table and are significantly smaller for all elements than their concentrations in the sample, in some cases up to 2 orders of magnitude.

#### 12.4.1.3 Example: Detection of Mercury in Water

Mercury is highly toxic. Its sources can be of natural origin, such as volcanic eruptions, but also industrial emissions such as the burning of coal and cement and gold production. In this way, Hg enters the environment and can then contaminate drinking water or even food.

Because of its high toxicity the allowable limits for Hg are very low. They are defined at 1  $\mu\text{g/l}$  in Europe according to Custo et al. (2006), and are thus only slightly above the limit of detection of TXRF. In addition, there is the risk that the volatile Hg can be lost from the sample by the preparation procedures. Therefore, a preparation technique was designed with no element losses (LabReport-XRF\_430, n.d.). This is achieved by forming a complex with ethylene-diamine-tetra-acetate (EDTA), which is added to the sample in a ratio

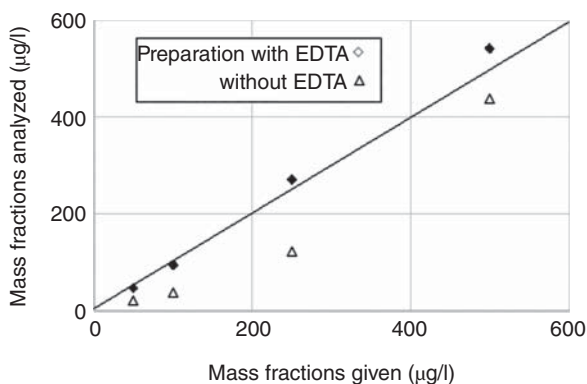


**Figure 12.8** Analysis results for Hg determined with and without EDTA-complexing. Source: According to LabReport-XRF\_430 (n.d.).

of 1 : 3. After a thorough homogenization of the mixture, the sample can be applied to a sample holder and dried. This process eliminates the underreporting of Hg, as shown in Figure 12.8.

Owing to the addition of EDTA, the limits of detection are somewhat reduced, since the lighter matrix of this complexing agent slightly increases the scattering, i.e. the spectral background. This is, however, only a small effect, which can easily be compensated by extending the measuring time.

## 12.4.2 Analysis of the Smallest Sample Quantities

### 12.4.2.1 Example: Pigment Analysis

Another very common application, which was one of the first uses for TXRF, is the analysis of the smallest pigment particles, for example the analysis of paintings (Klockenkämper et al. 2000; Salva et al. 1993). Pictures are painted with different pigments, which are often of inorganic origin. The individual pigments have a characteristic composition and they can be identified by a few elements only. This is important, for example, for the dating of paintings or for a customized restoration (see Section 16.5.4).

Since the damage of historical objects of art is prohibited, only small amounts of samples can be used for the analysis. For TXRF these small amounts are already sufficient. The sampling and preparation are carried out by removing only a very small sample quantity from the painting surface, for example, by swiping with a Q-Tip over the area to be examined. In this way, a sample quantity of about 1 µg can be taken. The transfer to a sample holder takes place by a single tap of the Q-Tip. If the amount deposited is 100 ng, it is already sufficient for collecting a spectrum.

For the characterization of a pigment, the identification of the elements present as well as their intensity ratios is sufficient. Complete quantification is difficult with these type of samples since no internal standards can be applied. However, it is possible to estimate the concentrations of the various elements by a normalization of all identified elements to 100% using the known elemental sensitivities. A prerequisite, however, is that there are no undetectable elements in the pigment.

#### 12.4.2.2 Example: Aerosol Analysis

Aerosols are particles or liquid droplets of natural or anthropogenic origin in the air. The size of the aerosols ranges from a few tens of micrometers to the sub-micrometer range. Depending on the particle size and the particle composition, different health hazards due to aerosols can be expected. The smaller the particles, the deeper they enter the respiratory system and can then penetrate into the body. Therefore, knowledge of the aerosol quantity as well as its composition is important for an assessment of the health hazard of dust pollution.

On the other hand, the contamination in clean rooms with aerosol can also be of analytical interest. They can contaminate the materials processed in the clean room. Determining the composition of such contaminants can be helpful in the identification of their sources and thus in their avoidance.

The sample collection can be carried out in various ways. The big advantage of TXRF for this analytical problem is the very small amount of sample material required. This means that the collection times for a sufficient sample quantity can be relatively short and therefore even time-dependent dust contaminations can be tracked.

The simplest way to collect the sample is through the deposition of the aerosol particles in an impactor. In this process, the particles are directed and deposited by an air stream onto an impact plate. In a multistage instrument, even size-dependent separation is possible by changing the air flow intensity with variations of the nozzle size. If the sample holders of the TXRF instrument are used as impact plates, they can directly be used for the analysis. In this case, for better adhesion of the aerosol particles, the sample plate may be treated with a silicon solution (LabReport-XRF\_438 n.d.).

Another possibility is the collection of aerosol particles on filters. The particles collected in this way can then be separated from the filter. For Nuclepore filters this is possible by separation in an ultrasonic bath, and for membrane filters by a digestion of the filter containing the aerosols. To the resulting solutions an internal standard can be added, applied to the sample holder, and analyzed after drying. Care must be taken when using these preparation methods that the filter material is very clean and that only pure solvents are used. For this purpose, blind sample analyses should continuously be carried out in order to detect impurities and, if necessary, to take them into account. The reproducibility of the method can be checked by repeated analyses.

The spectrum of an aerosol sample together with the quantities determined with the help of internal standards is shown in Figure 12.9, with the values in nanograms.

#### 12.4.2.3 Example: Analysis of Nanoparticles

Nanoparticles are particles with diameters of typically less than 100 nm, which often consist of only a single element, but they can also be coated. Nanoparticles have properties that differ significantly from those of larger particles or even from solids of the same composition. Owing to the large surface area, they are highly chemically reactive and have, due to the small size, very low weights so that molecular forces can already have an influence and gravitational forces are negligible. They are increasingly used for a wide variety of surface-active reactions, for

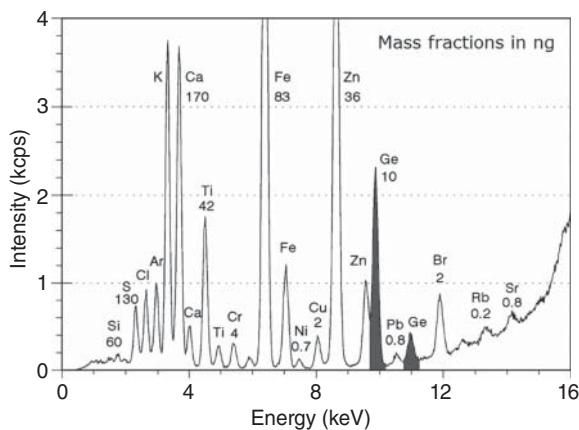


**Figure 12.9** TXRF spectrum of an environmental aerosol sample, particle size 2–4  $\mu\text{m}$ , with 10 ngGe as internal standard.

example, in catalysts or to prevent the growth of fungi or bacterial cultures. However, these particles can also cause health damages, since they can not only enter the lung due to their small size, but can even directly enter the cells through the blood. Therefore, the analysis of nanoparticles is of great importance – regarding both their quantity and composition (von Bohlen 2010).

For the analysis, the nanoparticles are deposited on the sample carrier. This can be done by direct application or by drying of a suspension. In the second case, the addition of internal standards for quantification is possible. If the nanoparticles are coated, the diameter of the particles and the coating thickness can be determined assuming spherical particles and uniform coating. Typical analysis times are again in the range of 1000 seconds.

Varying the incident angle of the excitation radiation (see Sections 4.3.3.8 and 14.4.6), intensity profiles can be measured, which are dependent of particle size and quantity, both for the fluorescence radiation of the element and for the elastically scattered radiation. These profiles can be used to determine particle size and quantity (LabReport-XRF\_77, n.d.). For the quantification, however, iterative calculation models for the particles will be necessary.

## 12.4.3 Trace Element Analysis on Human Organs

### 12.4.3.1 Example: Analysis of Blood and Blood Serum

The presence of trace elements in body fluids can be indicative of the health condition of people; missing essential elements such as Cr, Mn, Fe, Ni, Cu, Zn, or Se can lead to diseases, as well as to high concentrations of toxic elements such as As, Hg, or Pb.

A sample type that is often examined for this purpose is blood. Blood consists of about 40% of blood cells (erythrocytes, leukocytes, thrombocytes) and about 60% of blood plasma. Frequently, blood serum is analyzed, which is obtained when the liquid fraction is centrifuged from the blood.

The processing of the serum for the analysis is most easily accomplished by a tenfold dilution with ultrapure water and the addition of an internal standard, for example a Ga solution. Approximately 10  $\mu\text{l}$  of this solution needs to be pipetted

**Table 12.4** TXRF results of blood serum compared with certified values.

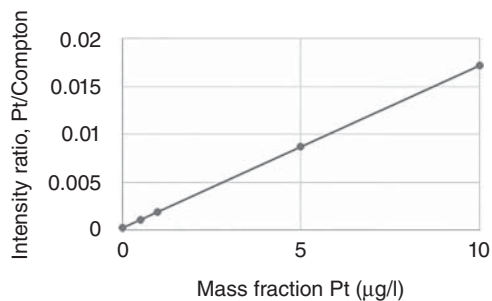
Element	$C_{\text{NIST}}$ ( $\mu\text{g}/\mu\text{l}$ )	$\Delta C_{\text{NIST}}$ ( $\mu\text{g}/\mu\text{l}$ )	$C_{\text{meas}}$ ( $\mu\text{g}/\mu\text{l}$ )	$\Delta C_{\text{meas}}$ ( $\mu\text{g}/\mu\text{l}$ )
K	137.6	4.3	133.4	2.8
Ca	120.8	3.5	109.1	1.8
Fe	1.98	0.27	2.14	0.021
Cu	1.10	0.10	1.08	0.02
Zn	—	—	1.21	0.04
Se	—	—	0.101	0.006
Pb	0.020	0.003	0.025	0.012

Source: According to Klockenkämper and von Bohlen (2015).

onto a sample holder and dried (Greaves et al. 2006). Another possibility, which can be applied to the blood constituents, i.e. to pure blood as well as to blood plasma, is microwave digestion in nitric acid. For this purpose, 1 ml of the sample is mixed with 5 ml of ultrapure nitric acid and the mixture is digested for about 15 minutes at 550 °C, and in a second step for 20 minutes at 400 °C. Then, an internal standard can be added. For the analysis an aliquot of 10  $\mu\text{l}$  of this solution can be pipetted at the sample carrier. The measurement times range from 600 to 1000 seconds. In Table 12.4 the analysis results of a serum standard (NIST SRM 909 human serum) are compared to the certified values. The results show very good correlation, even for the elements with lower concentrations.

An important medical application is the monitoring of blood from chemotherapy patients. Agents for chemotherapy often contain platinum, which generally has a high toxic potential. Since cancer patients often also suffer from kidney insufficiencies, the available functional window for the therapy is small. Monitoring patient blood requires a fast analysis to allow a quick reaction and accurate dosage adjustments. The analysis process starts already with the sample preparation. The preparation is carried out by centrifuging the serum at 10 000 rpm. The serum is then transferred to the sample holder with a pipette and dried at  $-4$  °C (von Bohlen et al. 1987). If the Pt intensity is normalized to the Compton peak of the tube radiation (Mo tube) no internal standard needs to be added. Preparing a calibration by adding an ultra-pure Pt solution to a serum resulted in a linear calibration curve (see Figure 12.10). The resulting detection limit was determined to

**Figure 12.10** Calibration curve for platinum in blood serum. Source: According to Greaves et al. (2006).



be  $0.67 \mu\text{g/l}$ . Therefore, the method is sensitive enough to detect Pt in the blood of chemotherapy patients.

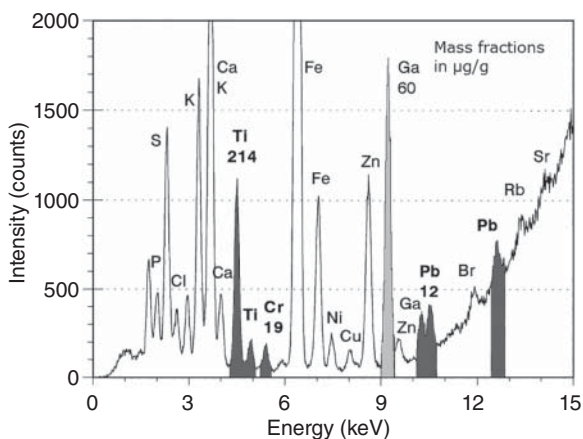
#### 12.4.3.2 Example: Analysis of Trace Elements in Body Tissue

The analysis of trace elements in body tissue can provide important information about the supply of vital elements or, on the contrary, about exposure to toxic elements. A possible preparation technique is an ashing or digestion of the tissue. However, the risk of contamination is relatively high as well as the possibility to lose volatile elements. Another possibility is the analysis of very thin tissue sections that are being directly applied to the sample carrier. For this purpose, a piece of the tissue with an approximate size of 4–8 mm is frozen to  $-15$  to  $-25^\circ\text{C}$ . The frozen tissue can then be cut with a microtome. The tissue sections are between 5 and  $15 \mu\text{m}$  thick. These sections can be transferred to a sample carrier, which is a hydrophobic surface and is slightly cooled. In this way, the tissue section can be prepared evenly and without any damage. When the sample carrier is then heated, the tissue slice dries quickly and adheres to the sample holder.

For quantification, usually an internal standard is required. In order to determine a suitable standard, a spectrum of the tissue should be measured after preparation. Then the element with the fewest peak overlaps can be selected. A  $10 \mu\text{l}$  solution of this element, for example, Ga or Y, can be pipetted as an internal standard to the already prepared sample. This solution is readily absorbed by the cut. The concentrations to be determined are usually in the  $1 \mu\text{g/ml}$  range. During the drying process by heating or evacuation, the sample size usually is slightly reduced; subsequently the sample can be measured. The analyzed sample quantity must be determined by a differential weighing of the sample holder with and without the sample. Typical weights are in the range of  $100 \mu\text{g}$ . Now the concentrations of the individual elements in the sample can be determined. A normalization of all concentrations to 100% is not possible since the elements with the highest concentration in the tissue are not measurable because of their small atomic number.

This preparation technique is applicable for different types of body tissue – for example, kidney, lung, or liver. An example is the analysis of a dust-loaded lung tissue (von Bohlen et al. 1987). For this purpose, the lungs of individuals without any heavy dust exposure were analyzed. The spectra of the samples were very similar and could be averaged to a “normal spectrum”. The comparison with the spectrum of a foundry worker who was heavily exposed to dust shows clear differences, especially for some heavy metals (see Figure 12.11). High loads of Ti, Cr, and Pb were detected in the upper microgram per gram range. The peaks of these elements as well as the peak of the internal Ga standard are marked in the spectrum.

**Figure 12.11** TXRF spectrum of lung tissue of a foundry worker. Source: Courtesy of A. von Bohlen.



The contamination with specific elements depends on the profession of the individuals examined. How much the spectrum deviates from the “normal spectrum” depends very much on the individual, their overall health, the duration of the exposure, and if any protective covers were used.

#### 12.4.4 Trace Analysis of Inorganic and Organic Chemical Products

The simplicity of the sample preparation makes TXRF ideal for the analysis of high-purity chemicals, such as acids, bases, solvents, ultra-pure water, or even organic materials such as oils, fuels, or pharmaceuticals.

For inorganic liquid chemicals, often only a dilution with ultra-pure water is required. Limits of detection down to 0.1 ng/ml are then achievable (Huber et al. 1988), which is similar to aqueous solutions (see Figure 12.6).

For organic material, the preparation is more material specific. Depending on their consistency, different methods are used. For highly volatile liquids, such as petrochemical products, pipetting the material to the sample holder is sufficient, along with the evaporation of the organic matrix. After adding an internal standard, the measurement can be carried out. Detection limits down to 5 ng/g are possible.

Macromolecular materials with stronger interlinking bonds vary in their consistency from liquid to viscous and even to solid. This means that both oils and fats and polymers cannot be prepared very easily as their high molar mass prevents an evaporation of the matrix. For these samples cold-plasma ashing is a suitable preparation technique. For this purpose, an internal standard is added to 1 ml of the sample, and it is then incinerated in a quartz vessel in an oxygen plasma (300 W for one hour at 500 Pa O<sub>2</sub> pressure). The ash is then dissolved in nitric acid; 50 µl of this solution can then be analyzed on the sample holder after drying.

With this method, the limits of detection can be improved by about 1 order of magnitude; however, the time required for the preparation, approximately two hours, is often too long, especially for process monitoring. Furthermore, volatile elements such as S, Se, As, or Hg can be lost. For the detection of these elements, a high-pressure digestion method with subsequent cold ashing is required. This increases the preparation time to about 10 hours, which further limits its use for process monitoring.

## 12.4.5 Analysis of Semiconductor Electronics

### 12.4.5.1 Ultra-Trace Analysis on Si Wafers with VPD

Si wafers are the raw material in the production of electronic components. The degree of integration has increased enormously in recent years, i.e. the dimensions of the individual components have been drastically reduced and their density has increased. Structure dimensions are now less than 20 nm and the distances between switching points are 500 nm. This requires not only high-tech for the structuring of features but also an extreme control of the cleanliness of the wafers, the manufacturing environment, and the influence it has on the production process.

Si wafers are cut from specifically grown crystals with diameters of up to 18 in. (approximately 450 mm) at thicknesses of up to 750  $\mu\text{m}$  and are polished to a roughness of 0.1 nm. This first process step already requires extreme cleanliness. Alkali metals such as Na and K can affect the breakdown voltage of the silicon; transition metals such as Cr, Fe, Co, Ni, Cu, or Zn can cause leakage currents or short-circuits; and radioactive elements such as U or Th can generate crystal defects by emission of  $\alpha$ -radiation, which can cause malfunctions. Therefore, such impurities are allowed only in the smallest concentration, the currently allowed value being  $2.5 \times 10^9$  atoms/cm<sup>2</sup> for all elements. If only Cu would be present as impurity, this would be about 43 fg/cm<sup>2</sup>. For a wafer with the above-mentioned diameter this corresponds to a total amount of approximately 7 ng.

TXRF for such examinations is used in two different ways (Klockenkämper and von Bohlen 2015). On the one hand, a direct analysis is possible. The detection limits are then in the range of  $10^9$  atoms/cm<sup>2</sup>, which is the range of the requirements for the sum of all elements. In this case, it is possible to examine the wafer nondestructively and to distinguish between particles just lying on the wafer and contaminations embedded within the very top layers by varying the incident angle of the excitation beam. The nondestructive nature of this method makes it suitable for process monitoring. However, the sensitivities are not good enough for an appropriate assessment of the contamination.

An increase in the sensitivities by about 2 orders of magnitude is possible by vapor phase deposition (VPD) yielding detection limits of  $10^7$  atoms/cm<sup>2</sup> (Klockenkämper et al. 2003). This method, however, can only be used for non-structured wafers since the method will influence the wafer surface. Using VPD, the impurities are collected from the entire wafer surface and then measured in a pre-concentrated state. The improvement in sensitivity results from the ratio of the size of an individually measurable surface to the total area of the wafer. For the collection



of the contaminants, the wafer surface is covered with a thin layer of hydrofluoric acid via vapor phase condensation. This dissolves the oxide layer deposited on the wafer, including embedded impurities and any other impurities on the wafer surface. Pure silicon automatically stops this etching process. As a result of this process, many small droplets are formed on the hydrophobic wafer surface, which contains the impurities. The individual droplets are collected by means of a droplet of ultra-pure deionized water, which is guided on a spiral inward path over the wafer surface. This drop can then either be directly dried for an analysis on the wafer or it can be removed and deposited on a quartz sample carrier for the measurement. Accordingly, this drop could also be used for other analytical methods, such as atomic absorption spectrometry (AAS) or inductive coupled plasma–mass spectrometry (ICP–MS). However, with AAS usually only one element can be analyzed, and the sample is consumed in the process by both methods. It is then no longer available for further analysis or for archiving for later control measurements. Since the sample is not consumed during the analysis, TXRF does not have that disadvantage.

#### 12.4.5.2 Depth Profile Analysis by Etching

Depth profile analysis of surface layers of a wafer is possible by a stepwise removal of the wafer surface and repeated measurements of the removed material or the surface composition (Klockenkämper and von Bohlen 2015). The removal of material can be carried out in various ways.

One way to do this is similar to the VPD method described in the previous section. In this case, the wafer is first oxidized in approximately 30%  $\text{H}_2\text{O}_2$  solution. This oxide layer can then be etched in 4% HF solution. Using the weight difference after each etching process, the thickness of the layer can be determined when the wafer surface is accurately known, and the density of pure Si is assumed. Determining the wafer area is possible with an uncertainty  $<0.01\%$ , and the weighing uncertainties are in the range of 2–5%. This results in accuracies for the determination of the layer thickness of approximately 5–10%. TXRF analysis can then be carried out directly on the wafer, or the etching solution is transferred to a sample holder and then analyzed. Repeating the described procedure, information about concentration gradients, for example, of implanted ions can be obtained.

Another possibility to remove material from a large area is by ion sputtering of the wafer surface, between the individual TXRF analyses (Klockenkämper et al. 2003). In this case, the wafer material is uniformly removed by  $\text{Ar}^+$  ions with relatively low energies of about 500 eV. The removal rate is proportional to the sputtering time; the layer thickness that is removed in each case can be determined by differential weighing as in the case of the etching method. Another possibility that permits the determination of the layer thickness with higher accuracy is the use of an interferometer. The height difference between the stripped surface and a surface that was masked off during the sputtering process can then be measured. This allows to control the removal of thicknesses of a few nanometers reproducibly. Sputtering eliminates the risk of any contamination from the chemicals that are required for the etching process. The surface composition can then again be measured with TXRF.

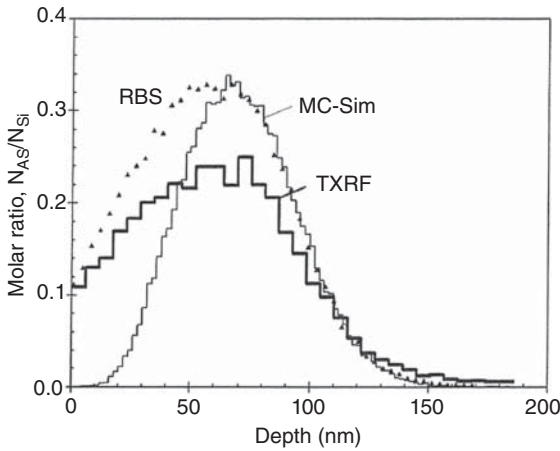


**Figure 12.12** Depth profiles of As ions in a Si wafer determined with TXRF, RBS, and by Monte Carlo (MC) simulation. Source: Courtesy of A. von Bohlen.

An example of such a depth profile determination is shown in Figure 12.12. Here, a Si wafer was implanted with about  $10^{17}$  As ions/cm<sup>2</sup> at an energy of 100 keV. Thirty two layers with thicknesses of about 6 nm were analyzed. The distribution of the As concentration (as molar ratio of As and Si) was determined by TXRF, Rutherford backscattering (RBS), and with the aid of a Monte Carlo simulation (Figure 12.12). It can be seen that the different profiles correlate well, except close to the surface. The deviations in this range can be partly explained by the limited depth resolution of the analytical methods.

## 13

### Nonhomogeneous Samples

Very often, the samples and parts to be analyzed are not homogeneous or cannot be homogenized by a corresponding preparation technique, because various manufacturing steps have already taken place during their production. Also prohibitive to homogenization are samples with potentially high monetary values or if they are integrated into production processes or their analysis result must be available very quickly. In these cases, a position-sensitive analysis may be the solution, which means only small sample areas will be analyzed. X-ray analysis offers this possibility by concentrating the incident beam on a small sample surface. Another possibility is to collect the fluorescence radiation from only a small area of a larger excited sample surface; however, in this case the excitation intensity must be rather high.

Instruments with spot sizes of various diameter are available. With collimators, the tube radiation can be restricted to diameters of about 0.3 mm. For smaller collimators, the intensity of the incident radiation is too low. With X-ray optics, spot sizes with sufficiently high excitation intensities, as low as 5–10  $\mu\text{m}$  can be achieved (Janssens et al. 2000; Kanngießner and Haschke 2006; Haschke 2014). Owing to the small area analyzed, these instruments are referred to as micro X-ray fluorescence ( $\mu\text{-XRF}$ ).

#### 13.1 Measurement Modes

$\mu\text{-XRF}$  spectrometers make it possible to analyze individual points due to the small areas being excited; this can be interesting for both inhomogeneous and irregularly shaped samples. These sample types cannot accurately be characterized when analyzing large areas. For inhomogeneous materials, an averaging of the composition would be the result; the not so well-defined geometry of irregularly shaped samples will influence the analysis result due to the variation of the sample–detector distances.

In contrast, if only a small sample area is analyzed, it is usually possible to find a homogeneous and plane sample area for the analysis.

A position-sensitive element analysis can also be used for the measurement of many points. If these points are arranged equidistantly on a line or on an area, one-dimensional or two-dimensional element distributions (line scan

or  $xy$ -maps) can be generated.  $\mu$ -XRF therefore allows for the comprehensive characterization of different materials. In particular, during the measurements of these samples, complete spectra for each measurement point are stored. In this way, the so-called HyperMaps are created, and they offer various opportunities for the evaluation of the measured data.

A special type of inhomogeneous samples are coated materials. In this case, the inhomogeneity exists perpendicular to the sample surface. For X-ray spectrometry, the layer material as well as the substrate layer will be excited during the measurement of the coated sample. Both fluorescence intensities depend on the layer thicknesses and under certain circumstances, they can be used for a nondestructive characterization of the layers, for the determination of both layer composition and layer thickness. Many products are coated with layers for decorative and/or functional purposes. These products are often inhomogeneous as well as irregularly shaped. This means that in order to obtain reliable quantitative results without destroying the sample by preparation, the analysis is often only possible on small sample surfaces.

## 13.2 Instrument Requirements

The available excitation intensity is limited as a result of the small spot sizes. When using collimators, the intensity is proportional to the diameter of the collimator squared, i.e. comparing an analysis with a diameter of the analyzed area of 30 mm to one with 1 mm diameter, the intensity is reduced approximately by a factor of 1000, and even by a factor of 10 000 for diameter of 0.3 mm. The excitation intensities cannot be increased substantially, since wavelength-dispersive spectrometers (WDSs) are already using high-performance X-ray tubes with a power of 3–4 kW. Energy-dispersive spectrometers (EDSs) are offering a solution for this problem. Because of the simpler EDS instrument design, the detector can be much closer to the sample than in a WDS instrument. The result is an increase in solid angle of up to a factor of 100, which allows for the collection of more fluorescence radiation. Consequently, sufficient fluorescence intensities can be collected even at low tube power, especially if the measurement geometry is very narrow. Suitable intensities can then already be generated with low power tubes with outputs of <50 W; they are also easier to handle and more cost effective, also because they have not to be cooled by an external system.

To achieve even smaller spot sizes, X-ray optics are required. With these, a larger amount of the primary radiation can be collected from the tube and then concentrated on the sample. Depending on the optics, spot sizes down to 5–10  $\mu\text{m}$  are possible. The increase in brilliance at the excited area can be up to 4 orders of magnitude. Capillary optics concentrate a broad energy spectrum into their focus. These optics provide efficient excitation conditions for a wide range of elements and can therefore be used for a wide range of applications. Additionally, optics such as shaped multilayer structures or curved crystals exist, which focus only a narrow energy band. They are used for the selective and efficient excitation of individual elements for their highly sensitive analysis.

For ideal sample positioning,  $\mu$ -XRF instruments excite samples from the top; this allows to adapt the measurement geometry to various sample shapes. The samples to be analyzed are placed on a programmable  $xy$ -stage with an additional programmable  $z$ -axis to adjust the distance of the sample to the focal plane of the X-ray spot. The sample can then be exactly positioned according to the beam in  $xy$ -stage and  $z$ -directions. Especially for very small spots, generated by X-ray optics, an optical microscope is useful for an exact positioning.

Depending on the analytical task, different detectors are used for position-sensitive analysis; they differ in the size of the active area, resolution, and impulse rate capability.

Proportional counters have large active areas and can therefore collect fluorescence radiation from a large solid angle; however, they have a limited energy resolution. For this reason, they are primarily used for monitoring production processes where the qualitative composition or the layer structure of the products to be inspected is known. With this knowledge, peak area calculation using a peak fitting algorithm yields sufficient accuracy, despite the peak overlap of individual X-ray lines. An important further limitation of the low-energy resolution is the limited peak-to-background ratio and thus a lower sensitivity for traces.

Solid-state detectors do not have the resolution and peak to background disadvantages. The detectors are usually made out of silicon, they have a much better resolution, but also smaller active areas. Otherwise, solid-state detectors have much higher count rate capabilities. The smaller detection solid angle, resulting from the smaller active surface area of the detector can be partially compensated by shorter distances to the sample. A comparison of the energy resolution of proportional counters and solid state detectors, in this case, a silicon drift detector (SDD), can be made looking at the spectra in Figure 4.4.

A summary of the most important properties of the commonly used energy-dispersive detectors is given in Table 13.1.

WDSs can also be used for point analysis; in this case the area to be analyzed is limited by a collimator. However, the fluorescence intensity decreases proportionally with the size of the area to be analyzed, resulting in reduced repeatability of the measurements. The lower intensity can be compensated by increasing the intensity of the incident radiation or by extending the measurement time or both. With such a system, the analysis of individual points, such as inclusions or individual particles, is possible. The determination of element distributions, however, is not useful with this method; the spatial resolution is limited by the relatively large beam size, and the increased analysis times for compensating the

**Table 13.1** Properties of energy-dispersive detectors.

Parameter	Proportional counter	PIN-diode	SDD
Effective area	Up to 1000 mm <sup>2</sup>	25 mm <sup>2</sup>	Up to 100 mm <sup>2</sup>
Energy resolution for Mn-K $\alpha$	Approx. 1000 eV	Approx. 180 eV	130 eV
Maximum count rate	Typical 10 kcps Up to 20 kcps	50 kcps	>500 kcps

low fluorescence intensities can become relatively large. This is in particular true because with WDS each element must be measured individually.

The spatial resolution of a distribution map primarily depends on the size of the excited area, but also influenced by the distance between the measurement points; the total accumulated intensity also affects the quality of the distribution images of the elements. For a given spot size, the spatial resolution can be improved by using small distances between measuring points. However, the number of points to be measured for a given area then increases, and therefore also the total measurement time and the size of the data file. To achieve good-quality images step sizes of about 30% of the spot size can be used (Haschke 2014).

High fluorescence intensities allow for the detection of small intensity differences as a result of the smaller statistical error. The required high fluorescence intensities can either be achieved by high excitation intensities or longer measuring times per measuring point.

### 13.3 Data Evaluation

A further special feature of a position-sensitive analysis is the evaluation of the spectra. For point analysis, comparable algorithms can be used as for conventional spectrometry (see Section 5.5). However, inhomogeneities of the material can influence the analysis result due to potential variations of the matrix at the measurement point, which restricts the analytical accuracy. It should be noted that calibration samples can also be nonhomogeneous, in particular for very small analyzed sample volumes. The certified concentrations of a reference sample are valid only for larger sample volumes; reference samples with defined inhomogeneities are very rare.

Moreover, different calibration sample sets would be required for a complete analysis of an inhomogeneous sample. Even if they would be available, using them would require much effort. Position-sensitive analysis methods therefore mostly use standard-free quantification models; they match the achievable accuracies that can be obtained from the nonhomogeneous samples. The analytical accuracies for inhomogeneous materials depend on the concentrations of the different elements – typically they are in the range of more than 10% relative.

For layer analysis, special evaluation methods are required; they have already been described in Section 5.6.

Many options exist for the presentation of element distribution data – especially for the evaluation of the multidimensional data sets consisting of the spatial coordinates, the energy, as well as the intensity. There are many different methods available which, however, must be adapted to the analytical problem at hand.

In the following chapters, examples of various applications of position-sensitive element analysis and their evaluation methods are presented. The various possibilities of data presentation and position-dependent analysis are demonstrated using specific applications. The methods can easily be transferred to comparable analytical tasks. Decision on the best evaluation strategy to be used must be based on the particular sample type and the analytical task.

## 14

### Coating Analysis

#### 14.1 Analytical Task

Layer analysis is a very common analytical problem for X-ray fluorescence (XRF). It is primarily used as a quality management tool in industrial control. Many products are coated for functional as well as for decorative reasons. A very large number of layer systems exist, and the main parameters of interest are the layer thicknesses and, in the case of alloy layers, their composition (DIN-EN-ISO-3497 2001-12; ASTM-B\_568-98 2014).

For a nondestructive layer analysis, the layer system is excited from above, which means that both the layer and the substrate are excited to emit fluorescence radiation, which can be used for the evaluation (see Figure 5.23). The fluorescence intensity from the layer increases with increasing thickness and approaches a saturation value, which corresponds to the value of an infinitely thick layer, in other words to the information depth of the radiation. On the other hand, with increasing layer thickness, the fluorescence radiation of the substrate decreases since more radiation is absorbed in the layer.

Depending on which signal is used for the evaluation, different measurement modes are possible:

- *The emission mode* uses the radiation emitted by the layer material for evaluation. This radiation is the most applied variant for layer analysis. Using the fluorescence of the layer material is the only possibility for the analysis of multilayer systems.
- *The absorption mode* uses the absorption of the substrate radiation in the layer. This mode is used preferentially for single-layer systems. It is especially interesting for layers made of light elements.
- *The relative mode* uses both layer and substrate radiation; it can be used just for single-layer systems. By utilizing both beam components, a layer characterization is possible where the given measurement geometry of the instrument is not maintained, for example, for variations of sample-detector distances or in the case that the instrument spot size does not match the measurement area.

The intensity of the fluorescence radiation is used for the quantitative determination of the layer parameters. It should be noted that with XRF, only mass per unit areas can be determined; they are then converted into layer thicknesses using the layer density (see Eq. (5.26)).

Layer analysis has some of its own characteristics:

- Layer systems must mostly be characterized on finished products. The products usually vary in shape and are often inhomogeneous. The analysis can therefore be only performed on small sample areas, resulting in low fluorescence intensities that are best analyzed with energy-dispersive (ED) instruments.
- Only layers that are not infinitely thick can be measured, i.e. the layer thickness has to be less than the information depth of the corresponding fluorescence radiation. Thicker layers cannot be analyzed with XRF.
- An independent signal must be available for each layer parameter to be analyzed, which means the elements in each layer and the substrate must be different. However, it is possible to evaluate the same element in different layers if they emit a measurable radiation at different energies (i.e. K-, L- or M-radiation or  $\alpha$ - and  $\beta$ -radiation). For alloyed layers, it is possible to reduce the number of required intensities by one, due to a normalization of the total element concentration to 100%.
- For quantification the layer structure (sequence and qualitative composition) must be known; only then a correct analysis of the measured intensities is possible. For practical purposes this is not a problem; for industrial process control, this information is known for the layers applied during the production process.

## 14.2 Sample Handling

The samples that are being analyzed are usually subassemblies or finished products; as already mentioned, they often are nonhomogeneous or irregularly shaped, and they should not be reworked for the analysis. Some products require even 100% inspection, which would not allow for a destructive sample preparation. This means the analysis for highly structured samples has to be done either on small sample surfaces in order to adjust the measurement point to the sample structure, or, in the case of coating applied to large areas, a large number of measurements must be done to get a representative characterization of the coating. Finished products can often be larger in size; the sample chamber of the instrument must be sufficiently large to hold the entire sample. Further, short analysis times are required for 100% inspection processes. The conclusion is: mostly sample preparation is not possible, but also not necessary.

In order to control a plating process, it is important that all measurements are done at the same sample position; only in this way results are comparable, and procedures for statistical process control can be implemented. Layer thicknesses can vary across shaped surfaces and are therefore dependent on plating location and plating method. For instance, thicker layers are often observed at edges and bends compared to flat surfaces (in electroplating, areas of high current density plate grow faster). In the case of vapor deposition, the layers are usually homogeneous, but they are dependent on the orientation of the coated surface with respect to the evaporation source. Thus, the deposition rate of several plating methods is dependent on the direction of material transport and sample



topology. On the other hand, very uniform coating of parts can be achieved by the electroless or autocatalytic plating process.

When small sample areas are to be measured, the exact positioning of the sample with respect to the incident beam is important. Therefore, the instruments use cameras and optics as well as high precision  $xy$  stages. The small sample areas are positioned according to the given measurement geometry, that is, parallel to the sample stage.

Slotted sample chambers are used when samples such as large printed circuit boards (PCBs) need to be measured. Sections of the PCB will protrude outside the sample chamber, which avoids the destruction of the sample. In this way it can be returned into the production process undamaged.

### 14.3 Measurement Technology

ED spectrometers are the preferred choice for layer analysis. The small areas and the thin layers analyzed only produce low fluorescence intensities. The spectrometers must therefore be capable to create high intensity primary beams. Only in the relatively rare case when the surfaces are flat and sufficiently large wavelength-dispersive (WD) spectrometers can be used for the analysis.

Energy-dispersive spectrometer (EDS) use both proportional counters and high-resolution semiconductor detectors. Proportional counters have the advantage of having a large effective area, hence they collect a large solid angle of fluorescence photons, but their limited energy resolution restricts the measurement sensitivity. In layer systems usually only a few known elements are found, which means that the determination of the individual peak areas by peak fitting algorithms is not a problem even with the limited spectrometer resolution. However, using high-resolution semiconductor detectors, the better peak-to-background ratios give better sensitivity, which results in the capability to measure very thin layers.

At the same time, due to fewer peak overlaps because of the better energy resolution, the errors in the peak area calculation are reduced. The slightly larger statistical error caused by the lower collected intensity due to the smaller effective area of these detectors is therefore compensated by the improved peak area calculations. Table 14.1 summarizes the results of 10 repeated measurements of an Au–Ni layer system measured with a proportional counter and a silicon drift detector (SDD) instrument. The measurements were performed with the same excitation conditions (40 kV, 600  $\mu$ A, 0.7 mm spot size, 15 second measurement time). For their evaluation the mean values of intensities and layer thicknesses were calculated, as well as the relative standard deviation of the repeated measurements.

The results show that with the same measuring conditions, the intensities are approximately by a factor of 10 lower for the high-resolution SDD compared with the proportional counter. Correspondingly the relative intensity fluctuations  $\sigma_{\text{Irel}}$  (see Eq. (6.3)) as well as their statistical errors  $\sigma_{\text{stat}}$  are larger by approximately a factor of 3. On the other hand, the absolute and relative standard deviations of

**Table 14.1** Detector influence on analytical results.

Detector	Prop counter		SDD	
	Au	Ni	Au	Ni
Intensity, counts (15 s)	27 000	78 000	2650	6500
$\sigma_{\text{irel}}$ (%)	0.87	0.42	2.04	1.31
$\sigma_{\text{stat}}$ (%)	0.61	0.36	1.94	1.24
Thickness ( $\mu\text{m}$ )	0.48	2.47	0.50	2.53
$\Delta s$ ( $\mu\text{m}$ )	0.0135	0.069	0.009	0.033
$\sigma_{\text{drel}}$ (%)	2.94	2.79	1.75	1.10
$d_{\text{LOD}}$ ( $\mu\text{m}$ )	0.1	0.5	0.005	0.02

the layer thicknesses  $\Delta s$  and  $\sigma_{\text{drel}}$  are better by a factor of 2 for the high-resolution SDD than for the proportional counter. This means the fitting process for the peak area determination contributes obviously additional errors to the measurement result of the proportional counter.

The better energy resolution also increases the instrument sensitivity, which is reflected in the significantly improved estimates for the detection limits  $d_{\text{LOD}}$  of the SDD setup.

The analyzed volume of very thin layers and very small features is very small; for a layer thickness of 10 nm, it is only a few cubic micrometers. To collect enough fluorescence intensity from these small volumes, it is necessary to focus an incident beam with high intensity onto these small areas. This is only possible using polycapillary X-ray optics. In addition, the detector must have an energy resolution sufficient enough to achieve the peak-to-background ratio necessary for the required sensitivity. Using a grazing incidence geometry or low-energy fluorescence lines, it is further possible to increase the analytical sensitivity. For the grazing incidence geometry, one can achieve higher fluorescence intensities since the path length of the incident radiation within the layer is increased. Using low-energy fluorescence lines requires the measurement in vacuum; the vacuum requirements, however, are not particularly high, and pressures in the range of 20–50 mbar are usually sufficient.

## 14.4 The Analysis Examples of Coated Samples

In the following the analysis of various coated samples and their layer systems will be discussed. The examples will cover different layer structures as well as the already briefly mentioned varying measuring modes.

### 14.4.1 Single-Layer Systems: Emission Mode

Single layers are applied for functional or decorative purposes. A Zn on steel coating, for example, is a functional layer used for corrosion protection,

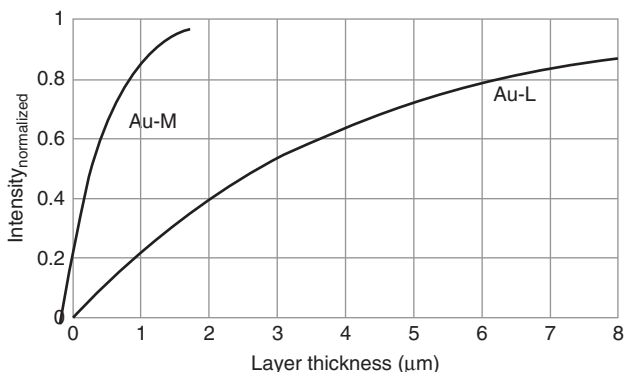


**Figure 14.1** Calibration curves for Au-layers for both Au-L- and Au-M-fluorescence.

Pd coatings on ceramics improve the effectiveness of catalysts, Au coatings on connectors ensure good electronic contact properties and solder pastes are used on PCBs, etc.

Decorative layers are used on consumer goods to improve their appearance (for example, Cr coatings on bathroom fixtures or in the automotive industry), as precious metal coatings on jewelry, or as paint coatings. Often these layer systems meet both application goals. Typical single-layer systems are:

*For the corrosion protection:* Cr/Fe, Cu/Fe, Cd/Fe, Ni/Fe, Ni/Cu, Ni/CuZn, Zn/Fe

*For electrical contact:* Ag/CuZnSnFe, Ag/Al, Au/Ni, Au/CuZnSnFe

It is also possible that the layer consists of an alloy, as in the case of electroless NiP coatings, ZnNi coatings, or solder coatings such as SnPb or a lead-free alloy (SnAgCu).

The excitation conditions are selected such that the elements of the layer are effectively excited. The X-ray lines appropriate for the analysis are selected depending on the layer system and the expected thicknesses of the layers. Figure 14.1 shows the intensities of the Au-L and Au-M radiation as function of the layer thickness normalized to the intensity of an infinitely thick sample.

These curves show the following:

- The fluorescence intensities for very thin layers increase linearly with increasing layer thickness, and the curve then flattens because of the self-absorption and then asymptotically approaches the value of an infinitely thick sample. For very thin layers, the change of intensity allows for high sensitivity because of the steep slope of the calibration curve; however, the statistics of the low intensity signal of the thin layer limits the analytical accuracy. The shallow slope of the calibration curve for thick layers goes along with a decrease in sensitivity, which means that small intensity fluctuations result in significant fluctuations of the measured thickness that causes a poor repeatability. An analysis with acceptable uncertainties is therefore only useful up to a maximum of about 90% of the infinite thickness. The lowest measurement uncertainties can be expected for mid-range layer thickness; however, the absolute values depend of course on the considered element.

- The low-energy Au-M radiation is more readily absorbed within the layer, and the saturation thickness therefore already occurs for much thinner layers than for the Au-L radiation. This can be easily seen by the steeper slope of the calibration curve. As a result, it can be concluded that the low-energy radiation of an element is more sensitive for the analysis of very thin layers.

The measurement time is set to meet the required accuracy. It should be considered that layer thicknesses are rarely homogeneous. Depending on the coating method, thicknesses can vary across a coated area between 1% and 10%. The measurement time should be selected in such a way that the expected statistical error is of the order of magnitude of the variation of the layer thickness. Measurement times of a few seconds are often enough. This is also evident from the example in Table 14.1. Measurement times of 15 seconds for the SDD detector were used to match the variation of the layer system, which means that the relative standard deviation from statistics and the coating thickness are of the same order of magnitude. For the proportional counter, the layer thickness results vary significantly due to the uncertainties in the peak area calculation; even for a measuring time of 5 seconds, the statistical error would not significantly contribute to the measurement uncertainty.

There are many different coating systems. Even for single-layer systems, the composition of the layer and its thickness and the composition of the substrate can vary. For multilayer systems, the combination of sample parameters becomes even greater. This makes the availability of suitable reference samples complicated; particularly for very thin layers of reactive materials, the layers are then not stable over a longer period of time, but they can corrode or diffuse.

A distinction is made between calibration foils and solid standards, i.e. hard-plated standards. Foils thicker than about 1  $\mu\text{m}$ , depending on the layer material, can be produced as self-supporting films, while foils as thin as 50 nm can be produced with thin polymer films as support. Foils can be stacked on substrates of different composition, and it is also possible to stack several layers of the same composition to produce thicker layers. Thin air layers between the individual films are negligible for layer thicknesses  $>1 \mu\text{m}$ . Calibration foils should not be stacked if low-energy lines are used for calibration. Stacking of multiple foils of various elements especially for thin PCB applications such as Au/Pd/Ni/Cu/PCB is also not recommended. In this case stacking multiple foils with several polymer films in between will have an absorption and geometry effect. The advantages of separate layers on foils are that they will not create intermetallic compounds with the substrate and that they can be used for calibration on different substrate materials. This is important since different substrates can have a big influence on the measured intensity especially for very thin films.

The advantage of hard-plated standards is that they are easier to produce and more robust. They are not as easily damaged as foils when used for contact measurement, for example, with handheld XRF. Hard standards can also have better uniformity since not all pure element standards can be easily rolled into thin films.

To achieve the best calibration results, it is recommended that the calibration samples closely represent the makeup and thickness range of the coating system

that needs to be analyzed. It is not advisable to calibrate thicknesses in the tens of nanometers with several micrometer thick foils.

National standards labs such as NIST or BAM only offer a very limited number of certified thickness standards. The whole range of commercially important thickness standards are offered by companies such as MicroMatter, Helmut Fischer GmbH, and Calmetrics Inc. (see Section B.2.2). The certification of layer thickness reference samples can be carried out, for example, with gravimetric methods, with Rutherford backscattering (Götz and Gärtner 1988), with profilometry, or with a reference-free evaluation of synchrotron measurements (Hönicke et al. 2015; Unterumsberger et al. 2011). The abovementioned companies offer calibration standards certified according to ISO 17025.

Quantification of layer systems can be performed standard-based or standard-less as discussed in detail in Section 5.6.3. The achievable accuracies are similar for both quantification methods. Under ideal test conditions, the repeatability and trueness for single-layer systems are in the range of 1–3% depending on the layer thickness.

#### 14.4.2 Single-Layer Systems: Absorption Mode

For light element layers whose fluorescence intensity is low and whose radiation in addition will be absorbed in air, the layer thickness can be determined by analyzing the absorption of the substrate radiation in the layer.

The absorption mode can preferably be used for single-layer systems since only one measurement parameter, the fluorescence intensity of the substrate, is available for evaluation.

Typical applications where the absorption mode is used are layer systems of Al and Si and even carbon-containing layers such as paints or plastics on different substrates. If the substrate is made of several elements, the fluorescence radiation of the element that has the largest measuring effect, i.e. sufficient absorption but enough fluorescence intensity, should be used.

The excitation conditions for the layer analysis must be selected such that the substrate radiation is effectively excited. The measuring time is selected in order to achieve the required accuracy.

Reference samples can be used in the same way as for the emission method. Similar restrictions apply regarding their availability, design, and stability.

If a vacuum capable instrument is available, the emission signal of the light elements may also be used for the evaluation, assuming that it is detectable.

An application example for the absorption method is the analysis of Al layers on an Fe substrate. The test conditions were 40 kV and 200  $\mu$ A with a measurement time of 20 seconds.

The right-hand side of the  $y$ -axis in Figure 14.2 shows the measured Fe intensities plotted against the layer thickness (open squares). The left-hand side of the  $y$ -axis gives the relation between the analyzed and given layer thicknesses of the plotted calibration line.

The achievable accuracies depend on the test conditions and the thickness of the coating. In the case of a careful calibration, they are essentially determined by the statistical error.

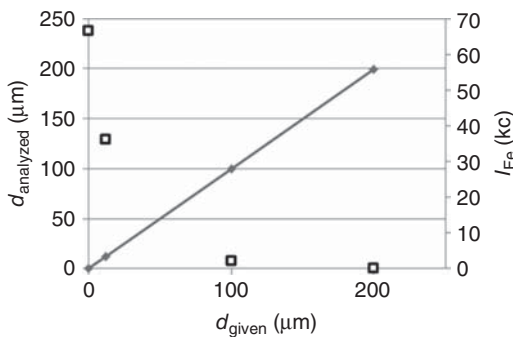


**Figure 14.2** Calibration curve for Al layer thickness based on Fe absorption.

At ideal measuring conditions, accuracies of about 3–5% can be achieved using the absorption mode for single-layer systems.

### 14.4.3 Single-Layer Systems: Relative Mode

#### 14.4.3.1 Analytical Problem

This measurement mode can be used to determine layer thicknesses as well as the composition of alloy layers, especially for cases where the given instrument geometry cannot be met, for example, for concave sample surfaces or for samples with a high aspect ratio, where the measurement distance cannot be adjusted as required. It even can be used if the structures that need to be measured are smaller than the exciting beam size, in which case the surrounding area of the measurement location will be excited too.

Any deviation from the measuring geometry results in a change to the intensity of the measured radiation, which will lead to an error during quantification. Using both emission and absorption signals, it is possible to correct such deviations with this relative method.

Preparing the sample is usually not possible because a preparation would destroy the sample. The relative mode allows for measurements where it is not necessary for the sample to be at the exact measurement geometry. Nevertheless, attempt should be made to carry out the measurements as close as possible to the required geometry and to surfaces that are parallel to the sample stage.

#### 14.4.3.2 Variation of the Specified Working Distance

By using the relative mode, variations in the working distance can be corrected. This is demonstrated in Figure 14.3, in which the layer thickness results of an approximately 50 nm thick gold layer were determined at varying working distances. The working distance changed by  $\pm 5$  mm. The results of the emission mode show a variation of the calculated thicknesses from 37 to 67 nm; this is a change of about  $6\% \text{ mm}^{-1}$ . On the other hand, the results for the relative mode change only little, and all results are close to the nominal thickness of the sample. The results are superimposed by the statistical variation of the analysis results, and the variation is only slightly larger than the normal measurement repeatability.

**Figure 14.3** Results of coating thickness measurements in relative and emission mode.

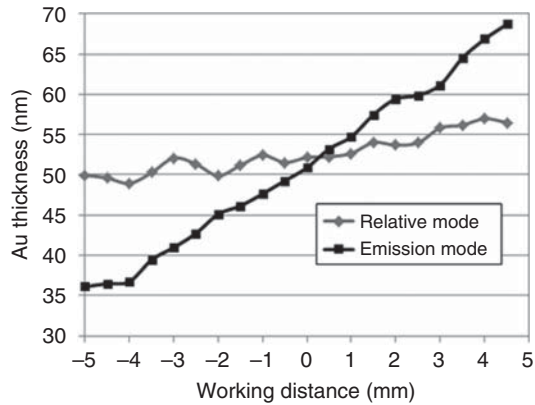
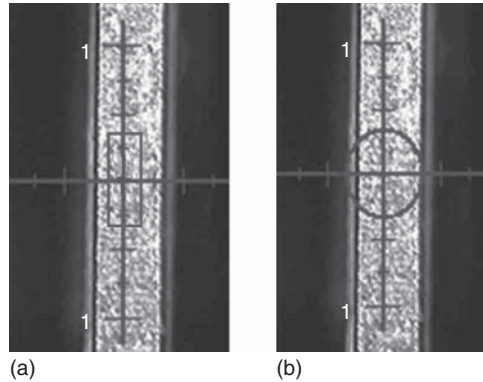


**Figure 14.4** 0.2 mm wide Au/Ni/Cu coated area on PCB using a spot size of  $0.1 \times 0.3 \text{ mm}^2$  (a) and  $\varnothing 0.3 \text{ mm}$  (b).



The achievable accuracies for the relative mode are comparable with those of the emission mode when using the same measurement geometry; for large deviations from the measurement geometry, slightly greater uncertainties are to be expected, which are, however, significantly smaller than those for the emission mode.

#### 14.4.3.3 Sample Size and Spot Size Mismatch

For very small homogeneous sample surfaces, it is possible that the X-ray spot size exceeds the size of the area to be analyzed, which means that not only the intended sample area but also the surrounding area is being irradiated and will contribute to the measured signal. If in this case the relative mode is used, a correction is possible too.

Measurements of Au and Ni coatings on a Cu base are used as an example. This application is typical for contact and bonding surfaces on PCBs. The 0.2 mm wide contact surface is shown with collimator images of two different sizes to the sample area mismatch in Figure 14.4.

The analysis results for the different spot sizes and quantification modes are summarized in Table 14.2. Additional collimator sizes were used where the mismatch between spot size and sample area varies between 70% and 100%. The relative standard deviations of the measurements  $\sigma_{\text{rel meas}}$  for the relative mode

**Table 14.2** Coating thickness results of an Au/Ni/Cu layer system evaluated in emission and relative mode.

Spot size (mm)	Sample area covered by spot size (%)	Au emission ( $\mu\text{m}$ )	Au relative ( $\mu\text{m}$ )	Ni emission ( $\mu\text{m}$ )	Ni relative ( $\mu\text{m}$ )
0.1 $\times$ 0.3	100	0.248	0.256	2.17	2.47
0.2 $\times$ 0.2	About 95	0.218	0.261	1.92	2.52
$\emptyset$ 0.3	About 80	0.181	0.265	1.65	2.51
$\emptyset$ 0.5	About 70	0.156	0.273	1.51	2.49
	$\sigma_{\text{rel meas}}$	16.3%	2.8%	13.5%	0.9%

are comparable to the statistical variation, i.e. 2.8% for the Au and 0.9% for the Ni layer thickness, and the variations of the values in the emission mode are significantly larger and for both layers in the range of 15%.

The data shows that when using the relative mode, it is possible to compensate intensity differences due to deviations from the given measurement geometry. Therefore an improved analytical accuracy is achieved.

#### 14.4.3.4 Non-detectable Elements in the Layer: NiP Layers

Nickel is an often used surface coating. It is usually electroplated; this of course requires an electrically conductive substrate. If the parts are not conductive, for example, plastics, electroless plating Ni plating, an autocatalytic plating process, is used. The process deposits a Ni–P alloy. Depending on the application and required properties, the NiP coating can contain between 2% and 14% P. For an accurate thickness analysis of the coating, both the Ni and P concentrations must be known. The P content changes the density of the coating and therefore the calculation of layer thickness. The P content also influences the mechanical and corrosion resistance properties of the coating; it is therefore important to be able to measure the content within an uncertainty of approximately 1 wt%. Because of the low energy of the P radiation, a direct determination of the P content usually requires the measurement in vacuum. However most coating thickness instruments do not have a vacuum chamber. The direct determination of P in air is only possible with instruments with SDD detectors with a thin detector window and at very close measurement distances. This adds additional costs to the instrument, and they are usually not common in general plating shops. It is however still possible to use non-SDD detector instruments if in addition to the Ni signal also the signal from the substrate is evaluated, i.e. a relative mode is used for the evaluation (ASTM-B\_733 2015). This works well for Fe substrate, Cu and Al substrates are already problematic because of the closeness in energy of Cu and Ni radiation, and Al does not give a measurable substrate signal.

Simulated spectra of a 5  $\mu\text{m}$  thick NiP/Fe system with different P contents are displayed in Figure 14.5. Due to the measurement in air and the thick detector window, there is no P signal. As can be seen, the P in the layer reduces the absorption of the Fe fluorescence from the substrate i.e. the Fe intensity increases with increasing P content. The Ni intensity, on the other hand, decreases with



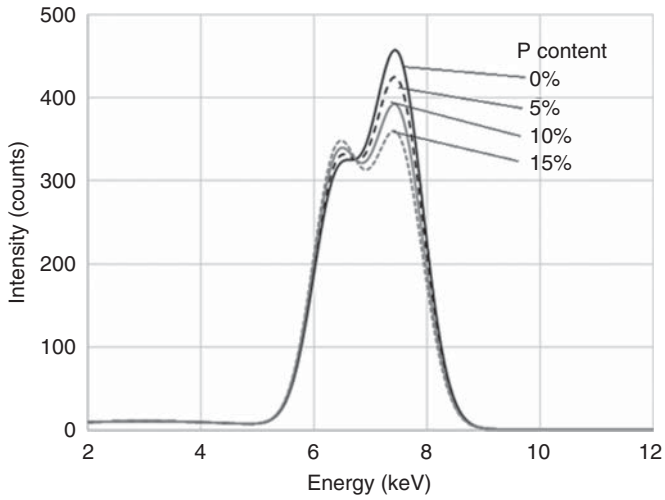


**Figure 14.5** Simulated spectra of a 5  $\mu\text{m}$  NiP/Fe system with different P content for a prop-counter instrument.

increasing P content caused by the reduced Ni content in the layer. The intensities of Ni and Fe as well as their intensity ratio can be used for the determination of both layer thickness and P content.

The analytical performance for the determination of the P content for different coating thicknesses and P contents is illustrated in Figure 14.6, and the measurement time was 30 seconds. It can be seen that for thick layers and high P content, the agreement is very good and the differences are less than 0.5 wt%. For these samples the effect of P is relatively large. For lower P concentration or thinner layers, the results deviate much more. It can be concluded that for thicker layers than 5  $\mu\text{m}$  and P contents greater than 4 wt%, an indirect determination of the P content for a NiP/Fe system is possible even with prop-counter instruments.

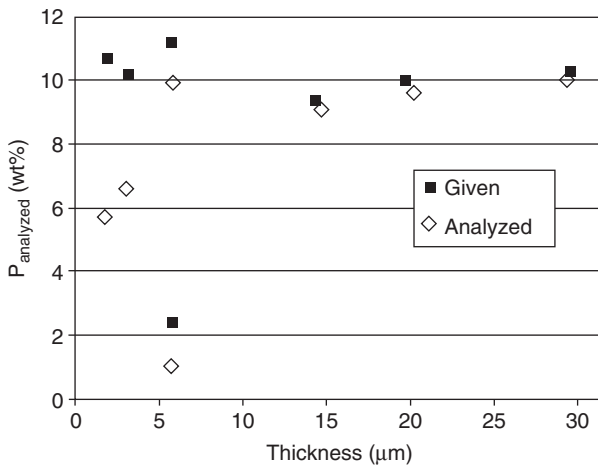


**Figure 14.6** Comparison of given and analyzed P contents in NiP layers.

For a measurement time of 30 seconds for 12 repeated measurements, the following results were obtained:  $12.9 \pm 0.1 \mu\text{m}$  and  $9.40 \pm 0.25 \text{ wt\% P}$ . The results are comparable with a direct analysis with more expensive instruments, with which only the uncertainty of the thickness can be slightly reduced (Rössiger and Conrad 1989).

#### 14.4.4 Characterization of Ultrathin Layers

Layer thicknesses below 50 nm require special measuring conditions because of the very low signal intensities the thin layers generate. Examples for such layer systems are found in microelectronics and leadframe applications where only a few nanometers of Au and Pd are plated IPC-4552 (n.d.), IPC-4556 (n.d.). Typical layer systems are ENIG (electroless nickel, immersion gold) and ENEPIG (electroless nickel, electroless palladium, immersion gold), which are plated on Cu/PCB and Cu alloys such as C19 or on Si<sup>4</sup>. In addition, the features that are plated are very small; they can have dimensions down to 50  $\mu\text{m}$  or even smaller.

High excitation intensities are required to obtain sufficiently fluorescence intensities from these small features and thin coatings. The applications are best measured using EDS instruments with X-ray optics. They are available with different detectors: prop counters with an energy resolution of approximately 1000 eV, PIN diodes with an energy resolution of 200 eV, or SDDs with an energy resolution of approximately 140 eV. Because of the thin layers and various peak overlaps, for example, Au-L $\alpha$  with Cu-K $\alpha$ , Au-L $\beta$  with Br-K $\alpha$  (used as fire retardant in PCBs), or Pd-L with Ar-K (for measurements in air), a high energy resolution detector is helpful. With an SDD, moreover, lower energies can be detected due to the available thin detector windows. For measurements where a vacuum system can be used, an additional improvement of the sensitivity is possible using low-energy lines. Their calibration curves have a steeper slope for thin layers (see Figure 14.1).

A spectrum measured with an SDD on an Au/Pd/Ni/Cu system in vacuum is shown in Figure 14.7. It illustrates the good energy resolution of the SDD that separates the different lines and allows the use of the higher sensitive Au-M and Pd-L radiation for the quantification.

Another possibility to increase the sensitivity for very thin layers is exciting under very small incident angles. In this case, a larger part of the primary radiation is absorbed in the upper surface layer, thus producing higher fluorescence intensities. However, there exist some restrictions: this special measurement geometry requires special instruments (see Section 4.3.3.8), and this type of analysis is possible only for larger areas because the excitation beam spot is enlarged by the grazing incidence.

Measurement results with three different detectors are summarized in Table 14.3. Shown are the absolute (nm) and relative (%) standard deviations for two Au/Pd/Ni-standards:

*Standard 1:* Au: 13 nm, Pd: 16 nm, Ni: 2000 nm

*Standard 2:* Au: 49 nm, Pd: 327 nm, Ni: 2700 nm

For both standards, 10 repeated analyses were done, 30 seconds each.

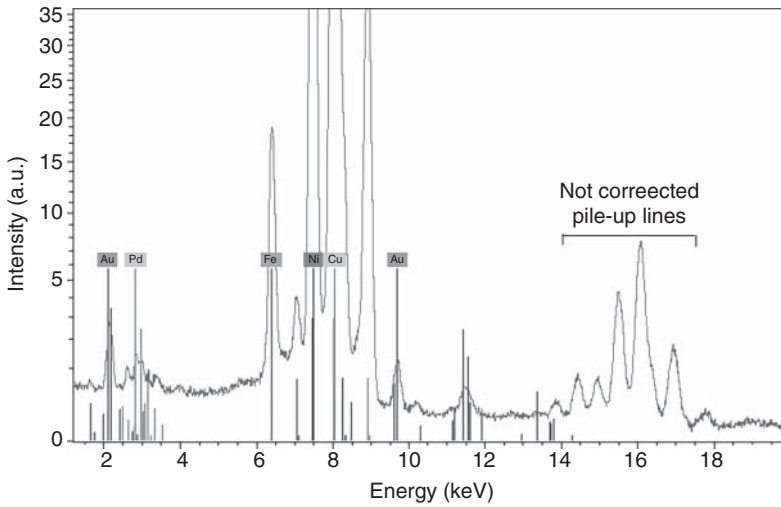


**Figure 14.7** Spectrum of an Au–Pd–Ni layer system.

**Table 14.3** Absolute and relative standard deviations of 10 repeated measurements on two Au/Pd/Ni standards 30 seconds each.

Detector	Prop-counter	PIN-diode	SDD
Energy resolution (eV)	950	200	150
Intensity (cps)	9500	4400	55 000
Spot size ( $\mu\text{m}$ )	250	350	60
Thicknesses of the reference samples	Absolute (nm) and relative (%) standard deviations For the 10 repeats		
Au: 13/49 (nm)	Abs.: 2.4/2.4 Rel.: 18/4.9	1.2/2.1 9.2/4.3	0.7/0.4 5.4/0.8
Pd: 16/327 (nm)	Abs.: 3.6/6.3 Rel.: 22/1.9	5/8 31/2.4	2.2/1.4 13/0.4
Ni: 2000/2700 (nm)	Abs.: 46/124 Rel.: 2.3/4.6	23/17 1.1/0.6	2.9/2.5 0.2/0.01

The following conclusions are possible from these results:

- With all three detectors, depending on the measurement specifications, the analysis is theoretically possible; however, the analysis quality is significantly improved with better energy resolution of the detector. In practice proportional counters should not be used.
- For SDDs this improvement is also a result of their higher count rate capability and higher excitation intensity by using X-ray optics that concentrates a high amount of primary radiation to the analyzed area.

**Table 14.4** Selection of reference standards and their uncertainties (95%).

Standard	Au (nm)	Pd (nm)	Ni (nm)
1	213.8 ± 2.6		103.6 ± 4.1
2	486.8 ± 4.7		250.4 ± 8.5
3	117.5 ± 1.3		2510 ± 35
4	114.1 ± 1.3		5710 ± 46
5	28.4 ± 0.6		2217 ± 32
6		21.6 ± 0.6	2101 ± 35
7		87.3 ± 0.9	2363 ± 33
8		333.2 ± 2.6	2263 ± 29
9	48.1 ± 0.7	21.1 ± 0.8	2211 ± 33
10	44.0 ± 0.7	92.1 ± 0.9	2354 ± 35
11	45.8 ± 0.7	331.7 ± 2.7	2693 ± 30
12	11.8 ± 0.2	18.7 ± 0.4	2425 ± 34

- A further improvement is caused by the use of the low-energy Au-M- and Pd-L-lines with their steeper slope of the calibration curve.
- The standard deviations of the hidden layers of comparable thickness are larger due to the error propagation from the upper layer(s).

The trueness of the analysis results can be assessed by measuring reference samples. Table 14.4 gives the analytical results of measurements for several reference samples. It demonstrates that even for these thin layers, adequate accuracies can be achieved.

#### 14.4.5 Multilayer Systems

##### 14.4.5.1 Layer Systems

Most coating systems for functional or decorative purposes are multilayer systems. Several layers can be used to ensure adhesion of the layers to the substrates, to ensure a cost-effective production, and to ensure the desired functionality of the layer systems.

For the vast amount of plating applications, hundreds of different layer systems are in use; therefore only a few selected can be mentioned here, for example:

- *Decorative coating systems:* Cr/Ni/Cu/ABS (bathroom fittings, automotive parts), Cr–Ni/Fe (corrosion protection)
- *Functional layer systems:* ZnO/CdS/CuInGaS/Mo/glass (solar cells), Pd/Cu/ZrO (catalysts)

Two examples will be discussed in more detail to demonstrate the complexity of these layer systems and the achievable analytical performance.

#### 14.4.5.2 Measurement Technology

For most applications the same instruments can be used as for single-layer applications. However, more and more spectrometers with high-resolution semiconductor detectors are being used for more challenging applications, in particular when multiple line overlaps occur. This allows for both better sensitivities and better accuracy of the analysis. However, high enough excitation intensities are required because of the small effective areas of the detectors.

The analytical accuracy that can be achieved depends very much on the individual layer system and on the sequence of the layers within the system. Higher accuracies can be expected for the top layers than for layers that are covered. The determination of the fluorescence intensities of the elements of covered layers has a higher statistical error and is also influenced by the uncertainty in the calculation for the covering layers. This results in a fault propagation from layer to layer. In general, the accuracies of the top layers are comparable with those of single-layer systems. The uncertainties for the covered layers increase by approximately 3–5% with each additional layer.

#### 14.4.5.3 Example: Analysis of CIGS Solar Cells

Modern thin film solar cells are often designed as a ZnO/CdS/CuInGaSe/Mo/glass layer system. In this case, the top layers are required for passivation (ZnO) and contact by a n-type semiconductor (CdS). In the p-type CuInGaSe (CIGS) semiconductor absorber layer, the conversion of light energy into electricity takes place, and the Mo layer is a contact layer again. This structure is shown in Figure 14.8 with thickness ranges typical for this layer system. The composition of the absorber layer is particularly important for the efficiency of the solar cells and must be monitored carefully. In-process monitoring of the composition is, therefore, a prerequisite in the production of the solar cells. This means that the analysis needs to be done in-line, directly after the deposition of the CIGS layer.

The X-ray lines representing the layer elements are well separated and can be easily determined. However, the determination of the In intensity is problematic because the K-radiation (24.2 keV) is poorly excited and the L-radiation (3.3 keV) is already significantly absorbed in air. Nevertheless, the determination of all layer parameters is possible with a single measurement.

Table 14.5 provides information on the accuracies that can be achieved. Here, the analysis results of the layer stack were obtained after each individual



Figure 14.8 Design of CIGS solar cells.

**Table 14.5** Measurement results of a CIGS layer system.

Layer system Elements	Mass fractions (wt%)				Coating thickness ( $\mu\text{m}$ )			
	Se	In	Ga	Cu	Mo	CIGS	CdS	ZnO
Mo-CIGS	52.7	19.6	8.9	18.8	0.27	1.51		
Mo-CIGS-CdS	52.5	20.0	8.8	18.7	0.27	1.53	0.10	
Mo-CIGS-CdS-ZnO	53.1	20.1	8.7	18.1	0.28	1.58	0.10	1.50
EDS	52.1	20.0	9.0	18.8				
Profilometer						1.5		

Source: Wittkopp et al. (2000).

production step was completed, i.e. the composition of the absorber layer and the thicknesses of the applied layers were determined each time subsequently after the application of the absorber layer, the CdS layer, and the ZnO layer. For validation, a direct determination of the composition of the absorber layer in an electron microscope with an EDS system and the layer thickness of the absorber layer with a profilometer was carried out. These measurements show that the results of the X-ray spectrometer are consistent independent of at what step in the production process the measurement were made; in addition, they also match the results of the reference methods well. This application demonstrates well the capabilities and the performance of X-ray spectrometry even for complex layer systems. However, no other analytical method can provide equivalent results in an in-line environment.

#### 14.4.5.4 Example: Analysis of Solder Structures

Electronic solder joints can be very complex in geometry, size, and thickness, depending on the type and shape of the electronic components being soldered. The characterization of both composition and thickness is important. This is only possible when for every parameter that is measured one separate fluorescence line is available. Since the analyzed volumes are again very small, the analysis is complicated by the low fluorescence intensities.

The application in this example is a multilayer system consisting of a SnPb solder on a Ni diffusion barrier on an AgPb metallization layer plated on a ceramic substrate. Two layers of this system contain Pb (Figure 14.9). For the determination of their thicknesses and composition, it is necessary to use different fluorescence lines of Pb. The low-energy Pb-M-radiation and the Sn-L-radiation can be used for the characterization of the upper layer because their information depth is very small, i.e. the fluorescence intensity detected can only be from the top SnPb layer. On the other hand, the Pb-L- and Sn-K-radiation with their higher energies can be used for the characterization of the AgPb metallization layer. Because the element concentration in an alloy layer needs to add up to 100%, it is only necessary to quantify one element in a binary alloy; therefore two signals are sufficient to determine both thickness and composition. A typical analytical result for such a layer system is summarized in Table 14.6.

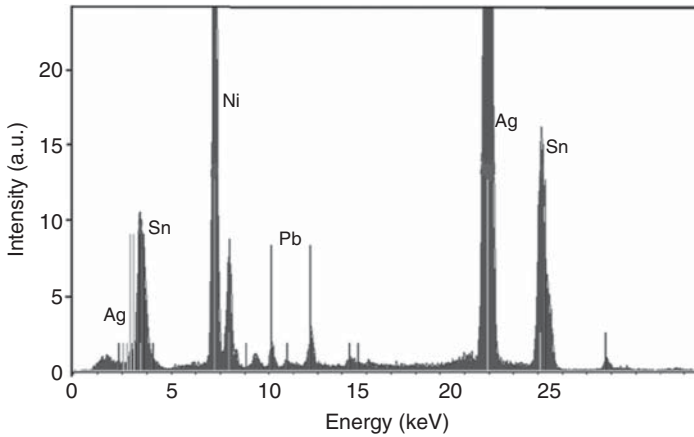


**Figure 14.9** Spectrum of a SnPb solder system.

**Table 14.6** Characterization of a SnPb/Ni/AgPb/ceramic system.

Layer	Thickness ( $\mu\text{m}$ )	Composition (wt%)
1. SnPb	$1.9 \pm 0.04$	Sn: $100.0 \pm 0.18$ Pb: $-0.02 \pm 0.02$
2. Ni	$1.3 \pm 0.007$	
3. AgPb	$33.0 \pm 0.5$	Ag: $98.3 \pm 0.05$ Pb: $1.74 \pm 0.05$

It should be noted that even though the application is defined to measure Sn and Pb in the top layer, the analysis correctly identified the top layer as a pure Sn solder. This is not trivial especially for Restriction of Hazardous Substances (RoHS) applications where lead-free solder needs to be identified. But even more important is that the Pb from the AgPb metallization layer is not attributed to the top Sn layer. This is important for high reliability applications where Sn whisker growth needs to be avoided, which is achieved for solders containing more than 3% Pb.

#### 14.4.6 Samples with Unknown Coating Systems

With the previously described measurement modes, only known layer structures can be investigated, which means that the layer sequence and the elements of the individual layers must be known to correctly interpret the fluorescence intensities. The advantage is that the method is nondestructive and the samples are available for further use after the analysis. If, however, layer systems need to be measured where neither the layer sequence nor the elements in the layers are known or where the layers have even a concentration gradient, other methods are required. Some of the methods that utilize XRF but require a special sample preparation or specific measurement geometries are briefly presented here. Further also fundamental-parameter based total pattern fitting algorithms with

an intelligent use of the goodness-of-fit parameters can be utilized to identify unknown layer structures.

#### 14.4.6.1 Preparation of Cross Sections

If a coated sample is cut perpendicular to the surface, the layer structure is visible in a cross section. The cross section can then directly be examined, for example, with microscopes. The layer thicknesses can be determined optically (ASTM-B\_487–85 2013); the composition of the layers can be determined using spatially resolved analysis methods. For this purpose, the spatial resolution of the instrument then must be adapted to the thickness of the layers. A frequently used method is the excitation of the XRF with electrons in an electron microscope. Very small spot sizes can be achieved since electrons can be strongly focused. However, the time and effort for such an analysis are relatively high, since the sample not only has to be cut but also needs to be polished and, if not conductive, needs to be coated to make it electrically conductive. Furthermore, the measurement needs to be done in vacuum, which puts additional demands on the sample type.

Another possibility is the excitation with X-rays; the smallest spots that currently can be achieved are in the 5–10  $\mu\text{m}$  range, which means that depending on the layer system, they are similar to the thicknesses but can also be significantly larger than the thicknesses to be measured. Care must be taken in the preparation of the cross sections, which needs experience and practice. The layer structures can be broadened if they are cut at an angle or tilted during polishing of the samples, as shown in Figure 14.10. This can also be done deliberately at a known angle in order to increase the measurable surface.

For the analysis of cross-sectioned samples as shown in Figure 14.10, commercially available  $\mu\text{-XRF}$  instruments can be used. Figure 14.11 shows an example of a low-alloy steel, which is coated with a Zn-Al coating for corrosion protection. The layer structure was polished at an angle of  $5.7^\circ$ . This broadens the structures by a factor of 10. The result of a distribution analysis of the polished sample is shown in Figure 14.11a for the elements Fe, Zn, and Al. The measurement technique used for the distribution analysis with  $\mu\text{-X-ray}$  is described in more detail in Chapter 16.

The distribution of the elements on a line perpendicular to the layer structure is shown in Figure 14.11b. It shows the Fe substrate (red), which has a Fe content of 99.4 and 0.6 wt% Mn. The substrate is coated with an approximately 2–3  $\mu\text{m}$  coating of Al and a final Zn cover layer. From the distribution curve, it can be

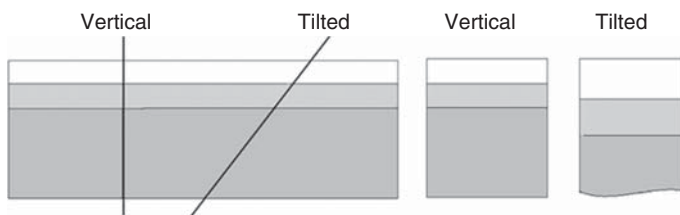
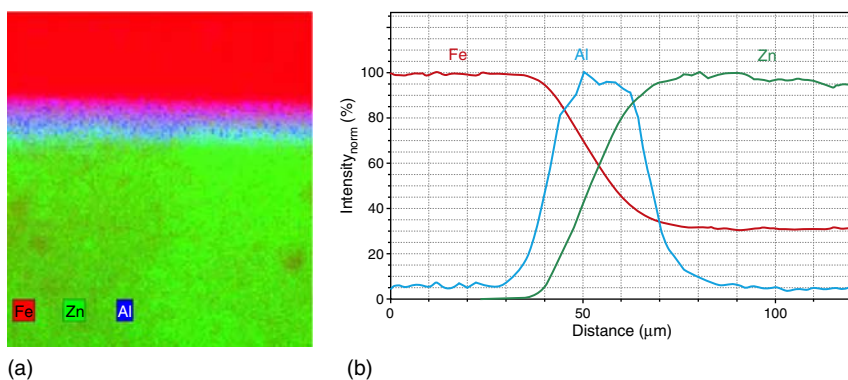


Figure 14.10 Layer structure form a vertical and tilted polished section.





**Figure 14.11** Element distribution in a cross section (a) and along a line perpendicular to the layer structure (b).

concluded that the layers are not clearly separated, but that the Al has diffused into both the Fe substrate and the Zn cover layer. In the element distribution map, this can be seen in the mixed colors; the line scan in Figure 14.11b shows the overlap of the individual distributions directly. The use of the Al intermediate layer improves the protection against electrochemical corrosion, especially when exposed to water, since the relatively large difference in the redox potential of Fe and Zn is reduced by Al.

#### 14.4.6.2 Excitation at Grazing Incidence with Varying Angles

When radiation hits a sample, it penetrates the sample and generates fluorescence radiation. The absorption length depends on the energy of the incident radiation and the mass attenuation coefficient of the analyzed sample. However, the penetration depth normal to the surface depends on the incident angle of the radiation with respect to the sample (see Figure 4.34). Here, the incident radiation hits the sample at different shallow angles, and the penetration depths for the same absorption length vary with the incident angle.

When the fluorescence radiation is detected perpendicular to the sample surface, different spectra as a function of the incident angle are produced. At higher incident angle, deeper layers are excited. This allows to determine the layer sequence as well as their composition by comparing spectra measured at different incident angles.

The grazing incidence of the primary radiation gave the method its name – grazing incidence X-ray emission (GIXE).

This analysis method is also nondestructive but requires an instrument that can vary the incident angle of the primary radiation. Commercially, instruments for coating thickness testing using this method are not yet available. However, this method is still primarily used in experimental setups, such as at synchrotrons. Moreover, newer total reflection X-ray fluorescence (TXRF) instruments will offer the possibility of tilting the sample or changing the tube position; in this way the measuring geometry can be adjusted.

The interpretation of the data requires complex calculations. They are currently only possible with a forward calculation based on an assumed layer model. Due

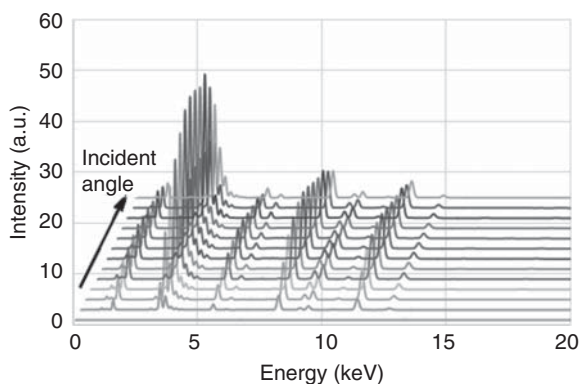


**Figure 14.12** Spectra of a CIGS layer system measured with grazing incidence. Source: Courtesy of B. Kanngießer, TU Berlin.

to this higher effort in data evaluation and collection, this method is currently primarily used for research purposes and is not yet available for routine analysis.

In the following, an application example of the method for the CuInGaSe system, which was already discussed in Section 14.4.5.3, is presented. Figure 14.12 shows spectra that were measured at different incident angles for this layer system (Spanier et al. 2016). The spectra were acquired at excitation voltages of 25 kV and with measurement times of 100 seconds each. A polycapillary optics with a small exit beam divergence was used to excite the sample. On the detection side an SDD with an effective area of 30 mm<sup>2</sup> was used. The incident angles were increased by 0.5° for small angles and by 1° and 5° for larger angles.

It was found that at very small angles the excitation of the sample was very low, with increasing angles; however, the fluorescence intensities of the absorber layer elements (Cu, In, Ga, Se) increase. These intensities decrease again at the larger angles because of the absorption of the incident radiation through the layers. Mo is the exception; it is the contact layer that is deposited directly on the glass substrate and it is covered by the CIGS layer. The intensity profiles, as a function of the incident angle normalized to the intensity maximum of each element, are shown in Figure 14.13. It shows that the intensity profiles of the elements of the absorber layer differ slightly from each other. As a result of the unfavorable excitation conditions for the Mo-K radiation, its fluorescence intensity is relatively small; however, it shows a noticeable increase at larger incident angles when Mo is excited sufficiently as the primary beam reaches the deeper layers of the sample.

The varying distribution of the intensities of the absorber elements depends on their different energies, but they will also be influenced by concentration gradients in the composition of the absorber elements. In the absorber layer, a gradient of the Ga concentration is desired to optimize the efficiency of the absorber for the respective radiation energy by adjusting the associated bandgap. The setting of this gradient must be adjusted by the production technology and therefore needs to be monitored. The intensity profiles of the fluorescence radiation of the absorber elements can be used for this purpose. Using a forward calculation for an assumed layer model, the intensity profiles for the individual elements are calculated and compared with the measured intensity profiles. To obtain correct results, for these calculations, corrections must be carried out with respect to the

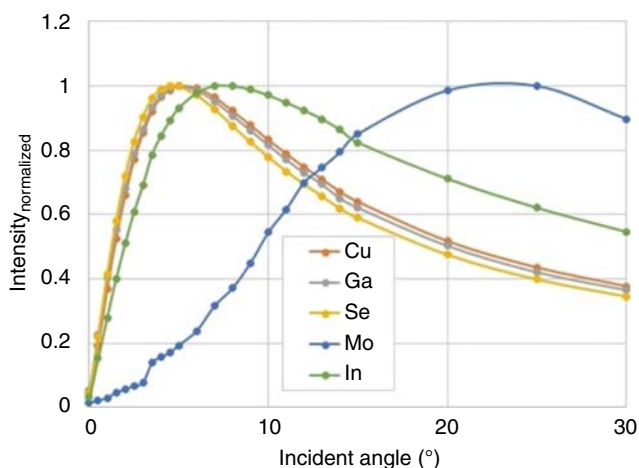


**Figure 14.13** Intensity profiles of the components of the CIGS layer system for different incident angles. Source: Courtesy of B. Kanngießer, TU Berlin.

excitation geometry and the excited sample volume as a function of the incident angle.

By means of iteratively changing the layer model, it can be presumed that the assumed layer model represents the analyzed layer system well if the calculated (solid line in Figure 14.13) and the measured (dots in Figure 14.13) intensity profile matches.

This method allows for the nondestructive characterization of unknown layer structures, including concentration gradients in the individual layers. The measurement and the computational effort, however, are very high, so the use as a process-oriented quality control method is not possible. Important information can nevertheless be gained during technology development.

#### 14.4.6.3 Measurement in Confocal Geometry

A further possibility to investigate unknown layer sequences is using a confocal measurement geometry (see also Figure 4.33). Here, both the incident radiation and the fluorescence radiation are localized by X-ray optics and define in this way a volume element that exclusively contributes to the measurement signal. If this volume element is moved all over the sample, it is possible to investigate both unknown and nonhomogeneous layer structures.

The focusing achievable with capillary optics allows volume element diameters down to 20  $\mu\text{m}$ . However, this is already close to penetration depth for many materials. Therefore, this analytical method can only be used for light matrices (see also Kanngießer et al. 2005; Mantouvalou et al. 2011; Mantouvalou 2016). This method, nevertheless, is very interesting for the characterization, for example, of pigment multilayers on art objects. With this method it is possible to determine three-dimensional element distributions; however, the measurements are very time consuming because several two-dimensional (2D) distribution maps at different sample depths must be acquired. Another possibility is the

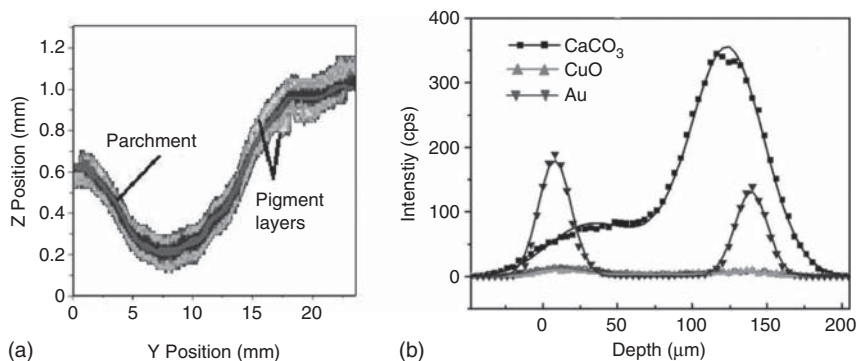


**Figure 14.14** Distribution of pigment layers on both sides of a parchment (a) and the depth profiles of few individual elements (b). Source: Lachmann et al. (2016).

measurement of depth profiles that can provide information about the layer sequence and composition of a layer system in a specific sample position.

Lachmann et al. (2016) describe the investigation of similar pigment layers that were painted on two sides of a parchment. Just a 2D distribution map does not allow to make a clear decision on which side of the parchment a specific pigment is because both excitation and fluorescence radiation penetrates the parchment. Being able to determine the element distributions at different sample levels allows for a clear separation of the pigments from both sides of the parchment, as can be seen in Figure 14.14a. The figure shows the distribution of the pigment elements in a vertical section through the sample, i.e. it shows the distribution on both sides of the parchment. It should be noted that the parchment was not flat and in order to avoid any damages to the parchment, it was neither flattened or tightly clamped down for the measurement (the scaling for y- and x-axis differ by a factor of approx. 20).

The depth profile, shown in Figure 14.14b, results from the measurement of the fluorescence intensities at a line with different depth positions within the sample. From the depth profile, it is then also possible to characterize the thickness of the individual pigment layer. Figure 14.14b shows the measured intensities at various depths in a specific sample position (dots) for the individual elements (or compounds) as well as the intensity profiles determined by a forward calculation for a presumed layer system (solid line).

The agreement between measured and calculated results is very good. It can therefore be assumed that the method allows for the characterization of unknown layer systems, keeping in mind the limitations imposed by the sample matrix and by the spatial resolution.

## 15

### Spot Analyses

#### 15.1 Particle Analyses

##### 15.1.1 Analytical Task

The characterization of individual particles may be necessary for a variety of reasons: it may be for analyzing contaminations in order to determine their origin, making it then possible to locate and eliminate the source of the contamination; it may be for analyzing wear particles in lubricants, which then provides information on the condition of engines or turbines; it may also be for analyzing fragments or chips, which are of forensic interest. Several other reasons exist for making a spot analysis. In Figure 15.1 a particle, whose largest dimension is about 150  $\mu\text{m}$ , is shown together with a 25  $\mu\text{m}$  diameter measurement spot.

When analyzing individual particles, it is essential to determine their material composition in order to make a positive identification. It should be noted, however, that the analysis and their quantification may be accompanied with some complications:

- The surfaces of the particles are usually not flat, which influences the absorption and thus the intensity of the fluorescence radiation, in particular of low-energy radiation.
- Very small particles have usually not the saturation thickness, which means that their thicknesses can be smaller than the information depth of the particular fluorescence radiation. Their intensity depends therefore not only on the concentration of the elements in the sample but also on the particle thickness.
- The surfaces of the particles may be contaminated with material from the source where they were embedded; this may influence the spectrum by an increase the scattering background, or additional elements may be present in the spectrum.

Often the objective of the investigation of particles is not the exact quantification, but the identification of their material, which can already be obtained from intensity or concentration ratios.

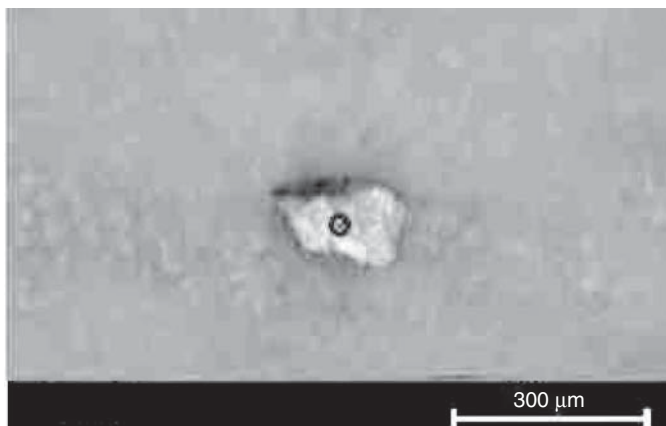


**Figure 15.1** Example of a metal particle; the analysis spot is marked.

### 15.1.2 Sample Preparation

The preparation of individual particles must be done very carefully:

- so that the preparation does not change the composition
- so that during the measurement only the particle contributes to the signal and not its sample holder and
- so that the often very small particles are not lost.

For this purpose, the particles can be positioned on a substrate whose fluorescent radiation is absorbed as far as possible by the particle itself and at the same time only contribute as little as possible to the scatter background. Figure 15.2 shows a sample cup that usually is used for the analysis of liquids, its top covered with a thin plastic foil. The particles can then be positioned on top of the thin foil. The contribution of the very thin foil to the scatter background of the spectrum is negligible, and the light elements of the polymer cannot be detected.

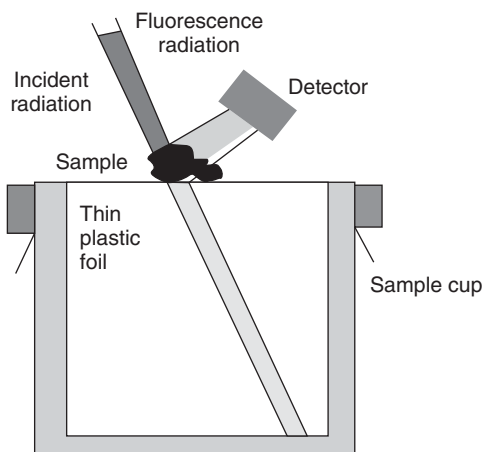


**Figure 15.2** Sample cup with particles.

Individual particles can also be fixed onto the supporting foil. For this purpose, materials must be used, which consist only of light elements and do emit only low-energy fluorescence. Hairsprays have proven to be usable for this purpose if the particle is sprayed with a fine mist of it. Since they are water soluble, the samples can later be easily removed. Before using any hairspray, their spectral purity should be checked.

### 15.1.3 Analysis Technology

Micro-X-ray fluorescence ( $\mu$ -XRF) spectrometers are particularly suitable for this type of analysis. Their spot sizes should be close to the particle sizes. For larger particles, instruments with collimators are sufficient, but for smaller particles, instruments with capillary optics should be used; they are of course also suitable for larger particles.

When using wavelength-dispersive spectrometers (WDSs) instruments, the collimation of the incident radiation onto the particle is necessary. The smallest available collimator sizes for these instruments are in the range of 0.5 mm. Then, however, only a small portion of the primary radiation can be used for the excitation of the sample because the total excitation intensity is only available over the entire sample area (e.g. 30 mm). The intensity decreases with the square ratio of the spot diameters, that is,  $(0.5/30)^2 = 0.03\%$ . This must be compensated with a longer measuring time for a sequential spectrometer even for every individual element.

The test conditions as well as the measurement times must be adjusted to the requirements of the analytical task, i.e. to the elements to be analyzed, as well as to the desired analytical accuracies.

### 15.1.4 Application Example: Wear Particles in Used Oil

As an example, the analysis of two different size steel wear particles, found in a used lubricating oil, is presented. One particle was rather small, close to the information depth, and the other was much larger. The spectra shown in Figure 15.3 were measured with an energy-dispersive spectrometer (EDSs) are normalized to the Ar intensity. The Ar peak is due to the measurement in air. Argon in the air is excited in the path from the sample to the detector and contributes to the overall signal. The peak is suitable for normalization, since for both measurements, the distance from the sample to the detector is constant, and therefore the Ar intensity will also be similar.

The spectrum of the larger particle resembles the spectrum of a bulk sample. No influence due to the size of the sample can be seen. The spectrum of the small particle, on the other hand, is influenced by the sample size, in particular by its thickness, which is close to the information depth of the heavier elements. It shows a larger spectral background for higher energies since the radiation is scattered by the sample holder. Further traces of Cl and Ca are visible due to the particle being contaminated with the used oil. The larger particle did not show these elements because these contaminations could be removed. Due to the overall low intensity of the signal of the small particle, elements of

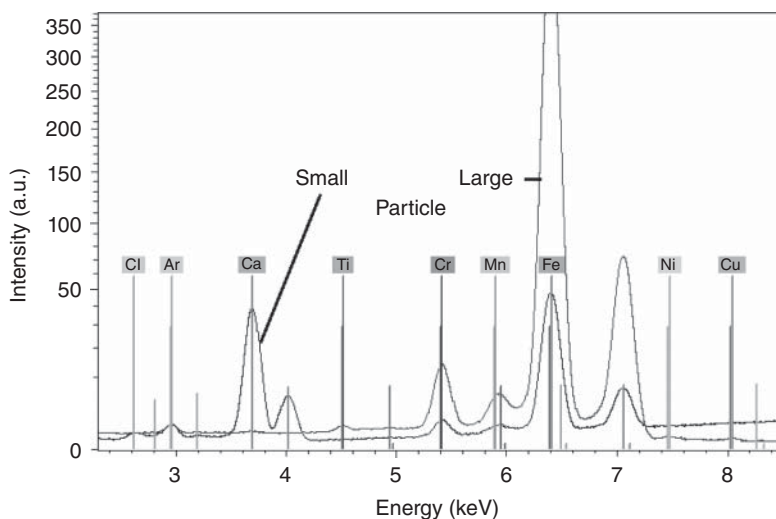


**Figure 15.3** Spectra of two particles of the same material but of different sizes (y-axis in square root scale).

low concentration (here, for example, Ti) cannot be detected. Nevertheless, in general, the spectra coming from the smaller particle are comparable with that of the larger particle and are sufficient to identify the material. This could be achieved, for example, by spectra matching; in addition the quantitative analysis of both particles does not differ significantly from the true composition of the material. This means that even small particles whose dimensions are close to information depth can be identified.

### 15.1.5 Application Example: Identification of Glass Particles by Chemometrics

For forensic applications very often small particles have to be identified. For this purpose  $\mu$ -XRF can be used (ASTM-1926-13 n.d.). Chemometric methods then can be used to characterize particles whose information depths for some of the analytes are larger than the particle dimensions. This demonstrates following example of the analysis of glass particles. The fluorescence intensities in this case will not only depend on the concentrations of the different elements but also on the particle size. In addition, a strong scatter background caused by the light glass matrix interferes with the fluorescent lines. The spectra can be used for element identification, i.e. for a qualitative analysis. However, the intensity ratios of the individual element lines are influenced by the particle size and preclude an exact quantification, sometimes even the positive material identification (PMI) using spectral matching procedures. For quantification it is in principle possible to take the size of particles into account; however this is problematic, since actual particles are usually irregularly shaped and are not ideal spheres or cubes.



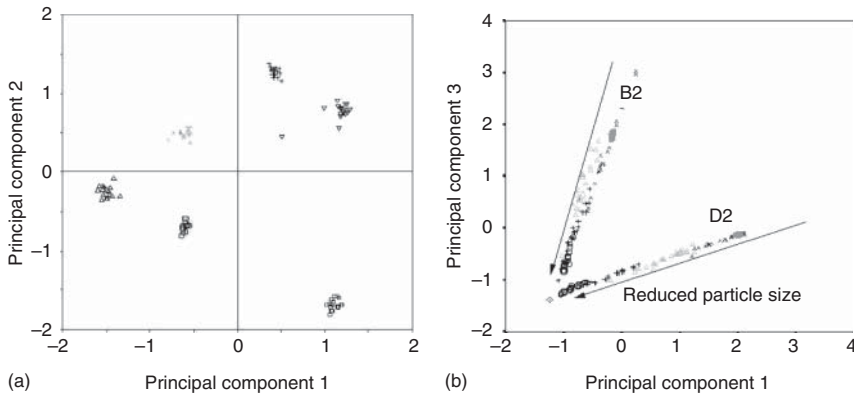


**Figure 15.4** Scores for different principal components for measurements on glass particles. Source: According to Rödel et al. (2002).

To demonstrate the potential of chemometric evaluation methods for material identification, many particles of different size, shape, and type of glass were characterized in terms of their size and then individually measured. Sorting for their size was carried out with a multistage sieve, and the measurements of the individual particles were done with a  $\mu$ -XRF instrument. Influences caused by the sample carrier are not negligible, since the incident radiation passes through the particles. It can be scattered or excite the sample carrier to fluoresce. The radiation from the sample carrier can affect the fluorescence intensity of the particle through secondary excitation, or it can contribute to the spectral background. This effect can be reduced if the sample carrier is a thin foil, as shown in Figure 15.2.

From a principal component analysis (PCA) of the spectra, different information as a function of the various relations between the principal components can be obtained (see, for example, Danzer et al. 2001). The results of such analysis are shown in Figure 15.4a (Rödel et al. 2002). The clusters of the six glass grades investigated can be clearly distinguished. This makes it possible to identify the glass particles according to their chemical composition. Figure 15.4b shows another score here for only two glass types; these results depend clearly on the particle size.

This example demonstrates that chemometric evaluation methods not only allow a material characterization, but even other analytical questions can be answered, which are not approachable for conventional algorithms of spectral processing. However, it must also be mentioned that the method requires both a comprehensive “training” of the system by measuring many test spectra and the appropriate evaluation routines to be adapted separately for each analytical problem. But then, thereafter, the results are available quickly and with high reliability.

Further, an application can always only be used for the “trained” analytical task; when adding a new material or changing the analytical question, the spectral library needs to be expanded with the new data, or a new design of the evaluation algorithms become necessary.

## 15.2 Identification of Inclusions

To identify inclusions in different materials requires, similar to particle analysis, the analysis of small sample surfaces. The analytical problem is therefore very similar to the characterization of small particles, as discussed in Section 15.1. In the case of inclusions, care must be taken that the surrounding material is not excited or that such contributions to the measured spectrum are recognized and not evaluated as part of the analysis of the inclusion itself. This holds also true for material layers that are located above or below the inclusions. Accurate quantification of inclusions is difficult for the same reason as it is for particles; it is very much dependent on the type and size of the inclusion. Material identification, however, is possible in most cases, which often is already sufficient to identify the type or the origin of the inclusion.

Compared to the analysis of particles, it is possible and sometimes even necessary to prepare the sample. The material can be polished until the inclusion is on the sample surface, thus eliminating any influence of material covering the inclusion. This then also simplifies positioning the sample since inclusions are inherently embedded in the sample.

The same instruments and similar measuring conditions are used as for the analysis of particles.

WDS instruments can also be used for the analysis of inclusions, if their incident radiation is collimated. This is a precondition for the analysis of small sample surfaces. The test conditions must be selected similar to the analysis of large samples. In order to achieve reasonable statistical errors for the measurement of the small sample areas, the measurement times must be increased. This can lead to measurement times of hours for sample areas of <1 mm in diameter, if the measuring time for the usual sample diameters of 30 mm is in the range of a few minutes (see also Section 15.1.3).

## 15.3 Material Identification with Handheld Instruments

### 15.3.1 Analytical Tasks

Often it is only necessary to identify a specific material without performing a full quantification. This may be the case in order:

- to ensure that the material used meets specified requirements, for example, steel is weldable or corrosion resistant
- to check whether the materials used in buildings or industrial plants have the correct composition and therefore meet the requirements and specifications for the intended use
- to determine the content of valuable alloying elements in scrap metal in order to quickly assess its value and to decide on its further use
- to select with a fast on-site analysis of, for example, environmental samples relevant samples for a more detailed laboratory analysis and avoid the effort for a lot of elaborated laboratory analyses of non-interesting samples

- to determine the content and thereby the value of precious metals in old jewelry (this application has become increasingly important as a result of their increasing prices)
- to characterize art objects according their composition by on-site analysis without damaging the object or its transportation to a laboratory
- to determine the course of ore veins during their exploration and mining in order to reduce the extraction and transportation of dead rock as well as a variety of other analytical questions (Potts and West 2008).

The focus in these applications is to rapidly generate analytical results that are available on-site, preferably without sample preparation, but above all without sample collection and transport of the sample for analysis to a laboratory. In addition, removing material from buildings, industrial plants, or even objects of art are too complex and often not even possible without damage.

However, one has to bear in mind that the analytical accuracy is often influenced in such analyses:

- as a result of contamination of the sample surface by corrosive layers or other contaminants from the measuring environment
- due to material changes on the surface caused by environmental pollutions
- because the correct measuring geometry cannot be met every time as a result of irregularly shaped sample surfaces or because the measuring instrument cannot be held by hand at the exact same position during the complete time of the measurement. Even small changes in angle have considerably impact on the element intensities.

Still, in many cases, it is sufficient to just carry out a PMI to solve the analytical problem. This means determining the material type based on measured intensities and their respective ratios and then comparing those with data from spectral libraries of the expected material types. As already mentioned, trueness and precision of the quantitative analysis are limited as a result of the described influences; nevertheless a material identification can often solve the assigned analytical task.

### 15.3.2 Analysis Technology

Handheld instruments are available for on-site material identification. They can measure a wide range of elements. Only the detection of light elements is limited since most handheld instruments operate in air. However, due to short measuring distances (detector and X-ray source are very close to the sample), this limitation has to be qualified, since the analysis down to Al is possible and even Mg can be detected under certain circumstances. For material identification, the measured spectrum can be compared with a spectral library. It is also possible to perform a complete quantitative analysis. However, the computational complexity and available analysis models for on-site analysis are somewhat restricted by the computing power of the portable instruments. Consequently, standardized models are primarily used. This limits the flexibility, and as a result, handheld instruments are usually set up for specific applications. For a more complex data analysis, the data can always be transferred to a laptop or benchtop computer.

For the handheld instruments the sample area analyzed has a diameter of up to 5 mm however, usually not smaller than 1 mm. For the measurement the instruments are placed directly onto the sample. Few instruments have even a camera to show the correct positioning at the sample. The measurement times can be very short because of the high counting rates that can be achieved by the closely coupled measurement geometry even with the available small tube powers of maximum 5 W.

Fast ED detectors like silicon drift detectors (SDDs) are state of the art for handheld instruments. They can capture a large solid angle of fluorescence radiation from the sample and can handle high count rates. Both tube and detector consume little power, and therefore these spectrometers can be operated by a battery and are able to work for up to eight hours, i.e. for one work shift.

The open beam path of these instruments requires careful handling in order to meet the requirements of radiation protection. Therefore, these instruments are usually designed for a two-hand operation, which is intended to prevent unintentional opening of the tube shutter. Further, they have sensors that check the distance of the instrument to the sample and allow the start of the measurement only if the instrument is in contact with the sample. Intensity thresholds can also be used for safety measures in order to avoid a shutter opening if the instrument is pointed in air.

### 15.3.3 Sample Preparation and Test Conditions

Usually no sample preparation is done for handheld instrument analyses. Occasionally, the sample surface can be roughly cleaned, removing coatings or contaminations at the analysis site. In the case of metals, it is advisable to remove corrosion products on the surface by grinding (i.e. with a roughing file). Since the analyzed areas have a diameter of 1–5 mm, one can expect that the sample to be analyzed is sufficiently representative; on the other hand, it is likely to find sample areas for the analysis that are mostly flat.

The test conditions should be set up according to the specifications of the instrument manufacturer for the respective analysis task. This is also necessary because the classification and quantification procedures are working only if the test conditions for the unknown samples and the references samples in the spectrum library are identical. For the handheld instruments, measurement conditions for the different material classes are often set automatically. The material class of a material that belongs to can be determined simply by experience of the analyst; by a given specific analytical task; or even from a short preliminary measurement.

### 15.3.4 Analytical Accuracy

How well a material can be identified depends strongly on the differences in composition between the individual material classes. If the differences are mainly in the composition of the light elements, a clear identification may be difficult for handheld instruments. However, in most cases, material identification is possible within seconds and also accurate.

In principle, for a quantitative analysis, accuracies can be achieved, which are comparable with those of laboratory ED spectrometers. The counting statistical error are comparable, however, the largest error contribution is due to errors in measuring geometry as already mentioned in Section 15.4.1. Other errors are due to the sample itself, i.e. the analyzed volume is not representative of the whole sample or the sample is contaminated or altered from environmental influences. The statistical errors can be very small due to the high intensities that are achievable with the handheld instruments; however, the measurement times are mostly relatively short, because the instrument has to be held by hand for measurement. Nevertheless, with a corresponding calibration effort, the correction models can give very good results. In summary the most relevant influences result from surface contaminations or from incorrect measuring geometries due to irregular-shaped sample surfaces. These influences can lead to significant increases in the measurement uncertainties.

### 15.3.5 Application Examples

#### 15.3.5.1 Example: Lead in Paint

The determination of lead in wall paint became the starting point for the development of handheld instruments. The high toxicity of lead required the replacement of lead-containing wall paints. However, in order to determine whether such lead containing color pigments were used, their identification is necessary. The effort to collect samples from different wall areas, transport them to a laboratory, and carry out the analyses is much too high. Therefore, a solution for an on-site analysis with a portable instrument was sought after. These instruments should not to be too heavy, be easy to handle, be radiation safe, and have a sufficient sensitivity as well as accuracy for the analysis. To this end, the first handheld instruments were developed – at that time still with a radioactive isotope source for excitation. The analysis of wall paints is regulated, for example, in ASTM-E\_2119-16 (n.d.), ASTM-F\_3078-15 (n.d.), and ASTM-D\_4764-01 (2016). From these early beginnings, a new and powerful X-ray instrument family was developed, which is now used for many other applications.

#### 15.3.5.2 Example: Scrap Sorting

The analytical problem of this application is the identification of scrap metal in order to decide on their further use and processing. For example, it is important to know the Cr and Ni content in steel alloys to determine their monetary value, or it is important to know if a steel has been coated with a Zn layer for corrosion protection, which would require special processing methods during a later remelting.

For these applications a very accurate quantification is not required; usually a material identification is already sufficient. It is required that the analyses are carried out quickly and on-site, without any sectioning of sample material and its transport to the laboratory. Using a handheld instrument, the analysis and material identification can take place directly at the material storage site or at the scrapyard.

Sample preparation might require the removal of thin contamination layers and other coatings in order to allow the detection of light elements. When elements are analyzed that account for most of the material value, it may be necessary to make a full quantitative analysis. However, the often not very reproducible on-site measuring conditions and sample impurities restrict the achievable analytical accuracies.

The measurement times for scrap sorting can be very short since the required analytical accuracies are not very high. When the analytical result is continuously updated on the display, it is even possible to stop the measurement upon reaching a clear positive result after few seconds.

#### **15.3.5.3 Example: Material Inspection and Sorting**

The number of different metal alloys is very large, and they partly have been developed for very specific applications. The differences in the alloys usually cannot be determined just by external characteristics. Therefore, a fast material identification is desirable, for example, in material stockpiles. Using a handheld instrument can help with these requirements. With just PMI analysis it is possible to correctly identify a material. For this purpose, it is sufficient to create a library from all possible materials in inventory; the correct material identification is then made by matching the measured spectrum against the spectra in the library. Also in this case the measuring time can be very short and adapted to the displayed analytical result.

#### **15.3.5.4 Example: Precious Metal Analysis**

The recent increase in precious metal prices created a new and significant market for XRF analysis, especially the analysis of scrap gold become important. The purchase of old jewelry or dental alloys is becoming increasingly important. Since jewelry or dental alloys have very different contents of gold (see Section 9.6), which considerably influences their value, an accurate analysis is necessary. Ideally the analysis should be done quickly and at the point of sale, independent of a professional analytical laboratory. Handheld instruments can be used for this application. For bulk gold analysis it is possible to do this by material identification, since the composition of jewelry alloys, in particular their gold content, is in many countries set by their karat value. With this information the determination of the monetary value can already be performed with sufficient reliability.

A complete quantitative analysis of all elements in the sample is possible as well. To achieve the necessary accuracies, the measurement times are adjusted in order to achieve very repeatable measurement results. For this purpose, the handheld instruments can be mounted in a holder, which then allow a well-defined positioning of the sample, or portable instruments are used (see Section 4.3.1.2). For longer measuring times, the measurement becomes operator independent, and the holder serves as an additional radiation protection instrument.

The value of a piece of jewelry is essentially determined by the material value of the gold (and the incorporated precious stones). For individual small pieces of jewelry, a limited analytical accuracy translates into a small error in monetary value. At a weight of 5 g, the current monetary value of gold is about US\$200, i.e. an analysis error of 1% corresponds to a miscalculation of US\$2. This however

becomes significant at a point of sale where large amounts of gold are exchanged each day.

#### 15.3.5.5 Example: Prospecting and Screening in Geology

In the exploration and mining of ore, a large quantity of dead rock is often excavated in addition to the real ore. In order to minimize this effort, it can be helpful to determine the course of an ore vein *in situ* and thus to define the direction of further mining activities while at the same time minimizing the excavation of dead rock material.

Handheld instruments can also support the sampling of geological samples. An example is the screening of soils on contaminations. Owing to the often nonuniform distribution of contaminations, with the capability of on-site screening, relevant samples can be identified and then taken to a laboratory for a more detailed analysis, whereas uncontaminated samples can remain in the field without further processing. This also considerably reduces the work at the laboratory, and it significantly accelerates the assessment of the specific state of contamination (Potts and West 2008; Young et al. 2016). Handheld instruments are also of great importance when the analysis site is far away from an analytical laboratory (Phillips and Speakman 2009; Zurfluh et al. 2011).

A special challenge in the quantification of geological materials are the many different compounds of individual elements and compounds that can be present, such as oxides, carbonates, sulfides, etc. and their mixtures. Quye-Sawyer et al. (2015) and de Winter (2017) investigated the requirements for the analysis of carbonates with handheld spectrometers. They found that a suitable characterization is possible if adequate reference samples are available.

Handheld instruments are very fitting for many of these tasks, since they enable a rapid on-site analysis. However, for each application, the measurement setups must be adjusted for the elements and their concentration ranges to be measured. The measurement times depend on the required sensitivities and accuracies. For the detection of traces, longer measuring times are necessary in order to achieve sufficient peak-to-background ratios. Then again, the analytical tasks often only require the monitoring of threshold values, which means that it must be determined whether the concentration of an element exceeds or falls below a certain threshold value. In each case it is good practice to always make several measurements in order to determine the influence of sample inhomogeneities or of irregularly shaped sample surfaces.

#### 15.3.5.6 Example: Investigation of Works of Art

To assess the authenticity of work of art, often an element analysis is necessary in order to gather information about the manufacturing technologies used, to provide information about probable restorations, etc. Removal of any material from these samples for an analysis is not possible due to their uniqueness or their value. Even transporting them to a laboratory can be impossible due to the size of the objects or because of the security required for them. Therefore, an on-site analysis with handheld instruments is interesting and often the only option. Recently handheld instruments have been frequently used for this purpose. The analytical tasks are very diversified. Various elements, even present only

in low concentrations, can even be of interest. The instruments are often used with special fixtures for easy positioning; they also allow for longer measurement times at the same position. The spectrometers are often only used to acquire the spectra, after transfer of data, evaluation can then be performed with a more powerful computer and with advanced algorithms. A comprehensive compendium of such analysis can be found, for example, in Moioli and Seccaroni (2000), Shugar and Mass (2012), Shakley (2010), Liritzis and Zacharias (2010), Schreiner (2004), and Mantler and Schreiner (2000).

## 15.4 Determination of Toxic Elements in Consumer Products: RoHS Monitoring

### 15.4.1 Analytical Task

Consumer protection and the conservation of the environment from exposure to toxic substances that can be present in consumer goods are becoming more and more important. Consumer goods are usually made out of many different parts and materials, making their overall composition very complex. Toxic substances are very often used as fire retardants or as pigments. How effective they are depends on their concentrations. Various rules and legislations were passed that limit the amount of these elements and substances.

A frequently cited directive related to the restriction of the use of certain hazardous substances in electrical and electronic equipment is the **Restriction of Hazardous Substances Directive**, in short referred to as RoHS. This regulation was originally recorded in the EU Directive 2002/95/EC, now EU-Richtlinie\_65 (2011), in the European Union. The directive establishes the maximum levels of toxic elements and substances in “homogeneous materials.” For the purpose of this directive, “homogeneous material” refers to materials of uniform composition throughout or materials, consisting of a combination of materials, that cannot be disjointed or separated into different materials by mechanical actions such as “unscrewing, cutting, crushing, grinding and abrasive processes.” Strictly following the directive means that for a plated part, both the plating and the substrate must each conform. The directive is intended both to reduce the exposure of toxic elements on the equipment user and to prevent the pollution of the environment by nondegradable toxic substances when the equipment is disposed.

The maximum concentrations of the toxic elements and substances covered by the regulation are summarized in Table 15.1. The concentrations cannot to be exceeded in any homogeneous material of the respective instrument. The highly complex design of electrical and electronic instruments establishes high requirements for the analytical technique to be used, since homogeneous components can be very small that only a sensitive and small-spot analysis technique can provide the desired information.

For these analyses there are different options. On the one hand, the element concentrations can be monitored by screening of the individual components of the instrument (DIN-EN-62321-3-1 2014) and (ASTM-F\_2617-15 n.d.). The analysis should be done, if possible, on-site in order to avoid having to transport



**Table 15.1** Maximum concentrations for toxic substances according to RoHS.

Toxic substance	Maximum content (mg/kg)	XRF analysis by:
Lead (Pb)	1000	Direct analysis
Mercury (Hg)	1000	Direct analysis
Cadmium (Cd)	100	Direct analysis
Hexavalent chromium (Cr <sup>6+</sup> )	1000	Total Cr content
Polybrominated biphenyl (PBB)	1000	Total Br content
Polybrominated diphenyl ether (PBDE)	1000	Total Br content

many samples to the laboratory. Only for inconclusive results a more elaborate analysis in a laboratory can be required. On the other hand, it could be necessary to investigate complex electronic components, such as printed circuit boards, by mapping over a large area.

#### 15.4.2 Analysis Technology

X-ray fluorescence (XRF) is a suitable method to detect these elements since the measurements can be performed without any special sample preparation and the detection limits for the elements in question are sufficient. The direct determination of hexavalent chromium and polybrominated biphenyls is not possible with XRF, but the detection of the marker elements Cr and Br. If their concentrations are below the given limits, the limits for their respective components are also met.

Depending on the specific analytical problem – screening or verification – different approaches are possible. In the beginning, the samples were broken up into small pieces and then analyzed as poured into a sample cup or as a pressed pellet (Brodersen et al. 1995). In this way, it is possible to determine whether toxic elements are present in the sample, but the process of breaking the whole sample into small pieces does not allow the assessment of homogeneous individual components in the sense of the regulation.

Another possibility is on-site analysis for which the handheld instruments are the most closest fit (see, for example, Shrivastava et al. 2005). For results that are unambiguously above or below the threshold values, decisions regarding the RoHS compliance are immediately possible. For values close to the limits, further investigations can be carried out in a laboratory. Using handheld instruments for this task depends to a large extent on the size of the components to be analyzed. If they are smaller than the area analyzed, a correct positioning as well as a clear evaluation of the measurement is difficult or not possible at all.

The manufacturers also subject their products and its components to a type test, which is usually done in a laboratory. Then the position where the toxic elements are located can be determined with  $\mu$ -XRF instruments with a good spatial resolution. Even for very complex assemblies, mapping and a distribution of the whole part can be performed (see Section 16.4). In this case, the time required

for the complete measurement is several hours; however, it is possible to monitor the concentration of all components simultaneously.

For the verification of the element concentration of the individual components, the analysis on small, possibly curved sample surfaces becomes necessary. This is possible with laboratory instruments with a small spot and accurate sample positioning (Wolf 2008).

The sensitivity requirements can already be achieved with basic instruments. The achievable count rates and therefore the statistical error depend on the setting of the tube parameters as well as on the spot size; they are proportional to the tube current and area of the spot size. The excitation voltage influences the sensitivity, especially for the detection of cadmium. Since RoHS measurements are usually performed in air, the high-energy Cd–K radiation must be used. Therefore, for an effective excitation of Cd, the excitation spectrum must have sufficiently high intensity at the K-absorption edge of Cd. This is ensured with an excitation voltage of 50 kV, or even better with 60 kV. Instruments using polycapillary optics deliver very small spots; however, sufficiently high excitation intensities are only achieved in the range of approximately 8–15 keV, the low transmission efficiency of polycapillary optics in the higher energy range limits the excitation of cadmium. This is clearly demonstrated in the spectra shown in Figure 15.5. They were measured with a polycapillary (30  $\mu\text{m}$  spot size) and with a collimator (0.7 mm diameter) on a polymer sample (here polyethylene) containing the RoHS elements at concentrations close to the respective limits of the directive.

The spectrum obtained with a polycapillary optic shows a significantly higher intensity of characteristic fluorescence lines and background in the medium energy range. The detection of Cr, Br, Hg, and Pb with the required sensitivity poses no problem. For Cd the situation is different. The low transmission of the optics at high energies reduces the excitation intensity, and the excitation with the straight spectrum of a W-tube with glass window using just a collimator is

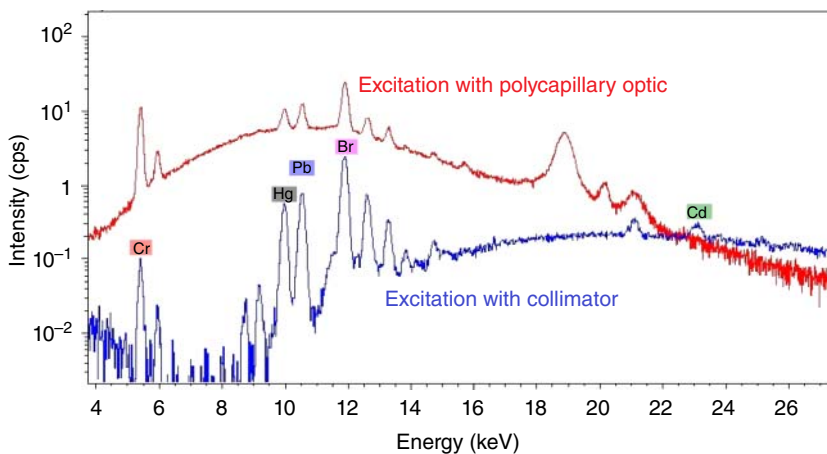


**Figure 15.5** Spectra of a PE specimen with toxic elements close to the RoHS limits (y-axis in logarithmic scaling).

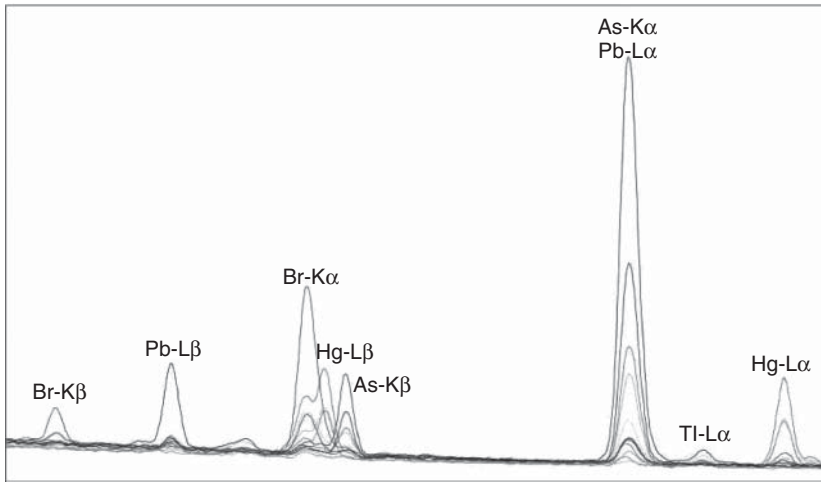


**Figure 15.6** Peak overlap of Br, As, Hg, and Pb.

more efficient. This is important since, according to the RoHS regulation, Cd has the smallest threshold to be monitored. Using a collimator for the detection of Cd can therefore be more effective especially if it is not necessary to analyze small sample areas.

From a spectroscopy standpoint, depending on the sample, the analysis of the elements such as Br, Hg, and Pb can also be quite challenging, as can be seen in Figure 15.6. While there is no overlap in the  $L\alpha$ -line of Hg, the  $Pb-L\alpha$ -line has the well-known overlap with the  $As-K\alpha$ -line. The  $Br-K\alpha$ -line overlaps with the  $Hg-L\beta$ -line. Therefore, for a careful determination of the element intensities, either a good resolution of the spectrometer is necessary, or in the case of energy-dispersive spectrometers, efficient deconvolution algorithms are required.

### 15.4.3 Analysis Accuracy

The accuracy requirements for the determination of the concentrations of toxic elements in consumer goods are relatively low. Usually only the decision is important if the threshold limits are exceeded or not. Relative errors of a few percent are not a problem. The detailed acceptance criteria based on the statistical errors of the measurement are given in the standard IEC 62321-1:2013. There the results are being classified into three categories: below limit, inconclusive, and over limit. For inconclusive results, further testing with more specific analytical methods are required.

Due to the very complex composition of the individual electronic components, it is important to correctly account for all matrix interactions. In particular, the common use of a wide variety of polymers of different compositions makes it challenging because the availability of reference samples is limited (Hanning et al. 2010).

A problem of using polymer standards is their durability when being exposed to X-ray radiation. Although ionizing radiation is not expected to deplete the elements, changes in the chemical bonding conditions can result in migrating effects of the elements, matrix's influence can be changed, and the strength of the samples can be affected. These effects can limit the lifetime of polymer standards. However, during normal usage as calibration standards, the effect become negligible (Wacker et al. 2008). It is further important to store the standards under a controlled environment.

## 15.5 Toxic Elements in Toys: Toys Standard

### 15.5.1 Analytical Task

A further regulation for the protection of consumers against toxic substances were implemented in the United States, in Germany, and many other countries. In Germany it is summarized in the "Spielzeugverordnung" (Toy Regulation [BGBl., II, Nr. 203/2011 und Nr. 38/2013] based on the EU-Richtlinie\_48 (2009)). In the United States the corresponding regulations are fixed in the ASTM-F\_963-17 2013. Standard Consumer Safety Specification for Toy Safety.

The German regulation does not only limit toxic elements but also several organic compounds. The list of toxic elements is more extensive than for the RoHS directive and refers to different parts of the toys, which can reach the digestive system of children when playing.

This includes specific fixed parts of toys as well as liquid materials or scrapable surface coatings. The much-differentiated upper limits for this regulation are significantly lower than for the RoHS regulation, because the limits to protect the children must be even lower.

These lower limits, summarized in Table 15.2, require a very sensitive analysis. The higher contents in the range of >1000 mg/kg are no problem; however, the small limit values for Sb, As, Pb, Cd, Cr, Co, or Hg are an analytical challenge. Their safe determination places particular demands on the analytics.

The US Consumer Product Safety Improvement Act (CPSIA) set out new regulations to limit the concentrations of certain heavy elements such as Sb, As, Ba, Cd, Cr, Pb, Hg, and Se as well as phthalates in toys. Full details can be found in the Standard Consumer Safety Specification for Toy Safety (ASTM-F\_963-17 2013). The heavy element limits are summarized in Table 15.3.

### 15.5.2 Sample Preparation

The preparation for these samples must be carried out according to the standards and specifications listed in Table 15.2 and Table 15.3, which means that the materials to be analyzed have to be separated from the toys or the entire toy must be analyzed at suitable locations. The preparation techniques must be adapted to the respective substances and shapes of the toys.

Dry, brittle, or flexible materials can directly be measured; if necessary, the parts must be made fit to the dimensions of the sample chamber of the spectrometer. Scraped materials can be poured into a sample cup or pressed into a

**Table 15.2** Maximum loads according to Toy Regulation (BGBl., II, Nr. 203/2011 und Nr. 38/2013 2013) in (mg/kg).

Element	Dry, brittle or flexible toy materials	Liquid or adhesive toy materials	Scrapable toy materials
Aluminum (Al)	5625	1406	70 000
Antimony (Sb)	45	11.3	560
Arsenic (As)	3.8	0.9	47
Barium (Ba)	4500	1125	56 000
Lead (Pb)	13.5	3.4	160
Boron (B)	1200	300	15 000
Cadmium (Cd)	1.3	0.3	17
Chromium (III) (Cr <sup>3+</sup> )	37.5	9.4	460
Chromium (VI) (Cr <sup>4+</sup> )	0.02	0.005	0.2
Cobalt (Co)	10.5	2.6	130
Copper (Cu)	622.5	156	7700
Manganese (Mn)	1200	300	15 000
Nickel (Ni)	75	18.8	930
Mercury (Hg)	7.5	1.9	94
Selenium (Se)	37.5	9.4	460
Strontium (Sr)	4500	1125	56 000
Tin (Sn)	15 000	3750	180 000
Organic tin compounds	0.9	0.2	12
Zinc (Zn)	3750	938	46 000

**Table 15.3** Maximum soluble migrated element in ppm (mg/kg) for surface coatings and substrates included as part of a toy according to ASTM F963.

Elements	Solubility limit (ppm)
Antimony (Sb)	60
Arsenic (As)	25
Barium (Ba)	1000
Cadmium (Cd)	75
Chromium (Cr)	60
Lead (Pb)	90
Mercury (Hg)	60
Selenium (Se)	500

pellet for the measurement. In doing so care must be taken that the samples and reference material used are comparable in regard to their amount and structure. For liquids the measurement in cuvettes is possible.

### 15.5.3 Analysis Technology

The low thresholds of some elements of the toy regulations require instruments with high sensitivity. Usually small sample amounts (for example, scraped sample parts) or the requirements to measure on curved sample surfaces can be best analyzed using position-sensitive methods. EDS met these requirements best; however their analytical sensitivity is limited by the limited energy resolution. Therefore, specific measurement conditions in order to increase the instrument sensitivity are necessary. This can be the use of monoenergetic or polarized radiation for sample excitation (see Section 4.3.3). If the energy of the incident monoenergetic radiation is close to the absorption edge of the element to be analyzed, the excitation is very effective, and the background of the spectra is very small due to any absence of the scattered bremsstrahlung. In this way high peak-to-background ratios and thus very good sensitivities are achieved. Excitation with monochromatic radiation is possible by using various secondary targets or monochromators in the primary beam path.

During excitation with polarized radiation, the incident radiation is not scattered within the polarization plane. This also reduces the spectral background and increases the sensitivity, not only for individual element groups but for a wider energy range.

Similar to the analysis of toxic elements in consumer products (see Section 15.4), the accuracy requirements for this task are not very high since the focus is more on compliance with the limits of the regulation.

## 16

# Analysis of Element Distributions

## 16.1 General Remarks

The investigation of element distributions becomes increasingly important as many raw materials and even more semifinished or final products are usually composed of different components. The quality of a raw material is determined by the individual components; however, the complex functionality of a final product is given by the interaction of their individual components. In order to ensure this functionality or to determine the reason of errors, large-area analysis is not suitable. However, the analysis of small sample surfaces or even better the determination of element distributions can be very helpful.

For these analytical tasks, micro-X-ray fluorescence ( $\mu$ -XRF) has become established. There are instruments available, which can determine element compositions of very small sample areas and also can scan extended sample areas to determine element distributions. In most cases energy-dispersive (ED) instruments are used for distribution analysis (see Section 4.3.3.6).

The image quality of element distributions depends on various measurement parameters, such as the size of the individual analyzed area, the step width, or the intensity collected from a sample point (Janssens et al. 2000; Kanngießner and Haschke 2006; Haschke 2014; Haschke and Kanngießner 2013). However, it also depends on the examined objects themselves, their structure, the differences in composition, etc.

In the following sections distribution measurements of some typical sample qualities will be described, which will demonstrate exemplarily the type of data acquisition, as well as their treatment and evaluation.

In general, distribution measurements often do not require any sample preparation or it is even not reasonable because the original sample has to be investigated. However, this means also non-planar and irregularly shaped samples have to be analyzed. Therefore, it is not always possible to maintain the ideal measuring geometry, in particular the sample-detector distance. This is not of great importance for distribution analyses since in this case only the qualitative composition of the different sample areas is of interest. For a quantification, specific point analyses can be carried out for which the required measuring geometry is exactly adjusted. Such point measurements are described in the previous chapter.

## 16.2 Measurement Conditions

The quality of the element distributions strongly depends on the measurement conditions. Therefore, it must be considered that in the case of an acquisition of element distributions, the number of measuring points increases rapidly by an enlargement of the scanned area as well as by reducing the pixel distance. This extended also the total measuring time, which is the pixel time multiplied by the number of measurement points. This means that for an acceptable total measuring time, the time for a single point also should be short. The following parameters can be used to influence the quality of element distributions:

- *Spot size and spacing*: The spot size is the essential parameter for the spatial resolution; however it is given by the design of the instrument and can be influenced only in special cases, for example, by changing the collimator or the working distance of the X-ray optics. Further, the pixel spacing influences the resolution. The best resolution for a given spot size is achievable for a step size of about 30% of the spot size. However, when pixel distances are very small, the number of pixels increases rapidly and therefore also the total measurement time. Therefore, pixel distances should be adapted to the sample structure. According to the sampling theorem, the pixel distance should be not more than half of the typical structure size of the distribution.
- *Number of pixels*: The number of pixels determines the image quality of the element distribution. Too small pixel numbers result in highly pixelated images that provide insufficient information about the element. Nevertheless, again it is to be mentioned that the total acquisition time increases proportionally with the number of pixels.
- *Measured intensity*: The acquired intensity in every pixel determines the separation between different mass fractions of an element. The acquired intensities have a statistical error, which determines also the contrast of the distribution. The pixel intensity can be improved by optimizing the measuring conditions or by increasing the measurement time, which would extend the total measurement time.

Based on these general considerations, it can be concluded that for distribution measurements, high intensities as possible should be acquired for all elements of interest. Even for short pixel times high intensities can be collected on a sufficiently large number of pixels. The optimal throughput of a measuring channel is achieved at dead times of 63%. For higher intensities of incident radiation, the dead time of the measuring channel and therefore its saturation are increased. Therefore, measurement conditions should be selected so that dead times are up to 50% for the sample areas with highest count rate.

For the analysis of element distributions, usually a complete spectrum is saved for every pixel; therefore so-called HyperMaps are generated, which typically are four-dimensional data packages (two spatial coordinates, energy, and intensity) for  $\mu$ -XRF and offer various possibilities for data evaluation and interpretation. Few of these possibilities will be demonstrated exemplarily in the following application examples.



## 16.3 Geology

### 16.3.1 Samples Types

Geological or mineral samples are available as compact samples and mostly inhomogeneous. The individual minerals can have different compositions, which can provide information, for example, about geological processes. Conclusions are then possible for the exploration of resources, for the assessment of valuable components in geological materials, or for the selection of optimal treatment technologies. Further, even paleoclimatological information can be obtained, which can be important for the interpretation of historical processes.

Geological specimens are often also available as thin sections, which have been applied to glass substrates and ground to a thickness of approximately 0.1 mm. These thin sections are used for microscopic inspections to determine the kind of minerals of individual grains. For that purpose, the knowledge of element distributions can provide further insights.

### 16.3.2 Sample Preparation and Positioning

In the case of distribution analyses, the priority is to recognize the element distributions; precise quantifications are usually not the main interest. Therefore, it is not always necessary to maintain the correct measurement geometry. This means that distribution analyses can be carried out also for irregular-shaped samples. Deviations from the measuring geometry, that means mainly changes of the sample-detector distance influence the measured intensities, however, not the element identification itself. Nevertheless, the sample roughness should not be too strong; otherwise collisions of the sample with the instrument are possible or shadowing can influence the measurements.

For quantitative analyses, on the other hand, a careful determination of the fluorescence intensities is necessary, which is only possible with an exact abundance of the measuring geometry. Additionally, longer measuring times are required in order to ensure a suitable counting statistical error. Such point measurements are already described in detail in Section 15.1.

Thin section samples are very flat but also very thin due to the special preparation process. They are positioned on a glass sample carrier. This preparation is very useful for microscopic investigation, however, for quantifications by  $\mu$ -XRF it offers few difficulties.

In the case of irradiation with X-rays, the glass support can also be excited, and the fluorescence of elements of the glass carrier superimposes and falsifies the measuring signal of the sample. The influence of light elements, such as Na, Mg, Al, or Si, in the sample carrier is negligible since their radiation is completely absorbed in the thin section. However, secondary excitation from the substrate (scattered primary radiation or fluorescence) is possible. Fluorescence radiation of heavy elements can penetrate the thin section and superimpose the spectrum of the sample. For even heavier elements, the information depth can be larger

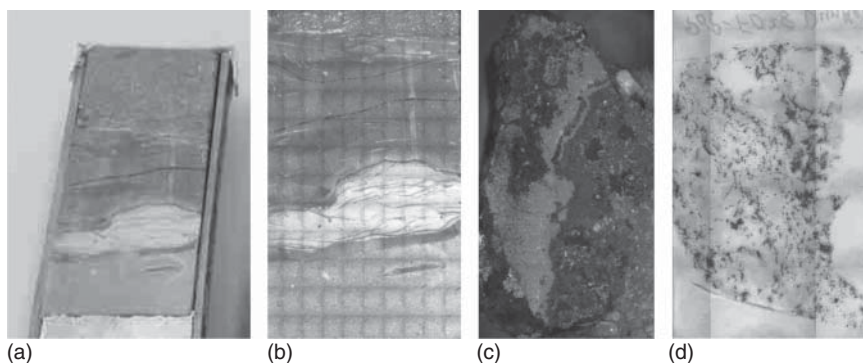


**Figure 16.1** Typical geological samples for distribution analyses: (a) bore core, (b) mosaic image of the bore core, (c) piece of a rock (pitchblende), and (d) thin section of a geological sample.

than the thickness of the thin section, i.e. the fluorescence intensity depends not only on the element content but also on the thickness. For all of these reasons thin sections are not suitable for quantitative assessments but can be very well used for the investigation of element distributions.

Figure 16.1 shows some typical geological samples, which will be used in the following to demonstrate the analysis of geological material regarding the test conditions as well as possible evaluation strategies. The first two pictures show the photograph of a bore core that is cut in half as well as its mosaic image, taken with a  $\mu$ -XRF spectrometer. The squares in this image represent the individually captured images. The next two pictures show a pitchblende, which is only roughly smoothed in the upper left part, but otherwise has a rough surface and the mosaic image of a thin section.

### 16.3.3 Measurements on Compact Rock Samples

The basic evaluation procedures for four-dimensional data cubes, called HyperMaps, which contain for every pixel a complete spectrum, will be demonstrated first for the bore core shown in Figure 16.1a,b. This sample with a size of about  $100 \times 170 \text{ mm}^2$  was measured with a pixel spacing of  $180 \mu\text{m}$ , which give  $545 \times 925$  pixel, or in total approximately 0.5 million. A measurement time of 15 ms per pixel yield in a total measurement time of approximately 2.5 hours for the complete mapping.

#### 16.3.3.1 Sum Spectrum and Element Distributions

The availability of the spectra of all pixels allows to sum spectra for specific sample areas from the data set. One of them is the sum spectra of all measured pixels, i.e. from the complete mapping. Figure 16.2 shows the sum spectrum of the bore core. This allows a rapid identification of all elements present in the sample.

Distributions can be calculated for all elements from the HyperMap. Such element distributions are shown in Figure 16.3 both for some individual elements

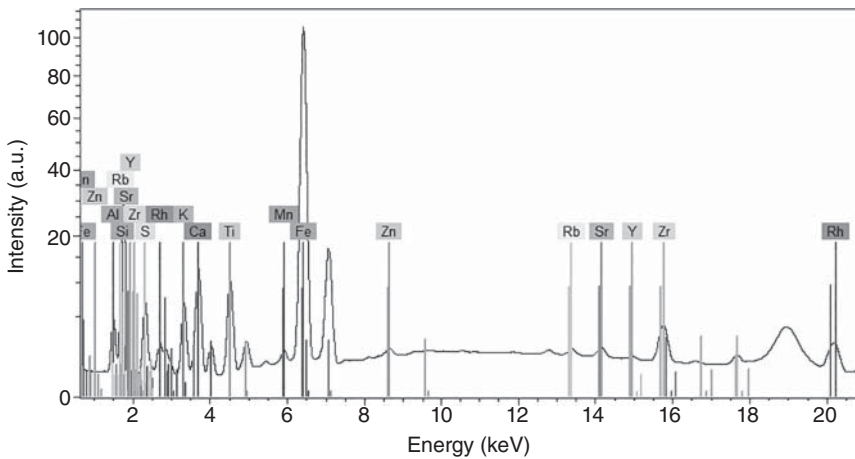


**Figure 16.2** Sum spectrum of the complete mapping (y-axis in square root scale).

and as superposition of several elements (Figure 16.3f). The distribution of an individual element can be represented in one color. In this case the brightness of the color is coding the measured intensity. However, then only few intensity levels are distinguishable by the human eye. Another possibility is a false color presentation, which can improve the contrast between the different intensity levels, as demonstrated in Figure 16.3d,e for the element Fe. The comparison of these two Fe distributions shows more clear differences in the false color representation, the contrasts are increased, and structures can be better recognized.

The simultaneous presentation of several elements is possible by the superposition of the distributions of these elements, each in an individual color and with an intensity coding by brightness, i.e. by an overlay of the different single-color representations. This results in the possibility for the identification of individual elements to sample structures and allows their better separation.

### 16.3.3.2 Object Spectra

For minerals it may be interesting to determine the composition of individual parts of the sample. A first approximation would be already possible by the availability of the pixel spectra of such a part. This is possible as demonstrated for the pitchblende from Figure 16.1c.

This sample was measured on an area of  $49 \times 26 \text{ mm}^2$  with a pixel spacing of  $50 \mu\text{m}$ . This resulted in  $970 \times 520$ , i.e. around 0.5 million pixels. The measuring time per pixel was 10 ms, which yield in a total measurement time of 1.5 hours.

The superposition of some elements is shown in Figure 16.4a. This figure contains two yellow marked objects in the center – a homogeneous sample area enclosed by a polygon as well as a single point in its center. In Figure 16.4b a limited energy range of the spectra of these two objects are shown.

These spectra illustrate that only a very small intensity is collected in a single pixel. Even not every background channel contains counts for the very short

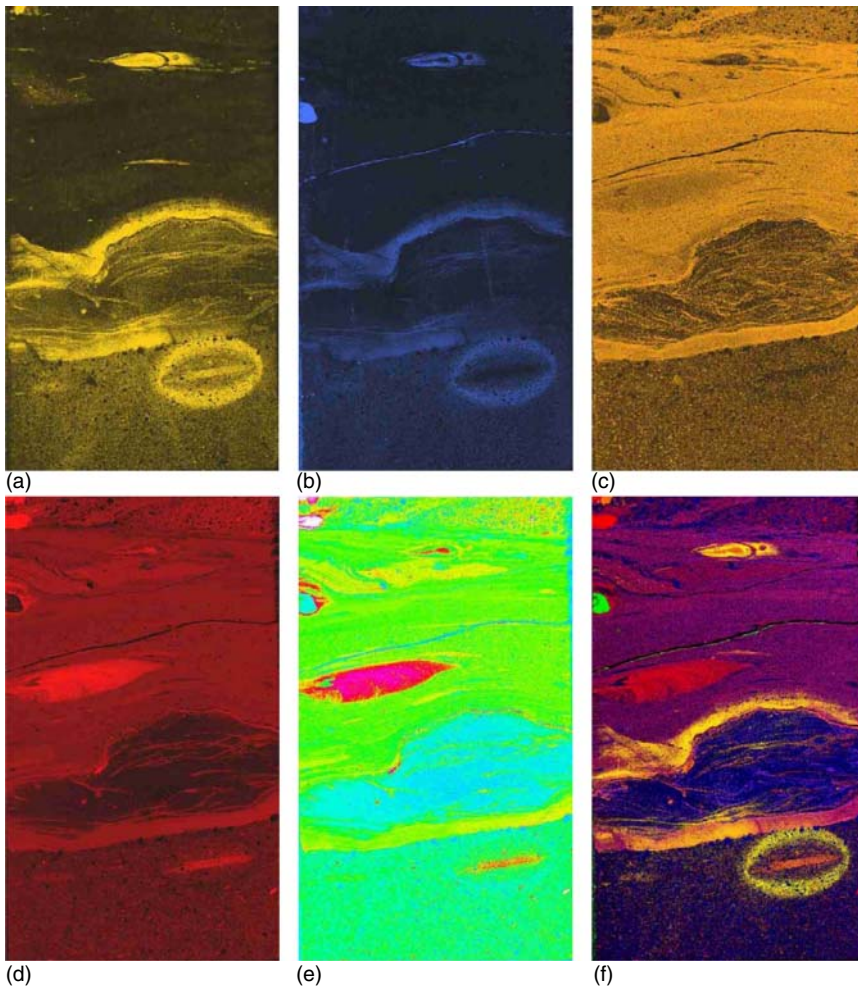


**Figure 16.3** Element distributions of the bore core for (a) Si, (b) Ca, (c) Ti, (d) Fe, and (e) Fe in false color; (f) element superposition with Si: blue, Ca: green, S: yellow, Ti: magenta, Fe: red.

measurement time of only 10 ms. On the other hand, the main components can already be clearly identified at these short measuring times. The spectrum of the polygonal area contains approximately 2300 pixels, i.e. the measurement time is already 2.3 seconds. This spectrum is somewhat smoothed and also shows already minor components.

#### 16.3.3.3 Treatment of Line Overlaps

The problems of the evaluation of single-pixel spectra are a clear peak recognition and the treatment of peak superposition, both due to the high statistical fluctuations caused by the small acquired intensities. Such overlaps will be of course reflected in the element distributions. For the pitchblende this is valid for

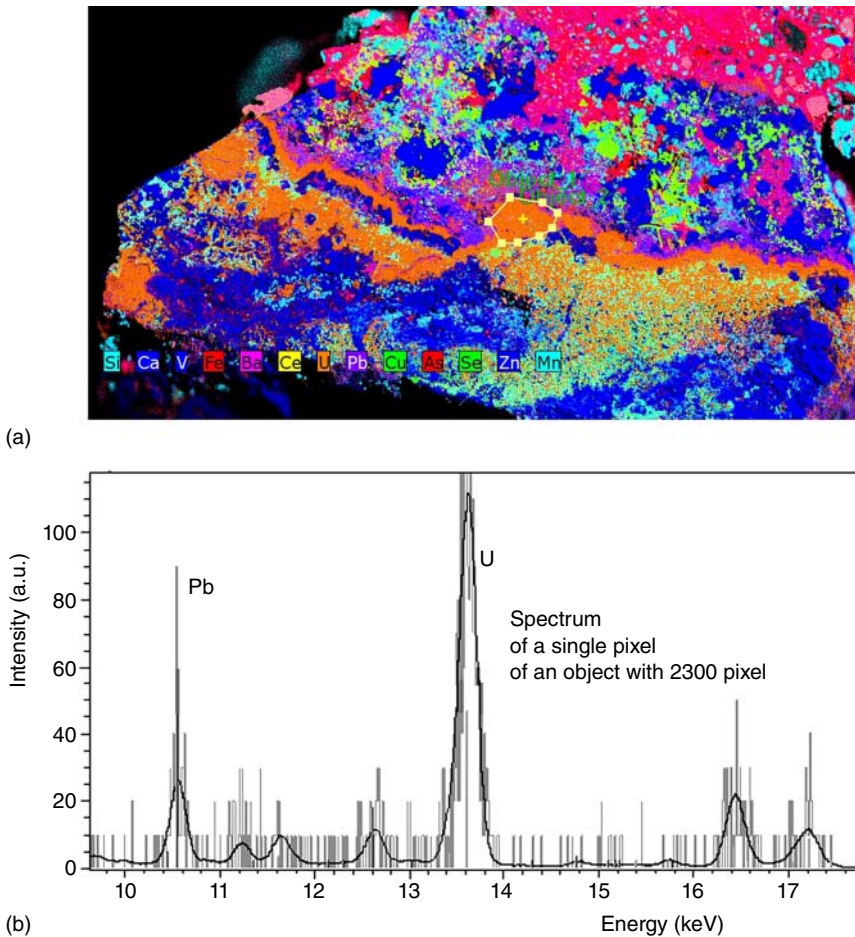
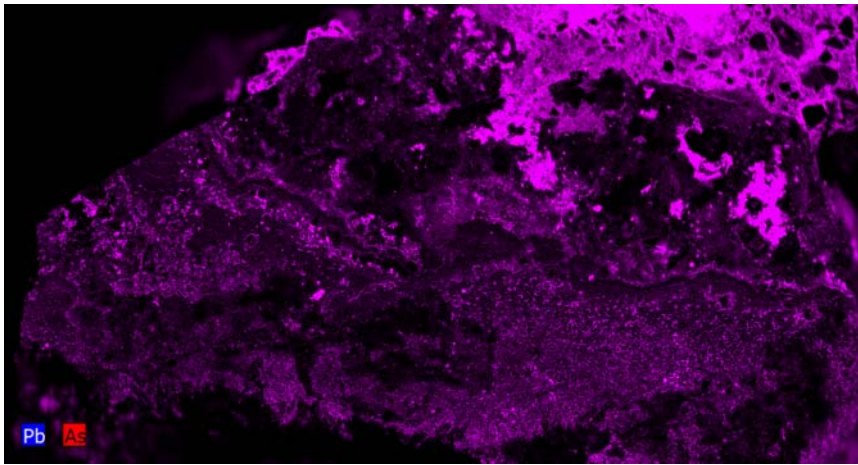
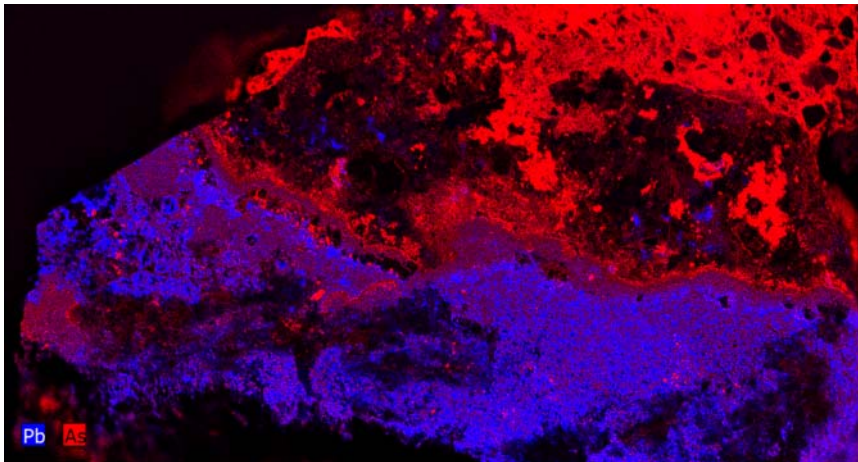


**Figure 16.4** Superposed element distribution of the pitchblende including inserted objects (single point and area marked by a polygon) (a) and spectra of these objects (b).

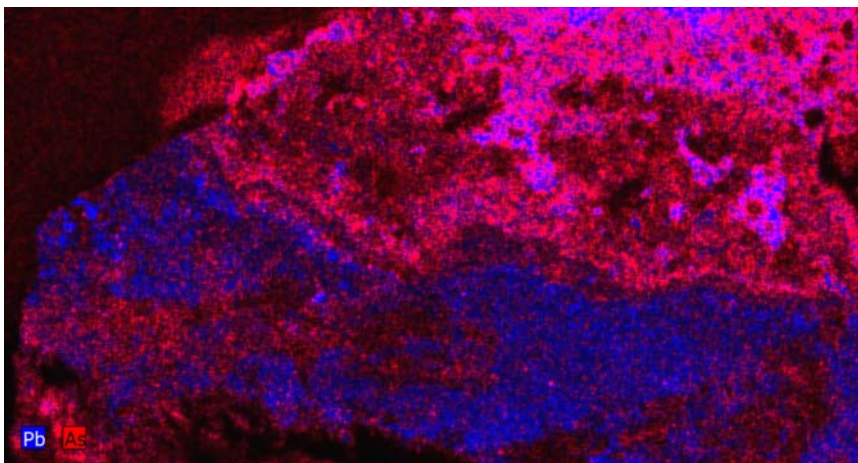
the overlay of the As-K $\alpha$ - and Pb-L $\alpha$ -lines. The distributions of these two lines are shown in Figure 16.5a, which shows the distributions of both elements in different colors. Since the mentioned lines used for the calculation of the distribution have a strong overlap, the distribution shows no differentiation between As and Pb. For a separation of the element distributions, non-overlapping lines of these elements can be used to calculate their distributions, in this case the As-K $\beta$ - and the Pb-L $\beta$ -line. Although the intensities of the  $\beta$ -lines are smaller than the peak intensity of the  $\alpha$ -lines, the different distributions can be well separated, as shown in Figure 16.5b. However, if there no lines of the elements available with different energies that can be used for the calculation of the distributions, another possibility would be the deconvolution of the individual pixel spectra. Figure 16.5c shows the distribution of As and Pb after such a deconvolution. This procedure can also separate the distributions of the two elements. However, the



(a)



(b)



(c)

**Figure 16.5** Element distributions of the overlapped As-K $\alpha$  and Pb-L $\alpha$ -lines (a) of the As-K $\beta$  and Pb-L $\beta$ -lines (b) and after a deconvolution process (c).

separation is not so clear since the pixel-wise deconvolution causes errors due to the small intensities and their high statistical error.

#### 16.3.3.4 Maximum Pixel Spectrum

The high number of accumulated spectra in the sum spectrum of the entire mapping can cover contributions of compounds that are concentrated at so-called hotspots, i.e. at only small sample areas or few pixels of the distribution. In this case, a comparison of the sum spectrum with the maximum pixel spectrum (MPS) can help. The MPS is an artificial spectrum that is calculated from the respective highest channel contents, regardless of the pixel.

The comparison of sum spectrum and MPS of the pitchblende in Figure 16.6a shows that in the MPS some element peaks have a significant higher intensity than in the sum spectrum. This is the result of the inhomogeneous composition of the sample. As long as these elements can be recognized in the sum spectrum

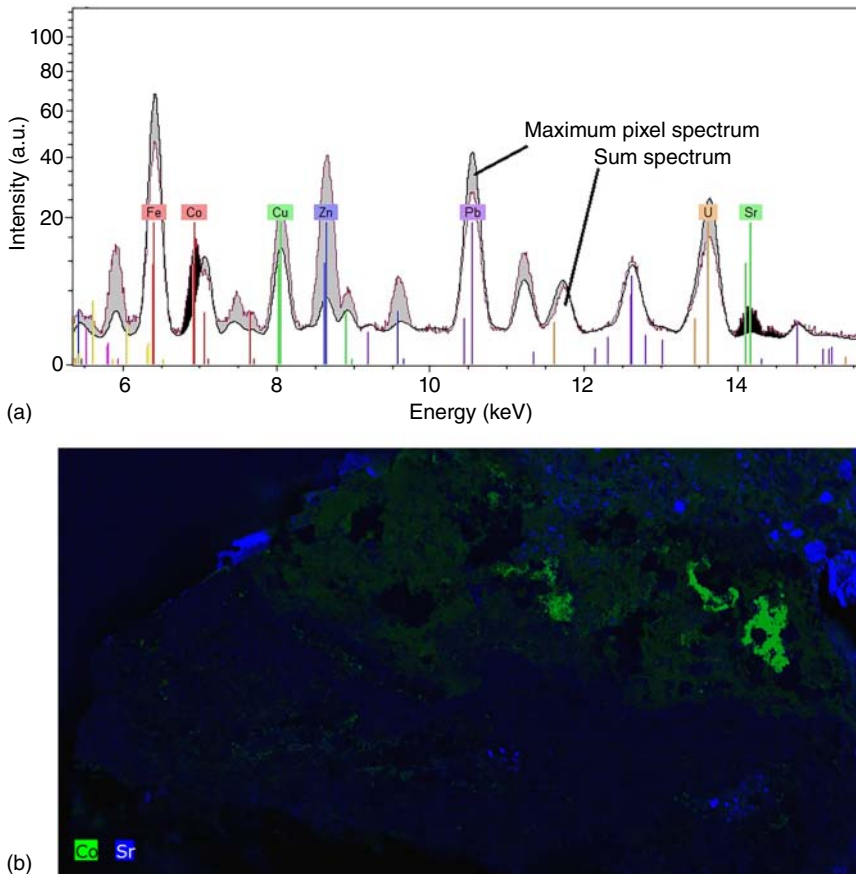


**Figure 16.6** Sum and maximum pixel spectrum of the pitchblende (a) (y-axis in square root scale) and distribution of Co (green) and Sr (blue) calculated after their identification (b).

(gray line), their identification and the calculation of the corresponding element distribution are no problem. However, if there are elements that have no peaks in the sum spectrum, there is also no reason to calculate their element distribution. This is valid here for the black highlighted peaks of Co (heavily superposed on the Fe-K $\beta$ -line) and Sr. With this information the calculation of the distribution of these elements is possible and is shown in Figure 16.6b. It can be seen that Co and Sr are concentrated in small sample areas.

### 16.3.4 Thin Sections of Geological Samples

There are a lot of thin sections of geological samples available since they are frequently used for an inspection with optical microscopes. However, the results of an optical inspection can be significantly improved and expanded by the knowledge of the elemental composition of the different identified minerals. To date, scanning electron microscopes with ED spectrometers are often used for this application. However, this method requires a special sample preparation; the samples must be provided with an electrically conductive layer, and the analysis process is time consuming because of introducing the samples into the vacuum.  $\mu$ -XRF offers the possibility for a faster and even more sensitive analysis. Nevertheless, it must be mentioned that the sample carrier can influence the measuring signal, since thickness of the thin section is only about 0.1 mm. This means that the incident radiation penetrates the sample and also the sample carrier and excites their fluorescence radiation. Although the radiation of light elements of the sample carrier is absorbed in the sample, the radiation of heavier elements as well as the scattered primary radiation penetrates the sample and is superimposed on the sample spectrum.

Further, it must be taken into account that as a result of the small sample thickness, particularly for heavier elements, the information depth can be larger than the actual sample thickness. Accordingly, the accumulated fluorescence intensities of sample elements can be smaller than for an infinite thick sample and can complicate a meaningful quantification. Additional effects are a decreased sensitivity for their detection and an influence to the contrast within the element distribution. However, the loss of intensity can be compensated by extended measuring times.

By means of measurements on the thin section shown in Figure 16.1d, these influences will be demonstrated. The size of the area analyzed here was about  $28 \times 45 \text{ mm}^2$ . The measurements were carried out with a step size of 50 and 200  $\mu\text{m}$ , respectively. In the case of same pixel times, this means an increase of the number of pixels by a factor of 16; therefore the pixel time of 3 ms for the measurements with a step size of 200  $\mu\text{m}$  was reduced to 1 ms for the 50  $\mu\text{m}$  step size. The total measurement times are then about 200 and 1000 seconds, respectively.

The results of these measurements are shown in Figure 16.7. The upper row shows the distributions obtained with a step size of 200  $\mu\text{m}$ , and the lower row with a step size of 50  $\mu\text{m}$ . In each row the first image shows the main components of the sample, the second image some minor components, and the third image some trace elements that are also found in the sample carrier.



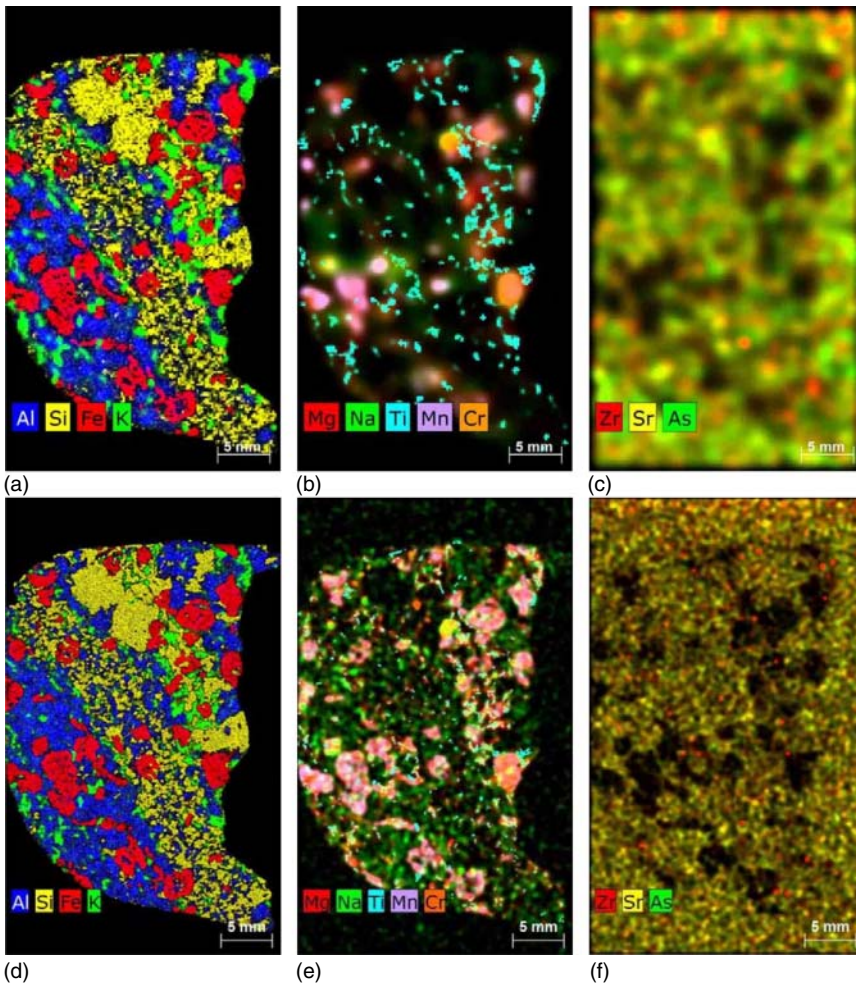


**Figure 16.7** Element distributions of thin sections measured with different step sizes, (a) to (c) 200  $\mu\text{m}$ , (d) to (f) 50  $\mu\text{m}$ , displayed for different element groups: (a) and (d) majors, (b) and (e) minors, (c) and (f) traces.

These distributions allow the following conclusions about the influence of the test conditions as well as for the interpretation of the element distributions:

- For the main components, the differences between the two test conditions are insignificant, in particular due to the relatively large grain sizes of the minerals in the sample. However, a more detailed inspection shows of course a stronger pixilation for the measurements with the larger step size in the upper row.
- The minors and traces show in contrast more significant differences. While for the measurement with the larger step size the structures are blurred and smaller structures even cannot be detected, these problems are eliminated in the measurements with the smaller step size; the structures are clearer, and even smaller ones are recognizable.

In general, it can be concluded that investigations of the element distributions of geological thin sections with  $\mu$ -XRF are possible. However, the test conditions have to be adjusted to the smaller sample thickness, and the influence of the sample carrier to the measured spectrum has to be taken into account. This problem can be avoided by using very clean quartz sample carriers, since the low-energy radiation of Si in the sample will be completely absorbed. However, in usual glasses, the fluorescence of heavy elements, such as As, Zr, or Ba, can overlap the sample spectrum.

For the investigation of thin sections, the possibility for quantification is limited since the intensities of not all sample elements originate from an infinitely thick sample, which means that high-energy fluorescence radiation is reduced because of the small sample thickness or the fluorescence intensities of the sample elements are falsified due to the overlay with the fluorescence of the same elements in the sample carrier or of due to secondary excitations by scattered radiation. However, the qualitative element distributions are clearly recognizable and can provide important information for solving various questions.

## 16.4 Electronics

Element analysis in electronics is mainly used for quality assurance and fault analysis, as well as for monitoring the load of electronic components with toxic elements. This can be achieved by the examination of individual components; however, as a result of the always smaller dimensions of electronic components, the analysis on smallest sample areas can be required. In the case of larger components, such as entire printed circuit boards (PCBs), distribution analysis can also be useful to examine the entire composition.

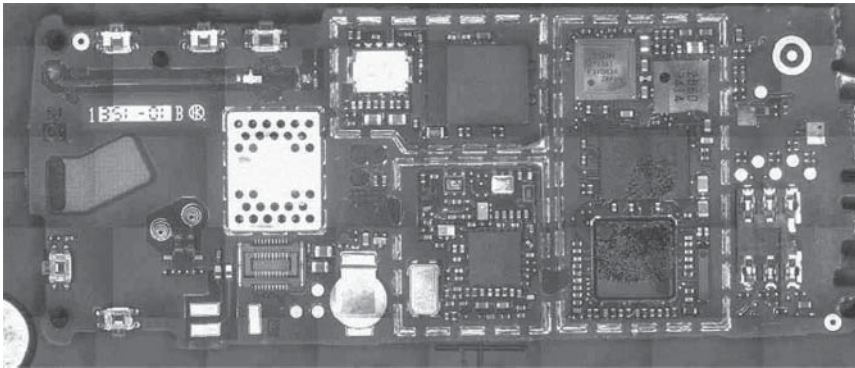
Point-like analyses of small sample surfaces have already been discussed in Chapter 15. Here, the analysis of element distribution of larger samples will be the focus.

For the distribution analysis, usually no preparation of the sample is necessary or even possible; the samples have to be measured directly. The sample-detector distances varying in the case of irregularly shaped samples can lead to shadows and minor falsifications, but the allocation of the individual structures of the components will not be affected. When detecting the intensities, errors can occur due to varying sample-detector distances. However, for individual pixels, these are on the order of magnitude of the statistical error, which is very large as a result of the short measurement times. For an acceptable quantification, a point analysis is therefore required in which both the correct observance of the sample geometry and the sufficient intensity can be collected.

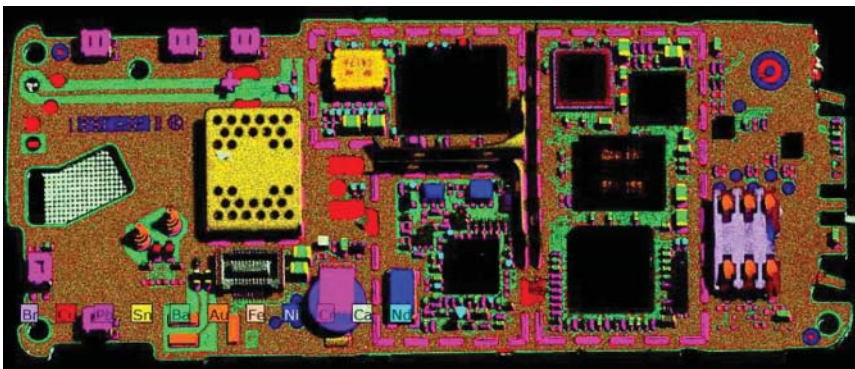
As an example, the study of the PCB of a mobile phone will be presented here. The size of the PCB is approximately  $1000 \times 424 \text{ mm}^2$ . The measurement

was performed with a step size of  $100\ \mu\text{m}$  and a pixel time of 10 ms. This resulted in a total measuring time of approximately 1.5 hours for the 0.4 million pixels.

Figure 16.8 shows the PCB itself as well as some element distributions. Due to these distributions, it is possible to recognize the composition of certain electronic components and to identify them. In particular, it is possible to identify components that contain toxic elements according to the Restriction of Hazardous Substances (RoHS) (Figure 16.8c) or valuable substances such as gold (Figure 16.8d) and, if necessary, to verify their contents with a subsequent point analysis. This information is important for monitoring compliance with consumer protection requirements or for recycling technologies.

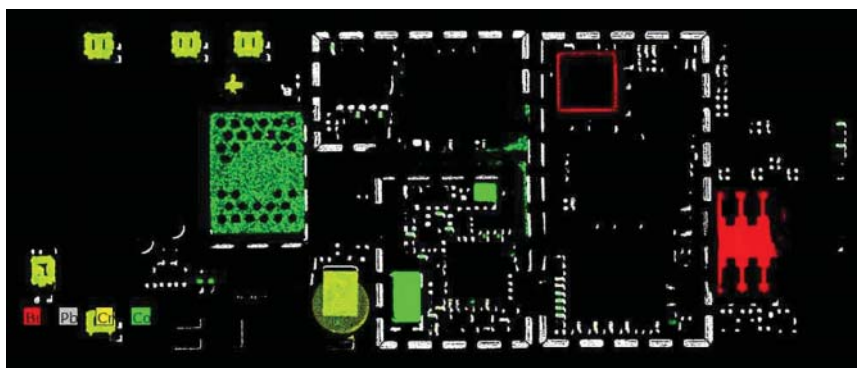


(a)

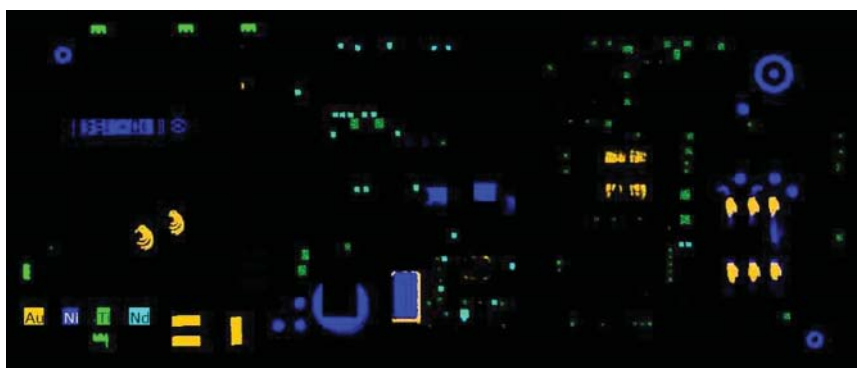


(b)

**Figure 16.8** (a) Photograph of a PCB of a mobile phone, (b) distribution of some main elements, (c) distribution of some toxic elements according to RoHS (Br: red, Pb: gray, Cr: yellow, Cr: green), and (d) distribution of valuable elements (Au: yellow, Ni: blue, Ti: green, Nd: light blue).



(c)



(d)

Figure 16.8 (Continued)

## 16.5 Archeometric Investigations

### 16.5.1 Analytical Tasks

The examination of work of arts as well as the related analytical tasks can be very diverse. One thing, however, is common to these investigations: the samples are usually unique and very valuable. This prohibits a preparation that altered or even damaged the samples. This means that the samples can only be analyzed without any alterations. Further, these samples are usually irregularly shaped; this means that no adaptation of the sample to the sample chamber of an instrument is possible and flat surfaces for a measurement are only rarely available. Therefore, either large sample chambers are required, or the analysis has to be carried out directly on the object. Further, art objects usually are nonhomogeneous, and therefore the analysis needs often to be done on small areas. In addition to the determination of the elemental composition of small sample areas, the determination of the element distributions can be a key interest. This requires scanning with position-sensitive methods.

Additionally, the high monetary value of work of arts makes a transport to laboratories very expensive caused by the necessary protection of the object

against damage or loss. Therefore, often transportable instruments are used for their analysis. This can be either handheld instruments (see Sections 4.3.1 and 15.3.5.6) or transportable macro-X-ray fluorescence spectrometers (see Section 4.3.3.5 and Alfeld et al. 2013).

A further important requirement is that the sample itself is not altered by the analysis itself. This concerns not only the preparation but also the irradiation with the incident radiation. However, the low excitation intensities of position-sensitive instruments and the short measuring times influence the sample only in very special cases. One example is the color changes of antique glasses; however, they are mostly reversible. Anyway, this should be tested before the analysis at positions that are not visible.

For the individual art objects, the analytical tasks can be very different. In the following, a few examples are given to illustrate this diversity:

- For historical statues or vessels, the element composition is interesting in order to make a dating of creation or a determination of the place of manufacturing or to understand the used technologies. Further, the composition may also be of interest in order to avoid damages, for example, by environmental influences, or to make appropriate restorations. Since such objects do not always fit into a sample chamber, investigations are often carried out using a handheld instrument (see, for example, Mass and Matsen 2012). In special cases also instruments with very large sample chambers are used (Greiff 2015).
- In the case of historical coins, the precise determination of the composition may be of interest because they allow conclusions about manufacturing technologies available at the time of coinage. Further, coin composition can give information about the economic situation during their issue or about the origin of the used precious metals. This would allow the retrace of historical trade routes or land conquests by means of the trace elements, since coins were produced not only from freshly extracted ores but often also by remelting from still older coins acquired by conquests or trade.  
In the case of more recent coins further, more forensic questions can be interesting. The collector's value of a coin substantially depends on the number of produced coins and their abrasion. The number of coins produced varies from year to year and also depends on the respective mint. This can provoke an intentional counterfeiting of the manufacturing markers in order to enhance the collector value. This can be a task for an element analysis by means of distribution analysis, which can make even small differences visible (Kämpfe and Haschke 1998).
- In the case of colored glass windows, the element composition of certain areas can be of interest. The used pigments and their location on the glass can provide information about the manufacturing technology but also deliver indications for appropriate restoration technologies. A proper restoration of environmental or other damages is only possible if the structure and the used technologies are exactly known. This allows also to prevent further damage by stabilizing the structures (Kaiser and Shugar 2012).
- For ceramics and porcelain, it is interesting to identify the basic material. Additionally, the pigments of surface paints and their structure can give notes about

the used technologies. This can help to identify the origin of the objects (Mantouvalou et al. 2011), but they can also be used for a proper restoration of damages (Bezur and Casadio 2012).

The main components of glass or ceramics are often light elements with low-energy fluorescence radiation. This is strongly absorbed in air as well as on surface layers, such as the enamels on the ceramics. Therefore, measurements in vacuum are required, or this absorption should be reduced by special conditions, such as short working distances or the flushing of the radiation path with helium.

- A very important analytical task for the investigation of paintings is the identification of used pigments and their distribution. In old paintings, predominantly inorganic pigments were used, which are characterized by specific elements, for example, blue by cobalt, cinnabar by mercury, or yellow by chromium; they can be measured with XRF. The composition and distribution of pigments can give information about the origin and the time of the creation of an art object, but help to understand the technology of painting and the history of the work, as well as to give valuable hints for an appropriate restoration.

Particularly in the case of paintings, an on-site investigation can be very important, since often their size, but also their value, can make transportation considerably difficult and can require a high logistical effort. Further, for well-known paintings, their continuous availability in an exhibition may also be of significance, i.e. an analysis on-site can be necessary. For such on-site analysis, special spectrometers are available (see Figure 4.32).

A few examples of these questions will be discussed in the following sections. They will demonstrate the possibilities to elucidate composition, structure, or origin of art objects by using  $\mu$ -XRF. In general, it has to be mentioned that various questions can be solved using XRF in the investigation of archeometric objects. However, in any case a careful preparation of the analysis has to be carried out. This applies to the selection of the appropriate measuring instrument, the selection of optimal measuring conditions, and the evaluation method depending on the analytical task.

### 16.5.2 Selection of an Appropriate Spectrometer

Small work of arts for example statues made of metals, ceramic vessels, jewelry made of enamel or precious metals, and coins, mostly requiring a point analysis in order to be able to analyze different parts of the objects and maintaining the measurement geometry.

Handheld instruments are suitable for such measurements since they can be used on-site as well as for the analysis of any point of the sample independent of their position. However, the disadvantages of handheld instruments are the not exact compliance with the measurement geometry and difficulties in detection of light elements due to the measurement in air. However, light elements are often the main components in ceramics and enamels; therefore this limitation can be significant.

Therefore, the use of  $\mu$ -XRF tabletop spectrometers can provide a solution. These instruments exist with sample chambers of different sizes, usually with

areas in the range of approximately  $0.2 \times 0.2 \text{ m}^2$ , but in special cases even up to  $0.4 \times 0.4 \text{ m}^2$ , as well as for sample heights in the range of 0.1–0.2 m, in which the samples can be positioned for the measurement. These instruments usually are evacuable for the measurement of light elements down to Na. Both the analysis of individual points and the determination of element distributions can be carried out since the sample usually is located on a motor-driven table (see Section 4.3.3.4).

For even larger and non-portable objects, macro-X-ray fluorescence spectrometers are available. In these instruments, excitation source, detector, and optical microscope are composed in a measuring head, which can move on a carriage horizontal or vertical in front of the sample (see Figure 4.32; Alfeld et al. 2013). They can be used for surfaces up to  $0.6 \times 0.8 \text{ m}^2$ ; however measurements are possible only in air.

### 16.5.3 Investigations of Coins

Analyses of coins are carried out for different purposes; historical coins are examined to determine their composition, which is important for an understanding of the used metallurgy technologies or for a tracking of trade routes.

On the other hand, coins with numismatic interest could be analyzed for more forensic reasons. The contemporary numismatic value of historical coins is not determined by their material value, but above all by the number of manufactured coins and by their condition. Therefore, sometimes their value is seemingly increased by specific alterations, i.e. by forgeries.

The number of minted coins depends on the year and the specific mint factory. Both details are indicated by mint marks on the coin. One possibility of a seemingly increase of the numismatic value of a coin is a change of the mint marks, for example, the mint year. Corresponding investigations were carried out on a coin of 2 Reichsmark minted in 1927. Depending on the condition of the coin, the collectors' value for these coins is around €100. However, for coins from the mint in Munich (marked with a "D"; see Figure 16.9) manufactured in 1927, the prices can go up to 50 times higher because the number of coins minted there in this year was only about 300 000 against several millions in all other years. This opens up possibilities for a "value increase" by changing the mark for the coinage year.

The coin from both sides is shown in Figure 16.9a. The investigation started with point measurements on the numbers "2" and "7" of the year date on the coin. The spectra are shown in Figure 16.9b.

The spectra show only small differences. The blue dot spectrum of the "7" shows a distinct peak of S, a result of a first but not successful wet chemical investigation with  $\text{H}_2\text{SO}_4$ . Further, there is a slightly higher silver intensity compared to the red bar spectrum collected on the "2." The nominal Ag content is 50 wt%. Quantification results for the two spectra are given in Table 16.1. They show a small difference between the two measuring positions, where the deviations for the "7" from the nominal composition are above the estimated uncertainty limits; however this allows no clear decision.

On the other hand, the element distribution shown in Figure 16.10 gives definite certainty about changes of the year data. The Ag distribution determined

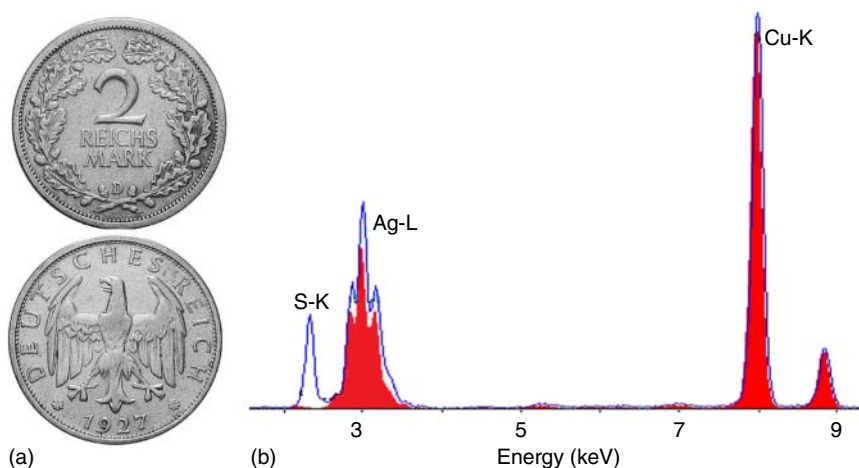


**Figure 16.9** Image of a coin of 2 Reichsmark minted in Munich (D) (a) and spectra measured on the figures “2” (red bars) and “7” (blue dots) of the coinage year (1927) (b).

**Table 16.1** Concentrations at the measuring points in wt%.

Element	“2”	“7”
Ag	49.9	51.3
Cu	51.1	48.7

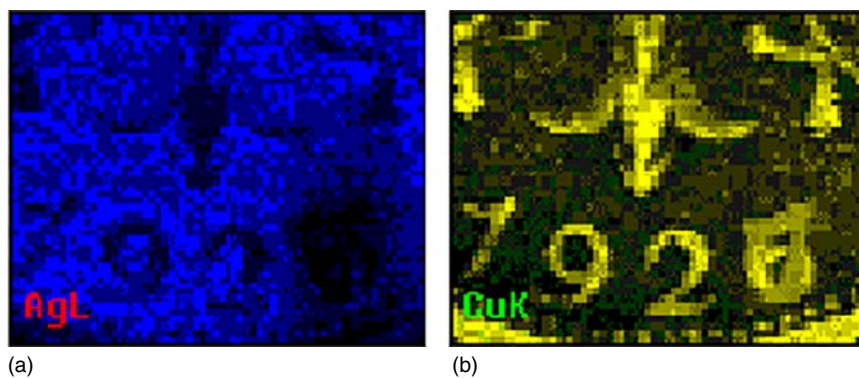


**Figure 16.10** Distribution of Ag (a) and Cu (b) of a 2 Reichsmark coin.

from the L-radiation in Figure 16.10a does not yet allow a clear statement. The thin salt layer of  $\text{Ag}_2\text{SO}_4$  caused by the mentioned wet chemical tests absorbs the low-energy Ag-L radiation. However, the Cu distribution in Figure 16.10b gives a clear indication: below the “7” was previously a “6.” This means that the numismatic value of the coin was originally lower, and now, due to this manipulation, its value is given only by the content of precious metal.



### 16.5.4 Investigations of Painting Pigments

The distribution of pigments of paintings can be tracked by the distribution of the elements characterizing the pigments. From such investigations, a variety of information about a painting can be obtained, for example:

- The verification of the authenticity and the determination of the period of manufacturing of a painting by the identification of the used pigments
- The approval of earlier restorations based on the identification of pigments
- The investigation of chemical transformations of pigments, for example, by environmental influences that are accompanied also by color changes
- The examination of hidden parts of paintings that can give information about the painting technology and about the history of a painting and the painter

Paintings are usually larger than the typical sample chambers of tabletop instruments, and, due to the often very high value of paintings, their transport to laboratories would also be very costly. Therefore, for such investigations, the spectrometer often has to be brought to the paintings for a direct examination, sometimes even in the hanging position at an exhibition.

Further it is important to be able to examine larger areas of a painting; otherwise a good spatial resolution is often required to make the painted structures visible by means of the element distributions. The size of the analyzed surfaces should be adaptable not only to the size of the painting but also to the size of their structures. In the case of large sample sizes and small steps, high pixel numbers need to be measured, and thus also long measuring times as well as large data sets are to be expected.

As an example, the detection of hidden pigment layers in paintings will be discussed in the following. Frequently, color layers are hidden under the upper visible layers since the artist sometimes repainted an already started works in order to adapt them to the time or to the wishes of the client as well as to use an old already used canvas for a new picture. These hidden distributions can also be made visible with X-ray fluorescence without destruction. However, the upper layers may not absorb the fluorescence radiation of hidden pigments too strongly, which means that they should not be too thick or consist of too heavy elements.

An example of such hidden pigment layers is shown in Figure 16.11. It shows in the left part (a) the photo of a painting by an old Flemish master, titled *St. Jerome with the Bible and the cross* (painting provided by Bastiaan Blok, Noordwijk). In the middle and in the right image, the distributions of some elements, i.e. of specific pigments, are shown.

The painting has a size of  $42 \times 58 \text{ cm}^2$ . The element distribution was measured with a step size of 0.5 mm and a pixel time of 15 ms, which results in a total measurement time of 5.5 hours for the approximately 1 million pixels.

The image in the middle (b) presents the distribution of the intensities of some elements with a relatively low-energy fluorescence radiation, for example, Mn (brown), Cr (green), Fe (yellow), Hg (red), and Pb (white). For the last two elements, the low-energy M-radiation is used. The fluorescence of these elements is emitted only from the upper pigment layers. The distribution of these elements

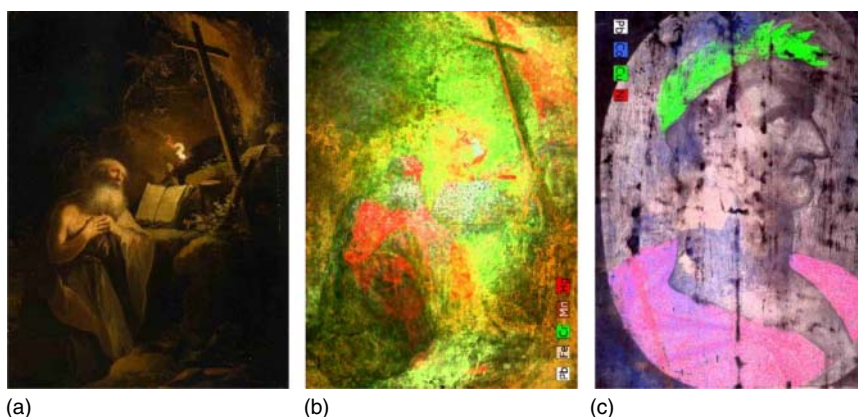


**Figure 16.11** St. Jerome with the Bible. (a) Photograph of the painting. (b) Distribution of the pigments on the surface. (c) Distribution of hidden pigments.

reflects the structure of the image, St. Jerome with the Bible, and the cross can be recognized.

The right-hand part (c) of the figure, on the other hand, shows the distribution of elements with higher-energy fluorescence radiation, in this case the L-radiation of Pb (white), the K-radiation of Co (blue), Ni (red), and Cu (green). This image is rotated by  $180^\circ$ . It shows a head with a laurel wreath and a stole. It is probably a portrait of Gaius Julius Civilis, the leader of the Batavian rebellion against the Romans in 69 AD in the territory of the Netherlands today. This picture was painted directly on the wooden block, with a white oval mirror of lead oxide.

The possibility to uncover hidden pigment layers can provide important information about the history of a painting or about the manner of painting of the painter. Frequently, the painters not only repainted older pictures with another motive but also made changes in the course of the creation of a work, which could provide interesting information for the understanding of the working conditions as well as for the respective living conditions.

## 16.6 Homogeneity Tests

### 16.6.1 Analytical Task

For many analytical tasks, the preparation of homogeneous samples is required. For example, for an accurate analysis of rocks, sand, slags, or ores, as well as metal chips or granulated polymers, the preparation of pressed pellets or fusion beads is necessary. In this case, at first it is necessary to ensure a sufficient representativeness and homogeneity of the material by a sufficient crushing and uniform mixture before further preparation procedures takes place.

When analyzing larger sample areas, smaller inhomogeneities are averaged; nevertheless, inhomogeneities can influence the analysis result. A control of the uniformity of the preparation procedure can be provided by the analysis on

repeatedly prepared samples. However, then it should be taken into account that possible fluctuations of the sample composition are superimposed by statistical deviations. Such measurements are common in the investigation of the homogeneity of samples of larger dimensions, for example, at pulled material, which is cut in disks, and the comparative measurements are made to monitor the homogeneity over the length.

If the analyses are carried out on only small sample surfaces, the homogeneity requirements are significantly higher. This is important, for example, for calibration samples used for a point analysis. Homogeneity tests are important in this case for an estimation of both the quality of the reference samples and thus the uncertainty of analysis.

The assessment of the homogeneity is also influenced by the measurement uncertainty of the used analytical method, which means that distinguishable differences between the individual measurements are superimposed by the measurement uncertainty  $U$  of the method, i.e.

$$U_{\text{Inhomogeneity}} = \sqrt{(U_{\text{total}}^2 - U_{\text{method}}^2)} \quad (16.1)$$

Statements on sample homogeneity thus strongly depend on the measurement uncertainty of the analytical method. The measurement uncertainty often increases with decreasing analyzed volume due to the fluctuations during the preparation procedure or due to a decrease of the measuring signal as a result of the smaller analyzed sample volume. This influence is negligible in  $\mu$ -XRF, since mostly a sufficient excitation intensity can be concentrated on small sample surfaces with X-ray optics.

A simple comparison of the individual measurements is possible with the accumulated element intensities  $I$ . The measurement uncertainty of a measurement is then determined essentially by the statistical error  $\Delta I = \sqrt{I}$ . This should be smaller than the expected or monitored intensity differences between individual sample areas.

Starting from these considerations, two possibilities of homogeneity investigations with high spatial resolution will be presented.

### 16.6.2 Homogeneity Studies Using Distribution Analysis

In the case of distribution analysis, relatively large sample areas are scanned with a small analyzed area. As a result of the high number of measuring points, for everyone only a short measuring time is possible, which results in a large statistical error. Nevertheless, concentration differences are noticeable with such measurements. This is demonstrated by means of a glass specimen. Glasses are generally considered to be very homogeneous, which means that only small intensity differences are expected. Here a glass sample with a diameter of 30 mm was mapped with a step size of 50  $\mu\text{m}$  and a pixel time of 5 ms. As can be seen in Figure 16.12, no differences are apparent in this sample for the main component Si (Figure 16.12a). For the secondary component Al, on the other hand, structures can be detected in the one-color representation of Figure 16.12b, which becomes even more obvious in the false color representation of Figure 16.12c.

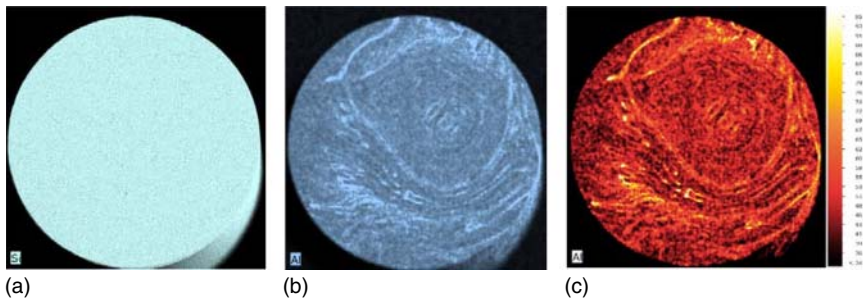


**Figure 16.12** Element distributions of a glass specimen: (a) Si distribution, (b) Al distribution, and (c) Al distribution in false color representation. Source: Courtesy by Hanning (2012).

From the intensity differences the concentration differences can be estimated. These vary for approximately 2.5–5 wt% for  $\text{Al}_2\text{O}_3$ . The Al intensities per pixel are in the range of only 1–4 counts, which means that the uncertainties of the individual counts about 50%. Nevertheless, these small differences are clearly visible and also significant. This is possible, since not only individual pixels are used for the evaluation but also the entire map. Then also these small differences in intensity are relevant.

### 16.6.3 Homogeneity Studies Using Multi-point Measurements

Another possibility for investigating inhomogeneities is the measurement at a limited number of measuring points, but then with a longer measuring time and thus a reduced statistical error.

For a demonstration, measurements were carried out on the polished surface of a Ni alloy. A first set of nine repeated measurements were carried out at the same sample position in order to determine the variation of the measurement procedure, as a second step measurements were then performed at different sample positions within a  $3 \times 3$  grid. The evaluation is then carried out according to Table 6.1, i.e. mean values as well as absolute and relative standard deviations of the absolute collected intensities are determined for the alloy elements. The relative deviations of the alloy elements of both measurement series are presented in Figure 16.13. As expected, the standard deviations for the repeated

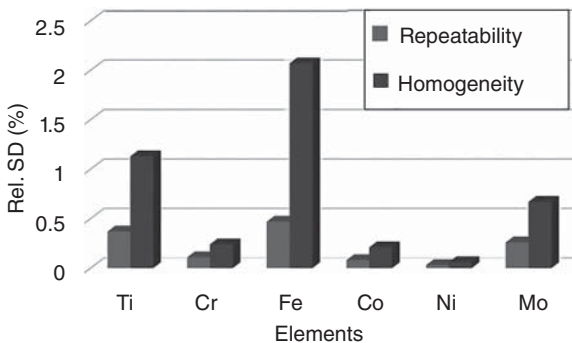


**Figure 16.13** Relative standard deviations of repeated measurements on the same position and on different positions of a Ni alloy.

measurements on the same position (repeatability) are inversely proportional to the concentrations of the elements or to the measured intensities. However, they are by a factor of approximately 4 larger for the measurements at different sample positions (homogeneity). This means that the homogeneous Ni alloy shows non-homogeneities when the analyzed sample areas are sufficiently small compared with the total sample; in this example the spot size diameter was about 30  $\mu\text{m}$ .

Similar measurements were also carried out for plastic reference materials (Mans et al. 2009) for homogeneity tests.

## 17

### Special Applications of the XRF

#### 17.1 High-Throughput Screening and Combinatorial Analysis

When relationships between material composition and material properties are not fully known and understood, the development of materials with new specific properties is often carried out by a “trial-and-error” procedure, which means by a stepwise change in the material composition, followed by a review of the desired properties. A multiple repeat of this cycle can optimize the material properties successively. Such processes are often used for the development of magnetic materials, of new catalysts, of high-temperature superconductors, of active agents, or others.

##### 17.1.1 High-Throughput Screening

Using high-throughput screening (HTS), this process can be made more effective by replacing the successive procedure by a parallel process. In this case, the compositions of the materials of a material bank are only slightly but purposefully modified, and then their composition as well as the desired material properties are checked. Through the correlation of material composition and material properties, tendencies for their optimization can be detected, and thus the process of material optimization can be significantly accelerated.

In addition, the reduction of the material consumption means that the process is not only faster but also cost-saving. However, then analytical methods are required, which can work with smaller amounts of material and which are also sufficiently fast. This can be, for example, focusing IR spectrometry for the elucidation of molecular composition or capillary X-ray diffractometry for structural determination.  $\mu$ -X-ray fluorescence ( $\mu$ -XRF) can be used for element analysis.

The methods used for HTS should meet a few further requirements:

- The high number of samples requires not only a fast analysis but also a fast and automated sample positioning, for example, by using motor-controlled sample magazines.

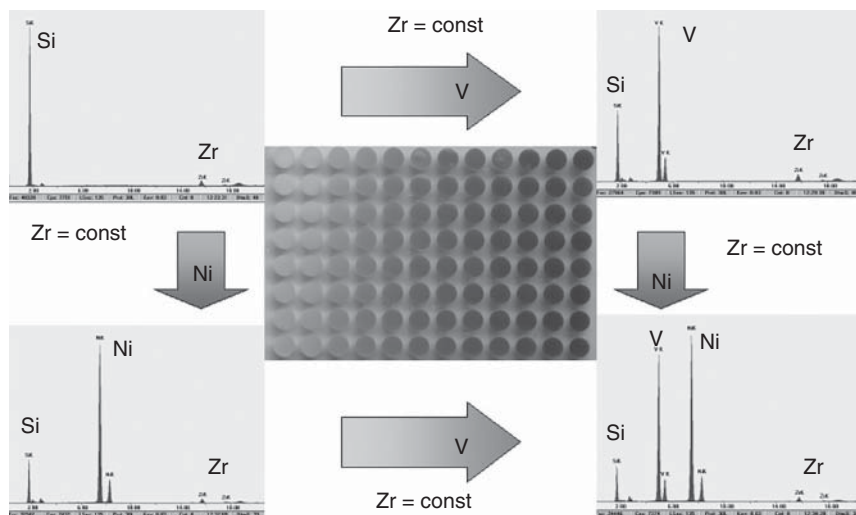


**Figure 17.1** High-throughput screening for the development of a catalyst.

- A further efficiency gain is achieved by reproducibly changing the sample magazines in the spectrometer.
- Variable information can be derived from the measurements, such as the composition of individual samples, changes in the sample composition within the material bank, homogeneity of the samples, correlation of the analytical result, and sample position.
- Possibilities for automation of measurement and data evaluation are indispensable when examining large sample collectives.

The following example for the development of catalysts illustrates the requirements and possibilities of HTS (Haschke et al. 2002; Klein et al. 2001). Here the samples were placed in an array, which is also used for other analytical methods. Figure 17.1 shows in the middle such an array with  $12 \times 8$  sample cups, each with a diameter of approximately 4 mm. The respective material quantity per vessel is then in the milligram range. The example shown is a  $\text{SiO}_2$  ceramic with a small content of Zr as base material, which was enriched with V and Ni solutions. The enrichment took place gradually with increasing concentrations in the sample field in the one direction for Ni and in the other for V. The spectra measured at the corner points of the array are shown also in Figure 17.1 at the respective corners. They show only Si- and Zr-lines in the upper left corner, since there are no additions of V and Ni. The intensity of the corresponding fluorescence radiation increases with the enrichment of V (horizontal) or Ni (vertical), but at the same time the intensity of the Si radiation decreases as a result of its stronger absorption in the heavier matrix.

Starting from the knowledge of the composition of the samples and taking into account the catalytic properties to be determined separately, the development of new catalysts and other functional materials can be significantly more effective.

### 17.1.2 Combinatorial Analysis for Drug Development

In the development of agents, not the development of new agents is in the focus, however, to a much greater extent the selection of agents with high efficiency. This depends primarily on the adsorption of the agents to a particular body protein. These investigations are also carried out conventionally with sequential methods, that is, generation and characterization of a certain agent and subsequent tests for its effect. The effect of an agent is, however, primarily dependent on the probability of its adsorption to a particular protein. The determination of this affinity is a time-consuming process, the acceleration of which can be achieved by means of X-ray analysis methods.

The active ingredients and proteins are predominantly composed of elements that are not accessible by X-ray spectroscopy, for example, hydrogen, carbon, oxygen, and nitrogen. However, in the active ingredients as well as in the proteins, some analytically detectable elements are also usually contained, e.g. halogens, sulfur, or other essential elements such as zinc, selenium, or others. These elements can be used for the determination of active agents. For this purpose, the procedure described in the following can be used (Miller et al. 2003; Minogue et al. 2005, 2006):

- First, various agents are introduced into a sample carrier, which separates individual samples from each other. For this purpose, styrofoam spheres can be used, which are coated with different agents. These spheres have a diameter of 0.08 mm. These agent carriers are embedded in a film that contains holes approximately of the size of the styrofoam spheres in a regular pattern. In this case a sample matrix with different but unknown agents is generated. This can be very tightly packed, with spacing of 0.5 mm. Then  $10 \times 10$  holes are placed on a surface of  $1/4 \text{ cm}^2$ , 10 000 holes on a surface of about  $5 \times 5 \text{ cm}^2$ . Such a sample carrier is shown in Figure 17.2a.
- In the next step, the agents are brought into contact with a protein. This may be by dipping the sample carrier in a solution of a particular protein. Depending on its affinity for the respective agent, the protein is deposited in varying amounts on the different agents on the styrofoam spheres.

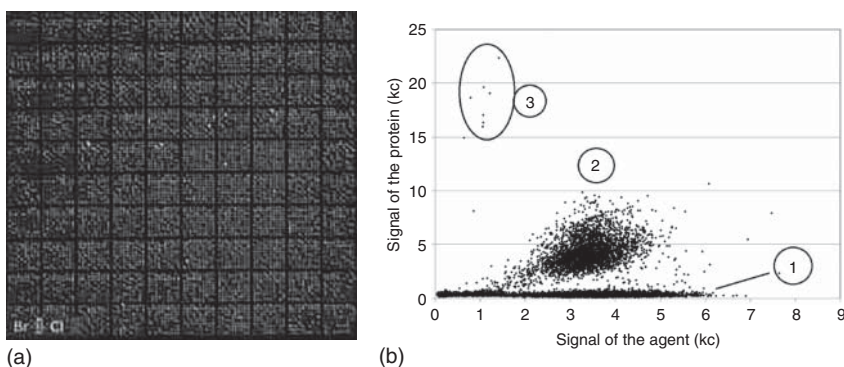


**Figure 17.2** (a) Sample carrier with  $10^4$  samples and (b) relations between agent signal and protein signal.



- By measuring X-ray spectra at the individual holes, information about the amount of the protein molecules attached to the different agents can be obtained from the fluorescence intensities of the elements characteristic for these specific proteins. Since no quantification but only an evaluation of the intensities is required, measurement times of about one second per sample are sufficient, which means that the entire array with 10 000 samples is measurable in only few hours. In this way, the interaction of a lot of different agents with one protein can be investigated quickly.
- The relationship of an agent signal to the substrate signal for the individual measuring points is shown in Figure 17.2b. The respective signals are to be selected as a function of the tested combination of the agents and the protein. In the distribution of Figure 17.2b, three groups can be distinguished:
  - Group 1 shows no or only a very low agent signal. These are holes in the sample carrier that contain no spheres with an agent, i.e. which have remained empty during the preparation.
  - Group 2 shows a low protein signal, which is largely proportional to the agent signal. Here, a normal adsorption of the protein to the respective agent takes place. Differences in signal correlation result from minor differences in the number of proteins molecules attached.
  - Group 3 has only very few participants, which can initially be considered as outliers. However, they are caused by a strong reaction between agents and protein. These are the measuring points of interest. The corresponding samples can be identified by assigning the measuring points to the sample position.
- After the dissection of one of these interesting styrofoam agent's carriers, the agent can be identified by means of a sequencer. In this way, an effective combination of an agent and the specific protein can be selected. On that basis a further decision can be made regarding their applicability for different task.

Compared with other methods, a drastic increase in efficiency and significantly cost reduction can be achieved with this type of agent selection.

However, this method cannot only test the efficiency of agents, but also the acceleration of other chemical reactions, such as catalytic processes or the effectiveness of precipitation reactions by changing the reaction conditions.

## 17.2 Chemometric Spectral Evaluation

As a result of the good understanding of the interaction of X-rays with matter, a complete calculation of X-ray spectra is possible (see Section 5.5.3). This, however, requires the knowledge of all elements present in the sample. This is not possible for any sample since light elements cannot be detected directly by X-ray fluorescence (XRF). On the other hand, these are elements that are present in many materials, and as in polymers, minerals, glasses, or ceramics, even in dominant concentrations.

Here, chemometric methods can provide a way for the spectral evaluation. These methods use all components of the spectrum, including the spectral

background for the evaluation (see Section 5.7). Examples for using chemometric methods for the quantification of polymers have already been discussed in Section 9.8.4.2 and for the identification of glass particles in Section 15.2.

Here this type of spectral processing will be discussed for the identification of various chemical compounds. These should be identified in their packaging, i.e. in polyethylene (PE) bags in order to avoid their unpacking and to identify them rapidly, and be cost effective (Kessler et al. 2000; Hoffmann et al. 2001; Hoffmann 2005; Henrich et al. 1999). The chemicals are various salts that contain only very few or even no elements, which can be detected directly with XRF. The measurements were carried out with an energy-dispersive (ED) spectrometer in order to detect the entire spectrum rapidly including the scattered radiation. As an example, the spectra of some Na salts are shown in Figure 17.3.

All spectra were measured under the same conditions, i.e. Rh target, 45 kV, Ag filter, and acquisition time of 20 seconds. They show only structures in the high energy range of the scattered tube radiation. The fluorescence radiation of sodium will be poorly excited due to the Ag filter and is completely absorbed on the way to the detector because the salts are in the PE bag and the measurements are carried out in air.

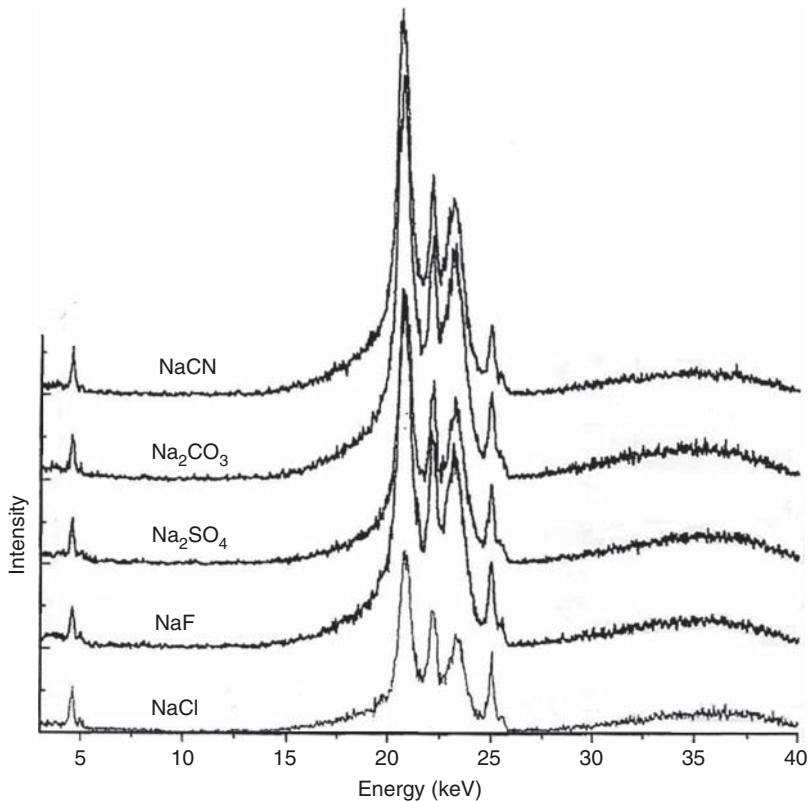


**Figure 17.3** Energy-dispersive measured X-ray spectra of few sodium salts. Source: Courtesy of P. Hoffmann.

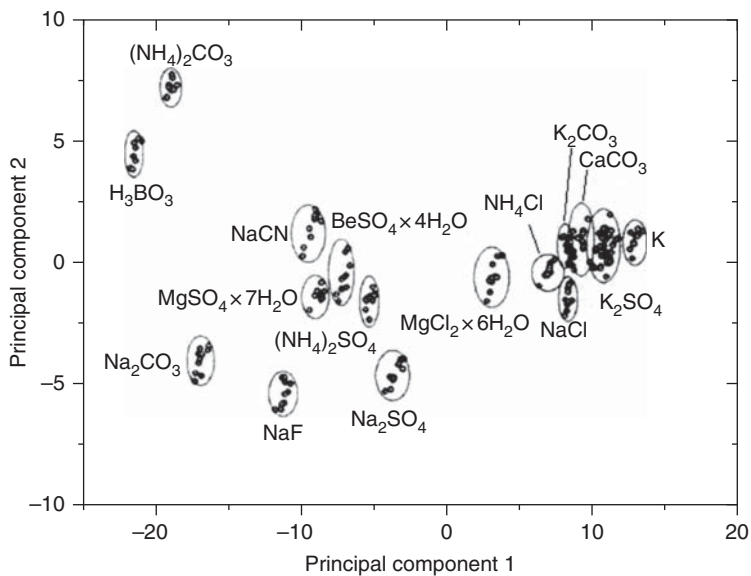


**Figure 17.4** Score plot of the principal components of different chemicals. Source: Courtesy of P. Hoffmann.

For the chemometric evaluation, these spectra were divided into 150 spectral ranges (principal components). With them all compounds under investigation could be clearly identified. For the “training” of the system, the spectra of all these chemicals need to be measured several times. As shown in Figure 17.4, a relatively reliable identification of the individual chemicals is possible with a simple principal component analysis (PCA); the individual material groups are highly distinguishable. Figure 17.4 contains not only the Na compounds but also other compounds. If they contain heavier elements, their fluorescence lines can be detected and of course also be used for the identification of the material.

This procedure can be applied not only for salts but also for complex organometallic compounds. If an additional material should be identified with this procedure, it must also be measured several times and can then be integrated into the spectral library. Then recalculation of the PCA is necessary.

This way allows a spectral evaluation even if individual element lines cannot be measured. Nevertheless, this is not a quantitation, rather a material identification, but with high reliability.

However, the application of chemometric methods strongly depends on the analytical problem and requires a special adaptation to every task, which includes the determination of the principal components, some steps of spectral evaluation, and then the training of the system. But then it offers a high potential for the determination of material or their properties. Other examples are the identification of wooden chipboards (here not only the type of the used wood but also the humidity grade of the chipboard could be determined [Kessler 2001]) or the identification of different types of beer (Brouwer 2015).

## 17.3 High-Resolution Spectroscopy for Speciation Analysis

### 17.3.1 Analytical Task

X-ray spectrometry is commonly used for element analysis. This task is independent of the bonding state of the elements since the electron levels involved for the mostly used fluorescence lines are close to the atomic nucleus and therefore only slightly influenced by the atomic environment. Furthermore, in many cases, the compound partners are not detectable by XRF, for example, for oxides, carbonates, nitrates, or other salts, since their fluorescence radiation has too low energy. In various cases, however, it is also interesting and necessary to know the binding forms, for example oxidation levels of the elements. Thus, a speciation analysis is required since the properties of the various compounds can be very different and their identification may be important for a correct assessment of the material.

The influence of the bonding on the electron configuration is relatively low and affects outer electron shells only. The very small changes in line energies can be detected by X-ray spectrometry only with high-resolution spectrometer and by using X-ray lines in which transitions from the outermost electron levels are involved. These are often high-energy satellite lines of a spectral series.

To ensure that the small influence of the atomic environment can be better detected, it is useful to use transitions to more outer electron shells, i.e. work in the low energy range. For this reason L-lines are often used for speciation analysis (see, for example, Urch 1996; Pappert et al. 1997; Geyer et al. 1997; Reisel et al. 2000; Schlesinger et al. 2015).

Another possibility of using high-resolution spectrometry is the examination of the precise spectrum shape. In solids the outer electron levels overlap each other and build bands with permissible electron states in a certain energy range with different state densities. These state densities are reflected in the form of the spectra. However, this shape is folded with the Gaussian distribution of the inner electron shell together with the spectrometer function, which is a result of its resolution. The state densities at the Fermi level are important for electrical and magnetic properties of the material, especially in transition metal alloys (Haschke and Weisbach 1973). The determination of electron densities at the Fermi level can contribute to the understanding of these macroscopic properties.

In order to determine the exact form of the spectra, the statistical error of the individual measurements should be very small. This must be ensured by appropriately long measuring times per wavelength range, but also by an effective excitation. This is particularly possible in the low energy range by means of electron excitation because they have a higher excitation efficiency for low-energy lines.

### 17.3.2 Instrument Technology

The energy shifts used for speciation analysis are in the range of some electronvolts. This requires a high spectrometric resolution, which is, however, achieved already by most of the commercially available wavelength-dispersive (WD) spectrometers. Especially in the low energy range, the resolution is high for WD

spectrometers (see Figures 4.1 and 4.2). This correlates well with the energies of the L-lines that are often used for speciation analysis. However, the fluorescence outputs of these lines are small, i.e. the achievable intensities are very small. In combination with the requirements for high resolution, i.e. small collimators and small angular steps during the measurement, relatively long measuring times are necessary.

A solution could be provided by simultaneous WD spectrometers, in which a relatively broad range of energy is covered with sufficient resolution. This would be possible with a von Hamos geometry in combination with a position-sensitive detector (Anklamm 2014).

### 17.3.3 Application Examples

#### 17.3.3.1 Analysis of Different Sulfur Compounds

Figure 17.5 shows the K $\beta$  spectra of different sulfur compounds (Urch 1996). They illustrate, depending on the bonding state, not only the line position changes but also its shape. In lithium sulfide ( $\text{Li}_2\text{S}$ ), sulfur is symmetrically incorporated as a simple  $\text{S}^-$  anion. This structure is also reflected in the spectrum. The binding situation of sulfur in pyrite ( $\text{FeS}_2$ ) is more complex, since here the sulfur is bound in a crystal and appears as a  $\text{S}_2^-$  anion. The binding conditions for dimethyl sulfide ( $\text{C}_2\text{H}_6\text{S}$ ), in which sulfur is asymmetrically bound between the two methyl groups, become even more complex. These environments influence the spectral shape.

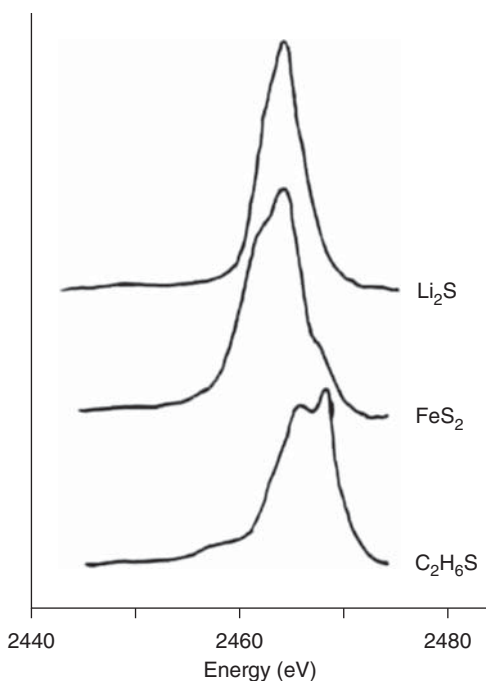


**Figure 17.5** S-K $\beta$  spectra of different sulfur compounds. Source: According to Urch (1996).

Already this simple example shows that the spectra with an appropriate resolution can reflect the particular binding conditions. On the other hand, information about the binding situation can be gained from the spectra. This is relatively simple for pure compounds if the statistical error of the individual measurements is sufficiently small. However, for mixtures of different compounds, the task becomes explicitly more complex. Nevertheless, it can be assumed that the spectra of the individual components of the mixture superimpose linearly. Therefore, the individual contributions can be determined by a fitting with the previously determined spectra of the pure compounds. The accuracy that can be achieved in this case, however, is limited by the propagation of the different errors, the low intensities of the used spectral lines, and the often high scattering background.

It should be noted that X-ray absorption spectrometry (X-ray absorption near edge structure [XANES] and extended X-ray absorption fine structure [EXAFS]) is also used for speciation analysis. In this method the speciation-dependent structures are usually stronger and thus more suitable for speciation analysis. However, X-ray absorption spectrometry up to now is possible only on synchrotrons and is therefore not available for a wide range of applications. Recently, X-ray absorption spectrometry in transmission, particularly for thin specimens, can also be performed in laboratories using a simultaneous WD spectrometer (Schlesinger et al. 2015).

### 17.3.3.2 Speciation of Aluminum Inclusions in Steel

Aluminum is used in steel production in order to deoxidize the melt, i.e. to bind the free oxygen in the melt and deposit it as alumina. The aluminum oxide swims upward due to its low specific weight and goes into the slag. However, Al is also incorporated into the steel, for example, after a reaction with nitrogen to AlN. Accordingly, Al can be found in steel in three different species: elemental Al, nitride (AlN), and oxide ( $\text{Al}_2\text{O}_3$ ) (Neuberger 1965). While dissolved Al and AlN positively influence the quality of steel,  $\text{Al}_2\text{O}_3$  forms, disturbing slag inclusions. AlN already crystallizes at elevated temperatures in iron and therefore binds the dissolved nitrogen, which avoids the formation of blowholes and segregations and thus counteracts an embrittlement of the steel (Wiegand 1977). At the same time, for austenitic steels, the grain size is reduced by AlN, which improves the resistance to mechanical stress.

On the other hand, the bonding of dissolved oxygen in the melt by the formation of  $\text{Al}_2\text{O}_3$  leads to surface defects in the material, which accelerate the fatigue of steel. Therefore, the content of  $\text{Al}_2\text{O}_3$  must be kept as small as possible. However, the determination of mass fractions of AlN and  $\text{Al}_2\text{O}_3$  in the steel with element analytical methods is difficult. Although the total proportion of Al can be determined by spark spectrometry or by XRF analysis, the contents of the both speciations are not accessible to these methods in a first approach. Conventionally, the determination of the speciation will be carried out with wet chemical methods (Beeghley 1949). However, this is time consuming and requires the use of harmful chemicals. Therefore, a spectroscopic method would be preferable. For the first time, the possibility of using X-ray spectrometry was described by

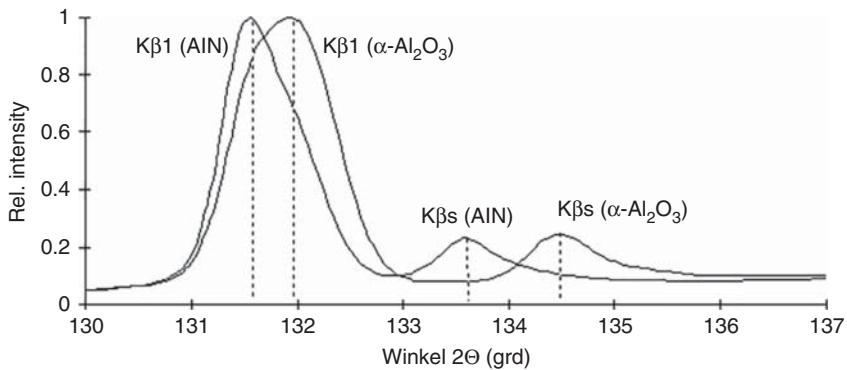


Figure 17.6 Al-K $\beta$  spectra of Al nitride and Al oxide.

Grimaldi et al. (1981). They used the dependence of the Al-K $\beta$  energy on its binding form. For this line, the electron transfer takes place from the M- to the K-shell. The external M-shell is influenced by the atomic environment, i.e. it depends on the binding form of Al. This becomes clear in the spectra shown in Figure 17.6. The energy difference between the two peaks is about 3.5 eV. This difference can be easily distinguished with WDS instruments. However, due to the overlapping of both peaks, an accurate determination of peak intensities would be erroneous. Therefore, the use of the satellite lines (K $\beta$ s) of both compounds is favored. Their energy difference is larger, and the lines are not overlapping; however, their intensities are drastically lower and will have a worse statistic.

A calibration using these satellite lines is illustrated in Figure 17.7. It shows the relation between the intensity ratios  $I\text{-K}\beta_5(\text{Al}_2\text{O}_3)/I\text{-K}\beta_5(\text{AlN})$  to the ratio of the concentrations of both compounds.

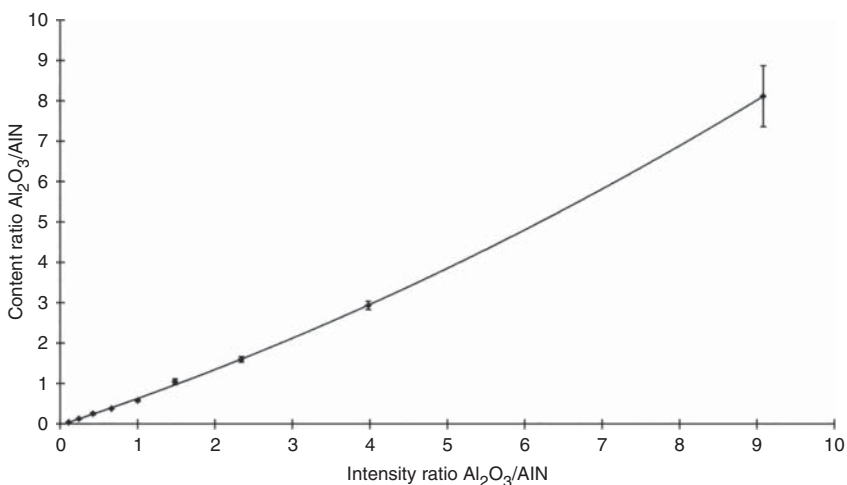


Figure 17.7 Calibration curve for the concentration ratio of  $\text{Al}_2\text{O}_3/\text{AlN}$  by using the Al-K $\beta$  satellites.

The low signal intensities allow only limits of determination for both aluminum compounds in the steel matrix of approximately 100  $\mu\text{g/g}$ , and the repeatability is about 10  $\mu\text{g/g}$ . This precision is not sufficient for a production control. If, however, the compounds are isolated by an electrolytic dissolution of the iron matrix and the residues are separated by a fine pore membrane filter, the direct analysis after drying by means of XRF is possible. Due to the associated enrichment, the statistics can be improved by a factor of approximately 5 (Pappert et al. 1996). However, due to the filtration of the electrolyte, it is possible that very small nitride particles ( $<0.1 \mu\text{m}$ ) cannot be separated, and thus the analytical result can be erroneous.

### 17.3.3.3 Determination of $\text{SiO}_2$ in SiC

Another example of using satellite lines in reasonable measuring times is the determination of the mixing ratio of  $\text{SiO}_2$  traces in SiC (Rüttimann 2008a).

The bonding influences can be determined here by the position of the Si-K $\beta$ -lines, since these are also generated by transitions of electrons from the outer M-shell. Compared with the Si-K $\alpha$ -line, their intensity is only approximately 10%. However, the K $\beta_{1,2}$ -lines are displaced only by approximately 0.3 eV for the two Si compounds. They are shown in Figure 17.8. The evaluation of this peak shift would be only possible by the measurement of the entire spectrum with a successive deconvolution. But it turns out that there is still a small Si-K $\beta'$ -line for  $\text{SiO}_2$ , which cannot be observed for SiC. When evaluating the intensity of this Si-K $\beta'$ -line in relation to the main line, the  $\text{SiO}_2$  content in SiC can be determined with sufficient accuracy.

For this purpose, however, the sample must be very fine-grained and pressed without binders in order to minimize grain size effects and any absorption by

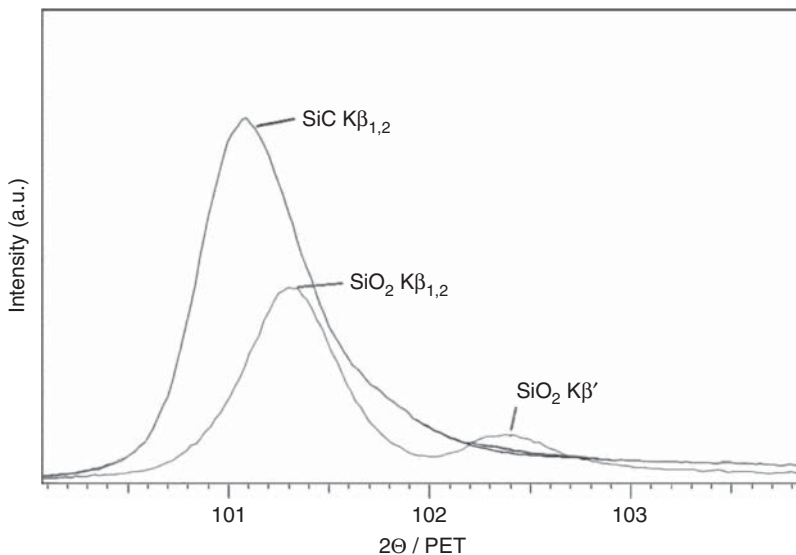


**Figure 17.8** Si-K $\beta$  spectra of  $\text{SiO}_2$  and SiC. Source: Courtesy of F. Rüttimann.



the binder. The preparation as a fusion pellet is not possible, since the chemical bonding of silicon could be changed. For an accurate determination of the net intensities, the spectral background was determined at two points on each side of the peak in addition to the peak position. The measurement times for all measuring positions were 30 seconds each; the tube power was relatively large with 30 kV voltage and 120 mA tube current, i.e. 3.6 kW.

In this way, detection limits for SiO<sub>2</sub> in SiC of about 0.5% could be achieved. The absolute errors in the mass fraction determination were approximately 0.03%, a factor of 3 better than by a determination with help of the concentration of the carbon in SiC, especially since additional additives can occur due to carbon-containing impurities.

## 18

# Process Control and Automation

## 18.1 General Objectives

The quality-checked manufacturing of products requires a comprehensive control of chemical and physical parameters throughout the entire manufacturing process. The driving force is the goal to optimize the overall process for a variety of aspects. In addition to the primary economic objectives, aspects such as sustainability and product liability are becoming increasingly important.

A look back in the history of chemistry reveals that analytical chemistry already laid in the Middle Ages the foundations for today's production processes with fundamental investigations on the characterization of raw materials. Chemical analysis provides information about the qualitative and quantitative composition as well as the structure of substances. A very special subdiscipline of analytics is process analysis, whose task is to use known analytical methods, considering the specific requirements resulting from the production processes and the customer-specific product properties. With the aim of a more efficient production, both continuous and discontinuous measuring methods are used to provide the necessary information for the monitoring and control of technical processes. Process analysis, together with the techniques used in the production process, must build an integrated system that meets the following requirements:

- Increased efficiency
- Reduction of operating and analyzing costs
- Reduction of the process and analysis time
- Improvement and equalization of product quality
- Improvement of environmental and health protection.

Looking at the economic aspects, a reduction of the cost of analysis also means a reduction in personnel costs. Accordingly, the automation of analytical processes, especially around process control, is of particular interest.

X-ray fluorescence (XRF) spectrometry is often used for process monitoring because of the automation capability of its measurement sequences, the relatively rapid availability of analytical results, and the possibility of continuous measurements. The carrying out of the measuring process requires, already with today's instrument technology, usually no external intervention. However, an automated process control requires also automatic sample preparation and feeding to the instrument. For this purpose, the analysis system must be integrated into the

production process by means of special engineering solutions, especially for sample preparation and sample handling.

Depending on the frequency of variation of process parameters, the type of samples to be examined, and the number of samples to be analyzed per time, there are different concepts for the design of process analysis:

- *Off-line analytics*: The classical approach of analytical chemistry in a production process is the central laboratory, in which all necessary test methods are available. This means that the samples taken from the process are transported to the laboratory located at a central location in the production plant, where they are examined. The methods available in this laboratory are not only oriented to the needs of an individual process, but rather represent a compromise since the available methods must be universally applicable. Off-line analysis is suitable for discontinuous and relatively slow processes.
- *At-line analysis*: At at-line analytics, sampling is, similar as the off-line analysis, not coupled to the analysis system. However, the analysis is carried out with special analysis systems in the immediate vicinity of the sampling site. This can be either a special operating laboratory or special, for example, mobile measuring systems whose measurement programs are adapted to the respective, mostly unique analytical problem and are often automated. The specialization to specific tasks allows shorter reaction times but is accompanied by a loss of flexibility since such measurement systems require special sample geometries or have restricted working ranges. In the case of at-line analysis, the time requirements can be stronger, but it is not yet a real-time monitoring.
- *On-line analysis*: In contrast to the concepts described previously, the sampling takes place automatically in the on-line analysis. This can be either continuous or discontinuous. The connection to the process stream can be, for example, a sampling bypass. In this material stream of the process, sampling can be carried out automatically under controlled conditions. The sample preparation, for example, the separation of interfering components, an enrichment or conditioning, is carried out automatically like the measurement. The measurement procedure is optimized to the special task. On-line analysis not only results in a further reduction of required time for the analytical process, but also an externalization of the analysis is achieved by means of the automated sample taking and preparation.
- *In-line analytics*: This is the next development stage of process analysis. The necessary test parameters are directly measured in the process stream by sensors and without direct contact to the sample by means of suitable measuring methods. For the non-contact analysis of the sample, spectrometric methods with X-rays are particularly suitable. In this case not only the fastest action times on the monitored process are achieved, but also a high degree of objectification of the results. However, the analytical accuracy can be limited by not ideal sample preparation, i.e. due to contaminations or not correct measurement geometry.

With increasing integration of analytics into the process, the effort to implement the process control also increases, both regarding the mechanical and analytical adaptation and the requirements for reliability.

In consideration of these concepts, there are different variants of the sample presentation for the measurements. Depending on the sample consistency, the sample type, its composition, and the time requirements for the provision of the material properties or information for the process, the appropriate concept must be selected. On-line and in-line analysis allows a continuous process control. The separate sampling and subsequent discontinuous measurement and evaluation of off-line and at-line analysis, on the other hand, result in a longer reaction time and are suitable for a discontinuous process control.

In process analysis often only the measured value itself is used for the process monitoring – in XRF, for example, the measured fluorescence intensity. If the relationship between signal intensity and material property is known and quantification is not required, a control variable that is approached to the process can be derived from the measured intensity with little effort. This is possible because the matrices in a production process usually do not vary widely, and thus already fluorescence intensities provide meaningful information. Often it is also only checked whether the values are within a certain range.

If this qualitative information is not enough and if the results are to be transmitted to the customer as quality characteristics, classical models of a quantification must be used.

The fields of applications of XRF for process control are very diverse and can therefore not be described in detail here. Spectroscopically, the requirements can be very different, but optimal excitation and test conditions always must be selected in order to obtain optimal measuring signals in the shortest possible measuring times. This means that a simultaneous detection of the complete spectrum is often required, this is possible both with multi-channel wavelength-dispersive spectrometers (WDSs) and energy-dispersive spectrometers (EDSs) instruments.

The possible applications for process control range from the automated central laboratory to the on-line measuring systems integrated directly into the production process.

## 18.2 Off-Line and At-Line Analysis

### 18.2.1 Sample Supply and Analysis

In the case of an automation of central labs, typically commercially available measuring technology is used. For the preparation of the sample, usually also commercially available components are used. The individual components must then be arranged according to the space available in the respective production process and, if necessary, adapted by design and coupled by means of robots (see Figure 18.1). The connection to the production process can be carried out by means of a tube mail system (see, for example, Figure 18.2). Nowadays also the transport from the tube mail gate to the analysis system can be realized by cobots. Such combinations reduce the effort required for the development of special instrument technology, enable the use for various analytical tasks, and ensure a high flexibility and simplify the adaptation also in the case of changes of the analytical problem (Koch and Flock 1990/91; Koch and Flock 1996; Sommer and Flock 1999).

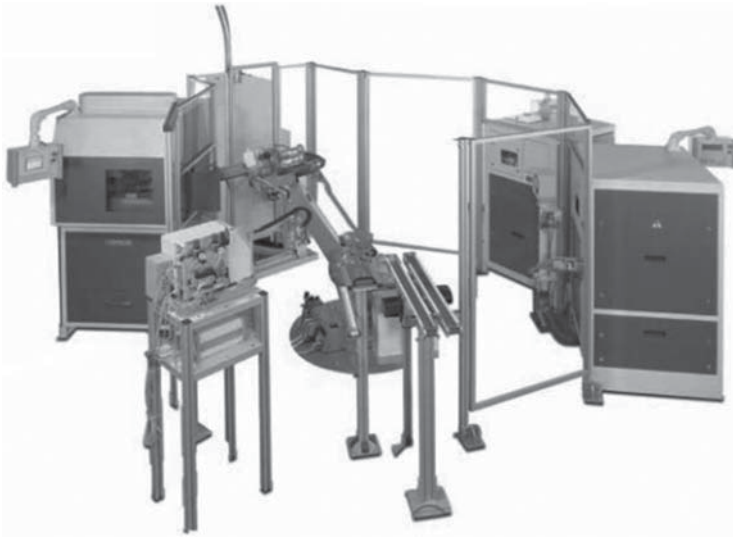


**Figure 18.1** Automated laboratory with instruments for sample preparation and measurement connected with a robot. Source: Courtesy of Herzog-Maschinenfabrik GmbH.

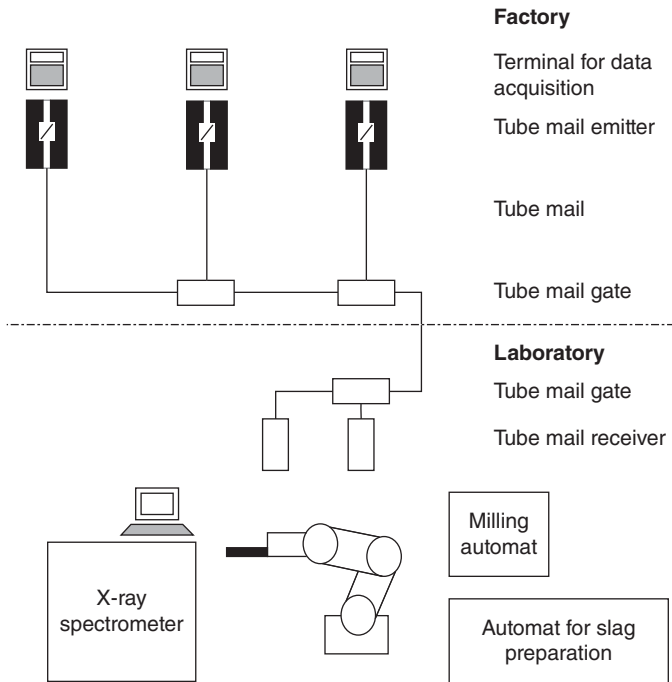


**Figure 18.2** Scheme of an automated blast furnace laboratory for the analysis of pig iron and slag samples. Source: According to Koch and Flock (1990/91).

In such systems, a certain sample quantity is removed from the process either directly or via a bypass, transported by means of a transport system to the central laboratory and there fed manually to the analysis system. The sample can be measured either directly or after a preparation procedure. Compared with on-line or in-line analysis, the time required for a complete analysis is longer, and the feedback to the process is therefore slower. However, in certain processes, a direct measurement is not possible due to the process conditions such as temperature or pressure, or a separate preparation is required for the material, for example, in the case of higher accuracy requirements. Nevertheless, even in these cases, by automation of the sample preparation, an acceleration of the workflows is possible, as well as an objectification of the results of the analysis and a reduction of costs.

Typical examples of off-line or at-line analytics are as follows:

- The analysis of powdered materials, for example, at the production of cement. Here material is taken from the material stream, grounded, weighed, pressed into pellets, and then fed into the measuring instrument for the analysis (Finney et al. 1998).
- The determination of the valuable part of minerals for the control and regulation of the enrichment processes necessary for the extraction (Noack et al. 1997).
- The analysis of materials in metallurgical processes, such as the control of the composition of alloys or slags. For this purpose, the samples are taken directly from the process, cooled, prepared, and analyzed (see Figure 18.1; van den Bosch et al. 2005).
- The monitoring of the product quality of finished products, such as glasses by a preparation after crushing and grinding as a pressed pellet (Buchmeyer 1997).
- The analysis of wafers and electronic components in the production process to monitor the quality of technological steps, such as coatings, with automated sample handling to avoid contamination through the analysis process.

The control of such automated analysis laboratory is carried out by means of laboratory information systems. These enable the control and monitoring of the individual instrument components, the control of the measurement procedures, and the evaluation of the measurement data and their feeding into the higher-level control system of the entire production process. Moreover, such systems have the necessary tools for generating and managing the required quality-relevant statistical parameters (defined in statistical process control – SPC), for example, by using monitor or reference samples as well as, if necessary, recalibration procedures. The monitoring of the entire analysis process as well as its externalization through automatic sample handling is carried out by repeated measurements of monitor samples. The subsequent corrections of the measured values or test conditions ensure the quality of the analysis and thus the product to be monitored.

### 18.2.2 Automated Sample Preparation

While the automation of the measurement is comparatively simple, the preparation of the samples often requires manual intervention. In addition to the

high personnel costs, the resulting disadvantage is, above all, a lower sample uniformity, which also affects the analysis quality. Therefore, considerable efforts are being made to find automated solutions for the preparation of powdered samples as pressed pellets or as fusion beads. However, such systems require very high operational availability. Already in the 1980s of the last century, corresponding systems were developed. In such systems, all relevant working steps are combined, that is, crushing, grinding, and pressing. In systems as shown in Figure 18.3, the sample material is fed into the system by means of a tube mail; then it is broken, portioned, mixed with a grinding aid, finely ground for the analysis, pressed into steel rings (Figure 18.4), and transferred to the analytical system. After the analysis, the steel rings are returned to the preparation machine for cleaning (Koch and Flock 1990/91; Koch and Flock 1996). In addition to the automatic sample feed, a manual sample feed is also implemented in order to be able for control measurements if necessary.

However, even complex sample preparation techniques, such as fusion, can be integrated into automation systems. In a manual operation, for that preparation, the sample is weighed with the flux agent and melted in the muffle furnace. During the heating in the muffle furnace, the fusion must be interrupted several times to homogenize the melt by swirling. At the end of the fusion, the melt is poured into a preheated platinum mold, cooled in a controlled manner, and the solidified pellet is demolded for measurement (see also Section 3.4.4). This manual operation requires the permanent presence of a laboratory technician. Therefore, the first gas-heated instruments were introduced into the laboratories for a mechanization of the fusion digestion already 30 years ago.

As an alternative to the gas-heated digestion instruments, there are also inductive heating instruments for about 25 years, which, in addition to safety

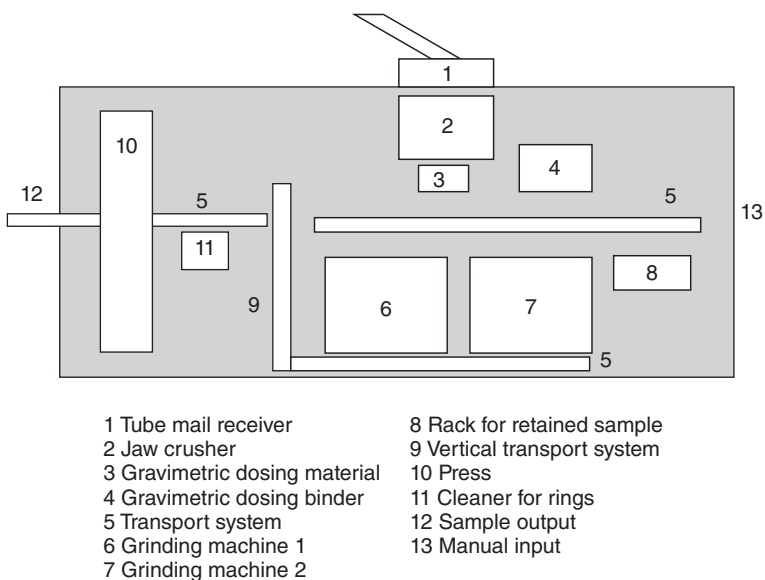


**Figure 18.3** Scheme of a preparation automat for oxidic materials.

**Figure 18.4** Pressed pellet from powder material in a ring of steel as a result of automated preparation process.



aspects and an automatic mixing, have the advantage of a much better control of the fusion parameters, like temperature and time regimes. Combining these instruments with an industrial robot has resulted in a powerful automated system with a sample rate of up to 8 samples/h (Figures 18.5 and 18.6). Both the pre-weighed samples and the empty crucibles are in a sample rack. The flux agent is weighed in via a dosing system, the sample is added, and the sample mass is determined. Flux agent and sample are homogenized in a mixer and then used in the fusion instrument. The complete fusion is automated. Shortly before the end of the fusion, a solid halogenide is added to the melt to ensure a complete pouring of the melt. After cooling the fusion beads, they are removed from the robot by means of a vacuum cup. Due to the capacity of the sample and crucible racks, an autonomous, unattended operation of such a system is possible over a period of up to four hours.

As an alternative to the already described inductive or gas-heated digestion systems, automated instruments with resistance furnaces are also available nowadays. Compared with other systems, these ones have a highly uniform temperature profile over the entire crucible. The temperature can be controlled within small ranges. Due to the small furnace volumes and the high heating rates, gradient programs, e.g. for the realization of oxidation steps, are programmable. Their time consumption is only slightly higher than for inductive or gas-heated systems.

Figure 18.7 shows the outer and inner view of an automation system with four furnace-based digestion instruments in which all work steps, i.e. weighing, controlled melting, pivoting of the melt, and its pouring, are carried out automatically. For the sample handling between the different stations, a conventional industrial robot is used. For the analysis a sequential wavelength-dispersive spectrometer (WDS) is integrated in the automation system.

Figure 18.8a shows the robot loading a furnace and Figure 18.8b the mold containing the sample. This system has two independent weighing systems. In difference to manual operation in which the digestion agent and sample are usually



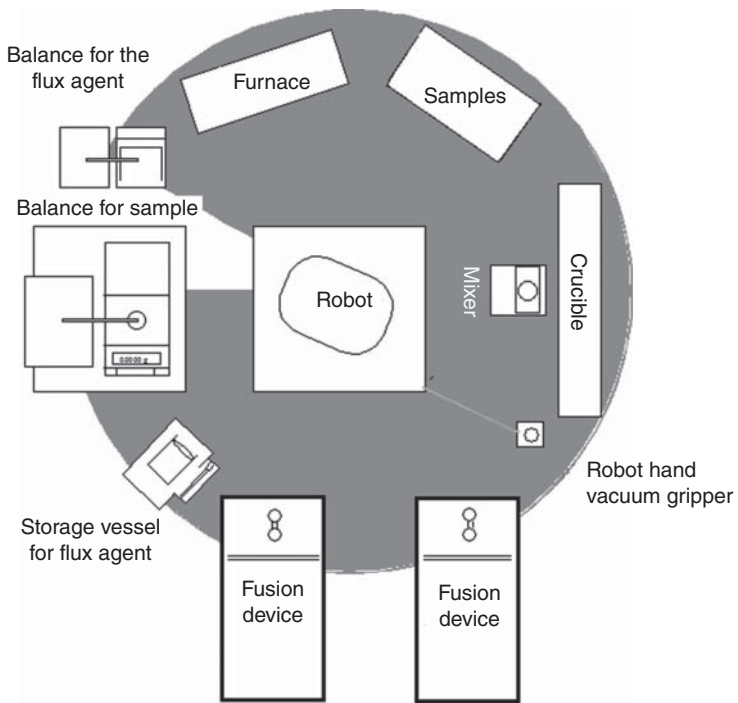


**Figure 18.5** Scheme of an automated fusion automat with inductive heated fusion instruments. Source: According to van den Bosch et al. (2005).



**Figure 18.6** Fusion automat with two inductive heated fusion instruments.

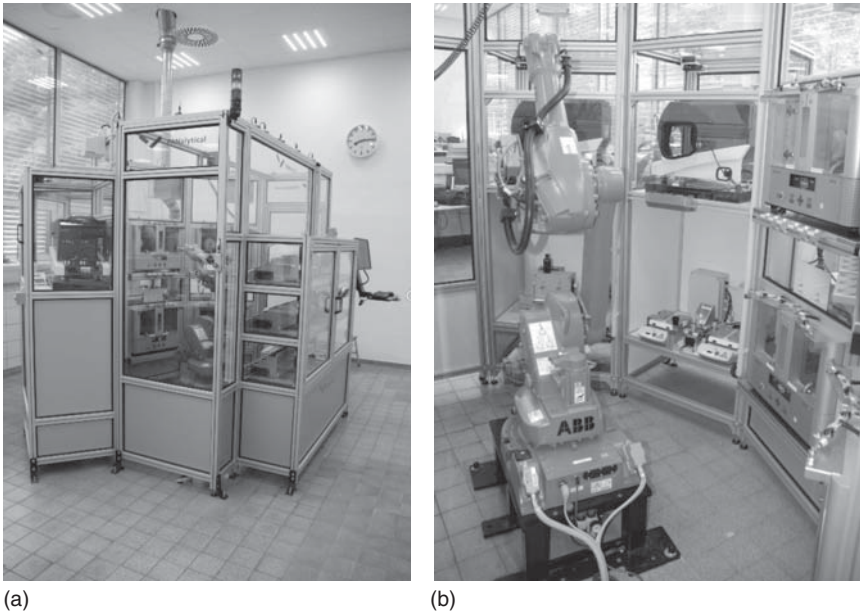


**Figure 18.7** External (a) and internal (b) view of an automated sample preparation system for fusion beads.

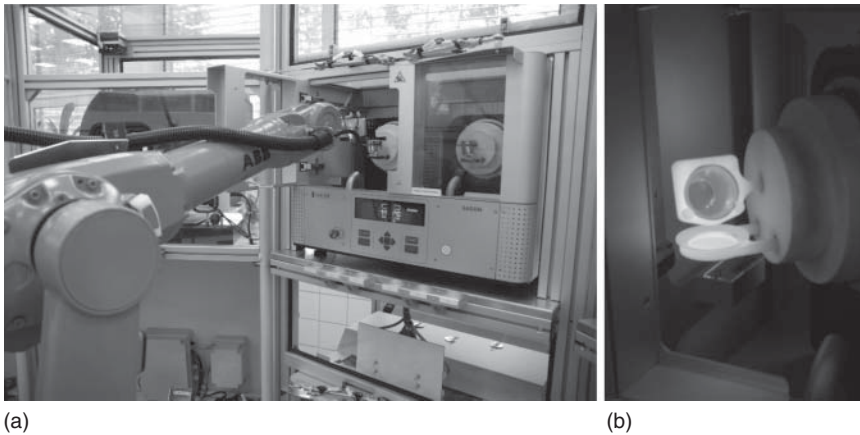


**Figure 18.8** Robot during loading of a resistance-heated fusion furnace (a) and mold during pouring (b).

weighed exactly in automatic systems, only the adherence of the exact mixing ratio is required. For this purpose, the sample is roughly weighed or volumetrically dosed before inserting into the system. With the help of the balance and a powder dispenser, a partial amount of the digestion agent is first added to the Pt crucible. The sample is then placed in the crucible, and the real sample mass is determined by differential weighing. Finally, the desired mass ratio between the sample and the digestion agent is precisely set with the aid of a powder dispenser.

By increasing the number of digestion positions and rack capacities and providing sufficient weighing capacity, the sample frequency can be increased up to 16 samples/h. With a rack capacity of 160 samples, a self-sufficient operation of over 12 hours is possible.

### 18.3 In-Line and On-Line Analysis

For in-line and on-line analysis, the measurements are carried out directly at the material stream or at a partial stream separated for the measurement. The material flow can be very different. Some examples are:

- small particle materials, for example, minerals or ores in the mining industry to monitor the value of the valuable substance and thus to control the exhaustion or separation of valuable material and waste material (see Figure 18.9)
- additives or waste materials in metallurgy for the control of material quality or for the determination of the further process technologies (Pilz et al. 2006)
- starting materials in the cement industry to ensure the quality of the end product by optimizing the mixing processes
- wastes to optimize the separation for a further use
- secondary raw materials for the determination of the content of toxic elements and thus to control their dosage in the incineration as well as their optimal temperatures
- the monitoring of layer thicknesses in continuous coating systems
- monitoring of powdered and liquid inputs to control the processes or to ensure product quality or to control the concentration of additives in liquids (see Figure 18.10; Graham 1996).

For these tasks, sometimes independent measuring instruments are developed that are unique. However, increasing effort is made to reduce the engineering

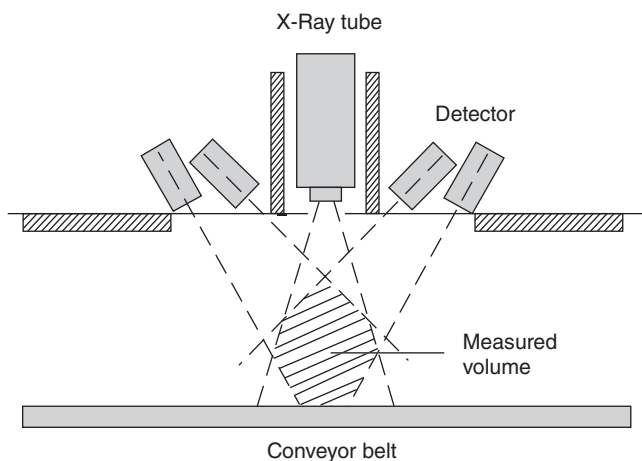
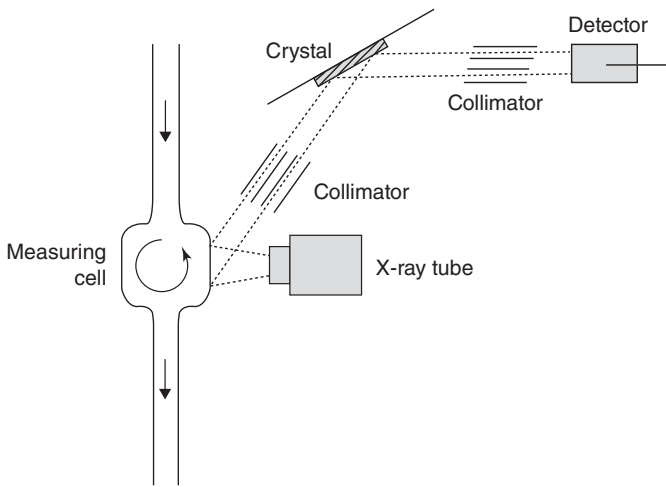
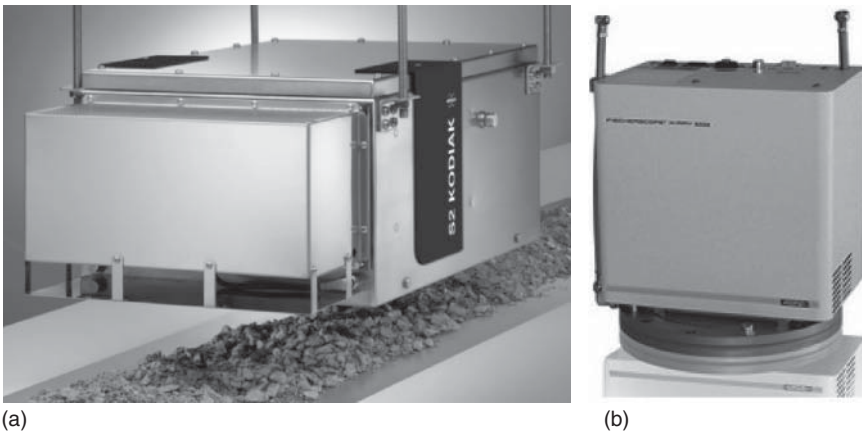


Figure 18.9 Scheme of an in-line analyzer for bulk material.



**Figure 18.10** Scheme of an on-line analyzer for liquids.



**Figure 18.11** Measuring heads for a continuous monitoring of material flow. (a) Kodiak, Bruker AXS GmbH. (b) FISCHERSCOPE X-RAY 5000, Helmut Fischer GmbH. Source: Courtesy of Bruker AXS GmbH and Helmut Fischer GmbH.

effort by using standardized components, such as sample holder, measuring heads, sample viewing systems, etc. However, these components, in particular the measuring heads, must meet special requirements. Above all, high robustness against external influences, for example, changing temperatures, mechanical vibrations, splashing water, or electric fields, is necessary. In addition, flexible adaptation and integration into various production processes must also be possible. A further feature of such measuring technology is the direct feeding of the measuring results into the process controlling networks to ensure a fast feedback to the process.

Examples of such measuring heads are shown in Figure 18.11. These can be integrated into a variety of process flows.

## 19

# Quality Management and Validation

## 19.1 Motivation

The demand for the assurance of a high analysis quality, that is, high repeatability and trueness of the analytical results, led to the development of different concepts and statistical methods. Starting with the zero-error strategies of some well-known American industrial companies, e.g. Ford and General Electric, in the 1980s of the last century, the actual concept of quality management (QM) has developed over the last decades by using the already mentioned Six Sigma tool, which nowadays is applied in most of the testing laboratories. The standard DIN-EN-ISO-17025 (2005), which is currently relevant for the laboratories active in analytical chemistry, has been developed from various standards and normative documents, for example, ISO 9001 (first version 2000), DIN-EN-45001 (1997), and ISO\_guide\_25 (1990), which are nowadays the basis for the quality-oriented assurance of precision and trueness in an analytical laboratory.

The basis of today's QM systems is the elements shown in Figure 19.1. In this context, a distinction is necessary between primarily organizational arrangements, such as test equipment, personnel, etc., and the more practical aspects, for example, monitoring of the test equipment, traceability, etc.

These elements of a QM system must implement in a QM manual, and the corresponding operating instructions need to be described and considered in the daily work. In addition to the actual test specifications, all quality-relevant processes, such as continuing training, order management, data documentation, calibration, etc., have to be extensively fixed in the operating instructions.

A particular challenge is the traceability to SI units for the control and calibration materials. Test laboratories must apply appropriate primary standards or primary substances or alternatively verify the traceability before their use. The so-called primary standards are usually certified reference materials (CRMs, see Section 5.5.8). On the other hand, primary substances are pure substances that can be used to reconstitute the analyte sample by weighing them in. Since these cost-intensive standards should only be used for calibration purposes for the daily laboratory practice, it is recommended to produce so-called secondary standards or laboratory internal reference materials ("house standard"), which can be

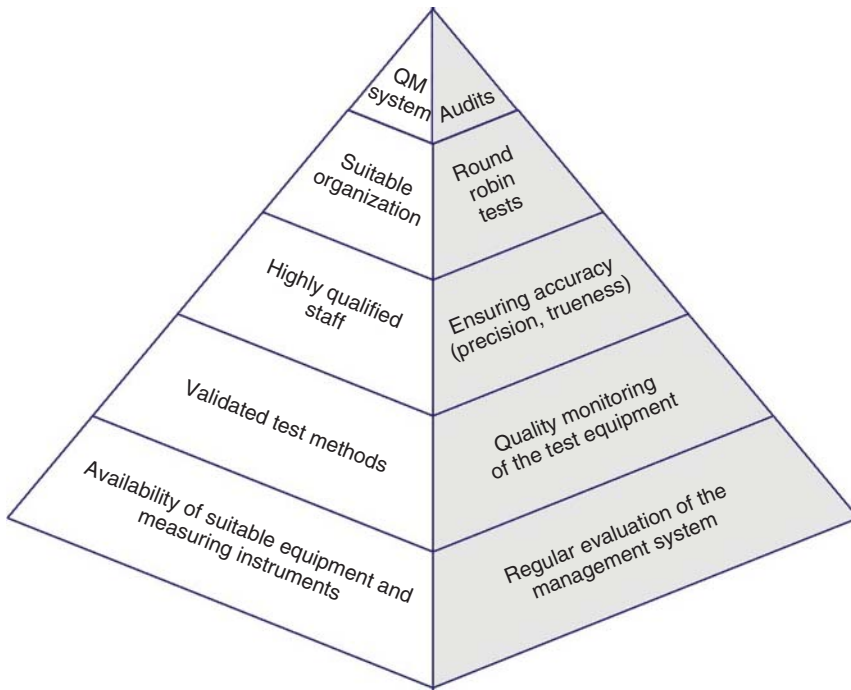


**Figure 19.1** Elements of a quality management system.

used for daily quality control. Figure 19.2 shows a possibility for connecting such materials to SI units. Calibration samples are prepared using the primary substances for the calibration of the analysis systems. The calibration shall be verified using one or more certified reference materials. Finally, the intended secondary standard can be analyzed. If the analysis results for the certified reference material are within the tolerance window of the certified specifications, the secondary standard can be used, for example, for further recalibrations.

Since not all aspects of a QM system can be dealt with in this book, refer to the relevant references (Funk et al. 2002; Dörffel 1966; Günzler 1994; Neitzel and Middeke 1994). In Germany the website of the Accreditation Office DAkkS ([www.dakks.de](http://www.dakks.de)) provides numerous documents on all relevant QM topics in the download area. It is recommended to use these documents.

## 19.2 Validation

The validation of a test procedure is intended to ensure that the test method used is suitable for the analytical problem and leads to trustworthy analysis values. In this case, the entire process from sampling to sample preparation, measurement, and data preparation is understood by means of analysis methods according to Figure 2.11. Within the framework of QM systems, validated testing procedures have a special significance since their results are highly reliable.

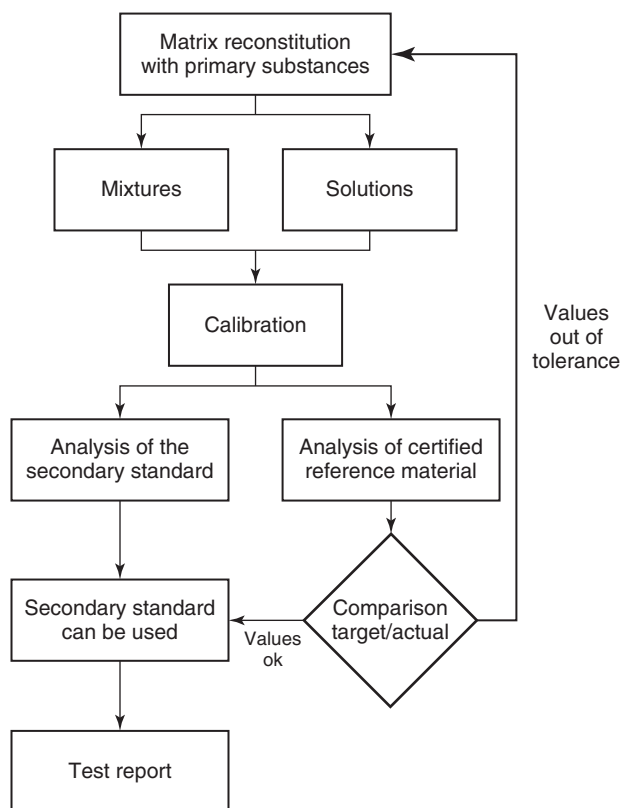


**Figure 19.2** Scheme for the connection of secondary references to SI units.

In the validation of a test procedure, an analytical method for a special analytical task must be confirmed for that analytical task. The steps required for this are shown in Figure 19.3.

Validation is by no means a new tool in analytical chemistry. Long before concepts such as “quality management” or “accreditation” were established, statistical methods were used to prove the quality of analytical methods. Already in the 1980s of the twentieth century, validation was implemented in international regulations such as ISO Guide 25 (ISO\_guide\_25 1990), DIN ISO 5725 Part 1–4 (DIN-ISO-5725 n.d.), and EN 45001 (DIN-EN-45001 1997, p. 06). DIN EN ISO/IEC 17025 (DIN-EN-ISO-17025 2005) was developed from these standards. It describes the “General requirement for the competence of testing and calibration laboratories.” In this standard the term “validation” is defined as follows:

Validation is the confirmation by examining and providing of the proof that the specific requirements for a particular intended use are met.

In an assigned sense, this means for the validation of an analytical test procedure to demonstrate that a test method is suitable for fulfilling a given test task.

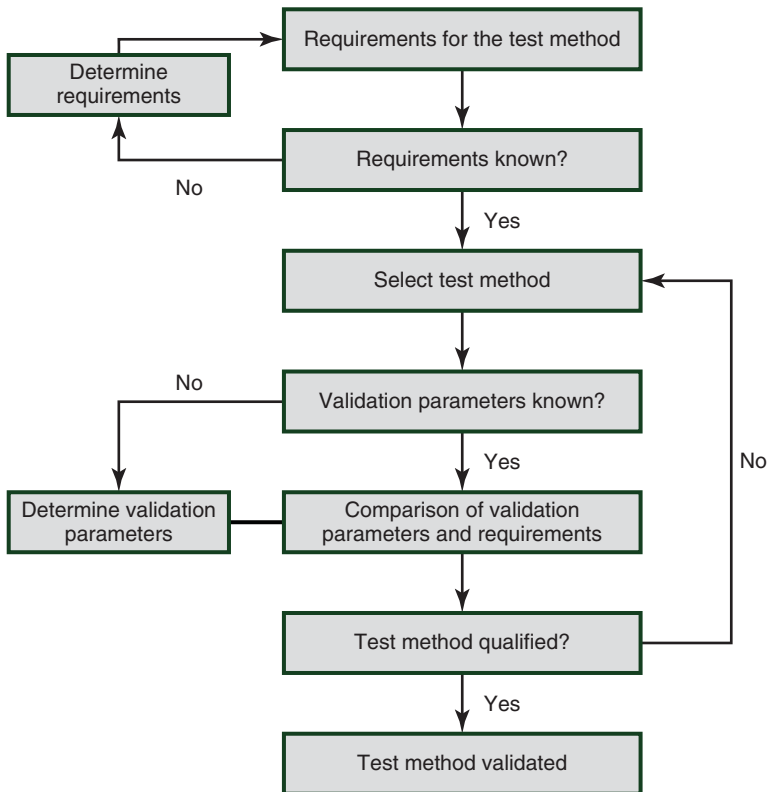


**Figure 19.3** Scheme of a validation process.

This proof refers to the special requirements of a customer for a specific intended use. In this sense, the validation can also be called a contract examination.

The prerequisite for validation is the definition of the customer-specific quality requirements for the analytical method. Usually, a customer orders at the laboratory to carry out an analysis. If no requirements have been defined with the contract, they must be laid down jointly (see Figure 19.3).

The selection of the test method can be carried out with knowledge of the requirements. The test method is characterized by various parameters. These must be determined if they are not yet known. The suitability of the test method can be derived from the comparison of these parameters with the requirements of the customer. If the test method is not suitable, an alternative method must be selected. A test procedure is validated if the characteristics of the test method meet the requirements or are even better.

The type and extent of the validation depend on the test method selected or applied (see Figure 19.4).

A basic validation (primary validation) requires the greatest effort and is carried out for the procedures developed in the laboratory (“house procedures”).



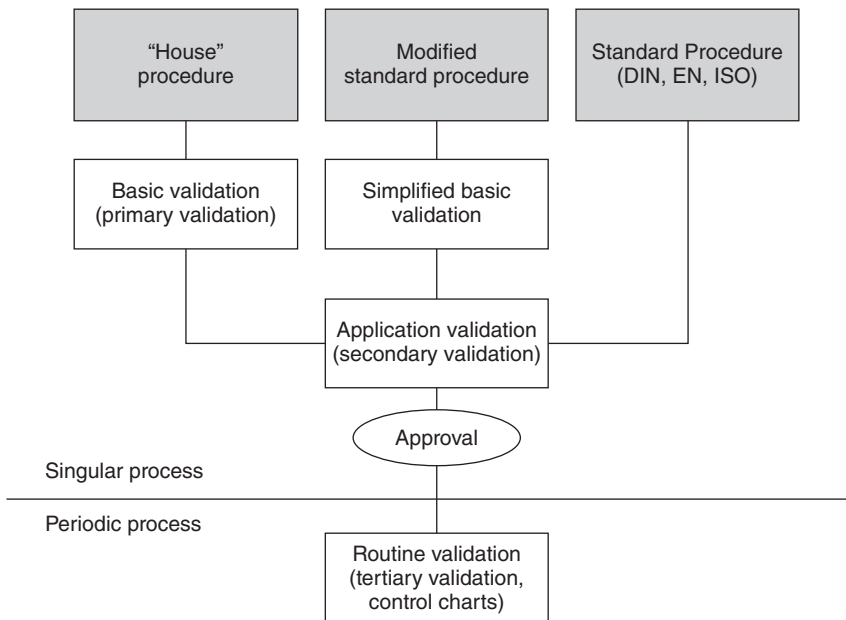


**Figure 19.4** Methods for a validation.

If a standard procedure (standardized or standard-like method) is used, which has already passed a validation during development, a basic validation is not necessary. It must only be verified that in the application in the laboratory, the specified parameters defined in the standard are achieved and that the users can handle the process (application validation, secondary verification).

If a standard procedure is modified, for example, in respect to the sample matrix or to the application, the extent to which the known method characteristics have changed has to be checked in a modified basic validation. This is followed by an application validation.

While all relevant parameters of a validation process are used for a basic validation depending on the purpose of the test, it is sufficient for the application validation to check parameters such as linearity, limit of detection and determination, repeatability and precision, and, if necessary, recovery.

While basic validation and application validation is a singular process, the results of which do not change under the same application conditions, the routine validation (tertiary validation) is used in a defined regularity to check the reliability of the procedure with routine use, for example:

- the regular use of reference material
- the management of control cards
- the participation in round robin tests and
- the verification of process parameters.

### 19.2.1 Parameters

The suitability of a test or calibration method is stated by the determination of characteristic parameters. The most important parameters are:

- limit of detection limit or determination
- precision (limit for comparison and repetition)
- trueness
- recovery rate
- specificity/selectivity
- robustness
- linearity and
- range of application.

With these data, the method can be adequately described, and a statement about the suitability can be made by comparison with the customer-specific requirements. Since the necessary professional competence is often only available in the laboratory, the laboratory must determine the requirements in certain cases.

Which parameters have to be evaluated within the scope of a validation depends on the respective test purpose. Depending on the complexity, the number of characteristic values increases and therefore also the scope of the test (see Table 19.1). Thus, for a trace analysis, the number of parameters to be determined is significantly higher than for a simple qualitative analysis.

The determination of the parameters and the measuring effort required for this is shown schematically in Table 19.2 and Figure 19.5. The statistical formulas and methods used for this purpose are to be taken from the corresponding literature (Kromidas 2011; Sucker 1983; EURACHEM-Guide 1998; DAkkS-Regel-71-SD-4-019 2010).

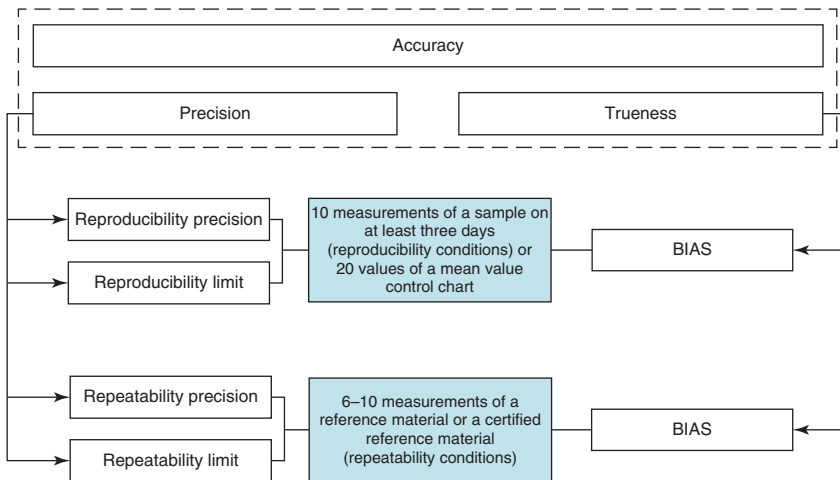
**Table 19.1** Parameters in dependence of the task for checking.

Parameter	Target of analysis			
	Qualitative	Quantitative (higher contents)	Quantitative (traces)	Physical parameters
Limit of detection	—	—	X	—
Limit of determination	—	—	X	—
Precision repeatability	—	X	X	X
Comparability	—	O	O	O
Trueness	—	X	X	X
Recovery rate	—	O	X	—
Selectivity	X	X	X	—
Robustness	—	O	O	O
Linearity (of calibration)	—	X	X	X
Range of application	X	X	X	X

X, necessary; —, not necessary; O, optional.

**Table 19.2** Determination of the parameter range of application, linearity, and limit of detection and determination.

Parameter	Method
Range of operation	Top and bottom point of the calibration curve
Limit of detection	6–10 measurements
Limit of determination	Blank or lowest sample of calibration curve (repeatability conditions) or calculation from the slope of the calibration curve or determination of signal-noise-ratio
Linearity	Determination of a calibration curve with 7–10 calibration samples or visual check – determination of the correlation coefficient and/or analysis of residues

**Figure 19.5** Determination of the parameter's precision and trueness.

### 19.2.2 Uncertainty

The estimation of the measurement uncertainty is important not only for the assessment of an analysis result, as described in Section 6.3.1, but is also of particular importance in the case of a validation.

According to DIN EN ISO/IEC 17025, test laboratories must have “procedures for the estimation of the measurement uncertainty” and apply them. The laboratory must “try to identify all components of the measurement uncertainty and make a reasonable estimate of the measurement uncertainty and ensure that the test report does not give a false impression regarding the uncertainty.”

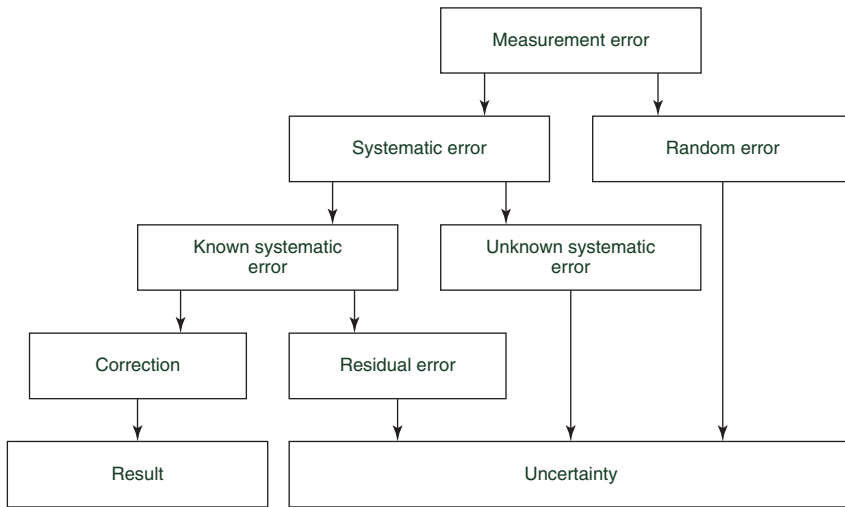


**Figure 19.6** Influence of deviations of the measurement to the determination of the analysis result as well as the uncertainty. Source: GUM (2008).

The quantitative determination of a measured value never delivers the actual “true” value, but a measured value, which is influenced by systematic and random errors and therefore has an uncertainty. This means that the measurement result fluctuates within the framework of the uncertainty determined around the “true” value. The measurement uncertainty thus is a measure of the quality of a measurement and finally a proof of the competence of the analyst.

In the communication with the client, measurement uncertainty can be a criterion of assessment, provided the customer has the competence to evaluate the results accordingly.

An analysis is influenced by various components, such as the used analytical instruments, environmental conditions, etc., which can lead to systematic as well as random errors. The determination of the measurement uncertainty can thus show which process step provides the greatest contribution to measurement uncertainty and thus requires special attention to improve the accuracy of the test method. The influence of the measurement deviation on the determination of the measurement uncertainty is shown schematically in Figure 19.6.

For the determination of measurement uncertainties, two approaches can be applied, which have already been described in detail in Section 6.3.3.

## Appendix A

### Tables

**Table A.1** Periodic table of elements with atomic number, atomic weight, and density (g/cm<sup>3</sup>) and information to measurability with X-ray spectrometry.

1 <b>H</b>				Not measurable						Measurable with EDS and WDS										2 <b>He</b>
3 <b>Li</b>	4 <b>Be</b> 9.01 1.84			Limited measurability with WDS						Limited measurability with EDS					5 <b>B</b> 10.81 2.33	6 <b>C</b> 12.01	7 <b>N</b> 14.00	8 <b>O</b> 15.99	9 <b>F</b> 18.99 1.11	10 <b>Ne</b> 20.18
11 <b>Na</b> 22.99 0.97	12 <b>Mg</b> 24.31 1.75			Non stable element					26 <b>Fe</b> 55.84 7.86	Atomic number <b>Element symbol</b> Atomic weight Density					13 <b>Al</b> 26.98 2.70	14 <b>Si</b> 28.08 2.42	15 <b>P</b> 30.97 1.82	16 <b>S</b> 32.07 2.07	17 <b>Cl</b> 35.45 3.21	18 <b>Ar</b> 39.95
19 <b>K</b> 39.10 0.87	20 <b>Ca</b> 40.08 1.41	21 <b>Sc</b> 44.96 3.10	22 <b>Ti</b> 47.87 4.49	23 <b>V</b> 50.94 5.96	24 <b>Cr</b> 51.99 6.92	25 <b>Mn</b> 54.94 7.20	26 <b>Fe</b> 55.84 7.86	27 <b>Co</b> 58.93 8.76	28 <b>Ni</b> 58.69 8.90	29 <b>Cu</b> 63.55 8.92	30 <b>Zn</b> 65.41 7.14	31 <b>Ga</b> 69.72 5.91	32 <b>Ge</b> 72.64 5.35	33 <b>As</b> 74.92 5.79	34 <b>Se</b> 78.96 4.79	35 <b>Br</b> 79.90 3.12	36 <b>Kr</b> 83.80			
37 <b>Rb</b> 85.47 1.52	38 <b>Sr</b> 87.62 2.54	39 <b>Y</b> 88.91 5.51	40 <b>Zr</b> 91.22 6.53	41 <b>Nb</b> 92.91 8.33	42 <b>Mo</b> 95.94 10.20	43 <b>Tc</b> 98	44 <b>Ru</b> 101.07 112.10	45 <b>Rh</b> 102.91 12.50	46 <b>Pd</b> 106.42 12.16	47 <b>Ag</b> 107.87 10.50	48 <b>Cd</b> 112.41 8.65	49 <b>In</b> 114.82 7.28	50 <b>Sn</b> 118.71 7.29	51 <b>Sb</b> 121.76 6.69	52 <b>Te</b> 127.60 6.24	53 <b>I</b> 126.90 4.93	54 <b>Xe</b> 131.29			
55 <b>Cs</b> 132.91 1.41	56 <b>Ba</b> 137.33 3.78	57* <b>La</b> 138.90 6.16	72 <b>Hf</b> 178.93 8.80	73 <b>Ta</b> 180.95 16.69	74 <b>W</b> 183.84 19.30	75 <b>Re</b> 186.21 20.53	76 <b>Os</b> 190.23 22.48	77 <b>Ir</b> 192.22 22.42	78 <b>Pt</b> 195.08 21.37	79 <b>Au</b> 196.97 19.32	80 <b>Hg</b> 200.59 13.55	81 <b>Tl</b> 204.38 11.85	82 <b>Pb</b> 207.21 11.35	83 <b>Bi</b> 208.98 9.78	84 <b>Po</b> 209	85 <b>At</b> 210	86 <b>Rn</b> 222			
87 <b>Fr</b> 223 2.5	88 <b>Ra</b> 226 5.5	89** <b>Ac</b> 227 10.07																		
* Lanthanides			58 <b>Ce</b> 140.11 6.90	59 <b>Pr</b> 140.91 6.80	60 <b>Nd</b> 144.24 7.00	61 <b>Pm</b> 145	62 <b>Sm</b> 150.36 6.90	63 <b>Eu</b> 151.96 5.20	64 <b>Gd</b> 157.25 7.90	65 <b>Tb</b> 158.93 8.30	66 <b>Dy</b> 162.50 8.60	67 <b>Ho</b> 164.93 8.80	68 <b>Er</b> 167.26 9.20	69 <b>Tm</b> 168.93 9.30	70 <b>Yb</b> 173.04 7.00	71 <b>Lu</b> 174.97 9.70				
** Actinides			90 <b>Th</b> 232.04 11.72	91 <b>Pa</b> 231.03 15.37	92 <b>U</b> 238.03 19.1	93 <b>Np</b>	94 <b>Pu</b>	95 <b>Am</b>	96 <b>Cm</b>	97 <b>Bk</b>	98 <b>Cf</b>	99 <b>Es</b>	100 <b>Fm</b>	101 <b>Md</b>	102 <b>No</b>	103 <b>Lr</b>				

**Table A.2** Atomic weight and density (in g/cm<sup>3</sup>) of all elements.

AN	Element	Symbol	Atomic weight	Density	AN	Element	Symbol	Atomic weight	Density	AN	Element	Symbol	Atomic weight	Density
4	<b>Beryllium</b>	Be	9.01	1.84										
5	<b>Boron</b>	B	10.81	2.33	20	<b>Calcium</b>	Ca	40.08	1.41	35	<b>Bromine</b>	Br	70.90	3.12
6	<b>Carbon</b>	C	12.01		21	<b>Scandium</b>	Sc	44.96	3.10	36	<b>Krypton</b>	Kr	83.80	
7	<b>Nitrogen</b>	N	14.00		22	<b>Titanium</b>	Ti	47.87	4.49	37	<b>Rubidium</b>	Rb	85.47	1.52
8	<b>Oxygen</b>	O	15.99		23	<b>Vanadium</b>	V	50.94	5.96	38	<b>Strontium</b>	Sr	87.62	2.54
9	<b>Fluorine</b>	F	18.99	1.11	24	<b>Chromium</b>	Cr	51.99	6.92	39	<b>Yttrium</b>	Y	88.91	5.51
10	<b>Neon</b>	Ne	20.18		25	<b>Manganese</b>	Mn	54.94	7.20	40	<b>Zirconium</b>	Zr	91.22	6.53
11	<b>Sodium</b>	Na	22.99	0.97	26	<b>Iron</b>	Fe	55.84	7.86	41	<b>Niobium</b>	Nb	92.91	8.33
12	<b>Magnesium</b>	Mg	24.31	1.75	27	<b>Cobalt</b>	Co	58.93	8.76	42	<b>Molybdenum</b>	Mo	95.94	10.20
13	<b>Aluminium</b>	Al	26.98	2.70	28	<b>Nickel</b>	Ni	58.69	8.90	43	<b>Technetium</b>	Tc	98	
14	<b>Silicon</b>	Si	28.08	2.42	29	<b>Copper</b>	Cu	63.55	8.92	44	<b>Ruthenium</b>	Ru	101.07	12.10
15	<b>Phosphorus</b>	P	30.97	1.82	30	<b>Zinc</b>	Zn	65.41	7.14	45	<b>Rhodium</b>	Rh	102.91	12.50
16	<b>Sulfur</b>	S	32.07	2.07	31	<b>Gallium</b>	Ga	69.72	5.91	46	<b>Palladium</b>	Pd	106.42	12.16
17	<b>Chlorine</b>	Cl	35.45	3.21	32	<b>Germanium</b>	Ge	72.64	5.35	47	<b>Silver</b>	Ag	107.87	10.50
18	<b>Argon</b>	Ar	39.95		33	<b>Arsenic</b>	As	74.92	5.79	48	<b>Cadmium</b>	Cd	112.41	8.65
19	<b>Potassium</b>	K	39.10	0.87	34	<b>Selenium</b>	Se	78.96	4.79	49	<b>Indium</b>	In	114.82	7.28

*(continued)*

Table A.2 Atomic weight and density (in g/cm<sup>3</sup>) of all elements.

AN	Element	Symbol	Atomic weight	Density	AN	Element	Symbol	Atomic weight	Density	AN	Element	Symbol	Atomic weight	Density
50	<b>Tin</b>	Sn	118.71	7.29	65	<b>Terbium</b>	Tb	158.93	8.30	80	<b>Mercury</b>	Hg	200.59	13.55
51	<b>Antimony</b>	Sb	121.76	6.69	66	<b>Dysprosium</b>	Dy	162.50	8.60	81	<b>Thallium</b>	Tl	204.38	11.85
52	<b>Tellurium</b>	Te	127.60	6.24	67	<b>Holmium</b>	Ho	164.93	8.80	82	<b>Lead</b>	Pb	207.21	11.35
53	<b>Iodide</b>	I	126.90	4.93	68	<b>Erbium</b>	Er	167.26	9.20	83	<b>Bismuth</b>	Bi	208.98	9.78
54	<b>Xenon</b>	Xe	131.29		69	<b>Thulium</b>	Tm	168.93	9.30	84	<b>Polonium</b>	Po	209	9.51
55	<b>Caesium</b>	Cs	132.91	1.41	70	<b>Ytterbium</b>	Yb	173.04	7.00	85	<b>Astatine</b>	At	210	8.75
56	<b>Barium</b>	Ba	137.33	3.78	71	<b>Lutetium</b>	Lu	174.97	9.70	86	<b>Radon</b>	Rn	222	9.73
57	<b>Lanthanum</b>	La	138.90	6.16	72	<b>Hafnium</b>	Hf	178.49	13.00	87	<b>Francium</b>	Fr	223	2.5
58	<b>Cerium</b>	Ce	140.11	6.90	73	<b>Tantalum</b>	Ta	180.95	16.69	88	<b>Radium</b>	Ra	226	5.5
59	<b>Praseodymium</b>	Pr	140.91	6.80	74	<b>Tungsten</b>	W	183.84	19.30	89	<b>Actinium</b>	Ac	227	10.07
60	<b>Neodymium</b>	Nd	144.24	7.00	75	<b>Rhenium</b>	Re	186.21	20.53	90	<b>Thorium</b>	Th	232.04	11.72
61	<b>Promethium</b>	Pm	145		76	<b>Osmium</b>	Os	190.23	22.48	91	<b>Proactinium</b>	Pa	231.03	15.37
62	<b>Samarium</b>	Sm	150.36	6.90	77	<b>Iridium</b>	Ir	192.22	22.42	92	<b>Uranium</b>	U	238.03	19.1
63	<b>Europium</b>	Eu	151.96	5.20	78	<b>Platinum</b>	Pt	195.08	21.37					
64	<b>Gadolinium</b>	Gd	157.25	7.90	79	<b>Gold</b>	Au	196.97	19.32					



**Table A.3** Energies of absorption edges (keV).

Element	Symbol	AN	K	L <sub>I</sub>	L <sub>II</sub>	L <sub>III</sub>	M <sub>I</sub>	M <sub>II</sub>	M <sub>III</sub>	M <sub>IV</sub>	M <sub>V</sub>
Beryllium	Be	4	0.116								
Boron	B	5	0.192								
Carbon	C	6	0.283								
Nitrogen	N	7	0.339								
Oxygen	O	8	0.531								
Fluorine	F	9	0.687								
Neon	Ne	10	0.874	0.048	0.022	0.022					
Sodium	Na	11	1.080	0.055	0.034	0.034					
Magnesium	Mg	12	1.303	0.063	0.050	0.049					
Aluminum	Al	13	1.559	0.087	0.073	0.072					
Silicon	Si	14	1.838	0.118	0.099	0.098					
Phosphorus	P	15	2.142	0.153	0.129	0.128					
Sulfur	S	16	2.470	0.193	0.164	0.163					
Chlorine	Cl	17	2.819	0.238	0.203	0.202	0.020				
Argon	Ar	18	3.203	0.287	0.247	0.245	0.026				
Potassium	K	19	3.607	0.341	0.297	0.294	0.033				
Calcium	Ca	20	4.038	0.399	0.352	0.349	0.040				
Scandium	Sc	21	4.496	0.462	0.411	0.406	0.046				
Titanium	Ti	22	4.964	0.530	0.460	0.454	0.054				
Vanadium	V	23	5.463	0.604	0.519	0.512	0.061				
Chromium	Cr	24	5.988	0.679	0.583	0.574	0.072				
Manganese	Mn	25	6.537	0.762	0.650	0.639	0.082				
Iron	Fe	26	7.111	0.849	0.721	0.708	0.093				
Cobalt	Co	27	7.709	0.929	0.794	0.779	0.104				
Nickel	Ni	28	8.331	1.015	0.871	0.853	0.120				
Copper	Cu	29	8.980	1.100	0.953	0.933	0.135	0.090		0.015	
Zinc	Zn	30	9.660	1.200	1.045	1.022	0.151	0.106		0.022	
Gallium	Ga	31	10.368	1.300	1.134	1.117	0.169	0.125	0.115	0.030	
Germanium	Ge	32	11.103	1.420	1.248	1.217	0.190	0.137	0.132	0.041	
Arsenic	As	33	11.863	1.529	1.359	1.323	0.211	0.156	0.150	0.052	
Selenium	Se	34	12.652	1.652	1.473	1.434	0.234	0.177	0.170	0.066	

*(continued)*

**Table A.3** Energies of absorption edges (keV).

Element	Symbol	AN	K	L <sub>I</sub>	L <sub>II</sub>	L <sub>III</sub>	M <sub>I</sub>	M <sub>II</sub>	M <sub>III</sub>	M <sub>IV</sub>	M <sub>V</sub>
Bromine	Br	35	13.475	1.794	1.599	1.552	0.265	0.198	0.191	0.082	
Krypton	Kr	36	14.323	1.931	1.727	1.675	0.294	0.225	0.217	0.095	
Rubidium	Rb	37	15.201	2.067	1.866	1.896	0.328	0.250	0.240	0.114	0.112
Strontium	Sr	38	16.106	2.221	2.008	1.941	0.358	0.280	0.270	0.136	0.134
Yttrium	Y	39	17.037	2.369	2.154	2.079	0.394	0.312	0.300	0.159	0.156
Zirconium	Zr	40	17.998	2.547	2.305	2.220	0.435	0.348	0.335	0.187	0.184
Niobium	Nb	41	18.987	2.706	2.467	2.374	0.468	0.379	0.362	0.207	0.204
Molybdenum	Mo	42	20.002	2.884	2.627	2.523	0.507	0.412	0.394	0.232	0.228
Technetium	Tc	43	21.054	3.054	2.795	2.677	0.551	0.449	0.429	0.260	0.257
Ruthenium	Ru	44	22.118	3.236	2.966	2.837	0.591	0.486	0.467	0.290	0.288
Rhodium	Rh	45	23.224	3.419	3.145	3.002	0.637	0.531	0.506	0.321	0.315
Palladium	Pd	46	24.347	3.617	3.329	3.172	0.684	0.573	0.546	0.354	0.349
Silver	Ag	47	25.517	3.810	3.528	3.352	0.734	0.619	0.588	0.389	0.383
Cadmium	Cd	48	26.712	4.019	3.727	3.538	0.781	0.666	0.632	0.423	0.420
Indium	Ir	49	27.928	4.237	3.939	3.729	0.839	0.716	0.678	0.464	0.456
Tin	Sn	50	29.190	4.464	4.157	3.928	0.894	0.772	0.720	0.506	0.497
Antimony	Sb	51	30.486	4.697	4.381	4.132	0.952	0.822	0.774	0.546	0.536
Tellurium	Te	52	31.809	4.938	4.613	4.341	1.010	0.873	0.822	0.586	0.575
Iodide	J	53	33.164	5.190	4.856	4.559	1.071	0.929	0.873	0.630	0.618
Xenon	Xe	54	34.579	5.462	5.104	4.782	1.147	0.989	0.926	0.677	0.662
Cesium	Cs	55	35.959	5.720	5.358	5.011	1.199	1.048	0.981	0.722	0.704
Barium	Ba	56	37.410	5.995	5.623	5.247	1.266	1.111	1.036	0.770	0.750
Lanthanum	La	57	38.931	6.283	5.894	5.489	1.330	1.173	1.092	0.823	0.801
Cerium	Ce	58	40.449	6.561	6.165	5.729	1.401	1.240	1.152	0.870	0.851
Praseodymium	Pr	59	41.998	6.846	6.443	5.968	1.476	1.305	1.210	0.923	0.898
Neodymium	Nd	60	43.571	7.144	6.727	6.215	1.544	1.372	1.266	0.969	0.946
Promethium	Pm	61	45.207	7.448	7.018	6.466	1.642	1.439	1.327	1.019	0.994
Samarium	Sm	62	46.846	7.754	7.281	6.721	1.689	1.512	1.388	1.073	1.048
Europium	Eu	63	48.515	8.069	7.624	6.983	1.767	1.584	1.450	1.129	1.101
Gadolinium	Gd	64	50.229	8.393	7.940	7.252	1.849	1.653	1.511	1.185	1.153

*(continued)*

**Table A.3** Energies of absorption edges (keV).

Element	Symbol	AN	K	L <sub>I</sub>	L <sub>II</sub>	L <sub>III</sub>	M <sub>I</sub>	M <sub>II</sub>	M <sub>III</sub>	M <sub>IV</sub>	M <sub>V</sub>
Terbium	Tb	65	51.998	8.724	8.258	7.519	1.937	1.737	1.583	1.245	1.211
Dysprosium	Dy	66	53.789	9.083	8.621	7.850	2.019	1.805	1.642	1.304	1.266
Holmium	Ho	67	55.615	9.411	8.920	8.047	2.104	1.886	1.715	1.365	1.327
Erbium	Er	68	57.483	9.776	9.263	8.364	2.184	1.973	1.783	1.430	1.385
Thulium	Tm	69	59.335	10.144	9.628	8.652	2.291	2.071	1.861	1.498	1.451
Ytterbium	Yb	70	61.303	10.486	9.977	8.943	2.387	2.165	1.948	1.566	1.518
Lutetium	Lu	71	63.304	10.867	10.345	9.241	2.488	2.262	2.025	1.637	1.586
Hafnium	Hf	72	65.313	11.264	10.734	9.556	2.601	2.366	2.109	1.718	1.664
Tantalum	Ta	73	67.400	11.676	11.130	9.876	2.698	2.459	2.184	1.783	1.725
Tungsten	W	74	69.508	12.090	11.535	10.198	2.812	2.566	2.273	1.864	1.803
Rhenium	Re	75	71.662	12.522	11.955	10.531	2.926	2.676	2.361	1.946	1.879
Osmium	Os	76	73.860	12.965	12.383	10.869	3.047	2.792	2.453	2.033	1.963
Iridium	Ir	77	76.097	13.413	12.819	11.211	3.171	2.908	2.551	2.119	2.040
Platinum	Pt	78	78.379	13.873	13.268	11.559	3.296	3.036	2.649	2.204	2.129
Gold	Au	79	80.713	14.353	13.733	11.919	3.379	3.149	2.744	2.307	2.220
Mercury	Hg	80	83.106	14.841	14.212	12.285	3.566	3.287	2.848	2.392	2.291
Thallium	Tl	81	85.517	15.346	14.697	12.657	3.702	3.418	2.957	2.483	2.389
Lead	Pb	82	88.001	15.870	15.207	13.044	3.853	3.558	3.072	2.586	2.484
Bismuth	Bi	83	90.521	16.393	15.716	13.424	4.003	3.709	3.186	2.694	2.586
Polonium	Po	84	93.112	16.935	16.244	13.817	4.147	3.863	3.312	2.798	2.681
Astatine	At	85	95.740	17.490	16.784	14.215	4.350	4.008	3.428	2.905	2.780
Radon	Rn	86	98.418	18.058	17.337	14.618	4.524	4.156	3.536	3.014	2.882
Francium	Fr	87	101.147	18.638	17.904	15.028	4.678	4.324	3.654	3.125	2.986
Radium	Ra	88	103.927	19.233	18.481	15.442	4.811	4.477	3.779	3.237	3.093
Actinium	Ac	89	106.759	19.842	19.978	15.865	5.019	4.637	3.892	3.352	3.202
Thorium	Th	90	109.630	20.460	19.688	16.296	5.176	4.810	4.030	3.474	3.313
Protactinium	Pa	91	112.581	21.102	20.311	16.731	5.355	4.993	4.164	3.597	3.416
Uranium	U	92	115.591	21.753	20.943	17.163	5.532	5.177	4.293	3.712	3.533

**Table A.4** K-line energies (keV).

Element	Symbol	AN	$K\alpha_1$	$K\alpha_2$	$K\beta_1$	$K\beta_2$	$K\beta_3$	$K\beta_4$	$K\beta_5$
Beryllium	Be	4	0.108						
Boron	B	5	0.183						
Carbon	C	6	0.277						
Nitrogen	N	7	0.392						
Oxygen	O	8	0.525						
Fluorine	F	9	0.677						
Neon	Ne	10	0.849						
Sodium	Na	11	1.040						
Magnesium	Mg	12	1.254	1.253	1.302				
Aluminum	Al	13	1.486	1.486	1.557				
Silicon	Si	14	1.740	1.739	1.837				
Phosphorus	P	15	2.010	2.010	2.139				
Sulfur	S	16	2.309	2.308	2.465		2.464		
Chlorine	Cl	17	2.622	2.620	2.812		2.812		
Argon	Ar	18	2.958	2.955	3.190		3.190		
Potassium	K	19	3.314	3.311	3.590		3.590		
Calcium	Ca	20	3.692	3.689	4.013		4.013		
Scandium	Sc	21	4.093	4.093	4.464		4.464		
Titanium	Ti	22	4.512	4.505	4.933		4.933	4.964	
Vanadium	V	23	4.953	4.945	5.428		5.428	5.463	
Chromium	Cr	24	5.415	5.405	5.947		5.947	5.987	
Manganese	Mn	25	5.900	5.889	6.492		6.492	6.537	
Iron	Fe	26	6.405	6.392	7.059		7.059	7.110	
Cobalt	Co	27	6.931	6.916	7.649		7.650	7.706	
Nickel	Ni	28	7.480	7.463	8.267		8.265	8.329	
Copper	Cu	29	8.046	8.027	8.904		8.902	8.974	
Zinc	Zn	30	8.637	8.614	9.570		9.568	9.649	
Gallium	Ga	31	9.251	9.224	10.267		10.264	10.348	
Germanium	Ge	32	9.886	9.855	10.982		10.978	11.073	
Arsenic	As	33	10.543	10.508	11.726	11.864	11.721	11.825	
Selenium	Se	34	11.224	11.184	12.497	12.655	12.492	12.602	

*(continued)*

Table A.4 K-line energies (keV).

Element	Symbol	AN	$K\alpha_1$	$K\alpha_2$	$K\beta_1$	$K\beta_2$	$K\beta_3$	$K\beta_4$	$K\beta_5$
Bromine	Br	35	11.924	11.878	13.292	13.471	13.285		13.494
Krypton	Kr	36	12.648	12.595	14.112	14.312	14.104		14.231
Rubidium	Rb	37	13.396	13.336	14.961	15.184	14.951		15.087
Strontium	Sr	38	14.165	14.098	15.835	16.093	15.825		15.969
Yttrium	Y	39	14.958	14.882	16.739	17.014	16.727		16.880
Zirconium	Zr	40	15.775	15.691	17.668	17.970	17.654		17.817
Niobium	Nb	41	16.615	16.521	18.625	18.953	18.610		18.731
Molybdenum	Mo	42	17.480	17.375	19.606	19.962	19.588		19.769
Technetium	Tc	43	18.367	18.251	20.625	21.002	20.596		20.786
Ruthenium	Ru	44	19.279	19.160	21.656	21.071	21.634		21.833
Rhodium	Rh	45	20.216	20.074	22.724	23.169	22.699	23.218	22.908
Palladium	Pd	46	21.177	21.020	23.818	24.294	23.790	24.348	24.009
Silver	Ag	47	22.163	21.990	24.941	25.450	24.910	25.510	25.140
Cadmium	Cd	48	23.173	22.984	26.093	26.647	26.058	26.699	26.299
Indium	Ir	49	24.210	24.002	27.275	27.866	27.237	27.922	27.489
Tin	Sn	50	25.271	25.044	28.485	29.115	28.444	29.175	28.707
Antimony	Sb	51	26.359	26.111	29.725	30.395	29.678	30.458	29.953
Tellurium	Te	52	27.473	27.202	30.993	31.711	30.943	31.772	31.231
Iodide	I	53	28.612	28.317	32.294	33.046	32.238	33.118	32.538
Xenon	Xe	54	29.775	29.454	33.620	34.414	33.559	34.492	33.872
Cesium	Cs	55	30.973	30.625	34.982	35.813	34.914	35.905	35.245
Barium	Ba	56	32.194	31.817	36.378	37.249	36.304	37.348	36.645
Lanthanum	La	57	33.442	33.034	37.797	38.719	37.719	38.820	38.072
Cerium	Ce	58	34.720	34.279	39.256	40.220	39.169	40.334	39.541
Praseodymium	Pr	59	36.027	35.551	40.749	41.755	40.654	41.876	41.043
Neodymium	Nd	60	37.361	36.847	42.272	43.325	42.166	43.449	42.566
Promethium	Pm	61	38.725	38.171	43.827	44.942	43.713	45.064	44.132
Samarium	Sm	62	40.118	39.522	45.414	46.568	45.293	46.705	45.723
Europium	Eu	63	41.542	40.902	47.038	48.235	46.905	48.385	47.360
Gadolinium	Gd	64	42.996	42.309	48.695	49.953	48.551	50.095	49.017

(continued)

**Table A.4** K-line energies (keV).

Element	Symbol	AN	$K\alpha_1$	$K\alpha_2$	$K\beta_1$	$K\beta_2$	$K\beta_3$	$K\beta_4$	$K\beta_5$
Terbium	Tb	65	44.482	43.744	50.385	51.574	50.228	51.846	50.719
Dysprosium	Dy	66	45.999	45.208	52.113	53.456	51.947	53.635	52.456
Holmium	Ho	67	47.547	46.700	53.577	55.275	53.695	55.458	54.225
Erbium	Er	68	49.128	48.222	55.674	57.120	55.480	57.318	56.033
Thulium	Tm	69	50.742	49.773	57.505	59.004	57.300	59.215	57.875
Ytterbium	Yb	70	52.388	51.354	59.382	60.943	59.159	61.141	59.755
Lutetium	Lu	71	54.070	52.965	61.290	62.902	61.050	63.108	61.675
Hafnium	Hf	72	55.790	54.612	63.244	64.913	62.986	65.131	63.635
Tantalum	Ta	73	57.535	56.280	65.222	66.953	64.947	67.178	65.623
Tungsten	W	74	59.318	57.981	67.244	69.035	66.950	69.269	67.653
Rhenium	Re	75	61.141	59.717	69.309	71.157	68.994	71.402	69.727
Osmium	Os	76	63.000	51.486	71.414	73.322	71.079	73.578	71.840
Iridium	Ir	77	64.895	63.287	73.560	75.533	73.202	75.799	73.995
Platinum	Pt	78	66.831	65.122	75.750	77.786	75.368	78.063	76.193
Gold	Au	79	68.805	66.991	77.982	80.082	77.577	80.372	78.434
Mercury	Hg	80	70.818	68.893	80.255	82.422	79.823	82.724	80.717
Thallium	Tl	81	72.872	70.832	82.573	84.809	82.114	85.124	83.045
Lead	Pb	82	74.970	72.805	84.999	87.243	84.451	87.571	85.419
Bismuth	Bi	83	77.107	74.815	87.349	89.721	86.830	90.062	87.838

**Table A.5** L-line energies (keV).

Element	Symbol	AN	$L\alpha_1$	$L\alpha_2$	$L\beta_1$	$L\beta_2$	$L\beta_3$	$L\beta_4$	$L\beta_5$	$L\beta_6$	$L\eta$	$L\gamma_1$	$L\gamma_2$	$L\gamma_3$	$L\gamma_4$	$L\gamma_5$	$L\gamma_6$	LI
Magnesium	Mg	12					0.088				0.048							0.047
Aluminum	Al	13					0.115				0.069							0.069
Silicon	Si	14					0.148				0.092							0.091
Phosphorus	P	15					0.183	0.182			0.124							0.123
Sulfur	S	16					0.224	0.223			0.150							0.148
Chlorine	Cl	17					0.260	0.260			0.184							0.182
Argon	Ar	18					0.311	0.310			0.221							0.219
Potassium	K	19					0.360	0.360			0.263							0.260
Calcium	Ca	20	0.341		0.345		0.413	0.413			0.305							0.302
Scandium	Sc	21	0.395		0.400		0.470	0.470			0.352							0.348
Titanium	Ti	22	0.452	0.452	0.458		0.528	0.528			0.402							0.395
Vanadium	V	23	0.510	0.510	0.518		0.590	0.590			0.454							0.446
Chromium	Cr	24	0.572	0.572	0.582		0.654	0.654			0.510							0.500
Manganese	Mn	25	0.637	0.637	0.648		0.722	0.722			0.568							0.556
Iron	Fe	26	0.705	0.705	0.718		0.792	0.792			0.629							0.616
Cobalt	Co	27	0.775	0.775	0.790		0.865	0.866			0.692							0.677
Nickel	Ni	28	0.849	0.849	0.866		0.942	0.941			0.759							0.742
Copper	Cu	29	0.928	0.928	0.947		1.022	1.019			0.830							0.810

(continued)

**Table A.5** L-line energies (keV).

Element	Symbol	AN	$L\alpha_1$	$L\alpha_2$	$L\beta_1$	$L\beta_2$	$L\beta_3$	$L\beta_4$	$L\beta_5$	$L\beta_6$	$L\eta$	$L\gamma_1$	$L\gamma_2$	$L\gamma_3$	$L\gamma_4$	$L\gamma_5$	$L\gamma_6$	LI
Zinc	Zn	30	1.012	1.012	1.035		1.108	1.105			0.905							0.882
Gallium	Ga	31	1.098	1.098	1.125		1.199	1.195			0.984		1.297					0.957
Germanium	Ge	32	1.188	1.187	1.218		1.294	1.290		1.212	1.068		1.412	1.412				1.037
Arsenic	As	33	1.282	1.282	1.317		1.386	1.381		1.316	1.154		1.524	1.524				1.119
Selenium	Se	34	1.379	1.378	1.419		1.491	1.486		1.422	1.245		1.649	1.649				1.204
Bromine	Br	35	1.481	1.480	1.526		1.600	1.593		1.523	1.339		1.779	1.779				1.293
Krypton	Kr	36	1.585	1.583	1.636		1.707	1.699		1.651	1.438		1.907	1.970		1.703		1.386
Rubidium	Rb	37	1.692	1.691	1.751		1.826	1.816		1.774	1.537		2.049	2.050		1.835		1.477
Strontium	Sr	38	1.806	1.804	1.871		1.946	1.936		1.901	1.648		2.194	2.196		1.969		1.581
Yttrium	Y	39	1.924	1.922	1.998		2.074	2.062		2.036	1.764		2.349	2.350		2.110		1.688
Zirconium	Zr	40	2.044	2.042	2.125	1.219	2.202	2.188		2.172	1.877	2.304		2.503	2.505		2.255	1.793
Niobium	Nb	41	2.169	2.166	2.260	2.367	2.337	2.322		2.315	1.998	2.462		2.665	2.667		2.407	1.904
Molybdenum	Mo	42	2.292	2.289	2.394	2.518	2.472	2.454		2.457	2.119	2.623		2.828	2.830		2.563	2.014
Technetium	Tc	43	2.423	2.419	2.535	2.670	2.625	2.595		2.607	2.249	2.790		3.001	3.003			2.133
Ruthenium	Ru	44	2.558	2.554	2.683	2.836	2.763	2.741		2.763	2.381	2.965		3.178	3.181		2.892	2.252
Rhodium	Rh	45	2.697	2.692	2.834	3.002	2.916	2.891		2.923	2.518	3.144		3.361	3.365		3.965	2.375
Palladium	Pd	46	2.838	2.833	2.990	3.171	3.072	3.044		3.086	2.658	3.328		3.548	3.553		3.244	2.501
Silver	Ag	47	2.983	2.977	3.150	3.347	3.233	3.202		3.254	2.805	3.520		3.742	3.748		3.428	2.632
Cadmium	Cd	48	3.133	3.126	3.315	3.526	3.400	3.355		3.428	2.955	3.715		3.954	3.954		3.619	2.766
Indium	In	49	3.286	3.279	3.487	3.712	3.573	3.535		3.607	3.111	3.920		4.165	4.165	4.237	3.818	2.903

(continued)



**Table A.5** L-line energies (keV).

Element	Symbol	AN	$L\alpha_1$	$L\alpha_2$	$L\beta_1$	$L\beta_2$	$L\beta_3$	$L\beta_4$	$L\beta_5$	$L\beta_6$	$L\eta$	$L\gamma_1$	$L\gamma_2$	$L\gamma_3$	$L\gamma_4$	$L\gamma_5$	$L\gamma_6$	LI
Tin	Sn	50	3.444	3.436	3.663	3.904	3.750	3.708		3.792	3.271	4.131	4.381	4.381	4.464	4.019	3.044	
Antimony	Sb	51	3.604	3.595	3.942	4.099	3.932	3.885		3.979	3.440	4.347	4.602	4.602	4.697	4.229	3.192	
Tellurium	Te	52	3.768	3.758	4.029	4.299	4.118	4.068		4.172	3.606	4.570	4.836	4.836	4.973	4.444	3.335	
Iodide	I	53	3.938	3.925	4.221	4.506	4.313	4.527		4.371	3.780	4.801	5.065	5.065	5.185	4.666	3.485	
Xenon	Xe	54	4.110	4.097	4.418	4.719	4.512	4.451		4.573	3.958	5.037	5.306	5.308			3.637	
Cesium	Cs	55	4.285	4.271	4.619	4.932	4.711	4.643		4.780	4.148	5.279	5.542	5.553	5.703	5.129	3.801	
Barium	Ba	56	4.465	4.451	4.828	5.154	4.926	4.852		4.994	4.331	5.531	5.797	5.810	5.937	5.371	3.954	
Lanthanum	La	57	4.647	4.630	5.038	5.378	5.238	5.057		5.208	4.529	5.785	6.060	6.070	6.252	5.621	4.121	
Cerium	Ce	58	4.839	4.821	5.262	5.614	5.361	5.274		5.432	4.728	6.055	6.325	6.341	6.528	5.875	4.287	
Praseodymium	Pr	59	5.035	5.016	5.492	5.849	5.593	5.498		5.660	4.929	6.325	6.599	6.617	6.815	6.136	4.453	
Neodymium	Nd	60	5.228	5.205	5.719	6.088	5.829	5.723		5.889	5.147	6.601	6.883	6.901	7.107	6.406	4.633	
Promethium	Pm	61	5.432	5.407	5.961	6.339	6.071	5.957		6.123	5.363	6.893	7.168	7.168			4.809	
Samarium	Sm	62	5.633	5.605	6.201	6.587	6.317	6.196	6.713	6.369	5.589	7.183	7.471	7.490	7.714	6.968	4.993	
Europium	Eu	63	5.849	5.818	6.458	6.844	6.571	6.438	6.975	6.617	5.817	7.484	7.768	7.795	8.030	7.257	5.177	
Gadolinium	Gd	64	6.053	6.021	6.708	7.100	6.832	6.688	7.237	6.864	6.049	7.787	8.090	8.105	8.355	7.554	5.362	
Terbium	Tb	65	6.273	6.237	6.975	7.364	7.097	6.940	7.509	7.118	6.284	8.101	8.386	8.424	8.685	7.853	5.546	
Dysprosium	Dy	66	6.498	6.457	7.248	7.636	7.370	7.204	7.806	7.376	6.534	8.427	8.713	8.753	9.020	8.166	5.743	
Holmium	Ho	67	6.720	6.679	7.525	7.911	7.653	7.471	8.052	7.639	6.790	8.758	9.050	9.086	9.374	8.481	5.943	
Erbium	Er	68	6.949	6.905	7.811	8.190	7.939	7.745	8.350	7.908	7.058	9.096	9.385	9.431	9.722	8.814	6.152	
Thulium	Tm	69	7.180	7.133	8.102	8.473	8.231	8.026	8.641	8.177	7.310	9.441	9.730	9.783	10.084	9.144	6.341	
Ytterbium	Yb	70	7.416	7.368	8.402	8.753	8.536	8.313	8.939	8.463	7.580	9.787	10.097	10.146	10.460	9.491	6.546	
Lutetium	Lu	71	7.655	7.605	8.710	9.038	8.845	8.605	9.240	8.737	7.858	10.143	10.458	10.511	10.843	9.843	6.753	
Hafnium	Hf	72	7.899	7.845	9.023	9.341	9.164	8.906	9.555	9.023	8.138	10.519	10.833	10.890	11.240	10.201	6.960	
Tantalum	Ta	73	8.146	8.088	9.343	9.643	9.488	9.213	9.875	9.318	8.428	10.898	11.219	11.281	11.645	10.570	7.173	
Tungsten	W	74	8.398	8.335	9.672	9.951	9.819	9.525	10.200	9.613	8.724	11.288	11.610	11.675	12.063	10.949	7.387	

(continued)

**Table A.5** L-line energies (keV).

Element	Symbol	AN	$L\alpha_1$	$L\alpha_2$	$L\beta_1$	$L\beta_2$	$L\beta_3$	$L\beta_4$	$L\beta_5$	$L\beta_6$	$L\eta$	$L\gamma_1$	$L\gamma_2$	$L\gamma_3$	$L\gamma_4$	$L\gamma_5$	$L\gamma_6$	LI
Rhenium	Re	75	8.652	8.586	10.010	10.261	10.150	9.845	10.532	9.910	9.027	11.685	12.008	12.080	12.492	11.334		7.603
Osmium	Os	76	8.911	8.840	10.354	10.578	10.511	10.176	10.871	10.213	9.336	12.092	12.419	12.497	12.923	11.730		7.822
Iridium	Ir	77	9.175	9.099	10.708	10.903	10.868	10.510	11.211	10.524	9.650	12.512	12.841	12.923	13.368	12.134		8.041
Platinum	Pt	78	9.442	9.362	11.071	11.232	11.235	10.853	11.561	10.839	9.977	12.941	13.271	13.361	13.828	12.552		8.268
Gold	Au	79	9.713	9.628	11.443	11.566	11.610	11.205	11.914	11.157	10.309	13.381	13.710	13.807	14.300	12.974	13.729	8.494
Mercury	Hg	80	9.989	9.899	11.824	11.905	11.992	11.560	12.274	11.482	10.647	13.831	14.159	14.262	14.778	13.410	14.199	8.722
Thallium	Tl	81	10.269	10.173	12.213	12.252	12.390	11.931	12.643	11.812	10.994	14.292	14.627	14.738	15.272	13.853	14.683	9.954
Lead	Pb	82	10.551	10.449	12.614	12.601	12.795	12.307	13.014	12.143	11.349	14.766	15.099	15.217	15.777	14.388	15.179	9.184
Bismuth	Bi	83	10.839	10.731	13.023	12.955	13.211	12.692	13.392	12.480	11.712	15.247	15.583	15.709	16.295	14.773	15.684	9.420
Polonium	Po	84	11.131	11.015	13.445	13.314	13.637	13.085	13.783	12.819	12.095	15.744	16.088	16.234			16.213	9.665
Astatine	At	85	11.427	11.305	13.876	13.681	14.067	13.485	14.174	13.172	12.468	16.252	16.607	16.753			16.745	9.897
Radon	Rn	86	11.727	11.597	14.315	14.052	14.511	13.890	14.571	13.522	12.855	16.770	17.120	17.281			17.289	10.137
Francium	Fr	87	12.031	11.895	14.771	14.428	14.975	14.312	14.973	13.878	13.255	17.304	17.659	17.829			17.849	10.379
Radium	Ra	88	12.339	12.196	15.235	14.808	15.445	14.747	15.376	14.236	13.662	17.848	18.179	18.358	19.084	17.274	18.416	10.622
Actinium	Ac	89	12.652	12.501	15.713	15.196	15.931	15.184	15.791	14.602	14.081	18.408	18.760	18.950			19.003	10.869
Thorium	Th	90	12.968	12.809	16.202	15.588	16.425	16.642	16.207	14.970	14.511	18.981	19.304	19.506	20.292	18.370	19.601	11.118
Protactinium	Pa	91	13.291	13.122	16.703	15.990	16.931	16.104	16.639	15.345	14.947	19.571	19.881	20.098	20.882	18.930	20.220	11.365
Uranium	U	92	13.614	13.438	17.220	16.428	17.454	16.575	17.063	15.727	15.400	21.170	20.486	20.714	21.562	19.507	20.845	11.618

**Table A.6** M-line energies (keV).

Element	Symbol	AN	M1N3	M2N1	M2N4	M3N1	M3O1	M3O45	M $\alpha_1$	M $\alpha_2$	M $\beta$	M $\gamma$	Mz1	Mz2
Rubidium	Rb	37												0.097
Strontium	Sr	38												0.114
Yttrium	Y	39												0.133
Zirconium	Zr	40												0.153
Niobium	Nb	41												0.172
Molybdenum	Mo	42												0.194
Technetium	Tc	43												0.215
Ruthenium	Ru	44												0.238
Rhodium	Rh	45										0.494		0.261
Palladium	Pd	46										0.530		0.285
Silver	Ag	47										0.569		0.310
Cadmium	Cd	48										0.608		0.337
Indium	In	49										0.648		0.366
Tin	Sn	50			0.733							0.691		0.397
Antimony	Sb	51			0.766							0.734		0.429
Tellurium	Te	52			0.830							0.780		0.464
Iodide	J	53			0.881							0.826		0.497
Xenon	Xe	54			0.936							0.873		0.525

*(continued)*

**Table A.6** M-line energies (keV).

Element	Symbol	AN	M1N3	M2N1	M2N4	M3N1	M3O1	M3O45	M $\alpha_1$	M $\alpha_2$	M $\beta$	M $\gamma$	Mz1	Mz2
Cesium	Cs	55			0.986							0.925		0.568
Barium	Ba	56			1.043	0.807			0.780		0.799	0.973		0.604
Lanthanum	La	57			1.101				0.836		0.849	1.026		0.640
Cerium	Ce	58			1.159				0.884		0.902	1.078		0.679
Praseodymium	Pr	59			1.224				0.927		0.946	1.127	0.712	0.712
Neodymium	Nd	60			1.285				0.979		1.002	1.177	0.753	0.753
Promethium	Pm	61			1.351				1.023		1.048	1.237	0.790	0.790
Samarium	Sm	62			1.412				1.078		1.105	1.291	0.832	0.831
Europium	Eu	63			1.481				1.131		1.153	1.353	0.875	0.875
Gadolinium	Gd	64			1.548				1.181		1.209	1.401	0.914	0.914
Terbium	Tb	65			1.620				1.240		1.269	1.450	0.955	0.955
Dysprosium	Dy	66			1.688				1.293		1.325	1.522	1.000	1.000
Holmium	Ho	67			1.762				1.348		1.383	1.576	1.048	1.048
Erbium	Er	68			1.829				1.404		1.448	1.644	1.087	1.087
Thulium	Tm	69			1.910				1.462		1.503	1.710	1.129	1.129
Ytterbium	Yb	70			1.975				1.525		1.573	1.768	1.187	1.187
Lutetium	Lu	71			2.059				1.580		1.630	1.828	1.227	1.227
Hafnium	Hf	72			2.141				1.646		1.170	1.895	1.278	1.278
Tantalum	Ta	73			2.225				1.712	1.710	1.770	1.968	1.331	1.330
Tungsten	W	74			2.314				1.775	1.773	1.838	2.038	1.383	1.379

(continued)

**Table A.6** M-line energies (keV).

Element	Symbol	AN	M1N3	M2N1	M2N4	M3N1	M3O1	M3O45	$M\alpha_1$	$M\alpha_2$	$M\beta$	$M\gamma$	Mz1	Mz2
Rhenium	Re	75			2.408				1.843	1.840	1.906	2.107	1.437	1.431
Osmium	Os	76			2.502				1.907	1.904	1.978	2.179	1.492	1.483
Iridium	Ir	77			2.594				1.980	1.975	2.052	2.255	1.546	1.537
Platinum	Pt	78	2.780		2.695	1.921		2.641	2.050	2.047	2.127	2.330	1.602	1.592
Gold	Au	79	2.883		2.797	1.981		2.742	2.123	2.118	2.203	2.408	1.662	1.648
Mercury	Hg	80	2.986		2.900	2.036		2.838	2.195	2.190	2.281	2.488	1.724	1.712
Thallium	Tl	81	3.089		3.013	2.107		2.386	2.271	2.266	2.363	2.572	1.778	1.763
Lead	Pb	82	3.202		3.124	2.174		3.045	2.342	2.340	2.444	2.654	1.840	1.823
Bismuth	Bi	83	3.315		3.234	2.239		3.153	2.423	2.427	2.526	2.737	1.901	1.883
Polonium	Po	84			3.351				2.499		2.614	2.829	1.947	
Astatine	At	85			3.473				2.577		2.699	2.919	2.023	
Radon	Rn	86			3.597				2.654		2.784	2.997	2.093	
Francium	Fr	87			3.723				2.732		2.868	3.0866	2.156	
Radium	Ra	88			3.852				2.806		2.949	3.189	2.190	
Actinium	Ac	89			3.983				2.900		3.051	3.270	2.290	
Thorium	Th	90	4.230	3.505	4.117	2.714	3.780	3.959	2.995	2.987	3.149	3.371	2.364	2.322
Protactinium	Pa	91			4.260	2.786	3.820		3.082	3.072	3.240	3.466	2.387	
Uranium	U	92	4.500	3.724	4.401	2.863	3.980	4.210	3.171	3.160	3.335	3.555	2.507	2.455

**Table A.7** Wavelengths of K-lines (nm).

Element	Symbol	OZ	$K\alpha_1$	$K\alpha_2$	$K\beta_1$	$K\beta_2$	$K\beta_3$	$K\beta_4$	$K\beta_5$
Beryllium	Be	4	11.481						
Boron	B	5	6.776						
Carbon	C	6	4.477						
Nitrogen	N	7	3.163						
Oxygen	O	8	2.362						
Fluorine	F	9	1.832						
Neon	Ne	10	1.461						
Sodium	Na	11	1.192						
Magnesium	Mg	12	0.989	0.990	0.952				
Aluminum	Al	13	0.834	0.834	0.796				
Silicon	Si	14	0.713	0.713	0.675				
Phosphorus	P	15	0.617	0.617	0.580				
Sulfur	S	16	0.537	0.537	0.503		0.503		
Chlorine	Cl	17	0.473	0.473	0.441		0.441		
Argon	Ar	18	0.419	0.420	0.389		0.389		
Potassium	K	19	0.374	0.375	0.345		0.345		
Calcium	Ca	20	0.336	0.336	0.309		0.309		
Scandium	Sc	21	0.303	0.303	0.278		0.278		
Titanium	Ti	22	0.275	0.275	0.251		0.251	0.250	
Vanadium	V	23	0.250	0.251	0.228		0.228	0.227	
Chromium	Cr	24	0.229	0.229	0.209		0.209	0.207	
Manganese	Mn	25	0.210	0.211	0.191		0.191	0.190	
Iron	Fe	26	0.194	0.194	0.176		0.176	0.174	
Cobalt	Co	27	0.179	0.179	0.162		0.162	0.161	
Nickel	Ni	28	0.166	0.166	0.150		0.150	0.149	
Copper	Cu	29	0.154	0.154	0.139		0.139	0.138	
Zinc	Zn	30	0.144	0.144	0.130		0.130	0.129	
Gallium	Ga	31	0.134	0.134	0.121		0.121	0.120	
Germanium	Ge	32	0.125	0.126	0.113		0.113	0.112	
Arsenic	As	33	0.118	0.118	0.106	0.105	0.106	0.105	
Selenium	Se	34	0.110	0.111	0.099	0.098	0.099	0.098	

*(continued)*

**Table A.7** Wavelengths of K-lines (nm).

Element	Symbol	OZ	$K\alpha_1$	$K\alpha_2$	$K\beta_1$	$K\beta_2$	$K\beta_3$	$K\beta_4$	$K\beta_5$
Bromine	Br	35	0.104	0.104	0.093	0.092	0.093		0.092
Krypton	Kr	36	0.098	0.098	0.088	0.087	0.088		0.087
Rubidium	Rb	37	0.093	0.093	0.083	0.082	0.083		0.082
Strontium	Sr	38	0.088	0.088	0.078	0.077	0.078		0.078
Yttrium	Y	39	0.083	0.083	0.074	0.073	0.074		0.073
Zirconium	Zr	40	0.079	0.079	0.070	0.069	0.070		0.070
Niobium	Nb	41	0.075	0.075	0.067	0.065	0.067		0.066
Molybdenum	Mo	42	0.071	0.071	0.063	0.062	0.063		0.063
Technetium	Tc	43	0.068	0.068	0.060	0.059	0.060		0.060
Ruthenium	Ru	44	0.064	0.000	0.057	0.059	0.057		0.057
Rhodium	Rh	45	0.061	0.062	0.055	0.054	0.055	0.053	0.054
Palladium	Pd	46	0.059	0.059	0.052	0.051	0.052	0.051	0.052
Silver	Ag	47	0.056	0.056	0.050	0.049	0.050	0.049	0.049
Cadmium	Cd	48	0.054	0.054	0.048	0.047	0.048	0.046	0.047
Indium	Ir	49	0.051	0.052	0.045	0.044	0.046	0.044	0.045
Tin	Sn	50	0.049	0.050	0.044	0.043	0.044	0.043	0.043
Antimony	Sb	51	0.047	0.047	0.042	0.041	0.042	0.041	0.041
Tellurium	Te	52	0.045	0.046	0.040	0.039	0.040	0.039	0.040
Iodide	J	53	0.043	0.044	0.038	0.038	0.038	0.037	0.038
Xenon	Xe	54	0.042	0.042	0.037	0.036	0.037	0.036	0.037
Cesium	Cs	55	0.040	0.040	0.035	0.035	0.036	0.035	0.035
Barium	Ba	56	0.039	0.039	0.034	0.033	0.034	0.033	0.034
Lanthanum	La	57	0.037	0.038	0.033	0.032	0.033	0.032	0.033
Cerium	Ce	58	0.036	0.036	0.032	0.031	0.032	0.031	0.031
Praseodymium	Pr	59	0.034	0.035	0.030	0.030	0.031	0.030	0.030

*(continued)*

**Table A.7** Wavelengths of K-lines (nm).

Element	Symbol	OZ	$K\alpha_1$	$K\alpha_2$	$K\beta_1$	$K\beta_2$	$K\beta_3$	$K\beta_4$	$K\beta_5$
Neodymium	Nd	60	0.033	0.034	0.029	0.029	0.029	0.029	0.029
Promethium	Pm	61	0.032	0.032	0.028	0.028	0.028	0.028	0.028
Samarium	Sm	62	0.031	0.031	0.027	0.027	0.027	0.027	0.027
Europium	Eu	63	0.030	0.030	0.026	0.026	0.026	0.026	0.026
Gadolinium	Gd	64	0.029	0.029	0.025	0.025	0.026	0.025	0.025
Terbium	Tb	65	0.028	0.028	0.025	0.024	0.025	0.024	0.024
Dysprosium	Dy	66	0.027	0.027	0.024	0.023	0.024	0.023	0.024
Holmium	Ho	67	0.026	0.027	0.023	0.022	0.023	0.022	0.023
Erbium	Er	68	0.025	0.026	0.022	0.022	0.022	0.022	0.022
Thulium	Tm	69	0.024	0.025	0.022	0.021	0.022	0.021	0.021
Ytterbium	Yb	70	0.024	0.024	0.021	0.020	0.021	0.020	0.021
Lutetium	Lu	71	0.023	0.023	0.020	0.020	0.020	0.020	0.020
Hafnium	Hf	72	0.022	0.023	0.020	0.019	0.020	0.019	0.019
Tantalum	Ta	73	0.022	0.022	0.019	0.019	0.019	0.018	0.019
Tungsten	W	74	0.021	0.021	0.022	0.018	0.019	0.018	0.018
Rhenium	Re	75	0.020	0.021	0.021	0.017	0.018	0.017	0.018
Osmium	Os	76	0.020	0.024	0.017	0.017	0.017	0.017	0.017
Iridium	Ir	77	0.019	0.020	0.017	0.016	0.017	0.016	0.017
Platinum	Pt	78	0.019	0.019	0.016	0.016	0.016	0.016	0.016
Gold	Au	79	0.018	0.019	0.016	0.015	0.016	0.015	0.016
Mercury	Hg	80	0.018	0.018	0.015	0.015	0.016	0.015	0.015
Thallium	Tl	81	0.017	0.018	0.015	0.015	0.015	0.015	0.015
Lead	Pb	82	0.017	0.017	0.015	0.014	0.015	0.014	0.015
Bismuth	Bi	83	0.016	0.017	0.014	0.014	0.014	0.014	0.014



**Table A.8** Wavelengths of L-lines (nm).

Element	Symbol	OZ	$L\alpha_1$	$L\alpha_2$	$L\beta_1$	$L\beta_2$	$L\beta_3$	$L\beta_4$	$L\beta_5$	$L\beta_6$	$L\eta$	$L\gamma_1$	$L\gamma_2$	$L\gamma_3$	$L\gamma_4$	$L\gamma_5$	$L\gamma_6$	LI
Magnesium	Mg	12					14.091				25.833							26.383
Aluminum	Al	13					10.783				17.971							17.971
Silicon	Si	14					8.378				13.478							13.626
Phosphorus	P	15					6.776	6.813			10.000							10.081
Sulfur	S	16					5.536	5.561			8.267							8.378
Chlorine	Cl	17					4.769	4.769			6.739							6.813
Argon	Ar	18					3.987	4.000			5.611							5.662
Potassium	K	19					3.444	3.444			4.715							4.769
Calcium	Ca	20	3.636		3.594		3.002	3.002			4.066							4.106
Scandium	Sc	21	3.139		3.100		2.638	2.638			3.523							3.563
Titanium	Ti	22	2.743	2.743	2.707		2.348	2.348			3.085							3.139
Vanadium	V	23	2.431	2.431	2.394		2.102	2.102			2.731							2.780
Chromium	Cr	24	2.168	2.168	2.131		1.896	1.896			2.431							2.480
Manganese	Mn	25	1.947	1.947	1.914		1.717	1.717			2.183							2.230
Iron	Fe	26	1.759	1.759	1.727		1.566	1.566			1.971							2.013
Cobalt	Co	27	1.600	1.600	1.570		1.434	1.432			1.792							1.832
Nickel	Ni	28	1.461	1.461	1.432		1.316	1.318			1.634							1.671
Copper	Cu	29	1.336	1.336	1.309		1.213	1.217			1.494							1.531

(continued)

**Table A.8** Wavelengths of L-lines (nm).

Element	Symbol	OZ	L $\alpha_1$	L $\alpha_2$	L $\beta_1$	L $\beta_2$	L $\beta_3$	L $\beta_4$	L $\beta_5$	L $\beta_6$	L $\eta$	L $\gamma_1$	L $\gamma_2$	L $\gamma_3$	L $\gamma_4$	L $\gamma_5$	L $\gamma_6$	L $\zeta$
Zinc	Zn	30	1.225	1.225	1.198		1.119	1.122			1.370							1.406
Gallium	Ga	31	1.129	1.129	1.102		1.034	1.038			1.260		0.956					1.296
Germanium	Ge	32	1.044	1.045	1.018		0.958	0.961		1.023	1.161		0.878	0.878				1.196
Arsenic	As	33	0.967	0.967	0.942		0.895	0.898		0.942	1.075		0.814	0.814				1.108
Selenium	Se	34	0.899	0.900	0.874		0.832	0.834		0.872	0.996		0.752	0.752				1.030
Bromine	Br	35	0.837	0.838	0.813		0.775	0.778		0.814	0.926		0.697	0.697				0.959
Krypton	Kr	36	0.782	0.783	0.758		0.726	0.730		0.751	0.862		0.650	0.629		0.728		0.895
Rubidium	Rb	37	0.733	0.733	0.708		0.679	0.683		0.699	0.807		0.605	0.605				0.840
Strontium	Sr	38	0.687	0.687	0.663		0.637	0.640		0.652	0.752		0.565	0.565		0.630		0.784
Yttrium	Y	39	0.644	0.645	0.621		0.598	0.601		0.609	0.703		0.528	0.528		0.588		0.735
Zirconium	Zr	40	0.607	0.607	0.584	1.017	0.563	0.567		0.571	0.661	0.538	0.495	0.495		0.550		0.692
Niobium	Nb	41	0.572	0.572	0.549	0.524	0.531	0.534		0.536	0.621	0.504	0.465	0.465		0.515		0.651
Molybdenum	Mo	42	0.541	0.542	0.518	0.492	0.502	0.505		0.505	0.585	0.473	0.438	0.438		0.484		0.616
Technetium	Tc	43	0.512	0.513	0.489	0.464	0.472	0.478		0.476	0.551	0.444	0.413	0.413				0.581
Ruthenium	Ru	44	0.485	0.486	0.462	0.437	0.449	0.452		0.449	0.521	0.418	0.390	0.390		0.429		0.551
Rhodium	Rh	45	0.460	0.461	0.438	0.413	0.425	0.429		0.424	0.492	0.394	0.369	0.368		0.313		0.522
Palladium	Pd	46	0.437	0.438	0.415	0.391	0.404	0.407		0.402	0.467	0.373	0.349	0.349		0.382		0.496
Silver	Ag	47	0.416	0.417	0.394	0.370	0.384	0.387		0.381	0.442	0.352	0.331	0.331		0.362		0.471
Cadmium	Cd	48	0.396	0.397	0.374	0.352	0.365	0.370		0.362	0.420	0.334	0.314	0.314		0.343		0.448
Indium	In	49	0.377	0.378	0.356	0.334	0.347	0.351		0.344	0.399	0.316	0.298	0.298	0.293	0.325		0.427

(continued)

**Table A.8** Wavelengths of L-lines (nm).

Element	Symbol	OZ	$L\alpha_1$	$L\alpha_2$	$L\beta_1$	$L\beta_2$	$L\beta_3$	$L\beta_4$	$L\beta_5$	$L\beta_6$	$L\eta$	$L\gamma_1$	$L\gamma_2$	$L\gamma_3$	$L\gamma_4$	$L\gamma_5$	$L\gamma_6$	LI
Tin	Sn	50	0.360	0.361	0.339	0.318	0.331	0.334		0.327	0.379	0.300	0.283	0.283	0.278	0.309		0.407
Antimony	Sb	51	0.344	0.345	0.315	0.303	0.315	0.319		0.312	0.360	0.285	0.269	0.269	0.264	0.293		0.388
Tellurium	Te	52	0.329	0.330	0.308	0.288	0.301	0.305		0.297	0.344	0.271	0.256	0.256	0.249	0.279		0.372
Iodide	J	53	0.315	0.316	0.294	0.275	0.288	0.274		0.284	0.328	0.258	0.245	0.245	0.239	0.266		0.356
Xenon	Xe	54	0.302	0.303	0.281	0.263	0.275	0.279		0.271	0.313	0.246	0.234	0.234				0.341
Cesium	Cs	55	0.289	0.290	0.268	0.251	0.263	0.267		0.259	0.299	0.235	0.224	0.223	0.217	0.242		0.326
Barium	Ba	56	0.278	0.279	0.257	0.241	0.252	0.256		0.248	0.286	0.224	0.214	0.213	0.209	0.231		0.314
Lanthanum	La	57	0.267	0.268	0.246	0.231	0.237	0.245		0.238	0.274	0.214	0.205	0.204	0.198	0.221		0.301
Cerium	Ce	58	0.256	0.257	0.236	0.221	0.231	0.235		0.228	0.262	0.205	0.196	0.196	0.190	0.211		0.289
Praseodymium	Pr	59	0.246	0.247	0.226	0.212	0.222	0.226		0.219	0.252	0.196	0.188	0.187	0.182	0.202		0.278
Neodymium	Nd	60	0.237	0.238	0.217	0.204	0.213	0.217		0.211	0.241	0.188	0.180	0.180	0.174	0.194		0.268
Promethium	Pm	61	0.228	0.229	0.208	0.196	0.204	0.208		0.203	0.231	0.180	0.173	0.173				0.258
Samarium	Sm	62	0.220	0.221	0.200	0.188	0.196	0.200	0.185	0.195	0.222	0.173	0.166	0.166	0.161	0.178		0.248
Europium	Eu	63	0.212	0.213	0.192	0.181	0.189	0.193	0.178	0.187	0.213	0.166	0.160	0.159	0.154	0.171		0.240
Gadolinium	Gd	64	0.205	0.206	0.185	0.175	0.181	0.185	0.171	0.181	0.205	0.159	0.153	0.153	0.148	0.164		0.231
Terbium	Tb	65	0.198	0.199	0.178	0.168	0.175	0.179	0.165	0.174	0.197	0.153	0.148	0.147	0.143	0.158		0.224
Dysprosium	Dy	66	0.191	0.192	0.171	0.162	0.168	0.172	0.159	0.168	0.190	0.147	0.142	0.142	0.137	0.152		0.216
Holmium	Ho	67	0.185	0.186	0.165	0.157	0.162	0.166	0.154	0.162	0.183	0.142	0.137	0.136	0.132	0.146		0.209
Erbium	Er	68	0.607	0.607	0.584	1.017	0.563	0.567		0.571	0.661	0.538	0.495	0.495		0.550		0.692
Thulium	Tm	69	0.572	0.572	0.549	0.524	0.531	0.534		0.536	0.621	0.504	0.465	0.465		0.515		0.651

(continued)

**Table A.8** Wavelengths of L-lines (nm).

Element	Symbol	OZ	$L\alpha_1$	$L\alpha_2$	$L\beta_1$	$L\beta_2$	$L\beta_3$	$L\beta_4$	$L\beta_5$	$L\beta_6$	$L\eta$	$L\gamma_1$	$L\gamma_2$	$L\gamma_3$	$L\gamma_4$	$L\gamma_5$	$L\gamma_6$	LI
Ytterbium	Yb	70	0.167	0.168	0.148	0.142	0.145	0.149	0.139	0.147	0.164	0.127	0.123	0.122	0.119	0.131		0.189
Lutetium	Lu	71	0.162	0.163	0.142	0.137	0.140	0.144	0.134	0.142	0.158	0.122	0.119	0.118	0.114	0.126		0.184
Hafnium	Hf	72	0.157	0.158	0.137	0.133	0.135	0.139	0.130	0.137	0.152	0.118	0.114	0.114	0.110	0.122		0.178
Tantalum	Ta	73	0.152	0.153	0.133	0.129	0.131	0.135	0.126	0.133	0.147	0.114	0.111	0.110	0.106	0.117		0.173
Tungsten	W	74	0.148	0.149	0.128	0.125	0.126	0.130	0.122	0.129	0.142	0.110	0.107	0.106	0.103	0.113		0.168
Rhenium	Re	75	0.143	0.144	0.124	0.121	0.122	0.126	0.118	0.125	0.137	0.106	0.103	0.103	0.099	0.109		0.163
Osmium	Os	76	0.139	0.140	0.120	0.117	0.118	0.122	0.114	0.121	0.133	0.103	0.100	0.099	0.096	0.106		0.159
Iridium	Ir	77	0.135	0.136	0.116	0.114	0.114	0.118	0.111	0.118	0.128	0.099	0.097	0.096	0.093	0.102		0.154
Platinum	Pt	78	0.131	0.132	0.112	0.110	0.110	0.114	0.107	0.114	0.124	0.096	0.093	0.093	0.090	0.099		0.150
Gold	Au	79	0.128	0.129	0.108	0.107	0.107	0.111	0.104	0.111	0.120	0.093	0.090	0.090	0.087	0.096	0.090	0.146
Mercury	Hg	80	0.124	0.125	0.105	0.104	0.103	0.107	0.101	0.108	0.116	0.090	0.088	0.087	0.084	0.092	0.087	0.142
Thallium	Tl	81	0.121	0.122	0.102	0.101	0.100	0.104	0.098	0.105	0.113	0.087	0.085	0.084	0.081	0.090	0.084	0.125
Lead	Pb	82	0.118	0.119	0.098	0.098	0.097	0.101	0.095	0.102	0.109	0.084	0.082	0.081	0.079	0.086	0.082	0.135
Bismuth	Bi	83	0.114	0.116	0.095	0.096	0.094	0.098	0.093	0.099	0.106	0.081	0.080	0.079	0.076	0.084	0.079	0.132
Polonium	Po	84	0.111	0.113	0.092	0.093	0.091	0.095	0.090	0.097	0.103	0.079	0.077	0.076			0.076	0.128
Astatine	At	85	0.109	0.110	0.089	0.091	0.088	0.092	0.087	0.094	0.099	0.076	0.075	0.074			0.074	0.125
Radon	Rn	86	0.106	0.107	0.087	0.088	0.085	0.089	0.085	0.092	0.096	0.074	0.072	0.072			0.072	0.122
Francium	Fr	87	0.103	0.104	0.084	0.086	0.083	0.087	0.083	0.089	0.094	0.072	0.070	0.070			0.069	0.119
Radium	Ra	88	0.100	0.102	0.081	0.084	0.080	0.084	0.081	0.087	0.091	0.069	0.068	0.068	0.065	0.072	0.067	0.117
Actinium	Ac	89	0.098	0.099	0.079	0.082	0.078	0.082	0.079	0.085	0.088	0.067	0.066	0.065			0.065	0.114
Thorium	Th	90	0.096	0.097	0.077	0.080	0.075	0.075	0.077	0.083	0.085	0.065	0.064	0.064	0.061	0.068	0.063	0.112
Protactinium	Pa	91	0.093	0.094	0.074	0.078	0.073	0.077	0.075	0.081	0.083	0.063	0.062	0.062	0.059	0.066	0.061	0.109
Uranium	U	92	0.091	0.092	0.072	0.075	0.071	0.075	0.073	0.079	0.081	0.059	0.061	0.060	0.058	0.064	0.059	0.107

**Table A.9** Wavelengths of M-lines (nm).

Element	Symbol	OZ	M1N3	M2N1	M2N4	M3N1	M3O1	M3O45	M $\alpha_1$	M $\alpha_2$	M $\beta$	M $\gamma$	Mz <sub>1</sub>	Mz <sub>2</sub>
Rubidium	Rb	37												12.784
Strontium	Sr	38												10.877
Yttrium	Y	39												9.323
Zirconium	Zr	40												8.105
Niobium	Nb	41												7.209
Molybdenum	Mo	42												6.392
Technetium	Tc	43												5.767
Ruthenium	Ru	44												5.210
Rhodium	Rh	45										2.510		4.751
Palladium	Pd	46										2.340		4.351
Silver	Ag	47										2.179		4.000
Cadmium	Cd	48										2.039		3.680
Indium	Ir	49										1.914		3.388
Tin	Sn	50			1.692							1.795		3.123
Antimony	Sb	51			1.619							1.689		2.890
Tellurium	Te	52			1.494							1.590		2.672
Iodide	I	53			1.407							1.501		2.495
Xenon	Xe	54			1.325							1.420		2.362

(continued)

**Table A.9** Wavelengths of M-lines (nm).

Element	Symbol	OZ	M1N3	M2N1	M2N4	M3N1	M3O1	M3O45	M $\alpha_1$	M $\alpha_2$	M $\beta$	M $\gamma$	Mz <sub>1</sub>	Mz <sub>2</sub>
Cesium	Cs	55			1.258							1.341		2.183
Barium	Ba	56			1.189	1.537			1.590		1.552	1.274		2.053
Lanthanum	La	57			1.126				1.483		1.461	1.209		1.938
Cerium	Ce	58			1.070				1.403		1.375	1.150		1.826
Praseodymium	Pr	59			1.013				1.338		1.311	1.100	1.742	1.742
Neodymium	Nd	60			0.965				1.267		1.238	1.054	1.647	1.647
Promethium	Pm	61			0.918				1.212		1.183	1.002	1.570	1.570
Samarium	Sm	62			0.878				1.150		1.122	0.960	1.490	1.492
Europium	Eu	63			0.837				1.096		1.075	0.916	1.417	1.417
Gadolinium	Gd	64			0.801				1.050		1.026	0.885	1.357	1.357
Terbium	Tb	65			0.765				1.000		0.977	0.855	1.298	1.298
Dysprosium	Dy	66			0.735				0.959		0.936	0.815	1.240	1.240
Holmium	Ho	67			0.704				0.920		0.897	0.787	1.183	1.183
Erbium	Er	68			0.678				0.883		0.856	0.754	1.141	1.141
Thulium	Tm	69			0.649				0.848		0.825	0.725	1.098	1.098
Ytterbium	Yb	70			0.628				0.813		0.788	0.701	1.045	1.045
Lutetium	Lu	71			0.602				0.785		0.761	0.678	1.011	1.011
Hafnium	Hf	72			0.579				0.753		1.060	0.654	0.970	0.970
Tantalum	Ta	73			0.557				0.724	0.725	0.701	0.630	0.932	0.932
Tungsten	W	74			0.536				0.699	0.699	0.675	0.608	0.897	0.899

(continued)

**Table A.9** Wavelengths of M-lines (nm).

Element	Symbol	OZ	M1N3	M2N1	M2N4	M3N1	M3O1	M3O45	M $\alpha_1$	M $\alpha_2$	M $\beta$	M $\gamma$	Mz <sub>1</sub>	Mz <sub>2</sub>
Rhenium	Re	75			0.515				0.673	0.674	0.651	0.589	0.863	0.867
Osmium	Os	76			0.496				0.650	0.651	0.627	0.569	0.831	0.836
Iridium	Ir	77			0.478				0.626	0.628	0.604	0.550	0.802	0.807
Platinum	Pt	78	0.446		0.460	0.645		0.470	0.605	0.606	0.583	0.532	0.774	0.779
Gold	Au	79	0.430		0.443	0.626		0.452	0.584	0.585	0.563	0.515	0.746	0.752
Mercury	Hg	80	0.415		0.428	0.609		0.437	0.565	0.566	0.544	0.498	0.719	0.724
Thallium	Tl	81	0.401		0.412	0.589		0.520	0.546	0.547	0.525	0.482	0.697	0.703
Lead	Pb	82	0.387		0.397	0.570		0.407	0.529	0.530	0.507	0.467	0.674	0.680
Bismuth	Bi	83	0.374		0.383	0.554		0.393	0.512	0.511	0.491	0.453	0.652	0.659
Polonium	Po	84			0.370				0.496		0.474	0.438	0.637	
Astatine	At	85			0.357				0.481		0.459	0.425	0.613	
Radon	Rn	86			0.345				0.467		0.445	0.414	0.592	
Francium	Fr	87			0.333				0.454		0.432	0.402	0.575	
Radium	Ra	88			0.322				0.442		0.420	0.389	0.566	
Actinium	Ac	89			0.311				0.428		0.406	0.379	0.541	
Thorium	Th	90	0.293	0.354	0.301	0.457	0.328	0.313	0.414	0.415	0.394	0.368	0.525	0.534
Protactinium	Pa	91			0.291	0.445	0.325		0.402	0.404	0.383	0.358	0.519	
Uranium	U	92	0.276	0.333	0.282	0.433	0.312	0.295	0.391	0.392	0.372	0.349	0.495	0.505

**Table A.10** Common line interferences, energies in keV.

Analytic line	Energy	Interference	Energy	Interference	Energy	Interference	Energy
F-K $\alpha$	0.677	Fe-L $\alpha$	0.704	Mn-L $\alpha$	0.636		
Na-K $\alpha$	1.041	Zn-L $\beta_1$	1.009	Cu-L $\beta_3$	0.948		
Al-K $\alpha$	1.487	Br-L $\alpha$	1.480				
Si-K $\alpha$	1.740	Sr-L $\alpha$	1.806	W-M $\alpha$	1.775		
P-K $\alpha$	2.015	Zr-L $\alpha$	2.041	Mo-LI	2.014		
S-K $\alpha$	2.308	Pb-M $\alpha$	2.342	Mo-L $\alpha$	2.292	Zr-L $\gamma$	2.302
Cl-K $\alpha$	2.622	Rh-L $\alpha$ (tube)	2.695	Mo-L $\gamma_1$	2.623		
Ca-K $\alpha$	3.691	K-K $\beta$	3.589	Sn-L $\beta_1$	3.662		
Ti-K $\alpha$	4.510	Sc-K $\beta$	4.460	Ba-L $\alpha_1$	4.467		
Ti-K $\beta$	4.931	V-K $\alpha$	4.950	Ba-L $\beta_3$	4.926	Cs-L $\beta_2$	4.936
V-K $\alpha$	4.950	Ti-K $\beta$	4.931	Ba-L $\beta_3$	4.926	Cs-L $\beta_2$	4.936
Cr-K $\alpha$	5.411	V-K $\beta$	5.427	Pr-L $\beta_1$	5.489	La-L $\beta_2$	5.384
Mn-K $\alpha$	5.888	Cr-K $\beta$	5.946				
Fe-K $\alpha$	6.400	Mn-K $\beta$	6.490				
Co-K $\alpha$	6.925	Fe-K $\beta$	7.057	Er-L $\alpha_1$	6.948	Hf-LI	6.960
Ni-K $\alpha$	7.471	Co-K $\beta$	7.649	W-LI	7.387		
Cu-K $\alpha$	8.040	Ni-K $\beta$	8.264	Ta-L $\alpha_1$	8.145		
Zn-K $\alpha$	8.631	Cu-K $\beta$	8.904	W-L $\alpha_1$	8.396	Ta-L $\eta$	8.428
Ga-K $\alpha$	9.245	Ta-L $\beta_1$	9.343	Ta-L $\beta_4$	9.213	Hf-L $\beta_2$	9.341
Ge-K $\alpha$	9.875	W-L $\beta_2$	9.951	Hg-L $\alpha_2$	9.896	W-L $\beta_3$	9.819
As-K $\alpha$	10.530	Pb-L $\alpha_1$	10.549	Hf-L $\gamma_1$	10.514		
As-K $\beta$	11.725	Br-K $\alpha$	11.905	Hg-L $\beta_1$	11.823	W-L $\gamma_3$	11.675
Se-K $\alpha$	11.208	W-L $\gamma_1$	11.288				
Br-K $\alpha$	11.905	As-K $\beta$	11.725	Hg-L $\beta_2$	11.923		
Rb-K $\alpha$	13.374	Br-K $\beta_1$	13.290	U-L $\alpha_2$	13.438		
Sr-K $\alpha$	14.112	Tl-L $\gamma_1$	14.288	Au-L $\gamma_4$	14.300		
Y-K $\alpha$	14.932	Rb-K $\beta_1$	14.960	Pb-L $\gamma_1$	14.762		
Zr-K $\alpha$	15.746	Sr-K $\beta_1$	15.834	Th-L $\beta_2$	15.620		
Nb-K $\alpha$	16.586	Y-K $\beta_1$	16.736	U-L $\beta_2$	16.425		
Mo-K $\alpha$	17.440	Zr-K $\beta_1$	17.666	U-L $\beta_1$	17.218		
Rh-K $\alpha$ Comp		Mo-K $\beta_1$	19.607	Nb-K $\beta_2$	18.953		
Rh-K $\beta$ Comp		Ag-K $\alpha$	22.102	Pd-K $\alpha$	21.103	Ru-K $\beta$	19.149
Ag-L $\alpha_1$	2.984	Rh-L $\beta_2$	3.001	Cd-L $\eta$	2.955		
Cd-L $\beta_1$	3.316	K-K $\alpha$	3.312	U-M $\beta$	3.336		
In-K $\alpha$	24.207	Pd-K $\beta_1$	23.816				
Sn-L $\alpha_1$	3.444	Sb-L $\eta$	3.440	Cd-L $\beta_6$	3.428		

(continued)



**Table A.10** Common line interferences, energies in keV.

Analytic line	Energy	Interference	Energy	Interference	Energy	Interference	Energy
Sn-K $\alpha$	25.270	Ag-K $\beta_1$	24.942				
Sb-K $\alpha$	26.357	Cd-K $\beta_1$	26.093				
I-L $\alpha_1$	3.937	Ba-LI	3.954	Sb-L $\beta_3$	3.932		
I-K $\alpha$	28.610	Sn-K $\beta_1$	28.483				
Cs-K $\alpha$	30.970	Te-K $\beta_1$	30.993				
Ba-La $_1$	4.467	Ti-K $\alpha$	4.508				
Ba-L $\beta_1$	4.828	Ti-K $\beta$	4.931	Ce-La $_1$	4.840		
La-L $\alpha_1$	4.651	Cs-L $\beta_1$	4.620				
La-L $\beta_1$	5.043	Pr-L $\alpha_1$	5.034				
Ce-L $\beta_1$	5.262	Nd-La $_1$	5.230				
Pr-L $\beta_1$	5.489	Ba-L $\gamma_1$	5.531				
Pr-K $\alpha_2$	35.548	Ba-K $\beta_1$	36.376				
Nd-La $_1$	5.230	Ce-L $\beta_1$	5.262				
Nd-K $\alpha_2$	36.845	Ba-K $\beta_1$	36.376	Ba-K $\beta_2$	37.249		
Sm-La $_1$	5.636	Ce-L $\beta_2$	5.613				
Sm-L $\beta_1$	6.206	Fe-K $\alpha$	6.400				
Gd-La $_1$	6.059	Nd-L $\beta_2$	6.090	Ce-L $\gamma_1$	6.052		
Tb-La $_1$	6.275	Sm-L $\beta_3$	6.317				
Ho-La $_1$	6.720	Gd-L $\beta_1$	6.714				
Tm-La $_1$	7.181	Dy-L $\beta_1$	7.249				
Yb-La $_1$	7.414	Ni-K $\alpha$	7.470				
Lu-La $_1$	7.654	Co-K $\beta$	7.649				
Hf-L $\beta_1$	9.021	Cu-K $\beta$	8.904				
Ta-La $_1$	8.145	Cu-K $\alpha$	8.040				
Os-La $_1$	8.910	Cu-K $\beta$	8.904				
Ir-La $_1$	9.173	Pb-LI	9.184				
Pt-La $_1$	9.441	W-L $\beta_4$	9.525	Ta-L $\beta_1$	9.341		
Au-L $\beta_1$	11.439	Pt-L $\beta_5$	11.561	Pb-L $\eta$	11.349		
Tl-L $\beta_1$	12.213	Pb-L $\beta_4$	12.307				
Pb-L $\beta_1$	12.611	Se-K $\beta_1$	12.495				
Bi-La $_1$	10.836	Ge-K $\beta_1$	10.981	W-L $\gamma_5$	10.949	Ta-L $\gamma_1$	10.898
Th-La $_1$	12.966	Pb-L $\beta_5$	13.014	Pt-L $\gamma_1$	12.939		
Th-L $\beta_1$	16.200	Nb-K $\alpha$	16.580	U-L $\beta_2$	16.425	Sr-K $\beta_2$	15.834
U-La $_1$	13.613	Rb-K $\alpha$	13.363	Br-K $\beta_2$	13.290		

Table A.11 Fluorescence yields.

AN	Element	Symbol	K	L	M	AN	Element	Symbol	K	L	M	AN	Element	Symbol	K	L	M
4	<b>Beryllium</b>	Be	0.00003														
5	<b>Boron</b>	B	0.0007			20	<b>Calcium</b>	Ca	0.142	0.001		35	<b>Bromine</b>	Br	0.604	0.016	
6	<b>Carbon</b>	C	0.0014			21	<b>Scandium</b>	Sc	0.168	0.001		36	<b>Krypton</b>	Kr	0.629	0.019	
7	<b>Nitrogen</b>	N	0.002			22	<b>Titanium</b>	Ti	0.197	0.001		37	<b>Rubidium</b>	Rb	0.653	0.021	0.001
8	<b>Oxygen</b>	O	0.003			23	<b>Vanadium</b>	V	0.227	0.002		38	<b>Strontium</b>	Sr	0.675	0.024	0.001
9	<b>Fluorine</b>	F	0.005			24	<b>Chromium</b>	Cr	0.258	0.002		39	<b>Yttrium</b>	Y	0.695	0.027	0.001
10	<b>Neon</b>	Ne	0.008			25	<b>Manganese</b>	Mn	0.291	0.003		40	<b>Zirconium</b>	Zr	0.715	0.031	0.001
11	<b>Sodium</b>	Na	0.013			26	<b>Iron</b>	Fe	0.324	0.003		41	<b>Niobium</b>	Nb	0.732	0.035	0.001
12	<b>Magnesium</b>	Mg	0.019			27	<b>Cobalt</b>	Co	0.358	0.004		42	<b>Molybdenum</b>	Mo	0.749	0.039	0.001
13	<b>Aluminium</b>	Al	0.026			28	<b>Nickel</b>	Ni	0.392	0.005		43	<b>Technetium</b>	Tc	0.765	0.043	0.001
14	<b>Silicon</b>	Si	0.036			29	<b>Copper</b>	Cu	0.425	0.006		44	<b>Ruthenium</b>	Ru	0.779	0.047	0.001
15	<b>Phosphorus</b>	P	0.047			30	<b>Zinc</b>	Zn	0.458	0.007		45	<b>Rhodium</b>	Rh	0.792	0.052	0.001
16	<b>Sulfur</b>	S	0.061			31	<b>Gallium</b>	Ga	0.489	0.009		46	<b>Palladium</b>	Pd	0.805	0.058	0.001
17	<b>Chlorine</b>	Cl	0.078			32	<b>Germanium</b>	Ge	0.520	0.010		47	<b>Silver</b>	Ag	0.816	0.063	0.002
18	<b>Argon</b>	Ar	0.097			33	<b>Arsenic</b>	As	0.549	0.012		48	<b>Cadmium</b>	Cd	0.827	0.069	0.002
19	<b>Potassium</b>	K	0.118			34	<b>Selenium</b>	Se	0.577	0.014		49	<b>Indium</b>	In	0.836	0.075	0.002

(continued)

Table A.11 Fluorescence yields.

AN	Element	Symbol	K	L	M	AN	Element	Symbol	K	L	M	AN	Element	Symbol	K	L	M
50	Tin	Sn	0.845	0.081	0.002	65	Terbium	Tb	0.924	0.210	0.009	80	Mercury	Hg	0.952	0.366	0.028
51	Antimony	Sb	0.854	0.088	0.002	66	Dysprosium	Dy	0.927	0.220	0.009	81	Thallium	Tl	0.953	0.376	0.030
52	Tellurium	Te	0.862	0.095	0.003	67	Holmium	Ho	0.930	0.231	0.010	82	Lead	Pb	0.954	0.386	0.032
53	Jodide	J	0.869	0.102	0.003	68	Erbium	Er	0.932	0.240	0.011	83	Bismuth	Bi	0.954	0.396	0.034
54	Xenon	Xe	0.876	0.110	0.003	69	Thulium	Tm	0.934	0.251	0.012	84	Polonium	Po	0.955	0.405	0.037
55	Cesium	Cs	0.882	0.118	0.004	70	Ytterbium	Yb	0.937	0.262	0.013	85	Astatine	At	0.956	0.415	0.040
56	Barium	Ba	0.888	0.126	0.004	71	Lutetium	Lu	0.939	0.272	0.014	86	Radon	Rn	0.957	0.425	0.043
57	Lanthanum	La	0.893	0.136	0.004	72	Hafnium	Hf	0.941	0.283	0.015	87	Francium	Fr	0.957	0.434	0.046
58	Cerium	Ce	0.898	0.143	0.005	73	Tantalum	Ta	0.942	0.293	0.016	88	Radium	Ra	0.958	0.443	0.049
59	Praseodymium	Pr	0.902	0.152	0.005	74	Tungsten	W	0.944	0.304	0.018	89	Actinium	Ac	0.958	0.452	0.052
60	Neodymium	Nd	0.907	0.161	0.006	75	Rhenium	Re	0.945	0.314	0.019	90	Thorium	Th	0.959	0.461	0.056
61	Promethium	Pm	0.911	0.171	0.006	76	Osmium	Os	0.947	0.325	0.020	91	Proactinium	Pa	0.959	0.469	0.060
62	Samarium	Sm	0.915	0.180	0.007	77	Iridium	Ir	0.948	0.335	0.022	92	Uranium	U	0.960	0.478	0.064
63	Europium	Eu	0.918	0.190	0.007	78	Platinum	Pt	0.949	0.345	0.024						
64	Gadolinium	Gd	0.921	0.200	0.008	79	Gold	Au	0.951	0.356	0.026						

**Table A.12** Transfer factors between elements and oxides.

Element	Oxide	Element $\Rightarrow$ Oxide	Oxide $\Leftarrow$ Element
C	CO <sub>2</sub>	3.6641	0.2729
Na	Na <sub>2</sub> O	1.3480	0.7417
Mg	MgO	1.6579	0.6032
Al	Al <sub>2</sub> O <sub>3</sub>	1.8895	0.5292
Si	SiO <sub>2</sub>	2.1392	0.4675
P	P <sub>2</sub> O <sub>5</sub>	2.2914	0.4364
S	SO <sub>3</sub>	2.5000	0.4000
K	K <sub>2</sub> O	1.2046	0.8302
Ca	CaO	1.3992	0.7147
CaO	CaCO <sub>3</sub>	1.7848	0.5603
Ti	TiO <sub>2</sub>	1.6681	0.5995
Cr	Cr <sub>2</sub> O <sub>3</sub>	1.4615	0.6843
Mn	MnO	1.2912	0.7745
Mn	Mn <sub>3</sub> O <sub>4</sub>	1.3883	0.7203
Fe	FeO	1.2865	0.7773
Fe	Fe <sub>2</sub> O <sub>3</sub>	1.4297	0.6994
Ni	NiO	1.2726	0.7858
Rb	Rb <sub>2</sub> O	1.0936	0.9144
Sr	SrO	1.1826	0.8456
Zr	ZrO <sub>2</sub>	1.3508	0.7403
Nb	Nb <sub>2</sub> O <sub>5</sub>	1.4305	0.6990
Ba	BaO	1.1165	0.8957

## Appendix B

### Important Information

#### B.1 Coordinates of Main Manufacturers of Instruments and Preparation Tools

Manufacturer	Address headquarter	Representation in Germany	Web-address/Phone
Bruker AXS GmbH	D-76181 Karlsruhe Östliche Rheinbrückenstr. 49	D-76181 Karlsruhe Östliche Rheinbrückenstr. 49	www.bruker.com Tel: +49-721-50997.0
Bruker Nano GmbH	D-12489 Berlin Am Studio 2d	D-12489 Berlin Am Studio 2d	www.bruker.com Tel: +49-30-670.990.0
EDAX Inc. (Ametek)	USA NJ-07430 Mahwah 91 McKee Drive	AMETEK GmbH, EDAX Division D-64331 Weiterstadt Rudolf-Diesel-Str. 16	www.edax.com Tel: +49-6150-543.7050
Helmut Fischer GmbH & Co, KG	D-71069 Sindelfingen Industriestr. 22	D-71069 Sindelfingen Industriestr. 22	www.helmut-fischer.com Tel: +49-7031-303.0
Oxford Instruments Industrial Analysis	Oxford Instruments plc Tubney Woods Abingdon, OX13 5QX, UK	D- 47589 Uedem Wellesweg 31	www.oxford-instruments.com Tel: +49-2825-9383.0

<b>Manufacturer</b>	<b>Address headquarter</b>	<b>Representation in Germany</b>	<b>Web-address/Phone</b>
Panalytical B.V.	NL-7602 EA Almelo Lelyweg 1	Panalytical GmbH D- 34123 Kassel Nürnberger Str. 113	www.panalytical.com Tel: +49-561-5742.0
Rigaku Corporation	Tokyo 196-8666, Japan 3-9-12, Matsubara, Akishima-shi	Rigaku Europe SE D-76275 Ettlingen Am Hardtwald 11	www.rigaku.com Tel: +49-7243-94936.0
Hitachi Corporation	24-14, Nishi-Shimbashi, 1-chome, Minato-ku, Tokyo 105-0003, Japan	Hitachi High-Technologies Europe GmbH D-47807 Krefeld Europapark Fichtenhain 12A	www.hitachi-hightech .com Tel: 02151-6435.0
Shimadzu Corporation	3, Kanda-Nishikicho 1-chome Chiyoda-ku, Tokyo 101-8448, Japan	Shimadzu Europa GmbH D-47269 Duisburg Albert-Hahn-Straße 6	www.shimadzu.com Tel: +49-203-7687.0
SkyRay Instruments Co. Ltd.	Skyray Building, Tsinghua Science Park, 1666 South Weicheng Road, Kushan, Jiangsu Province, China		www.skyrayinstrument .com
SPECTRO Analytical Instruments GmbH (Ametek)	D-47533 Kleve Boschstr. 10	D-47533 Kleve Boschstr. 10	www.spectro.com Tel.: +49-2821-892.0
Thermo Fisher (Niton)	USA MA-01821 Billerica 900 Middlesex Tpke	Analyticon D-61191 Rosbach v.d.Höhe Dieselstr. 18	www.analyticon.eu Tel.: +49-6003-9355.20
Thermo Fisher Scientific	Thermo Fisher Scientific 1024 Ecublens, Switzerland	Thermo Fisher Scientific GmbH D-63303 Dreieich Im Steingrund 4-6	www.thermo.com Tel.: +49-6103-4080
XOS	USA NY-12062 East Greenbush 15 Tech Valley Drive		www.xos.com

Manufacturer	Address headquarter	Representation in Germany	Web-address/Phone
<i>Sample preparation</i>			
Chemplex Industries Inc.	Palm City, FL 34990-5573 USA 2820 SW 42nd Avenue	LGC Standards GmbH D-46485 Wesel Mercatorstraße 51	www.chemplex.com Tel. +49-281-319.391.0
Corporation Scientifique Claisse	Ville de Québec, QC G1P 4P3, Can 350 Rue Franquet #45	Impexron GmbH D-72793 Pfullingen Gönningerstr. 99	www.claisse.com Tel:+49-7121-305.9012
Fluxana GmbH + Co KG	47551 Bedburg-Hau Borschelstraße 3		www.fluxana.com Tel.: +49-2821.997.320
Fritsch GmbH	55743 Idar-Oberstein Industriestrasse 8		www.fritsch.de Tel.: +49-6784-70.153
LGC Standards GmbH	LGC Standards GmbH D-46485 Wesel Mercatorstraße 51		www.lgcstandards.com Tel. +49-2 81-319.391.0
Retsch Technology GmbH	42781 Haan Retsch-Allee		www.retsch.de Tel.: +49-2104-233.330
Sigma-Aldrich Corp.			www.sigma-aldich.com
Spex SamplePrep LLC	Metuchen, NJ 08840, USA 65 Liberty St	C3 Analysentech- nik GmbH D-85540 Munich Peter-Henlein-Str. 20	www.spexsampleprep .com Tel.: +49-89-4560.0670
XRF Scientific Ltd.	Osborne Park, West. Aus 6017 98 Guthrie St	D-63791 Karlstein Seligenstädter Straße 100	www.xrfscientific.com Tel.: +49-6188-954.276
<i>Automation</i>			
Herzog- Maschinenfabrik GmbH & Co. KG	49086 Osnabrück Auf dem Gehren 1		www.herzog- maschinenfabrik.de/ Tel.: +49-541-9332.0
Pfaff AQS GmbH	42232 Wuppertal Lennep Str. 23-25		www.flsmidth.com/
Thyssenkrupp Industrial Solutions	45143 Essen Thyssenkrupp Allee 1		www.thyssenkrupp- industrial-solutions.com/

## B.2 Main Suppliers of Standard Materials

### B.2.1 Geological Materials and Metals

Issuer/country	Name	Link to the corresponding catalog	Prevailing materials
NMI, Australia	National Measurement Institute	<a href="http://www.measurement.gov.au">www.measurement.gov.au</a>	Metals, minerals
GEOSTATS, Australia	Geostats Pty Ltd.	<a href="http://www.geostats.com.au">www.geostats.com.au</a>	Minerals
IAEA, Austria	International Atomic Energy Agency	<a href="http://www.iaea.org/">www.iaea.org/</a>	Database for natural reference materials
IRMM, Belgium	Institute for Materials and Measurements	<a href="https://ec.europa.eu/jrc/en/science-update/welcome-irmm-reference-materials-catalogue">https://ec.europa.eu/jrc/en/science-update/welcome-irmm-reference-materials-catalogue</a>	Metals, minerals
IPT, Brasilia	Instituto de Pesquisas Technologicas	<a href="http://www.ipt.br/nmr.htm">www.ipt.br/nmr.htm</a>	Metals, minerals
CCRPM, Canada	Canadian Certified Reference Materials Project	<a href="http://www.nrcan.gc.ca">www.nrcan.gc.ca</a>	Metals, minerals, coal
IMB, Canada	Institute for Marine Biosciences	<a href="http://www.nrc-cnrc.gc.ca">www.nrc-cnrc.gc.ca</a>	Metals
Conostan, Canada	SCP Science Corporate	<a href="http://www.scpscience.com/en/corporate">www.scpscience.com/en/corporate</a>	Oil
NSC, China	China Iron & Steel Research Institute Group (CISRI)	<a href="http://www.ncsstandard.com">www.ncsstandard.com</a>	Ferroalloys, coal, metals, minerals, slags
CRPG, France	Centre de Recherches Pétrographiques et Géochimiques	<a href="http://www.crpq.crns-nancy.fr">www.crpq.crns-nancy.fr</a>	Minerals
BAM, Germany	Bundesanstalt für Materialforschung und -prüfung	<a href="http://www.bam.de">www.bam.de</a>	Ceramics, metals
Breitländer, Germany	Breitländer GmbH	<a href="http://www.breitlander.com">www.breitlander.com</a>	Metals, minerals, ferroalloys
NMIJ, Japan	National Metrology Institute of Japan	<a href="https://unit.aist.go.jp/nmij/english/service/database">https://unit.aist.go.jp/nmij/english/service/database</a>	Metals, minerals
GSI, Japan	Geological Survey of Japan	<a href="http://www.gsj.jp/en">www.gsj.jp/en</a>	Minerals



Issuer/country	Name	Link to the corresponding catalog	Prevailing materials
JSS, Japan	Iron and Steel Institute of Japan	<a href="http://www.seishin-syoji.co.jp">www.seishin-syoji.co.jp</a>	Metals, ores, ferroalloys
CENAM, Mexico	Centro Nacional de Metrologia	<a href="http://www.gob.mx/cenam">www.gob.mx/cenam</a>	Metals, minerals
Rocklabs, New Zealand	Rocklabs Ltd.	<a href="http://www.rocklabs.com">www.rocklabs.com</a>	Precious metals ores
SGS, Switzerland	Societe Generale de Surveillance	<a href="http://www.sgs.com">www.sgs.com</a>	prevailing materials: Metals, minerals
MINTEK, South Africa	National Mineral Research Organization	<a href="http://www.mintek.co.za/technical-divisions/analytical-services-asd">www.mintek.co.za/technical-divisions/analytical-services-asd</a>	Ores, minerals
AMIS, South Africa	African Minerals	<a href="http://www.african-minerals.com/">http://www.african-minerals.com/</a>	Minerals
SABS, South Africa	South African Bureau of Standards	<a href="http://www.sabs.co.za">www.sabs.co.za</a>	Metals, minerals
BAS, UK	Bureau of Analysed Samples Ltd.	<a href="http://www.basrid.co.uk/">www.basrid.co.uk/</a>	Minerals, ferroalloys, metals
BGS, UK	British Geological Survey	<a href="http://www.bgs.ac.uk">www.bgs.ac.uk</a>	Minerals
MBH, UK	MBH Analytical Ltd	<a href="http://www.mbh.co.uk">www.mbh.co.uk</a>	Metals
NIST, USA	National Institute of Standards and Technology	<a href="http://www.nist.gov/srm/index.cfm">www.nist.gov/srm/index.cfm</a>	Ores, metals, minerals, coal,
Brammer, USA	Brammer Standard Company Inc.	<a href="http://www.brammerstandard.com/">www.brammerstandard.com/</a>	Metals

### B.2.2 Stratified Materials

Issuer/country	Name	Link to the corresponding catalog	Prevailing materials
Micro-Matter, Canada	Micromatter thin film standards	<a href="http://www.micromatter.com">www.micromatter.com</a>	Thin films
Fischer, Germany	Helmut-Fischer GmbH	<a href="http://www.helmut-fischer.de/de/deutschland/schichtdicke/roentgenfluoreszenz-verfahren/fischerscope-kalibrierstandards-X-ray/">www.helmut-fischer.de/de/deutschland/schichtdicke/roentgenfluoreszenz-verfahren/fischerscope-kalibrierstandards-X-ray/</a>	Layer thickness, metals
Calmetrics, USA	Calmetrics Inc	<a href="http://calmetricsinc.com/#">http://calmetricsinc.com/#</a>	Layer thickness

### B.2.3 Polymer Standards

Issuer/country	Acronym of the reference set	Link to the corresponding catalog	Polymer matrix
Analytical Reference Material, Int. Corp., USA	ARMI	<a href="http://www.armi.com">www.armi.com</a>	PE – polyethylene PVC – polyvinyl chloride
Institute for Reference Materials and Measurement, Europ. Union	ERM	<a href="https://crm.jrc.ec.europa.eu/">https://crm.jrc.ec.europa.eu/</a>	PE – polyethylene
Japan Society for Analytical Chemistry, Japan	JSAC	<a href="http://www.jsac.jp/english-page/">www.jsac.jp/english-page/</a>	ABS – acrylonitrile butadiene styrene PVC – polyvinyl chloride
DSM, Netherlands	ADPOL, TOXEL, RoHS	<a href="http://www.panalytical.com">www.panalytical.com</a>	LDPE – low density polyethylene PE – polyethylene PVC – polyvinyl chloride
R.T.Corp., USA	RTC	<a href="http://www.rt-corp.com/products/">http://www.rt-corp.com/products/</a>	PE – polyethylene
Bundesanstalt für Materialforschung, Germany	BAM	<a href="http://www.bam.de">www.bam.de</a>	PE – polyethylene PVC – polyvinyl chloride ABS – acrylonitrile butadiene styrene
Verband der Automobilindustrie, Germany	VDA	<a href="http://www.vda.de/en">www.vda.de/en</a>	PE – polyethylene

### B.2.4 High Purity Materials

Supplier	Name	Web-address
AA, USA	Alfa Aesar (high purity reagents)	<a href="http://www.alfa.com">www.alfa.com</a>
AE, USA	American Elements (high purity reagents)	<a href="http://www.americanelements.com">www.americanelements.com</a>
Sigma-Aldrich, USA	Sigma-Aldrich Corp. (now Merck)	<a href="http://www.sigmaaldrich.com">www.sigmaaldrich.com</a>
Wirsam, South Africa	Wirsam Scientific & Precision Equipment Ltd.	<a href="http://www.wirsam.com">www.wirsam.com</a>
Goodfellow	Goodfellow GmbH	<a href="http://www.goodfellow.com">http://www.goodfellow.com</a>

## B.2.5 Precious Metal Alloys

Supplier	Name	Web-address
Fluxana GmbH	Fluxana GmbH	www.fluxana.de
Fischer, Germany	Helmut-Fischer GmbH	www.helmut-fischer.de/de/deutschland/ schichtdicke/roentgenfluoreszenz-verfahren/ fischerscope-kalibrierstandards-X-ray/
Goodfellow	Goodfellow GmbH	www.goodfellow.com
Valcambi	Valcambi SA	www.valcambi.com

## B.3 Important Websites

### B.3.1 Information About X-Ray Analytics and Fundamental Parameters

Website	Information
www.exsa.hu	General information about X-ray fluorescence
<a href="http://www.csrri.iit.edu/periodic-table.html">http://www.csrri.iit.edu/periodic-table.html</a>	Line energies, jump ratios, and fluorescence yield for all elements
<a href="http://physics.nist.gov/PhysRefData/contents.html">http://physics.nist.gov/PhysRefData/contents.html</a>	Information about element data for a wide energy range
<a href="http://xdb.lbl.gov/">http://xdb.lbl.gov/</a>	Compilation of X-ray data
<a href="http://ftp.esrf.fr/pub/scisoft/xraylib/">http://ftp.esrf.fr/pub/scisoft/xraylib/</a>	Interaction cross sections for X-ray
<a href="http://physics.nist.gov/asd">http://physics.nist.gov/asd</a>	Fundamental parameters
<a href="https://github.com/tschoonj/xraylib">https://github.com/tschoonj/xraylib</a>	Fundamental parameters and functions for their calculation
<a href="https://github.com/tschoonj/xmimsim">https://github.com/tschoonj/xmimsim</a>	Monte Carlo algorithm for calculation of X-ray transport phenomena
<a href="http://pymca.sourceforge.net/">http://pymca.sourceforge.net/</a>	Free share program for spectra evaluation and quantification with different algorithms

### B.3.2 Information About Reference Materials

Web page	Materials
<a href="http://www.ipt.br/nmr.htm">http://www.ipt.br/nmr.htm</a>	Metals, minerals, geological materials
<a href="http://www.comar.bam.de/home/login.php">http://www.comar.bam.de/home/login.php</a>	All
<a href="http://www.helmut-fischer.de/de/deutschland/schichtdicke/roentgenfluoreszenz-verfahren/fischerscope-kalibrierstandards-X-ray/">http://www.helmut-fischer.de/de/deutschland/schichtdicke/roentgenfluoreszenz-verfahren/fischerscope-kalibrierstandards-X-ray/</a>	Layers
<a href="http://www.scpscience.com/en/corporate">http://www.scpscience.com/en/corporate</a>	Sample preparation, pure materials, solutions
<a href="http://www.ncsstandard.com/">http://www.ncsstandard.com/</a>	Metals, geological materials, coal, slag, environmental materials
<a href="https://ec.europa.eu/jrc/en/reference-materials/catalogue">https://ec.europa.eu/jrc/en/reference-materials/catalogue</a>	Metals, geological material, coal, slag, environmental material
<a href="https://unit.aist.go.jp/nmij/english/service/database">https://unit.aist.go.jp/nmij/english/service/database</a>	Metals, geological material, coal, slag, environmental material
<a href="http://www.mintek.co.za/technical-divisions/analytical-services-asd">http://www.mintek.co.za/technical-divisions/analytical-services-asd</a>	Metals, geological material, coal, slag
<a href="http://www.basrid.co.uk/">http://www.basrid.co.uk/</a>	Metals, geological material
<a href="http://www.nist.gov/srm/index.cfm">http://www.nist.gov/srm/index.cfm</a>	Metals, geological material, coal, slag, environmental material, pure materials, food, cement
<a href="http://www.brammerstandard.com/">http://www.brammerstandard.com/</a>	Metals
<a href="http://calmetricsinc.com/#">http://calmetricsinc.com/#</a>	Layers
<a href="https://fluxana.de/produkte/referenzmaterialien">https://fluxana.de/produkte/referenzmaterialien</a>	Metals, geological material, coal, slag, environmental material
<a href="https://www.fh-muenster.de/fb1/laboratorien/ia/instrumentelle_analytik_php?p=7,6">https://www.fh-muenster.de/fb1/laboratorien/ia/instrumentelle_analytik_php?p=7,6</a>	Polymers
<a href="http://gorem.mpch-mainz.gwdg.de">http://gorem.mpch-mainz.gwdg.de</a>	Information about geological references

### B.3.3 Scientific Journals

Journal	Web page
X-Ray Spectrometry	<a href="http://onlinelibrary.wiley.com/journal/10974539">onlinelibrary.wiley.com/journal/10974539</a>
Spectrochimica Acta Part B: Atomic Spectroscopy	<a href="http://www.sciencedirect.com/science/journal/05848547">www.sciencedirect.com/science/journal/05848547</a>
Radiation Physics and Chemistry	<a href="http://www.sciencedirect.com/science/journal/0969806X">www.sciencedirect.com/science/journal/0969806X</a>
Journal of Analytical Atomic Spectrometry	<a href="http://www.rsc.org">www.rsc.org</a> ⇒ Journals: JAAS
Nuclear Instruments and Methods in Physics Research A: Accelerators, Spectrometers, Detectors and Associated Equipment	<a href="http://www.sciencedirect.com/science/journal/01689002">www.sciencedirect.com/science/journal/01689002</a>
Atomic Data and Nuclear Data Tables	<a href="http://www.sciencedirect.com/science/journal/0092640X">www.sciencedirect.com/science/journal/0092640X</a>
Journal of Physical and Chemical Reference Data	<a href="https://aip.scitation.org/journal/jpr">https://aip.scitation.org/journal/jpr</a>
Review of Scientific Instruments	<a href="https://aip.scitation.org/journal/rsi">https://aip.scitation.org/journal/rsi</a>
Advances in X-Ray Analysis	<a href="http://www.icdd.com/axa-allvolumes/">http://www.icdd.com/axa-allvolumes/</a>
Journal of Applied Physics	<a href="https://aip.scitation.org/journal/jap">https://aip.scitation.org/journal/jap</a>

## B.4 Laws and Acts, Which Are Important for X-Ray Fluorescence

### B.4.1 Radiation Protection

AtG, Atomgesetz (1985). *Gesetz über die friedliche Verwendung der Kernenergie un den Schutz gegen ihre Gefahren. s.l.: Bundesgesetzblatt I, Nr. 41, S. 1565.*

RöV (2003). *Verordnung über den Schutz vor Schäden durch Röntgenstrahlen; BGBl Nr.17, S. 604.*

StrlSchV (2001) *Verordnung über den Schutz vor Schäden durch ionisierende Strahlung in Deutschland; BgBl Nr.38, 1714.*

ASTM-E\_1167-15 (2015). *Standard Guide for Radiation Protection Program for Decommissioning Operations.*

ASTM-F\_3094-14 (2014). *Standard Test Method for Determining Protection Provided by X-ray Shielding Garments Used in Medical X-ray Fluoroscopy from Sources of Scattered X-Rays.*

ASTM-F\_2547-06 (2006). *Standard Test Method for Determining the Attenuation Properties in a Primary X-ray Beam of Materials Used to Protect Against Radiation Generated During the Use of X-ray Equipment.*

ASTM-ISO/ASTM-52628-13 (2013). *Standard Practice for Dosimetry in Radiation Processing.*

## B.4.2 Regulations for Environmental Control

AbfklärV (2018). Klärschlammverordnung vom 15. April 1992 (BGBl. I S. 912). [www.gesetze-im-internet.de/bundesrecht/abfkl\\_rv\\_1992/gesamt.pdf](http://www.gesetze-im-internet.de/bundesrecht/abfkl_rv_1992/gesamt.pdf) (accessed 17 April 2020).

EU-2002/32/EG (2002). *Richtlinie über unerwünschte Stoffe in der Tierernährung. s.l.: Europäisches Parlament.*

ICH Guideline, Q3D on elemental impurities (2016). [ema.europa.eu/docs/en\\_GB/document\\_library/Scientific\\_guideline/2015/01/WC500180284.pdf](http://ema.europa.eu/docs/en_GB/document_library/Scientific_guideline/2015/01/WC500180284.pdf) (accessed 17 April 2020).

TrinkwV\_2001 (2001). *Verordnung über die Qualität von Wasser für den menschlichen Gebrauch.*

EPA\_10-3.3 (1999). *Compendium of Methods for the Determination of Inorganic Compounds in Ambient Air.*

## B.4.3 Regulations for Performing Analysis

ISO/IEC Guide, 98-3 (2008). *Uncertainty of Measurement (Part 3), Guide to the expression of uncertainty in measurement (GUM:1995).*

JCGM\_100:2008 (2008). *Evaluation of measurement data - Guide to the expression of uncertainty in Measurement.*

DIN-EN-ISO/IEC\_17025 (2005). *Allgemeine Anforderungen an die Kompetenz von Prüf- und Kalibrierlaboratorien*, Beuth-Verlag, Berlin.

DIN-EN-ISO\_9001 (2015-11). *Qualitätsmanagementsysteme*, Beuth-Verlag, Berlin.

DIN-EN-45001 (1997-06). *Allgemeine Anforderungen an die Kompetenz von Prüf- und Kalibrierlaboratorien – Dokument zurückgezogen*, Beuth-Verlag, Berlin.

ISO Guide 25 (1990). *General requirements for the competence of calibration and testing laboratories.*

## B.4.4 Use of X-ray Fluorescence for the Chemical Analysis

### B.4.4.1 General Regulations

ASTM-E\_1172-16 (2016) *Standard Practice for Describing and Specifying a Wavelength-dispersive X-Ray Spectrometer.*

ASTM-E\_1361 (2014). *Standard Guide for Correction of Inter-element Effects in X-Ray Spectrometric Analysis.*

ASTM-E\_1621-13 (2013). *Standard Guide for Elemental Analysis by Wavelength-dispersive X-Ray Spectrometry.*

DIN\_32633 (2013-05). *Chemische Analytik - Verfahren der Standardaddition - Verfahren, Auswertung*, Beuth-Verlag, Berlin.

DIN\_32645 (2008-11). *Chemische Analytik - Nachweis-, Erfassungs- und Bestimmungsgrenze unter Wiederholbedingungen - Begriffe, Verfahren, Auswertung*, Beuth-Verlag, Berlin.

DIN\_5030-1 (1985-06). *Spektrale Strahlungsmessung; Begriffe, Größen, Kennzahlen*, Beuth-Verlag, Berlin.

- DIN\_5030-2 (1982-09). *Spektrale Strahlungsmessung; Strahler für spektrale Strahlungsmessungen; Auswahlkriterien.*
- DIN\_5030-3 (1984-12). *Spektrale Strahlungsmessung; Spektrale Aussonderung; Begriffe und Kennzeichnungsmerkmale,* Beuth-Verlag, Berlin.
- DIN\_5030-5 (1987-12). *Spektrale Strahlungsmessung; Physikalische Empfänger für spektrale Strahlungsmessungen; Begriffe, Kenngrößen, Auswahlkriterien,* Beuth-Verlag, Berlin.
- DIN\_51003 (2004-05). *Totalreflektions-Röntgenfluoreszenz-Analyse (TXRF) - Allgemeine Grundlagen und Begriffe,* Beuth-Verlag, Berlin.
- DIN\_51418-1 (2008-08). *Röntgenspektralanalyse - Röntgenemissions- und Röntgenfluoreszenz-Analyse (RFA) - Teil 1: Allgemeine Begriffe und Grundlagen,* Beuth-Verlag, Berlin.
- DIN\_51418-2 (2014-06). *Röntgenspektralanalyse - Röntgenemissions- und Röntgenfluoreszenz-Analyse (RFA) - Teil 2: Begriffe und Grundlagen zur Messung, Kalibrierung und Auswertung,* Beuth-Verlag, Berlin.
- DIN-EN-ISO/IEC\_17025 (2005). *Allgemeine Anforderungen an die Kompetenz von Prüf- und Kalibrierlaboratorien,* Beuth-Verlag.
- DIN-EN-ISO\_21747 (2007). *Statistische Verfahren - Prozessleistungs- und Prozessfähigkeitskenngrößen für kontinuierliche Qualitätsmerkmale,* Beuth-Verlag, Berlin.

#### **B.4.4.2 Analysis of Minerals**

- AS\_2503.6 (2007). *Australian standard: Refractories and refractory materials – Chemical analysis Part 6: Refractories, refractory mortars and silicate materials – Determination of major and minor elements – Wavelength-dispersive X-ray fluorescence spectrometry using Lithium-borate fusion.*
- ASTM-C\_114 (2015). *Standard Test Methods for Chemical Analysis of Hydraulic Cement.*
- ASTM-C\_1255-11 (2011). *Standard Test Method for Analysis of Uranium and Thorium in Soils by Energy-dispersive X-Ray Fluorescence Spectroscopy.*
- ASTM-C\_1605-04 (2014). *Standard Test Methods for Chemical Analysis of Ceramic Whiteware Materials Using Wavelength-dispersive X-Ray Fluorescence Spectrometry.*
- ASTM-E\_2119-16 (2016). *Standard Practice for Quality Systems for Conducting In Situ Measurements of Lead Content in Paint or Other Coatings Using Field-Portable X-Ray Fluorescence (XRF) Devices.*
- ASTM-E\_2926-17 (2017). *Standard Test Method for Forensic Comparison of Glass Using Micro X-ray Fluorescence ( $\mu$ -XRF) Spectrometry.*
- ASTM-F\_3078-15 (2015). *Standard method for Identification and Quantification of Lead in Paint and Similar Coating Materials using Energy-dispersive X-Ray Fluorescence Spectrometry.*
- ASTM-D\_4764-01 (2016). *Standard Test Method for Determination by X-ray Fluorescence Spectroscopy of Titanium Dioxide Content in Paint.*
- ASTM-D\_8064-16 (2016). *Standard test method for Elemental Analysis of Soil and Solid Waste by Monochromatic Energy-dispersive X-ray Fluorescence Spectrometry Using multiple monochromatic Excitation beams.*

- DIN\_4021 (1990). *Aufschluß durch Schürfe und Bohrungen sowie Entnahme von Proben*, Beuth-Verlag, Berlin.
- DIN\_51001 (2003-08). *Prüfung oxidischer Roh- und Werkstoffe - Allgemeine Arbeitsgrundlagen zur RFA*, Beuth-Verlag, Berlin.
- DIN\_51010-2 (1987-08). *Prüfung keramischer Roh- und Werkstoffe; Ungeformte feuerfeste Erzeugnisse; Herstellung von Probekörpern*, Beuth-Verlag, Berlin.
- DIN\_51081 (1996-07). *Prüfung oxidischer Roh- und Werkstoffe; Massenveränderungen beim Glühen*, Beuth-Verlag, Berlin.
- DIN\_66165-1 und -2 (1987). *Partikelgrößenanalyse; Grundlagen und Durchführung*, Beuth-Verlag, Berlin.
- DIN-EN\_15309 (2007-08). *Charakterisierung von Abfällen und Böden, Bestimmung der elementaren Zusammensetzung durch RFA*, Beuth-Verlag, Berlin.
- DIN-EN-ISO\_12677 (2013-02). *Chemische Analyse von feuerfesten Erzeugnissen durch RFA – Schmelzaufschlussverfahren*, Beuth-Verlag, Berlin.
- DIN-EN\_955-5 (1955). *Chemische Analyse von feuerfesten Erzeugnissen. Teil 5: Röntgenfluoreszenzanalyse von Schmelztabletten*, Beuth-Verlag, Berlin.
- ISO\_9516-1 (2003). *Iron Ores – Determination of various elements by X-ray fluorescence spectrometry, Part 1: Comprehensive procedure*, Beuth-Verlag, Berlin.

#### **B.4.4.3 Analysis of Oils, Liquid Fuels, Grease**

- ASTM-D\_2622–08 (2010). *Standard Test Method for Sulfur in Petroleum Products by Wavelength-dispersive X-ray Fluorescence Spectrometry*.
- ASTM-D\_4294-16 (2016). *Standard Test Method for Sulfur in Petroleum and Petroleum Products by Energy-dispersive X-ray Fluorescence Spectrometry*.
- ASTM-D\_4927 – 15 (2015). *Standard Test Methods for Elemental Analysis of Lubricant and Additive Components—Barium, Calcium, Phosphorus, Sulfur, and Zinc by Wavelength-Dispersive X-ray Fluorescence Spectrometry*.
- ASTM-D\_5059-14 (2014). *Standard Test Method for Lead in Gasoline by X-ray Fluorescence Spectrometry*.
- ASTM-D\_5839-15 (2015). *Standard Test Method for Trace Element Analysis of Hazardous Waste Fuel by Energy-Dispersive X-Ray Fluorescence Spectrometry*.
- ASTM-D\_6052 (2008). *Standard Test Method for Preparation and Elemental Analysis of Liquid Hazardous Waste by Energy-Dispersive X-ray Fluorescence*.
- ASTM D6247-10 (2010). *Standard Test Method for Determination of Elemental Content of Polyolefins by Wavelength-dispersive X-ray Fluorescence Spectrometry*.
- ASTM-D\_6334-12 (2012). *Standard Test Method for Sulfur in Gasoline by Wavelength-dispersive X-ray Fluorescence Spectrometry*.
- ASTM-D\_6376-10 (2010). *Standard Test Method for Trace Metals in Petroleum Coke by Wavelength-dispersive X-ray Fluorescence Spectrometry*.
- ASTM-D\_6443 (2014). *Standard Test Method for Determination of Calcium, Chlorine, Copper, Magnesium, Phosphorus, Sulfur, and Zinc in Unused Lubricating Oils and Additives by Wavelength-dispersive X-ray Fluorescence Spectrometry (Mathematical Correction Procedure)*.
- ASTM-D\_6481-14 (2014). *Standard Test Method for Determination of Phosphorus, Sulfur, Calcium, and Zinc in Lubrication Oils by Energy-dispersive X-ray Fluorescence Spectrometry*.



- ASTM-D\_7212-13 (2013). *Standard method for Low Sulfur in automotive Fuels by Energy-dispersive X-Ray Fluorescence Spectrometry Using a Low Background Proportional Counter.*
- ASTM-D\_7343-12 (2017). *Standard Practice for Optimization, Sample handling, Calibration, and Validation of X-Ray Fluorescence Spectrometry Methods for Elemental Analysis of Petroleum and Petroleum Products.*
- ASTM-D\_7455-14 (2014). *Standard Practice for Sample Preparation of Petroleum and Lubricant Products for Elemental Analysis.*
- ASTM-D\_7751 (2011). *Standard Test Method for Determination of Additive Elements in Lubricating Oils by EDXRF Analysis.*
- DIN\_51750-1 (1990-12). *Prüfung von Mineralölen; Probenahme; Allgemeines, Beuth-Verlag, Berlin.*
- DIN\_51750-2 (1990-12). *Prüfung von Mineralölen; Probenahme; Flüssige Stoffe, Beuth-Verlag, Berlin.*
- DIN\_51750-3 (1991-02). *Prüfung von Mineralölen; Probenahme; Salbenartig-konsistente und feste Stoffe, Beuth-Verlag, Berlin.*
- DIN\_51363 (2003-02). *Prüfung von Mineralölen - Bestimmung des P-Gehaltes von Schmierölen und Schmierölwerkstoffen, Teil 2: RFA, Beuth-Verlag, Berlin.*
- DIN\_51390 (1997-11). *Prüfung von Mineralölerzeugnissen - Bestimmung der Si-Gehaltes, Teil 2: RFA, Beuth-Verlag, Berlin.*
- DIN\_51391 (1994-03). *Prüfung von Schmierstoffen, bestimmung des Gehaltes an additivelementen RFA, Beuth-Verlag, Berlin.*
- DIN\_51396 (2008-11). *Prüfung von Schmierstoffen - Bestimmung von Abriebelementen, Teil 2: RFA, Beuth-Verlag, Berlin.*
- DIN-51399 (2010-01). *Prüfung von Schmierölen - Bestimmung des Elementgehalte aus Additiven, Abrieb und sonstigen Verunreinigungen, Teil 2: RFA, Beuth-Verlag, Berlin.*
- DIN-51440 (2003-03). *Prüfung von Ottokraftstoffen - Bestimmung des P-Gehaltes Teil 1: RFA, Beuth-Verlag, Berlin.*
- DIN-51577 (1994-02). *Prüfung von Kohlenwasserstoffen und ähnlichen Erzeugnissen, Bestimmung des Cl- und Br-Gehaltes EDRFA, Beuth-Verlag, Berlin.*
- DIN-51769-10 (2013-04). *Mineralölerzeugnisse - Bestimmung niedriger Pb-Gehalte in Kraftstoffen, Teil 10: RFA, Beuth-Verlag, Berlin.*
- DIN-51769-6 (1990-11). *Prüfung von Mineralölerzeugnissen, Bestimmung de Pb-Gehaltes von Ottokraftstoffen mit einer Massenkonzentration über 25 mg/l RFA, Beuth-Verlag, Berlin.*
- DIN-51790-07 (2002-01). *Prüfung flüssiger Brennstoffe - Bestimmung des V- und Ni-Gehaltes, Teil 7: RFA mit FP-Modellen, Beuth-Verlag, Berlin.*
- DIN-51829 (2013-03). *Mineralölerzeugnisse - Bestimmung von Additiv- und Abriebelementen in Schmierfetten, RFA, Beuth-Verlag, Berlin.*
- DIN-EN\_13723 (2002-10). *Mineralölerzeugnisse - Bestimmung niedriger Pb-Gehalte in Kraftstoffen, RFA, Beuth-Verlag, Berlin.*
- DIN-EN-ISO\_14596 (2007-12). *Mineralölerzeugnisse - Bestimmung des S-Gehalte, RFA, Beuth-Verlag, Berlin.*
- DIN-EN-ISO\_14597 (1999-03). *Mineralölerzeugnisse - Bestimmung des V- und Ni-Gehaltes, WDRFA, Beuth-Verlag, Berlin.*

DIN-EN\_15485 (2007-11). *Ethanol zur Verwendung als Blendkomponente in Ottokraftstoff, Pb-Komponente in Ottokraftstoff - Bestimmung des S-Gehaltes mit RFA*, Beuth-Verlag, Berlin.

DIN-EN-ISO 20847 (2004-07). *Mineralölerzeugnisse - Bestimmung des S-Gehaltes von Kraftstoffen für Kraftfahrzeuge – EDRFA*, Beuth-Verlag, Berlin.

DIN-EN-ISO\_20884 (2011-07). *Mineralölerzeugnisse - Bestimmung des S-Gehaltes von Kraftstoffen für Kraftfahrzeuge – WDRFA*, Beuth-Verlag, Berlin.

DIN-EN-ISO\_3170 (2004-06). *Flüssige Mineralölerzeugnisse - Manuelle Probenahme*, Beuth-Verlag, Berlin.

DIN-EN-ISO\_4259 (2006-10). *Mineralölerzeugnisse - Bestimmung und Anwendung der Werte für die Präzision von Prüfverfahren*, Beuth-Verlag, Berlin.

DIN-EN-ISO\_8754 (2003-12). *Mineralölerzeugnisse - Bestimmung des S-Gehaltes, EDRFA*, Beuth-Verlag, Berlin.

ISO\_14596 (2007). *Petroleum products: Determination of Sulfur content – Wavelength-dispersive X-Ray spectrometry*, Beuth-Verlag, Berlin.

ISO\_14597 (1997). *Petroleum products: Determination of Vanadium and Nickel content – Wavelength-dispersive X-Ray spectrometry*, Beuth-Verlag, Berlin.

ISO\_20884 (2011). *Petroleum products: Determination of Sulfur content of automotive fuels – Wavelength-dispersive X-Ray spectrometry*, Beuth-Verlag, Berlin.

#### **B.4.4.4 Analysis of Solid Fuels**

DIN-51700 (2010-07). *Prüfung fester Brennstoffe - Allgemeines und Übersicht über Prüfverfahren*, Beuth-Verlag, Berlin.

DIN\_51701-2 (2006-09). *Prüfung fester Brennstoffe - Probenahme und Probenvorbereitung - Teil 2: Durchführung der Probenahme*, Beuth-Verlag, Berlin.

DIN\_51701-3 (2006-09). *Prüfung fester Brennstoffe - Probenahme und Probenvorbereitung - Teil 3: Durchführung der Probenvorbereitung*, Beuth-Verlag, Berlin.

DIN\_51701-4 (2006-09). *Prüfung fester Brennstoffe - Probenahme und Probenvorbereitung - Teil 4: Geräte*, Beuth-Verlag, Berlin.

DIN\_51718-06 (2002). *Prüfung fester Brennstoffe - Bestimmung des Wassergehaltes und der Analysenfeuchtigkeit*, Beuth-Verlag, Berlin.

DIN\_51719-07 (1997). *Prüfung fester Brennstoffe - Bestimmung des Aschegehaltes*, Beuth-Verlag, Berlin.

DIN\_51720-03 (2001). *Prüfung fester Brennstoffe - Bestimmung des Gehaltes an flüchtigen Bestandteilen*, Beuth-Verlag, Berlin.

DIN\_51729-10 (2011-04). *Prüfung fester Brennstoffe - Bestimmung der chemischen Zusammensetzung von Brennstoffasche*, Beuth-Verlag, Berlin.

DIN\_51729-10 (2011-04). *Prüfung fester Brennstoffe - Bestimmung der chemischen Zusammensetzung von Brennstoffasche, Teil 10: RFA*, Beuth-Verlag, Berlin.

DIN-EN-ISO\_16967 (2004-07). *Feste Biobrennstoffe - Bestimmung von Hauptelementen - Al, Ca, Fe, Mg, P, K, Si, Na und Ti*, Beuth-Verlag, Berlin.

DIN-EN-ISO\_4257 (2002-03). *Flüssiggase – Probenahme*, Beuth-Verlag, Berlin.

DIN-ISO\_12980 (2006-05). *Kohlenstoffmaterialien für die Herstellung von Al, Grünkoks und kalzinierter Koks für Elektroden*, WDRFA, Beuth-Verlag, Berlin.

RAL-GZ-724 (2012). *Sekundärrohstoffe - Gütesicherung*. Beuth-Verlag, Berlin.

**B.4.4.5 Coating Analysis**

ASTM-B\_487-85 (2013). *Standard Test Method for Measurement of Metal and Oxide Coating Thickness by Microscopical Examination of Cross Section.*

ASTM-B\_568-98 (2014). *Standard Test Method for Measurement of Coating Thickness by X-Ray Spectrometry.*

ASTM-B-659 (2014). *Standard Guide for Measuring Thickness of Metallic and Inorganic Coatings.*

ASTM-D\_7639-10 (2014). *Standard Test Method for Determination of Zirconium Treatment Weight or Thickness on Metal Substrates by X-Ray Fluorescence.*

DIN-EN\_1071-4 (2006-05). *Hochleistungskeramik - Verfahren zur Prüfung keramischer Schichten, Teil 4: Bestimmung der Zusammensetzung durch ESMA,* Beuth-Verlag, Berlin.

DIN-EN-ISO\_1513 (2010-10). *Beschichtungsstoffe - Prüfung und Vorbereitung von Proben,* Beuth-Verlag, Berlin.

DIN-EN-ISO\_15528 (2013-12). *Beschichtungsstoffe und Rohstoffe für Beschichtungsstoffe – Probenahme,* Beuth-Verlag, Berlin.

DIN-EN-ISO\_3497 (2001-12). *Metallische Schichten - Schichtdickenmessung – RFA,* Beuth-Verlag, Berlin.

**B.4.4.6 Metallurgy**

ASTM-B\_890-07 (2012). *Standard Test Method for Determination of Metallic Constituents of Tungsten Alloys and Tungsten Hard-metals by X-Ray Fluorescence Spectrometry.*

ASTM-E\_322-12 (2012). *Standard Test Method for Analysis of Low-Alloy Steels and Cast Irons by Wavelength-dispersive X-Ray Fluorescence Spectrometry.*

ASTM-E\_539-11 (2011). *Standard Test Method for Analysis of Titanium Alloys by X-Ray Fluorescence Spectrometry.*

ASTM-E\_572-13 (2013). *Standard Test Method for Analysis of Stainless and Alloy Steels by Wavelength-dispersive X-Ray Fluorescence Spectrometry.*

ASTM-E\_1085-16 (2016). *Standard Test Method for Analysis of Low-Alloy Steels by Wavelength-dispersive X-Ray Fluorescence Spectrometry.*

ASTM-E\_2465-13 (2013). *Standard Test Method for Analysis of Ni-Based Alloys by Wavelength X-Ray Fluorescence Spectrometry.*

DIN-EN\_10315 (2006-10). *Standardverfahren zur Analyse von hochlegiertem Stahl mittels RFA unter Anwendung eines Vergleichs-Korrekturverfahrens,* Beuth-Verlag, Berlin.

DIN-EN\_15063-1 (2013-11). *Cu und Cu-Legierungen - Bestimmung von Hauptbestandteilen und Verunreinigungen durch RFA, Teil 1: Anleitung für das Routineverfahren,* Beuth-Verlag, Berlin.

DIN-ISO\_4503 (1991-07). *Hartmetalle, Bestimmung des Gehaltes metallischer Elemente durch RFA in fester Lösung,* Beuth-Verlag, Berlin.

DIN-ISO\_4883 (1991-06). *Hartmetalle, Bestimmung des Gehaltes metallischer Elemente durch RFA, Lösungsverfahren,* Beuth-Verlag, Berlin.

DIN-EN-15063-2 (2007-01). *Kupfer und Kupferlegierungen - Bestimmung von Hauptbestandteilen und Verunreinigungen durch wellenlängndispersive Röntgenfluoreszenz (RFA): Routineverfahren.* Berlin, Beuth-Verlag.

DIN-EN-10020 (2000-07). *Begriffsbestimmungen für die Einteilung der Stähle*, Beuth-Verlag, Berlin.

EN-573\_3-2013-12 (2013). *Aluminium und Aluminiumlegierungen - Chemische Zusammensetzung und Form von Halbzeug - Teil 3: Chemische Zusammensetzung und Erzeugnisformen*, Beuth-Verlag, Berlin.

#### **B.4.4.7 Analysis of Electronic Components**

ASTM-F\_2617-15 (2017). *Standard Test Method for Identification and Quantification of Chromium, Bromine, Cadmium, Mercury, and Lead in Polymeric Material Using Energy-dispersive X-ray Spectrometry*.

ASTM-D\_7611/D7611M-13 (2013). *Standard Practice for Coding Plastic Manufactured Articles for Resin Identification*.

DIN-EN\_23270 (1991-09). *Lacke, Anstrichstoffe und deren Rohstoffe; Temperaturen und Luftfeuchten für Konditionierung und Prüfung*, Beuth-Verlag, Berlin.

DIN-EN\_62321-3-1 (2014-10). *Verfahren zur Bestimmung von bestimmten Substanzen in Produkten der Elektrotechnik, Teil 3-1: Screening Pb, Cd, Hg, Gesamt-Cr und Gesamt-Br durch RFA*, Beuth-Verlag, Berlin.

DIN-IEC\_62495 (2011-12). *Strahlungsmessgeräte - Tragbare Röntgenfluoreszenz-Analysengeräte mit Kleinströntgenrohren*, Beuth-Verlag, Berlin.

Directive 2002/95/EC (2003-01). *Restriction of the use of Hazardous Substances in Electrical and Electronic Equipment*.

Directive 2002/96/EC (2003-01). *Waste Electrical and Electronic Equipment*.

Directive 2000/53/EC (2000-09). *End of Life Vehicles*.

## References

- AbfklärV (2016). Klärschlammverordnung vom 15. April 1992 (BGBl. I S. 912), letzte Änderung von 2015 [Online]. [www.gesetze-im-internet.de/bundesrecht/abfkl\\_rv\\_1992/gesamt.pdf](http://www.gesetze-im-internet.de/bundesrecht/abfkl_rv_1992/gesamt.pdf) (accessed February 2016).
- Aiginger, H. and Wobrauschek, P. (1974). A method for quantitative X-ray fluorescence analysis in the nanogram region. *Nucl. Instrum. Methods* 114: 157.
- Alfeld, M., Haschke, M., Dik, J. et al. (2013). A mobile instrument for in situ scanning macro-XRF investigation of historical paintings. *J. Anal. At. Spectrom.* 3: 760.
- AltholzV (2002). Verordnung über Anforderungen an die Verwertung und Beseitigung von Altholz. Bundesministeriums der Justiz und für Verbraucherschutz.
- Anklamm, L. (2014). *Ein hocheffizientes von-Hamos-Spektrometer für Röntgenemissionsspektroskopie im Labor*. TU Berlin.
- ApplBrief-Airborne\_particles (n.d.). Elemental Analysis of Airborne Particles Using ED-XRF. Spectro.
- ApplBrief-Animal-feed (n.d.). At-Line Analysis of Lead in Animal Feed Using EDXRF-Spectroscopy. Spectro Analytical Instruments GmbH.
- ApplBrief-Geology (2015). Analyzing Trace Elements in Pressed Pellets of Geological Materials Using ED-XRF. Kleve: Spectro Analytical Instruments GmbH.
- ApplNote-Bauxite (n.d.). Analysis of major and minor elements in Bauxite samples prepared as fused beads. Panalytical.
- ApplNote-Cereals (n.d.). Analysis of infant cereals. Panalytical.
- ApplNote-Coal (n.d.). Analysis of inorganic major and minor compounds in unashed coals samples prepared as pressed pellet. Panalytical.
- ApplNote-EDXRF\_Cement\_beads (n.d.). Analysis of major and minor elements of cement fused beads. Panalytical.
- ApplNote-EDXRF-Cast\_Iron (n.d.). Carbon analysis in Cast iron. Panalytical.
- ApplNote-EDXRF-Cement\_Pressed\_Pellets (n.d.). Analysis of major and minor elements in cement pressed powders. Panalytical.
- ApplNote-EDXRF-Iron\_ore (n.d.). Analysis of Iron ore samples prepared as fused beads. Panalytical.
- ApplNote-EDXRF-Mn-Ore (n.d.). Analysis of Manganese ore samples prepared as fused beads. Panalytical.
- ApplNote-EDXRF-Mn-ore\_Pellets (n.d.). Analysis of Manganese samples prepared as pressed pellets. Panalytical.

- ApplNote-EDXRF-Ni\_ore\_Pellets (n.d.). Analysis of Nickel ore samples prepared as pressed pellets. Panalytical.
- ApplNote-EDXRF-Ni-ore\_Beads (n.d.). Analysis of Nickel ore samples prepared as fused beads. Panalytical.
- ApplNote-Ferrosilicon (n.d.). An analysis of major and minor elements in Ferrosilicon. Panalytical.
- ApplNote-Rare\_earth\_elements (n.d.). Analysis of Cd, Sn, Sb, Cs, Ba, La, Ce and Nd in rocks and soils - improved detection limits using K-series lines. Panalytical.
- ApplNote-Slags\_Pellets (n.d.). Quick and precise analysis of major and minor elements of slag samples prepared as pressed pellets. Panalytical.
- ApplNote-WDXRF\_Cement (n.d.). Cement analysis using CEMOXI standards. Panalytical.
- ApplNote-WDXRF-Al-alloy (n.d.). Wide range calibration for Al-alloy. Panalytical.
- ApplNote-WDXRF-Cast\_Iron (n.d.). Analysis of cast iron. Panalytical.
- ApplNote-WDXRF-Low-Steel (n.d.). Analysis of low alloy steel. Panalytical.
- ApplNote-WDXRF-Stainless\_Steel (n.d.). Analysis of stainless steel. Panalytical.
- ApplNote-WDXRF-Tool\_Steel (n.d.). Analysis of tool steel. Panalytical.
- ASTM-1926-13 (n.d.). *Standard Test Method for Forensic Comparison of Pieces of Glass Using  $\mu$ -XRF*.
- ASTM-6376\_110 (2010). *Standard Test Method for Determination of Trace Metals in Petroleum Coke by Wavelength Dispersive X-Ray Fluorescence Spectroscopy*. ASTM International, West Conshohocken, PA. [www.astm.org](http://www.astm.org).
- ASTM-B\_487-85 Standard Test Method for Measurement of Metal and Oxide Coating Thickness by Microscopical Examination of Cross Section 2013.
- ASTM-B\_568-98 (2014). *Standard Test Method for Measurement of Coating Thickness by X-Ray Spectrometry*.
- ASTM-B\_890-07 (2012). *Standard Test Method for Determination of Metallic Constituents of Tungsten Alloys and Tungsten Hardmetals by X-Ray Fluorescence Spectrometry*.
- ASTM-C\_114 (2015). *Standard Test Methods for Chemical Analysis of Hydraulic Cement* [Online].
- ASTM-B733-15 (2015). *Standard Specification for Autocatalytic (Electroless) Nickel-Phosphorus Coatings on Metal*.
- ASTM-C\_1255-11 (n.d.). *Standard Test Method for Analysis of Uranium and Thorium in Soils by Energy Dispersive X-Ray Fluorescence Spectroscopy*.
- ASTM-D\_2622-08 (2010). *Standard Test Method for Sulfur in Petroleum Products by Wavelength Dispersive X-Ray Fluorescence Spectrometry*.
- ASTM-D\_3173-17 (2017). *Standard Test Method for Moisture in the Analysis Sample of Coal and Coke*. NIST.
- ASTM-D\_4294-16 (n.d.). *Standard Test Method for Sulfur in Petroleum and Petroleum Products by Energy Dispersive X-Ray Fluorescence Spectrometry*.
- ASTM-D\_4764-01 (2016). *Standard Test Method for Determination by X-Ray Fluorescence Spectroscopy of Titanium Dioxide Content in Paint*.
- ASTM-D\_4927:2015 (n.d.). *Prüf-Elementaranalyse von Schmiermittel- und Zusatzkomponenten - Barium, Calcium, Phosphor, Schwefel und Zink - mittels wellenlängendispersiver Röntgenfluoreszenzspektroskopie*.

- ASTM-D\_5059-14 (2014). *Standard Test Method for Lead in Gasoline by X-Ray Spectroscopy*. ASTM International, West Conshohokocken, PA. [www.astm.org](http://www.astm.org).
- ASTM-D\_5839-15 (n.d.). *Standard Test Method for Trace Element Analysis of Hazardous Waste Fuel by Energy-Dispersive X-Ray Fluorescence Spectrometry*.
- ASTM-D\_6052 (2008). *Standard Test Method for Preparation and Elemental Analysis of Liquid Hazardous Waste by Energy-Dispersive X-Ray Fluorescence*.
- ASTM-D\_6334-12 (2012). *Standard Test Method for Sulfur in Gasoline by Wavelength Dispersive X-Ray Fluorescence*. ASTM International, West Conshohokocken, PA. [www.astm.org](http://www.astm.org).
- ASTM-D\_6443-14 (2010). *Standard Test Method for Determination of Calcium, Chlorine, Copper, Magnesium, Phosphorus, Sulfur, and Zinc in Unused Lubricating Oils and Additives by Wavelength Dispersive X-Ray Wavelength Dispersive (Mathematical Correction Procedure)*. ASTM International, West Conshohokocken, PA. [www.astm.org](http://www.astm.org).
- ASTM-D\_6481:2014 (n.d.). *Standard Test Method for Determination of Phosphorus, Sulfur, Calcium, and Zinc in Lubrication Oils by Energy Dispersive X-Ray Fluorescence Spectroscopy*.
- ASTM-D\_7039-15a (n.d.). *Standard Test Method for Sulfur in Gasoline, Diesel Fuel, Jet Fuel, Kerosine, Biodiesel, Biodiesel Blends, and Gasoline-Ethanol Blends by Monochromatic Wavelength Dispersive X-Ray Fluorescence Spectrometry*.
- ASTM-D-8064-16 (2016). *Standard Test Method for Elemental Analysis of Soil and Solid Waste by Monochromatic Energy Dispersive X-Ray Fluorescence Spectrometry Using Multiple Monochromatic Excitation Beams*. [www.astm.org](http://www.astm.org).
- ASTM-E\_1085-16 (n.d.). *Standard Test Method for Analysis of Low-Alloy Steels by Wavelength Dispersive X-Ray Fluorescence Spectrometry*.
- ASTM-E\_1167-15 (n.d.). *Standard Guide for Radiation Protection Program for Decommissioning Operations*.
- ASTM-E\_2119-16 (n.d.). *Standard Practice for Quality Systems for Conducting In Situ Measurements of Lead Content in Paint or Other Coatings Using Field-Portable X-Ray Fluorescence (XRF) Devices*.
- ASTM-E\_2465-13 (n.d.). *Standard Test Method for Analysis of Ni-Based Alloys by Wavelength X-Ray Fluorescence Spectrometry*.
- ASTM-E\_322-12 (n.d.). *Standard Test Method for Analysis of Low-Alloy Steels and Cast Irons by Wavelength Dispersive X-Ray Fluorescence Spectrometry*.
- ASTM-E\_539-11 (n.d.). *Standard Test Method for Analysis of Titanium Alloys by X-Ray Fluorescence Spectrometry*.
- ASTM-E\_572-13 (n.d.). *Standard Test Method for Analysis of Stainless and Alloy Steels by Wavelength Dispersive X-Ray Fluorescence Spectrometry*.
- ASTM-F\_2617-15 (n.d.). *Standard Test Method for Identification and Quantification of Chromium, Bromine, Cadmium, Mercury, and Lead in Polymeric Material Using Energy Dispersive X-Ray Spectrometry*.
- ASTM-F\_3078-15 (n.d.). *Standard Test Method for Identification and Quantification of Lead in Paint and Similar Coating Materials Using Energy Dispersive X-Ray Fluorescence Spectrometry (EDXRF)*.
- ASTM-F\_963-17 (2013) *Standard Consumer Safety Specification for Toy Safety*.
- AtG and Atomgesetz (1985) *Gesetz über die friedliche Verwendung der Kernenergie und den Schutz gegen ihre Gefahren: Bundesgesetzblatt I, Nr. 41, S. 1565*.

- Banerjee, S. and Olsen, B.G. (1978). Rapid analysis of Chrome ores, Chrome-Magnesia and Magnesia-Chrome materials by XRF. *Appl. Spectrosc.* 32: 376.
- Beckhoff, B., Kanngießer, B., Langhoff, N. et al. (2006). *Handbook of Practical X-Ray Fluorescence Analysis*. Berlin: Springer-Verlag. ISBN-10: 3540286039.
- Beebe, K.R. and Pell, R.J. (1998). *Chemometrics: A Practical Guide*. Wiley.
- Beeghley, H.F. (1949). Determination of aluminium nitride nitrogen in steel. *Anal. Chem.* 21: 1513.
- Bezur, A. and Casadio, F. (2012). The Analysis of Porcelain using handheld and portable XRF spectrometers. In: *Handheld XRF for Art and Archeology* (eds. A.N. Shugar and J. Mass), 249. Leuven: University Press Leuven.
- BGBI., II, Nr. 203/2011 und Nr. 38/2013 (2013). Verordnung des Bundesministers für Gesundheit über die Sicherheit von Spielzeug. *II, Nr. 203/2011 und Nr. 38/2013*.
- Bianchi, U., Falk, H.; Heckel, J et al. (2002). Vergleichende analytische Untersuchungen an festen Schlackeproben mittels ED-RFA und LIBS. Dortmund: RFA-Anwendertreffen.
- Blackwell, T. et al. (2005). *Inductively Coupled Plasma Mass Spectrometry Handbook* (ed. S.M. Nelms). Oxford. ISBN: 0-8493-2381-9.
- Bleymüller, J., Weißbach, R., Gehlert, G., and Gülicher, H. (2015). *Statistik für Wirtschaftswissenschaftler*. München: Vahlen.
- de Boer, D.K.G. and Brouwer, P.N. (1989). Angular dependence of X-ray fluorescence intensities. *X-Ray Spectrom.* 18 (3): 119.
- de Boer, D.K.B. (1990). Calculation of X-ray fluorescence intensities from bulk and multilayer samples. *X-Ray Spectrom.* 19: 145.
- de Boer, D.K.G. and Brouwer, P.N. (1990). Fundamental parameter-based X-ray fluorescence analysis of thin and multilayer samples. *Adv. X-Ray Anal.* 33: 237.
- von Bohlen A. (2010). TXRF an partikelförmigen Feststoffen (PhD thesis). Dissertation. Dortmund.
- von Bohlen, A. (2015). Fast Analysis, fast richtig - Zur Probenaufgabe bei der TXRF. Dortmund: RFA-Anwendertreffen.
- von Bohlen, A., Klockenkämper, R., Otto, H. et al. (1987). Qualitative survey analysis of thin layers of tissue samples - heavy metal traces in human lung tissue. *Int. Arch. Occup. Environ. Health* 59: 403.
- van den Bosch, S., Flock, J., and Sommer, D. (2005). Werkstoffanalytik in der Stahlindustrie. Dortmund: RFA-Anwendertreffen.
- Bragg, W.H. and Bragg, W.L. (1913). The reflection of X-rays by crystals. *Proc. R. Soc. London, Ser. A* 88: 428.
- Brinkmann, B. (2012). *Internationales Wörterbuch der Metrologie. Grundlegende und allgemeine Begriffe und zugeordnete Benennungen (VIM)*. Berlin: Beuth Verlag.
- Brodersen, K., Tartler, D., and Danzer, B. (1995). Wertstoffrückgewinnung aus Vielstoffgemischen am Beispiel Computerschrott. Dortmund: RFA-Anwendertreffen.
- Brouwer, P. (2015). Identification of Beer Types by Chemometric Methods. Berlin: PRORA.



- Brown, S., Tauler, R., and Walczak, B. (eds.) (2009). *Comprehensive Chemometrics*. Amsterdam: Elsevier.
- Brumme, M. (n.d.). Die BARKLA-Polarisationscinrichtung in der energiedispersiven Röntgenfluoreszenzanalyse (PhD thesis). Dissertation. TU Dresden.
- Buchmeyer J. (1997). Röntgenfluoreszenzanalyse in der Prozesskontrolle. Dortmund: RFA-Anwendertreffen.
- Budzikiewicz, H. and Schäfer, M. (2005). *Massenspektrometrie – Eine Einführung*. Weinheim: Wiley-VCH. ISBN: 3-527-30822-9.
- Bühler, A. (2002). Optimale Analysen-Strategien bei der Röntgenfluoreszenzanalyse von Ölen. Dortmund: RFA-Anwendertreffen.
- Cammann K. (2000) Instrumentelle Analytische Chemie: Spektrum Akademischer Verlag. - ISBN 3-8274-0057-0.
- Claisse, F. (1957). Accurate X-ray fluorescence analysis without internal standard. *Norelco Rep. III* 1: 3.
- Crone, R., Flock, J., and Thurmann, U. (2005). Direkte Analyse von Hochofenschlacken mittels RFA. Dortmund: RFA-Anwendertreffen.
- Custo, G., Litter, M.I., Rodriuez, D. et al. (2006). Total reflection X-ray fluorescence trace mercury determination by trapping complexation: application in advanced oxidation technologies. *Spectrochim. Acta, Part B* 61: 1119.
- Cybik, M. (2003). RFA-Bestimmung von Spurenelementen in Wässern nach Anreicherung auf Festphasensorbentien. Steinfurt: RFA-Anwendertreffen.
- DAkS-Regel-71-SD-4-019 (2010). Validierung von Prüfverfahren im Geltungsbereich des Scopes des SK-Chemie und Umwelt.
- Danzer, K., Hobert, H., Fischbacher, C. et al. (2001). *Chemometrik – Grundlagen und Anwendungen*. Berlin: Springer-Verlag.
- DEV-AV-4 (2006). Deutsches Einheitsverfahren DEV AO-4 Leitfaden zur Abschätzung der Messunsicherheit aus Validierungsdaten.
- DIN-32645 (2008-11). *Chemische Analytik - Nachweis-, Erfassungs- und Bestimmungsgrenze unter Wiederholbedingungen - Begriffe, Verfahren, Auswertung*. Beuth Verlag.
- DIN-38406 (1998:07). *Deutsche Einheitsverfahren zur Wasser-, Abwasser- und Schlammuntersuchung - Kationen (Gruppe E) - Teil 6: Bestimmung von Blei mittels Atomabsorptionsspektrometrie (AAS)*. Berlin: Beuth Verlag.
- DIN-38414-7 (1983:01). *Deutsche Einheitsverfahren zur Wasser-, Abwasser- und Schlammuntersuchung - Schlamm und Sedimente (Gruppe S) - Aufschluss mit Königswasser zur nachfolgenden Bestimmung des säurelöslichen Anteils von Metallen*. Berlin: Beuth Verlag.
- DIN-4021 (1990). *Aufschluß durch Schürfe und Bohrungen sowie Entnahme von Proben*. Beuth Verlag.
- DIN-51003 (2004-05). *Totalreflektions-Röntgenfluoreszenz-Analyse (TXRF) - Allgemeine Grundlagen und Begriffe*. Beuth Verlag.
- DIN-51396 (2008:11). *Prüfung von Schmierstoffen - Bestimmung von Abriebelementen*, Teil 2: RFA. Berlin: Beuth Verlag.
- DIN-51399 (2010:01). *Prüfung von Schmierölen - Bestimmung des Elementgehalte aus Additiven, Abrieb und sonstigen Verunreinigungen*, Teil 2: RFA. Berlin: Beuth Verlag.

- DIN-51418-1 (2008). *Röntgenspektralanalyse - Röntgenemissions- und Röntgenfluoreszenz-Analyse (RFA)*, Teil 1: Allgemeine Begriffe und Grundlagen. Berlin: Beuth Verlag.
- DIN-51418-2 (2014). *Röntgenspektralanalyse - Röntgenemissions- und Röntgenfluoreszenz-Analyse (RFA)*, Teil 2: Begriffe und Grundlagen zur Messung, Kalibrierung und Auswertung. Berlin: Beuth Verlag.
- DIN-51440 (2003:03). *Prüfung von Ottokraftstoffen - Bestimmung des P-Gehaltes*, Teil 1: RFA. Berlin: Beuth Verlag.
- DIN-51577 (1994:02). *Prüfung von Kohlenwasserstoffen und ähnlichen Erzeugnissen, Bestimmung des Cl- und Br-Gehaltes EDRFA*. Berlin: Beuth Verlag.
- DIN-51718-06 (2002). *Prüfung fester Brennstoffe - Bestimmung des Wassergehaltes und der Analysenfeuchtigkeit*. Berlin: Beuth Verlag.
- DIN-51719-07 (1997). *Prüfung fester Brennstoffe - Bestimmung des Aschegehaltes*. Berlin: Beuth Verlag.
- DIN-51720-03 (2001). *Prüfung fester Brennstoffe - Bestimmung des Gehaltes an Flüchtigen Bestandteilen*. Berlin: Beuth Verlag.
- DIN-51729-10 (2011-04). *Prüfung fester Brennstoffe - Bestimmung der chemischen Zusammensetzung von Brennstoffasche*. Berlin: Beuth Verlag.
- DIN-51750-02 (1990:12). *Prüfung von Mineralölen; Probenahme; Probennahme*. Berlin: Beuth Verlag.
- DIN-51769-10 (2013:04). *Mineralölerzeugnisse - Bestimmung niedriger Pb-Gehalte in Kraftstoffen*, Teil 10: RFA. Berlin: Beuth Verlag.
- DIN-51769-2 (1990-12) DIN-51750-1 Prüfung von Mineralölen.
- DIN-51829 (2013:03). *Mineralölerzeugnisse - Bestimmung von Additiv- und Abriebelementen in Schmierfetten, RFA*. Berlin: Beuth Verlag.
- DIN-EN-10315 (2006-10). *Standardverfahren zur Analyse von hochlegiertem Stahl mittels Röntgenfluoreszenzspektroskopie (RFA) unter Anwendung eines Vergleichs-Korrekturverfahrens*. Berlin: Beuth Verlag.
- DIN-EN-13723 (2002:10). *Mineralölerzeugnisse - Bestimmung niedriger Pb-Gehalte in Kraftstoffen, RFA*. Berlin: Beuth Verlag.
- DIN-EN-15063-1/2 (2007-01). *Kupfer und Kupferlegierungen - Bestimmung von Hauptbestandteilen und Verunreinigungen durch wellenlängndispersive Röntgenfluoreszenz (RFA): 1. Anleitungen für das Routineverfahren 2: Routineverfahren*. Berlin: Beuth Verlag.
- DIN-EN-15309 (2007-08). *Charakterisierung von Abfällen und Böden - Bestimmung der elementaren Zusammensetzung durch Röntgenfluoreszenz-Analyse*. Berlin: Beuth Verlag.
- DIN-EN-15485 (2007:11). *Ethanol zur Verwendung als Blendkomponente in Ottokraftstoff, Pb-Komponente in Ottokraftstoff - Bestimmung des S-Gehaltes mit RFA*. Berlin: Beuth Verlag.
- DIN-EN-1652 (1998:03). *Kupfer- und Kupferlegierungen*. Berlin: Beuth Verlag.
- DIN-EN-45001 (1997:06). *Allgemeine Anforderungen an die Kompetenz von Prüf- und Kalibrierlaboratorien*. Berlin: Beuth Verlag.
- DIN-EN-62321-3-1 (2014:10). *Verfahren zur Bestimmung von bestimmten Substanzen in Produkten der Elektrotechnik*, Teil 3-1: Screening Pb, Cd, Hg, Gesamt-Cr und Gesamt-Br durch RFA. Berlin: Beuth Verlag.

- DIN-EN-62321-3-1 (2014-10). *Verfahren zur Bestimmung von bestimmten Substanzen in Produkten der Elektrotechnik: Screening von Pb, Hg, Cd, Cr und Br durch Röntgenfluoreszenz-Spektroskopie*. Beuth Verlag.
- DIN-EN-955-5 (n.d.). *Chemische Analyse von feuerfesten Erzeugnissen*, Teil 5: Röntgen-fluoreszenzanalyse von Schmelztablette. Berlin: Beuth Verlag.
- DIN EN 10020:2000-07 (n.d.) Begriffsbestimmung für die Einteilung der Stähle; Deutsche Fassung EN 10020:2000 Beuth, Berlin.
- DIN-EN-ISO-11352 (2011:03). *Wasserbeschaffenheit - Bestimmung der Messunsicherheit basierend auf Validierungsdaten*. Berlin: Beuth Verlag.
- DIN-EN-ISO-11885 (2007). *Wasserbeschaffenheit - Bestimmung von ausgewählten Elementen durch induktiv gekoppelte Plasma-Atom-Emissionsspektrometrie (ICP-OES)*. Berlin: Beuth Verlag.
- DIN-EN-ISO-12677 (2013-02). *Chemische Analyse von feuerfesten Erzeugnissen durch Röntgenfluoreszenz-Analyse (RFA)*. Berlin: Beuth Verlag.
- DIN-EN-ISO-16967 (2013-03). *Feste Biobrennstoffe - Bestimmung von Hauptelementen - Al, Ca, Fe, Mg, P, K, Si, Na, Ti*. Berlin: Beuth Verlag.
- DIN-EN-ISO-17025 (2005). *Allgemeine Anforderungen an die Kompetenz von Prüf- und Kalibrierlaboratorien*. Berlin: Beuth Verlag.
- DIN-EN-ISO-20847 (2004:07). *Mineralölerzeugnisse - Bestimmung des S-Gehaltes von Kraftstoffen für Kraftfahrzeuge - EDRFA*. Berlin, Beuth Verlag.
- DIN-EN-ISO-20884 (2011:07). *Mineralölerzeugnisse - Bestimmung des S-Gehaltes von Kraftstoffen für Kraftfahrzeuge - WDRFA*. Berlin: Beuthg Verlag.
- DIN-EN-ISO-21747 (2007). *Statistische Verfahren - Prozessleistungs- und Prozessfähigkeitskenngrößen für kontinuierliche Qualitätsmerkmale*. Berlin: Beuth Verlag.
- DIN-EN-ISO-3170 (2004:06). *Flüssige Mineralölerzeugnisse - Manuelle Probenahme*. Berlin: Beuth Verlag.
- DIN-EN-ISO-3497 (2001-12). *Metallische Schichten - Schichtdickenmessung - RFA*. Berlin: Beuth Verlag.
- DIN-EN-ISO-4259 (2006:10). *Mineralölerzeugnisse - Bestimmung und Anwendung der Werte für die Präzision von Prüfverfahren*. Berlin: Beuth Verlag.
- DIN-EN-ISO-9001 (2015:11). *Qualitätsmanagementsysteme*. Berlin: Beuth Verlag.
- DIN-ISO-12980 (2000). *Kohlenstoffmaterialien für die Herstellung von Aluminium - Grünkoks und kalzinierter Koks für Elektroden - Wellenlängendispersive Röntgenfluoreszenz-Analyse (RFA)*. Berlin: Beuth Verlag.
- DIN-ISO-4883 (1991-06). *Hartmetalle: Bestimmung des Gehaltes metallischer Bestandteile durch Lösungsverfahren*. Berlin: Beuth Verlag.
- DIN-ISO-5725 (n.d.). *Genauigkeit (Richtigkeit und Präzision) von Messverfahren und Messergebnissen*, Teil 1–4. Berlin: Beuth Verlag.
- DIN-V-ENV\_13005 (1999:06). Leitfaden zur Angabe der Unsicherheit beim Messen.
- Dörffel, K. (1966). *Statistik in der analytischen Chemie*. Leipzig: VEB Deutscher Verlag für Grundstoffindustrie.
- Doujak, G., Ramb, W., and Mertens, R. (2002). *Die betriebliche Schlackeanalytik - ein Methodenvergleich mit Ausblick*. Dortmund: RFA-Anwendertreffen.
- Eggert, F. (2005). *Standardfreie Elektronenstrahl-Mikroanalyse mit dem EDX im Rasterelektronenmikroskop*. Morderstedt: Book on Demand. ISBN: 3-8334-2599-7.

- Elam, W.T., Ravel, B.D., and Sieber, J.R. (2002). A new atomic database for X-ray spectroscopic calculations. *Radiat. Phys. Chem.* 63: 121.
- EN-573\_3-2013-12 (2013). *Aluminium und Aluminiumlegierungen - Chemische Zusammensetzung und Form von Halbzeug*, Teil 3: Chemische Zusammensetzung und Erzeugnisformen. Beuth.
- EPA IO-3.3 Determination of metals in ambient particulate matter using X-ray fluorescence (XRF) spectrometry 1999.
- Erhardt, H. (1989). *Röntgenfluoreszenzanalyse: Anwendung in Betriebslaboratorien*. Berlin: Springer-Verlag.
- EURACHEM\_CITAC\_GUIDE (2004). *Ermittlung der Messunsicherheit bei analytischen Messungen*.
- EURACHEM-Guide (1998). *The Fitness for Purpose of Analytical Methods*.
- EU-regulation\_22 (2001). Sampling methods and the methods of analysis for the official control of the levels of Pb, Cd, Hg and 3-MCPD in foodstuff. European Commission. [http://www.megapesca.com/eu\\_regulations\\_update/Directive\\_2001\\_22\\_EC\\_8\\_March\\_2001.pdf](http://www.megapesca.com/eu_regulations_update/Directive_2001_22_EC_8_March_2001.pdf) (accessed 2 March 2020).
- EU-regulation\_32 (2002). Richtlinie über unerwünschte Stoffe in der Tierernährung. Europäisches Parlament.
- EU-regulation\_466 (2001). Setting maximum levels for certain contaminants in foodstuff. EU-Commission. [http://ec.europa.eu/food/fs/sfp/fcr/fcr02\\_en.pdf](http://ec.europa.eu/food/fs/sfp/fcr/fcr02_en.pdf) (accessed 2 March 2020).
- EU-Richtlinie\_48 (2009). Über die Sicherheit von Spielzeug. Europäisches Parlament. <http://eur-lex.europa.eu/LexUriServ/LexUriServ.do?uri=OJ:L:2009:170:0001:0037:de:PDF> (accessed 24 April 2020).
- EU-Richtlinie\_65 (2011). Beschränkung der Verwendung bestimmter gefährlicher Stoffe in Elektro- und Elektronikgeräten. Europäisches Parlament. <http://www.ce-zeichen.de/templates/ce-zei/richtlinien/rohs-richtlinie-2011.pdf> (accessed 2 March 2020).
- EUROLAB-TB\_2 (2006). *Leitfaden zur Ermittlung von Messunsicherheiten bei quantitativen Prüfergebnissen*.
- European-Pharmacopoeia (2008). Section 2.2.37.
- Finney, M.S., Field, K.M., and Tyrrel, S.G. (1998). A New In-Line Analyzer FPR the Analysis of Powdered Materials. Dortmund: RFA-Anwendertreffen.
- Fischer (n.d.). [www.helmut-fischer.de](http://www.helmut-fischer.de) (accessed 2 March 2020).
- Fittschen, U.A.E.; Sparks, C.; Havrilla, G.J.; Strelt, C.; (2011). Picoliter Pipette deposition in TXRF-Analysis. Steinfurt: RFA-Anwendertreffen.
- Fittschen, U.A.E. and Havrilla, G.J. (2010). Picoliter droplet deposition using a prototype picoliter pipette: control parameters and application in  $\mu$ -XRF. *Anal. Chem.* 82: 297.
- Flock, J. and Ohls, K. (1987). Automatischer Schmelzaufschluß zur schnellen Vorbereitung fester und flüssiger Analysenproben für die Röntgenfluoreszenz- und ICP-Spektroskopie. *Fresenius Z. Anal. Chem.* 328: 560.
- Flock, J. and van den Bosch, S. (2016). *Handbuch für das Eisenhüttenwesen*, Bd. 1. Verlag StahlEisen.
- Flock, J., Langbein, D., and Loepp, H. (2009). Wieviel Probe Braucht Die RFA?. Steinfurt: RFA-Anwendertreffen.

- Flock, J., Langbein, D., and Sternberg, M. (2008). Analyse von feuerfesten Baustoffen mit fundamental-Programmen. Dortmund: RFA-Anwendertreffen.
- Fluxana (n.d.). <http://www.fluxana.de/> (accessed 2 March 2020).
- Frechette, G., Heert, J.C., Thinh et al. (1979). X-ray fluorescence analysis of cement. *Anal. Chem.* 51: 1957.
- Friedrich, W., Knipping, P., and von Laue, M. (1912). Interferenz-Erscheinungen bei Röntgenstrahlen. Bayerische Akademie der Wissenschaften, Sitzungsberichte.
- Füchtjohann, L., Jayiy, B., and Kwarteng, W. (2004). Bestimmung von Schwermetallen, Fluor und Chlor in Althölzern mit Hilfe der Röntgenfluoreszenzanalyse. Duisburg: RFA-Anwendertreffen.
- Funk, W., Dammann, V., and Donnevert, G. (2002). *Qualitätssicherung in der Analytischen Chemie*. Wiley-VCH.
- Gelman, A. (2005). Analysis of variance? Why it is more important than ever. *Ann. Stat.* 33 (1): 1.
- Geyer, J., Flock, J., and Broekaert, J.A.C. (1997). Bestimmung der Bindungsformen des Eisens in Einsatz- und Nebenprodukten der Stahlindustrie. Dortmund: RFA-Anwendertreffen.
- Giles, H.L., Hurley, P.W., and Webster, H.W. (1995). Simple approach to the analysis of oxides, silicates and carbonates using X-ray fluorescence spectrometry. *X-Ray Spectrom.* 24: 205.
- Gill, P., Murray, W., and Wright, M. (1981). *Practical Optimization*. Academic Press.
- Glocker, R. and Schreiber, H. (1928). Quantitative Röntgenspektralanalyse mit Kalanregung des Spektrums. *Ann. Phys.* 85: 1089.
- Goodfellow (n.d.). [www.goodfellow.com/de/](http://www.goodfellow.com/de/) (accessed 2 March 2020).
- Götz, G. and Gärtner, K. (1988). *High Energy Ion Beam Analysis of Solids*. Berlin: Akademie Verlag.
- Graham, S. (1996). On-line Messungen von Schwefel in Raffinerieprodukten mittels RFA. Dortmund: RFA-Anwendertreffen.
- Greaves, E.D., Angeli-Greaves, M., Jaehde, U. et al. (2006). Rapid determination of Platinum plasma concentrations of chemotherapy patients using TXRF. *Spectrochim. Acta* 61B: 1194.
- Greiff, S. (2015). Die Anwendung der Mikro-Röntgenfluoreszenz zur Herkunftsanalyse roter Edelgranate. In: *Archäologie in NRW 2010-2015* (eds. T. Otten, J. Kunow, M. Rind and M. Trier).
- van Grieken, R. and Markowicz, A. (2002). *Handbook of X-Ray Spectrometry, Practical Spectroscopy*. Marcel Dekker. ISBN-10: 0824706005.
- Grimaldi, R., Paris, V., and Mariani, E. (1981). Quantitative determination of various forms of aluminium in steel by XRF. *X-Ray Spectrom.* 4: 163.
- Gross, J.H. (2013). *Massenspektrometrie - Ein Lehrbuch*. Berlin/ Heidelberg: Springer-Verlag. ISBN: 978-3-8274-2980-3.
- GUM (2008). *Guide to the Expression of Uncertainty in Measurement*. Bureau International des Poids et Mesures, BIPM [www.bipm.org/en/publications/guides/gum.html](http://www.bipm.org/en/publications/guides/gum.html).
- Günzler, H. (1994). *Akkreditierung und Qualitätssicherung in der Analytischen Chemie*. Heidelberg: Springer-Verlag.
- Hahn-Weinheimer, R., Hirner, A., and Weber-Diefenbach, K. (2012). *Röntgenfluoreszenz-analytische Methoden: Grundlagen und praktische*

- Anwendung in den Geo-, Material- und Umweltwissenschaften*. Berlin: Springer-Verlag. ISBN-10: 3540670211.
- Hanning, S. (2012). Messungen an Glasstandards. Persönliche Mitteilung.
- Hanning, S. and Bühler, A. (2014). Vom ppm bis zu Prozenten - über den Einsatz der RFA im 'Leichtgewicht' Kunststoffanalytik. Dortmund: RFA-Anwendertreffen.
- Hanning, S. and Janssen, A. (2005). Anwendbarkeit der WDRFA bei der Bestimmung ausgewählter Elemente im Abfall des DSD. Dortmund: RFA-Anwendertreffen.
- Hanning, S.; Wacker, G.; Mans, C.; Kreyenschmidt, M. (2010). Herstellung von 'in House' Kunststoffstandards für die RFA. Dortmund: RFA-Anwendertreffen.
- Haschke, M. (2014). *Micro-X-Ray Fluorescence - Instrumentation and Application*. Berlin: Springer-Verlag.
- Haschke, M. and Kanngießer, B. (2013). Multidimensionale analysedaten (1). *Opt. Photon.* 8 (3): 60.
- Haschke, M. and Weisbach, J. (1973). Untersuchungen zur Elektronenstruktur und den Werkstoffeigenschaften ausgewählter Widerstands- und Magnetlegierungen (PhD thesis). Dissertation. TU Dresden.
- Haschke, M., Scholz, W., and Theis, U. (1998). X-ray fluorescence in the  $\mu\text{m}$ -range using capillary lenses. In: *Proceedings of EDXRF-Conference*, 157. Bologna.
- Haschke, M., Waldschläger, U., and Scheller, S. (2012). Energieauflösung vs. Zählraten - was ist der beste Kompromiss?. Dortmund: RFA-Anwendertreffen.
- Haschke, M., Klein, J., Vietze, U., and Stichert, W. (2002). High Throughput Experimentation mit der Mikro-Röntgenfluoreszenz. *GIT Labor-Fachzeitschr.* 2: 2.
- Haschke, M.; Scheller, S.; Langbein, D.; Flock, J. (2016). Präzisionsanalyse mit Röntgenfluoreszenz - Vergleich von WDS und EDS. Dortmund: RFA-Anwendertreffen.
- Heckel, J. and Ryon, R.W. (2002). *Polarized Beam X-Ray Fluorescence Analysis. Handbook of X-Ray Spectrometry*. New York: Marcel Dekker.
- Heckel, J., Haschke, M., Brumme, M., and Schindler, R. (1992). Principles and applications of energy-dispersive X-ray fluorescence analysis with polarized radiation. *J. Anal. At. Spectrom.* 7 (2): 281.
- Henrich, A.; Hoffmann, P.; Ortner, H.; Itzel, H. (1999). Chemometrische Unterscheidung und Klassifizierung von Substanzen ohne detektierbare Röntgenfluoreszenzlinien durch Röntgenstreustrahlung. Dortmund: RFA-Anwendertreffen.
- Hevesy G.v. and Böhm, J. (1927). Die quantitative Bestimmung des Tantals auf röntgenspektroskopischem Wege. *Z. Anorg. Chem.* 164: 69.
- von Hevesy, G., Böhm, J., and Fassler, A. (1930). Quantitative röntgenspektroskopische Analyse mit Sekundärstrahlen. *Z. Phys.* 63: 74–105.
- Hoffmann, P. (2005). Non-invasive identification of chemical compounds by EDXRF. In: *Handbook of Practical X-Ray Fluorescence Analysis* (eds. B. Beckhoff, B. Kanngießer, N. Langhoff, et al.). Heidelberg: Springer-Verlag.
- Hoffmann, P., Kessler, T., and Ortner, H. (2001). Identifikation von Substanzen durch chemometrische Auswertung von EDRFA-Spektren. *Anwendertreffen Röntgenfluoreszenz*, Steinfurt.

- Hönicke, P., Beckhoff, B., Kolbe, M. et al. (2015). Depth profile characterization of ultra shallow junction implants. *Anal. Bioanal. Chem.* 396: 2825, <http://www.claisse.com/>.
- Huber, A., Rath, H.J., Eichinger, P. et al. (1988). Sub-ppb monitoring of transition metal contamination of silicon wafer surfaces by VPD-TXRF. *Proc. Electrochem. Soc.* (88): 109.
- ICH Guideline Q3D on elemental impurities (2016). [ema.europa.eu/docs/en\\_GB/document\\_library/Scientific\\_guideline/2015/01/WC500180284.pdf](http://ema.europa.eu/docs/en_GB/document_library/Scientific_guideline/2015/01/WC500180284.pdf) (accessed 3 March 2020).
- IEC\_62321-1 (2013) Determination of certain substances in electrotechnical products; <https://webstore.iec.ch/searchform&q=IEC%2062321>. - International Electrotechnical Commission.
- IPC-4552 (n.d.). Specification for Electroless Nickel/ Immersion Gold (ENIG) Plating for Printed Circuit Boards. <http://www.ipc.org/TOC/IPC-4552.pdf> (accessed 3 March 2020).
- IPC-4556 (n.d.). Specification for Electroless Nickel/ Electroless Palladium/ Immersion Gold (ENEPIG) Plating for Printed Circuit Boards. <http://www.ipc.org/TOC/IPC-4556.pdf> (accessed 3 March 2020).
- ISO/IEC Guide 98-3 (2008). Uncertainty of Measurement (Part 3), Guide to the expression of uncertainty in measurement (GUM:1995).
- ISO\_guide\_25 (1990). General requirements for the competence of calibration and testing laboratories.
- Janßen, A. and Flock, J. (2004). Anreicherungsverfahren in der Probenvorbereitung für die RFA. Duisburg: RFA-Anwendertreffen.
- Janßen, A., Protzer, A., and Priggemeyer, St. (1997). Röntgenfluoreszenzanalyse von Kupferlegierungen nach Auflösung in Säure. Dortmund: RFA-Anwendertreffen.
- Janßen, A., Werning, A.J., and Rethfeld, H. (1998). Schwermetallbestimmungen in Klärschlamm - Vergleich von RFA und ICP-OES. Dortmund: RFA-Anwendertreffen.
- Janßen, A.; Erftmeier, P.; Flock J. (1994). Vergleich von Borataufschluss und Pulverpressverfahren als Probenvorbereitung für die Eisenerzanalytik mit der RFA. Dortmund: RFA-Anwendertreffen.
- Janssens, K.H.A., Adams, F.C.V., and Rindby, A. (2000). *Micro-X-Ray Fluorescence Analysis*. Wiley.
- JCGM\_100:2008 (2008). *Evaluation of Measurement Data - Guide to the Expression of Uncertainty in Measurement*. IUAPC.
- Jenkins, R. and de Vries, J.L. (1967). *Practical X-Ray Spectrometry*. London: McMillan. ISBN: 0333006135.
- Jenkins, R., Gould, R.W., and Gedcke, D. (1981). *Quantitative X-Ray Spectrometry*. New York: Marcel Dekker. ISBN8: 0-8247-1266-8.
- Jonkers, A. (2006). Luftfilteranalytik mit RFA. Münster: RFA-Anwendertreffen.
- Kaiser, B. and Shugar, A.N. (2012). Glass analysis utilizing handheld XRF. In: *Handheld XRF for Art and Archeology* (eds. A.N. Shugar and J. Mass), 449. Leuven: University Press Leuven.
- Kämpfe, B. and Haschke, M. (1998). *Röntgenstrahlen zur Untersuchung von Münzen*. MGM-Magazine.

- Kanngießer, B., Malzer, W., Fuentes, A., and Reiche, I. (2005). Three-dimensional  $\mu$ -XRF investigations of paint layers with a table top setup. *Spectrochim. Acta, Part B* 60: 41.
- Kanngießer, B. and Haschke, M. (2006). Micro X-ray fluorescence spectroscopy. In: *Practical Handbook of X-Ray Fluorescence* (eds. B. Beckhoff, B. Kanngiesser, N. Langhoff, et al.), 433–474. Berlin: Springer-Verlag.
- Kessler, T. (2001). Multivariat-statistische Auswertung von energiedispersiven Röntgenfluoreszenzspektren zur Identifizierung von Substanzen (PhD thesis). Dissertation: TU Darmstadt.
- Kessler, T., Hoffmann, P., and Ortner, H. (2000). Optimierung der Identifikation von Substanzen durch chemometrische Auswertung von EDXRF-Spektren. *Anwendertreffen Röntgenspektroskopie*, Dortmund.
- Klein, J.; Vietze, U.; Stichert, W.; Haschke, M. (2001). Die  $\mu$ -RFA als effektive Analysenmethode in der kombinatorischen Chemie. Steinfurt: RFA-Anwendertreffen.
- Klockenkämper, R. and von Bohlen, A. (2015). *Total-Reflection X-Ray Fluorescence Analysis and Related Methods*. Wiley.
- Klockenkämper, R., von Bohlen, A., and Moens, L. (1993). Analytical characterization of artists' pigments used in old and modern paintings by TXRF. *Spectrochim. Acta, Part B* 48: 239.
- Klockenkämper R. and von Bohlen A (1996). Total-Reflection X-Ray Fluorescence Analysis: John Wiley & Sons; 1. Auflage. - ISBN-13: 978-0471305248.
- Klockenkämper, R., von Bohlen, A., and Moens, L. (2000). Analysis of pigments and inks on old paintings and historical manuscripts using TXRF. *X-Ray Spectrom.* 29: 119.
- Klockenkämper, R., Krzyzanowska, H., and von Bohlen, A. (2003). Tiefenprofilanalyse von nm-dünnen Schichten durch sanftes planares Ionenätzen und TXRF. Steinfurt: Anwendertreffen RFA.
- Knoth, J. and Schwenke, H. (1978). Total-reflection X-ray fluorescence with totally reflecting sample support for trace analysis at the ppb-level. *Fresenius Z. Anal. Chem.* 291: 200.
- Koch, K.H. and Flock, J. (1996). Rationalisierung der metallurgischen Prozeßanalytik durch Automation und Dezentralisierung. *Stahl Eisen* 116: 71.
- Koch, K.H. and Flock, J. (1990/91). *Steel Technology International*. London: Sterling Publications International.
- Körber, H. (1998). Einsatz der RFA zur Qualitätssicherung für feuerfeste und keramische Rohstoffe und Produkte. Dortmund: RFA-Anwendertreffen.
- Kromidas, S. (2011). *Handbuch Validierung in der Analytik, Wirtschaftlichkeit, Praktische Fallbeispiele, Alternativen*. Wiley-VCH.
- LabReport-XRF\_053 (n.d.). Analysis with Blast Furnace Slags with EDXRF. Bruker.
- LabReport-XRF\_079 (n.d.). Process and Quality Control in Cement Production (ASTM C 114). Bruker.
- LabReport-XRF\_093 (n.d.). Fastest Process and Quality Control in Cement Production by Simultaneous WDXRF (ASTM C 114).
- LabReport-XRF\_094 (n.d.). Rapid Free-Lime Quantification in Clinker. Bruker.
- LabReport-XRF\_096 (n.d.). The Analysis of Pb and Cd in Lead-Free Solder for RoHS Compliance Testing. Bruker.



- LabReport-XRF\_100 (n.d.). Grade Control of Bauxite for Aluminium and Refractory Production by XRF. Bruker.
- LabReport-XRF\_101 (n.d.). ASTM D6443 Standard Test Method for Determination of Ca, Cl, Cu, Mg, P, S and Zn in Unused Lubricating Oils and Additives. Bruker.
- LabReport-XRF\_105 (n.d.). Accurate and Precise Analysis of Ferroalloys for Steel Production. Bruker.
- LabReport-XRF\_110 (n.d.). Accurate and Flexible Analysis of Iron Ores as Fused Beads by EDXRF. Bruker.
- LabReport-XRF\_111 (n.d.). Fast and Dedicated Analysis of Iron Ores as Pressed Pellets by EDXRF. Bruker.
- LabReport-XRF\_115 (n.d.). Quality Control of Anode Cokes - Trace Analysis by WDXRF. Bruker.
- LabReport-XRF\_425 (n.d.). Trace Element Analysis of Fresh Water Samples by TXRF Spectrometry. Bruker Nano Berlin.
- LabReport-XRF\_430 (n.d.). Analysis of Mercury in Tap Water and Orange Juice by TXRF Spectrometry. Bruker.
- LabReport-XRF\_438 (n.d.). Ultratrace Element Analysis of Nanoparticles. Bruker Nano Berlin.
- LabReport-XRF\_77 (n.d.). Trace Element Analysis of Blood Samples. Bruker Nano Berlin.
- Lachance, G. and Claisse, F. (1994). *Quantitative X-Ray Fluorescence Analysis*. Wiley. ISBN: 0-471-95167-6.
- Lachance, G.R. and Traill, G.J. (1966). A practical solution to the matrix problem in X-ray analysis. *Canadian Journal of Spectroscopy* 11 43 und 63.
- Lachmann, T., van der Snickt, G., Haschke, M., and Mantouvalou, I. (2016). Combined micro-XRF techniques for the analysis of illuminated manuscripts. *J. Anal. At. Spectrom.* 31 (10): 1941.
- Levenberg, K. (1944). A method for the solution of certain problems in least squares. *Q. Appl. Math.* 2: 164.
- LGC-Standards (n.d.). [www.lgcstandards.com](http://www.lgcstandards.com) (accessed 3 March 2020).
- Lienemann, P. (2008). Abriebspartikel des Schienen- und Strassenverkehrs. Dortmund: RFA-Anwendertreffen.
- Lienemann, P. (2009). Holzaschen aus Kleinf Feuerungsanlagen - Elementanalytik mit der RFA. Steinfurt: RFA-Anwendertreffen.
- Lira, I.H. and Wöger, W. (1998). Evaluation of the uncertainty associated with a measurement result not correct for systematic effects. *Meas. Sci. Technol.* 9: 1010–1011.
- Liritzis, I. and Zacharias, N. (2010). Portable XRF of archaeological artifacts: current research potentials and limitations. In: *X-Ray Fluorescence Spectrometry in Archaeology*, vol. 109 (ed. M.S. Shakley), 109–142. New York: Springer.
- Love, G., Cox, M.G., and Scott, V.D. (1978). The surface ionisation function phirhoz derived using a Monte Carlo method. (Correction procedure development for electron-probe microanalysis). *J. Phys. D: Appl. Phys.* 11 (1): 23.
- Lück, D., Scharf, H., and Ostermann, M. (2012). Einsatz und Eignung von RFA-Handgeräten für die Bodenanalytik. Dortmund: RFA-Anwendertreffen.
- Lunau, S. (2013). *Six Sigma+Lean Toolset*. Springer-Verlag.
- M2-Automation (2016). <http://www.m2-automation.com>.

- C. Mans, C. Simons, S. Hanning, A. Janßen, A. Bühler, M. Kreyenschmidt (2009). Homogenitätsuntersuchungen an Kandidatenreferenzmaterialien. Steinfurt: RFA-Anwendertreffen.
- Mantler, M. (1986). X-ray fluorescence analysis of multiple-layer films. *Anal. Chim. Acta* 188: 25.
- Mantler, M. (2006). *Handbook of Practical X-Ray Fluorescence Analysis* (eds. B. Beckhoff et al.). Berlin, Heidelberg: Springer-Verlag.
- Mantler, M. and Schreiner, M. (2000). X-ray fluorescence spectrometry in art and archaeology. *X-Ray Spectrom.* 29: 3.
- Mantouvalou, I. (2016). Visualisierung von Elementverteilungen mit polychromatischer 3D-Röntgen-Fluoreszenzanalyse. Dortmund: RFA-Anwendertreffen.
- Mantouvalou, I., Lange, K., Wolff, T. et al. (2011). 3D micro-XRF for cultural heritage objects: new analysis strategies for the investigation of the dead sea scrolls. *Anal. Chem.* 83: 6308.
- Marquardt, D. (1963). An algorithm for least-squares estimation of nonlinear parameters. *SIAM J. Appl. Math.* 11: 431.
- Marx, T. (2000). Analyse von flüssigen Sekundärbrennstoffen. Dortmund: RFA-Anwendertreffen.
- Mass, J. and Matsen, C. (2012). Quantitative non-destructive analysis of historic silver alloys: XRF approaches and challenges. In: *Handheld XRF for Art and Archeology* (eds. A.N. Shugar and J. Mass), 215. Leuven: Leuven University Press.
- Michaelis, M. (2005). Einsatz der RFA bei der Zertifizierung von Referenzmaterialien. Dortmund: RFA-Anwendertreffen.
- Miller, T.C. and Havrilla, G. (2004). Nanodroplets: a new method for dried spot preparation and analysis. *X-Ray Spectrom.* 33: 101.
- Miller, T.C., Mann, G., Havrilla, G. et al. (2003). Micro-X-ray fluorescence as a general high-throughput screening method for catalyst discovery and small molecule recognition. *J. Comb. Chem.* 5: 245.
- Minogue, E.M., Taylor, T.P., Burrell et al. (2005). A high throughput screening method for the selection of zeolites for binding cations. *Chem. Commun.* 4167.
- Minogue, E.M., Taylor, T.P., Burrell et al. (2006). An ultra high throughput, double combinatorial screening method of peptide–metal binding. *New J. Chem.* 30: 1145.
- Miziolek, A.W., Palleschi, V., and Schechter, I. (2006). *Laser Induced Breakdown Spectroscopy*. Cambridge: Cambridge Press.
- Moioli, P. and Seccaroni, C. (2000). Analysis of art objects using a portable X-ray fluorescence spectrometer. *X-Ray Spectrom.* 29 (1): 48.
- Musazzi, S. and Perini, V. (2014). *Laser-Induced Breakdown Spectroscopy: Theory and Applications*. Heidelberg: Springer-Verlag.
- Nakano, K.; Tsuji, K.; Kakita, K.; Ono, A.; Nakamura, T. (2006). Development of plastic certified materials for XRF analysis containing Pb, Cd, Cr: Part 1: Sample preparation and homogeneity test. <http://iccd.com>.
- Neitzel, V. and Middeke, K. (1994). *Praktische Qualitätssicherung in der Analytik*. Weinheim: Wiley-VCH.

- Nerin, C. et al. (1995). Trapping efficiency of polyurethane foam and Amberlite XAD-2 for various organochlorine compounds. *Fresenius J. Anal. Chem.* 352 (6): 609.
- Neuberger, A. (1965). Die Ermittlung des Aluminiums und seiner Bindungsformen in unlegierten Stählen. *Stahl Eisen* 85: 1446.
- Niese, S. (2007). Die Entdeckung der Röntgenfluoreszenzanalyse. *Mitt. FG Gesch. Chem. GDCh* 19: 217.
- Noack, S. (2012). Messunsicherheit bei Funken-OES und RFA - eine sichere Sache?. Dortmund: RFA-Anwendertreffen.
- Noack, R., Krefß, S., and Dunkel, L. (1997). Röntgenfluoreszenzanalyse in der Prozesskontrolle. Dortmund: RFA-Anwendertreffen.
- NordtestReport-TR537 (2004-02). Handbook for calculation of uncertainty in environmental laboratories.
- Norrish, K. and Hutton, J.T. (1969). An accurate X-ray spectrographic method for the analysis of a wide range of geological samples. *Geochim. Cosmochim. Acta* 33: 431.
- Norrish, K. and Thompson, G.M. (1990). X-ray analysis of sulphides by fusion methods. *X-Ray Spectrom.* 19: 67.
- Otto, M. (2007). *Chemometrics*. Wiley. ISBN: 978-3-527-31418-8.
- Pappert, E., Flock, J., and Broekaert, J.A.C. (1996). Bestimmung von AlN und Al<sub>2</sub>O<sub>3</sub> mittels RFA nach elektrolytischer Voranreicherung. Nichtmetalle in Metallen, Hrsg. D. Hirschfeld, p. 61.
- Pappert, E., Flock, F., and Broekaert, J.A.C. (1997). Bestimmung der Bindungsform und des Oxidationszustandes von Chrom in Feststoffen mittels soft-X-Ray Spectroscopy. Dortmund: RFA-Anwendertreffen.
- Perrier, C. and Segrè, E. (1947). Technetium: the element of atomic number 43. *Nature* 159: 24.
- Peters, J. and Schröder, J. (1996). Probenpräparation für die quantitative Analyse mittels RFA an Rohstoffen und pulverförmigen Produkten von Refraktärmetallverbindungen. Dortmund: RFA-Anwendertreffen.
- Peters, J. and Schröder, J. (1997). Probenpräparation für die quantitative Analyse mittels RFA an Rohstoffen und pulverförmigen Produkten von Refraktärmetallverbindungen. Dortmund: RFA-Anwendertreffen.
- Phillips, S.C. and Speakman, R.J. (2009). Initial source evaluation of archeological obsidian from the kuril islands of the russian far east using portable XRF. *J. Archaeol. Sci.* 36: 1256.
- Pilz, K., Heiss, J., Haschke, M. et al. (2006). On-Line Messungen zur Bestimmung des Zinkgehaltes von Konverterstaub bei Temperaturen im Bereich von 250 °C. Steinfurt: RFA-Anwendertreffen.
- Potts, P.J. and West, M. (2008). *Portable X-Ray Fluorescence Spectrometry: Capabilities for in Situ Analysis*. Cambridge: The Royal Society of Chemistry.
- Prange, A., Kramer, K., and Reus, U. (1991). Determination of trace element impurities in ultrapure reagents by TXRF. *Spectrochim. Acta* 338: 891.
- Quye-Sawyer, J., Vandeginste, V., and Johnston, K.J. (2015). Application of handheld energy-dispersive X-ray fluorescence spectrometry to carbonate studies: opportunities and challenges. *J. Anal. At. Spectrom.* 30: 1490.
- RAL-GZ-724 (2012). Sekundärrohstoffe - Gütesicherung. Berlin: Beuth Verlag.

- Reisel, J. (2001). Bestimmung nichtmetallischer Einschlussverbindungen in Stählen mit Hilfe der Röntgenfluoreszenz- und Röntgenemissionsspektrometrie (PhD thesis). Dissertation: Universität Dortmund.
- Reisel, J., Flock, J., and Broekaert, J.A.C. (2000). Bestimmung von AlN und Al<sub>2</sub>O<sub>3</sub> in Stählen mit Hilfe der wellenlängendispersiven RFA. Dortmund: RFA-Anwendertreffen.
- Rödel, T.C., Bronk, H., and Haschke, M. (2002). Investigation of the influence of particle size on the quantitative analysis of glasses by energy-dispersive micro X-ray fluorescence spectrometry. *X-Ray Spectrom.* 31 (1): 16.
- Rössiger, V. and Conrad, G. (1989). Metalloberfläche. - München 43 12: 569.
- Rössiger, V. and Nensel, B. (2006). *Handbook of Practical X-ray Fluorescence Analysis* (eds. B. Beckhoff et al.), 554. Berlin: Springer-Verlag.
- Rüttimann, F. (2008a). SiC Bestimmung mittels Röntgenfluoreszenz. Dortmund: RFA-Anwendertreffen.
- Rüttimann, F. (2008b). Verfahren für die Probenpräparation flüssiger oder pastöser Stoffe zur Messung mittels Röntgenfluoreszenz und dafür geeigneter Probenkörper. EP 2 149 043 B1.
- Rüttimann, F. (2011). LiTrap - Analyse von Flüssigkeiten. Seinfurt: RFA-Anwendertreffen.
- Saiz-Zens, A., Flock, J., and Geyer, J. (1998). Eingangskontrolle von Ferrolegierungen mittels Röntgenfluoreszenzanalyse von Pulverschüttungen. Dortmund: RFA-Anwendertreffen.
- Salva, A., von Bohlen, A., and Klockenkämper, R. (1993). Multielement analysis of airborne particulate matter by TXRF. *Quim. Anal.* 12: 57.
- Schlesinger, C., Malzer, M., and Kanngießer, B. (2015). Chemische Speziationsanalyse mit Röntgenabsorptionsspektroskopie im Labor - Stand und Potential. Steinfurt: RFA-Anwendertreffen.
- Schmeling, M., Klockenkämper, R., and Klockow, D. (1995). Sammlung von Luftstäuben auf Filtern und deren nachfolgende Analyse mit der TRFA. Dortmund: RFA-Anwendertreffen.
- Scholze, F. and Procop, M. (2009). Modelling the response function of energy dispersive X-ray spectrometers with silicon detectors. *X-Ray Spectrom.* 38 (4): 312.
- Schoonjans, T. (2017). <https://github.com/tschoonj/xmimsim> (November 2017).
- Schoonjans, T., Brunetti, A., Golosio, B. et al. (2011). The xraylib library for X-ray-matter interactions. *Spectrochim. Acta, Part B* 66: 776.
- Schoonjans, T., Sole, V.A., Vincze, L. et al. (2013). A general Monte Carlo simulation of energy-dispersive X-ray fluorescence spectrometers - Part 6: Quantification through iterative simulations. *Spectrochim. Acta, Part B* 82: 36.
- Schramm, R. (2016). Praxisbericht - Herstellung neuer Referenzmaterialien. Dortmund: RFA-Anwendertreffen.
- Schramm, R. (2018). Neues 3D-Druckverfahren zur Herstellung von RFA-Kongrollproben. *Anwendertreffen Röntgenspektroskopie*, Steinfurt.
- Schreiner, M., Fruhmann, B., Jembrih-Simburger, D., and Linke, R. (2004). X-rays in art and archaeology: an overview. *Powder Diffr.* 19 (1): 3.
- Sear, L.G. (1997). The fusion of difficult materials including chromite, Casserite and reduced sulphur. *X-Ray Spectrom.* 26: 105.

- Shakley, M.S. (2010). An introduction to X-ray fluorescence spectrometry for archaeologists. In: *X-Ray Fluorescence Spectrometry in Geoarchaeology*. New York: Springer.
- Sherman, J. (1955). The theoretical derivation of fluorescent X-ray intensities from mixtures. *Spectrochim. Acta* 7: 283.
- Shrivastava, P., O'Connell, S., and Whitley, A. (2005). Handheld X-ray fluorescence: practical application as screening tool to detect the presence of environmentally-sensitive substances in electronic equipment. *Proceedings of the 2005 IEEE International Symposium on Electronics and Environment*, Volume 157.
- Shugar, A.N. and Mass, J.L. (2012). *Studies in Archaeological Sciences - Handheld XRF for Art and Archaeology*. Leuven: Leuven University Press.
- Siegbahn, M.K. (1923). *Spektroskopie der Röntgenstrahlen*. Springer-Verlag.
- Sigma-Aldrich (n.d.). [www.sigmaaldrich.com/germany.html](http://www.sigmaaldrich.com/germany.html) (accessed 3 March 2020).
- Skoog, D. and Leary, J. (1996). *Instrumentelle Analytik. Grundlagen, Geräte, Anwendung*. Berlin: Springer-Verlag. ISBN: 3-540-60450-2.
- Slickers, K. (1992). *Die automatische Atom-Emissions-Spektralanalyse*. Gießen.
- Sommer, D. and Flock, J. (1999). Automatisierte produktionsbegleitende Analytik in der Stahlindustrie. *Nachr. Chem. Tech. Lab.* 47: 330.
- Spanier, M., Herzog, C., Groitzsch, D. et al. (2016). A flexible setup for angle-resolved X-ray fluorescence spectrometry with laboratory sources. *Rev. Sci. Instrum.* 87: 035108.
- Staats, G. and Noack, S. (1996). *Qualitätssicherung in der Analytik: Die Rekonstitution Eine Methode zur Optimierung der Richtigkeit von Analysen*. Düsseldorf: Stahl Eisen. ISBN-10: 3514005818.
- Sucker, H. (1983). *Praxis der Validierung*. Wissenschaftliche Verlagsgesellschaft.
- Tacke, I. (1925). Zur Auffindung der Ekamangane. *Z. Angew. Chem.* 38 (51): 1157.
- Taylor, H.E. (2001). *Inductively Coupled Plasma-Mass Spectrometry. Practices and Techniques*. San Diego, CA: Academic Press. ISBN: 0-12-683865-8.
- Thomas, R. (2004). *Practical Guide to ICP-MS*. New York: Marcel Dekker. ISBN: 0-8247-5319-4.
- TrinkwV\_2001 (2001). Verordnung über die Qualität von Wasser für den menschlichen Gebrauch. BMJV.
- Unterumsberger, R., Pollakowski, B., Mueller, M., and Beckhoff, B. (2011). Complementary characterization of buried nanolayers by quantitative x-ray fluorescence spectrometry under conventional and grazing incidence conditions. *Anal.Chem.* 83: 8623.
- Urch, D.S. (1996). *Chemical Speciations by X-Ray Fluorescence Spectroscopy*. Dortmund: RFA-Anwendertreffen.
- Van Espen, P., Nullens, H., and Adams, F. (1980). An in-depth study of energy-dispersive X-ray spectra. *X-Ray Spectrom.* 9 (3): 126.
- Verma, H. (2007). *Atomic and Nuclear Analytical Methods*. Springer-Verlag. ISBN: 978-3-540-30279-7.
- Vincze, L., Janssen, K., and Adams, F. (1993). A general Monte Carlo simulation of energy-dispersive X-ray fluorescence - I. Unpolarized radiation, homogeneous samples. *Spectrochim. Acta, Part B* 48: 553.

- Wacker, G. (2015). Bestimmung der Polymermatrix von Kunststoffen mit der Röntgenfluoreszenzanalyse unter Anwendung der Partial Least Squares Regression. Phd-Theses. Bergakademie Freiberg.
- Wacker, G.; Hanning, S.; Mans, C. et al. (2008). Alterung und Eignung von polymeren Standardmaterialien für die Röntgenfluoreszenzanalyse. Dortmund: RFA-Anwendertreffen.
- Waldschläger, U. (2016). Personal information.
- Waldschläger, U. (n.d.). Persönliche Mitteilung.
- Walther, A. (2005). Untersuchungen zur Zuverlässigkeit der Borbestimmung in Gläsern mit der RFA. Dortmund: RFA-Anwendertreffen.
- Walther, A. and Anderson, O. (2002). Einsatz der RFA in der Schmelzwannenkontrolle. Dortmund: RFA-Anwendertreffen.
- Welz, B. and Sperling, M. (1999). *Atomabsorptionsspektroskopie*. Weinheim: Springer-Verlag. ISBN: 3-527-28305-6.
- Wiegand, H. (1977). *Eisenwerkstoffe*. Weinheim: VCH.
- Willis, J. (2010). *XRF - Sample Preparation - Glass Beads by Borate Fusion*. Almelo: Panalytical.
- Willis, J., Feather, C., and Turner, K. (2014). *Guidelines for XRF Analysis*. Cap Town. ISBN: 978-0-620-62961-4.
- de Winter, N.J., Sinnesael, M., Makarona, C. et al. (2017). Trace element analyses of carbonates using portable and micro-X-ray fluorescence: performance and optimization of measurement parameters and strategies. *J. Anal. At. Spectrom.* 32: 1211.
- Wittkopp, A., Haschke, M., and Eicke, A. (2000). Schichtanalytik mit der Röntgenfluoreszenz. *Metall* 54: 662.
- Wolf, M. (2008). RoHs-Analytik in der Praxis: Möglichkeiten und Grenzen des RFA-Screenings. Dortmund: RFA-Anwendertreffen.
- Wolff, T.; Reinhardt, F.; Nitsche, F.; Docenko, D. (2018). Invited - full spectrum modeling: understanding the matter. *Denver X-Ray Conference*, Big Sky.
- Young, K.E., Evans, C.A., Hodges, K.V. et al. (2016). A review of the handheld X-ray fluorescence spectrometer as a tool for field geologic investigations on Earth and in planetary surface exploration. *Appl. Geochem.* 72: 77.
- Zurfluh, F.J., Hofmann, B.A., Gnos, E., and Eggenberger, U. (2011). Evaluation of the utility of handheld XRF in meteoritics. *X-Ray Spectrom.* 40: 449.

## Index

### a

- abrasion analysis 209–211
- absorption 16, 44, 99, 134
  - detector window 70
  - measurement medium 107–110
  - sample cup 57
- absorption edge 90, 104, 256
  - energy 269, 391
- absorption length 121, 309
- absorption mode 291, 297
- accuracy 10
  - obtainable 133
- analysis of
  - abrasion 209–211
  - abrasion particles in waste oil 315–316
  - additives 261
  - Al-alloys 191–192
  - animal food 243–244
  - archeometric objects 344
  - bauxite 218–219
  - boron in glasses 201
  - cement 223–227
  - ceramics, refractories 237–239
  - CIGS 305–306
  - coal 227–230
  - coke 227–230
  - compact samples 189
  - consumer goods 324–325
  - Cu-alloys 189–191
  - dust in work environments 241
  - dusts 239–242
  - element distributions 331
  - ferroalloy 230–235
  - float glass 200
  - food stuff 242–245
  - free lime 227
  - fuels 255–260
  - geological samples 213–216
  - glass 199–203
  - glass particles 316–317
  - hidden pigment layers 349
  - high-alloyed steel 187–188
  - historical coins 347–348
  - inclusions 318
  - infant food 244–245
  - iron alloy 183–188
  - iron ore 216–217
  - layer systems 291
  - light element in liquids 263–265
  - liquids 253–255
  - low-alloyed steel 185–187
  - lubricating oils 258–260
  - medium dust loads 239–240
  - Mn, Co, Ni, Zn, Pb ores 217–218

- analysis of (*contd.*)
  - non-destructive 8
  - nonhomogeneous samples 287–290
  - oils 255–260
  - ores 216–221
  - particles 313–317
  - Pb in paint 321
  - pharmaceuticals 245–246
  - polymers 203–209
  - powder samples 213
  - precious metal 322–323
  - precious metal jewelry 195–199
  - precious metal ores 219–221
  - pure elements 198–199
  - qualitative 10, 28
  - quantitative 10, 28
  - quartz 223
  - rare earth element ores 219–221
  - refractories 192–194
  - scrap sorting 321–322
  - secondary fuels 246–252
  - sewage sludge 221–223
  - slags 235–237
  - soil 221–223
  - solder alloys 194–195
  - solder structures 306–307
  - solid samples 183
  - Ti-alloys 194
  - toxic elements 324–328
  - toxic elements in fuel 256–258
  - toys 328–300
  - traces in liquids 261–263
  - unknown coating systems 307–308
  - waste 246
  - wear debris 260
- analysis of variance (ANOVA) 152
- analysis report 27, 29
- analysis task 28, 144, 204, 252, 256
- analyte line 70, 102, 115, 145
  - layer analysis 136
- analytical errors 149
  - randomly 157–158
  - systematic 158–159
- analytical method 27, 31, 74, 126, 127, 146, 156
- analytical performance
  - abrasion analysis 211
  - Al-alloys 191–192
  - Bauxite 219
  - cement 226
  - ceramics, refractories 238
  - coal 230
  - consumer goods 327
  - Fe-ores 217
  - ferro-alloys 235
  - float glass 203
  - fuels 258
  - geological samples 216
  - handheld 320
  - high alloy steel 188
  - layer systems 293
  - low alloy steel 187
  - lubricating oils 259
  - metal solutions 191
  - Ni-Fe-Co alloys 189
  - pig and cast iron 185
  - polymers 206
  - precious metals 198
  - secondary materials 251
  - slags 237
  - soils, sludges 223
  - solder alloys 195
- analytical procedure 27, 31, 143



- analytical question 4, 32, 143, 290, 319
- analytical task 1, 26, 28, 189, 195–196
- analyzed mass 35, 126
- analyzed volume 32–36
- ashing, biological materials 59
- at-line analysis 368
- Atomic Absorption Spectrometry (AAS) 168–169
- atomic number  
dependence of important parameters 7
- atomic weight 388, 389
- automation 10, 86, 356, 371
- average value 39, 151
- b**
- background correction  
ED spectra 115
- background position 74, 108, 115
- ball mill 42, 231
- bandpass filter  
excitation beam 93
- binder 45
- binder tray 46, 59
- blank sample 32, 116, 127, 132, 271
- bracketing technique 124
- Bragg angle 63, 66, 86, 202
- Bragg's equation 61, 68
- Bragg's law 20
- c**
- calibration models  
conventional 118–121  
fundamental parameter based 121–123  
standard based 118
- calibration sample 32, 118
- cellulose 48
- Certified Reference Material 131
- characteristic lines  
intensity ratios 14
- characteristic spectrum 11
- chemometric method  
glass particles 316–317  
polymers 206–209  
spectra evaluation 358–360
- cluster analysis 142
- coherent scattering 18
- collimator 81, 93, 287, 315
- collimator size 67
- combinatorial analysis 355  
for drug development 357–358
- Compton electron 76, 178
- Compton peak 18, 220, 281
- Compton–Rayleigh ratio 18, 256
- Compton scattering 18, 104, 120, 123, 204
- concentration range 8
- confocal geometry 311
- continuous spectrum 11
- costs 49, 367
- count number 108, 112
- count rate 62, 102, 104, 110, 129, 289
- count rate capability 23, 71, 74, 105
- creation of an application 143
- cross-contamination 38
- crystal-collimator combination 87, 113
- crystalline samples 77
- crystalline structure 19
- crystal, WD-spectrometer 62, 67
- curved crystals 93
- cutting mill 42

**d**

- dead time 72, 109
  - optimal throughput 71–72
  - pile-up probability 77
- degree of determination 126
- density 12, 16, 45, 134, 135, 177, 388
  - sample 43
- depth of penetration 9
- detection efficiency 70, 81
- detection limit 8, 126, 127
  - blank value method 128
  - geological samples 215
  - layer systems 136
  - TXRF 89
- detector 21
  - development 23
  - types 68
- detector saturation 110, 184
  - WD instruments 72
- difference method 199
- diffraction peak 77
  - elimination 107
- disk mills 42
- drift correction 131
- drift correction sample 32
- dust collection 239

**e**

- EDS instruments
  - principle layout 81
- elastic scattering 18
- electrolyte manganese 230
- electronic noise contribution 68
- element analysis methods 167, 175
- element distribution 10, 93, 287
  - archeometric objects 344–350
  - art objects 349

- electronic components
  - 342–344
- geological samples 333
- homogeneity tests 351
- image quality 332
- line overlap 337
- maximum pixel spectrum
  - 339–340
- object spectra 335–336
- printed circuit board 343
- sum spectrum 334–335
- element identification 21, 28, 99
- element range 8
- emission mode 291, 294, 298
- empirical model
  - linear, quadratic 119
- energies
  - K-line 394
  - L-lines 397
  - M-lines 401
- energy-dispersive spectrometer
  - 21
- energy resolution 15, 112, 289, 302
  - EDS 68–71, 289, 303
  - high 96
  - WDS 66–68
- enrichment
  - by absorption 264–265
  - by complexing 265
  - by drying 261–262
- equipment for fusion beads 52
- equivalent dose 177, 178
- error 149
  - absolute 164
  - propagation 160–162
  - randomly 157–158
  - relative 164
  - statistical 102, 152
  - stochastic 157

- systematic 158–159
- error information
  - recording 164–165
- escape peak 76
- ESMA 23, 173
- excitation conditions 10, 86, 92, 99, 103, 145, 295
  - tube voltage and current 104
- excitation geometry 36
  - confocal geometry 95–96
  - ED-spectrometers 81–85
  - grazing incidence 97
  - monoenergetic radiation 90–91
  - polarized radiation 91–93
  - position sensitive 93–94
  - total reflection 88–90
  - WD-spectrometers 85–87
- f**
- Fano factor 69
- Ferro-Chromium 230
- Ferro-Manganese 230
- Ferro-Molybdenum 230
- Ferro-Niobium 230
- Ferro-Silicon 230
- Figure of Merit (FOM) 129
- filter
  - dust collection 60, 240, 279
  - excitation beam optimizing 63, 73, 78, 106
  - selection 145
- fixed channel
  - Boron in glass 202
- fluorescence intensity 36
  - fundamental calculation 117
  - grinding time 43
  - matrix dependence 101
  - sample density 44
  - sample morphology 44
  - surface roughness 40
- fluorescence yield 15, 19, 117, 416
- flux 50, 51, 236
- free lime 227
- fusion beads 48
  - crystallization 54
- fluxes 50
- instrumentation 49
- oxidizing agents 50
- quality criteria 53–54
- temperature profile 52
- g**
- Gaussian distribution 155, 157
- Gauss statistics 102
- grain size 31, 42, 43
  - distribution 46
  - for fusion beads 49
- Gray (Gy) 177
- grazing incidence 269, 309
- grazing incidence X-ray emission (GIXE) 97, 309
- grinding time 43
  - ferro alloys 231
- grinding tools 42
- gross intensity 115
- h**
- half-width 178
- handheld
  - archeometric objects 345
  - art objects 323–324
  - prospecting in geology 323
  - sample preparation 320
- handheld devices
  - material identification 318–324
- hidden layers 304, 306
  - of pigments 350

- hidden layers (*contd.*)
- high-throughput screening 355
- homogeneity 38
  - by elemental distribution 351
  - fusion beads 53
  - by multi point measurement 352–353
- house standard 379
- i***
- impactor 239
- incident angle 35, 97, 269, 309
- incoherent scattering 18
- Inductively Coupled Plasma (ICP) 170
- inelastic scattered bremsstrahlung 105
- inelastic scattering 18, 124, 206
- infinite thickness 36
- information depth 9, 31, 32, 36, 136, 263, 292, 316
  - layer systems 291
  - small particles 313
  - TXRF 271
- in-line analysis 368
- instrument types 61, 81, 98
- intensity normalized to
  - current 112
  - time 112
- intensity ratio 114
  - quant models 122
  - quant of coatings 135, 301
  - for speciation analysis 363
- internal standard 120
  - analysis of dust 240
  - analysis of liquids 263
  - TXRF 89, 121, 269, 278
- k***
- Kramers' law 12
- l***
- laboratory sample 26–28, 31, 32, 149, 159, 170, 231
- Lambert-Beer's law 15, 34, 134, 272
- laser induced breakdown spectroscopy (LIBS) 171–172
- layer analysis 9, 25, 133, 135–139, 290, 291–293, 297
- layer systems 24, 28, 291
  - absorption mode 297
  - characterization 133–140
  - CIGS 305–306
  - GIXE 97
  - measurement technology 293–294
  - mono-layers 294–302
  - multi layers 304–307
  - NiP-layers 300–302
  - relative mode 298–302
  - sample handling 292–293
  - ultra-thin layers 302–304
- limit of detection 127, 174, 384
  - sulfur 257
- line energies 13
  - dependence on atomic number 17
- line intensity 99, 102
- line interferences 7, 110, 414
- line-like spectra 11, 12, 113
- liquids
  - analysis 253–265
  - direct measurement 55–58
  - measurement medium 107–110
  - multielement analysis 254–255
  - preparation 54–55
  - trace analysis 261–263

- trace analysis by enrichment 264–265
  - lithium-metaborate 40, 50, 52, 55, 225
  - lithium-tetraborate 40, 50, 51, 193, 201, 222, 225, 239
  - LiTrap 263, 264
  - live time 109–110
  - loss of ignition 50, 53, 218, 225
- m**
- macro X-ray spectrometer 94–95
  - majors 133, 164, 341
  - mass-absorption coefficient 99
  - mass attenuation coefficient 12, 16, 103, 104, 117, 134, 139, 177, 272, 309
  - mass per area 291
  - mass spectrometry (MS) 1, 3, 167, 168, 171, 172–173
  - matrix correction 119, 129, 216, 255
    - concentration-corrected 119
    - intensity-corrected 120
  - matrix dependence 8
  - matrix influence
    - correction 120
    - fluorescence intensity 205
  - matrix interaction 99
    - change by absorbers 51
    - quantification 102
    - reduction by fluxe 54
    - secondary and tertiary effects 101
    - for TXRF 89
  - measurement
    - conditions 102
    - long term stability 153–154
    - precision 151–153
    - reproducibility 154
    - time 108
    - uncertainty 28, 29, 159
  - measuring sample 32
  - measuring time 1, 10, 56, 63, 64, 73, 74, 83, 86, 96, 110, 112, 128, 145, 158, 190, 278, 290, 297, 318, 332, 335, 336, 345, 352
  - melting, surface tension 52
  - micro-X-ray fluorescence ( $\mu$ -XRF) 2, 106, 315, 331
  - minerals 213, 333, 335, 358, 371, 376
  - minors 133, 341
  - Monte Carlo quantifications 124
  - mortar 42, 223
  - Moseley's law 13, 99, 110
  - multi-point measurements 352–353
- n**
- net intensity 112, 115
  - neutron activation analysis (NAA) 168
  - noise, energy dependence 68
  - nomenclature
    - IUPAC 15
    - Siegbahn 15
  - nonhomogeneous samples
    - measurement modes 287–288
  - normal distribution 152, 155, 157
- o**
- off-line analysis 368, 369
  - on-line analysis 368, 376–377
  - operating costs 79–80
  - optical emission spectrometry (OES) 1, 167, 169–172

- optimization criteria 102–103
- optimum throughput 71–72
- ores
  - Mn, Co, Ni, Cu, Zn, Pb 217–218
  - precious metals 219–221
- overlap factors 113
  
- P**
- paraffin wax 48
- peak fitting 75, 110, 113, 158, 289, 293
  - influence to uncertainty 75, 78
- peak intensity
  - determination 112–116
- peak overlaps 62, 64, 74, 75, 102, 110, 112–114, 119, 188, 197, 198, 217, 252, 271, 289, 327
- peak-to-background ratio 64
  - assessment criteria 129
  - measuring conditions 73
  - optimal sensitivity 73
  - polarized excitation 91–93
  - primary spectrum 105–107
  - requirements 102
- penetration depth 9, 31, 34, 96, 97, 173, 177, 194, 263, 309, 311
- preparation small particles,
  - fusion bead 41
- periodical system 192, 214, 388
- phase analysis 141–142
- photo-absorption coefficient 13, 117
- pigment investigations 349
- pile-up peak 77
- PIN-diode 68, 302, 303
- planet mill 42
- point analyses 4, 183, 289, 290, 331, 342, 343, 346
- Poisson statistics 102
- positive material identification (PMI) 28, 83, 141, 211, 316
- precision 162
  - process capability 154–156
- preparation
  - by cutting 42
  - by drying 55
  - by grinding 42
  - of hard-metals 192
  - of organic tissues 59
  - by polishing 40
  - of precious metal jewelry 195–198
  - by pre-oxidation 50
  - by remelting 39
- preparation small particles,
  - pouring 43–44
- pressed pellet 44–49, 54, 213–220, 222–229
  - stability 46
- pressing die 214
- press mold 44
- principal component analysis 141–142, 317, 360
- process control 367–377
- prop-counter 68, 70, 301, 303
- proton-induced X-ray emission (PIXE) 173
- pulse throughput
  - influence to measuring time 74–75
  
- q**
- qualitative analysis 7, 10, 21, 28, 81, 99, 316, 384

- quality management 5, 291,  
379–386
- quantification  
chemometric methods  
140–143  
by reconstitution 124–125
- quantification models 117  
comparison 129–131  
layer systems 138
- quantitative analysis 10, 18, 21,  
28, 99, 239, 316, 319, 321,  
322
- r**
- radiation damages  
clinical effects 180  
genetic 178  
relative sensitivities 179  
somatic 178  
teratogenic 178
- radiation exposure by  
cosmic radiation 180  
inhalation of Radon 180  
natural 179–180  
terrestrial 180
- radiation protection 177  
dose 177  
half-width thickness 177  
handheld instruments 320  
regulations 181
- raw data 28
- Rayleigh scattering 17, 104
- real time 109, 110, 368
- recalibration sample 32
- reference materials 109, 118,  
125, 131–133, 167, 170,  
205, 223, 353, 376, 380, 381,  
426
- reference sample 4, 8, 28, 29, 90,  
117, 118, 120, 122, 131, 145,  
146, 163, 204
- reflections, higher order 76
- relative mode 291, 298–302
- relative standard deviation 151  
statistical error 152
- repeatability 29, 125, 150, 154,  
186, 187, 226, 258–260,  
289, 295, 365
- Restriction of Hazardous  
Substances (RoHS) 194,  
307, 324, 343
- rocks 33, 41, 51, 213, 216, 350
- rotating mill 42
- s**
- sample  
blank 32  
calibration 32  
drift correction 32  
recalibration 32
- sample cup 56  
foil, transmission 57  
window materials 56
- sample preparation 8, 26, 27  
adjust to device geometry 9  
aerosols 59–60  
aids 31  
automated 371  
binders 48  
biological materials 58–59  
carbonates 55  
contaminations 37–38  
dust 59  
fusion beads 48  
generation of homogeneous  
samples 31  
glasses 40–41  
grain size effects 47

- sample preparation (*contd.*)
  - liquids 55–58
  - metallic compounds 55
  - metals 39–40
  - micro droplets 262, 270, 285
  - particles 314
  - pouring loose powder 43–44
  - powder-like materials 41
  - pressed pellets 44
  - representativity 41
  - small particles 59–60
  - small part materials 41–55
  - sulfide minerals 55
  - surface contamination 36
  - surface roughness 36
  - targets 31
  - techniques 33
  - TXRF 269–271
- sample thickness 36, 37, 46, 52, 86, 205, 225, 228, 271–273, 340
- sample volume 9, 28, 36, 97, 99, 121, 158, 188, 222, 252, 351
- sampling 4, 26, 27, 39, 63, 79, 82, 83, 133, 149, 185, 210, 216, 222
- saturation thickness 127, 210, 291, 296
  - influence to intensity 36
- scattered radiation
  - dependence on energy 20
  - dependence on scatter direction 20
- scattering 16, 17, 26
  - background 60, 115, 363
- scintillation counter 62, 70
- secondary fuels
  - toxic elements 247
- secondary raw materials
  - liquids 249–250
  - solid 247–249
- self-absorption 134, 295
- sensitivity 10, 64
  - improvement 89–92, 265
  - for light elements 107, 202
  - optimal for EDS 73
- setting parameters 64, 80
- shaping time 71–73
- shelf 79
- Sherman equation 117, 121–123, 134, 138, 209
- Si(Li) detector 68, 70, 71, 91
- Sievert (Sv) 177
- significant figures 133, 164, 165
- silico-manganese 230
- silicon drift detectors (SDD) 23, 68, 71, 74, 129, 137, 289, 293, 320
- sodium-borate 192
- sodium-tetraborate 50, 236
- solid samples
  - coating reference 296
- speciation analysis 361
  - Al-inclusions in steel 363–365
  - S-compounds 362–363
  - SiO<sub>2</sub> in SiC 365
- spectra acquisition 63
- spectra artifacts 76–79
- spectra deconvolution 113–114
- spectra evaluation, chemometric 358–360
- spectral background, WD spectra 115
- spectrometer
  - coating thickness 94
  - monoenergetic excitation 90
  - polarized radiation 91–93
  - position-sensitive 93–94
  - tabletop 84–85
  - total reflection 88–90



- spectroscopy
  - energy-dispersive 63
  - wavelength-dispersive 62
- spectrum
  - characteristic 11
  - continuous 11
  - tube 12
- spot size 93, 94, 96, 136, 194, 196, 287, 288, 290, 291, 293, 299, 332
- standard deviation 39, 74, 75, 102, 108, 109, 128, 151–153, 155, 157, 185, 188, 201, 236, 252
- standard reference material 118, 131
- statistical error 8, 23, 69, 74, 75, 102, 103, 125, 127, 129, 144, 152, 185, 188, 198, 208, 225, 226, 238, 252
- Student's distribution 152, 153
- surface roughness 10, 31, 36, 38, 40, 43, 48, 158, 187
- surface tension 52
- synchrotron 2, 11, 91, 297, 309, 363
- synthetic multilayer systems (SML) 67
- t**
- tail 79
- target disc model 149
- target material 18, 103
  - tube 103
- thickness ranges 37, 136, 137, 296, 305
- thin section, geology 333, 340–342
- threshold control 10, 28, 215
- threshold value 28, 215, 242, 255, 323, 325
- tolerance limits 155
- tolerance window 380
- total reflection X-ray fluorescence (TXRF) 88, 90, 120, 210, 263, 269
  - analysis by VPD 284–285
  - analysis of aerosols 279
  - analysis of aqueous solutions 274–278
  - analysis of blood and blood serum 280–282
  - analysis of depth profiles 285–286
  - analysis of drinking water 275
  - analysis of HG in water 277
  - analysis of high-purity chemicals 283
  - analysis of nanoparticles 279–280
  - analysis of pigments 278
  - analysis of traces in body tissues 282–283
  - critical sample thickness 272
  - detection limits 273–274
  - incidence angle 269
  - matrix interaction 272–273
  - measurement geometry 271
  - measuring time 269
  - quantification 271–272
  - sample quantities 269
  - special features 271
- traceability to SI-units 379
- traces 1, 38, 44, 54, 133, 171, 184, 190, 191, 194, 199, 202, 228, 237, 254
- transfer factors, element-oxide 418
- transition probability 13, 117

- transmission, sample cup foil 57
- trueness 126, 127, 150, 156, 170, 189, 196, 198, 215, 216
- tube parameter
  - voltage and current 105
- tube power 25, 73, 74, 82, 86, 103, 105, 288, 320, 366
  
- u**
- uncertainty 385
  - bottom-up method 161–162
  - layer systems 140
  - top down method 162–163
- uncertainty budget 147, 161, 418
  
- v**
- validation 28, 380
  - parameters 384–385
  - procedure 382
- vapor phase deposition (VPD) 284
  
- w**
- wavelength-dispersive spectrometer 20
  - multi-channel 87
  - sequential 85–87
  - simultaneous 87
- wavelength-dispersive spectrometers (WDS) instruments
  - principle layout 85
- wavelengths 11
- wavelengths
  - K-lines 404
  - L-lines 407
  - M-lines 411
- wax 45, 48, 201, 218, 225, 228, 231
- working range 127–129
  
- x**
- X-ray lines, frequency 110
- X-ray microanalysis 23
- X-ray optics 1, 8, 11, 80, 88, 93, 95, 288
- X-ray spectra 7, 20–21, 99–147
- X-ray spectrometer
  - energy dispersive 63
  - energy resolution 64
  - general design 61–63
  - handheld 25, 82, 98, 215
  - multichannel 98
  - portable instruments 83–84
  - sequential 98
  - table top 98
  - total reflection 98
  - wavelength dispersive 66
- X-ray spectrometry
  - history 21